

Hemicelluloses: Science and Technology

ACS SYMPOSIUM SERIES **864**

Hemicelluloses: Science and Technology

Paul Gatenholm, EDITOR
Chalmers University of Technology

Maija Tenkanen, EDITOR
University of Helsinki

**Sponsored by the
ACS Division of Cellulose and Renewable
Materials**



American Chemical Society, Washington, DC

In Hemicelluloses: Science and Technology; Gatenholm, P., et al.;
ACS Symposium Series; American Chemical Society: Washington, DC, 2003.

International Symposium on
Xylans, Mannans and Other
Hemicelluloses



Library of Congress Cataloging-in-Publication Data

International Symposium on Xylans, Mannans and Other Hemicelluloses (1st : 2002 : Orlando, Fla.)

Hemicelluloses : science and technology / Paul Gatenholm, editor, Maija Tenkanen, editor ; sponsored by the ACS Division of Cellulose and Renewable Materials.

p. cm.—(ACS symposium series ; 864)

Includes bibliographical references and index.

ISBN 0-8412-3842-1

1. Hemicellulose—Congresses.

I. Gatenholm, Paul. II. Tenkanen, Maija. III. American Chemical Society. Division of Cellulose and Renewable Materials. IV. American Chemical Society. Meeting (223rd : 2002 : Orlando, Fla.) V. Title. VI. Series.

QD323.I58 2002
547.782—dc21

2003052411

The paper used in this publication meets the minimum requirements of American National Standard for Information Sciences—Permanence of Paper for Printed Library Materials, ANSI Z39.48-1984.

Copyright © 2004 American Chemical Society

Distributed by Oxford University Press

The photograph of the image on the cover was taken by Mariitta Svanberg of VTT Biotechnology. The molecular model was provided by Paul Gatenholm of Chalmers University of Technology.

All Rights Reserved. Reprographic copying beyond that permitted by Sections 107 or 108 of the U.S. Copyright Act is allowed for internal use only, provided that a per-chapter fee of \$24.75 plus \$0.75 per page is paid to the Copyright Clearance Center, Inc., 222 Rosewood Drive, Danvers, MA 01923, USA. Reproduction or reproduction for sale of pages in this book is permitted only under license from ACS. Direct these and other permission requests to ACS Copyright Office, Publications Division, 1155 16th St., N.W., Washington, DC 20036.

The citation of trade names and/or names of manufacturers in this publication is not to be construed as an endorsement or as approval by ACS of the commercial products or services referenced herein; nor should the mere reference herein to any drawing, specification, chemical process, or other data be regarded as a license or as a conveyance of any right or permission to the holder, reader, or any other person or corporation, to manufacture, reproduce, use, or sell any patented invention or copyrighted work that may in any way be related thereto. Registered names, trademarks, etc., used in this publication, even without specific indication thereof, are not to be considered unprotected by law.

PRINTED IN THE UNITED STATES OF AMERICA
American Chemical Society
Library
1155 16th St., N.W.
Washington, D.C. 20036

Foreword

The ACS Symposium Series was first published in 1974 to provide a mechanism for publishing symposia quickly in book form. The purpose of the series is to publish timely, comprehensive books developed from ACS sponsored symposia based on current scientific research. Occasionally, books are developed from symposia sponsored by other organizations when the topic is of keen interest to the chemistry audience.

Before agreeing to publish a book, the proposed table of contents is reviewed for appropriate and comprehensive coverage and for interest to the audience. Some papers may be excluded to better focus the book; others may be added to provide comprehensiveness. When appropriate, overview or introductory chapters are added. Drafts of chapters are peer-reviewed prior to final acceptance or rejection, and manuscripts are prepared in camera-ready format.

As a rule, only original research papers and original review papers are included in the volumes. Verbatim reproductions of previously published papers are not accepted.

ACS Books Department

Preface

Hemicelluloses are polysaccharides that are biosynthesized in large quantities in the majority of trees and terrestrial plants. An estimated annual production of hemicelluloses on the earth is in the range of 60 billion tons. No statistics on the production of hemicelluloses in oceans and other aquatic systems are available. Hemicelluloses are the world's second most abundant family of polymers after cellulose and thus represent an enormous renewable resource that until now has been almost completely unused.

In contrast to hemicelluloses, cellulose plays a very important role in human life. Cellulosic materials are used in a wide variety of industrial applications ranging from paper, cloths and packaging to plastics, cosmetics, pharmaceuticals, and food additives. Hemicelluloses are nearly always intimately interconnected with cellulose. They are important constituents in plants holding together the cellulosic microfibrils and acting as an interphase toward the lignin matrix. Unlike cellulose, which is a high molecular weight linear homopolymer organized in a crystalline state, the hemicelluloses are often branched and composed of different sugar units. Their molecular weight is not as high as that of cellulose and the consequence of their heterogeneous and branched chemical structure is a non-crystalline morphology in the native state. This makes hemicelluloses much more susceptible to chemical and enzymatic reactions. For this reason, hemicelluloses are often degraded during fiber liberation processes such as pulping. Although the hemicelluloses are sometimes present in an almost unmodified state, such as in mechanical pulps, our understanding of the effects of the hemicelluloses on the fiber properties is poor.

Only recently have new processes been developed where biomass components are separated and isolated. Access to hemicelluloses on the pilot scale opens a new world of applications of hemicelluloses as materials. A new generation of plastics, coatings, hydrogels, and so on based on this renewable resource is waiting to be discovered. We are convinced that the hemicelluloses will play an important role in moving society from its petrochemical dependency into a sustainable economy.

The wake-up call for this enormous renewable resource has gone through Scandinavia and Europe to North America. The editors organized a 1st International Symposium on Xylans, Mannans and Other Hemicelluloses as a Symposium of the American Chemical Society Division of Cellulose and Renewable Material in Orlando, Florida in April 2001. The meeting was very successful and resulted in fruitful interaction between scientists and resulted in this book, which covers topics dealing with the isolation processes of the hemicelluloses and the characterization of their structure. The development of new analytical tools for determining the molecular architecture of hemicelluloses is described. The assembly characteristics and the interactions of hemicelluloses with cellulose are recurrent themes in this book, and the enzymatic and chemical modifications of hemicelluloses along with new applications for materials based on hemicelluloses are also covered. We hope that this book will play an important role in the process of utilization of hemicelluloses.

Acknowledgments

We thank all the contributing authors for excellent collaboration. Paul Gatenholm acknowledges the Swedish funding agency Vinnova for supporting him in his research activities in the field of hemicelluloses. Without this support it would have been difficult to make a priority of taking time to edit this book. Special thanks go to Ann Jakobsson for handling all correspondence with authors and reviewers and getting all the manuscripts in a timely manner.

Paul Gatenholm

Department of Materials and Surface Chemistry
Biopolymer Technology
Chalmers University of Technology
SE-412 96 Göteborg, Sweden

Maija Tenkanen

Department of Applied Chemistry and Microbiology
University of Helsinki
P.O. Box 27
FIN-00014 Helsinki, Finland

Chapter 1

Hemicelluloses and Their Derivatives

RunCang Sun^{1,3}, X. F. Sun², and J. Tomkinson³

¹State Key Laboratory of Pulp and Paper Engineering, South China University of Technology, Guangzhou 510640, People's Republic of China

²College of Forestry, The North-Western Science and Technology University of Agriculture and Forestry, Yangling 712100, People's Republic of China

³The BioComposites Centre, University of Wales, Bangor, Wales LL57 2UW, United Kingdom

Hemicelluloses are a large group of polysaccharides found in the primary and secondary cell walls of all land and fresh water plants, and in some seaweeds. The hemicelluloses, isolated from cereal straws, are largely represented as complex heteropolysaccharides whose structure varies in the nature and degree of branching of the β 1,4-linked xylopyranosyl main chain. Hemicelluloses interconnect other cell wall components *via* covalent linkages and also secondary forces. In this review, the structural features and complexity of the hemicelluloses are illustrated. Alkaline peroxide treatment provides a suitable and environmental friendly procedure for the isolation of hemicelluloses from different cereal straws and other agricultural residues. The esterification of hemicelluloses prepared under homogeneous reaction conditions in the presence of 4-dimethylaminopyridine or *N*-bromosuccinimide as a catalyst is summarized.

Introduction

Hemicelluloses rank second to cellulose in abundance in wood and cereal straws, comprising roughly one-fourth to one-third of most plant materials, and this amount will vary according to the particular plant species, such as maize stems (28.0%), barley straw (34.9%), wheat straw (38.8%), rice straw (35.8%), and rye straw (36.9%) (1). They, unlike cellulose, which is a unique molecule differing only in degree of polymerization and crystallinity, are non-crystalline heteropolysaccharides and classically defined as the alkali soluble material after removal of the pectic substances. This definition of hemicelluloses is very generic, but is accepted at present (2). Hemicelluloses, however, are the most complex components in the cell wall of woods, straws, and grasses. They form hydrogen bonds with cellulose, covalent bonds (mainly α -benzyl ether linkages) with lignins and ester linkages with acetyl units and hydroxycinnamic acids. In addition, hemicelluloses are formed through biosynthetic routes different to the glucose-UDP route of cellulose (a homopolysaccharide). They are branched polymers of low molecular weight with a degree of polymerization of 80-200. Their general formulae are $(C_5H_8O_4)_n$ and $(C_6H_{10}O_5)_n$ and called pentosans and hexosans, respectively (3). Hemicelluloses consist of various different sugar units, arranged in different proportion and with different substituents (4-9). The principle sugars are D-xylose, L-arabinose, D-glucose, D-galactose, D-mannose, D-glucuronic acid, 4-O-methyl-D-glucuronic acid, D-galacturonic acid, and to a lesser extent, L-rhamnose, L-fucose, and various O-methylated neutral sugars. Hemicelluloses of Gramineae such as cereal straws have a backbone of (1 \rightarrow 4)-linked β -D-xylpyranosyl units. The chain may be linear, but is often branched and usually has other glycosidically bound sugar units. Some xylan chains have D-glucopyranosyluronic acid units attached, but the most important acidic hemicelluloses are O-acetyl-4-O-methyl-D-glucuronoxylans and L-arabino (4-O-methyl-D-glucurono)xylans. In Dicots, where the hemicelluloses are mostly xyloglucan, hydroxyproline-rich glycoproteins also comprise a substantial amount of the cell wall and cross-link the carbohydrate polymers to form a rigid matrix (10). The predominant hardwood hemicelluloses are partially acetylated acidic xylans; as much as 35% of birchwood is composed of these hemicelluloses, while cottonwood contains only 13%. A small percentage of hardwood is also composed of mannan. The predominant softwood hemicelluloses are galactoglucomannans, which are partially acetylated. In addition to these hemicelluloses, 10-20% of the dry weight of the heartwood of larch comprises an arabinogalactan (11). Xylans from grasses and cereal straws have the same backbone as the wood xylans. However, they contain smaller proportions of uronic acids, but are more highly branched and contain large proportions of L-arabinofuranosyl units. In general,

arabinofuranosyl units are attached to some C-3 position of the main xylan chain and glucuronic acid and/or its 4-*O*-methyl ether linked to some xylose units. The latter are probably mainly linked to the C-2 position (12). The fact that the arabinose units generally seem to be furanosidically linked as terminal groups makes them particularly sensitive towards acid hydrolysis (2,12). The arabinose and uronic acid xylans of these hemicelluloses vary considerably from the cereal grain arabinoxylans which have an arabinose: xylose ratio of about 1 to esparto xylan which has no arabinose at all. During botanical aging, the percentage of side chains on xylans decreases markedly hence (13) straw xylans are found to have a relatively lower arabinose content as compared to the xylans from cereal grains (14). In the primary wall the 4-*O*-methyl-D-glucuronic side chains seems to be absent (15). However, oligomeric side chains containing other glycosyl residues, e.g. galactose, are also found. An acid galactoarabinoxylan has been isolated from the cell wall of Gramineae by Buchala et al. (16).

The hemicelluloses are potentially very useful. Studies on utilization of hemicelluloses from cereal straws have demonstrated to be a potential fermentation feedstock in production of ethanol, acetone, butanol, and xylitol. The current uses of xylan on an industrial scale involve their conversion to xylose, xylitol and furfural. Xylitol is produced by hydrolysis of xylan, crystallization of xylose, and hydrogenation. This has been tested in a variety of food products (17). Properties of wheat straw hemicelluloses being worth exploiting are their ability to serve as adhesives, thickeners, and stabilizers, and as film formers and emulsifiers (18). Based on an extensive study of hemicelluloses from wheat straw, we found that native hemicelluloses latexes showed good properties for making decorative paints, which indicated a possibility of using straw hemicelluloses for real commercial decorative paint systems (19). In addition, some important applications for xylans have been discovered. These include uses in chiral separations (20), cholesterol depressant (21), table disintegrant (22), HIV inhibitor (23), and dietary fibre (24). Evidently, hemicellulosic biopolymers have a very wide variety of direct food and non-food applications. In particular, some hemicelluloses from higher plants and herbs represent a potential source of pharmacologically active polysaccharides. Glucuronic acid-containing (acidic) xylans isolated from annual plant residues such as bamboo leaves, corn stalks, wheat straw (25) as well as hardwood (26,27) have been reported to inhibit markedly the growth of sarcoma-180 and other tumors, probably due to the indirect stimulation of the non-specific immunological host defense (28,29). Arabino-(glucurono) xylans isolated from *Echinacea purpurea*, *Eupatorium perfoliatum* have been reported to have immunostimulating effects (30,31). Similarly, 4-*O*-methylglucuronoxylan from *Chamomilla recutita* (32) and the acetic, highly

branched heteroxylan from *plantago* species (33,34) have been found to have anti-inflammatory activity.

Structure

Like most polysaccharides from plant origin hemicelluloses display a large polydiversity and polymolecularity. This corresponds to their being present in a variety of plant species and to their distribution in several types of tissues and cells. All straw hemicelluloses are characterized by a β 1,4-linked-D-xylopyranosyl main chain which carries a variable number of neutral or uronic monosaccharide substituents (35). For example, the hemicellulosic fraction, isolated with 0.5 M NaOH at 37°C for 2 h from wheat straw, was confirmed to be a β (1-4) xylan with side chains consisting of L-arabinofuranosyl and D-xylopyranosyl groups attached in position 3, and D-glucopyranosyluronic acid or 4-O-methyl-D-glucopyranosyluronic acid group attached at position 2. For every 15 D-xylopyranosyl residues in the main chain, there was one L-arabinofuranosyl group. For 19 such D-xylopyranosyl residues, there was one D-xylopyranosyl group, and for ~26 such D-xylopyranosyl residues, there was one uronic acid unit (Fig. 1) (36). In addition, the hemicelluloses obtained from wheat straw have also been subfractionated into hemicelluloses A, B, and C. Hemicellulose A is a more linear and less acidic fraction, while hemicellulose B is a more acidic and branched fraction. Hemicelluloses containing a high degree of side-chain substitution are more water-soluble and bind less tightly to cellulose, whereas molecules with infrequent side chains are less water-soluble and bind more tightly to cellulose (37).

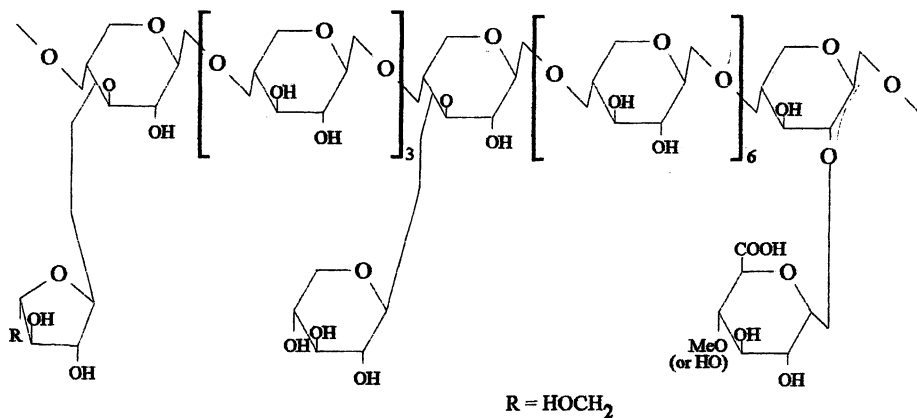


Fig. 1. A structure of wheat straw hemicelluloses.

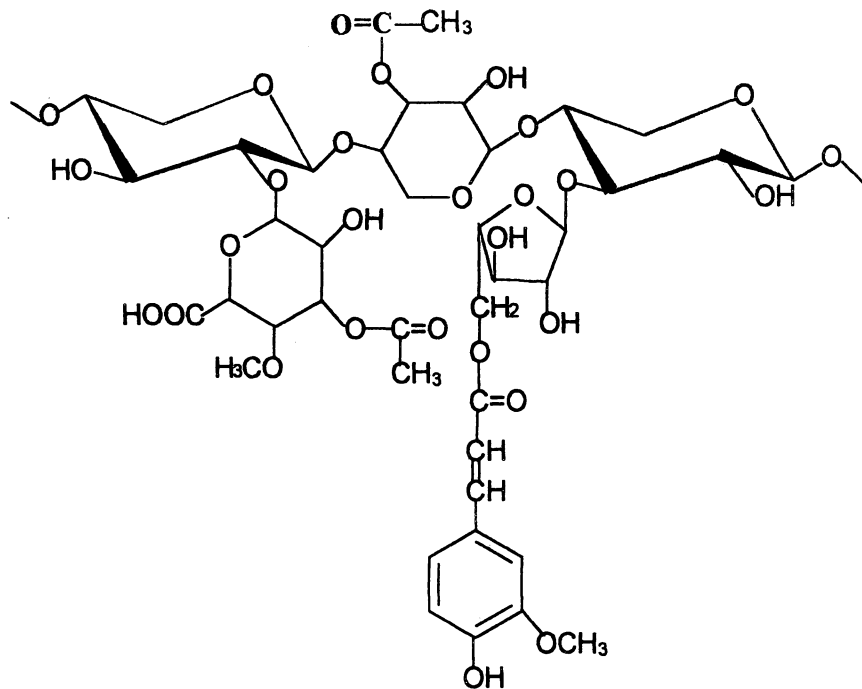


Fig. 2. A tentative 4-*O*-methylglucuronoarabinoxylan with esterified acetic acid and ferulic acids.

Timell (8,9) reviewed the chemistry of hemicelluloses from Angiosperms and Gymnosperms whereas Wilkie (38) described the structural characteristics of the different hemicelluloses from Monocotyledonous species. However, a lot less is known about their true primary structure, that is if the arabinosyl, uronic acid or acetyl substituents are attached to the xylosyl backbone randomly or as regular repeating sequences. A significant portion of the xylose in cereal straw cell walls was found to be acetylated, mainly on C-2 but also on C-3 (8). Bacon et al. (39) mentioned that cell walls of *Gramineae* plants account for 1-2% of the acetyl groups. Acetyl groups occur to the extent of 3-17% of wood hemicelluloses and are at highest content in hardwoods. Dimethyl sulfoxide extraction of angiosperm woods yields hemicelluloses with 16.9% acetate groups corresponding on the average to 7.1 ester groups per ten D-xylose units (40). These acetylated hemicelluloses are soluble in water and in solvents such

as dimethyl sulfoxide, formamide, and *N,N*-dimethylformamide. Furthermore, cell walls of cereal straws also contain 1-2% phenolic acids, which are esterified to hemicelluloses. *p*-Coumaryl and ferulyl groups are attached to the xylan through the arabinose residues at C-5 position (Fig. 2) (41). It is estimated that one out of 121 pentose residues in ferulylated and one of 243 is *p*-coumarylated in barley straw (42).

It was reported that ferulic acid ether-linked to lignin formed a cross-link to hemicelluloses through an ester linkage (Hemicelluloses-ester-FA-ether-lignin bridges). In these cases, ferulic acid ethers might form cross-links between lignin (at the β -position of the side chains) and hemicelluloses by simultaneous esterification of their carboxyl group to the C-5 position of arabinose substituents of arabinoglucuronoxylans (Fig. 3) (43-54).

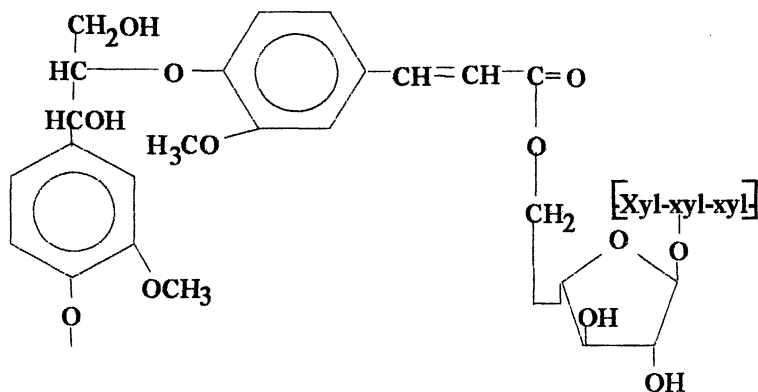


Fig. 3. Simple representative hemicelluloses-ester-FA-ether-lignin bridges.

Diferulic acids were also identified in the wheat straw cell walls by the cross-linking of arabinoxylans to lignin (Fig. 4). There are between nine and ten ferulic acid ester-ether bridges for every 100 C₆-C₃ lignin monomers (55,56). While most of the *p*-coumaric acids are mainly ester-linked to lignin at the γ -position of the side chains (Fig. 5). Only few of them are esterified to hemicelluloses at arabinose substituents of arabinoglucuronoxylans (Fig. 6). It should be noted that *p*-coumaric acid does not have a lignin/hemicelluloses cross-linking function (57-58).

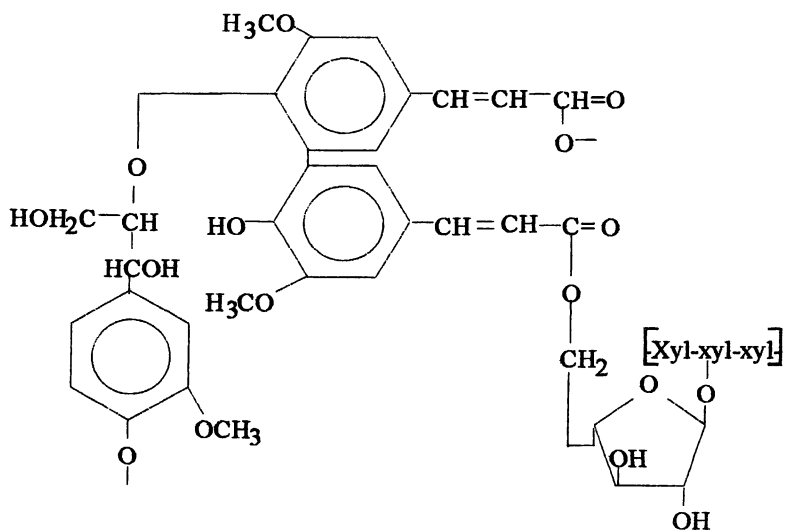


Fig. 4. A simple representative hemicelluloses-ester-diFA-ether-lignin bridge.

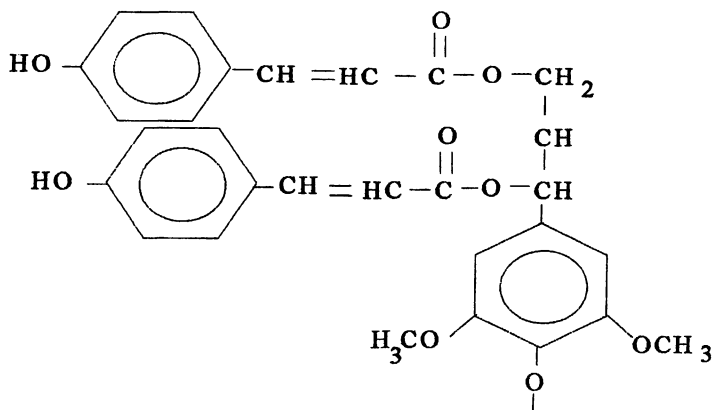


Fig. 5. A simple representative PCA-ester-lignin.

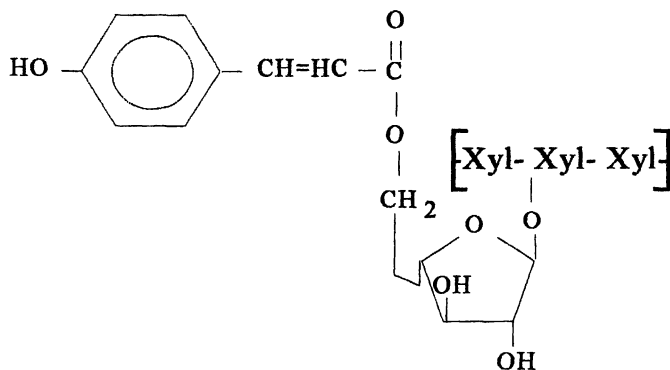


Fig. 6. A simple representative PCA-ester-hemicelluloses.

In addition to the linkages between hemicelluloses and hydroxycinnamic acids, the association of xylans with other components of the cell wall also have commercial significance and have been studied. There is evidence that, during the assembly, the synthesis and deposition of xylan is intimately linked with cellulose (59). Hemicelluloses have also been shown to be linked with secondary wall proteins. One example of specific secondary wall proteins located directly other than inferred from cDNA sequence, have been shown in Loblolly pine (60), hypocotyl of French bean (61) and in differentiating Zinnia cells (62,63). A particular protein (extensin), of which the uncommon amino acid hydroxyproline constitutes up to 20% of the amino acid content, is found in many dicots (64) as well as monocots (65). This protein makes up 2-10% of the primary cell wall and most of the hydroxyproline residues are glycosylated by a tri- or tetraarabinoside (64). Many of the serine residues are also glycosylated but with galactose residues. Hydroxyproline-rich glycoproteins containing arabinose residues have been isolated from monocotyledonous plants (66).

More importantly, the deposition of lignin in these walls involves generation of mesomeric phenoxy-radicals from the hydroxy-cinnamyl-alcohol precursors. These will rapidly form linkages with the hemicelluloses of the wall and these linkages may take place randomly (62). Our previous studies found that the majority of lignins in cereal straw cell walls are directly linked to arabinose side chains of xylan by ether bonds (67-70). Chemical studies on these linkages between lignin and hemicelluloses, especially arabinoxylans, have emphasized the important role of arabinose residues in forming these linkages. Chesson et al. (71) indicated the presence of a covalent association between arabinose side

chains of xylan and phenolic substances including lignin in forage species. The presence of lignin-arabinose linkages was also reported from spruce wood (72). The majority of these benzyl ether linkages in wheat straw cell walls are etherified to the α -position of the side chain of lignin molecules, hydrolysable by alkali (67) (Fig. 7). Another potential lignin-hemicellulosic linkage is an ester bond between the lignin and carboxyl (C-6) group of a uronic acid residue (Fig. 8). During the studies of lignin-carbohydrate complexes from *fagus crenata*, Imamura and co-workers (73) demonstrated that a part of the glucuronic acid residue is esterified in the lignified wood cell walls, and the frequency of ester bonds between the lignin and glucuronic acid residue of glucuronoxylan was determined to be 1.6 per molecular of lignin-hemicellulose complex obtained from the beech wood. The occurrence of ester bond between lignin and glucuronic acid or 4-*O*-methylglucuronic acid in the cell walls of wheat straw was corroborated by the chemical analyses and was confirmed by ^{13}C -NMR spectroscopy studies (74-77). In other words, in cereal straw cell walls, hemicelluloses are usually ester-linked through the glucuronic acid side chains to lignin, and lignin polymers are attached to arabinosyl residues by aryl-ether linkages.

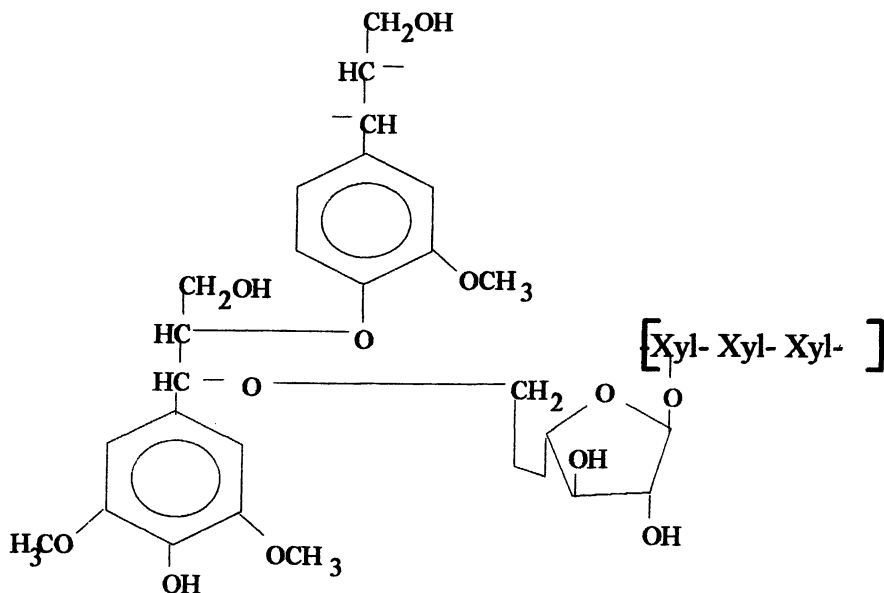


Fig. 7. A simple representative benzyl ether linkage.

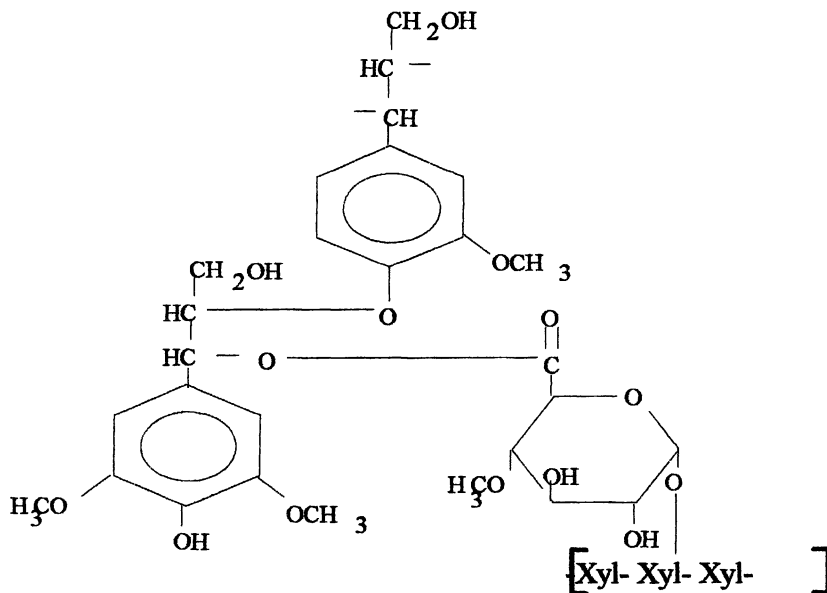


Fig. 8. A simple representative benzyl ester linkage.

Isolation

Isolation of hemicelluloses actually involves alkaline hydrolysis of ester linkages to liberate them from the lignocellulosic matrix followed by extraction them into aqueous media. However, the liberation of the xylan component from the cell wall of cereal straws is restricted by the presence of lignin network as well as ester and ether lignin-hemicellulose linkages. Furthermore, extensive hydrogen bonding between the individual polysaccharide cell wall components may impede isolation of the hemicellulosic component (17). For quantitative isolation of hemicelluloses from straw, the material must first be, therefore, pre-extracted, preferably with ethanol-toluene (2/1, v/v), so as to remove all lipophilic and hydrophilic non-structural components. As a second step, the material is delignified, after which the resulting holocellulose is extracted with alkali. The delignification is usually effected with chlorine (78), chlorine dioxide (79) or peroxyacetic acid (80). No completely satisfactory method for preparation of holocellulose is available. Some loss of the hydroxycinnamic acid appendices and degradation of the hemicelluloses is apparently inevitable.

In order to avoid saponification of ester linkages, the holocellulose is extracted in succession with dimethylsulphoxide and water. As the yield obtained using this procedure seldom exceeds 50%, most commercial hemicelluloses are usually extracted with alkali. In the case of the product obtained, except for the fact that acetyl, feruloyl-, and *p*-coumaroyl appendices have been saponified, is quite similar to the native polysaccharide (81). In recent years, the hazardous and expensive NaClO_2 -delignification step is substituted by such procedure of aqueous alcohol treatment, which yields xylan-rich polysaccharide fractions contaminated to various extent with lignin and degradation products of the cell wall components. However, the yield of the prepared hemicelluloses was lower in comparison to those obtained from partially delignified straw meal (17). Another potential method for isolation of hemicelluloses has been proposed recently by Gabrielli et al. (82), in which the wood material was extracted by an alkali followed by hydrogen peroxide treatment and ultrafiltration. The hemicelluloses were then recovered by spray drying.

The isolation of hemicelluloses by steam explosion is another potential method in an industrial separation of the polymers from cereal straw and wood samples (83,84). The use of an extruder-type twin-screw reactor makes the extraction more feasible (85). The extractability of hemicelluloses from annual plants is easier than that of wood hemicelluloses due to the lower amounts and different structure of lignin. It can be affected by the alkali type and isolation conditions and improved by a multistep mechanical-chemical treatment (86). The mechanical and chemical effect of ultrasonication on the cell wall material during alkaline extraction of annual plants was shown to be very effective. Higher yields of hemicelluloses can be achieved at lower temperatures and shorter extraction times (87-89). On the basis of extractability of the wheat straw hemicelluloses with and without application of ultrasonic irradiation in 0.5 M KOH aqueous solution, the result showed that ultrasonically assisted extraction in a period of 20-35 min produced a slightly higher yield of hemicelluloses and lignin than those of the classical alkali procedure by 0.8-1.8% of the original hemicelluloses and 0.6-5.3% of the original lignin, respectively. The hemicelluloses, obtained by ultrasound-assisted extraction, seemed more linear and less acidic than that of the hemicelluloses extracted by alkali in the absence of ultrasonic irradiation. In addition, the hemicellulosic preparations obtained by ultrasound-assisted extractions showed a relatively lower content of associated lignin, but a higher molecular weight and a slightly higher thermal stability in comparison with the hemicelluloses isolated by alkali without ultrasonic irradiation (90).

The hemicelluloses isolated by aqueous alkali from wheat straw were, in general, brown and this impedes their industrial utilization. The aim in our laboratory is to develop a commercial process for fractionation of cereal straw components using an environmental friendly procedure for the extraction of

hemicelluloses in a large scale with a light color. Based on our recent ten years' study on hemicelluloses, we found that alkaline peroxide is an effective agent for both delignification and solubilization of hemicelluloses from straws and grasses. It is generally accepted that the hydroperoxide anion (HOO^-), formed in alkaline media, is the principal active species in hydrogen peroxide bleaching systems. In contrast, hydrogen peroxide is unstable in alkaline conditions and readily decomposes into hydroxyl radicals ($\text{HO}\cdot$) and superoxide anion radicals ($\text{O}_2^{\cdot-}$). This is particularly true in the presence of certain transition metals such as manganese, iron, and copper. These radicals are thought to cause the oxidation of lignin structures which lead to the introduction of hydrophilic (carboxyl) groups, cleavage of some interunit bonds and eventually, the dissolution of lignin and hemicelluloses (91,92). The results obtained from our laboratory found that alkaline peroxide is an effective agent for both delignification and solubilisation of hemicelluloses from cereal straws. The data showed that more than 80% of the original hemicelluloses and lignin were solubilized during the treatment of cereal straws such wheat, rice, and rye straws as well as maize stems with 2% H_2O_2 at 48°C for 16 h at pH 12.0-12.5 (68,93,94). Furthermore, the hemicelluloses are much whiter in colour and contained very smaller amounts of associated lignin (3-5%) than those obtained from the traditional alkali extraction process.

Modification

The preparation and properties of new polymers from hemicelluloses are an important part of any research program aimed at utilizing annually renewable, agricultural derived polymers as extenders and replacements for polymers prepared from petrochemicals. In other words, the modification or derivatization of these polymers creates novel opportunities to maximally exploit the various valuable properties of hemicelluloses for previously unperceived applications. However, the hemicelluloses with one or two free hydroxyl groups are hydrophilic, while synthetic polymers are usually hydrophobic. This results in significantly different solubility characteristics of the hemicelluloses, i.e., solubility in aqueous alkali but insolubility in virtually all organic solvents. Furthermore, due to their different chemical and molecular structure, e.g. branched, amorphous, composed of several different types of monosaccharides (heteropolysaccharides), and consisting of different types of functional groups (e.g., OH groups, acetoxy groups, carboxyl groups, methoxyl groups, etc.), hemicelluloses represent a different type of polysaccharide that behaves differently as compared to cellulose and starch. These limited their utilization in industry. However, these shortcomings can be overcome by their modification, such as by partial hydrolysis, oxidation, reduction, etherification

or esterification of the hydroxyl groups, and cross-linking. Up to now, cellulose and starch are the main starting materials for the bulk production of modified polysaccharides, and their derivatives have been found to use in the industrial production of food, textiles, paper and cosmetics, while analogous polymerization with hemicelluloses as the substrates have received comparatively little attention. It is presumed due to the different behaviours of the hemicelluloses during modification than cellulose and/or starch derivatives (95).

Chemical modification of hemicelluloses, mainly on xylan, was investigated as early as in the 1960s as a means of making xylan solvent soluble for molecular weight determination (96-98). Glaudemans and Timell (96) succeeded in preparing the acetate of a birch xylan, which was fully soluble in chloroform. However, only 60-80% of two butyrate derivatives of xylan could be brought into solution, and it was shown that this portion had a lower molecular weight. Other esters, such as benzoate, caprate, laurate, myristate, and palmitate of xylan isolated from corncobs have been prepared (99,100). Interestingly, esterified xylan acetate with low DS is subject to biodegradation by xylanolytic enzymes in relation to DS. Cellulose and xylan acetates lose enzyme degradability at a rate of about 45% per DS-unit with DS rising, but starch acetate loses this degradability approximately twice as fast. No interpretation currently explains why cellulose and xylan derivatives have apparently greater tolerance to chemical modification than modified starch, when esterified. As early as 1967, Church (101) reported the preparation of aspenwood 4-*O*-methylglucuronoxylan graft copolymers by the ammonium persulfate-sodium thiosulfate-initiated reaction with sodium acrylate. One year later, O'Malley and Marchessault (102) prepared and characterized graft copolymers of aspenwood 4-*O*-methylglucuronoxylan by allowing the fully methylated polysaccharide to react with either living polystyrene or living poly(2-vinylpyridine). Fanta et al. (103) and EI-Shinnawy and EI-Kalyoubi (104) independently investigated the graft copolymerization of acrylonitrile onto hemicelluloses using ceric ammonium nitrate as an initiate and stated that the graft yield depends on the monomer and initiator concentration as well as reaction time and temperature. In addition, a series of structural different xyans have recently been modified to make the hemicellulosic polymers as novel materials for industries. The trimethylammonium-2-hydroxypropyl (TMAHP) xylan from aspen wood also may be used as a beater additive. This substance doubled the beating resistance and increased significantly the tear strength of a bleached spruce organosolv pulp (105). The TMAHP derivatives prepared from beechwood xylan and corn cob xylan, in particular, were shown to be useful in papermaking (106). Both derivatives improved the strength properties of bleached hardwood kraft pulp and unbleached thermomechanical spruce pulp and increased the retention of fines. The modification of

beechwood xylan (107) as well as other heteroxylans with *p*-carboxybenzyl bromide in aqueous alkali imparted water-solubility to xylans as well as moderate hydrophobic properties demonstrated by emulsifying and foam-sterilizing actives (108). Recently, Vincendon (109) has described the preparation of xylan-2,3-bis (phenyl carbamate), xylan-2,3-bis (tolyl carbamate) and the benzyl ether of xylan. These derivatives are reported to be thermoplastic materials. The substitution of xylan's hydroxyl groups by alkoxy or acetoxy substituents generally induces solubility in water and/or organic solvents, as is the case for cellulose. Water-soluble hydroxypropyl cellulose and starch derivatives find numerous applications in industry (110,111). More recently, thermoplastic xylan derivatives with propylene oxide have been prepared by reaction of polymeric xylan with propylene oxide in aqueous alkali solution. The hydroxypropyl xylan is a low molecular weight, branched, water-soluble polysaccharide with low intrinsic viscosity and thermoplasticity (100,112). In addition, hemicellulose/poly(2-hydroxyethyl methacrylate) (PHEMA)-based hydrogels have been prepared by the radical polymerization of HEMA with hemicellulose purposely modified with well-defined amounts of methacrylic functions using a redox initiator system. The resulting hydrogels after a 30 min reaction are homogeneous, elastic, and transparent materials (113).

Another potential utilization of the hemicellulosic derivatives is in pharmaceuticals. For examples, a novel drug for prophylaxes and treatment of degenerative articulator disease is based on polysaccharides, including hemicelluloses, that have been substituted with non-aromatic long-chain esters and sulfate groups in the form of a physiological tolerated cation (114). Pentosan polysulfate (PPS), usually derived from beechwood glucuronoxylan, has been known as anticoagulant for nearly thirty years in Europe. PPS has been suggested to be more effective as an anti-cancer agent when it is given intermittently and on a weekly schedule (115). It is very efficient in the treatment of pain, urgency, and frequency associated with interstitial cystitis (116). PPS also decrease the cholesterol and triglyceride level in the serum of stone forming rats (117). Meanwhile, Fan and Feng (26) reported that carboxymethyl-modified hemicelluloses can be used as a new antitumor drug in which the modified hemicellulose augment cellular immunity by enhancing the number and activity of immunocytes.

To improve the properties of hemicellulose derivatives, such as increase hydrophobicity, we have investigated to find suitable reaction media to perform derivatation reactions in homogeneous phase, in which the substitutions along the hemicellulose backbone can be achieved with satisfactory yields and with little depolymerization of the hemicellulose chains. Strongly polar aprotic solvents, such as *N,N*-dimethylformamide (DMF), were found to be able to prevent the aggregation of flexible hemicellulose chains, promoting the

interactions between substrate and reagents in our recent studies. The products were prepared under homogeneous reaction conditions in the system DMF/lithium chloride by reacting the native hemicelluloses with various acyl chlorides (C_3 - C_{18}) in the presence of 4-dimethylaminopyridine (DMAP) as a catalyst and triethylamine (TEA) as a base within 30 min at 70-75°C. The degree of substitution of esterified hemicelluloses can be controlled with high accuracy by adjusting the concentration of TEA and the molar ratio of reagent and hydroxyl functionality. The reaction conditions were optimized to give high degrees of substitution under mild reaction conditions with a short period of reaction time. Under an optimum reaction condition (molar ratio 1:3, TEA 160%, 75°C, 30 min), a high DS value of 1.75 was obtained, in which about 95% of the free hydroxyl groups in native hemicelluloses were esterified (95). The results obtained by GPC analysis showed that no significant degradation occurred during the reaction. The thermal stability of the product is increased by chemical modification (118-121).

More recently, based on the study of acetylation of alcohols under mild reaction conditions, by using *N*-bromosuccinimide (NBS) as a catalyst (122), we found that NBS, an inexpensive and commercially available reagent, is a novel and highly effective catalyst for acetylation of hemicelluloses under nearly neutral reaction conditions, in which acetic anhydride gave an advantage on the high reactivity to OH group. Acetylation between DS 0.27 and 1.15 could be prepared by varying reaction temperature between 25 and 80°C and reaction duration from 0.5 to 2 h using 1.0% NBS as a catalyst (unpublished data).

The actual role of NBS is not clear but a plausible explanation is that NBS might act as a source for Br^+ , which in turn activates the carbonyl groups of acetic anhydride to produce the highly reactive acylating agent ($CH_3-CO-N-(OCCH_2CH_2CO-)$). This acylating agent reacts with hydroxyl groups of hemicelluloses, which upon elimination of NBS produces acetylated hemicelluloses ($Xyl-O-CO-CH_3$) (Fig. 9). However, the possibility of NBS generating HBr, which may activate the carbonyl group for further reaction, can not be ruled out (123). The actual role of this reagent should be further investigated.

In short, alkylation of the hydroxyl groups of hemicelluloses to increase hydrophobicity is one approach toward increasing the water resistance of hemicelluloses. Derivatization of hemicellulose hydroxyl groups may also reduce the tendency of hemicelluloses to form strong hydrogen-bonded networks and increase film flexibility. This increasing hydrophobic capacity would lead to potential use of esterified hemicelluloses in the production of plastic, especially biodegradable and/or environmentally degradable plastics, resins, films, and coatings in the food industry. That is, the hydrophobicity of the esterified hemicelluloses is advantageous for maintaining a large surface on

dry from water and would make the polymers compatible with other hydrophobic materials. This feature could be exploited in developing new biopolymer materials from renewable resources.

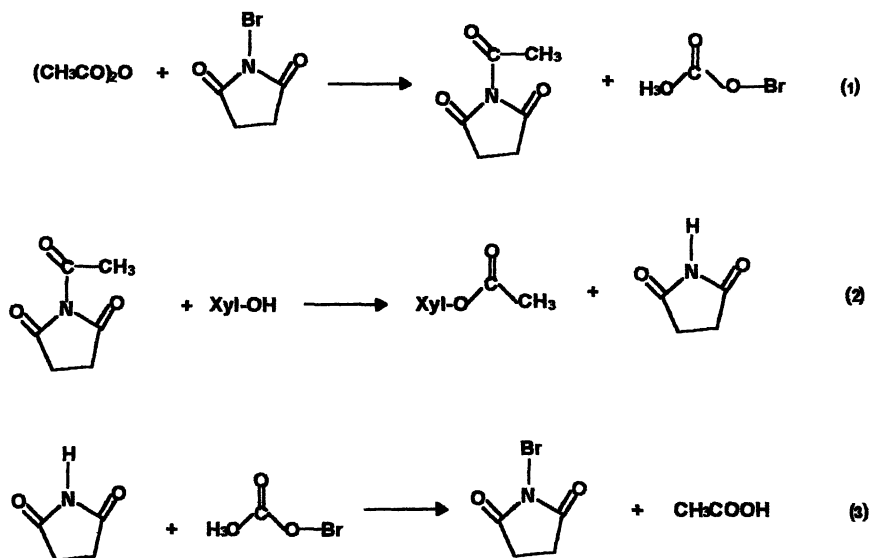


Fig. 9. Scheme mechanism of acetylation of hemicelluloses by using NBS as a catalyst.

Acknowledgments

The authors are grateful for the financial support of this research from National Natural Science Foundation of China (No. 30271061 and No. 30025036) and Guangdong Natural Science Foundation (No. 013034).

References

1. Fang, J. M.; Sun, R. C.; Tomkinson, J.; Fowler, P. *Carbohydr. Polym.* **2000**, *41*, 379.
2. Aspinall, G. O. *Adv. Carbohydr. Chem.* **1959**, *14*, 429.
3. Cai, Z. S.; Paszner, L. *Holzforschung* **1988**, *42*, 11.

4. Whistler, R. L. *Adv. Carbohydr. Chem.* **1950**, *5*, 269.
5. Aspinall, G. O.; Mahomed, R. S. *J. Chem. Soc.* **1954**, *76*, 1731.
6. Ehrental, I.; Montgomery, R.; Smith, F. J. *J. Chem. Soc.* **1954**, *76*, 5509.
7. Glaudemans, C. P. J.; *J. Chem. Soc.* **1958**, *80*, 1209.
8. Timell, T. E. *Adv. Carbohydr. Chem.* **1964**, *19*, 247.
9. Timell, T. E. *Adv. Carbohydr. Chem.* **1965**, *20*, 409.
10. Sun, R. C.; Tomkinson, T. In *Encyclopedia of Separation Science*; Wilson, I. D., Adlard, T. R., Poole, C. F., Cook, M., Eds.; Academic Press: London, 2000; Vol. 6, pp 4568-4574.
11. Puls, J.; Schuseil, J. In *Hemicellulose and Hemicellulases*; Coughlan, M. P., Hazlewood, G. P., Eds.; Portland Press: London and Chapel Hill, 1993; pp 1-13.
12. Theander, O. In *New Approaches to Research on Cereal Carbohydrates*; Hill, R. D., Elsevier, L. M., Eds.; Science Publishers B. V.: Amsterdam, 1985; pp 217-230.
13. Morrison, I. M. *Carbohydr. Res.* **1974**, *36*, 45.
14. Morrison, I. M. In *Straw Decay and its Effect on Disposal and Utilization*; Grossbard, E., Ed.; Wiley: Chichester, 1979; pp 237-245.
15. Aspinall, G. O. In *The Biochemistry of Plants 3*; Presis, J., Ed.; Academic Press: New York, 1980; pp 473-500.
16. Buchala, A. J.; Fraser, C. G.; Wilkie, K. C. B. *Phytochemistry* **1972**, *11*, 2803.
17. Ebringerova, A.; Heinze, T. *Macromol. Rapid Commun.* **2000**, *21*, 542.
18. Doner, L. W.; Hicks, K. *Cereal Chem.* **1997**, *74*, 176.
19. Sun, R. C.; Fang, J. M.; Goodwin, A.; Lawther, J. M.; Bolton, J. J. *Agric. Food Chem.* **1998**, *46*, 2817.
20. Okamoto, Y.; Kawashima, M.; Hatada, K. *J. Amer. Chem. Soc.* **1984**, *106*, 5357.
21. Chinen, I.; Sadoyama, K. Japanese Patent JP 89 40,502, 1989.
22. Juslin, M.; Paronen, P. J. *Pharm. Pharmacol.* **1984**, *36*, 256.
23. Magerstaedt, M.; Meichsner, C.; Schlingmann, M.; Schrinner, E.; Walch, A.; Wiesner, M.; Winkler, I. Ger. Patent DE 3,921,761 A1, 1991.
24. Barnett, E. R.; Dikeman, R.; Pantaleone, D. P.; Liao, S. Y.; Gill, J. Eur. Patent EP 0,301,440 A1, 1989.
25. Whistler, R. L.; Bushway, A.; Singh, P. P.; Nakahara, W.; Tokuzen, R. *Adv. Carbohydr. Chem. Biochem.* **1976**, *32*, 235.
26. Fan, Y. R.; Feng, Z. H.; *Acta Pharmacol. Sin.* **1987**, *8*, 166.
27. Hashi, M.; Takeshita, T. *Agric. Biol. Chem.* **1979**, *43*, 951.
28. Hashi, M.; Takeshita, T. *Agric. Biol. Chem.* **1979**, *43*, 961.
29. Ebringerova, A.; Kardosova, A.; Hromadkova, Z.; Malovikova, A.; Hribalova, V. *Int. J. Biol. Macromol.* **2002**, *30*, 1.

30. Wanger, H.; Proksch, A.; Riess-Mauter, I.; Vollmar, A.; Odenthal, S.; Stuppner, S.; Stuppner, H. *Arzneimittelforschung*, **1985**, *35*, 1069.
31. Proksch, A.; Wanger, H. *Phytochemistry*, **1987**, *26*, 1989.
32. Fuller, E.; Sosa, S.; Tubaro, A.; Franz, G.; Loggia, R. D. *Planta Med.* **1993**, *59*, 666.
33. Yamada, H.; Nagai, T.; Cyong, T. G.; Otsuka, Y. *Carbohydr. Res.* **1985**, *144*, 101.
34. Samuelsen, A. B.; Paulsen, B. S.; Wold, J. K.; Otsuka, H.; Yamada, H.; Espevik, T. *Phytother. Res.* **1995**, *9*, 211.
35. Joseleau, J. P.; Comtat, J.; Ruel, K. In *Xylans and Xylanases*; Visser, J., Ed.; Science Publishers B. V.: Amsterdam, 1992; pp 1-15.
36. Sun, R. C.; Lawther, J. M.; Banks, W. B. *Carbohydr. Polym.* **1996**, *29*, 325.
37. Lawther, J. M.; Sun, R. C.; Banks, W. B. *J. Agric. Food Chem.* **1995**, *43*, 667.
38. Wilkie, K. C. B. *Adv. Carb. Chem.* **1979**, *36*, 215.
39. Bacon, J. S. D.; Gordon, A. H.; Morris, E. J. *Biochem. J.* **1975**, *149*, 485.
40. Bouveng, H. O.; Garegg, P. J.; Lindberg, B. *Chem. Ind. London* **1958**, *1*, 1727.
41. Hartley, R. D. *Phytochemistry* **1973**, *12*, 661.
42. Mueller-Harvey, I.; Hartley, R. D. *Carbohydr. Res.* **1986**, *148*, 71.
43. Scalbert, A.; Monties, B.; Lallemand, J. Y.; Guittet, E.; Rolando, C. *Phytochemistry* **1985**, *24*, 1359.
44. Scalbert, A.; Monties, B.; Guittet, E.; Lallemand, J. Y. *Holzforschung* **1986**, *40*, 119.
45. Ahmad, M.; Khan, L. *J. Chem. Soc. Pak.* **1988**, *10*, 299.
46. Almendros, G.; Martínez, A. T.; González, A. E.; González-Vila, F. J.; Fründ, R.; Lüdemann, H.-D. *J. Agric. Food Chem.* **1992**, *40*, 1297.
47. Helm, R. F.; Ralph, J. *J. Agric. Food Chem.* **1992**, *40*, 2167.
48. Grabber, J. H.; Hatfield, R. D.; Ralph, J.; Zon, J.; Amrhein, N. *Phytochemistry* **1995**, *40*, 1077.
49. Fidalgo, M. L.; Terron, M. C.; Martinez, A. T.; Gonzalez, A. E.; Gonzalez-vila, F. J.; Galletti, G. C. *J. Agric. Food Chem.* **1993**, *41*, 1621.
50. Crestini, C.; Argyropoulos, D. S. *J. Agric. Food Chem.* **1997**, *45*, 1212.
51. Iiyama, K.; Lam, T. B. T. *J. Sci. Food Agric.* **1990**, *51*, 481.
52. Jacquet, G.; Pollet, B.; Lapiere, C.; Mhamdi, F.; Rolando, C. *J. Agric. Food Chem.* **1995**, *43*, 2746.
53. Kondo, T.; Ohshita, T.; Kyuma, T. *Anim. Feed Sci. Technol.* **1992**, *39*, 253.
54. Ralph, J.; Grabber, J. H.; Hatfield, R. D. *Carbohydr. Res.* **1995**, *275*, 167.

55. Lam, T. B. T.; Iiyama, K.; Stone, B. A. *J. Sci. Food Agric.* **1990**, *51*, 493.
56. Lam, T. B. T.; Iiyama, K.; Stone, B. A. *Phytochemistry* **1992**, *31*, 1179.
57. Shimada, M.; Fukuzuka, T.; Higuchi, T. *Tappi* **1971**, *54*, 72.
58. Sun, R. C.; Lawther, J. M.; Banks, W. B. *J. Appl. Polym. Sci.* **1998**, *68*, 1633.
59. Taylor, J. G.; Haigler, C. H. *Acta Botanica Neerland* **1993**, *42*, 153.
60. Bao, W.; O'malley, D. M.; Sederoff, R. R. *Proceedings of the National Academy of Sciences*, **1992**, USA89, 6604.
61. Wojtaszek, P.; Bolwell, G. P. *Plant Physiol.* **1995**, *108*, 1001.
62. Gregory, A. C. E.; O'Connell, A. P.; Bolwell, G. P. *Biotechnol. Genet. Eng. Rev.* **1998**, *15*, 439.
63. Stacey, N. J.; Roberts, K.; Carpita, N. C.; Wells, B.; McCann, M. C. *Plant J.* **1995**, *8*, 891.
64. Lamport, D. T. A.; Atona, L.; Roerig, S. *Biochem. J.* **1973**, *133*, 125.
65. Meuser, F.; Suckow, P. *Royal Society Chem.* **1986**, *56*, 42.
66. Lamport, D. T. A.; Miller, D. A. *Plant Physiol.* **1971**, *48*, 454.
67. Sun, R. C.; Fang, J. M.; Goodwin, A.; Lawther, J. M.; Bolton, A. J. *J. Sci. Food Agric.* **1999**, *79*, 1091.
68. Sun, R. C.; Tomkinson, J.; Mao, F. C.; Sun, X. F. *J. Appl. Polym. Sci.* **2001**, *79*, 719.
69. Sun, R. C.; Lawther, J. M.; Banks, W. B. *Holzforschung* **1997**, *51*, 244.
70. Sun, R. C.; Tomkinson, J.; Zhu, W.; Wang, S. Q. *J. Agric. Food Chem.* **2000**, *48*, 1253.
71. Chesson, A.; Gordon, A. H.; Lomax, J. A. *J. Sci. Food Agric.* **1983**, *34*, 1330.
72. Eriksson, O.; Lindgren, B. O. *Svensk Papperstidn* **1977**, *80*, 59.
73. Imamura, T.; Watanabe, T.; Kuwahara, M.; Koshijima, T. *Phytochemistry* **1994**, *37*, 1165.
74. Lawther, J. M.; Sun, R. C.; Banks, W. B. *Cellulose Chem. Technol.* **1996**, *30*, 395.
75. Sun, R. C.; Lawther, J. M.; Banks, W. B. *Ind. Crops Prod.* **1997**, *6*, 1.
76. Sun, R. C.; Lawther, J. M.; Banks, W. B. *J. Agric. Food Chem.* **1996**, *144*, 3965.
77. Sun, R. C.; Lawther, J. M.; Banks, W. B. *J. Appl. Polym. Sci.* **1996**, *62*, 1473.
78. Stephen, A. M. In *The Polysaccharides*; Aspinall, G. O., Ed.; Academic Press: New York and London, 1983; pp.98-102.
79. Wong, K. K. Y.; Tan, I. U. I.; Saddler, J. N. *Microbiol. Rev.* **1988**, *52*, 305.
80. Biely, P. *Trends Biotechnol.* **1985**, *3*, 286.
81. Theander, O.; Aman, P. *Swedish J. Agric. Res.* **1978**, *8*, 189.

82. Gabrielli, I.; Gatenholm, P.; Glasser, W. G.; Jain, R. K.; Kenne, L. *Carbohydr. Polym.* **2000**, *43*, 367.
83. Glasser, W. G.; Kaar, W. E.; Jain, R. K.; Sealey, J. *Cellulose* **2000**, *7*, 299.
84. Ibrahim, M.; Glasser, W. G. *Bioresource Technol.* **1991**, *70*, 181.
85. N'Diaye, S.; Rigal, L.; Laroque, P.; Vidal, P. E. *Bioresource Technol.* **1996**, *57*, 61.
86. Lawther, J. M.; Sun, R. C.; Banks, W. B. *J. Appl. Polym. Sci.* **1996**, *60*, 1827
87. Ebringerova, A.; Hromadkova, Z. *Biotechnol. Genet. Eng. Rev.* **1999**, *16*, 325.
88. Hromadkova, Z.; Ebringerova, A.; Machova, E. *Proceedings of the 8th Bratislava Symposium on Saccharides*, September, 1-5, Smolenice, 1997; p 95.
89. Hromadkova, Z.; Kovacikova, J.; Ebringerova, A. *Ind. Crops Prod.* **1999**, *9*, 101.
90. Sun, R. C.; Tomkinson, J. *Ultras. Sonochem.* **2002**, *9*, 85.
91. Dence, C. W. In *Pulp Bleaching-Principle and Practice*; Dence, C. W., Reeve, D. W., Eds.; TAPPI Press: Atlanta, 1996, pp 349-361.
92. Pan, G. X.; Bolton, J. L.; Leary, G. J. *J. Agric. Food Chem.* **1998**, *46*, 5283.
93. Sun, R. C.; Tomkinson, J.; Wang, Y. X.; Xiao, B. *Polymer* **2000**, *41*, 2647.
94. Sun, R. C.; Tomkinson, J.; Ma, P. L.; Liang, S. F. *Carbohydr. Polym.* **2000**, *42*, 111.
95. Fang, J. M.; Sun, R. C.; Fowler, P.; Tomkinson, J.; Hill, C. A. S. *J. Appl. Polym. Sci.* **1999**, *74*, 2301.
96. Glaudemans, C. P.; Timell, T. E. *Svensk Papperstidn* **1958**, *61*, 1.
97. Timell, T. E.; Glaudemans, C. P.; Gillham, J. K. *Tappi* **1959**, *42*, 623.
98. Koshijima, A.; Timell, T. E.; Zinbo, M. *J. Polym. Sci.* **1965**, *C-11*, 265.
99. Carson, J. F.; Maclay, W. D. *J. Amer. Chem. Soc.* **1948**, *70*, 293.
100. Jain, R. K.; Sjostedt, M.; Glasser, W. G. *Cellulose* **2001**, *7*, 319.
101. Church, J. A. *J. Polym. Sci.* **1967**, *5*, 3183.
102. O'Malley, J. J.; Marchessault, R. H. *J. Polym. Sci.* **1968**, *C 24*, 179.
103. Fanta, G. F.; Burr, R. C.; Doane, W. M. *J. Appl. Polym. Sci.* **1982**, *27*, 4239.
104. EI-Shinnawy, N. A.; EI-Kalyoubi, S. F. *J. Appl. Polym. Sci.* **1988**, *30*, 2171.
105. Antal, M.; Ebringerova, A.; Micko, M. M. *Das Papier* **1991**, *45*, 232.
106. Antal, M.; Ebringerova, A.; Hromadkova, Z.; Pikulik, II.; Laleg, M.; Micko, M. M. *Das Papier* **1997**, *51*, 223.
107. Ebringerova, A.; Novotna, Z.; Kacurakova, M.; Machova, E. *J. Appl. Polym. Sci.* **1996**, *62*, 1043.

108. Sroková, I.; Talaba, P.; Hromádková, Z.; Ebringerová, A.; Alfoldi, J. *Proceedings of the 8th Bratislava Symposium on Saccharides*, September 1-5, Smolenice, Slovakia, 1997, p 97.
109. Vincendon, M. *J. Appl. Polym. Sci.* **1998**, *67*, 455.
110. Whistler, R. L.; Daniel, J. R. In *Encycl. Chem. Technol.*; Mark, H. F., Othmer, D. F., Overberger, C. G., Seaborg, G. T., Eds.; 3rd edn; Wiley: NY, 1983; Vol. 21, pp 492-496.
111. Majewicz, T. G.; Podlas, T. J. In *Encycl. Chem. Technol.*; Howe-Grant, M., Ed.; 4th edn; Wiley: NY, 1993; Vol. 5, pp 541-545.
112. Glasser, W. G.; Ravinfran, G.; Jain, R. K.; Samaranayake, G.; Todd, J. *Biotechnol. Progr.* **1995**, *11*, 552.
113. Lindblad, M. S.; Ranuci, E.; Albertsson, A. C. *Macromol. Rapid Commun.* **2001**, *22*, 962.
114. Raiss, R.; Wiesner, M. *PCT Int. Appl.* **1992**, *13*, 541.
115. Marshall, J. L.; Wellsten, A.; Rae, J.; Delap, R. J.; Phipps, K.; Hanfelt, J.; Yunmbam, M. K.; Sun, J. X.; Duchin, K. L.; Hawkins, M. J. *Clinical Cancer Res.* **1997**, *3*, 2347.
116. Hwang, P.; Auclair, B.; Beechinor, D.; Diment, M.; Einarson, T. R. *Urology* **1997**, *50*, 39.
117. Shuba, K.; Sivamurugesan, A.; Varabakshmi, P. *Biochem Int.* **1992**, *27*, 1011.
118. Sun, R. C.; Fang, J. M.; Tomkinson, J.; Jones, G. L. *Ind. Crops Prod.* **1999**, *10*, 209.
119. Sun, R. C.; Sun, X. F.; Zhang, F. Y. *Polym. Int.* **2001**, *50*, 803.
120. Sun, R. C.; Fang, J. M.; Tomkinson, J. *Polym. Degrad. Stabil.* **2000**, *67*, 345.
121. Sun, R. C.; Tomkinson, J.; Liu, J. C.; Geng, Z. C. *Polym. J.* **1999**, *31*, 857.
122. Karimi, B.; Seradj, H. *Synlett* **2001**, *4*, 519.
123. Kamal, A.; Chouhan G.; Ahmed K. *Tetrahedron Lett.* **2002**, *43*, 6947.

Chapter 2

Industrially Isolated Hemicelluloses

Juergen Puls and Bodo Saake

Federal Research Centre of Forestry and Forest Products, Institute of Wood Chemistry and Chemical Technology of Wood, D-21002 Hamburg, Germany

Sources for hemicellulose recovery are discussed, which explicitly include the option to obtain this interesting polysaccharide from lignocellulosic materials in a large scale and in only slightly degraded form. Many attempts have been made for hemicellulose fractionation in organosolv pulping and steaming-pretreatment. Unfortunately not all of these processes are in operation at any time, which may give rise to supply problems. On a long term it may be wiser to focus on hemicelluloses, which accumulate in side streams during production of thermomechanical pulp or viscose fibres. A newly developed conversion process for dissolving pulps, based on the extraction of xylan from paper grade pulps might be a further source for hemicelluloses. As far as data are available technical occurring hemicelluloses are characterized regarding their composition and molar masses.

The most important chemical processes based on lignocellulosic materials are the production of chemical and mechanical pulps. In the ongoing discussions about a possible use of by-products from pulping processes hemicelluloses only play a minor role compared to lignin utilization. Hemicellulose is the term for the particular polysaccharides of the cell wall, which are, at least partly, alkali-extractable. In contrast to crystalline cellulose hemicelluloses are highly accessible towards acid and alkaline reagents, specially under heat. Accordingly the major proportion of hemicelluloses being solubilized in the pulping process are degraded, either under the acid conditions of the sulphite process or under the alkaline conditions of the kraft process, although differences exist in the extent and degradation pattern between both processes (1, 2, 3). Those hemicelluloses, which survive the sulphite process, may be recovered as monosaccharides, whereas part of the hemicelluloses, being solubilized in kraft pulping, reprecipitate on the surface of the pulp fibres as partly modified polysaccharides (mainly xylan), improving the total pulp yield (4). The conventional production of dissolving pulps too is no suitable procedure for recovery of hemicelluloses as polymers. Both processes, sulphite pulping and prehydrolysis kraft pulping only include the option to obtain the hemicelluloses as monosaccharides. As a rule the degraded hemicelluloses are burnt together with lignin, although the contribution of the hemicelluloses to the overall heating value is small compared to lignin.

However during the last 15 years two different routes for wood fractionation have been developed, which include the option to separate cellulose, lignin and polymeric hemicelluloses. One route is based on the application of organic solvents, originating in the pioneering work of Kleinert and von Tayenthal (5). The other option is based on steaming lignocellulosic materials at elevated temperatures, which has been considered for biomass fractionation more than 30 years ago (6). Both concepts led to the development of pilot plants (steaming) or production plants (organosolv pulping), guaranteeing the availability of hemicelluloses in a large scale. Not all of these plants are in operation anymore. However at any time hemicelluloses are available from the steeping liquor of the viscose process, in case the price for the recovered hemicellulose justifies its recuperation. The process water from mechanical pulp production might be another source, although no technology has been suggested for their utilisation. A new attempt opens the option for hemicellulose recovery from paper pulp, using a metal complex. It is the intention of this paper to describe chemical and physical properties of hemicellulose fraction obtained from these processes. Hemicelluloses from the tubers, bulbs and seeds of different plant, where they function as energy reserve material, are not considered in this chapter.

Hemicelluloses from Organosolv Pulping

Conventional pulping processes can only economically operate in a very large scale. Consequently raw material supply may become a critical issue, specially in highly populated regions. Sulfur-free pulping procedures, especially

organosolv methods are less complicated in recovery of their pulping chemicals. Therefore they offer the chance to operate economically small-sized pulp mills, which may precisely cover the need of one paper factory. Organic solvents like alcohols, phenol, amines, and organic acids have been intensively tested for their pulping efficiency, from which methanol, ethanol, acetic acid, and formic acid have reached the pilot scale. Organic acid pulping should not be considered here, since hemicelluloses are being degraded under the influence of acid and heat. The organosolv pulping procedure, using methanol or ethanol as pulping reagent, is based on simultaneous hydrolysis and extraction of lignin. When water is added to the system, the hemicelluloses are also dissolved. These true organosolv processes with no addition of chemicals besides of the organic solvents seem to have the biggest potential for hemicellulose recovery due to the easy separation from lignin by its precipitation. A fine example for an ideal organosolv process was the Alcell process, being developed in Canada (7), but not any more in operation. The Organocell process was only partly such an ideal pulping process, because it was a two-stage process, from which only the first stage was alkali-free, whereas alkali was added in the second stage (8). However both stages were methanol-based and sulphur-free. The implementation of two stages can be explained by historical reasons as well as by the requirements on adequate strength properties of the pulps. In the 1970's the Organocell company picked up Kleinert's idea about a one-stage alcohol-water pulping process. The company found out quite early that hardwoods could be pulped with methanol:water or ethanol:water alone. However pulping experiments with Norway spruce or Scots pine proved to be unsuccessful. When alkali was added to the second stage, pulps from spruce and pine were obtained, that had reasonable strength properties and that could be bleached. The concept of the pilot plant was a two-stage process with an alkaline-free cooking zone as a first stage, where the wood chips were extracted with 50 % aqueous methanol and temperatures up to 195 °C for 20 to 50 min (9).

Composition of Aqueous Phase from Spruce, derived from the First Stage of the Organocell Process

Analytical acid hydrolysis followed by analysis of the sugar composition revealed that the aqueous phase from spruce (*Picea abies*), derived from the first stage of the Organocell process had a sugar content of 16.5 g x l⁻¹ with mannose as the predominant monomer, indicating a galactoglucomannan to be the principal polysaccharide (Table 1). Surprisingly there was more arabinose than xylose in solution, although the native xylan from Norway spruce carries only one L-arabinofuranose residue per 7.4 xylose residues (10). This phenomenon can only be explained by selective cleavage of L-arabinofuranose side groups from those xylan chains which remained in the pulps. The hemicellulose solution was obtained after methanol recovery. The dry-matter content was 38 g x l⁻¹, from which 6.6 g (17.3%) was ether-soluble.

Table I. Carbohydrate composition of the aqueous phase of the first stage of the Organocell process

	<i>Man</i>	<i>Ara</i>	<i>Gal</i>	<i>Xyl</i>	<i>Glu</i>	Σ Carb.	Acetyl
Original aqueous phase (g x l ⁻¹)	6.2	3.3	2.7	2.6	1.7	16.5	n.d.
Precipitated fraction (%) based on dry matter content)	41.6	0.0	13.4	7.6	9.6	72.2	4.6
Supernatant (g x l ⁻¹)	4.7	3.3	2.1	2.2	1.3	13.6	n.d.

NOTE: Figures obtained after posthydrolysis

The latter fraction consisted of different classes of components, namely carbohydrate degradation products (5-hydroxymethylfurfural, 5-HMF), lignin monomers (vanillin and syringol), and wood extractives (5-hydroxymateiresinol).

Investigations on the chain length distribution of the hemicellulose indicated that a substantial amount of them were oligomeric or even polymeric, although also monomeric sugars were present. Accordingly a separation of the more or less polymeric galactoglucomannan from the degradation products and wood extractives by precipitation seemed to be advisable. After filtering through fritted glass, one litre crude hemicellulose solution was poured into three litre ethanol containing 100 ml formic acid. The precipitate was recovered by centrifugation and was washed in succession with methanol and petroleum ether. A white product was obtained (4 g), which represented about 10% of the dry material in the crude fraction. The sugar composition of the polysaccharide is given in Tab. I. In the purified hemicellulose product no arabinose could be found, which supports the theory of selective cleavage of this substituent from the xylan chain during methanol-water pulping. The acetyl content of the hemicellulose fraction was 4.6%, which is in good agreement with Häggglund et al. (11), who reported an acetyl content of 5.0 % for a dimethyl sulfoxide extracted hemicellulose fraction from Norway spruce. Indeed the galactoglucomannan in the Organocell hemicellulose fraction seemed to be acetylated, since softwood arabino-4-0-methylglucuronoxylans do not carry acetyl substituents.

Figure 1 gives the SEC elution curves from the re-precipitated Organocell fraction as well as the corresponding curve of a water-soluble glucomannan from white spruce (*Picea glauca*). The degree of polymerisation of this glucomannan was reported to be 107 (12). It becomes apparent that only a small amount of the originally long chains persisted the organosolv treatment. The major amount of the precipitated hemicellulose fraction was smaller in molecular weight than the original.

So far the aqueous fraction of the Organocell process seems to be a valuable source for an easy recovery of acetylated galactoglucomannan. The precipitated hemicellulose fraction was re-dissolved in citrate buffer pH 5 and incubated with purified xylanase (Fig. 2). Xylanase incubation led to the liberation of some xylose and xylo-oligomers (Fig. 3 bottom). The humpback present in the SEC elution curve (7.5 h) of the starting material may be derived from xylan impurities, since it disappeared after xylanase treatment. Therefore, specific xylanase treatment of the original hemicellulose solution prior to the precipitation seems to be the method of choice to obtain a pure acetylgalactoglucomannan.

In the first commercial Organocell plant in southern Germany the first stage was eliminated. Now a single stage process with sodium hydroxide, methanol and anthraquinon was performed (13). This change prevented the utilisation of hemicelluloses in the process. In addition it led to increased lignin condensation and reduced the performance in bleaching operations.

Hemicelluloses from Heat Fractionation Processes

Steaming of wood at elevated temperature and pressure is a common process in fibreboard and rayon pulp production. By this treatment lignin becomes plasticised. The steamed material can therefore be easily fiberized, and carbohydrates, mainly derived from hemicelluloses, can be extracted with water. Concentrated extracts from hardboard production, so called "wood molasses" have been used as a liquid feed for cattle (14). The carbohydrate portion of steamed and washed material is mainly cellulose. Bender and coworkers have steamed hardwoods and straw to increase their digestibility to ruminants (6). For aspen wood steamed at 165-200 °C and wheat straw steamed at 170°C for ½ - 1 hour they reached digestibilities of hay (in vitro 45-57%). Steaming at higher temperatures and pressures (up to 254 °C, 21 to 42 bar) were also tried to increase the rumen digestibility of lignocellulosic materials (15) or as a pretreatment method to improve the enzymatic hydrolysis yield for the production of fermentable sugars and ethanol from lignocelluloses (16, 17). However this is a severity range, which leads to a more or less complete hydrolysis and further degradation of the hemicelluloses. Actually in these early developments hemicelluloses have only been regarded as a by-product. Consequently little attention have been given neither to their structure nor to their yield. In wood-to-ethanol processes the steamed material has not been washed in order to recuperate the hemicelluloses, but to remove inhibitory substances, which could negatively influence the fermentation (18). Only at a later time special attention was given to hemicellulose structure and recovery yield in the development of pretreatment processes (19, 20, 21). The use of steam at elevated temperatures without addition of any other chemicals for

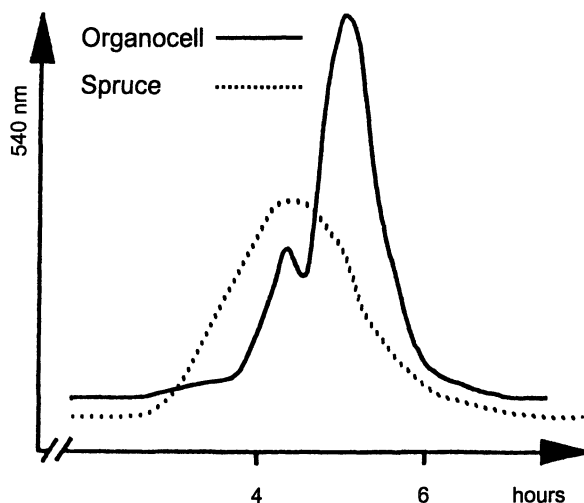


Figure 1. SEC elution curves of the precipitated hemicellulose fraction from the Organocell process and a glucomannan, both from Norway spruce. SEC: TSK HW 55 (100 x 2,5 cm); 1 ml/min 0.1 M phosphate buffer pH 7.2; detection: 540 nm after reaction with 0.2% 3,5 dihydroxytoluene in 72% H_2SO_4 .

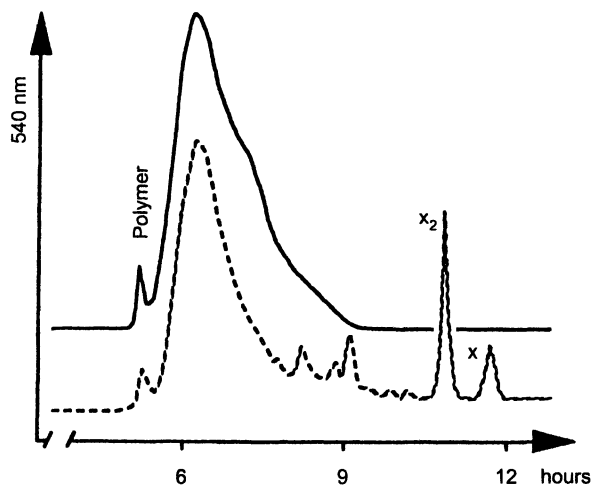


Figure 2. SEC curves of the precipitated Organocell white spruce hemicellulose fraction (top) and after xylanase incubation (bottom). SEC: TSK HW 40 (100 x 2.5 cm) and TSK HW 50 (100 x 2.5 cm) coupled in line. For mobile phase and carbohydrate detection see Fig. 1.

pretreatment of lignocellulosics was restricted to hardwood and low-lignified residues of annual plants. Steaming pretreatment of softwoods required the addition of sulfuric acid, sulfur dioxide (22, 23, 24), or Lewis acids and other chemicals (25, 26). The addition of these compounds strongly modified and intensified the steam-treatment including the advantage of a substantial reduction in temperature requirements. However the solubilized sugars were mainly composed of monosaccharides and low molecular weight oligosaccharides. The polymeric nature of the hemicelluloses was completely destroyed. Recently the addition of sodium hydroxide during heat fractionation of spruce has been optimized in order to recover acceptable quantities of only partly degraded O-acetyl-galactoglucomannan (27). This aim could only be achieved after additional separation of the low molecular weight compounds by preparative size exclusion chromatography.

Hemicelluloses from Steaming Pretreatment

The mass balance of fragments derived from xylan after steaming birchwood for 10 min in the temperature range between 170-210°C is given in Tab. II. The pH-values were taken from the original extracts, whereas all other figures were based on extracted freeze-dried material. The pH values indicate a shift to lower pH from 4.3 at 170°C to 3.5 at 210°C, which could be deduced to enhanced deacetylation or decarboxylation. The xylose content in the extracts increased steadily from 170°C to 200°C and amounted up to 54.5%, based on

Table II. Chemical characteristics of the hemicellulose fraction of birchwood after steaming for 10 min

<i>Steaming Temp. °C</i>	<i>pH</i>	<i>Xylose original extract</i>	<i>Xylose after enzymatic hydrolysis</i>	<i>0-Acetyl</i>	<i>4-O-MeGlcA</i>
170	4.3	0.9	38.5	6.5	3.8
180	3.8	1.5	51.3	8.5	3.3
190	3.6	4.0	53.2	8.7	1.9
200	3.6	5.9	54.5	7.8	1.5
210	3.5	13.2	48.0	7.2	0.7

NOTE: Figures in % of extract dry weight

extracted material. This amount was obtained after enzymatic posthydrolysis of the extracts. An additional increase in temperature by 10°C led to a decrease in xylan survival. Only 48% of the extract were still xylan and xylan fragments. The proportion of free xylose in the extract increased markedly only at 210°C. At this temperature it comprised 13.2% of the extract dry matter, suggesting a

shift from higher to lower oligomers as a function of the steaming temperature, which was verified by size exclusion chromatographic investigations of the extracts (Fig. 3). Surprisingly the 4-0-methylglucuronic acid substituents were more labile with increasing steaming temperatures compared to the acetyl substituents. In the steaming extract of 170°C every 14th xylose unit remained substituted by a 4-0-methylglucuronic acid side group (0.07 substituents per xylose unit). At 190°C every 38th xylose unit was substituted by a 4-0-methylglucuronic acid residue, whereas only every 90th xylose unit was substituted, when birchwood was processed at 210°C. The amount of acetyl groups are ranging between 6.5% and 8.7% with an optimum of bound acetyl at 190°C steaming temperature. The corresponding acetyl values per xylose units in the steaming extracts are in the range between 0.36 and 0.42. The results make clear that more than half of the acetyl groups remained bound with little temperature dependence.

Generally the degree of polymerization (DP) of hemicelluloses obtained after steaming can be influenced by the severity of the steaming conditions. A partial degradation of the hemicellulose chain length can never be avoided, although, at least for wheat straw, an initial increase in molecular weight (M_w) from 6200 to 11000 g/mol was obtained, when the steaming temperature was increased from 170°C to 190°C. However a further increase to 200°C led to a sudden M_w reduction as low as 1800 g/mol, corresponding to a DP of 14. This effect can be explained by an initial recovery of easily extractable low molecular weight material, when milder conditions are applied. Longer xylan chains become only water-extractable at higher severity of the pretreatment conditions with a high risk of degradation (Fig. 3).

The reduction in chain length seems also to be dependent on the acetyl content of the starting material, being partly cleaved off and moderately autohydrolysing hemicelluloses and also cellulose (19). Hardwoods like beech and birch contain as much as 6% acetic acid, leading to an efficient acid degradation of polysaccharides from 2300 g/mol to 1000 g/mol, when the steaming temperature is being increased from 170°C to 200°C. Cereal straws however contain much less bound acetic acid. Consequently the reduction in chain length with increasing steaming temperature is less dramatic and hemicelluloses of much higher molar masses can be recovered from straw with an acceptable yield compared to birchwood. As can be deduced from Figure 3 the chain length of the required hemicelluloses can be influenced by the steaming conditions in a wide range.

For most raw materials $\frac{2}{3}$ of the hemicelluloses present in the raw materials can be extracted under optimal conditions, which are dependent on the composition of the raw material and must be determined individually. Unfortunately the conditions for optimal hemicellulose recovery are not necessarily identical with the conditions for optimal enzymatic accessibility of the fibre fraction.

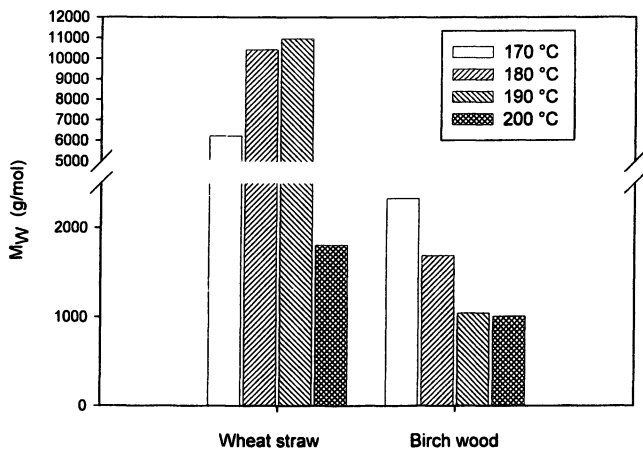


Figure 3. Effect of steaming temperature on the chain length distribution of xylo-oligomers in the aqueous extract of steamed birchwood and wheat straw. Steaming time 10 min. Molar mass by SEC in DMSO:H₂O (90:10) 0.05 M LiBr according to (29).

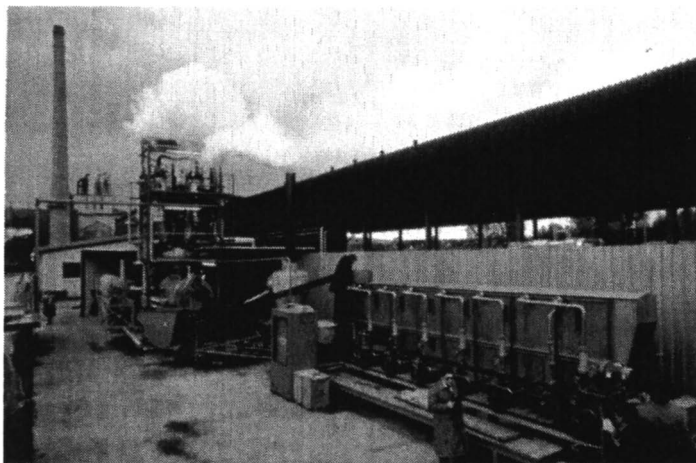


Figure 4. Semi-industrial plant for steaming hardwoods (capacity ~600 kg x h⁻¹) and annual plants, equipped with a counter-current extraction unit for hemicellulose recovery (FRITZ WERNER GmbH, Geisenheim/Germany). The horizontally operating reactor (background) is optionally fed from two pressured vessels in top or from an extruder, located parallel at the left side of the reactor. Steam is released from the blow tank in front of the extraction unit.

Steaming processes have been developed independently and tested in the pilot or semi-industrial scale in different countries e.g. Canada, Austria, France, Germany and Italy (28, 29, 30). The individual plants differed by their feeding systems, steaming conditions and extent of additional equipment for fibre and extract processing, hydrolysis and fermentation. Figure 4 gives the view of a semi-industrial plant in Germany, being in operation in the 1980'ies, which included a counter-current extraction plant and a thin film concentration unit for hemicelluloses.

The literature on isolation and further refining of hemicelluloses from steaming pretreatment has been reviewed recently by Glasser et al. (31). Due to the polydispersity of the hemicellulose material from steaming processes a further purification step may be advisable in order to remove low molecular weight material including lignin fragments. Figure 5 demonstrates the impact of ultrafiltration using hollow fibre membranes of a molecular weight cut-off of 10.000 Daltons on the SEC elution profiles of an aqueous hemicellulose extract from birchwood with a molar mass (M_w) of 1400 g/mol. The low-molecular weight materials could easily be separated and resulted in an ultrafiltrate (M_w : 740 g/mol), which also included most of the solubilized lignin. The molar mass

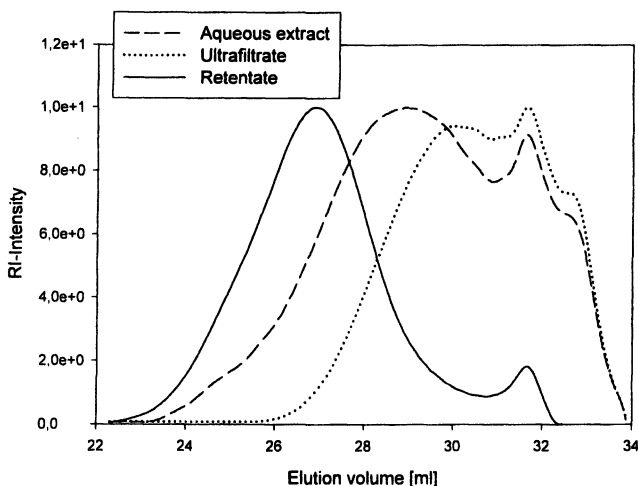


Figure 5. Size exclusion chromatographic separation of hemicelluloses in the aqueous extract after steaming birchwood at 190°C for 10 min. The original extract has been ultrafiltrated (M_w cut-off 10.000 daltons) resulting in a retentate and an ultrafiltrate. SEC in DMSO:H₂O (90:10) 0.05 M LiBr according to (32).

of the hemicelluloses in the retentate was increased to 3100 g/mol corresponding to a DP of 24.

Hemicelluloses Dissolved from Softwood in Thermomechanical Pulping

The severity of the refining conditions in the production of thermomechanical pulps are much milder compared to steaming pretreatment. Nevertheless a small but distinct quantity of hemicelluloses is released from wood and accumulates in the white water system, representing a possible source for hemicellulose recovery. The polysaccharides released from unbleached TMP were comprised of neutral (88 %) and anionic (12 %) polysaccharides. The neutral polysaccharides were mostly O-acetyl-galactoglucomannans and the anionic polysaccharides were mostly arabinogalactans (33). The molar ratio between the monosaccharide units and the acetyl groups for a high molecular mass fraction of TMP-galactoglucomannan was measured to be 1.1 : 1 : 3.9 : 2.4 (Gal:Glu:Man:Ac) (34). The O-acetyl galactoglucomannans were deacetylated by the alkaline conditions of peroxide bleaching, thereby causing their substantial adsorption onto the TMP fiber (33).

Hemicelluloses from the Steeping Liquor of the Viscose Process

Viscose pulps are mainly produced by the acid sulphite process, which causes not only lignin removal, but also the degradation of the major quantity of the initial hemicellulose content. After bleaching the hemicellulose content in viscose pulp exceeds not more than 5%. In the viscose process the pulp is treated with 18% sodium hydroxide, causing a dissolution of the residual hemicellulose content and part of the cellulose. The lye is recycled for economic reasons and a steady state of dissolved compounds is created. Due to the drastic conditions in this process the major proportion of low molar mass cellulose is being degraded, whereas part of the xylan is resistant to complete degradation and can be recovered (35). The degree of polymerization of the viscose xylan is about 35 and the material has nearly lost all its substituents (36, 37). This may be the reason for the poor water-solubility of the viscose xylan.

Hemicelluloses from Paper Pulps

Many attempts have been made to convert paper pulps into dissolving pulps by removing hemicelluloses either by alkaline extraction or by acid or enzymatic

hydrolysis. Most of them were unsuccessful due to the fact that the required purity in terms of residual hemicelluloses in the pulp did not meet the requirements of the particular cellulose derivatization process. Recently a range of solvents like NMMO, DMA/LiCl, Cuen, DMA/LiCl and Nitren have been tested for their ability to specifically improve the α -cellulose content by removing the hemicellulose proportion from paper pulp. This goal was achieved with Nitren, which is a 1:1 complex of tris(2-aminoethyl)amine and nickel-II-hydroxide. Nitren forms relatively stable olate complexes with dioles, e.g. sugar alcohols, which is the reason for the solvation capacity of Nitren for polysaccharides. The favourable concentration for hemicellulose–Nitren-complexes is in the range between 1 and 3 % Nitren. Higher concentration lead to cellulose solvation, lower concentrations are missing the capacity for hemicellulose solubilization. The dissolved polymeric hemicellulose fraction can be precipitated by pH-reduction, whereas Nitren can be recovered by nanofiltration (38). The isolated polymers excel by high purity regarding the xylan content. The chain length is not shortened significantly during the extraction and a DP of 100 could be determined for a xylan isolated from Eucalyptus kraft pulp.

Conclusion

A variety of industrial processes are available for hemicellulose recovery in large scale. They can be classified into processes with lignocelluloses as starting materials or pulps as a source for hemicellulose extraction. Of course the hemicellulose source and the recovery process are of major importance for the chemical and physical properties of the recovered polysaccharides. Hemicellulose fractionation from lignified materials mostly yields polysaccharides which are associated with major proportions of lignin. Hemicellulose separation from bleached pulps, however, results into products, which may be rather pure. Harsh treatments, partly applied in heat fractionation processes, may lead to hemicellulose products, which are heavily degraded in chain length and excel by a rather high polydispersity. Although partly degraded these hemicelluloses have preserved most of their side chains e.g. acetyl-, feruloyl-, p-coumaroyl- and arabinofuranosyl substituents, which makes them highly water-soluble. In the utilization of hemicelluloses extracted from pulps the removal of ester-linked and glycosidically linked side groups, dependent on the pulping process and the extraction procedure, must be considered. All these factors influence the physical properties of polysaccharides. Accordingly the choice of the industrial process, where to recover the hemicellulose from, is highly dependent on the final application of the recovered hemicelluloses.

References

1. Sjöström, E.; Enström, B. *Tappi* 1967, 50, 32-36.
2. Sjöström, E. *Wood Chemistry, Fundamentals and Applications*; Academic Press: San Diego, 1993.
3. Alen, R.; Lahtela, M.; Niemelä, K.; Sjöström, E. *Holzforschung* 1985, 39, 235-238.
4. Aurell, R. *Tappi* 1965, 48, 80-84.
5. Kleinert, Th.; von Tayental, K. *Zeitschr. angew. Chem.* 1931, 11, 788-791.
6. Bender, F.; Heaney, D.P.; Bowden, A. *Forest Prod. J.* 1970, 20 (4), 36-41.
7. Pye, E.K.; Lora, J.H. *Tappi* 1991, 74 (3), 113-118.
8. Dahlmann, G.; Schroeter, M. C. *Tappi* 1990, 73, 237-240.
9. Leopold, H. *Papier* 1993, 47 (10A), 1-5.
10. Zinbo, M.; Timell, T.E. *Svensk Papperstidn.* 1967, 70, 597-606.
11. Hägglund, E.; Lindberg, B.; McPherson, J. *Acta Chem. Scand.* 1956, 10, 1160-1164.
12. Tyminski, A.; Timell, T.E. *J. Am. Chem. Soc.* 1960, 82, 2823-2827.
13. Stockburger, P. *Tappi* 1993, 76 (6), 71-74.
14. Galloway, D. *Forest Ind.* 1976, 103 (2), 62-63.
15. Hart, M.R.; Graham, R.P.; Hanni, P.F.; Rockwell, W.C.; Walker, M.G.; Kohler, G.O.; Waiss, A.C.; Garrett, W.N. *Feedstuffs* 1975, 47, 39.
16. Lora, J.H.; Wayman, M. *Tappi* 1978, 61 (6), 47-50.
17. Saddler, J.N.; Brownell, H.; Clermont, L.P. *Biotechnol. Bioeng.* 1982, 24, 1389-1402.
18. Tengborg, C.; Galbe, M.; Zacchi, G.; Mosier, N.S.; Sarikaya, A.; Ladisch, C.M.; Ladisch, M.R. *Enzyme Microb. Technol.* 2001, 2, 835-844.
19. Puls, J.; Poutanen, K.; Körner, H.-U.; Viikari, L. *Appl. Microbiol. Biotechnol.* 1985, 22, 416-423.
20. Zhuang, Q. and Vidal, P.F. *Cell. Chem. Technol.* 1996, 30, 371-384.
21. Glasser, W. G.; Wright, R. S. *Biomass & Bioenergy* 1998, 14, 219-235.
22. Schell, D.; Nguyen, Q.; Tucker, M.; Boynton, B. *Appl. Biochem. Biotechnol.* 1998, 70, 17-24.
23. Tengborg, C.; Stenberg, K.; Galbe, M.; Zacchi, G.; Larsson, S.; Palmqvist, E.; Hahn-Hägerdal, B. *Appl. Biochem. Biotechnol.* 1998, 70, 3-15.
24. McDonald, A.G.; Clark, T.A. *J. Wood Chem. Technol.* 1992, 12, 53-78.
25. Aoyama, M.; Seki, K. *Bioresource Technol.* 1999, 69, 91-94.
26. Rughani, J.; Wasson, L.; Prewitt, L.; McGinnis, G. J. *Wood Chem. Technol.* 1992, 12, 79-90.
27. Lundqvist, J.; Teleman, A.; Junel, L.; Zacchi, G.; Dahlman, O.; Tjerneld, F.; Ståhlbrand, H. *Carbohydr. Polym.* 2002, 48, 29-39.
28. Heitz, M.; Capek-Menard, E.; Koeberle, P.G.; Gagne, J.; Chornet, E.; Overend, R.P.; Taylor, J.D.; Yu, E. *Bioresource Technol.* 1991, 35, 23-32.

29. Ropars, M.; Marchal, R.; Pourquoi, J.; Vandecasteele, J.P. *Bioresource Technol.* **1992**, *42*, 197-204.
30. Hayn, M.; Steiner, W.; Klinger, R.; Steinmüller, H.; Sinner, M.; Esterbauer, H. *Biotechnol. Agric. Ser.* **1993**, *9*, 33-72.
31. Glasser, W.G.; Kaar, W.E.; Jain, R.K.; Sealey, J.E. *Cellulose* **2000**, *7*, 299-317.
32. Saake, B.; Kruse, Th.; Puls, J. *Bioresource Technol.* **2001**, *80*, 195-204.
33. Thornton, J.; Ekman, R.; Holmbom, B.; Örsa, F. J. *Wood Chem. Technol.* **1994**, *14*, 159-175.
34. Hannuksela, T.; Holmbom, B. *Proceed. 11th ISWPC Vol.I.*, **2001**, 379-382.
35. Gamerith, G.; Strutzenberger, H. In *Xylans and Xylanases*; Visser, J.; Beldman, G.; Kusters van Someren, M.A.; Voragen, A.G.J. Eds.; Elsevier Science Publishers B.V., **1992**; pp 339-348.
36. Lenz, J.; Schurz, J.; Bauer, J. *Papier* **1984**, *38*, 45-54.
37. Lenz, J.; Noggler, E.; Leibetseder, J. *Nahrung* **1986**, *30*, 959-965.
38. Rhodia Acetow AG. DE-OS 10109502, **2002**.

Chapter 3

Twin Screw Extrusion and Ultrafiltration for Xylan Production from Wheat Straw and Bran

P. Maréchal, J. Jorda, P.-Y. Pontalier*, and L. Rigal

**Laboratoire de Chimie Agro-Industrielle (LCA-CATAR), ENSIACET,
118 Route de Narbonne, F31077 Toulouse Cedex 4, France**

Xylans can be coextracted from wheat straw and bran in a twin-screw extruder. The best results for both the production yield and the extract properties are obtained with low alkali content, as the majority of the xylans comes from bran. The desired concentration of the extract solution can be achieved by ultrafiltration. The membrane configuration and molecular weight cut off (MWCO) must be adapted to each solution to limit fouling and concentration polarisation. A permeate flux of 20 dm³/h.m² was obtained at a final concentration ratio of 2. Ultrafiltration allows for a partial demineralization of the solutions but does not change the properties of the final powder.

Wheat bran is a by-product of wheat grain milling, with a production of about 1.2 million metric tons per year in France in the late 1990's mainly used as cattle feed. Wheat bran from mills is partly composed of residual starch, easily removed by hot water washings (1). Destarched wheat bran is mainly composed of natural polymers of xylose and arabinose, sometimes called hemicelluloses or xylans, which can be used as thickening, emulsifying or film-forming substances (2). Industrial xylans extraction is done primarily in alkaline conditions, the key conditions being the pH of the media, the extraction time

and the temperature of the reaction (3-4). Extraction is usually carried out in two steps: i) alkaline hydrolysis of ester linkage between the hemicelluloses and the other parietal components with sodium hydroxide (5); potassium hydroxide (6) or barium hydroxide (7), ii) water extraction. After ester links hydrolysis, xylans are liberated in the aqueous media at a low percentage concentration where they form a gel and remain associated to the vegetable matrix. A large liquid/solid ratio (L/S) (between 25 and 200 for wheat bran) is therefore needed to achieve an efficient batch reactor extraction. Centrifugation (for the elimination of the remaining solids) is usually followed by an evaporation step to reduce the volume of the extract. The solution is precipitated with several volumes of ethanol (to reach an alcohol concentration of 60-70%) and filtrated to retain xylans, which are then dried. Two obstacles impede industrial development: i) the large L/S ratio, which implies a concentration phase and a consumption of large quantities of sodium hydroxide, ii) and the precipitation step with (three volumes).

The aim of this work was therefore to develop a process for direct atomization of the extract by considering twin-screw extrusion and ultrafiltration. Twin-screw extrusion is very efficient for alkali impregnation of wheat bran, but xylan extraction is achieved only with large L/S ratios. As xylan extraction from wheat bran alone is not feasible by twin-screw extrusion with a low L/S, the coextrusion of wheat bran and wheat straw was investigated.

This study compares wheat bran extraction in a stirred reactor and combined wheat straw and bran extrusion and then focuses on the influence of the origin of the extract on ultrafiltration performance.

Materials

Extraction

Batch extraction of destarched wheat bran was carried out on 2.2 kg of vegetable matter under continuous stirring in an 80L stainless steel reactor devoid of any heating or cooling device.

Xylans were coextracted from wheat straw and wheat bran with a BC 45 twin screw extruder (Clextral). The 1.4 m long barrel is composed of seven different sections (figure 1), each cooled by cold water and four of which are heated by induction belts. Straw and bran were introduced at the beginning of the first section of the barrel and water in the fourth section. The corotative intermeshing screws are composed of small modular screw elements and present

a profile dedicated to alkaline treatment of vegetable matter. Our experiments were carried out with two reverse-pitch screw elements in which peripheral slots were grooved in the screw flight for leakage flow. A series of 1 cm long bilobal elements with a neutral pitch, splayed 90° from one another, was used to knead the matter. The screw profile is identical to the profile optimized by (8) for refining straw fibres. Conical holes (1 mm inlet, 2 mm outlet) formed the 10 cm long filter element mounted down the last section. This element was used for a first L/S separation.

Wheat bran and sodium hydroxide were blended at room temperature in a separate reactor one hour before each experiment. The initial L/S ratio was seven and the mixture was stirred for five minutes. The L/S ratio was increased to ten just before the introduction of the mixture into the twin screw extruder with a Nemo excentric-screw pump. Straw was introduced in the extruder's first section with a screw feeder. Straw was mixed with the alkaline dough in the first zone of the barrel through the neutral pitch element and the reverse-pitch screw element successively. The washing water was injected downstream from this zone, and the mixture was conveyed through the second reverse pitch located just downstream from the filtration module. The filtrate was collected and kept in a cold room before further processing, while the refined cellulosic fibres were gathered at the barrel outlet.

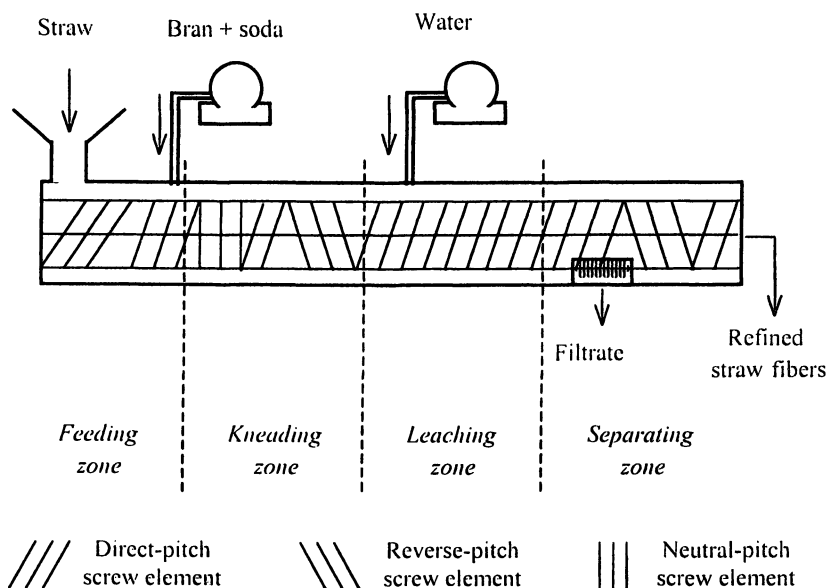


Figure1 : Twin-screw extruder configuration for the alkaline treatment of vegetable matter

The alkaline extract, either from batch or continuous process was separated from the vegetable matrix by centrifugation. In the classic treatment developed in the laboratory, the filtrate was then evaporated under reduced pressure at 50°C. Acetic acid was added to the remaining solution up to a pH of 5.0 before the addition of 2 volumes of ethanol for 1 volume of solution and storage at 4°C overnight for precipitation. Aggregated xylans were sieved and ground with an ultraturax at 4000 rpm and then mixed with 1 volume of ethanol. The blend was filtered under vacuum, and the precipitate was then dried at 50°C, ground and stored.

Despite two distinct populations of xylans that appeared during the precipitation, these were not separated. The procedure using an ethanol concentration of 60-70%, described above, led to a precipitation yield around 60% (9). Ultrafiltration and spray-drying were investigated to replace this time consuming procedure.

Destarched wheat bran of an average particle size of 600 µm was provided by Ardeval-Reims (France). Wheat straw harvested in the Toulouse region was chopped in a hammer-mill until the morsels passed through a 6-mm screen.

Ultrafiltration

The filtration apparatus was composed of a feed tank, a pump, an ultrafiltration cartridge and pressure gauges for feed, retentate and permeate. The membranes (table I) were polysulfone (Polymem and Pall) or cellulose acetate (Amicon) with a molecular weight cut-off ranging between 1 kDa and 50 kDa. The module was a flat sheet cassette (Pall) or hollow fibres (Amicon and Polymem).

Table I. Membrane properties

<i>Name</i>	<i>Reference</i>	<i>Composition</i>	<i>MWCO (kDa)</i>	<i>Area</i>
<i>Amicon</i>	H10P10-20	CA	10	0.9 m ²
<i>Pall</i>	Omega	PES	1, 5, 10, 30, 50	0.09 m ²
<i>Polymem</i>	SI1156FM6	PS	6	0.006 m ²

CA: cellulose acetate; PES: polyethersulfone; PS: polysulfone.

The volume of the tank was 20 dm³ for Amicon membrane, 500 cm³ for Polymem membrane and 1.2 dm³ for Pall membranes. Peristaltic and piston pumps were respectively used for Polymem membranes and for Pall and Amicon membranes.

All the trials were done in a concentration mode, as the aim was to reduce the volume of the solution in order either to limit the amount of alcohol used for the precipitation or to replace precipitation by spray-drying. Concentration mode means that the retentate is recycled in the feed tank but the permeate is eliminated, thus leading to a volume decrease. Permeate flow rate was periodically evaluated by weight measurements and concentration ratios (CR) calculated from these measures. After concentration, extracts were precipitated with alcohol to evaluate the influence of ultrafiltration on the final powder composition.

The ultrafiltered solutions were obtained under optimal conditions for stirred extraction ($L/S = 25$, bran/alkali = 1, 2 hour at 35°C) and twin-screw extrusion ($L/S = 25$, bran/alkali = 1, 1 hours at 35°C) and are described in table II.

Membranes were cleaned according to the following procedure: i) water rinsing ii) sodium hydroxide washing iii) water rinsing. Sodium hydroxide had a concentration of 0.4% for Pall and Polymem membranes and 0.5% for Amicon membranes.

Analytical

Analyses were done on the extract after centrifugation (feed for ultrafiltration), ultrafiltration permeate and ultrafiltration retentate. Dry matter was determined gravimetrically at 105°C over a period of 24h and the ash content was determined by thermogravimetric analysis after incineration at 550°C for 3 hours. Lignin concentration was measured according to the Tappi norm T222 om 88 for acid-insoluble lignin. Matter treated with sulphuric acid was filtered on Wattman pre-weighed glass-fibre filters, washed with deionized water and dried at 105°C overnight before being weighed. Proteins (%N*5.7) in all samples were measured on a Kjeldhal semi-automated device.

Monomeric sugar composition was determined by HPLC after a mild hydrolysis (H_2SO_4 , 1N at 120°C, kinetic over 30, 60, and 90 min.) using a Dionex DX300 HPLC fitted with a Carbopac PA1 column. Xylose, arabinose, glucose and galactose contents were investigated. The sugar content is the sum of the maximal contents of each of the 4 sugars over the 3 durations. The sum of the percentages {ashes + lignins + proteins + sugars} was always around 95%.

The hemicellulosic powders recovered were characterized according to their composition, thickening and film-forming properties. The thickening ability of the hemicellulosic powder was evaluated as the viscosity under a defined strain of an aqueous solution containing 3.5 % organic matter. These

measurements were made on a Carrimed rheometer using a cone-plate spindle geometry. All samples exhibited a clear shear-thinning behaviour. 20 g of the former solution was cast in a 100-cm² plastic tray, and the water was allowed to evaporate at room temperature. The film-forming abilities were evaluated as the mechanical properties of small dumbbell-shaped test pieces cut into films obtained according to this procedure. Their thickness was approximately 55 μm . The mechanical tests were done on a computer-driven RHEO TA-XT2 Texturometer using a traction method at 0.1mm/s and an average moisture content of 10%. The initial length between the grips was 55 mm.

Results

Extraction

The twin-screw extruder has proved to be a versatile tool for continuous treatment of vegetable matter, either for food or non-food applications. Trials for the direct alkaline extraction of xylans from wheat bran in a twin-screw extruder were unsuccessful. Bran impregnation with sodium hydroxide in the twin-screw extruder was very efficient, but it was necessary to make the separation between the hemicellulosic gel and the lignocellulosic matrix in another apparatus and remained difficult without a dilution to a L/S ratio of 50. Bran and straw co-extrusion was therefore investigated to be able to reduce the L/S ratio. Straw fibres form a dynamic plug in the restrictive elements of the screw profile just after the filtration zone. The pressure induced in the extruder sheath by the cellulosic fibres enabled the liquid/solid separation.

The xylan extraction yields and the purity of the precipitate are given as functions of the vegetable matter. The NaOH quantities used are shown in the form of isoresponse curves, computed from the results of 20 experiments and plotted using NEMROD software (10). Several trials have shown that the best results for the co-extraction of xylans from wheat bran and straw are obtained when working with a low screw speed and a high washing water flow rate. All the isoresponse curves are therefore given for a washing water flow of 90 l/h and a screw speed of 150 rpm.

The yield in organic matter swept along in the filtrate versus the total quantity of organic matter introduced in the system (figure 2) depends on two factors: first, the quantity of NaOH available and second the quality of the dynamic filtration tap in the twin screw extruder. A low rate of NaOH (bran/soda = 7) with low straw concentration seems to be sufficient to extract

most of the alkaline soluble compounds. Filtration with such a soda rate remains possible for every straw/bran ratio. High straw feed rates give the best filtration tap efficiency but also yield a lower organic matter recovery because of the decrease in the global soda/vegetable matter rate.

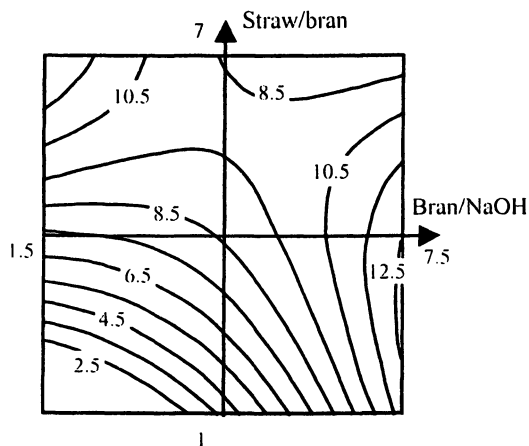


Figure 2. % of solubilized organic matter recovered in the filtrate / total of introduced organic matter

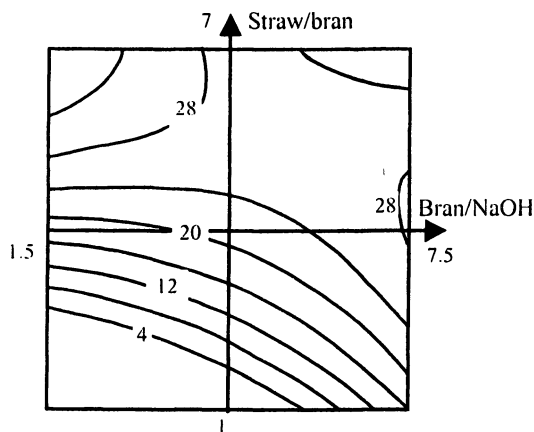


Figure 3. % of precipitated hemicellulosic powder / introduced bran

Experimental conditions combining a high soda content (bran/soda = 2) with a high straw introduction rate also give good yields in extracted organic matter as long as the vegetable matter/soda rate is kept around 15-20 to allow the formation of the fibrous tap. If this ratio is too low (when smaller quantities

of straw are used), the quantity of cellulosic fibres is not sufficient and the high lubricating effect of soda prevents the formation of the dynamic tap in the extruder. Since the pressure in the sheath does not build up, the filtrate flow rate drops and is followed by a drop in the yield of extracted hemicelluloses.

The isoresponse curves showing the proportion of recovered hemicellulosic powder (figure 3) are similar to the figure 2 curves, which means that the yield during the organic precipitation phase remains almost constant throughout the experiment. A large amount of lignin and protein seem to remain embedded in the hemicelluloses molecular network formed during the precipitation phase.

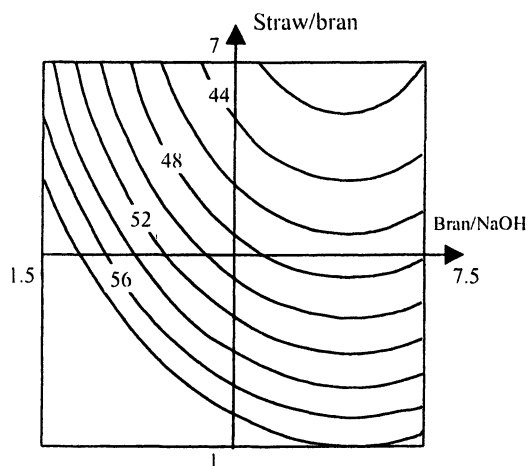


Figure 4. Sugar content of the hemicellulosic powder (in %)

The isoresponse curves representing the properties of the hemicelluloses co-extracted from straw and bran as thickener or film-former are very similar in pattern to sugar content curves. High sugar contents correspond to high viscosities and high tensile strength. Figure 4 shows the isoresponse curves representing the sugar content of the hemicellulosic powder as a function of the mass ratios of straw/bran and bran/NaOH, at a high water flow and a low screw speed.

The sugar content of the hemicellulosic powder increases with the rise in alkalinity and the decrease in straw content. The first can be explained by a more efficient action of NaOH on bran before coextrusion, which favours the release of more hemicelluloses, and by an increase of protein hydrolysis at high soda content. In fact, the rise in the sugar content is correlated with the decrease in the proteic material (data not shown). The second aspect is linked to the extraction of lignin from straws by soda, which is known to be very efficient in

a twin-screw extruder (8; 11). An increase in straw content implies more lignin swept along and partially co-precipitated with the hemicelluloses.

Xylans seem to originated mainly from bran during the combined extrusion of wheat straw and bran. This conclusion is made on the basis of the study of the xylose/arabinose ratio. Hemicelluloses from wheat bran have an approximate xylose/arabinose ratio of 2 (12) with a ramified structure. These ramifications give a rigid structure to the molecules, which cannot align under strain and therefore show a high viscosity. On the contrary, hemicelluloses from wheat straw have a high xylose content (xylose/arabinose = 7) (8) and can easily wrap or align under strain, showing poor properties in aqueous solutions. Viscosities up to 2000cp, at 20°C, under a strain of 5N/m² have been measured with the hemicelluloses from twin-screw extrusion. The increase in the lignin content (and the attendant decrease in the sugar content) of the powder induces a viscosity drop because of the hydrophobic nature of the lignin structure. The hemicellulosic sample collected for the experiment showing the best yield had a viscosity of 450cp (Table II).

Table II. Xylan aqueous solutions and film properties

	<i>Stirred reactor</i>	<i>Twin-screw extruder</i>
<i>Viscosity (Pa.s)</i>	70.10 ⁻³	450.10 ⁻³
<i>Elasticity (%)</i>	2.4	1.3
<i>Tensile strength (MPa)</i>	31.3	31.4
<i>Young's modulus (MPa)</i>	1790	2760

Xylans extracted by combined twin-screw extrusion of straw and bran are good film formers. For each experimental condition, film elasticity is low (around 2%), which means that oxidative gelation took place, thus leading to 3-dimensionnal cross-linking (9). The Young's modulus of such films are between 1.5 and 2.5 GPa, which are typical values for polymers linked mainly by H-bonds. The changes in the tensile properties are closely associated to the sugar content and, as a consequence, to the lignin content of the hemicellulosic powder, which hindered the H-bond network.

The best results for both the extraction yield in the hemicellulosic powder and the sugar purity in the case of xylan extraction from wheat bran in a twin-screw extruder are obtained for a low NaOH ratio (bran/soda = 7) and a low straw content.

The best results were obtained with a straw/bran ratio of 2 and a bran/soda ratio of 7 at a temperature of 50°C. Extraction was carried out with a L/S ratio

of 10. Extract was recovered after centrifugation with a concentration of 2.3% (dry matter) 65% of this dry mater being organic matter.

After the precipitation stage, the final powder from twin screw extrusion (92% dry matter), contains 91% organic matter. The global yield of this process is about 24 % of the potential in hemicelluloses of wheat bran, if it is considered that arabinoxylans represents 60 % organic matter 26% protein and 5.3% lignin (originating from straw) (table III). These results should be compared with extraction conditions in the stirred reactor, where the best results are obtained with a molar soda and a L/S ratio of 50. The chemical charge is reduced by a factor of 14 and the L/S ratio by a factor of 15 when twin-screw extruder is used.

Table III. Composition of the extract for the most favourable conditions in stirred reactor and twin-screw extruder.

	<i>Stirred reactor</i>	<i>Twin screw extrusion</i>
<i>Dry matter (%)</i>	93	92
<i>Ash (%)</i>	9.5	9.4
<i>Organic matter (%)</i>	90	91
<i>Sugar (%)</i>	80.7	53
<i>Proteins (%)</i>	6.9	26
<i>Lignins (%)</i>	2.9	5.3

When a stirred reactor is used, the final powder (93% dry matter) contains 90% organic matter. The alcohol precipitation also acts as a purification step during which salts are almost eliminated. The remaining salts are imbedded during the precipitation of hemicelluloses. The global yield of this process is about 59% of the potential in wheat bran hemicelluloses, if arabinoxylans are considered to represent 80% of the organic matter in the final powder (table III).

Some differences appear between the final powders resulting from the two processes. The differences are confirmed by slight differences in their physico-chemical properties. Extracts seem more limpid after twin-screw extrusion than those obtained after stirred reactor extraction. The sharpest difference between the xylan powders is the viscosity of the aqueous solutions. This difference may be partly due to the protein content (table III and IV).

Xylans from batch extraction are also good film formers, even though the tensile properties of these films differ slightly from the twin-screw extracts. The difference might be a result of the composition in minor compounds liable to oxidative cross linking in the twin-screw extract, thus leading to a more rigid film. Combined extrusion of wheat straw and bran leads to an extract with a

American Chemical Society
Library
1155 16th St., N.W.

concentration (2.3 % dry matter) lower than the concentration of the extract obtained in a stirred reactor (7%). Nevertheless, the organic matter concentration is similar in both cases due to the high mineral content of the stirred extract.

Ultrafiltration

As the L/S ratio remains high, a concentration stage must be kept in the purification process. Evaporation is an expensive step that may be replaced by membrane filtration. Ultrafiltration was therefore investigated for its capability to achieve purification (in the same way as the alcohol precipitation) and concentration at the same time. Ultrafiltration was tested using different membranes with an MWCO ranging from 1 to 50 kDa in order to obtain a minimum concentration ratio (CR) of 2 with a minimal organic matter loss.

At the beginning of the filtration, the permeate flux drops (figure 5) in every case because of the development of a concentration polarisation layer. The flux then decreases smoothly over a long period until another sharp decrease appears as the result of an increase in the viscosity of the solution.

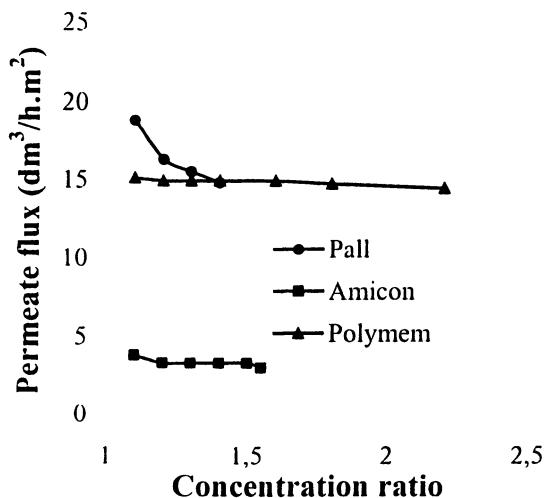


Figure 5. Influence of volume concentration ratio on permeate flux with 10 kDa membranes (Pall and Amicon) or 6 kDa membrane (Polymem) when filtering a twin-screw extract at 25°C. Pressure was 0.1 MPa with Amicon and Polymem and 0.4 MPa with Pall membrane.

The higher permeate fluxes were obtained with the 50 kDa Pall membrane (Table IV) when filtering stirred reactor extracts. Eleven liters were concentrated to a CR of 2 over 350 minutes with a 13% organic loss, as compared to the 38% loss with the 1 kDa and the 43% loss with the 5 kDa membranes. The final permeate flux was 20 L/h.m² at a pressure of 4 bars.

Table IV. Influence of the MWCO of the ultrafiltration membranes on the filtration properties and the properties of the final powder from the stirred reactor.

	Membranes		
	1 kDa	5 kDa	50 kDa
Final CR	1.8	2	2
Final permeate flux (L/h.m ²)	21	29	20
Dry matter yield (%)	60	55	87
Demineralization rate (%)	40	43	46

Ultrafiltration allows for a partial reduction of salt content in the retentate, approximately 50% of the initial salt content. Salts are partly retained because of electrostatic interactions (Donnan effect) with the biopolymers, which are polyelectrolytes. Nevertheless, this demineralization does not really change the salt concentration in the final powder, which decreases from 15% (treatment without UF) to 10% (UF step).

When ultrafiltering twin screw extracts, the 6 kDa membrane from Polymem was the only one to reach a CR of 2. At this point, the flux was 15L/h.m² with a 44% dry matter loss and a 34% demineralisation rate. The salt concentration of the final powder remained the same because it depends on the salt solubility in alcohol.

Table V: Ultrafiltration performance during the concentration step of the twin-screw extract.

	Membranes		
	1 kDa	5 kDa	50 kDa
Final CR	1.3	1.5	2.4
Final permeate flux (L/h.m ²)	15	3	14
Dry matter yield (%)	90	63	56
Demineralization rate (%)	18	18	34

Ultrafiltration can be introduced in the polysaccharide purification scheme instead of the alcohol precipitation step, but the membranes must be optimized in each case. Fouling of the membrane can completely change its selectivity, and the fouling properties of the solution depend on the way the extract is obtained. Twin-screw extrusion or stirred extraction leads to solutions with partially hydrolyzed molecules. The size spectra of the molecules is very large, and the small molecules produced can be a source of membrane fouling. The best performance is obtained with the 50 kDa membrane for the stirred extract and with the 10 kDa, as concerns the twin-screw extract. It can be concluded from these results that the twin-screw extract contains smaller molecules than the stirred extract.

Concentration polarization is another key parameter of polysaccharide filtration. When the MWCO of the membrane is adapted to the composition of the extract, hollow fibers seem to be more efficient than flat sheet membranes. Flat sheet membranes with turbulence promoters in the feed channel are used with low tangential velocity because turbulences are created by the screen. When filtering polysaccharides extracts, the viscosity of the solution is high, particularly in concentration mode, and the efficiency of the turbulence promoters is too low to avoid the creation of a gel layer. Hollow fibre membranes, which are used with high tangential velocity, thus give the higher permeate fluxes.

Conclusion

The trials with a twin-screw extruder showed that hemicelluloses, originating mainly from bran, with the best sugar purity can be obtained using both a high NaOH rate and a low straw/bran ratio. This combination of conditions gives lower extraction yield and is not interesting from an industrial point of view. Working with a lower soda rate leads to good extraction yield, and keeps the valuable properties of the precipitated xylans, although sugar purity is slightly lower. A twin-screw extruder allows to strongly lower consumption of chemicals and waste water volumes. Extraction was done with a sodium hydroxide consumption 14 times lower in the extruder than in the stirred reactor. This technique, combining wheat straw and wheat bran extraction, is attractive because it allows valorization of both liquid extract and solid raffinate (agromaterials) and because it is a continuous process, useful for the treatment of large quantities of organic matter.

In optimal conditions, stirred extraction of wheat bran combined with alcoholic precipitation leads to a powder containing 93% dry matter and

showing a 51% final yield. When introducing the 50 kDa membrane (for concentration) prior to alcohol precipitation, the final yield is 49% with a similar powder. Xylan extraction in a twin-screw extruder by coextrusion of wheat straw and wheat bran is achieved with a production yield of about 8% (compared to the total xylan quantity introduced with bran and straw). When the 10kDa membrane is introduced, the final production yield is only 4%, half the percentage obtained in treatment without ultrafiltration.

The fluxes obtained with ultrafiltration membranes are not very high (about 20 L/h.m²) because of the viscosity of the solutions and because of fouling. Ultrafiltration can be introduced for concentration and partial purification, but the final concentration does not allow direct atomization. New trials must be done to reach a CR of 4 using other membranes with a higher MWCO perhaps up to 100 kD, and under optimized hydrodynamic conditions.

References

1. Raynal, R. PhD thesis, INP, Toulouse, Fr, 1996.
2. Ebringerova, A. and Hromadkova, Z. *Bio. Gen. Eng. Rev.* 1999, 16, pp325-346.
3. Bataillon, M.; Mathaly, P.; Numes Cardinali A. and Duchiron F. *Ind. Cro. Prod.* 1998, 8, pp37-43.
4. Schooneveld-Bergmans M.E.; Beldman G. And Voragen A.G.J. 1999 *J. Cer. Sci.*, 29, pp49-61.
5. Brioullet, J.M. and Mercier, C. *J. Sci. Food Chem.* 1981, 32, pp243-251.
6. Du Pont, S. and Selvendran, R. *Car. Res.* 1987, 163, pp99-113.
7. Gruppen, H.; Hamer, R.J. and Voragen, A.G. *J. Cer. Sci.* 1991, 13, pp275-290.
8. Magro, C. PhD thesis, INP, Toulouse, Fr, 1995.
9. Schooneveld-Bergmans M.E., Van Dijk Y.M., Beldman G. And Voragen A.G.J. 1997 *J. Cer. Sci.*, 29, 63-75.
10. Mathieu, D. and Phan-Tan-Luu, R. Nemrod Software Université Aix-Marseille, Fr 1992.
11. Scalbert, A.; Monties, B.; Guittet, E. and Lallemand, J.Y. *Holzforschung* 1986, 40, pp119-126.
12. Shiiba, K.; Yamada, H.; Hara, H.; Okada, K. and Nagao, S. *Cer. Chem.* 1993, 70(2), pp209-214.

Chapter 4

Isolation and Characterization of Arabinoxylan from Oat Spelts

B. Saake, N. Erasmy, Th. Kruse, E. Schmekal, and J. Puls

Institute of Wood Chemistry and Chemical Technology of Wood, Federal Research
Centre of Forestry and Forest Products, 21031 Hamburg, Germany

Oat spelts contain high amounts of xylan whereas the lignin content is comparatively low. Accordingly this raw material is an interesting candidate for the isolation of xylan. The variation in chemical composition of oat spelts from different sources was investigated. Xylans were isolated by alkaline extraction under various conditions. A NaOH concentration of 5% (w/v) at a temperature of 90 °C enabled the isolation of xylan in high yield and purity. The total alkali charge, based on the raw material, could be reduced by lowering the liquid to solid ratio. With a simple H₂O₂ bleaching procedure high brightness values of 90 % ISO could be reached. Bleached xylan powders excelled by a high brightness stability.

Oat spelts are a raw material rich in xylan. They are collected at the factory sides of oat mills in large quantities since they can make up to almost 40% of the total weight of grain processed in a mill. In the seventies oat spelts were a major source for the production of furfural accounting for about 22% of the total production (1). However, the importance of oat spelts for this application has declined due to lower production costs in countries of Afrika and Asia, where bagasse or rice residues are the raw materials of choice. In addition the utilisation of furfural is in general declining in industrialized countries. Today oat spelts are mainly used as an additive for animal feed, in most cases after grinding and pelleting. However, the price of this product is rather low, especially considering the energy input for production. Lehrfeld reported in 1996 that 70 US \$ per ton can be obtained and prices today should be even lower (2).

During the last years there exists an emerging interest for the application of xylan as a polymer. Xylans were tested as gel forming or thermoplastic material (3,4,5), as filler for polypropylene (6), and as a component for paint formulation (7) or for the coating of cellulosic fibres (8). For higher value products the application for pharmaceuticals might be of interest for instance as tableting material (9), for the treatment of wounds (10) or for preventing blood coagulation (11). Some biological and physiological effects of xylans are summarized by Ebringerova and Hromadkova (12). Further studies have focused on the derivatisation of xylans to ethers and esters (13). Besides of the large number of possible applications xylan is not yet available in large quantities on the market.

Xylans are components of many plant groups including monocotyls, dicotyls and even algae. However, for a technical isolation procedure not all raw materials are favourable. In recent years several groups tried to pursue the development of isolation procedures of xylan based on raw materials, like wood (14), corn cobs (15), corn hulls (16), or straw from various agricultural plants (17, 18).

In generell xylans from different raw materials show a wide variation in their structure, which are summarized in several reviews for wood hemicelluloses (19, 20), grass hemicelluloses (21) and cereals (22). Arabinoxylans from cereals cell walls are of importance for cereal utilisation or flour properties. These arabinoxylans often have a high amount of side groups or side chains, and molar masses can reach several hundred thousands or even millions (23). For xylan isolated from oat spelts molar masses of 22,000 g/mol have been reported (24). The ratio of xylose, arabinose and 4-O-methyl glucuronic acid for those sample was 7.6:1:0.03. Accordingly, these xylans resemble xylans isolated from different straw types, which is in accordance with the fact that both, straw and spelts, are lignified plant tissues.

For lignocellulosic materials there are some arguments in favour of grasses compared to wood as raw material. The first mentioned materials have higher xylan and lower lignin contents, while the lignin structure is easier degradable.

For the isolation procedure several techniques have been applied which normally include an alkaline extraction as the main step. Sodium hydroxide or

aqueous ammonia are the most common extraction media. Mild steaming treatment (25), refining (14,26) or milling (17,18) of the raw material have been applied to increase accessibility or reduce the necessary reactor volume. For lignocellulosic materials extraction yields can be further improved by delignification treatments which reduce the hindrance of extraction by lignin carbohydrate bonds. Treatments with sodium chlorite (18) and hydrogen peroxide (17) have been applied prior to extraction while hydrogen peroxide, peracetic acid and performic acid have been used as well during the extraction stage (27). Extraction yields can be improved as well by the application of ultrasound during the extraction (15), while twin screw extrusion might be a technical approach to design a high throughput process (28).

Experimental

Raw Material

All oat spelts were provided by Peter Kölln KGaA (Elmshorn/Germany). Starch residues were reduced by removing material smaller than 1 mm by sieving. Prior to xylan extraction oat spelts were treated in a Sprout Waldron refiner.

Xylan Extraction and Precipitation

Climatized oat spelts, corresponding to a dry weigh of 50 g were mixed with the NaOH solution. The NaOH concentration was varied from 2-19% (w/v) and the consistency from 10-30%. Extraction treatments were performed in autoclaves, rotating in an oil bath for 60 min including the heating up period. The autoclaves were equipped with valves for the application of oxygen pressure, if needed. After the reaction, autoclaves were cooled down. The reaction mixture was transferred into a hollow steel cylinder, containing a filter cloth on a perforated steel plate on the bottom of the cylinder. A plunger fitting into the cylinder was used to apply a pressure of 10 MPa using a hydraulic press. The alkaline extraction liquor passed the perforated plate on the bottom of the cylinder and was collected in a tray.

The liquor was neutralised using acetic acid and slowly precipitated in the threefold volume of ethanol. The pH was adjusted to 5.5 and the precipitate was recovered by filtration. The xylan was re-dispersed in water, the volume equivalent to the volume of the starting liquid. The solution was re-precipitated in the threefold volume of ethanol, the pH adjusted to 4.0 and the precipitate recovered by filtration. The xylan was washed first with ethanol and then with ether. Samples were dried in the fume hood from ether. During this procedure the particles size was reduced every now and then to insure the formation of a fine powder.

The extracted oat spelts residue was mixed with 100 ml acetic acid (20%) in a glass beaker. After 10 min the residue was transferred on a buchner funnel and

the acetic acid was washed out with water. The samples were climatized for yield determination and further analysis.

Bleaching of Xylans

Peroxide bleaching of extracted xylans was performed analogously to the procedures used for pulp bleaching in polyethylen bags in a thermostated water bath at 80 °C for 2 hours at a consistency of 10%. The NaOH, water glass, and peroxide charges were calculated, based on dry xylan. After the treatment xylans were recovered by one precipitation step into the threefold volume of ethanol. The pH of the liquid was adjusted to 4.0. The xylan was recovered by filtration and drying from ether, analogously to the procedure for extracted xylan.

Monosaccharide Analysis

Prior to carbohydrate analysis oat spelts and extraction residues were ground in a vibration grinding mill (HSM 100, Herzog, Osnabrück/Germany). A two step hydrolysis was used for spelts and extraction residues applying 72% sulphuric acid in the first and 2.5% sulphuric acid in the second step. Extracted xylans were analysed in a one step procedure applying 4% of sulphuric acid. Monosaccharides were then determined by borate-complex anion exchange chromatography. Details of the hydrolysis and chromatography procedures were reported previously (29, 30). Starch was analysed by aqueous extraction, enzymatic hydrolysis and chromatographic determination of the glucose (31)

Size Exclusion Chromatography

SEC was performed on the following column set: GRAM 30, 100, 3000 (8x300 mm) and guard column (8x50 mm, Polymer Standard Service, Mainz/Germany). 0.05 M LiBr in DMSO:water (90:10) was chosen as mobile phase with a flow rate of 0.4 ml/min at 60 °C. The amount of the soluble material passing the column was determined by concentration calibration with xylopentaose as a standard. Molar mass data were calculated from viscosity-detection and universal calibration as published previously (24).

Brightness and Brightness Stability of Xylans

3 g of xylan powder was pressed into a pellet of 45 mm diameter and 5 mm heights using a small press for the production of BaSO₄ brightness standards. The measurements were then performed with an Daticolor 2000 instrument. Brightness stability was tested placing xylan powder in a large crystallizing dish to maximise the surface exposed to the light source. A daylight source was used for irradiation. Every day the powder was transformed into a pellet for

brightness measurement and afterwards dispersed in the dish for further exposure.

Results and Discussion

Analysis of Different Oat Spelts

Oat spelts from different sources were analysed regarding their chemical composition. The samples were not collected according to botanical species, since the grain wholesaler are collecting and mixing products from several farmers. Nevertheless, between spelts from oats purchased from Finland, Australia and two German sources major differences occurred. The hydrolysis residues listed in Table I are an indication for the lignin content of the spelts. The sample with the highest lignin content were spelts from Finnish oats while the lowest content was determined for quality B from Germany and the material produced from Australian oats. The maximum difference accounted to 5% which is a substantial advantage for low lignin content material. In view of the fact that oat spelts contain an arabinoxylan, the possible product yield can be compared after adding up the xylose and arabinose content for each sample. Here the lowest amount was found for quality B from Germany (21.9%) while the highest content was determined for the spelts from Australian oats (33%). Again this difference of more than 10% clearly demonstrates that a comparison of different oat varieties has to be considered for further studies. For all samples the glucose contents in Tabel I not only reflects the cellulose but as well the starch. Therefore the residual starch content was investigated separately. Here a variation between 0.8 and 10.2% was found. For the extraction work a

Table I. Hydrolysis residue, monosaccharide composition, and starch content of oat spelts from different sources

<i>Origin</i>	<i>Hydrolysis residue</i>	<i>Xylose</i>	<i>Arabinose</i>	<i>Total glucose</i>	<i>Glucose from starch</i>
<i>% based on raw material</i>					
Finland	23.6	29.7	2.9	34.0	0.8
Australia	18.8	30.1	2.9	35.4	4.9
Germany-A	22.9	27.0	2.6	37.9	10.2
Germany-B	18.5	19.7	2.2	46.7	2.6
Material for extraction	21.3	29.5	2.7	36.5	4.5

representative sample was taken from the oat mill, which was a mixture of different raw materials representing the production process. This material is listed in the last line of Table I and had a hydrolysis residue of about 21.3% and a arabinoxylan content of 32.7%, not adjusted for water addition. The acetyl, ferulic and p-coumaric acid content of xylans was not determined, since these side groups are removed in an alkaline extraction and cannot contribute to the product yield. 4-O-methyl glucuronic acid contents are low in these xylans. Only 0.2-0.3% survive the hydrolysis procedure used for the raw materials. Assuming a xylan yield of 30% this would amount to 0.8 to 1%, based on the xylan. A ¹H-NMR study of xylan extracted in this work indicated about 1-1.5% of 4-O-methyl glucuronic acid in the xylan. Accordingly a significant proportion of these substituents are destroyed under the hydrolysis conditions applied for the raw materials. Since the total amount is still low the analysis of 4-O-methyl glucuronic acid was not included in the study as a routine analysis. Galactose and rhamnose are present in small quantities adding up to less than 2 % and will not be discussed in detail. The ester groups (acetyl, feruloyl, p-coumaroyl) were not quantified. These groups are saponified under the alkaline extraction conditions applied and therefore not relevant for the characteristics and the yield of arabinoxylan in this study.

Non-Pressurized Alkaline Extraction

First the alkaline extraction at ambient temperature was investigated using NaOH concentrations from 5 to 12.5% (w/v) and consistencies of 10% for 1 hour extraction time. However, under those conditions xylan yields were very low and did not exceed 8%, based on raw material. Therefore the effect of reaction temperatures was investigated using different NaOH concentrations. The results for 5% (w/v) NaOH are summarized in Table II.

Table II. Yield, carbohydrate composition and molar mass of xylans extracted at different temperatures

Temp. °C	Xylan- yield %	Carbohydrate analysis				SEC <i>M_w</i> g/mol
		Hydrolysis residue %	Xylose % based on total carbohydrates	Arabinose %	Glucose %	
70	34.6	14.5	70.1	11.2	16.7	29,300
80	38.5	13.7	74.7	12.7	10.2	30,200
90	40.4	15.4	72.4	11.7	13.4	30,080

NOTE: Extraction at 10% consistency, 5% (w/v) NaOH, 1 h

At 70 °C a yield of 34.6% extracted powder could be achieved while a further increase of the reaction temperature up to 90 °C enabled a maximum yield of 40.4%. The hydrolysis residue of roughly 14-15% indicated that the xylans still have a high amount of lignin impurities. The carbohydrate fraction was made up to more than 80% by arabinoxylan, while between 10-17% of the carbohydrates were glucose, which resulted mainly from starch impurities and to a minor extent from low molar mass cellulose. Molar masses were in the magnitude of 30,000 g/mol, which is equivalent to 227 monosaccharide units per molecule. Considering the xylose:arabinose ratio of 5.9 to 6.4 for these samples the polymer backbone, calculated as weight average degree of polymerisation (DP_w), amounted to roughly 195 xylose units while every sixth unit was substituted by arabinose.

In general the results indicate that an effective extraction of oat spelt xylan requires the application of elevated temperatures. It can be assumed that even at the high alkaline concentration applied, elevated temperatures are needed to effectively cleave lignin carbohydrate bonds in the limited time of the alkaline treatment.

Oxygen Aided Alkaline Extraction

Alternatively to non-pressurized extraction the application of 0.6 MPa O_2 pressure was investigated. These experimental conditions should generate an alkaline oxygen bleaching effect and lower the lignin content in both, the extracted xylan powder and the extraction residue.

Effect of Consistency and Alkaline Concentration on O_2 -Aided Extraction

The total alkaline charge required for xylan extraction was of major importance for the feasibility of the isolation process. These factors were dependant on the alkalinity of the extraction liquor and the consistency used in the process. In Figure 1 the effect of alkalinity on the yield of xylan and extraction residue is depicted for 10% and 25% consistency. The upper picture for 10% consistency demonstrates that an increase of NaOH concentration from 2.2 to 5% resulted in a continuous increase of xylan yield. Totalling the yield of xylan and residue it became apparent that up to 20% of the starting materials were not recovered. This material remained in the precipitation liquid and should consist of extractives, lignin fragmentation products, and low molar mass carbohydrates. A further analysis of those components was not pursued at this stage of the project.

By comparison of the upper and lower x-axis it became apparent that 5% NaOH concentration at 10% consistency resulted in an enormous total alkali charge of more than 45%, based on raw material. Rising the consistency to 25% (Figure 1, lower graph), enabled far higher alkali concentrations up to 15%,

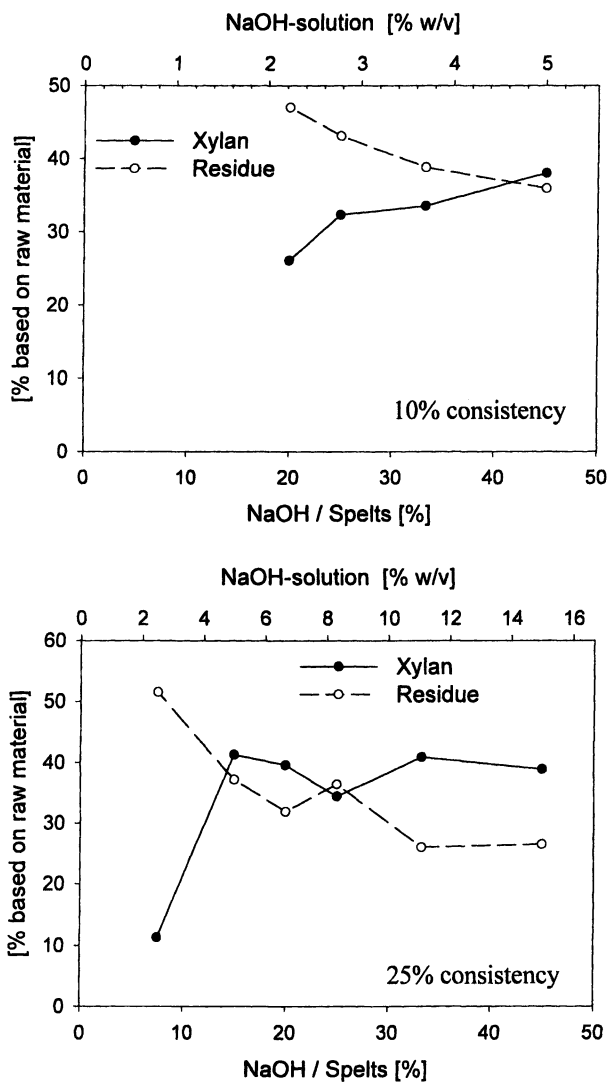


Figure 1. Influence of NaOH concentration on the extraction yield at 10% and 25% consistency (oxygen aided extraction 0.6 MPA, 90 °C, 1 h)

when the same total NaOH charge was applied. However, for NaOH solutions from 2-15% (w/v) it became apparent that in the range from 2 to 5% a strong increase of xylan yield could be achieved. Higher alkali concentration could not provide a further improvement. Therefore the NaOH concentration should be limited to 5% (w/v) and high consistencies are an effective measure to lower the total alkali consumption in the extraction process.

SEC investigations of isolated xylans revealed that the polymers were very stable under the conditions of alkaline oxygen treatment. Applying an alkaline solution of 8.6% (w/v) at 30% consistency, these experimental condition represented a total NaOH charge of 20%, based on raw material. The xylan isolated under those harsh conditions had still a molar mass of 27,300 g/mol (Table III). Increasing the alkalinity up to 19.3% (w/v) resulted in a reduction of molar mass down to values of 20,400 to 21,000 g/mol. While the combination of high alkaline charges and high consistencies resulted in a reduction of molar mass, the polydispersity (M_w/M_n) was not yet negatively affected. Applying 5% NaOH solution no negative effect of high consistencies on molar mass could be determined up to 25% (data not shown).

The carbohydrate composition and hydrolysis residue were not significantly effected by application of high consistencies. However, the experimental deviation regarding the extraction yield was quite large due to difficulties with a reproducible removal of the alkaline solution. This effect is documented in the course of the xylan yields in the lower graph of Figure 1. For this reason further studies were conducted at 10% consistency. Nevertheless according to these results there is no restriction to the application of high consistencies from a chemical standpoint. Engineering solutions for application of high consistencies and counter current extraction will be crucial for the feasibility of the process.

Table III. Viscosity and molar mass data of xylans extracted with different NaOH concentrations at 30% consistency

<i>NaOH concentration</i>		<i>SEC analysis</i>			
<i>% [w/v]</i>	<i>% / spelts</i>	<i>SEC-recovery</i>	<i>[η]</i>	<i>M_w</i>	<i>M_w / M_n</i>
		<i>%</i>	<i>ml/g</i>	<i>g/mol</i>	
8.6	20	73.5	41	27,300	4.5
10.8	25	71.2	39	23,500	2.9
14.3	33	81.4	39	20,400	2.5
19.3	45	80.4	35	21,000	3

NOTE: Extraction at 0.6 MPa O₂, 90 °C, 1 h

Comparison of Non-Pressurized and Oxygen Aided Alkaline Extraction

Further experiments were performed with a new batch of raw material which excelled by a higher content of arabinoxylan (39%) and a low content of

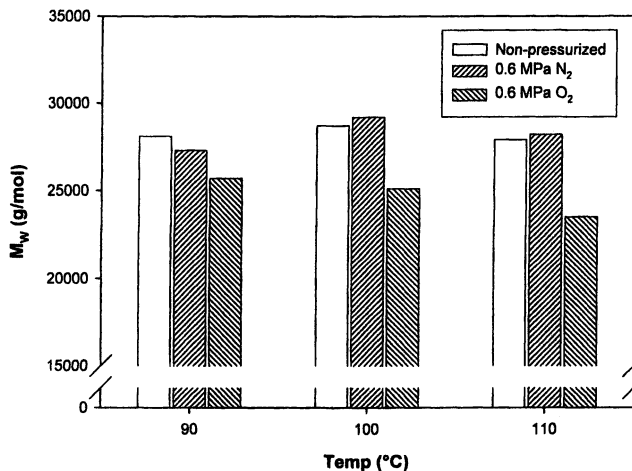


Figure 2. Influence of O₂ and N₂ pressure on the molar mass of xylan extracted at different reaction temperatures with 25% consistency

starch impurities. To evaluate the effect of oxygen and pressure on xylan yield and quality extractions were performed non-pressurized and pressurized with N₂ and O₂. The application of temperatures of 100 or 110 °C partly resulted in extraction yields above 40%. However the carbohydrate analysis revealed that those samples were heavily contaminated with cellulose. This indicates that under these harsh alkaline conditions at temperatures above 100 °C a degradation, of cellulose occurs. In addition a reduction of the spelt particle size and a reduced retention on the filter cloth might be responsible for this effect. The analysis of molar masses for xylans extracted at 10% and 25% consistency showed now significant difference between the extraction with N₂ pressure and without pressure. In contrast the O₂ resulted in a significant reduction, which was more pronounced at the high consistency of 25%. The data in Figure 2 demonstrate that the O₂ induced reduction of molar mass was increasing with the reaction temperature, while without O₂ no negative effect of temperature on molar mass of xylans could be determined. Nevertheless, due to the contamination of xylan with cellulose at higher temperatures, reaching quantities up to 9% based on raw material, 90 °C can be considered as the optimum temperature for extraction.

Non-pressurized and O₂ aided extraction were further compared at 90 °C and 10% consistency, performing the extraction eight times for each condition. The results in Table IV demonstrate that a high reproducibility of ± 0.3-0.4% could be achieved regarding the extraction yield. The non-pressurized extraction had a 1.4% higher yield of xylan powder compared to the O₂-aided procedure. However, this difference resulted from a higher lignin content as indicated by

the hydrolysis residue. The carbohydrate composition showed no differences regarding the arabinoxylan purity which amounted 95% of the carbohydrate fraction for these samples. The residual sugars were made up of glucose and galactose in even proportions. According to these results the O₂-aided extraction offers only a benefit regarding the lignin content, but not regarding the extraction yield.

Table IV. Comparison of non-pressurized and O₂-aided extraction at 10% consistency (90 °C, 1 h, O₂ pressure 0.6 MPa)

<i>Extraction procedure</i>	<i>Extraction yield</i>	<i>Hydrolysis residue</i>	<i>Xylose</i>	<i>Arabinose</i>
	<i>% based on raw material</i>	<i>% based on xylan</i>	<i>% based on total carbohydrates</i>	
non-pressurized	40.4 ± 0.4	11.2	82.8	12.9
O ₂ - aided	39.0 ± 0.3	9.2	82.8	12.2

Hydrogen Peroxide Bleaching of Xylans from Non-Pressurized and O₂-Aided Extraction

H₂O₂ bleaching experiments of the xylans listed in Table IV were performed at 80 °C for two hours, using 2% NaOH and 2% water glass as alkali source. The carbohydrate composition of xylans was not effected by the bleaching operation. However, with increasing H₂O₂ concentration the hydrolysis residue was reduced while the brightness increased up to 90% ISO. From Figure 3 it is apparent that both xylans reached the same brightness level.

However, the 2% lower lignin content of the xylan derived from O₂-aided extraction can be maintained through the bleaching procedure resulting in values of 4.1 -5.4 at high H₂O₂ charge compared to 7.1-7.4 for the xylan from non-pressurized extraction. Since the residual lignin might be a drawback for some applications, this might be a point in favour of the pressurized extraction procedure. Molar masses (M_w) of starting materials and bleached xylans were determined by SEC (Figure 4).

The starting xylan from O₂-aided extraction had a molar mass about of 15% below the sample from non-pressurized extraction. The latter sample was very stable under bleaching conditions and lost only 5-6% its molar mass even at high H₂O₂ concentration, while the xylan extracted with O₂ was more intensively degraded losing about 16% of its molar mass. Comparing samples at a brightness level of 90% ISO the material derived from the non-pressurized extraction had a molar mass of 28.300 g/mol compared to 21.100 g/mol for the corresponding sample from O₂-aided extraction.

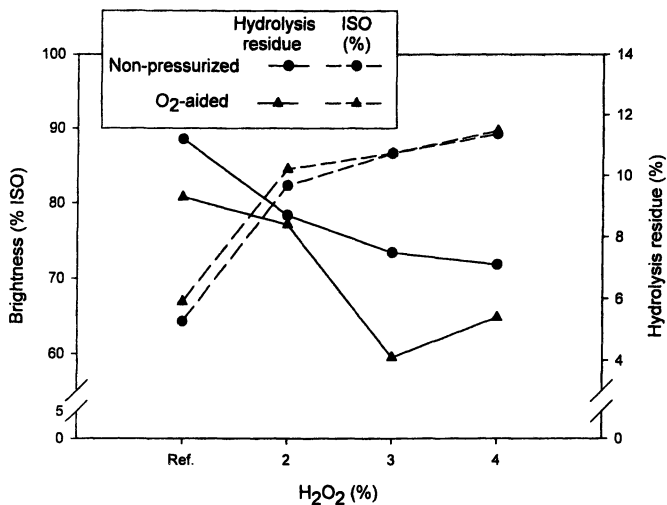


Figure 3. Effect of H₂O₂ charge on brightness and hydrolysis residue of xylans derived from non-pressurized and O₂-aided extraction (Ref. = starting xylans)

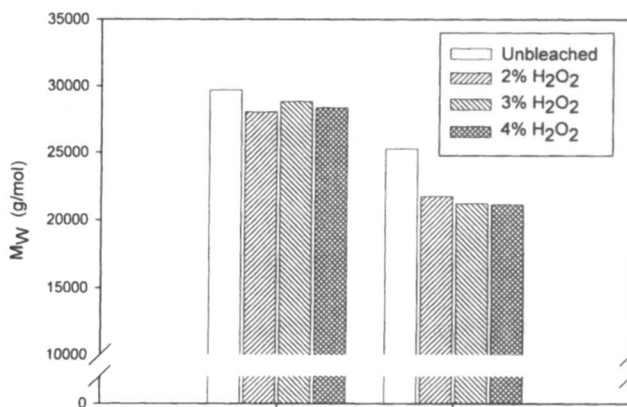


Figure 4. Effect of H₂O₂ bleaching on the molar mass (M_w) of xylans derived from non-pressurized and O₂-aided extraction.

Since the bleached xylans still contain a significant amount of lignin the brightness stability of xylans bleached with 4% H₂O₂ was investigated by light induced yellowing. Even after a period of three weeks xylans from both extraction procedures excelled by a high brightness stability. The bleached sample derived from non-pressurized extraction lost 1.5% ISO, while for the

sample from O₂-aided extraction no significant brightness loss could be determined.

Conclusion

Oat spelts are an interesting raw material for the isolation of xylan. They are available in large quantities at oat mills and have a comparatively low price. The xylan content showed a large variation from 22% to 39% for different oat spelts investigated in this study. This aspect deserves further attention and might help to establish a xylan isolation process on a technical scale. A temperature of 90 °C and a NaOH-concentration about 5% (w/v) seem to be most suitable to reach high xylan purities and high extraction yields. The total chemical charge in the process can be reduced by applying high consistencies in the extraction. Here, engineering solutions for handling high consistencies will be of major importance for the economical evaluation.

O₂-aided extraction can reduce the lignin content of the isolated xylan. However, molar masses of xylans are reduced compared to a non-pressurized extraction. Xylans from both extraction concepts can easily be bleached to a high brightness level of 90% ISO. In H₂O₂ bleaching operations the xylan from O₂-aided extraction was more severely degraded, resulting in a degree of polymerisation of about 160 monosaccharide units compared to 214 for the sample extracted without O₂. Surprisingly the bleached xylans from both isolation methods excel by a high brightness stability, also a significant amount of lignin is retained in the samples. A major focus of future research will be on the role of lignin in various end products and the possibility to increase delignification in bleaching stages.

Acknowledgement

This project was supported by the German Agency of Renewable Resources (FNR e.V. Güstrow, Project: 00NR097). We thank the P. Kölln KGaA (Elmshorn, Germany) for providing the oat spelt raw materials.

References

1. Shukla, T.P. *Crit. Rev. Food Sci.* **1975**, *6*, 383-431.
2. Lerfeld, J. *J. Appl. Polym. Sci.* **1996**, *61*, 2099-2105.
3. Lenz, J.; Schurz, J.; Bauer, J. *Papier* **1984**, *38*, 45-54.
4. Ebringerová, A.; Hromádková, Z. *Food Hydrocolloid* **1992**, *6*, 437-442.
5. Rajesh, K.J.; Sjöstedt M.; Glasser W.G. *Cellulose* **2001**, *7*, 319-336.

6. Amasch, A.; Zugenmaier, P. *Polym. Bull.* **1998**, *40*, 251-258.
7. Fang, J.M.; Sun, R.C.; Salisbury, D.; Fowler, P.; Tomkinson, J. *Polym. Degrad. Stabil.* **1999**, *66*, 423-432.
8. Henriksson, Å; Gatenholm, P. *Holzforschung*, **2001**, *55*, 494-502.
9. Paronen, P.; Juslin, M.; Käsnänen, K. *Drug. Dev. Ind. Pharm.* **1985**, *11*, 405-429.
10. Methacanon, P.; Kennedy, J.F.; Lloyd, L.L.; Paterson, M.; Knill, C.J. *Carbohydr. Polym.* **1998**, *34*, 435-436.
11. Kindness, G.; Williamson, F.B.; Long, W.F. *Biochem. Biophys. Res. Commun.* **1979**, *88*, 1062-1068.
12. Ebringerová, A.; Hromádková, Z. *Biotechnol. Genet. Eng.* **1992**, *16*, 325-346.
13. Ebringerová, A.; Heinze, T. *Macromol. Rapid. Comm.* **2000**, *21*, 542-556.
14. Glasser, W.G.; Jain, R.K.; Sjöstedt, M.A. US Patent 5,430,142, 1995.
15. Hromádková, Z.; Kováčiková, J.; Ebringerová, A. *Ind. Crop. Prod.* **1999**, *9*, 101-109.
16. Chanliaud, E.; Saulnier, L.; Thibault, J.F. *J. Cereal. Sci.* **1995**, *21*, 195-203.
17. Sun, R.C.; Thomkinson, J.; Ma, P.L.; Liang, S.F. *Carbohydr. Polym.* **2000**, *42*, 111-122.
18. Sun, R.C.; Fang, J.M.; Thomkinson, J. *J. Agric. Food Chem.* **2000**, *48*, 1247-1252.
19. Timell, T.E. *Wood Sci. Technol.* **1967**, *1*, 45-70.
20. Puls, J. *Macromol. Symp.* **1997**, *120*, 183-196.
21. Wilkie, K.C.B. *Adv. Carbohydr. Chem. Biochem.* **1979**, *36*, 215-264.
22. Fincher, G.B.; Stone, B.A. Advances in cereal science and technology VIII (5) **1986**, 207-295.
23. Izydorczyk, M.S.; Biliaderis, C.G. *Carbohydr. Polym.* **1995**, *28*, 33-48.
24. Saake, B.; Kruse, Th.; Puls, J. *Bioresource Technol.* **2001**, *80*, 195-204.
25. Košíková, B.; Ebringerová, A. *Apitta* **1991**, *45*, 425-430.
26. Sun, R.; Lawther, J.M.; Banks, W.B. *Ind. Crop. Prod.* **1998**, *7*, 121-128.
27. Sun, R.C.; Thomkinson, J.; Geng, Z.C.; Wang, N.J. *Holzforschung* **2000**, *54*, 349-356.
28. N'Diaye, S.; Rigal, L.; Laroque, P.; Vidal, P.F. *Bioresource Technol.* **1996**, *57*, 61-67.
29. Puls, J.; Poutanen, K.; Körner, H.-U.; Viikari, L. *Appl. Microb. Biotechnol.* **1985**, *22*, 416-423.
30. Puls, J.; Dokk Glawischnig, T.; Hermann, A.; Borchmann, A.; Saake, B. *Proceedings: "8th Intern. Symp. on Wood and Pulping Chemistry" Vol I, Helsinki, Finland, June 6-9, 1995*, 503-510.
31. Rademacher, P.; Bauch, J.; Puls, J. *Holzforschung*, **1986**, *40*, 331-338.

Chapter 5

Isolation, Characterization, and Enzymatic Hydrolysis of Acetyl-Galactoglucomannan from Spruce (*Picea abies*)

H. Stålbrand¹, J. Lundqvist¹, A. Andersson¹, P. Hägglund¹,
L. Anderson¹, F. Tjerneld¹, A. Jacobs², A. Teleman², O. Dahlman²,
M. Palm³, and G. Zacchi³

¹Department of Biochemistry, Lund University, P.O. Box 124,
SE-221 00 Lund, Sweden

²Swedish Pulp and Paper Research Institute (STFI), Box 5604, S114 86, Stockholm,
Sweden

³Department of Chemical Engineering I, Lund University, Lund, Sweden

Water-soluble hemicelluloses were extracted from spruce chips by heat-fractionation using microwave treatment. A screening of conditions (pH, temperature and residence time) was performed for the extraction of *O*-acetyl-galactoglucomannan (AcGGM). The yield and the average molecular weight of the extracted mannan were analysed using HPLC, size-exclusion chromatography (SEC) and mass-spectrometry. The pH during heat fractionation influenced the yield and the structure of AcGGM. The highest yield (78%) of AcGGM (average molecular weight 3800) was achieved with heat-fractionation in water at 190° C for 5 minutes. With 0.025% NaOH, an average molecular weight of 9500 was obtained at a yield of 30%. AcGGM molecular weight standard molecules were prepared using SEC. The structure of the AcGGM was determined using ¹H-NMR. The enzymatic hydrolysis of AcGGM was studied using β-mannanase and α-galactosidase.

The different components in lignocellulose are tightly associated and one of the difficulties in the fractionation of the native components is the risk of chemical modifications. Consequently, in several fractionation processes it has been proven difficult to separate the lignin from the cellulose and hemicellulose without modifying the hemicellulose (19). The extraction of hemicelluloses often includes different hydroxide solutions (20, 21). However, under alkaline conditions the acetyl sidegroups are rapidly cleaved off (22). This problem can be avoided; acetylated hemicellulose may be isolated from softwood holocellulose (in these cases the residue after chemical delignification) by treatment with dimethyl sulfoxide, followed by hot-water extraction of the residue (23-27). Recently, soft-wood AcGGM was isolated by hot-water extraction of defatted and chlorite delignified soft-wood followed by gelchromatography (28).

The current paper summarizes and discusses our work, which is directed toward the extraction of hemicellulose as an environmental friendly raw material with potential for different polymer applications (2, 3). Here, we present the fractionation of softwood hemicellulose from lignocellulose using heat. After a screening of microwave heat-fractionation conditions, we achieved the extraction of acetylated hemicellulose (AcGGM) employing heat-fractionation of milled spruce-chips in water (2). AcGGM was isolated from the obtained filtrate using size-exclusion chromatography (SEC). The structure, size and enzymatic hydrolysis of the isolated AcGGM was studied (2). Purified and well characterised AcGGM fractions were further applied as molecular weight standard molecules (3). The yield, the molecular weight, the degree of acetylation (DS) and the content of galactosyl sidegroups were influenced by the pH during the heat-fractionation (3). The results are informative in further studies directed toward the preparation of higher molecular weight AcGGM.

Materials and Methods

Impregnation and Heat-fractionation

The starting material was spruce-chips with a mannan content of 12.9% (2). The heat-fractionation of milled spruce-chips was performed in a closed vessel in a microwave oven (MLS 1200 Microwave workstation, Milestone) with 9.1 g dry weight of wood chips in 100 ml of water solution (1, 2). Prior to the heat-fractionation, the milled spruce chips were impregnated (soaked) in either water or water solutions of sodium hydroxide (0.025-2%), potassium hydroxide (0.05%) or sulfuric acid (0.05%) (2). The heat-fractionation was performed at different temperatures and times, ranging from 170° to 220° C and 2 to 20 minutes, respectively. The solids were discarded by filtration and the filtrates were analyzed further.

Size-Exclusion Chromatography (SEC)

Subsequently, the content of the filtrates from the heat-fractionation were size-fractionated by SEC using a Superdex 75 column connected in series with a Superdex 200 column (Pharmacia Biotech., Uppsala, Sweden) (2).

Carbohydrate Analysis and Yield

The concentrations of monomeric carbohydrates were determined using high performance anion-exchange chromatography (HPAEC, Dionex). The content of mannose in the filtrate and in the filtrate after acid hydrolysis (using 0.5 M sulfuric acid at 120° C for 4 hours) was determined. Using this data and data from raw material analysis, the yield of mannose residues in oligo- and polysaccharides in the filtrates were determined (2, 3).

Nuclear Magnetic Resonance (NMR) spectroscopy

The purified carbohydrates in two SEC-fractions were analysed with one dimensional and two dimensional ^1H NMR spectroscopy (MMBruker DPX 400 MHz) (2). The molar ratio of the sugar residues, the degree of acetylation (DS) and the degree of polymerization (DP) were calculated from the integrated signals in the ^1H NMR spectra (2).

Mass Spectrometry

Matrix assisted laser desorption/ionization time-of-flight mass-spectrometry (MALDI-TOF MS) analysis of AcGGM fractions was performed using a Hewlett-Packard G2025 A spectrometer equipped with a linear detector (3). Positive and negative spectra were recorded, representing the sums of 20-50 laser shots.

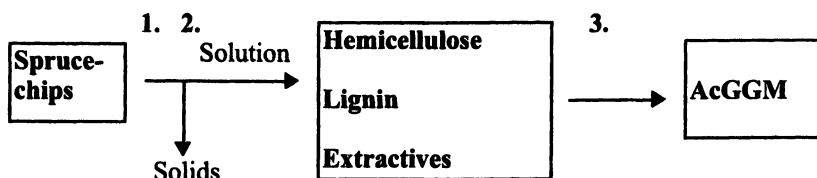
Enzymatic Hydrolysis

The isolated fractions of AcGGM were separately incubated with the *Aspergillus niger* endo-1,4- β -mannanase of family 5 (29) and the family 27 α -galactosidase (30) at enzyme loadings of 5 or 10 nkat/mg substrate incubated at 40 C for 48 hours at pH 5.0 and 4.8, respectively (2). The produced saccharides were analyzed either by determination of reducing sugars or by HPAEC (2).

Results and Discussion

Heat-Fractionation for Hemicellulose Extraction

With the aim to find conditions allowing the isolation of intact or fragmented AcGGM free from lignin, spruce chips were first impregnated in water media and then heat-fractionated using microwave irradiation. The solids were removed by filtration and the obtained filtrate was then further processed and analyzed (2, 3) as schematically shown in Figure 2.



1. IMPREGNATION

2. HEAT-FRACTIONATION (MICROWAVE OVEN)

3. SIZE-SEPARATION (SEC)

Figure 2. Scheme over the procedure used for the isolation of AcGGM from spruce chips using micro-wave heat-fractionation and SEC.

Molecular Weight Distribution

The solubilized material in the obtained filtrates was analyzed for molecular weight distribution with SEC, calibrating the column using dextran molecular weight standard molecules. The filtrates were expected to consist of carbohydrates (mainly hemicellulose) and lignin (19). Thus, refractive index and absorbance at 280 nm were used in order to detect both the carbohydrates and possible lignin residues. The latter is expected to have absorbance maximum in the UV region where carbohydrates do not absorb (31).

Figure 3 shows an example of the RI and UV signals for a SEC chromatogram obtained on analysis of a filtrate. The heat-fractionation time and temperature was in this case 2 minutes at 200° C and the impregnation was done in water. Other impregnation media were tested as well. Impregnation with sodium hydroxide gave a shift toward higher molecular weights of the RI-signal trace, but at these lower elution volumes also peaks with UV-absorbance eluted. Impregnation with potassium hydroxide at the same temperature and time gave no improvement (2). The filtrates from impregnation with sulfuric acid contained predominantly monomeric sugars due to acid hydrolysis.

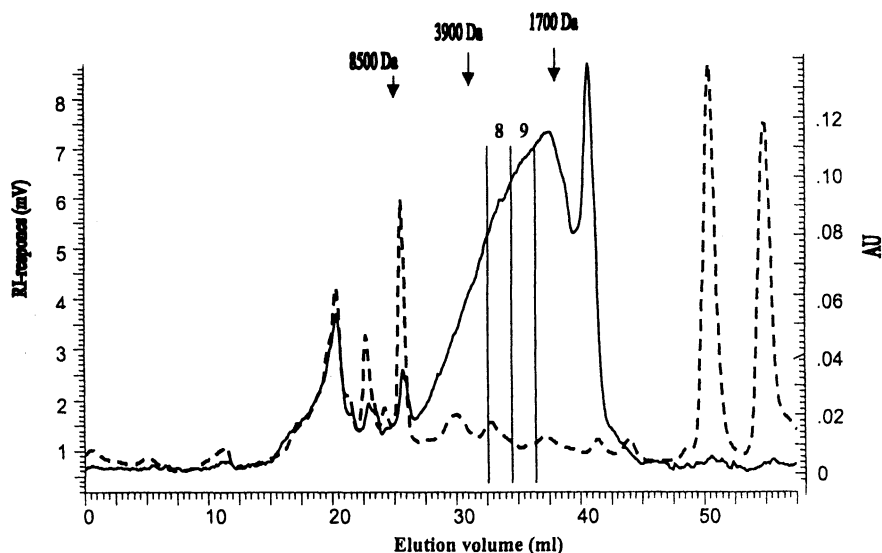


Figure 3. Elution profile of water-soluble material from microwave oven treated (200°C for 2 min) milled spruce chips after SEC using Superdex 75 and 200 columns. RI-detection (solid line) and absorbance at 280 nm (hatched line) is shown (AU: Absorbance units). The applied sample volume was 100 μ l. The arrows mark the elution volumes from fractions of AcGGM analyzed with MALDI-MS (M_p 8500, 3900 and 1700). Monomeric sugars eluted at 39–40 ml. The elution volumes using dextran standards of molecular weights 70 000, 16 000, 1600 and mannitriose (molecular weight 504) were 20, 24 37 and 40 ml, respectively. AcGGM from fractions 8 and 9 (marked with vertical lines) were characterized in detail (see text and reference 2).

Yield

Heat-fractionation of milled spruce chips after impregnation with either water or 0.05% sodium hydroxide was further evaluated. The spruce chips were heat-fractionated at 170°-200° C for 2-20 minutes (for impregnation with sodium hydroxide, heat-fractionation up to 220° C was used) (2). The sugars in the obtained filtrates, analyzed after acid hydrolysis, were mainly mannose (70-80%). The yield of oligomeric and polymeric mannan was determined as well. Generally, up to a temperature of 200° C and a time of 5 minutes the yield of mannan increased with increased residence time and temperature both for the water-impregnated and the sodium hydroxide impregnated spruce chips. The highest yield of mannan was 75-80% which was obtained for water impregnated spruce-chips heat-fractionated at 190-200° C for 5 minutes (2,3). The carbohydrates present in filtrates obtained from heat-fractionation of spruce chips in water at 200° C were further characterized.

Isolation of AcGGM

As a first step to characterize the extracted carbohydrates from heat-fractionation with water at 200° C, the filtrate from 2 min residence time was analysed further. With this filtrate preparative SEC-separations were performed (2). Two fractions (fractions 8 and 9) with assumed substantial carbohydrate content but no UV-absorbance were collected (Figure 3). These fractions with an estimated molecular weight from the SEC-run of 5000 and 1600, respectively, were subject to acid hydrolysis with subsequent analysis of monomeric sugars. The obtained approximate molar galactosyl:glucosyl:mannosyl ratio was roughly what is expected for AcGGM (0.3:1:3 and 0.5:1:4, for fraction 8 and 9, respectively) (2).

Structure of the Isolated AcGGM

The carbohydrates in fraction 8 and 9 (see above) were subsequently studied with ¹H NMR spectroscopy (2). On the basis of the the NMR analysis it could be concluded that the carbohydrates in fraction 8 and 9 consist of a backbone of linear β-1,4-linked glucomannan, *O*-acetylated at the C-2 or C-3 position of some mannose residues. The presence of α-1,6-linked galactosyl sidegroups was indicated (2).

The obtained galactosyl:glucosyl:mannosyl ratio for both fraction 8 and 9 (about 0.1:1:4) is in rough agreement with that for galactoglucomannan with low galactosyl content, found in softwoods (5). Some of the mannose residues were acetylated (DS 0.28 and 0.25 for fraction 8 and 9, respectively). The acetyl substitutions were almost equally distributed at the C-2 and the C-3 positions (2). However, it cannot be ruled out that *O*-acetyl migration between C-2 and

C-3 (32) occur during the isolation procedure. The obtained acetyl content is somewhat lower than previously reported for pine glucomannan (DS 0.36, reference 33) and spruce AcGGM (DS 0.32, reference 27).

Using the NMR data, the approximate degree of polymerization of the *O*-acetyl-galactoglucoamannan present in fraction 8 and fraction 9, was calculated to DP 20 and 11, respectively (2).

Enzymatic Hydrolysis of AcGGM

The overall structural features, typical for AcGGM were also further confirmed by the use of highly purified hydrolytic enzymes. The *Aspergillus niger* endo- β -1,4-mannanase (29) was incubated with isolated AcGGM (fraction 8) and the obtained hydrolysate analyzed with ^1H NMR spectroscopy and HPAEC (2). The results clearly showed that the polysaccharide has β -1,4-mannosidic bonds accessible to the active site of the enzyme. The β -mannanases from *Trichoderma reesei* (34) and *Cellulomonas fimi* (35) also readily degraded the AcGGM (unpublished). Furthermore, an *A. niger* α -galactosidase from family 27 (30), appeared to release all galactose sidegroups from AcGGM (fraction 8) (2). The use of enzymes may be optimized further as attractive tools in the modification of the structure and the molecular weight of hemicelluloses.

Improved Molecular Weight Determination.

Both heteroxylyan and heteromannan oligo- and polysaccharides are extracted from spruce using heat-fractionation (2). In order to allow a better analysis of the AcGGM in filtrates by the use of SEC, the mannan containing polysaccharides need to be distinguished from other material. This was done by analyzing the mannan and xylan content in the SEC fractions using acid hydrolysis and HPAEC (3). The distribution of acidic heteroxylyan only partly overlapped with AcGGM, thus these two polysaccharides could be separated from each other using SEC (3).

Furthermore, a more accurate determination of the average molecular weight using SEC was developed. Initially in our investigations, dextran molecular weight standard molecules were used in the SEC-analysis of AcGGM. However, due to differences in the elution behavior of different polysaccharides this approach may introduce errors in molecular weight determinations (36). The lack of accessibility of standard molecules having a narrow molecular weight distribution and the right size-range is a general problem for many water-soluble polysaccharides. In order to overcome these limitations in the analysis of AcGGM, we isolated a range of AcGGM fractions. The peak-average molecular weight (Mp) for each fraction were determined using MALDI-TOF MS (3, 37). Thus, the fractionation of AcGGM and the determination of Mp made it possible to use well-defined AcGGM fractions as

standards (Figure 3). A more accurate weight-average molecular weight (Mw) of the extracted AcGGM could therefore be determined, which improved further the evaluation of heat-fractionation conditions (below).

In Table I a comparison of the different molecular weights obtained for fraction 8 and fraction 9 is shown. For the fraction with the lowest molecular weight, fraction 9, a limited discrepancy of the data obtained with SEC using the different standards and the data generated by NMR spectroscopy was observed (obtained molecular weights between 1600 and 1900). With fraction 8, on the other hand, a significant discrepancy was obtained with SEC using the two different types of standard molecules. The NMR data agreed somewhat better with the SEC-values obtained using AcGGM standards. This is consistent with the observation that the disagreement of the SEC molecular weight standard curves when comparing dextran and AcGGM standards is greater at higher molecular weights (38).

Table I. Size-determination of the purified AcGGM with different methods

	SEC-D (Mw)	SEC-G (Mw)	NMR (DP)
Fraction 8	5000	2500	20*
Fraction 9	1600	1700	11*

Summary of the size-determination of the purified AcGGM using SEC with dextran standard molecules (SEC-D) and AcGGM standard molecules (SEC-G) and using NMR spectroscopy. *)These number-average DPs are equivalent to approx. calculated molecular weights of 3500 (Fraction 8) and 1900 (fraction 9). Data from reference 2 (SEC-D and NMR) and reference 3 (SEC-G).

Influence of pH During the Heat-Fractionation

The heat-fractionation conditions were subsequently further studied in order to find conditions which allowed extraction of a higher molecular weight AcGGM and a higher yield (3). Such a polysaccharide would be more useful as a raw material. The degree of galactosyl substitution has been shown to influence the gelling properties of carob galactomannan (39). Thus, besides the molecular weight, also the side-group content and composition is likely to influence the properties and usefulness of the polysaccharide.

The influence of the pH during the heat-fractionation on the molecular weight, yield, and composition of the galactoglucomannan in the filtrates was studied. Heat-fractionation at 190°C for 5 minutes was used after impregnation at a sodium hydroxide concentration of 0-2% (3). The pH decreased 0.5-3 pH units during the heat-fractionation. The results are summarized in Table II. Generally, an increase of the Mw but a decrease of the mannan yield was obtained with increased pH. The highest yield of AcGGM was 78% , obtained

using water impregnation (pH 3.4 after heat-fractionation). However, a relatively low Mw, 3800, was obtained. A higher Mw (9500) but a lower yield (31%) was obtained with impregnation in 0.025% sodium hydroxide (pH 4.2 after heat-fractionation). Under these conditions the galactoglucomannan was acetylated, but at pH values above approx. 5, it appeared to be deacetylated (Table II). Also the galactosyl side-group content of the galactoglucomannan appeared to vary with pH. At the lower pH values a lower content of galactosyl side-groups, present in oligo- and polysaccharides, was observed (3).

Table II. Influence of pH during heat-fractionation

% NaOH	pH	Mw	Yield (%)	Acetylation
0	3.4	3800	78	yes
0.010	3.6	5900	36	yes
0.020	4.0	5700	29	yes
0.025	4.2	9500	31	yes
0.05	4.6	8700	16	yes
0.1	5.1	6400	1.5	no
0.5	6.9	10800	2.0	no
1	11.7	11000	2.2	no
2	12.7	14000	3.0	no

Summary of the Mw, the mannan yield (%) and the composition of extracted (Ac)GGM which was obtained from heat-fractionation at 190 C for 5 minutes. Impregnation was with 0-2% NaOH. The pH after heat-fractionation is given. The Mw of the (Ac)GGM was determined with SEC using AcGGM standard molecules. Galactosyl groups were present in all cases, but to a lower extent when impregnation in 0-0.05% NaOH was used. The presence of acetylation is indicated. Data from reference 3.

Conclusions.

It is possible to extract acetylated galactoglucomannan from spruce-chips employing heat-fractionation by microwave irradiation after impregnation in aqueous solutions. We have also shown that steam may be employed instead of microwave irradiation (data not shown). AcGGM of DP 20 (equivalent to approx. molecular weight of 3500) was isolated from milled spruce-chips, microwave heat-fractionated in water at 200° C for 2 minutes (2). It had a structure, carbohydrate composition and degree of acetylation, which is typical for softwood AcGGM with low galactosyl content (5, 40). Thus, this would indicate that at least most of the acetyl groups remain after the heat-fractionation. The comparably short chain length, however, indicates that fragmentation occurs. Heat-fractionation in water at 190° C for 5 minutes gave

the highest yield of AcGGM (78%), which had an approx. molecular weight of 3800 (3). In order to produce AcGGM with a higher molecular weight (9500) heat-fractionation in 0.025% sodium hydroxide but otherwise at the same conditions may be used. However, the yield is lower (31%). The pH decreased 0.5-3 pH units during the heat-fractionation. At pH values above approx. 5 (after heat-fractionation), the extracted galactoglucomannan was deacetylated (3). Furthermore, the galactosyl content was lower at the lower pH values. Thus, both types of side-groups are sensitive to the pH during the heat-fractionation. The degree of substitution of some heteromannans, such as carob galactomannan (galactosyl side-groups) and konjac glucomannan (acetyl side-groups), has been shown to greatly influence the water solubility of the polysaccharides (39, 41, 42, and reviewed in reference 38). Our results are consistent with the assumption of a similar behavior for AcGGM, where a decrease in water solubility due to deacetylation at the higher pH values may lead to the observed decrease of the yield. Analysis of the heteromannan content in the solid remains would help further to understand the influence of the substitutions on the extraction process. Enzymes are attractive tools which may be used in the preparation of AcGGM of different sizes and degrees of substitution. Furthermore, also heat-fractionation at different pH values may serve as a way to obtain AcGGM with different molecular weights and side-group content, which in turn, will influence the properties with potentially different applications.

References

1. Junel, L. Fractionation of lignocellulosic materials for production of hemicellulosic polymers. Licentiate thesis. Department of Chemical Engineering I. Lund university, Lund, 1999.
2. Lundqvist, J.; Teleman, A.; Junel, L.; Zacchi, G.; Dahlman, O.; Tjerneld, F.; Stålbrand, H. Isolation and characterization of galactoglucomannan from spruce (*Picea abies*). *Carbohydr. Polymers*, **2002**, *48*, 281-289.
3. Lundqvist, J.; Jacobs, A.; Palm, M.; Zacchi, G.; Dahlman, O.; Stålbrand, H. Characterization of galactoglucomannan extracted from spruce (*Picea abies*) by heat fractionation at different conditions. *Carbohydr. Polymers*, **2003**, *51*, 203-211
4. Söderqvist Lindblad, M.; Ranucci, E.; Albertsson, A.-C. *Macromol. Rapid Commun.* **2001**, *22*, 962.
5. Timell, T.E. *Wood Science Technol.* **1967**, *1*, 45-70.
6. Sjöström, E. *Wood chemistry; Fundamentals and applications. Academic press: San Diego, CA, 1993.*
7. Biermann, C.J.; Schulz, T.P.; McGinnis, G.D. *J. Wood Chem. Technol.*, **1984**, *4*, 111-128.
8. Lamprey, J.; Robinson, C.W.; Moo-Young, M. *Biotechnol. Lett.*, **1985**, *7*, 531-534.

9. Lipinsky, E.S. *Wood Agricult. Res.*, **1983**, 489-501.
10. Puls, J.; Poutanen, K.; Körner, H.-U.; Viikari, L. *Appl. Microbiol. Biotechnol.*, **1985**, *22*, 416-423
11. Schulz, T.P., McGinnis, G.D.; Biermann, C.J. *Energy Biomass Wastes.*, **1984**, *8*, 1171-1198.
12. Teh-an, H. In *Handbook of Bioethanol: Production and utilization*; Wyman, C.E., Ed. 1996; pp 179-212
13. Eklund, R.; Galbe, M.; Zacchi, G. *J. Wood Chem. Technol.* **1988**, *8*, 379-392.
14. Bennani, A.; Rigal, L.; Gaset, A. *Biomass Bioenergy* **1991**, *1*, 289-296.
15. Paszner, L.; Jeong, C.; Quinde, A.; Awardel-Karim, S. *Energy Biomass Wastes* **1993**, *16*, 629-664.
16. Azuma, J.-I.; Katayama, T.; Koshijima, T. *Wood res.*, **1986**, *72*, 1-11.
17. Azuma, J.-I.; Tanaka, F.; Koshijima, T. *J. Ferment. Technol.* **1984**, *62*, 377-384.
18. Magara, K., Ueki, S., Azuma, J.-I., Koshijima, T. *Mokuzai Gakkaishi* **1988**, *34*, 462-468.
19. Puls, J.; Schuseil, J. In *The Second TRICEL93 Symposium on Trichoderma reesei Cellulases and Other Hydrolases*; Suominen, P.; Reinikainen, T., Eds.; The Foundation for Biotechnical and Industrial Fermentation Research; Espoo, 1993, vol 8, pp 51-60.
20. Hamilton, J.K.; Quimby, G.R. *Tappi* **1957**, *40*, 781-786.
21. Timell, T.E. *Tappi* **1961**, *44*, 88-96.
22. Lai, Y.Z. In *Wood and Cellulosic Chemistry*; Hon, D.N.-S.; Shiraishi, N., Eds.; Marcel Dekker: New York and Basel, 1991, vol 10, pp. 455-522.
23. Hägglund, E.; Lindberg, B.; McPherson, J. *Acta Chem. Scand.* **1956**, *10*, 1160-1164.
24. Lindberg, B.; Rosell, K.-G., Svensson, S. *Svensk papperstidning* **1973**, *76*, 30-32.
25. Meier, H. *Acta Chem. Scand.* **1958**, *12*, 1911-1918.
26. Meier, H. *Acta Chem. Scand.* **1961**, *15*, 1381-1385.
27. Tenkanen, M., Puls, J., Rättö, M.; Viikari, L. *Appl. Microb. Biotech.* **1993**, *39*, 159-165.
28. Capek, P.; Alföldi, J.; Lisková, D. *Carbohydr. Res.* **2002**, *337*, 1033-1037
29. Ademark, P.; Varga, A.; Medve, J.; Harjunpää, V.; Drakenberg, T.; Tjerneld, F.; Stålbrand, H. *J. Biotechnol.* **1998**, *63*, 199-210.
30. Ademark, P.; Larsson, M.; Tjerneld, F.; Stålbrand, H. *Enz. Microb. Technol.* **2001**, *441-448*.
31. Morohoshi, N. In *Wood and Cellulosic Chemistry*; Hon, D.N.-S.; Shiraishi, N., Eds.; Marcel Dekker: New York and Basel, 1991, vol 10, pp. 331-392.
32. Garegg, P.J. *Arkiv Kemi* **1965**, *23*, 255-268.
33. Lindberg, B.; Rosell, K.-G., Svensson, S. *Svensk papperstidning*, **76**, 383-384.
34. Stålbrand, H.; Saloheimo, A.; Vehmaanperä, J.; Henrissat, B.; Penttilä, M. *Appl. Env. Microb.* **1995**, *61*, 1090-1097.

35. Stoll, D.; Stålbrand, H.; Warren, R.A.J. *Appl. Env. Microb.* **1999**, *65*, 2598-2605.
36. Kato, T.; Tokuya, T.; Takahashi, A. *J. Chrom.*, **1983**, *256*, 61-69.
37. Jacobs, A.; Dahlman, O.; *Biomacromolecules*, **2001**, *2*, 894-905.
38. Lundqvist, J. *Isolation, characterization and enzymatic hydrolysis of water-soluble wood polysaccharides*. Ph.D. Thesis; 2002, Lund university, Lund
39. Rol, F. In *Industrial Gums: Polysaccharides and Their Derivatives*; Whistler, R.L., Ed.; 2nd ed., Academic press: New York, 1973, pp. 323-337.
40. Shimizu, K. In *Wood and Cellulosic Chemistry*; Hon, D.N.-S.; Shiraishi, N., Eds.; Marcel Dekker: New York and Basel, 1991, vol 10, pp. 177-214.
41. McCleary, B.V. In *Enzymes in Biomass Conversion*, American Chemical Society: Washington, DC, 1991. Chapter 34.
42. Nishinari, K.; Williams, P.A.; Phillips, G.O. *Food Hydrocoll.* **1992**, *6*, 199-222.

Chapter 6

Characterization of Hemicelluloses from Wood Employing Matrix-Assisted Laser Desorption/Ionization Time-of-Flight Mass Spectrometry

Olof B. Dahlman, Anna Jacobs, and Maria Nordström

Swedish Pulp and Paper Research Institute, STFI, Box 5604, S-114 86, Stockholm, Sweden

This chapter describes some analytical procedures employing Matrix-Assisted-Laser-Desorption/Ionization Time-Of-Flight (MALDI-TOF) mass spectrometry for the characterization of hemicelluloses. The molar mass parameters for glucuronoxylans, hexenuronoxylans and glucomannans were determined by using an analytical procedure involving size exclusion chromatography followed by off-line MALDI-MS analysis. In the case of *O*-acetylated glucuronoxylans and glucomannans, the degree of substitution with acetyl moieties was determined on the basis of the MALDI spectra obtained prior to and following deacetylation. By using this MALDI-MS procedure *O*-acetyl residues were found to be present in hardwood glucomannans. The distribution of 4-*O*-methylglucuronic acid residues along the polysaccharide chains of hardwood and softwood xylans was studied employing MALDI-MS analysis. In the case of softwood xylans, the 4-*O*-methylglucuronic acid residues were distributed regularly within the polysaccharide. In contrast, the corresponding uronic acid residues in hardwood xylans were found to be distributed irregularly along the polysaccharide chains.

In 1996 we described (1) the successful application of Matrix-Assisted-Laser-Desorption/Ionization Time-Of-Flight Mass Spectrometry (MALDI-TOF-MS) for characterizing hemicelluloses isolated from wood and pulps. Since then this approach has been improved considerably (2,3) and several different procedures for wood and pulp constituents have been reported (3-8). In the present article, a selection of our previously reported analytical procedures are discussed together with some hitherto unpublished results from our laboratory.

MALDI is a soft ionization and desorption technique that was first described in 1988 by Karas and Hillenkamp (9,10). Among other applications, they employed this new technique for characterizing biomacromolecules (e.g., proteins and polysaccharides) and synthetic polymers (10,11).

The major advantages associated with the use of MALDI-MS include a high level of sensitivity; applicability to molecules exhibiting a wide range of masses; little or no fragmentation of the molecules being analyzed and the rapidity with which results can be obtained. Interpretation of data is facilitated by the fact that almost only single-charged ions are generated. This fact also implies that the mass to charge ratios of the ions formed in connection with MALDI analysis are directly related to the absolute molar masses of the molecules present.

The present article discusses the analytical information that can be obtained by MALDI-MS analysis of different types of non-acetylated and *O*-acetylated hemicelluloses derived from wood and pulp. Furthermore, a procedure for analyzing the molar mass parameters for hemicelluloses, utilizing size exclusion chromatography (SEC) followed by MALDI-MS analysis, is discussed.

MALDI-MS analysis of glucomannans

The glucomannans are linear polysaccharides composed of β -(1-4)-linked glucopyranosyl and mannopyranosyl residues. Several kinds of glucomannans, which might contain β -(1-6)-linked galactopyranosyl residues, have been isolated from both soft- and hardwoods. Glucomannans from softwood have galactose and *O*-acetyl groups linked to the mannose residues and a glucose-to-mannose ratio of 1:3 to 1:4.

The MALDI-MS spectrum of a low molar mass fraction of an alkali-treated glucomannan from spruce wood is depicted in Figure 1. This spectrum contains a distribution of well-resolved signals separated by 162 mass units (i.e., the mass of a hexose residue). These peaks originate from different oligomers with varying chain length. From the mass (i.e., the *m/z* ratio) associated with its MALDI-MS signal, the number of hexose residues present in each oligomer can

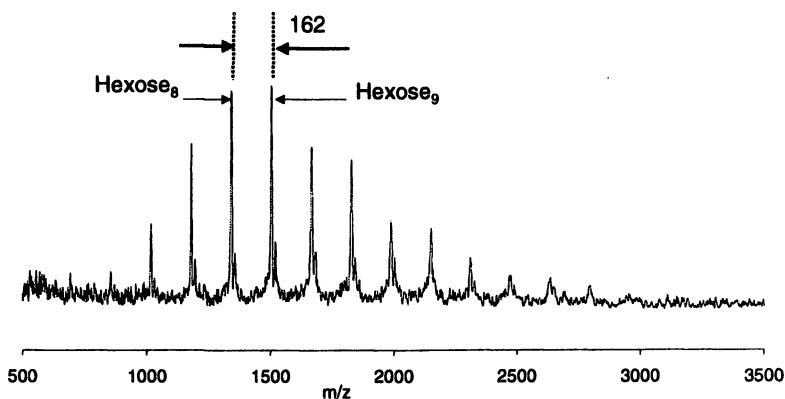


Figure 1. MALDI-MS spectrum (positive-ion mode) of a partly depolymerized alkali-treated spruce glucomannan demonstrating a distribution of well-resolved signals corresponding to oligo- and polysaccharide chains of increasing lengths.

be calculated. In Figure 1, the mass peaks corresponding to hexose₈ and hexose₉ are indicated. The precise sugar composition of each oligomer cannot be derived since the constituent sugars, i.e., glucose, mannose and galactose residues, all have same molar mass (i.e., 162). However, the absolute molar mass, the molar mass distribution and the degree of polymerization (DP) for this glucomannan sample are obtained with a high accuracy from the MALDI-MS spectrum.

Glucomannan present in softwood contains *O*-acetyl substituents at certain of the mannose residues. In Figure 2 (upper spectrum), the MALDI-MS spectrum of a partly depolymerized *O*-acetyl-glucomannan, obtained by hydrothermal treatment of spruce wood, is depicted (7). This spectrum demonstrates a number of partially overlapping series of signals separated by 42 mass units (i.e., the mass of an acetyl group). These signals originate from *O*-acetyl-glucomannans with different numbers of hexose residues and *O*-acetyl groups. The number of hexose residues and *O*-acetyl groups in each oligomer can be calculated from the *m/z* ratio of its MALDI-MS peak. The mass peaks corresponding to hexose₁₄-Ac₃ and hexose₁₄-Ac₄ are indicated in the spectrum. As expected for softwood glucomannan, the signal pattern indicates an irregular distribution of the acetyl groups along the polysaccharide chains. After alkaline hydrolysis, the MALDI-MS spectrum (lower spectrum, Figure 2), contained only a single series of sharp peaks originating from the sodiated molecular ions, [M-Na]⁺, of glucomannan polysaccharide chains. The average degree of substitution (DS~0.3) with acetyl substituents of the *O*-acetyl-glucomannan was determined from the difference in the peak-average mass, *M_p*, values obtained by MALDI-MS prior to and following removal of the *O*-acetyl substituents.

Hardwoods contain small amounts of glucomannans with a glucose-to-mannose ratio 1:1 to 1:2. Galactose substituents can also be present in hardwood glucomannans. We recently reported (7) the MALDI-MS identification of *O*-acetyl moieties present in glucomannan isolated from aspen wood. The MALDI-MS spectra of *O*-acetyl-glucomannans from aspen and birch demonstrate similar pattern of signals as that of the *O*-acetyl-glucomannan from spruce. Figure 3 (upper spectrum), depicts the MALDI-MS spectrum of the *O*-acetyl-glucomannan isolated from birch by extraction with water. The signals in this spectrum, assigned to *O*-acetylated oligosaccharides with increasing numbers of hexose residues, indicate an irregular distribution of the acetyl groups along the polysaccharide. The assignment was supported by the MALDI-MS spectrum of the glucomannan following alkaline deacetylation (lower spectrum, Figure 3). This spectrum demonstrates signals corresponding to the molecular ions, $[M+Na]^+$, of glucomannans with chain lengths ranging up to 18 hexose residues. Also in this case, the degree of substitution with acetyl moieties (DS~0.3) was determined from the MALDI-MS analyses prior to and following deacetylation.

MALDI-MS analysis of glucuronoxylans

The glucuronoxylans are composed of linear chains of β -(1 \rightarrow 4) xylopyranosyl residues branched with α -(1 \rightarrow 2)-linked 4-*O*-methylglucuronopyranosyl residues (4-*O*-MeGlcA). The 4-*O*-MeGlcA-to-xylose ratio is ~1:6 for softwood and ~1:10 for hardwood xylans. *O*-acetyl-(4-*O*-methylglucurono)-xylan is the major hemicellulose present in hardwood, whereas arabino-(4-*O*-methylglucurono)-xylan is present in softwood.

During acidic sulfite cooking of softwood, the β -(1 \rightarrow 3) arabinofuranosyl side-groups are cleaved off from the backbone while some of the 4-*O*-methylglucuronic acid residues remain linked to the xylan chains. The MALDI-MS spectrum of a 4-*O*-methyl-glucuronoxylan, isolated from a softwood sulfite pulp, is depicted in Figure 4 (3,12). The spectrum contains a broad range of well-resolved peaks, which originate from different oligomers with varying sugar compositions. The composition of each oligomer can be derived from the mass associated with its MALDI-MS signal (i.e., the *m/z* ratio), since xylose and 4-*O*-MeGlcA residues have different masses (i.e., 132 and 190, respectively).

This MALDI-MS spectrum is evidently composed of two major, partially overlapping series of mass peaks, in which the distance between adjacent peaks in each series corresponds to 132 mass units (the mass of a xylose residue). The first series contains oligosaccharides with an odd number of 4-*O*-MeGlcA residues linked to the xylan chains (denoted *o* in Figure 4). In contrast, the second series contains oligosaccharides containing an even number of 4-*O*-MeGlcA moieties as substituents on the backbone (denoted *x* in Figure 4).

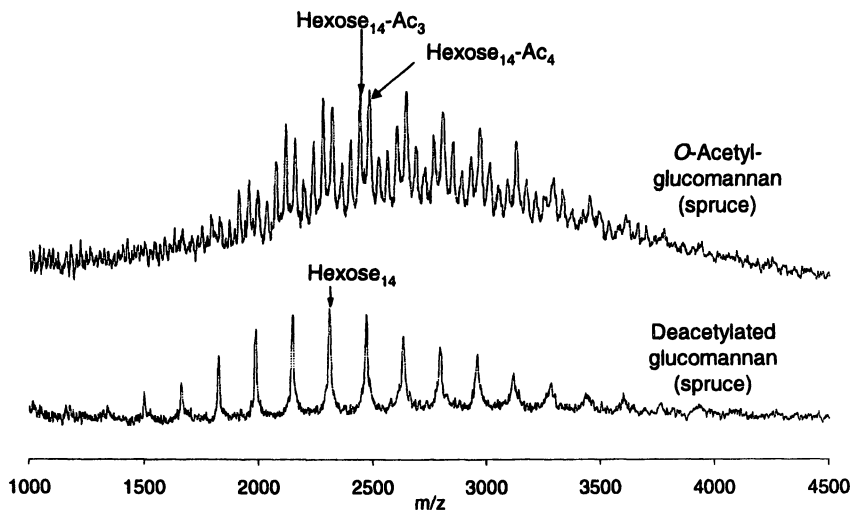


Figure 2. MALDI-MS spectrum (positive-ion mode) of an O-acetyl-glucomannan (upper spectrum) isolated from hydrothermally treated spruce wood. Spectral analysis of the same spruce glucomannan following alkaline hydrolysis (lower spectrum).

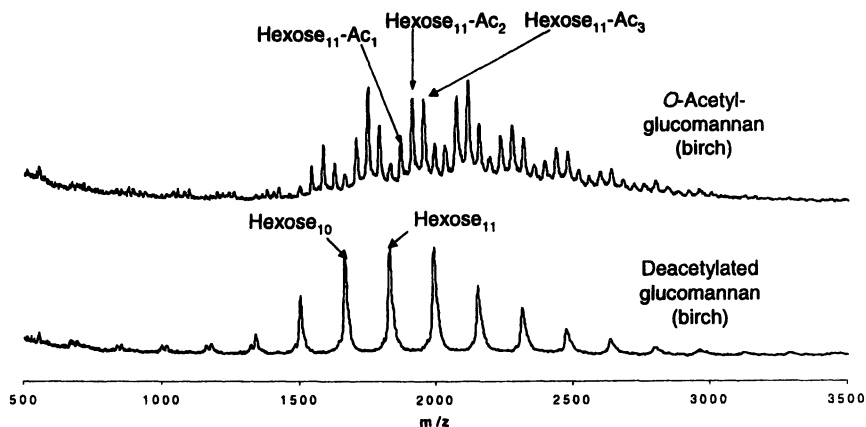


Figure 3. MALDI-MS spectrum (positive-ion mode) of an O-acetyl-glucomannan (upper spectrum) isolated by water extraction from birch wood. Spectral analysis of the same birch glucomannan following alkaline hydrolysis (lower spectrum).

In the case of 4-*O*-methyl-glucuronoxylan from hardwood, which, in addition to 4-*O*-MeGlcA residues, has different numbers of *O*-acetyl groups linked to the polysaccharide backbone, the differences in molar mass between different oligosaccharides chains were often too small to be resolved by the MALDI instrument at our laboratory. The MALDI-MS spectrum of a partly depolymerized xylan isolated from hydrothermally treated aspen wood, is depicted in Figure 5 (upper spectrum) (7). This spectrum contains a distribution of more-or-less poorly resolved mass peaks, but it is possible to observe several signals separated by 42 mass units (i.e., the mass of an acetyl moiety). Hence, these mass peaks originate from *O*-acetyl-(4-*O*-methylglucurono)xylan oligosaccharides with different DP values and numbers of *O*-acetyl substituents.

After deacetylation by alkaline hydrolysis, the MALDI-MS spectrum of the aspen xylan (Figure 5, lower spectrum) revealed that this xylan contained acidic xylooligosaccharides with one or two 4-*O*-MeGlcA substituents (DP 10-28). Thus, the molar mass parameters (i.e., average molar masses) and the degree of polymerization and the degree of acetyl substitution of this xylan could be conveniently determined by this MALDI-MS analysis procedure.

In a recent study (6), the distributions of 4-*O*-MeGlcA residues along the xylan chains of softwood and hardwood xylans were characterized by employing partial acid hydrolysis and subsequent MALDI-MS analysis of the oligosaccharides obtained. The negative-ion MALDI-MS spectrum of the oligosaccharides obtained from a softwood xylan (spruce) after such hydrolysis is presented in Figure 6. The contents of xylose and 4-*O*-MeGlcA in the acidic oligosaccharides present could be calculated without ambiguity on the basis of their molar masses determined by MALDI-MS. Thus, the signals in the spectrum originated from oligo- and polysaccharides containing increasing numbers of xylose residues and from one up to five 4-*O*-MeGlcA substituents.

It is evident from this spectrum (Figure 6) that each series of uronic acid-containing xylosaccharides exhibits a quite limited range of sizes. Thus, the peak patterns revealed by MALDI-MS analysis indicate that the 4-*O*-MeGlcA substituents are distributed periodically along the backbones of the original softwood xylan. If the 4-*O*-MeGlcA residues were randomly distributed instead, the distributions of xylosaccharides containing 4-*O*-MeGlcA substituents would have been considerably broader (as in the case for hardwood xylan in Figure 7).

The positive-ion MALDI mass spectrum obtained for the oligo- and polysaccharides obtained from a hardwood (birch) xylan after mild acid hydrolysis is shown in Figure 7 (upper spectrum). This spectrum consists of several partially over-lapping series of peaks, which were identified on the basis of their exact molar masses as corresponding to neutral xylosaccharides with DP up to 30 and acidic xylosaccharides with one or two 4-*O*-MeGlcA substituents.

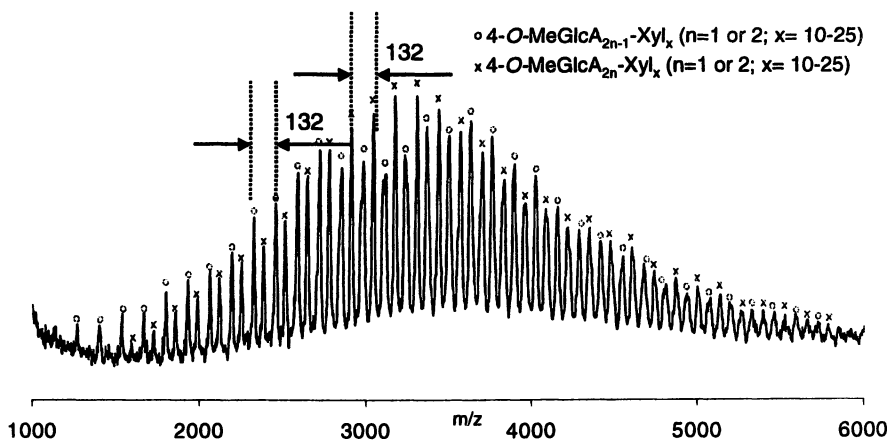


Figure 4. MALDI-MS spectrum (negative-ion mode) of a 4-O-methylglucuronoxylan from a sulfite pulp (spruce). The mass peaks correspond to xylooligosaccharides of increasing lengths containing an odd (o) or even (x) number of 4-O-methylglucuronic acid residues. Reproduced from Reference 3. Copyright 2001 American Chemical Society.

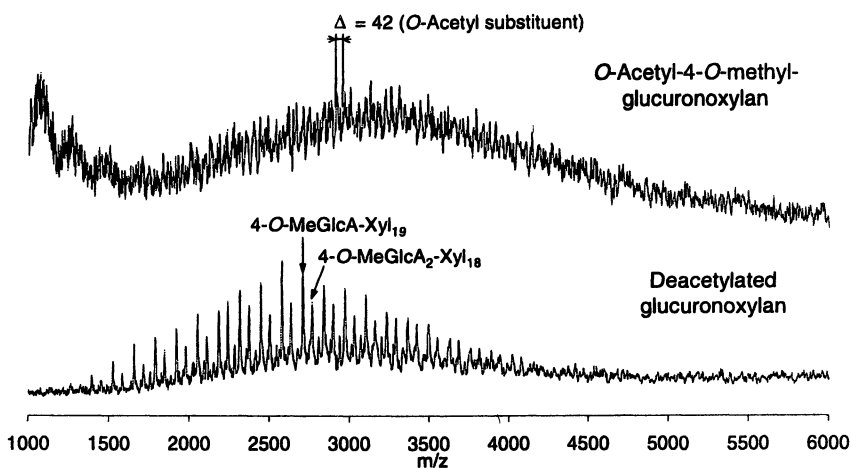


Figure 5. MALDI-MS analysis of O-acetyl-4-O-methylglucuronoxylan obtained from hydrothermally treated aspen (upper spectrum) showing series of weak signals (Δ) separated by 42 mass units (i.e., the mass of an acetyl substituent). Following deacetylation (lower spectrum) acidic xylooligosaccharides with one or two 4-O-methylglucuronic acid residues are detected.

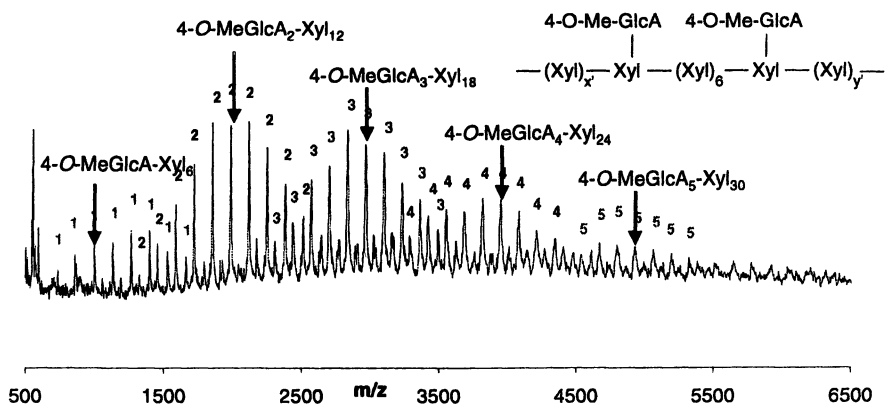


Figure 6. MALDI mass spectrum (negative-ion mode) of the oligosaccharides obtained from a spruce xylan after mild acid hydrolysis. Reproduced from Reference 6. Copyright 2001 American Chemical Society.

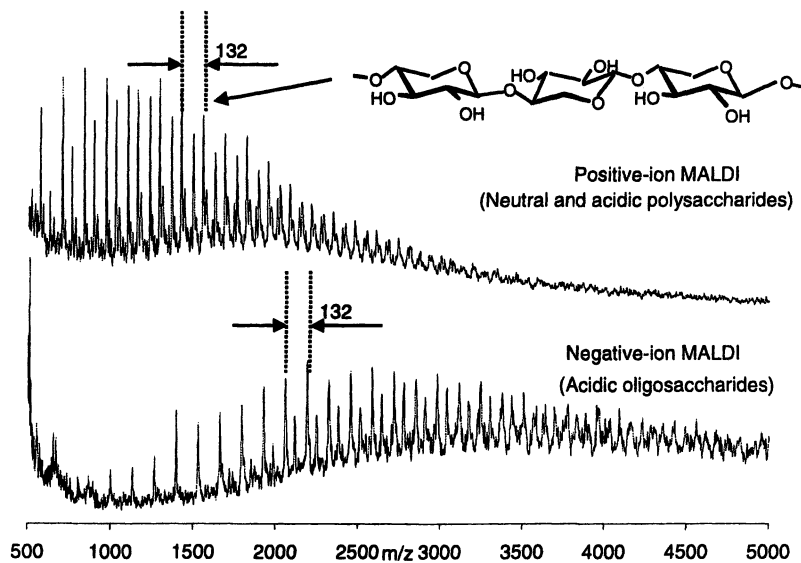
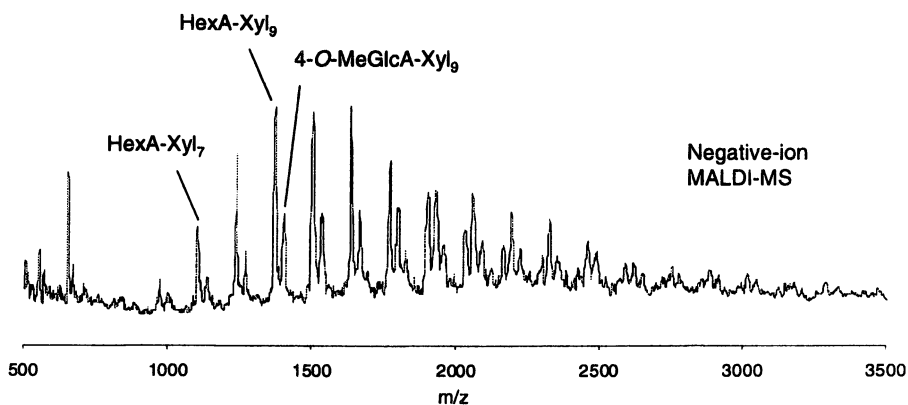


Figure 7. Positive- (upper) and negative- (lower) ion MALDI mass spectra of the oligosaccharides obtained from birch wood xylan by mild acid hydrolysis. In positive ion mode, both neutral and acidic oligosaccharides are detected, whereas acidic oligosaccharides only are detected by negative-ion MALDI-MS. Reproduced from Reference 6. Copyright 2001 American Chemical Society.

The lower spectrum in Figure 7 depicts the corresponding negative-ion MALDI-MS for the oligosaccharides in the hydrolysate obtained from the birch wood xylan. In MALDI-MS, only the oligo- and polysaccharides containing acidic groups generate negative ions. Consequently, this spectrum contains two broad series of peaks corresponding to acidic xylosaccharides of increasing chain-length and with one or two 4-*O*-MeGlcA residues. Altogether, these MALDI spectra indicate that the 4-*O*-methylglucuronic acid residues are distributed irregularly along the backbones of hardwood xylans.

MALDI-MS analysis of hexenuronoxylans

Under alkaline cooking conditions some of the 4-*O*-MeGlcA residues present in hardwood and softwood xylans are converted into unsaturated hexenuronic acid residues (HexA) by β -elimination of methanol. In an early study (4) employing MALDI-MS, we were able to identify a number of different HexA and 4-*O*-MeGlcA containing xylooligosaccharides in the hydrolysate obtained after endoxylanase treatment of an unbleached hardwood kraft pulp.



*Figure 8. MALDI mass spectrum (negative-ion mode) of the acidic xylooligosaccharides obtained by endoxylanase treatment of a hexenuronoxylan isolated from alkaline peroxide bleached hardwood kraft pulp. The spectrum consists of two series of peaks assigned to the molecular ions $[M-H]^-$ of xylooligosaccharides with varying chain lengths and containing one hexenuronic acid (HexA) residue or one 4-*O*-methylglucuronic acid (4-*O*-MeGlcA) residue.*

Figure 8 depicts the negative-ion MALDI-MS spectrum of a partly depolymerized enzymatically (endoxylanase) treated hexenuronoxylan, originating from an oxygen delignified and alkaline peroxide bleached hardwood kraft pulp. This MALDI-MS spectrum demonstrates a broad distribution of mass peaks, which originates from HexA and 4-*O*-MeGlcA containing xylo-oligosaccharides. The composition of each oligosaccharide can be derived from its MALDI-MS peak, since xylose, HexA and 4-*O*-MeGlcA residues all have different molar masses (i.e., 132, 158 and 190, respectively). The MALDI-MS spectrum is evidently composed of two partially overlapping series of signals, in which the distance between adjacent signals in each series corresponds to one xylose residue. The first series originates from oligosaccharides with one HexA residue linked to the xylan backbone. The second series corresponds to oligosaccharides containing one 4-*O*-MeGlcA residue on the backbone. Furthermore, in the high mass part of the spectrum several oligosaccharides containing both HexA and 4-*O*-MeGlcA residues, can be detected.

SEC/MALDI-MS analysis of hemicelluloses

It has been reported that in the case of mixtures of polymers exhibiting a wide range of molar masses, MALDI-MS may yield somewhat inaccurate values for the average molar mass, due to discrimination of signal from the larger polymers (8). However, this problem can be minimized or eliminated simply by separating the polymer mixture into fractions each containing components within a relatively narrow size range by SEC prior to MALDI-MS analysis (so-called SEC/MALDI-MS) (3,7,8).

Figure 9 depicts a schematic representation of the analytical procedure developed by us to characterize the absolute molar mass parameters of hemicelluloses derived from wood and pulp. In this procedure, SEC separates the hemicellulose into fractions each containing components with a narrow range of molar masses and the accurate peak-average molar mass (M_p) of each fraction is subsequently determined by MALDI-MS. The molar mass parameters for the hemicelluloses are then calculated on basis of the SEC distribution curve and utilizing the MALDI-MS calibrated mass scale.

In the case of water-soluble *O*-acetylated xylans and glucomannans, an ammonium acetate solution with a pH of 7 was employed as eluent in connection with the SEC separation step (7). However, for alkali extracted xylans and glucomannans, a more alkaline (pH 13) sodium hydroxide/acetate eluent was required (3). In all cases pretreatment of the SEC fractions by passage through a cation-exchange resin prior to MALDI-MS analysis and/or the use of MALDI probes coated with a Nafion film (2), were necessary in order to minimize the disturbance by buffer ions during the MALDI analysis step.

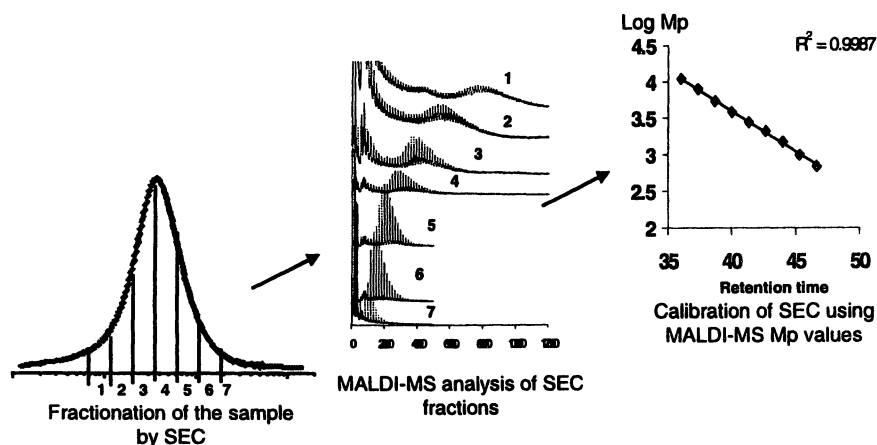


Figure 9. Schematic representation of the analytical procedure employed to characterize the molar mass parameters for hemicelluloses. SEC separates the hemicellulose into fractions with a narrow range of molar masses, the absolute molar mass (M_p) of each fraction is determined by MALDI-MS and, finally, the molar mass parameters for the entire hemicellulose are calculated from the SEC distribution curve using the MALDI-MS calibrated mass scale.

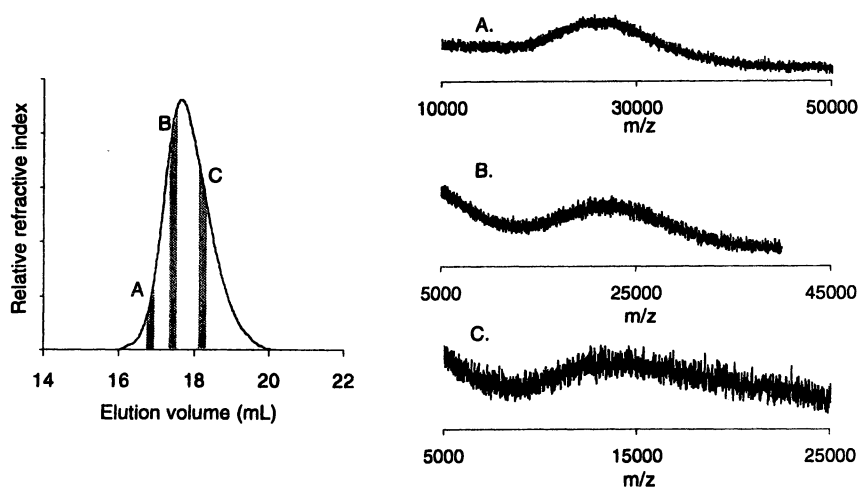
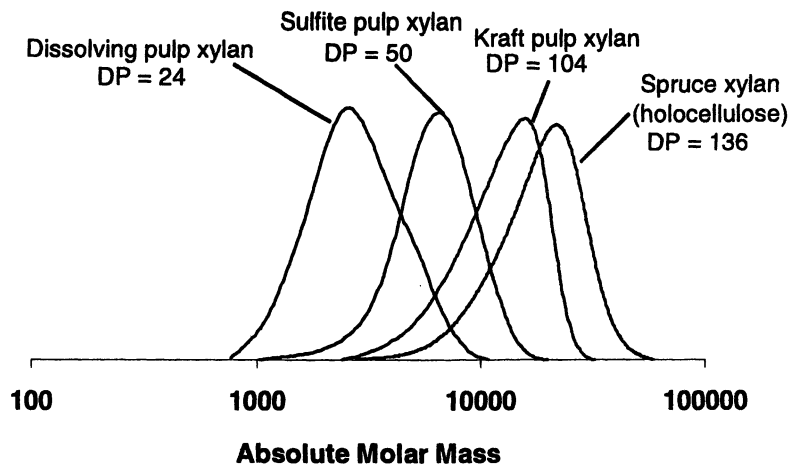


Figure 10. SEC chromatogram and MALDI-MS spectra of three sequential fractions (a, b and c; shaded) obtained with an arabino-4-O-methylglucuronoxylan from spruce wood. Reproduced from Reference 3. Copyright 2001 American Chemical Society.



*Figure 11. The SEC molar mass distribution curves for arabino-4-*O*-methylglucuronoxylan (from spruce holocellulose), arabinohexenuronoxylan (kraft pulp) and two different 4-*O*-methylglucuronoxylans (sulfite and dissolving pulp) obtained by the SEC/MALDI-MS procedure. Each xylan was analyzed separately employing the alkaline (pH 13) buffer SEC system and subsequently graphed on the same MALDI-MS calibrated absolute molar mass scale.*

Figure 10 illustrates fractionation of an arabino-4-*O*-methylglucuronoxylan by SEC and the subsequent MALDI-MS analysis of three of the fractions obtained. These fractions gave rise to relatively symmetric distributions of MALDI signals up to a m/z value of at least 35 000. However, no signals originating from individual polysaccharide constituents can be resolved in this case. These MALDI-MS spectra are nonetheless of sufficiently high quality to provide reliable values for the peak-average molar mass (M_p). Subsequently, the logarithms of the M_p values determined by MALDI-MS were used together with the SEC distribution curve to obtain the average molar mass values and the polydispersity index for this xylan from spruce (3).

The SEC distribution curves and the degree of polymerization (DP) values for four different softwood xylans, determined by this SEC/MALDI-MS procedure with the sodium hydroxide/acetate (pH 13) eluent system are documented in Figure 11. As can be seen from this figure, the arabino-4-*O*-methylglucuronoxylan extracted from the spruce holocellulose demonstrates a higher DP than does the arabinohexenuronoxylan extracted from the softwood kraft pulp. The 4-*O*-methylglucuronoxylan extracted from the sulfite pulp exhibited a much lower DP, which is as expected, since sulfite cooking under acidic conditions depolymerizes xylans more extensively than under alkaline kraft cooking conditions. The degree of polymerization of the dissolving pulp 4-*O*-methylglucuronoxylan, which had been subjected to prolonged acidic sulfite cooking conditions, was considerably lower than the corresponding values for all the other xylans investigated (3).

Concluding remarks

The new MALDI-MS based analytical procedures described in this chapter have been employed successfully for; (i) determining the accurate molar mass and molar mass distribution for different types of xylans and glucomannans, (ii) characterizing the distribution of uronic acid residues in hard- and softwood xylans and (iii) determining the content and distribution of *O*-acetyl substituents in xylans and glucomannans.

The MALDI-MS procedures described here, which were developed for wood and pulp hemicelluloses, should also be suitable for characterizing hemicelluloses isolated from annual plant materials and such studies are currently being carried out in our laboratory.

Experimental

The MALDI analyses were performed using a Hewlett-Packard G2025 A MALDI-TOF mass spectrometer equipped with a linear detector, employing 1-5 μJ energy pulses of the UV (337 nm) laser beam. The mesa surface of the MALDI probes employed was coated with a Nafion perfluorosulfonated ionomer film (2) prior to application of the hemicellulose sample and the matrix 2,5-dihydroxybenzoic acid (DHB). A saturated, aqueous solution of the matrix DHB was added to the sample and approximately 0.5 μL of the sample/matrix mixture was applied to the MALDI probe. In the case of SEC fractions containing the sodium hydroxide/acetate eluent, pretreatment with a cation-exchange resin (NH_4^+ -form) was performed prior to mixing with the matrix solution. Both positive- and negative-ion spectra were obtained. The peak-average molar mass (M_p) of the sample was determined as the molar mass at the maximal peak intensity in the MALDI-MS spectrum.

The SEC system consisted of three columns containing Ultrahydrogel 120, 250 and 500 (Waters Assoc. USA) linked in series with each other and with an instrument for measuring the refractive index of the eluate (Waters Assoc. USA). Two different mobile phases were employed, i.e., 0.05 M ammonium acetate, pH 7 for *O*-acetylated hemicelluloses and sodium hydroxide/acetate (0.2 M hydroxide and 0.1 M acetate) pH 13 for non-acetylated hemicelluloses. The hemicelluloses were dissolved in the eluting solution to obtain final concentrations of 0.2 - 1 % (w/v). All solutions were filtered through syringe filters with 0.45 μm pores prior to injection into the SEC column system. 100 μL samples were injected into the SEC system and 0.13 mL fractions containing components with a narrow range of molar masses were collected from the outlet of the refractometer. The peak-average molar mass (M_p) values of the fractions were determined by MALDI-MS analysis. For each fraction, the logarithm of the

Mp value determined by MALDI-MS was graphed as a function of the time required for elution from the SEC system. The linear relationship between log Mp and elution time was subsequently employed to determine the number and weight-average molar masses (Mn and Mw) of the entire hemicellulose sample. In this manner the weight- and number-average molar masses (Mw and Mn) for various types of xylans and glucomannans could be obtained employing SEC and MALDI-MS.

Acknowledgements

Financial support from VINNOVA and Jacob Wallenbergs Research Foundation are gratefully acknowledged.

References

1. Dahlman, O.; Rydlund, A.; Lindquist, A. *The European conference on pulp and paper research. The present and the future. October 9-11, 1996*; Arabatzis, A., Eriksson, L., Seoane, I., Eds.; The European Commission: Brussels, **1997**; pp 231-237.
2. Jacobs, A.; Dahlman, O. *Anal. Chem.* **2001**, *73*, 405.
3. Jacobs, A.; Dahlman, O. *Biomacromolecules* **2001**, *2*, 894.
4. Rydlund, A.; Dahlman, O. *Carbohydr. Res.* **1997**, *300*, 95.
5. Lindquist, A.; Dahlman, O. *Adv. Lignocellul. Chem. Ecol. Friendly Pulping Bleaching Technol., 5th Eur. Workshop Lignocellul. Pulp.* University of Aveiro, Aveiro, Port., 1998; p 483.
6. Jacobs, A.; Larsson, P. T.; Dahlman, O. *Biomacromolecules* **2001**, *2*, 979.
7. Jacobs, A.; Lundqvist, J.; Stålbrand, H.; Tjerneld, F.; Dahlman, O. *Carbohydrate Res.* **2002**, *337*, 711
8. Jacobs, A.; Dahlman, O. *Nord. Pulp Pap. Res. J.* **2000**, *15*, 120.
9. Karas, M.; Hillenkamp, F. *Anal. Chem.* **1988**, *60*, 2299.
10. Hillenkamp, F.; Karas, M. *Int. J. Mass Spectrom.* **2000**, *200*, 71.
11. Hillenkamp, F. *Adv. Mass Spectrom* **1995**, *13*, 95.
12. Dahlman, O.; Rydlund, A.; Lindquist, A. *The 9th international symposium on wood and pulp chemistry*: CPPA, Montreal, Canada, **1997**; Vol. 1, pp L5-1-L5-4.

Chapter 7

Characterization of Alkali-Soluble Hemicelluloses of Hardwood Dissolving Pulps

Ursula Mais¹ and Herbert Sixta^{2,*}

¹Competence Center Wood, Werkstrasse 1, A-4860 Lenzing, Austria

²R & D, Lenzing AG, Werkstrasse 1, A-4860 Lenzing, Austria

In the first step of the viscose process, pulp is steeped in aqueous sodium hydroxide of about 18% at temperatures up to 50 °C removing alkali-soluble carbohydrates. After pressing off the cellulose, which is converted to its alkoxide, the so-called press lye is enriched with undesirable short chain material which is removed by membrane separation processes. A more profound knowledge of the fractions is necessary to improve the separation system and to possibly use them as source for new products. Here, hemicellulose fractions of two pulps extracted at different sodium hydroxide concentrations and fractions obtained from press lye have been characterized with respect to macromolecular properties, functionalities and carbohydrate composition. The results show that the properties of alkali-soluble hemicelluloses depend on the pulp origin and the steeping conditions. The molecular mass and molecular weight distribution were determined and detailed carbohydrate analysis revealed both the building units of the heteropolysaccharides and the amount of fragmentation products. Effort has also been undertaken to elucidate the presence of side chains in the high molecular weight fraction.

Introduction

Hemicelluloses are important cell wall components being associated with cellulose microfibrils and the lignin matrix. In hardwoods they constitute almost one third of the total organic material present with O-acetyl-(4-O-methylglucurono)xylan as the major component.

The chemistry of hemicelluloses is currently undergoing a surge of interest as hemicelluloses are promising starting materials for the production of a variety of valuable chemical products both under destruction and preservation of the polymeric structure (1,2).

During acid sulphite cooking for dissolving pulp production, hardwood xylan is hydrolyzed into acetic acid on the one hand, and monomer xylose on the other. Part of the xylose is oxidized to xylonic acid by bisulphite ions as oxidizing agent. Therefore the yield of xylonic acid strongly depends on the ratio of combined (HSO_3^-) to free, hydrated sulphur dioxide ($\text{SO}_2 \cdot \text{H}_2\text{O}$). Depending on both the acidity of the cooking acid and the temperature, xylose is further dehydrated to furfural. In the final cooking phase furfural can polymerize, with its precursors and degraded lignin moieties giving rise to condensation products (3,4). In a typical acid sulphite cook using beechwood as a raw material, 40-45% of the wood's xylose (in xylan) is converted to monomeric xylose, 10-12% to xylonic acid (as xylose), 6-8% to furfural (as xylose) and 28-30% to unspecific condensation products (as xylose) (5). The residual 10-12% are preserved as polymeric xylan in the unbleached pulp. To meet the specifications for viscose pulp, hemicelluloses have to be further decreased in the course of a hot caustic extraction stage prior to bleaching. Finally, a fully bleached beech sulphite dissolving pulp typically contains 6-7% of the xylan present in the wood.

In commercial practice of viscose fibre production, pulp is steeped in aqueous sodium hydroxide of about 18% concentration at temperatures up to more than 50°C to form alkali cellulose after pressing off the slurry. During steeping, alkali-soluble hemicelluloses are largely removed, the extent of removal depending on the R18 of the pulp (13), on the process conditions and on the equilibrium hemicellulose level established in the recycled steeping liquor. Approximately 1-1.5% of the xylose present in beechwood remains alkali-resistant and stays with the final product. Due to economic reasons, steeping is a closed loop operation, which in turn results in hemicellulose accumulation. When exceeding a certain concentration, hemicelluloses have to be removed from the press lye system, which presently can only be achieved by means of dialysis. The dialysis system, however, has the disadvantage of rather low separation efficiency, the dilution of the treated sodium hydroxide solution with water, and rather poor specific performance of the membrane (6).

Also the steeping liquor is discussed as a potential source of new products based on xylans, xylooligosaccharides, xylose and different xylose degradation

products. The isolation of new products from the steeping lye as well as the potential use of unrefined and thus cheaper pulp as a raw material in the viscose process are certainly driving forces for the development of appropriate, new pressure-driven membrane separation processes (7).

A deeper knowledge of the chemical composition and macromolecular properties of the alkali-soluble hemicellulose fraction is a prerequisite to both the development of a new process technology, and characterization of product properties. As the amount of hemicellulose fraction removed is proportional to the R18 values for pulps, experiments were carried out based on the alkali-insoluble R- and alkali-soluble S-fractions for comparative studies.

Only a few attempts have been made so far to determine the molecular weight properties of hemicellulose fractions from viscose-grade pulps isolated at the mercerization stage (8,9). The viscosity- and weight-average molecular weight (MW) values were determined to range between 5.000 and 10.000 g/mol and were thus significantly lower as compared to the hemicelluloses directly isolated from wood and annual plants, due to more severe degradation reactions during cooking and bleaching (10).

Recently, we have employed a variety of analytical approaches to determine the chemical composition and the molecular weight distribution (MWD) of alkali-soluble pulp fractions (11). Size-exclusion chromatography (SEC) revealed a bimodal molecular weight distribution reflecting the low-molecular-weight gamma- and the higher-molecular-weight beta-cellulose fractions. Dynamic light scattering experiments confirmed a negligible amount of aggregates asserting that MWD determination was not impaired. Both carbohydrate and HPAEC-PAD measurements demonstrated a significantly higher degree of fragmentation products in the press lye as compared to the S18-fraction. Two thirds of the hemicelluloses in the press lye (46% in S18) were attributed to the gamma-fraction, with a carbohydrate content of only 33% (88% in S18). Surprisingly, the latter also contained rather high-molecular weight-material which has an important impact on the development of new membrane separation processes.

The aim of the present study was to investigate the structural composition of the hemicellulose fractions, e.g. the presence of uronic acid side chains by means of MALDI-MS analysis, FT-IR- and solid-state NMR-spectroscopy. For comparison also a softwood-derived starting material was used.

Experimental Part

Materials. TCF-bleached beech Mg-sulphite dissolving pulp (BS), with 93.8% R18, 2.9% pentosan, and 1.7 copper number, and Eucalypt prehydrolysis kraft pulp (EK), with 96.6% R18, 3.6% pentosan and 0.2 copper number, were

extracted according to the sample preparation methods described below. Press lye was obtained from a commercial steeping lye system, supplied by Lenzing AG. For comparison, unbleached hemicellulose fraction (beta-cellulose) isolated from the steeping lye by Lenzing AG contained 78% of xylan with 79.8% pentosan. All commercial reagents used were of analytical grade (12).

Isolation of hemicellulose fractions. A standard method for R/S-fraction determination (13) was adapted and conducted as follows: Pulp samples were swollen for 2 min in aqueous sodium hydroxide solution (10 or 18%), then pulped for 3 min and incubated for 60 min at 20 °C. Next, the slurry was separated by filtration into the alkali-insoluble R-fraction and the alkali-soluble S-fraction. For quantitative separation of the beta-cellulose, fractionation was done by precipitation with sulphuric acid and subsequent centrifugation, gamma-cellulose remained in the filtrate.

Carbohydrate analysis. Anion-exchange chromatography (AEC) with pulsed amperometric detection (PAD) was applied directly (for monomers) or after total hydrolysis (TH) with H₂SO₄ (for polymers) as described in (11).

Carboxyl group determination. A solution of methylene blue was added to the fraction and the amount of bound methylene blue was measured photometrically at 665 nm (14).

Size-exclusion chromatography (SEC). The SEC system consisted of two 2 MCX, 1000 Å, 300*8 mm (PSS) columns with refractive index and UV (262 nm) detection at a flow rate of 0.5 M NaOH of 1 mL/min. Calibration was carried out with a set of cello-oligomers and pullulan standards (11). The R-fractions were determined by SEC according to (15) in 0.9% LiCl/DMAc as eluent, employing pullulan standards for calibration.

FT-IR spectroscopy. FT-IR spectra were recorded on a Bruker IFS 66 spectrometer in a transmission mode using KBr pellets. This method is based on WAXS and NMR-techniques as reference measurement. Crystallinity and amount of cellulose I/II were determined as described earlier (16).

Solid-state NMR spectroscopy (¹³C CP/MAS NMR). The ¹³C CP/MAS NMR measurements were performed on a 400 MHz Bruker DSX-Spectrometer with a 4 mm probe head at a MAS-frequency of 12.5 kHz and 256 scans. Initially the experiments were conducted at cross polarization time of 1 ms and repeating times of 2 s and 10 s to determine different T1-times in the proton domain.

MALDI-TOF-MS. MALDI-TOF mass spectra were obtained using a Dynamo system from Thermo Bioanalysis with 2,5-dihydroxybenzoic acid as the matrix. Spectra were recorded in the positive ion mode with an average of 50 shots.

Methylation of hemicellulose fractions. Methylation of the beta-cellulose fractions and xylan was carried out according to (17,18).

Results and Discussion

Carbohydrate composition

Hemicelluloses extracted from a hardwood and softwood source, namely beech wood sulphite pulp (BS) (19) and Eucalyptus prehydrolysis kraft pulp (EK) (20) respectively, were characterized and the results were compared to the press lye obtained from the viscose process. Table I contains the standard specification of the starting materials. The characteristic data of press lye (PL) are summarized in Table II.

Table I. Standard specification of starting materials

<i>Parameter</i>	<i>Unit</i>	<i>BS</i>	<i>EK</i>
Kappa number		0.36	0.37
Brightness	% ISO	91.2	89.0
Viscosity	mL/g	565	447
R18	%	93.8	96.6
R10	%	88.1	93.3
Glucan	%	93.7	93.9
Xylan	%	3.00	3.7
Mannan	%	1.00	0.4
Copper number	%	1.51	0.21
Carboxylic groups	mmol/kg	24.4	30.8
DCM extractives	%	0.18	0.26
GPC-data Mw	kg/mol	219.5	135.8
Mw/Mn		8.13	3.13

For better evaluation the hemicellulose fractions were extracted using a sodium hydroxide concentration of 18 and 10% which corresponded to the R18 and R10 values of pulp tests (13). After separation of the alkali-soluble S-fraction and the alkali-insoluble R-fraction the carbohydrate compositions were determined by anion exchange chromatography. The data are presented in Table III.

The differences between the fractions of press lye and the S-fractions are clearly visible. Two thirds of press lye consisted of the gamma-cellulose-

Table II. Characteristic data of press lye (PL)

<i>Parameter</i>	<i>Unit</i>	<i>PL</i>
Density (20 °C)	g/ml	1.2
Total alkali	%	16.7
Total alkali	g/l	201.5
Sodium carbonate	%	0.47
Sodium carbonate	g/l	5.7
Sodium hydroxide	%	16.4
Sodium hydroxide	g/l	197.2
Total Hemicellulose	g/l	36.2
Gamma-Cellulose	g/l	24.4
Beta-Cellulose	g/l	11.8

Table III. Carbohydrate composition of R- and S-fractions

[% dry substance]	<i>BS</i>				<i>EK</i>				<i>PL</i>
	<i>S18</i>	<i>R18</i>	<i>S10</i>	<i>R10</i>	<i>S18</i>	<i>R18</i>	<i>S10</i>	<i>R10</i>	
β-fraction	53.7		91.2		80.0		97.3		32
Glucan	53.7	95.3	80.0	95.8	23.7	93.4	59.9	94.0	2.6
Xylan	42.6	0.7	17.7	0.7	69.4	2.1	34.7	1.4	91.6
Mannan	2.0	0.0	2.2	0.0	0.6	0.0	0.9	0.0	0.0
Sugar in β	98.3		99.9		93.7		95.5		94.2
γ-fraction	46.3		8.8		20.0		2.7		68
Glucan	17.6		2.0		10.4		0.0		6.9
Xylan	45.8		57.0		54.6		69.4		17.9
Mannan	24.8		15.8		13.4		0.0		8.4
Sugar in γ	88.2		74.8		78.4		69.4		33.2
Total sugar	93.6	96.0	97.7	96.5	90.6	95.5	94.8	95.4	52.7

fraction, whereas the S-fractions from pulp are mainly beta-cellulose. From the original pentosan content of 3% and 3.7% for BS and EK, respectively, more hemicelluloses (percentage of xylan, mannan) could be extracted from BS than from EK. Beta-hemicellulose appeared to be the dominant fraction extracted with 10% sodium hydroxide for both substrates, but contained a rather high amount of glucan (80% and 60% for BS and EK, respectively) and hence a low amount of xylan. The difference between the pulps was more significant in the S18-fractions: here, half of the S-fraction of BS was attributed to beta-cellulose, whereas in EK still 80% was isolated as the high molecular fraction. Concerning

the carbohydrates present in the beta-cellulose of S18-fractions, the amount of xylan increased significantly compared to S10-fractions, and in press lye almost only xylan was found as intact carbohydrate. On the other hand, in gamma-fractions a decrease in xylan content was observed in the following order: S10-EK > S10-BS ~ S18-EK > S18-BS >> press lye. It is also obvious that in the alkali-soluble S-fractions the total amount of carbohydrates was relatively high (90-98%), in contrast, only half of the press lye could be attributed to intact sugar components. There, due to this low total sugar content, a strong formation of non-monosaccharide portion was assumed. However, no further characterization of these components was attempted so far.

Carboxyl group determination

Relatively low amounts of COOH-groups were present in the alkali-insoluble fraction as these groups should be found linked to xylan (Table IV).

Table IV. Carboxyl group content in R- and beta-fractions

<i>Sample</i>	<i>COOH [$\mu\text{mol/g}$]</i>	<i>COOH [weight %]</i>	<i>Ratio β:R</i>
BS-R18	15.4	0.07	
BS- β -S18	157	0.7	10:1
BS-R10	14.4	0.07	
BS- β -S10	113	0.51	8:1
EK-R18	22.1	0.1	
EK- β -S18	221	0.99	10:1
EK-R10	19.3	0.09	
EK- β -S10	161	0.73	8.4:1
PL	315	-¹	-¹

¹ calculation was not possible

The ratio of COOH in beta:R-fractions was about 8:1 for S10 to 10:1 for S18. It appeared that more COOH-groups were detected in EK, but with respect to the amount of xylan in the S-fractions the COOH-value was higher in extracted BS samples. The amount of COOH-groups found in PL was in the range of the BS-S18-beta-fraction.

Molecular weight distribution

Molecular weight distribution of all fractions is summarized in Table V.

Table V. Molecular weight determination of hemicellulose fractions

	<i>BS-20°C-18</i>			<i>BS-20°C-10</i>			<i>BS-50°C-18</i>		
	<i>S</i>	β	γ	<i>S</i>	β	γ	<i>S</i>	β	γ
MWD	6.7	9.9	3.7	16.6	10.1	3.9	7.9	12.2	5.1
PDI	2.2	1.8	1.8	4.4	1.8	1.6	1.9	1.4	1.9

	<i>EK-20°C-18</i>			<i>EK-20°C-10</i>			<i>PL</i>		
	<i>S</i>	β	γ	<i>S</i>	β	γ	<i>S</i>	β	γ
MWD	13.9	13.2	4.3	25	14.7	3.2	9.1	12.8	4.4
PDI	2.4	1.6	1.9	2.4	1.6	1.9	1.8	1.4	1.5

values in [kg/mol]

Acid sulphite cooking depolymerized xylan more extensively than kraft cooking. Also the treatment with a higher concentrated sodium hydroxide solution resulted in increased degradation. A fraction was also extracted at elevated temperature and gave a better approximation of the press lysate data. In Figure 1, a typical molecular weight distribution of the beta and gamma-cellulose fraction of press lysate is depicted.

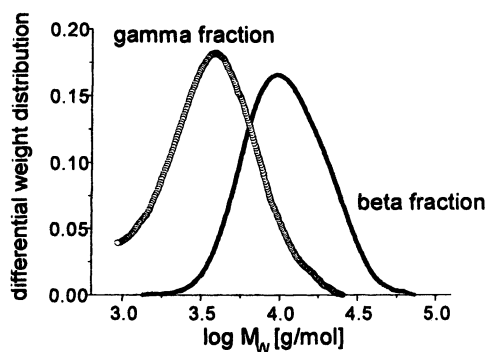


Figure 1. Typical molecular weight distribution for PL (beta- and gamma-fraction)

The low-molecular part of the gamma-fraction could not be evaluated because of the interfering salt peak. After separation into the alkali-soluble and alkali-insoluble fraction an overlapping of the molecular weight fractions was detected showing that parts of the same molecular weight are both acid soluble and insoluble.

MALDI-TOF-MS

Another technique suitable for providing more information about the presence of substituents in oligosaccharides is MALDI-TOF-MS. The advantages of MALDI-TOF-MS include its ability of mass measurements of extremely large biomolecules (>500 kDa) with a high degree of precision and sensitivity (21,22). Furthermore, sample preparation is relatively easy, only single-charged ions are generated with negligible fragmentation of the molecules, and results are obtained quite fast (21-23). However, limitations occur regarding the quantitative determination of the molecular weights if the polymer consists of a mixture with a wide molar range (21). Some investigations have already been done concerning the determination of the molecular weight of hemicelluloses from various pulps. Size-exclusion chromatography was applied prior to MALDI to fractionate the samples (24-26). Also the distribution of 4-*O*-methylglucuronic acid residues along the chain was studied, and it was found that the residues are irregularly distributed along the polymer chain using hardwood as substrate (25). Also the combination of HPAEC with MALDI-TOF-MS was investigated to identify the nature of unknown oligosaccharides (21,27). There, an on-line desalting step and automated handling of the fractions made peak identification relatively easy (21,27).

In this study, MALDI-TOF-MS was employed to determine the structure and amount of side chains as the presence of uronic acid is known to have effects on the molecular properties of xylan (25). The MALDI-TOF-MS spectrum of an acid-insoluble hemicellulose fraction isolated from the press lye, which was methylated (17,18) prior to measurement, is shown in Figure 2.

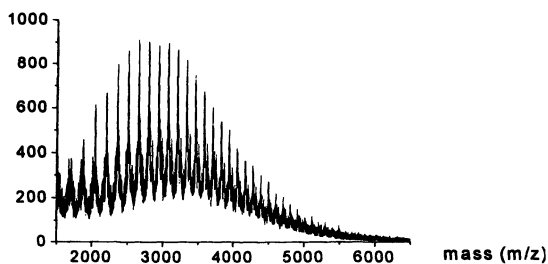


Figure 2. MALDI-TOF-MS spectrum of PL

The spectrum exhibits a broad distribution with maximum intensity at 2950 mass units (m/z). The distance between the peaks was 160 which is one unit of a completely methylated xylose. Complete methylation of the sample was also confirmed by FT-IR (28). The maximum mass peak therefore corresponded to one 4-*O*-methylglucuronic (4OMeGlcA) residue linked to the xylo-oligomer backbone with a DP of 17. Two series of oligosaccharides were found with

either one or two 4OMeGlcA residues bound to the xylan backbone with the increasing chain length corresponding to a composition of 4OMeGlcA₁(Xyl)₁₂₋₃₀ and 4OMeGlcA₂(Xyl)₁₅₋₂₆, respectively. So MALDI-TOF-MS analysis confirmed the presence of 4OMeGlcA side chains, and the ratio of 4OMeGlcA to xylose was calculated to be about 5:100. This result was in agreement to the carboxyl group determination, assuming the 4OMeGlcA residue as source of the COOH-groups. It is particularly pointed out that the average molecular weight determined by MALDI analysis can deviate from that of other determination methods if a polymer mixture is present. Deviations of the molecular weights obtained from SEC and MALDI analysis could partly be attributed to the standard calibration used in the SEC and also to the fractionation that could have occurred during methylation and subsequent extraction.

Structural characterization by FT-IR spectroscopy

FT-IR spectroscopy proved to be an adequate method for the qualitative and quantitative analysis of lignocellulosics (29-32). In Figure 3, typical deconvoluted spectra of BS, BS-S18-beta-fraction and PL-beta-fraction are given.

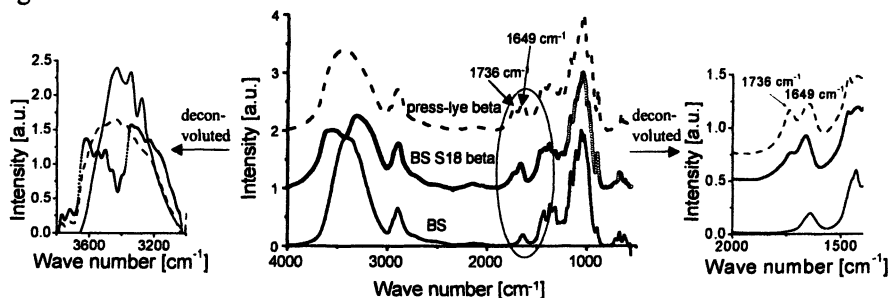


Figure 3. FT-IR spectra of BS, BS-S18-beta-fraction and PL-beta-fraction

The carboxyl bands at 1736 cm^{-1} can clearly be seen in the xylan-containing S-fractions (33). Also the range of OH-resonances showed the characteristic differences for xylan and cellulose. An estimation of the crystallinity in the R-fractions was possible as well as a rough evaluation of the ratio of Cellulose I and II in R10-fractions (see Table VI)(16,30,34-36).

This method is calibrated for cellulose I/II ratio comparing the bands at 1370 and 670 cm^{-1} . The starting materials consisted of cellulose I with a crystalline fraction of 45.3% and 51% for BS and EK, respectively. In the R18-fractions the conversion of cellulose I into cellulose II was already completed, whereas with 10% NaOH parts of cellulose I still remained. The crystallinity decreased to 44% and 47%, respectively.

Table VI. Percentage of cellulose modifications present and degree of crystallinity (italics in parenthesis) in samples obtained from IR- and NMR-analysis

<i>Sample</i>	<i>IR</i>			<i>NMR</i>
	<i>Cellulose I</i>	<i>Cellulose II</i>	<i>Crystallinity</i>	<i>Cellulose I</i>
BS	100%	-	45.3	-
BS-R10	41% (18%)	59% (2.6%)	44	17.4%
BS-R18		100%	44.9	
EK	100%		50.8	
EK-R10	79% (37.1%)	21% (9.9%)	47	37.9%
EK-R18			47	

Structural characterization by solid-state NMR spectroscopy

The structural composition of the fractions was also examined by solid-state NMR spectroscopy which has already been applied extensively for cellulose, cellulose derivatives and xylan (37-42). For example, determination of the crystallinity of pulps was achieved, and it was found that the amount of hemicelluloses in sulphite pulp was higher than in kraft pulp because of the more intensive resonances present in amorphous region where also hemicellulose resonances can be monitored (43). Spectra of alkali-insoluble and alkali-soluble products were compared with a spectrum recorded from press lye (Figure 4). The spectrum of press lye gave very sharp signals (where, for C-1, C-2, C-3,4, and C-5 the chemical shifts δ are: 102 ppm, 73 ppm, 75 ppm and 64 ppm, respectively) compared to signals resulting from cellulose (with shifts at 105 ppm for C-1, region around 89 ppm for C-4 highly ordered and around 84 ppm less ordered cellulose, 72-77 ppm for C-2, 3, 5 and 62-66 ppm for C-6) (40-45).

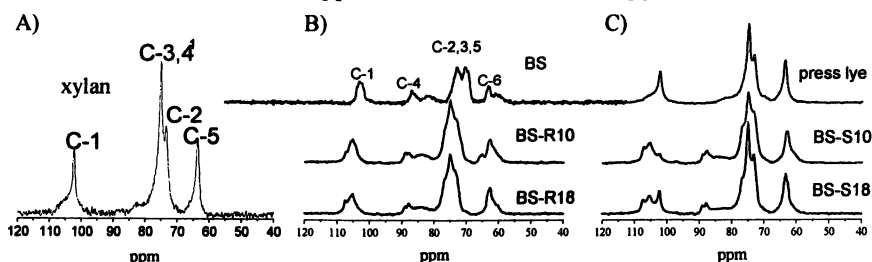


Figure 4. Solid-state NMR spectra of A) PL (xylan), B) R-fractions of BS, BS-R10 and BS-R18 and C) S-fractions of BS-S10 and BS-S18 and PL (Reprinted with permission from Mais, Milacher, Baldinger, Röder and Sixta 2002 Copyright 2002 European Workshop on Lignocellulosics and Pulp)

In the present spectrum of beech wood the amorphous part was clearly noticeable due to the relatively broad peaks besides the crystalline cellulose I form. In the alkali-insoluble fraction R18 partly amorphous cellulose II was predominant.

The difference between xylan and cellulose could clearly be seen at the chemical shift of 102 ppm originating from C-1. Comparing the spectra it could be assumed that press lye consisted of pure xylan. It has also been described that the structure of xylan is very sensitive to the close environment having an influence on the spectra (40). No indication for residual lignin could be found in the samples. Also by this method the alkali-insoluble fractions from 10% NaOH extraction were composed of cellulose I besides cellulose II as indicated by the presence of the signal at 66 ppm. By difference spectra the amount of xylan could be estimated, and the results matched the data from the carbohydrate analysis (Table VII).

Table VII. Comparison of carbohydrate analysis data obtained from solid-state NMR spectroscopy and HPLC

<i>Sample</i>	¹³ C-CP/MAS NMR		<i>AEC-PAD after TH</i>	
	<i>Cellulose (%)</i>	<i>Xylan (%)</i>	<i>Glucan (%)</i>	<i>Xylan (%)</i>
BS-S18-beta	52	48	54	43
BS-S10-beta	80	20	80	18
EK-S18-beta	28	72	24	69
EK-S10-beta	57	43	60	35
PL-beta ¹	0	100	2	81

¹ PL-Beta was assumed to consist of pure xylan and the spectrum was subtracted from all other spectra for carbohydrate estimation

The degree of crystallinity strongly depends on the amount of hemicellulose and lignin present in the sample (41,44). The crystalline amount of cellulose I of the R-fractions was assessed and was found comparable to the crystallinity values calculated from the IR-spectroscopy data. The percentage of crystalline cellulose I was about 18% for BS and twice as much in softwood-derived samples (see Table VI).

Conclusions

Alkali-soluble hemicellulose fractions from press lye and different pulps have been investigated. The carbohydrate composition strongly depended on the pulp and sodium hydroxide concentration. Employing 10% NaOH the S-fraction

contained almost only beta-hemicelluloses with a higher percentage of glucan compared to the S18-fractions, whereas press lye consisted of two thirds of gamma-cellulose. Using solid-state NMR spectroscopy the beta-fraction of press lye was determined as rather pure xylan and the sugar composition was comparable to the values obtained by AEC-PAD. The presence of 4-O-methylglucuronic acid in the beta-fraction of press lye as detected by FT-IR-spectra and COOH-analysis was confirmed by MALDI-MS with a similar 4OMeGlcA:Xylose-ratio of 5:100 at the maximum. In a subsequent work the influence of storage conditions (time, temperature) on the S18-fractions will be investigated to furnish a better model system for the press lye composition.

Acknowledgement. The authors wish to thank the Austrian Kompetenzzentrum Holz GmbH, Linz, Austria and the Lenzing AG, Lenzing, Austria for financial support. We would also like to thank Dr. A. Potthast for MALDI measurement and Prof. C. Jäger for NMR analysis.

References

1. Garves, K.; Wehlte, S.; Faix, O.; Puls, J. *Mitteilungen d. Bundesforschungsanstalt f. Forst- u. Holzwirtschaft Hamburg*, 1997 Nr. 187
2. Ebringerová, A.; Heinze, Th. *Macromol. Rapid Commun.* **2000**, *21*, 542-556
3. Carrasco, F.; Roy, C. *Wood Sci. Technol.* **1992**, *26*, 189-208
4. Masura, V. *Wood Sci. Technol.* **1987**, *21*, 89-100
5. Sixta, H.; Harms, H. Final report of partner 3, Lenzing AG, of the EU-Project FAIR-CT 98-3855: (2000).
6. Hurlen S.; Olsen, A. *Proceed.*, 5th Int. Dissolving Pulp Conf. 1980, 54-58
7. Sihtola, H.; Blomberg, L. *Proceed.*, Dissolving Pulps Conf., Oct. 24-26, 1973, pp21-24
8. Eremeeva, T. E.; Bykova, T. O. *J. Chromatogr.* **1993**, *639*, 159-164
9. Bandel, W. *Das Papier* **1953**, *15/16 (8)*, 306-209
10. Puls, J.; Kruse, Th.; Saake, B. Proceedings of the 10th ISWPC, Yokohama, June 7-10, 1999, p.54-57
11. Sixta, H.; Schelosky, N.; Milacher, W.; Baldinger, T.; Röder, Th. Proceedings of the 11th ISWPC 2001, Vol. 3, pp. 655-658
12. Lenz, J.; Noggler, E.; Leibetseder, J. *Nahrung* **1986**, *30 (9)*, 959-965
13. ISO 692:1982, Pulps-Determination of alkali solubility and ISO 699:1982, Pulps-Determination of alkali resistance, International Organisation for Standardization;1982
14. Philipp, B.; Rehder, W.; Lang, H. *Das Papier* **1965**, *19 (1)*, 1-9
15. Schelosky, N.; Röder, T.; Baldinger, T. *Das Papier* **1999**, *53 (12)*, 728-738
16. Baldinger, T.; Moosbauer, J.; Sixta, H. *Lenzinger Berichte* **2000**, *79*, 15-17
17. Kern, H. *Carbohydr. Res.* **2000**, *326*, 67-79
18. Ciucanu, I.; Kerek, F. *Carbohydr. Res.* **1984**, *31*, 209-217

19. Sixta, H. *Lenzinger Berichte* **2000**, *79*, 119-128
20. Sixta, H.; Borgards, A. *Das Papier* **1999**, *53*(4), 21-34
21. Harvey, D. H. *J. Chromatogr. A* **1996**, *720*, 429-446
22. Harvey, D. J. *Mass Spectrom. Rev.* **1999**, *18*, 349-451
23. Schols, H.; Kabel, M.; Bakx, E.; Daas, P.; Alebeek, G. J.; Voragen, F. AVH Association- 7th Symposium- Reims, March, 2000, 39-45
24. Jacobs, A.; Dahlman, O. *Biomacromolecules* **2001**, *2*, 894-905
25. Jacobs, A.; Larsson, P. T.; Dahlman, O. *Biomacromolecules* **2001**, *2*, 979-990
26. Jacobs, A.; Lundquist, J.; Stalbrand, H.; Tjerneld, F.; Dahlman, O. *Carbohydr. Res.* **2002**, *337*, 711-717
27. Kabel, M. A.; Schols, H. A.; Voragen, A. G. J. *Carbohydr. Polym.* **2001**, *44*, 161- 165
28. Fang, J. M.; Fowler, P.; Tomkinson, J.; Hill, C. A. S. *Carbohydr. Polym.* **2002**, *47*, 285-293
29. Kacuráková, M.; Wellner, N.; Ebringerová, A.; Hromádková, Z.; Wilson, R.H.; Belton, P.S. *Food Hydrocolloids* **1999**, *13*, 35-41
30. Evans, R.; Newman, R.H.; Roick, U. C.; Suckling, I. D.; Wallis, A.F.A. *Holzforchung* **1995**, *49*(6), 498-504
31. Higgins, H. G.; Stewart, C. M.; Harrington, K. J. *J. Polym. Sci.* **1991**, *51*, 59-84
32. Fengel, D. *Das Papier* **1992**, *46*(1), 7-11
33. Fengel, D. *Holzforchung* **1993**, *47*, 103-108
34. Kondo, T.; Sawatari, C. *Polymer* **1996**, *37*(3), 393-399
35. Hulleman, S.H.D.; van Hazendonk, J.M.; van Dam, J.E.G. *Carbohydr. Res.* **1994**, *261*, 163-172
36. Fink, H.P.; Dantzenberg, H.; Kunze, J.; Philipp, B. *Polymer* **1984**, *27*, 944-948
37. Dybowski, C. *Anal. Chem.* **1998**, *70*, 1R
38. Dybowski, C.; Lichter, R.L. NMR spectroscopy techniques, Marcel Dekker: New York, 1987
39. Atalla, R.H.; Ranua, J.; Malcolm, E. W. Int. Dissolving and Speciality Pulps **1983**, 217-221
40. Teleman, A.; Larsson, P. T.; Iverson, T. *Cellulose* **2001**, *8*, 209-215
41. Liitiä T.; Maunu, S.L.; Hortling, B. *Holzforchung* **2001**, *55*, 503-510
42. Kunze, J.; Fink, H.P. *Das Papier* **1999**, *53* (12), 753-764
43. Maunu, S.; Liitiä, T.; Kauliomäki, S.; Hortling, B.; Sundquist, J. *Cellulose* **2000**, *7*, 147-159
44. Hult, E.L.; Larsson, P. T.; Iverson, T. *Holzforchung* **2002**, *56*, 179-184
45. Hult, E.L.; Larsson, P. T.; Iverson, T. *Cellulose* **2000**, *7*, 35-55

Chapter 8

Identification of Structural Features of Various (*O*-Acetylated) Xylo-Oligosaccharides from Xylan-Rich Agricultural By-Products: A Review

Mirjam A. Kabel, Henk A. Schols, and Alphons G. J. Voragen

Department of Agrotechnology and Food Sciences, Laboratory of Food Chemistry,
Wageningen University, Bomenweg 2, 6703 HD, Wageningen, The Netherlands

Hydrolysates obtained by hydrothermal treatment of four xylan rich by-products (wheat bran, brewery's spent grain, corn cobs and *Eucalyptus* wood) were characterised. Depending on the feedstock material studied, a wide variety of differently substituted xylo-oligosaccharides (XOS) and xylan-fragments were obtained. The structural features of the this way obtained arabinose, 4-*O*-methylglucuronic acid and *O*-acetyl substituted XOS are reviewed. High performance anion-exchange chromatography (HPAEC), reversed phase (RP)-high performance liquid chromatography (HPLC), mass spectrometry (MS), NMR spectroscopy, RP-HPLC-MS and RP-HPLC-NMR showed to be very useful for the separation and characterisation of the detailed structures of the substituted XOS.

1. Introduction

Alternative applications of agricultural by-products are of interest, because their economic value as animal feed compounds is decreasing. One of the possibilities is to perform a hydrothermal treatment of these by-products with emphasis on minimising the environmental impact (avoiding acid, alkali or organosolv additions). Such a treatment will result in a selective fractionation of (partially) degraded hemicelluloses from the ligno-cellulosics present, which can be used for different product applications (1).

In this publication the research performed within the framework of the PhD-research concerning the characterisation of complex xylo-oligosaccharides from xylan rich by-products (2) is reviewed. The separation and structural features of differently substituted xylo-oligosaccharides obtained from hydrothermally treated wheat bran, brewery's spent grain, corn cobs and *Eucalyptus* wood is described.

2. Hydrothermal treatment of xylan rich by-products

2.1 Structural features of xylans originally present in by-products

The main products resulting from the depolymerisation of the xylans during hydrothermal treatment are xylose and xylo-oligosaccharides (XOS) (3,4). Depending on the source of the by-product various (amounts of) substituents are linked to the xylans present (5).

In a previous publication we described the structural features of the xylans originally present in the by-products studied (5). In general, alkali extracted xylan from the wheat bran used was mainly substituted at *O*-3 and both *O*-2 and *O*-3 of the xylosyl residues with arabinose. For xylans from the brewery's spent grain and corn cobs studied (5) arabinosyl substituents are present at *O*-3 or *O*-2 and both *O*-2 and *O*-3 of the xylosyl residues. Additionally, besides substitution with arabinoses corn cob xylan was substituted with (4-*O*-methyl-)glucuronic acid in a ratio of uronic acid to xylose of 0.1 and 0.3 for alkali extract and residue respectively. Alkali extracted *Eucalyptus* wood xylan (5) was mainly substituted with 4-*O*-methylglucuronic acid residues (UA/Xyl-ratio=0.16) and some indications for the presence of the linkage 2-*O*- α -galactopyranosyl-4-*O*-methyl- α -D-glucuronic acid were obtained. Furthermore, the *O*-acetyl content of the wood is the highest for the four by-products studied (3 % (w/w)) representing a ratio of *O*-acetyl to xylose of 0.65. Usually, for hardwoods the

content of *O*-acetyl substituents is 3-5 % (w/w) of the total wood (6). These *O*-acetyl substituents are mainly linked to the 2-*O*- and/ or 3-*O*-positions of the xylosyl residues in the backbone of xylan in hardwoods (7,8).

2.2 Composition of hydrothermally treated by-products

Taking into account the structural features of the xylans originally present the composition of the hydrolysates obtained after hydrothermal treatment of the four by-products is studied (5,9). The results of the composition of hydrolysates of each of the four by-products obtained at similar process conditions are summarised in Table I (5,9).

Table I Sugar content and composition of the hydrolysates obtained after hydrothermal treatment (160 °C; 60 min; 8-10 g/g) of wheat bran, brewery's spent grain, corn cobs and *Eucalyptus* wood (5,9).

<i>Hydrolysates</i>	<i>Wheat bran</i>	<i>Brewery's spent grain</i>	<i>Corn cobs</i>	<i>Eucalyptus wood</i>
Mw-range (Da) ^a	150- 5·10 ⁴	150-1·10 ⁵	150- 5·10 ⁴	150-1·10 ⁴
Monomers (Ara+Xyl) ^b	8	6	7	9
Oligo- & polymers ^b	25	38	50	56
Molar composition:				
Ara	4	18	3	0
Xyl	64	56	78	68
Gal	4	5	5	9
Glc	21	16	7	2
UA	7	6	7	17
Substitution ^c :				
Total	22	54	35	73
Ara	6	32	4	0
UA	11	11	9	25
Ac	5	11	22	48

^a based on HPSEC (pullulan standards).

^b expressed as weight percentage (dry weight).

^c amount of substituents per 100 xylosyl residues (Ara = arabinose; UA = uronic acid; Ac = *O*-acetyl).

In this table the estimated molecular weight (Mw) ranges are shown as well. The estimation of the Mw-ranges of the hydrolysates is determined by high-performance size-exclusion chromatography (HPSEC; based on pullulan standards).

The hydrolysate obtained after treatment of wheat bran mainly contains low-substituted XOS and polymeric xylan-fragments. This indicates that during hydrothermal treatment almost all arabinose originally present is removed from the xylans and XOS, and partially converted into degradation products like hydroxymethylfurfural (HMF). In the wheat bran hydrolysate both monomeric xylose and arabinose are present.

As for wheat bran, during the hydrothermal treatment of brewery's spent grain and corn cob arabinose is released from the xylans present. However, in the hydrolysates of brewery's spent grain still quite some XOS and xylan-fragments containing arabinose are present (Ara/Xyl-ratio=0.3).

In the hydrolysates of corn cobs non-substituted and *O*-acetylated xylan-fragments are accumulated. In both the hydrolysates of brewery's spent grain and corn cobs monomeric xylose and arabinose are present as well.

During the hydrothermal treatment of *Eucalyptus* wood some non-substituted XOS are released. Furthermore, XOS substituted with 4-*O*-methylglucuronic acid and/ or *O*-acetyl substituents represent a remarkable part of all XOS present.

3. Separation and identification of oligosaccharides

3.1 Chromatographic methods

To study the material released from the by-products during treatment, the hydrolysates obtained were analysed (5,9). Herefor, both high performance anion-exchange chromatography (HPAEC) and high performance size exclusion chromatography (HPSEC) appeared to be useful methods. HPSEC is performed to study the hydrodynamic volume of the released xylan-fragments, giving information about the depolymerisation of the xylans during treatment. Its use is a fairly well established technique and it has been used to estimate the weight-average molecular weights of (enzymatic degraded) wheat flour arabinoxylans (10), the molecular weight distribution of extracted wheat bran arabinoxylans (11), and the homogeneity of extracted maize and sorghum (glucurono)-arabinoxylans (12).

By using HPAEC, giving much higher resolutions for oligosaccharides compared to HPSEC, (substituted) XOS (DP 2-10) were separated well (13,14). In combination with the HPAEC-elution behaviour of the previously purified and fully identified enzymatically derived XOS from wheat flour xylan (15-17), barley xylan (18) and sorghum xylan (19), (part of) the XOS substituted with arabinose and (4-*O*-methyl)-glucuronic acid present in the hydrolysates studied is identified (5,9).

The off-line coupling of HPAEC to MALDI-TOF MS was established to overcome the rather unpredictable elution behavior of HPAEC (20).

A disadvantage of performing HPAEC in the characterisation of oligosaccharides substituted with ester groups (e.g. *O*-acetyl substituents) is that typically eluents with a high pH are used. Hereby, alkali-labile esters (*O*-acetyl) will be removed. To be able to characterise the *O*-acetyl substituted XOS other chromatographic methods were tested.

First, analytical HPAEC at pH 5 was performed by using instrumentation according to Daas et al. (21). An example of a HPAEC-elution pattern at pH 5 of the complex *Eucalyptus* wood hydrolysate containing (*O*-acetylated) neutral and (*O*-acetylated) negatively charged XOS is shown in Figure 1.

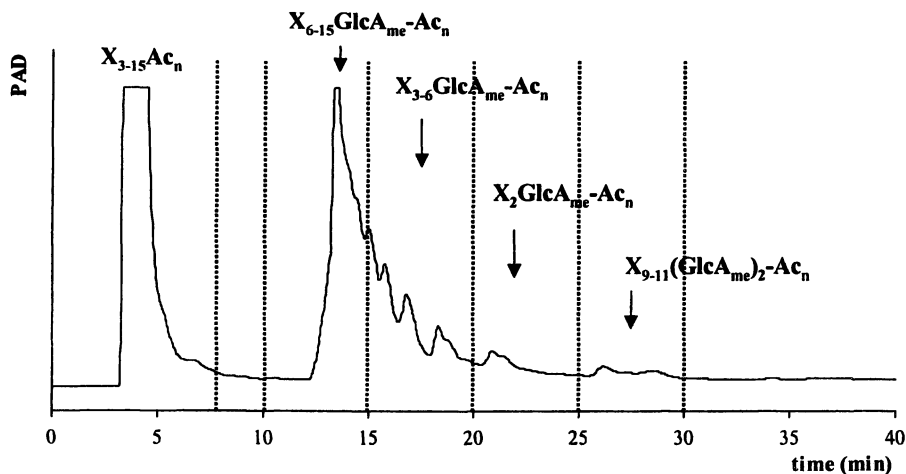


Figure 1 HPAEC (pH 5) elution pattern of an *Eucalyptus* wood hydrolysate; a gradient was used of 0-17 mM of sodiumacetate buffer (pH 5) during 5 min followed by 17-30 mM of buffer during 35 min at 0.5 ml/min (X = xylose; $GlcA_{me}$ = 4-*O*-methylglucuronic acid; Ac = *O*-acetyl).

The eluent was collected and combined in six pools, which were subjected to MALDI-TOF MS (9) to reveal the molecular mass of the XOS present (Figure 1). HPAEC at pH 5 in combination with MALDI-TOF MS has recently been used for the separation and identification of oligogalacturonides as well (21,22). From Figure 1 it can be seen that besides separation of the (*O*-acetylated) neutral and (*O*-acetylated) negatively charged XOS based on the presence of 4-*O*-methylglucuronic acid substituents, also the charge density influenced the separation. XOS containing one 4-*O*-methylglucuronic acid substituent having a lower Mw were more retained than higher Mw ones having also one 4-*O*-methylglucuronic acid substituent, while XOS containing two 4-*O*-methylglucuronic acid substituents were eluted only at much higher salt concentrations.

The conditions used for HPAEC at pH5 were applied to preparative anion-exchange chromatography using Source Q-column material (9). Hereby, larger amounts of neutral XOS separated from acidic XOS were obtained.

Further separation of the neutral and *O*-acetylated XOS was performed by using reversed phase (RP) HPLC (23). In general, separation by RP-HPLC is based on differences in hydrophobicity (24). The eluents can be monitored by using an evaporating light scattering (ELS) detector. ELS detection allows the use of methanol as eluent, while UV detection is not compatible with this eluent. Additionally, by using standards and comparing similar fractions ELS detection also allows quantification of oligosaccharides in different mixtures. The *O*-acetylated XOS present in the hydrolysates of *Eucalyptus* wood were separated based on the number and position of the *O*-acetyl substituents (23). The higher the number of *O*-acetyl substituents per oligomer the higher was the affinity with the hydrophobic column material. However, XOS having a different DP, but the same number of *O*-acetyl substituents mostly coeluted. Similar observations were described by Pauly et al. for acetylated xyloglucan oligosaccharides (25). They showed that the presence of an *O*-acetyl substituent on the galactosyl-residue significantly increases the retention time.

Another column, a TSKGel amide-80 column (Tosohaas; 4.6mm x 250mm; 5 μ m) was tested as well to separate *O*-acetylated XOS (Figure 2). Again, a separation based on the number of *O*-acetyl substituents per oligomer was achieved. In contrary with reversed phase chromatography, on the TSKGel amide-80 column the highly *O*-acetylated oligomers eluted first followed by XOS containing less *O*-acetyl substituents. However, also by using the TSKGel amide-80 column some coelution occurred, which makes the separation of complex oligosaccharide-mixtures more difficult.

The results obtained by the RP-HPLC as well as the results obtained by using the TSK Gel Amide-80 column reflect the potential of these methods in the separation of oligosaccharides.

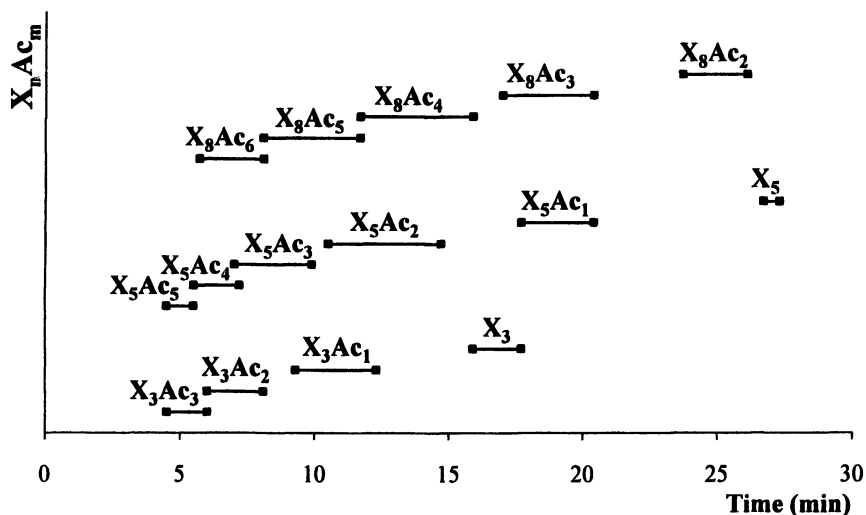


Figure 2 Part of a TSKGel Amide-80 elution pattern of several *O*-acetylated xylo-oligosaccharides monitored by MALDI-TOF MS in fractions collected (0.3 min/fraction); a gradient was used of acetonitril/water from 75/25v/v% to 50/50v/v% in 50 minutes at 1 ml/min (X = xylose; Ac = *O*-acetyl; n = number of xyloses; m = number of *O*-acetyl substituents).

Additionally, these two methods provided a good alternative for the commonly used HPAEC at high pH, especially for the separation of oligosaccharides substituted with alkali-labile esters. For the separation of complex mixtures a pre-separation by size-exclusion chromatography might be needed. Also, combining the RP-HPLC and TSKGel Amide-80 separation could be helpful in a complete separation of a variety of *O*-acetylated XOS in complex mixtures.

3.2 Spectrometric and spectroscopic methods

In the early nineties nuclear magnetic resonance (NMR) spectroscopy was the preferred technique in order to fully characterise structures of oligosaccharides. Nowadays, both matrix assisted laser desorption/ ionisation time-of-flight (MALDI-TOF) and electrospray MS have become routine and powerful techniques in the identification of structural features of oligosaccharides (26-28), even to determine the positions of residues within oligosaccharides (29,30).

The arabino-xylo-oligosaccharides mainly present in hydrolysates of brewery's spent grain and corn cobs were difficult to identify in detail by MS, because the mass of an arabinosyl and xylosyl residue is the same (m/z 132). However, the presence of *O*-acetyl and (4-*O*-methyl-)glucuronic residues could be confirmed using MS. Especially, regarding the hydrolysate of *Eucalyptus* wood establishing the number of substituents (*O*-acetyl and 4-*O*-methylglucuronic acid) per oligomer present in a complex mixture was rather straightforward by using MS (9).

An advantage of the use of RP-HPLC in the identification of oligomers is that in general solutions without salts, like pure water and methanol, enable the on-line coupling to a mass spectrometer. RP-HPLC coupled on-line to both an electrospray mass spectrometer and an ELS detector provided information about the order of elution of the various *O*-acetylated xylo-oligomers in the *Eucalyptus* wood hydrolysate (23).

Furthermore, tandem mass spectrometry (MS^n) is reported to be useful in the identification of the order of sugar residues within oligosaccharides (29,30). On MS^n -analysis of oligosaccharides a range of fragment ions is observed that are the result of the breaking of one or more bonds in the oligosaccharide ion that was selected as precursor. In general, the glycosidic bond between sugar residues is rather weak and therefore masses of fragment ions that are the result of breaking these bonds are predominantly observed in MS^n -spectra. However, fragmentation of the *O*-acetylated XOS in the *Eucalyptus* wood hydrolysate studied was most likely hindered by the *O*-acetyl substituent(s) present. The higher the number of *O*-acetyl substituents per oligomer the less fragment ions as a result of breaking glycosidic bonds between the monomers were observed in the MS^n -spectra. Therefore, the position of the *O*-acetyl substituted xylose or xylosyl residues within the xylo-oligomers was difficult to distinguish (23).

The use of the fragmentation of oligosaccharides by using post-source decay (PSD) MALDI-TOF MS was shown by Van Alebeek et al. (31). This technique was reported to permit the determination of the positions of methyl esters or other substituents in the sequencing of methyl-esterified oligogalacturonides (31). Nevertheless, also by using PSD MALDI-TOF MS no fragmentation of *O*-acetylated XOS was obtained.

Since the use of RP-HPLC-MS and MS^n was not successful in the identification of the location of the *O*-acetyl substituents within XOS in the hydrolysate of *Eucalyptus* wood, NMR spectroscopy was used. NMR spectroscopy is a commonly used and powerful method in the identification of oligosaccharides (16,32-35). First, a pool of several xylo-tetramers was obtained from the *Eucalyptus* wood hydrolysate by size exclusion chromatography. These xylo-tetramers all contained one *O*-acetyl substituent but located at different positions. Subsequently, these *O*-acetylated xylo-tetramers were separated by RP-HPLC based on the position of the *O*-acetyl

substituent and were analysed by NMR analysis (23). In stead of one signal indicating the position of the *O*-acetyl substituent, for each *O*-acetylated xylo-tetramer ¹H-NMR chemical shifts were obtained corresponding to both 2-*O*- and 3-*O*-acetylated xylosyl residues. In these *O*-acetylated tetramers *O*-acetyl migration was proven to have occurred (23). The migration was expected to have occurred during sample pre-treatment for NMR spectroscopy (evaporating methanol at room temperature, freeze-drying and freeze-drying in D₂O). To avoid such *O*-acetyl migration RP-HPLC coupled to a NMR unit without further sample treatment was used.

A disadvantage of LC-HPLC-NMR is that still relatively high amounts of sample are needed for the NMR analysis (50-150 µg per RP-HPLC peak applied to NMR), while often only very low amounts of pure material are available. Furthermore, the amount of sample applied to RP-HPLC is limited because of the risk of overloading the column. However, the development of nano-technology is on-going and most likely a reduction in the amount of sample needed for HPLC-NMR will be reached in the near future (32,36).

4 Structural characteristics of xylo-oligosaccharides present in brewery's spent grain and *Eucalyptus* wood hydrolysates

4.1 Arabinoxyloligosaccharides from barley are *O*-acetylated

Fractionation by using preparative anion-exchange and size-exclusion chromatography of the hydrothermally treated brewery's spent grain resulted in three pools of which two contained relatively high molecular weight xylan-fragments (pool 1A and B), singly and doubly branched with arabinose, separated from a pool of XOS (DP < 50) less branched with arabinose (pool 1C) (9). In all pools obtained the arabinosyl residues were located at the 3-*O*- and/ or 2-*O*-positions of the xyloses present.

Interestingly, endoxylanase I (*Aspergillus awamori*)-digestions (15,37) of all three brewery's spent grain-pools (1A-C) resulted in oligomers, which contained *O*-acetyl substituents. The content of *O*-acetyl substituents present in pool 1A, B and C was 0.7, 1 and 3 % (w/w) respectively. In the original brewery's spent grain hydrolysate this content was 0.9 % (w/w). A MALDI-TOF mass spectrum of endoxylanase I-treated pool 1B, also representative for similarly treated pool 1A and 1C, is shown in Figure 3. To confirm the presence of the *O*-acetyl substituents the endoxylanase I-digested material was treated with alkali, which removes alkali-labile *O*-acetyl esters. By MALDI-TOF MS it

was indeed confirmed that after treatment with alkali the masses of the *O*-acetylated XOS indicated in Figure 3 lacked, leaving only masses of a series of non-acetylated pentoses (not shown).

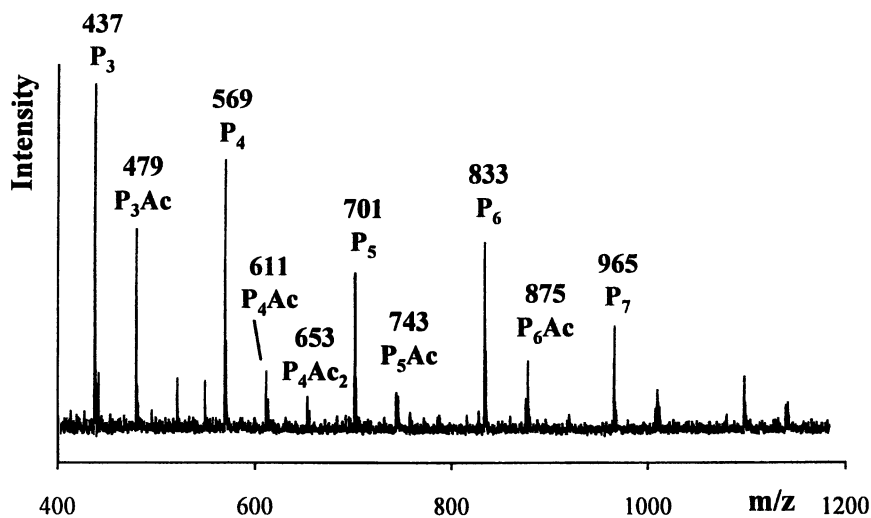


Figure 3 MALDI-TOF mass spectrum of endoxylanase I-digested brewery's spent grain pool B. Oligosaccharides are analysed as sodium-adducts (*P* = pentose; *Ac* = *O*-acetyl).

In the MALDI-TOF mass spectra of the original hydrolysate of brewery's spent grain used for fractionation the masses corresponding with *O*-acetylated XOS were hardly present. Most likely, if *O*-acetylated XOS (DP < 20) were present in the hydrolysate their concentration was too low to detect by MALDI-TOF MS. Additionally, *O*-acetylated xylan-fragment having a DP higher than 20 are difficult to detect by MALDI-TOF MS.

The precise location of the *O*-acetyl substituents within the (arabino-)xylo-oligosaccharides has not been established yet. To our knowledge only few publications reported the presence of *O*-acetyl substituents in xylans from grasses (38,39) and is it for the first time that *O*-acetyl substituents are presented to occur in xylan-fragments obtained from cereals. A reason to explain the fact that the *O*-acetyl substituents are overseen in general can be that studies regarding the structural features of xylans normally include alkali-extractions to

purify the xylans prior to characterisation. This way, information about the presence of ester-linked substituents (e.g. *O*-acetyl) is lost.

Purification of the hydrothermally treated brewery's spent grain also resulted in a pool containing charged xylan-material (9). Most likely, the recovered xylan-fragments were still partly substituted with (4-*O*-methyl-)glucuronic acid residues. However, the charged pool represented less than 1 % of the material obtained after hydrothermal treatment of brewery's spent grain and was not studied in more detail.

4.2 *O*-acetylated and/ or 4-*O*-methylglucuronic acid containing xylo-oligosaccharides

The fractionation of the hydrothermally treated *Eucalyptus* wood resulted in a neutral pool, mainly consisting of *O*-acetylated XOS, and three pools of charged 4-*O*-methylglucuronosyl containing xylan-fragments (9). Two of these pools contained a series of (*O*-acetylated) XOS carrying *one* 4-*O*-methylglucuronic acid, while the third charged pool contained (*O*-acetylated) XOS and xylan-fragments substituted with *two* 4-*O*-methylglucuronic acids. Additionally, a series of XOS containing both 4-*O*-methylglucuronic acid and a hexose, most likely galactose, was detected in the charged pools. The linkage 2-*O*- α -galactopyronosyl-4-*O*-methyl- α -D-glucuronic acid is described for xylan extracted from *Eucalyptus globulus* Labill as well (40).

The neutral *O*-acetylated XOS were characterised in more detail by using a combination of RP-HPLC, MS and NMR. Knowing the positions of the *O*-acetyl substituents of the released XOS might be helpful in understanding the mechanisms occurring during hydrothermal treatment. Within 6 xylo-tetramers and 4 xylo-trimers each containing one *O*-acetyl substituent, the precise residue and position (2-*O* or 3-*O*) to which the *O*-acetyl substituent was linked was determined (23).

The *O*-acetyl migration (§3.2) described to have occurred in XOS (23) already might have occurred during hydrothermal treatment of the *Eucalyptus* wood. Therefore, the position and distribution of the *O*-acetyl substituents in the xylo-oligomers analysed could not be extrapolated directly to the xylan-structures originally present and does therefore not allow conclusions about the mechanisms of degradation during hydrothermal treatment. It even could be possible that *O*-acetylation in native xylans occurs at only one position (2-*O*- or 3-*O*-) of the xylosyl residues and that external circumstances influences migration and the distribution of the *O*-acetyl substituents further on.

5. Conclusions

From this research it was concluded that by performing hydrothermal treatments of the xylan-rich by-products a variety of differently substituted XOS (DP 2-50) and xylan-fragments (DP >50) can be obtained. These XOS included linear XOS, xylan-fragments substituted with arabinoses, *O*-acetylated XOS and (*O*-acetylated) XOS substituted with one or two 4-*O*-methylglucuronic acid(s).

HPLC, RP-HPLC, RP-HPLC-MS, MS, RP-HPLC-NMR and NMR spectroscopy showed to be very useful for the separation and characterisation of the detailed structures of the substituted XOS. Furthermore, the use of these methods resulted in the recognition of some structural features, which have not been reported before to our knowledge. *O*-acetyl substituents were found to occur not only in hardwood xylans as shown in literature, but also in xylan-fragments obtained from cereals (brewery's spent grain). Additionally, 2-*O*- or 3-*O*-acetyl substituted terminal xylosyl residues were analysed by NMR to occur in XOS present in the *Eucalyptus* wood hydrolysates. The complete structural characterisation of several *O*-acetylated XOS obtained from *Eucalyptus* wood hydrolysates was established by using (RP-HPLC-)NMR.

6. References

1. Koukios, E.G., Pastou, A., Koullas, D.P., Sereti, V., Kolosis, F. In *Biomass: a growth opportunity in green energy and value-added products*; Overend, R.P., Chornet, E., Ed.; New green products from cellulose. Pergamon: Oxford, 1999; pp 641.
2. Kabel, M.A. Ph.D. thesis, Wageningen University, Wageningen, The Netherlands, 2002.
3. Korte, H.E., Offermann, W., Puls, J., *Holzforchung*, **1991**, *45*, 419-425.
4. Puls, J., Poutanen, R., Korner, H.U., Viikari, L., *Appl. Microbiol. Biotechnol.*, **1985**, *22*, 416-423.
5. Kabel, M.A., Carvalheiro, F., Garrote, G., Avgerinos, E., Koukios, E., Parajó, J.C., Gírio, F.M., Schols, H.A., Voragen, A.G.J., *Carbohydr. Polym.*, **2002**, *50*, 47-56.
6. Timell, T.E., *Adv. Carbohydr. Chem. Biochem.*, **1964**, *19*, 247-302.
7. Timell, T.E., Syracuse, N.Y., *Wood Sci. Technol.*, **1967**, *1*, 45-70.
8. Teleman, A., Lundqvist, J., Tjerneld, F., Stalbrand, H., Dahlman, O., *Carbohydr. Res.*, **2000**, *329*, 807-815.
9. Kabel, M.A., Schols, H.A., Voragen, A.G.J., *Carbohydr. Polym.*, **2002**, *50*, 191-200.

10. Gruppen, H., Kormelink, F.J.M., Voragen, A.G.J., *J. Cereal Sci.*, **1993**, *18*, 111-128.
11. Schooneveld-Bergmans, M.E.F., Beldman, G., Voragen, A.G.J., *J. Cereal Sci.*, **1999**, *29*, 63-75.
12. Huisman, M.M.H., Schols, H.A., Voragen, A.G.J., *Carbohydr. Polym.*, **2000**, *43*, 269-279.
13. Lee, Y.C., *Anal. Biochem.*, **1990**, *189*, 151-162.
14. Lee, Y.C., *J. Chromatogr. A*, **1996**, *720*, 137-149.
15. Gruppen, H., Hoffmann, R.A., Kormelink, F.J.M., Voragen, A.G.J., Kamerling, J.P., Vliegthart, J.F.G., *Carbohydr. Res.*, **1992**, *233*, 45-64.
16. Kormelink, F.J.M., Hoffmann, R.A., Gruppen, H., Voragen, A.G.J., Kamerling, J.P., Vliegthart, J.F.G., *Carbohydr. Res.*, **1993**, *249*, 369-382.
17. Van Laere, K.M.J., Hartemink, R., Bosveld, M., Schols, H.A., Voragen, A.G.J., *J. Agric. Food Chem.*, **2000**, *48*, 1644-1652.
18. Vietor, R.J., Hoffmann, R.A., Angelino, S.A.G.F., Voragen, A.G.J., Kamerling, J.P., Vliegthart, J.F.G., *Carbohydr. Res.*, **1994**, *254*, 245-255.
19. Verbruggen, M.A., Beldman, G., Voragen, A.G.J., *Carbohydr. Res.*, **1998**, *306*, 275-282.
20. Kabel, M.A., Schols, H.A., Voragen, A.G.J., *Carbohydr. Polym.*, **2001**, *44*, 161-165.
21. Daas, P.J.H., Arisz, P.W., Schols, H.A., de Ruiter, G.A., Voragen, A.G.J., *Anal. Biochem.*, **1998**, *257*, 195-202.
22. Van Alebeek, G.-J.W.M., Zabolina, O., Beldman, G., Schols, H.A., Voragen, A.G.J., *Carbohydr. Polym.*, **2000**, *43*, 39-46.
23. Kabel, M.A., De Waard, P., Schols, H.A., Voragen, A.G.J., *Carbohydr. Res.*, **2002**, *accepted*.
24. Vervoort, R.J.M., Debets, A.J.J., Claessens, H.A., Cramers, C.A., De Jong, G.J., *J. Chromatogr. A*, **2000**, *897*, 1-22.
25. Pauly, M., York, W.S., *Am. Biotech. Lab.*, **1998**, *14*,
26. Bahr, U., Pfenninger, A., Karas, M., Stahl, B., *Anal. Chem.*, **1997**, *69*, 4530-4535.
27. Cancilla, M.T., Gaucher, S.P., Desaire, H., Leary, J.A., *Anal. Chem.*, **2000**, *72*, 2901-2907.
28. Harvey, D.J., *J. Chromatogr. A*, **1996**, *720*, 429-446.
29. Huisman, M.M.H., Brull, L.P., Thomas-Oates, J.E., Haverkamp, J., Schols, H.A., Voragen, A.G.J., *Carbohydr. Res.*, **2001**, *330*, 103-114.
30. Brull, L.P., Huisman, M.M.H., Schols, H.A., Voragen, A.G.J., Critchley, G., *J. Mass Spectrom.*, **1998**, *33*, 713-720.
31. Van Alebeek, G., Zabolina, O., Beldman, G., Schols, H.A., Voragen, A.G.J., *J. Mass Spectrom.*, **2000**, *35*, 831-840.
32. Broberg, A., Thomsen, K.K., Duus, J.O., *Carbohydr. Res.*, **2000**, *328*, 375-382.

33. Casteren, W.H.M., Kabel, M.A., Dijkema, C., Schols, H.A., Beldman, G., Voragen, A.G.J., *Carbohydr. Res.*, **1999**, *317*, 131-144.
34. Homans, S.W. In *Molecular Glycobiology*; Fukada, M., Hindsgaul, O., Ed.; Conformational studies on oligosaccharides; Oxford University Press, 1994.
35. Okada, Y., Matsuda, K., Koizumi, K., Hamayasu, K., Hashimoto, H., Kitahata, S., *Carbohydr. Res.*, **1998**, *310*, 229-38.
36. Wolfender, J.-L., Ndjoko, K., Hostettmann, K., *Phytochem. Anal.*, **2001**, *12*, 2-22.
37. Kormelink, F.J.M., Gruppen, H., Vietor, R.J., Voragen, A.G.J., *Carbohydr. Res.*, **1993**, *249*, 355-367.
38. Ishii, T., *Phytochemistry*, **1991**, *30*, 2317-2320.
39. Wende, G., Fry, S.C., *Phytochemistry*, **1997**, *44*, 1011-1018.
40. Ebringerova, A., Heinze, T., *Macromol. Rapid Commun.*, **2000**, *21*, 542-556.

Chapter 9

Proton NMR Methods in the Compositional Characterization of Polysaccharides

David J. Kiemle, Arthur J. Stipanovic, and Kelly E. Mayo

Faculty of Chemistry, College of Environmental Science and Forestry (SUNY-ESF),
E. C. Jahn Chemistry Laboratory, State University of New York, One Forestry Drive,
Syracuse, NY 13210

We have developed a new analytical method based on ^1H -Nuclear Magnetic Resonance (proton NMR) spectroscopy to quantify the monosaccharide sugars released from lignocellulosic biomass (wood, pulp, agricultural residues, etc.) upon acid hydrolysis. Compared to other carbohydrate analysis procedures, the NMR protocol is relatively fast since actual acidic hydrolyzates are used, it requires no sample derivatization and provides excellent resolution of complex sugar mixtures. Using the α and β anomeric C1 protons of specific sugars as “probes” of their concentration, we have developed a computational algorithm which enables us to quantify the relative molar concentration of the following sugars in complex hydrolyzates: glucose, mannose, galactose, xylose, rhamnose, arabinose, glucuronic acid.

Introduction

The 21st century is envisioned to become the “age of biology” as renewable biomass resources begin to replace petroleum in the production of energy and industrial products including fuels, chemicals and new biodegradable materials (*1*). Despite its relative abundance and renewability, the hemicellulosic fraction of woody plants has not been fully developed into a commercially attractive feedstock for the production of biobased products. Although differences exist between hardwoods, softwoods and other plants, the hemicellulose component of

woody materials typically comprises 20-40 dry wt% (2-4) and contains 2-3 different polysaccharides, each with a unique chemical composition capable of providing a different distribution of constituent sugars when hydrolyzed by acids or enzymes. As a result, the ultimate application of hemicelluloses as a feedstock for the production of fuels, chemicals and materials requires a careful analysis of the carbohydrates contained within this resource. Further, the accurate analysis of the hemicellulose fraction of wood pulp has important implications in papermaking, especially as fungal or enzyme biodelignification and bleaching evolve into commercial processes.

The carbohydrate composition of woody feedstocks is typically analyzed by first treating the solid materials with high concentrations of sulfuric acid (72% H₂SO₄) to hydrolyze the native polysaccharides (cellulose and species specific hemicelluloses) into their constituent sugars (D-glucose, D-xylose, D-galactose, D-mannose, D-glucuronic acid, L-arabinose, L-rhamnose, etc.). In most cases, these sugars are then quantified using High Pressure Liquid Chromatography (HPLC; 5-7) or Gas Chromatography / Mass Spectrometry (GC/MS) techniques (5). This report represents a preliminary study aimed at determining the utility of proton (¹H) NMR spectroscopy in the quantification of sugars resulting from the acid hydrolysis of complex polysaccharides without the need to neutralize the hydrolysis reaction products, separate the sugars chromatographically, or to prepare volatile derivatives for GC/MS analysis.

Sugar Analysis by Proton (¹H) NMR

Proton NMR methods have been widely employed to probe the composition, stereochemistry and mutarotation kinetics of sugars in aqueous solution for many years (8,9). Although various one and two dimensional (1D, 2D) NMR techniques have been applied in the elucidation of monomeric sugar composition and linkage stereochemistry for oligosaccharides (5,10), less attention appears to have been focussed on using simple 1D proton NMR to quantify individual sugars in complex mixtures resulting from the acid or enzymatic hydrolysis of biomass. In part, this may be due to the fact that residual water (H₂O) contributes a strong resonance in the anomeric proton region of the NMR spectrum for such hydrolyzates (11). In addition, certain NMR resonances that result from common sugars may overlap, as shown in Figure 1, and a resolution algorithm is needed. As a result, the NMR method under development in our laboratory, which exploits acidic sugar solutions and an empirical quantification protocol (based on standard sugar model compounds), appears to be a unique approach in carbohydrate analysis.

As discussed above, the NMR method offers many advantages compared to techniques such as HPLC and a related technique, High Performance Anion Exchange Chromatography with Pulsed Amperometric Detection (HPAEC-PAD) which are widely applied in the analysis of lignocellulosic hydrolyzates (5). Since most carbohydrate chromatography columns separate molecules based

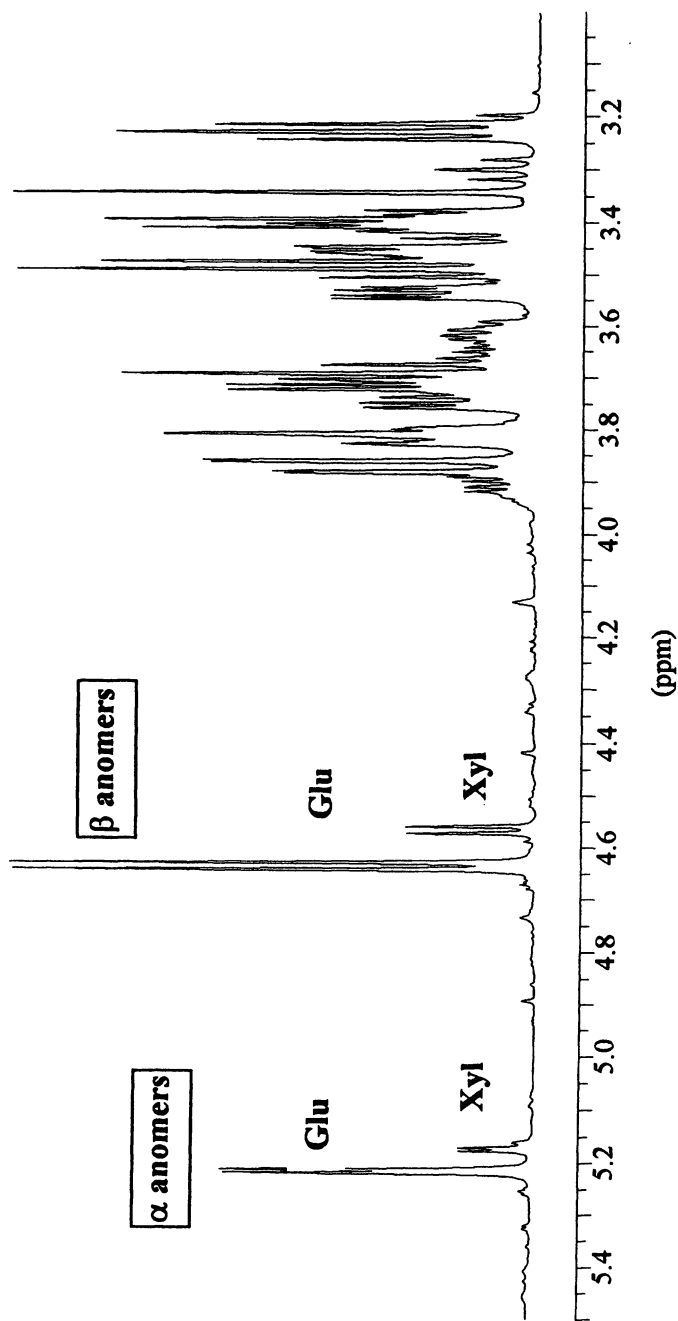


Figure 1. 600 MHz ^1H NMR spectrum of hydrolyzed willow wood (*Salix* sp.) in acidic D_2O .

on the slightly acidic character of sugars in neutral or alkaline solution (12), acidic biomass hydrolyzates must be neutralized before analysis and columns must be flushed with alkali after chromatography to release the bound sugars. Although HPLC and HPAEC-PAD generally provide excellent results for abundant sugars such as glucose and xylose, in some cases they offer only modest separation of minor sugars such as arabinose, rhamnose, galactose and mannose and quantification of these sugars may be limited by detector sensitivity (12). In addition, analysis times are typically long (up to 60 minutes) and column flushing between runs requires additional time for sugar desorption and re-equilibration with mobile phase. Using a so-called "pusher ion" solution following elution with the basic mobile phase, several groups have observed both an increase in resolution and faster elution times for carbohydrates (6, 7). In these procedures, the chromatography experiment is significantly more complex.

GC/MS has also been widely used to characterize the carbohydrate profile of lignocellulosic materials (5). However, this technique requires that sugar analytes be relatively volatile so manpower-intensive chemical derivatization is needed prior to analysis. Typical volatile derivatives include alditol acetates, silyl derivatives and methylated sugars (5). Compared to all of the chromatography-based techniques discussed above, the NMR method is an attractive alternative because it provides excellent resolution of sugars, including minor components, does not require sample derivatization or neutralization, and is very fast (instrument time 15-30 minutes).

Disadvantages of the NMR method compared to other techniques include: (1) the very high cost of a NMR instrument compared to HPLC or GC/MS systems, (2) some signal overlap of sugar resonances results in the need to adopt a quantification algorithm in which several assumptions are made (see below), (3) an additional step or internal standard is required to obtain absolute quantification of sugar concentration for hydrolyzates and, (4) no linkage information is derived.

Experimental Section

Wood or other lignocellulosic biomass samples are typically ground to a fine powder using a Wiley Mill with 20 mesh screens followed by drying at 110°C for 8-16 hours. Samples of microcrystalline cellulose, guar gum, larch arabinogalactan, and gellan gum were obtained as powders from the following sources, respectively: FMC Corp., Halliburton Oil Services, St. Regis Paper Company, and Kelco. Wood samples were obtained from a collection maintained at SUNY-ESF. For NMR analysis, 0.2ml of 72% H₂SO₄ was added to 0.040 g of dried biomass. After stirring, the dispersion was allowed to digest at 40°C for 1 hour in a bath or oven with additional stirring every 15 min. Following this digestion, 5.4 ml of D₂O (NMR solvent) was added to the dispersion which was then autoclaved in a high pressure sealed glass tube at 121°C for 1 hour. After cooling, an additional 0.42 ml of 96% H₂SO₄ is added for reasons discussed below. Hydrolyzates prepared in this fashion were then

filtered into NMR tubes without neutralization of the H_2SO_4 . For “model” sugar compounds, NMR analysis was performed at 3.3 wt % concentration in a solvent containing H_2SO_4 and D_2O in same ratio as used for the hydrolysis procedure although these samples were not autoclaved. Since the H_2SO_4 employed in the digestion contains 28% H_2O , the samples tested by NMR contained approximately 1% water (in D_2O) which can interfere with the observation of ^1H signals resulting from the sugars. However, the low pH of the acidic hydrolysis medium shifts the “water” NMR resonance (due to H_2O) away from the region of C1 anomeric proton resonances which are used to quantify each sugar. The magnitude of this water peak shift is illustrated in Table I. Specific NMR details and conditions include: Bruker AVANCE 600 MHz NMR system (proton frequency = 600.13 MHz), Broadband Observe probe type (BBO), 30°C , 90° Pulse = 11μ sec, delay between pulses = 10 sec, acquisition time = 2.73 sec, sweep width = 10 ppm, center of spectrum = 4.5 ppm, reference = acetone at 2.2 ppm ($1\mu\text{l}$ added to sample tube). Baseline corrections were made using a polynomial procedure.

Table I. Influence of Acid Concentration on Water Peak Chemical Shift

H_2SO_4 (%)	H_2O Chemical Shift (ppm)
0	4.6-4.7
4	5.2-5.4
8	5.7-5.9
15	6.1-6.3

Results and Discussion

Sugar Quantification Algorithm

In this analysis, both the cellulose and hemicellulose fractions of woody biomass are ideally hydrolyzed to monomeric sugars in aqueous acidic solution. Under these circumstances, sugars undergo a mutarotation process whereby an equilibrium is established between the α and β C1 anomer of the five and six-member ring forms of the sugars and the open chain form (13). As shown in Table II, for most common sugars, the 6-membered α and β ring form of the sugar predominates, suggesting that quantification of only the pyranose forms will provide an adequate estimate of sugar concentration. (This assumption is less appropriate for galactose and arabinose where the furanose form approaches 5-6%).

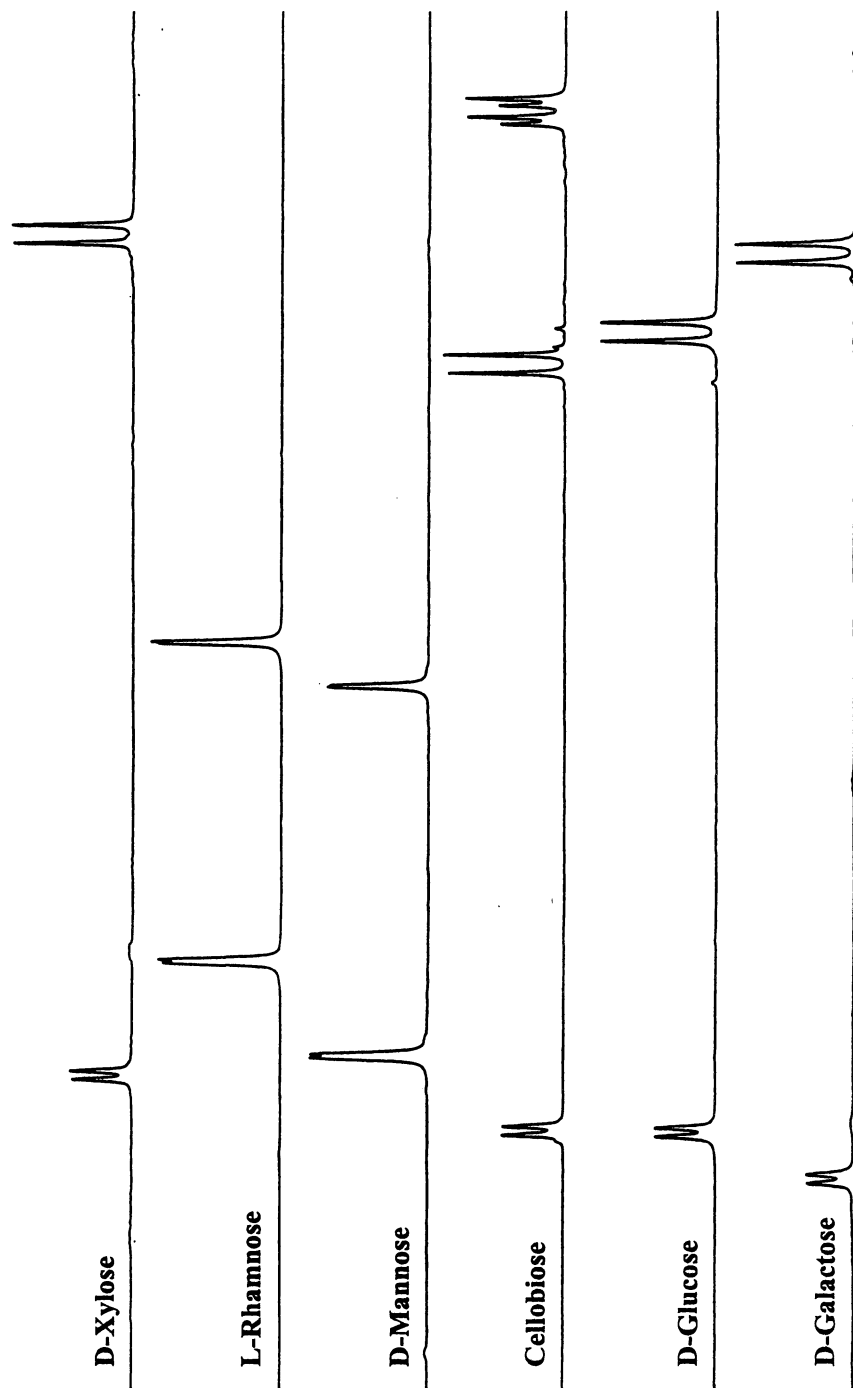
Figure 1 shown below is the proton NMR spectrum of an acid hydrolyzed sample of a fast-growing species of willow (*Salix spp.*). Although the spectral region from 3.2-4.0 ppm is very complex, the well resolved resonances centered near 5.2 ppm and 4.6 ppm can be assigned to the α and β anomeric C1 protons of D-glucose and D-xylose. The higher intensity resonance of each pair is D-

Table II. Conformation of Sugars in Aqueous Solution at 30-40°C (13)

Sugar	α and β Pyranose	α and β Furanose	Open Chain
	%	%	%
D-Glucose	99	1	0.002
D-Mannose	99	1	0.005
D-Galactose	94	6	0.02
D-Xylose	99.4	0.6	0.002
D-Rhamnose	99	1	0.005
L-Arabinose	95.5	4.5	0.03

glucose. These doublet signals are shifted away from the “complex” region of the spectrum since the C1 protons are adjacent to two electron withdrawing oxygen atoms (the pyranose ring oxygen and the C1 hydroxyl). By summing up the integrated intensity of the α and β doublets, the relative molar concentration of xylose and glucose can be easily determined.

Figure 2 contains the proton NMR spectra, recorded under acidic conditions, for a series of “model” sugar compounds commonly found in woody plant polysaccharides. For all sugars, the observed α and β peaks are “doublets” because the anomeric proton attached at C1 is coupled to a single proton at C2 of the pyranose ring. Figure 3 superimposes these sugar spectra onto one axis in a fashion that simulates the mixture of sugars resulting when an actual cellulose and hemicellulose-containing biomass sample is hydrolyzed by aqueous acid. Although excellent resolution of sugar types is achievable in most cases, peak overlaps do exist. The relative concentration of each sugar is determined by summing up the total integrated intensity from its respective α and β anomeric proton doublets (the α doublet occurs above 5.00 ppm and the β doublet occurs below 4.95 ppm) and dividing by the total spectral intensity observed for the α and β doublets of all sugars in the mixture. In our current quantification algorithm, α and β signal intensities for D-glucose (Glu), D-mannose (Man) and D-rhamnose (Rha) are summed directly since they are well resolved. In normal practice for woody materials, the arabinose (Ara) α peak is significantly lower in intensity compared to the nearby glucose α peak and it is not resolved (See Figure 3). To determine the total NMR intensity associated with arabinose, the β doublet between 4.5 and 4.55 ppm is integrated while the α intensity is calculated from the measured α / β ratio determined for this compound (from data in Figure 2). The observed β signal is then added to the calculated α intensity to yield the total arabinose contribution. The calculated α intensity for arabinose is also subtracted from the α intensity of the glucose peak since these peaks overlap. As shown in Figure 3, β peak overlaps for D-xylose (Xyl) and D-galactose (Gal) are also observed at 4.57 ppm. To alleviate this conflict, the well resolved “right” β resonance of xylose is doubled to yield a total β intensity which is added to the α doublet intensity. Similarly, for galactose, the “left” β resonance intensity is doubled and it is added to the α doublet. In order to determine the exact chemical shift of the α and β peaks associated with D-glucuronic acid (GluA), a 2D HSQC experiment was performed as shown in Figure 4. The spectral region between 4.3 and 5.4 ppm is significantly more



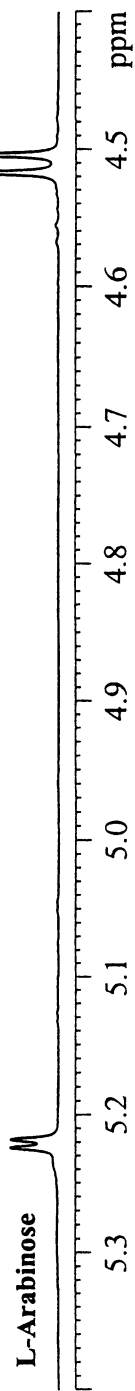


Figure 2. ^1H NMR spectra of common sugars in the C1 anomeric proton region. α resonances are > 5.00 ppm and β resonances are < 4.95 ppm (reversed for L-arabinose).

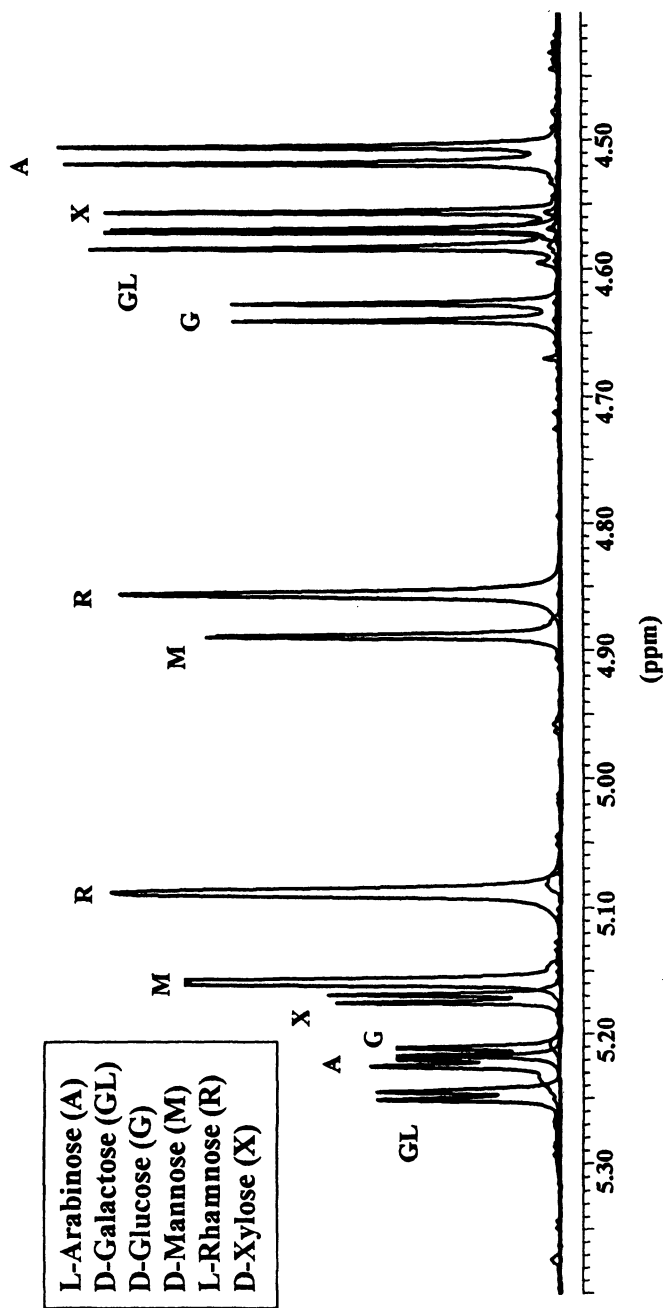


Figure 3. Superimposed ^1H NMR spectra of common sugars simulating a complex mixture.

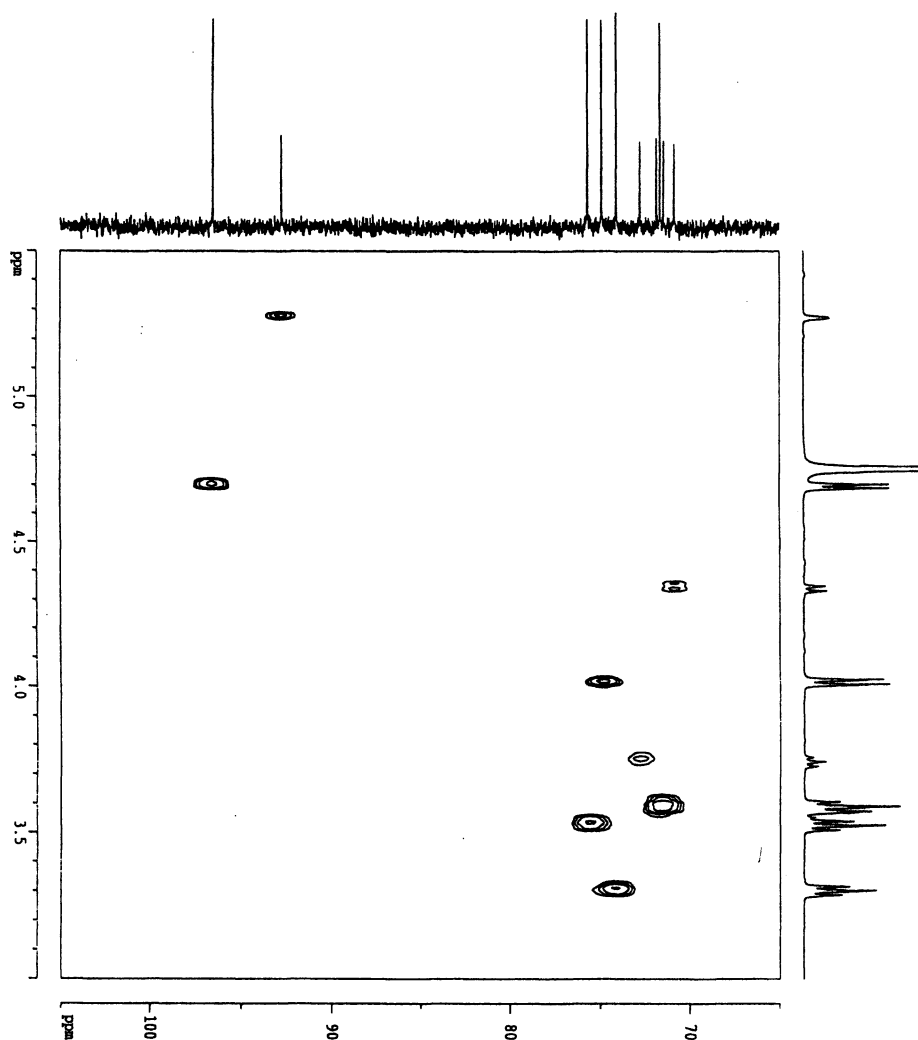


Figure 4. A 2D HSQC spectrum of GlucA. Horizontal axis is the proton spectrum dimension and the vertical axis is the ^{13}C dimension. Off axis peaks represent protons attached to specific carbon atoms in the sugar structure. The ^{13}C peaks at > 90 ppm correspond to C1 while the C2-C6 peaks are located between 70 and 80 ppm.

complicated for GluA compared to other sugars, perhaps due to lactone formation. Figure 4 reveals that the proton resonances observed near 4.7 and 5.3 ppm are attributable to C1 anomeric protons. In the quantification algorithm, these intensities are summed to provide an estimate of GluA concentration. Once all of the α and β doublets in a complex mixture are resolved and / or estimated, the algorithm sums these to yield a total sugar intensity from which the contribution of individual sugars can be calculated as a relative mol % or wt % since the molecular weight of each sugar is known.

To test the quantification procedure, solutions of sugar mixtures were prepared by weighing out a known amount of several sugars followed by proton NMR analysis under acidic conditions. Results shown in Table III compare the estimates of sugar concentration provided by NMR to the actual concentrations of two separate mixtures. It appears that the NMR method provides a reasonably good estimate of sugar concentration over the range of concentrations that might be expected for woody biomass hydrolyzates. To test the repeatability of the biomass hydrolysis / sugar quantification procedure, a sample of wood pulp was subjected to acid hydrolysis followed by NMR analysis a total of 5 times. Results presented in Table IV illustrate that the repeatability of the combined hydrolysis / analysis protocol is excellent.

Table III. Sugar Mixture Quantification by NMR (wt%)

<i>Sugar</i>	<i>Actual %</i>	<i>NMR %</i>	<i>Actual %</i>	<i>NMR %</i>
	<i>Mix 1</i>	<i>Mix 1</i>	<i>Mix 2</i>	<i>Mix 2</i>
Glucose	49.5	51.5	50.5	51.4
Xylose	24.9	23.7	23.9	24.2
Mannose	9.9	9.3	10.6	10.1
Galactose	10.6	10.1	7.5	7.2
Arabinose	2.5	2.5	3.3	3.1
Rhamnose	2.5	2.9	4.2	4.0

Table IV. Repeatability of Hydrolysis / NMR Analysis for Wood Pulp

<i>Sugar</i>	<i>Avg. Mole % - 5 Runs</i>	<i>Standard Deviation</i>
Glucose	90.0	0.24
Xylose	3.11	0.14
Mannose	5.89	0.12
Galactose	0.38	0.07
Arabinose	0.64	0.05

One source of potential variability in the overall analysis protocol is the degree to which each cellulose or hemicellulose molecule in the original woody biomass is degraded by acid to oligomers, monomeric sugars, and then to degradation products such as 2-furaldehyde (furfural; derived from xylose) or hydroxymethylfurfural (from glucose). Typically, hydrolysis conditions such as the duration of each temperature stage, are optimized for each type of sample (ground wood, isolated polysaccharides, plant stalks, pulp, etc) by monitoring NMR signals associated with “under-converted” cellobiose (cellulose dimer), specifically, the resonances near 4.65 – 4.67 and 4.45 – 4.48 (See Figure 2). At the same time, we attempt to avoid the over-conversion of xylose to furfural, which is a much faster reaction compared to glucose conversion (14). Furfural exhibits four well-resolved resonances from 6.7 to 9.5 ppm, as shown in Figure 5, that can be used to monitor its presence in the hydrolyzate. Although our algorithm is designed to compute relative concentrations based on monomeric sugars, it is possible to integrate both the cellobiose and furfural resonances and to “correct” the relative concentrations of glucose and xylose, respectively, by adding in these under- and over-converted species. The hydrolysis conditions summarized in the Experimental Section are typical for ground wood samples.

Analysis of Model Polysaccharides and Wood Samples

To test the NMR quantification protocol, a number of “model” polysaccharides were studied for which the monomeric sugar composition has been determined by other techniques. Table V shows that the NMR method agrees well with the known structures of microcrystalline cellulose, guar gum and the arabinogalactan polysaccharide from western larch. However, the GluA content observed for the microbial polysaccharide gellan, as well as xylan from birch, is consistently lower than reported by others. Since it is well known that the linkage between GluA and other sugars is very resistant to acid hydrolysis (5), it is likely that the underestimation of this sugar by NMR occurs because it is not hydrolyzed to a monomeric form but remains linked in higher molecular weight oligomers that are not adequately quantified by our procedure.

Table V. Sugar Composition of “Model” Polysaccharides (Dry wt. %)

Polysaccharide	Man	Gal	Ara		Observed NMR Ratio	Reference Ratio
Guar Gum	61%	36%			1.69 / 1	1.66 / 1 (15)
Larch Arabinogalactan		87%	13%		6.41 / 1	6.14 / 1 (16)
	Glu	Rha	Xyl	GluA		
MCC	100%				100% Glu	100%
Gellan	61%	27%		12%	2.25 / 1 / 0.44	2 / 1 / 1 (17)
Xylan			96%	3%	32 / 1	7 / 1 (18)

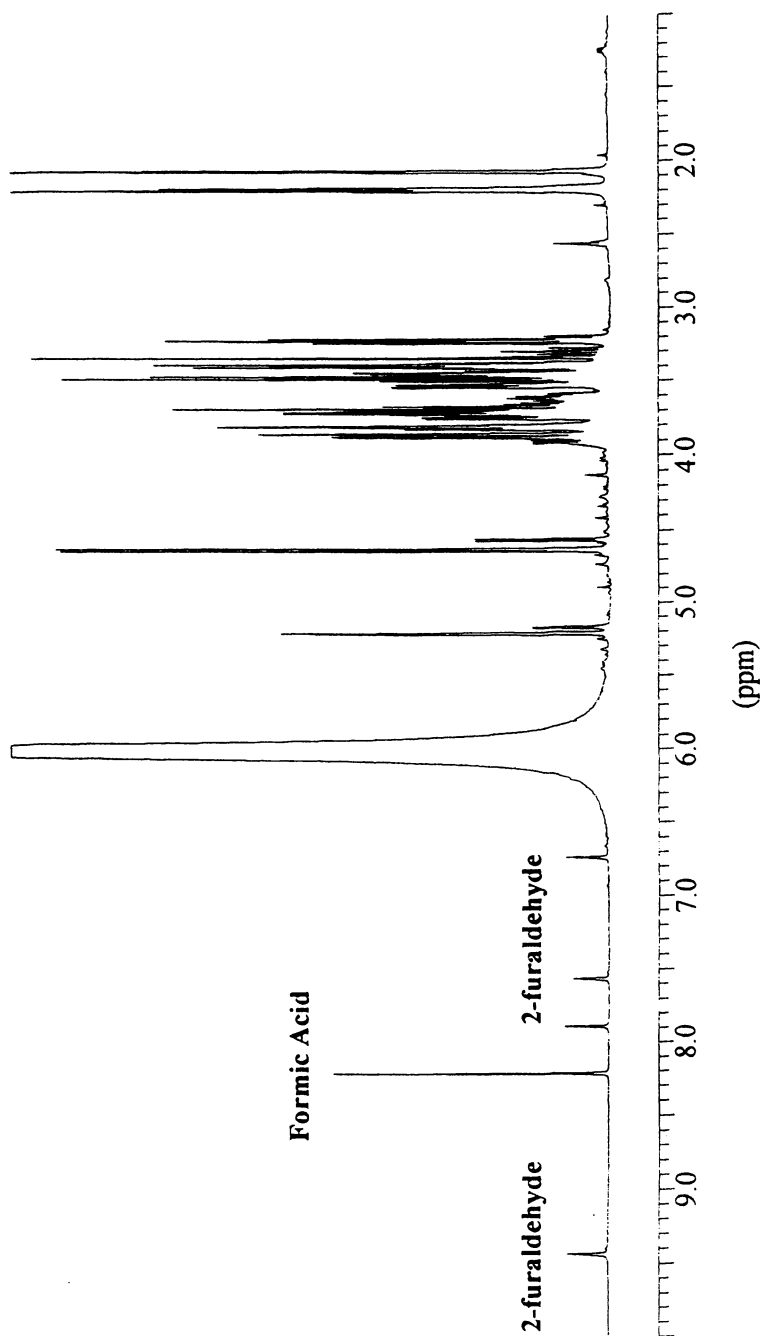


Figure 5. ^1H NMR spectrum of acid hydrolyzed willow wood. Peak at 6 ppm is due to H_2O .

To resolve this limitation of the current protocol, enzymatic digestion (19) or an acid methanolysis procedure could be employed to more completely liberate GluA (20) from polysaccharides. Since this NMR method has been developed to rapidly characterize biomass samples with minimal sample treatment, the added complexity of additional treatment or derivatization is not consistent with the objectives of the present work. It should also be noted that we have not resolved the effect of 4-O-methylation on the chemical shift of the GluA anomeric protons. Typically wood xylans contain 4-O-methyl-GluA in their structure and not unsubstituted GluA which generally occurs in microbial polysaccharides. It is anticipated that a substituent on O4 in the GlucA structure will have only a minor effect on the chemical shift of the C1 protons.

Having successfully demonstrated the utility of the NMR technique for model sugar compounds and polysaccharides, attention was focused on the characterization of wood samples. A ^1H NMR spectrum recorded for balsam fir hydrolyzate is provided in Figure 6. A summary of results for several wood samples is provided in Table VI along with "reference" values published for the same species. Good agreement exists between the NMR method and published results for the major sugars (glucose, xylose and mannose for softwoods only) while deviations may exist for sugars present in lower concentrations. Based on the repeatability data shown in Table IV, it is possible that the results determined by other techniques are not as sensitive to low sugar concentrations as NMR. For wood samples, we also observe a systematic underestimation of GlucA by our acid hydrolysis / NMR procedure (except balsam fir) as seen for isolated polysaccharides (See Table V). Since GluA underestimation is most likely the result of incomplete acid hydrolysis, it should also be noted that "observed" GluA would be linked to other sugars in an oligomer so the quantification of these other sugars would also be adversely influenced. It also appears that the NMR estimate of galactose is consistently high compared to other methods. Based on the results in Table III, however, we do not believe that this an "artifact" of the NMR method itself.

Table VI. Sugar Composition of Acid Hydrolyzed Wood Samples (% of Carbohydrate Fraction)

Sample	Glu	Xyl	Man	Gal	Ara	GluA
Sugar Maple (SM)	70.9	20.9	2.9	0.8	0.6	4.0
<i>SM - Ref (18)</i>	70.4	20.3	3.1	<0.1	1.1	6.0
Paper Birch (PB)	56.4	35.1	1.1	3.2	1.1	3.0
<i>PB- Ref. (18)</i>	56.2	34.0	2.4	0.8	0.7	6.0
Balsam Fir (BF);1	63.5	8.1	15.4	4.0	1.7	5.4
<i>BF-Ref (18)</i>	66.4	9.2	17.3	1.4	0.7	4.9
Loblolly Pine (LP)	66.6	10.6	14.1	4.2	2.2	2.4
<i>LP-Ref. (18)</i>	63.5	9.9	15.5	3.2	2.4	5.3

1. Also includes 1.9% rhamnose

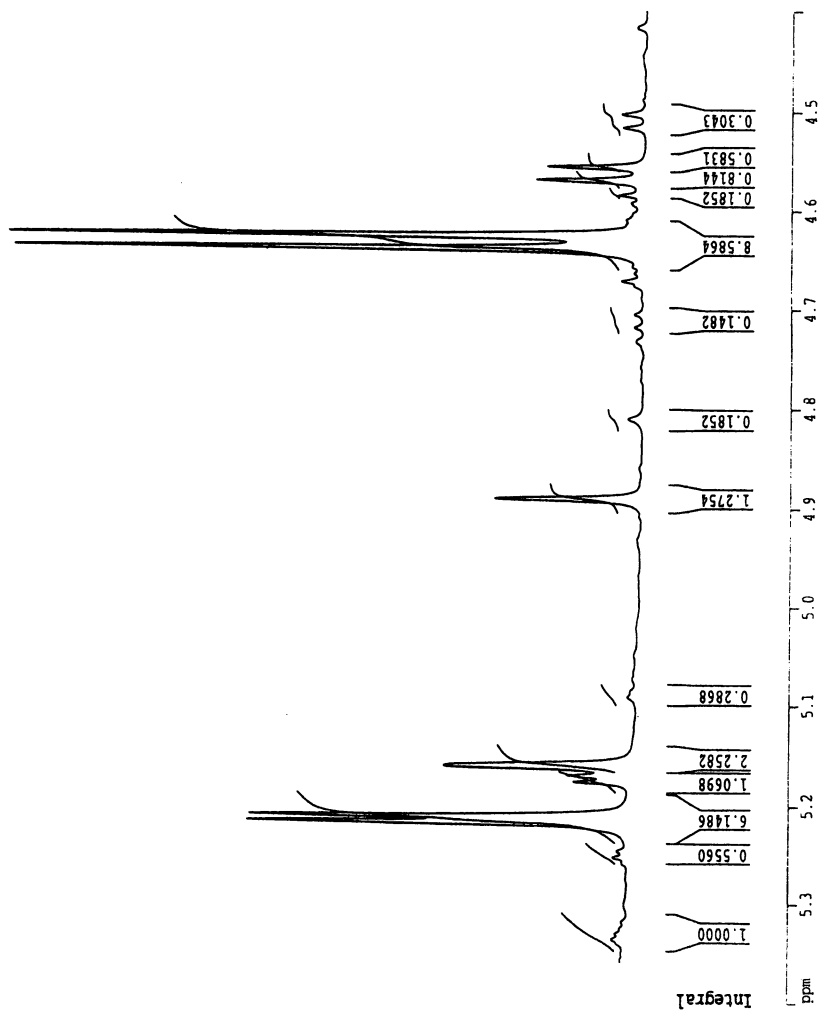


Figure 6. ¹H NMR spectrum of acid hydrolyzed balsam fir.

“Round Robin” Analysis of Woody Samples

To establish a degree of reproducibility for carbohydrate compositional analysis between several independent laboratories, three lignocellulosic samples were identified for comparison: (1) a species of shrub willow (*Salix sp.*), (2) paper birch and, (3) a recycled paper product. Three laboratories participated in this exercise: SUNY-ESF, the analytical laboratory of another academic institution designated as DC and the testing lab of a pulp / paper company denoted as AA. Each of the three laboratories utilized the same samples, their own acid hydrolysis protocol and a different method of hydrolyzate analysis. SUNY-ESF employed the NMR technique described herein, DC utilized HPLC with a refractive index (RI) detector, and AA employed HPLC coupled to a PAD detector. Results are compiled in Table VII. A comparison of these results for each sample suggests that the sugar distributions determined by ESF and AA are relatively similar while the data provided by DC, based on RI detection, differs to a greater degree. It is not possible to determine if these differences arise from the acid hydrolysis procedure or the analysis technique.

A future “round robin” is planned where each participant works with the same hydrolyzate so only the analytical techniques are compared.

“Absolute” Sugar Concentration Determination by ^1H NMR

The NMR analysis procedure discussed thus far provides a relative molar concentration of carbohydrates in the aqueous hydrolyzate resulting from the acidic saccharification of woody materials. In many cases, it is desirable to also determine the absolute concentration of sugars in a hydrolyzate, especially if the sugars are used for the production of chemicals or fuels in a subsequent process.

Table VII. Round Robin Analysis of Lignocellulosic Samples (wt % of Carbohydrate Fraction)

<i>Material</i>	<i>Glu %</i>	<i>Xyl %</i>	<i>Man %</i>	<i>Other Sugars %</i>
Willow	67	27	3	3
ESF				
AA	70	26	3	1
DC	60	18	5	17
Paper Birch	56	35	1	8
ESF				
AA	63	33	1	3
DC	58	27	3	12
Recycled Paper	77	21	2	0
ESF				
AA	80	17	2	1
DC	87	8	3	2

For absolute quantification, a known amount of a solid sugar such as rhamnose can be added to the hydrolyzate before NMR analysis, assuming that rhamnose is not present in the sample being analyzed, and the actual concentrations of other sugars can be calculated by comparing peak intensities. Alternatively, absolute concentrations can also be determined by adding a known amount of solid glucose to a specific volume of hydrolyzate sample after an initial NMR spectrum is recorded. A second spectrum is required, however, for the sample containing the extra glucose. The original concentration of glucose can then be “back calculated” based on the increase of the glucose peak intensities from spectrum 1 to spectrum 2.

Conclusions

This paper describes a new proton NMR-based method to determine the distribution of common sugars in complex mixtures such as would result from the acid hydrolysis of woody biomass containing cellulose and species specific hemicelluloses. This technique requires no sample derivatization and is very sensitive to low concentrations of certain sugars that are not well resolved by other techniques. Although the NMR analysis can easily detect and quantify glucuronic acid, the acid hydrolysis procedure employed in this study does not quantitatively liberate this sugar as a monosaccharide so its observed concentration is typically underestimated. A “round robin” analysis involving three laboratories suggests that the lab-to-lab reproducibility of sugar analysis for woody materials should be improved as renewable biomass resources are used more widely as feedstocks for new biobased industrial products.

References

1. *Biobased Industrial Products—Priorities for Research and Commercialization*; National Research Council Committee on Biobased Industrial Products; National Academy Press: Washington, DC, 2000; pp 1-14.
2. Sjostrom, E., *Wood Chemistry – Fundamentals and Applications*, 2nd ed.; Academic Press: New York, NY, 1993.
3. Stenius, P., *Forest Products Chemistry*; Papermaking Science and Technology Book 3; TAPPI Press: Gummerus Printing, Finland, 2000; pp 28-39.
4. Klass, D.L.; *Biomass for Renewable Energy, Fuels, and Chemicals*; Academic Press: San Diego, CA, 1998; pp 82-85.
5. *Analytical Methods in Wood Chemistry, Pulping and Papermaking*; Sjostrom, E.; Alen, R., Eds.; Springer Series in Wood Science; Springer-Verlag: Berlin, 1999.
6. Edwards, W.T.; Pohl, C.A.; Rubin, R.; *TAPPI Journal* **1987**, *6*, 138-140.
7. Suzuki, M.; Sakamoto, R.; Aoyagi, T; *TAPPI Journal* **1995**, *7*, 174-177.
8. Morohoshi, N.; In *Wood and Cellulosic Chemistry*, Hon, D.N.-S.; Shiraishi, N., Eds.; Marcel Dekker: New York and Basel, 1991; pp 331-392.

9. Angyal, S.J.; *Advances in Carbohydrate Chemistry and Biochemistry* **1984**, *42*, 15-62.
10. Van Halbeek, H.; *Methods In Enzymology* **1994**, *230*, 132-168.
11. Copur, Y.; Kiemele, D.J.; Stipanovic, A.J.; Makkonen, H.; *Paperi ja Puu*, **2002**, In Press.
12. Wright, P.J.; *Holzforschung* **1996**, *50* (6), 518-524.
13. Robyt, J.F.; *Essentials of Carbohydrate Chemistry*; Springer Advanced Texts in Chemistry, Springer-Verlag: New York, NY, 1998; pp 48-50.
14. Wenzl, H.F.J.; *The Chemical Technology of Wood*; Academic Press: NY, 1970; pp 169-172.
15. Halliburton Oil Services, Personnel Communication, 2001.
16. STRactan Technical Literature, St. Regis Paper Company, circa. 1980.
17. Chandrasekaran, R.; Puigjaner, R.; Joyce, L.C.; Arnott, S.; *Carbohydrate Res.* **1992**, *224*, 1-17.
18. Pettersen, R.C.; In *The Chemistry of Solid Wood*; Rowell, R., Ed.; *Advances in Chemistry Series 207*, American Chemical Society: Washington, DC, 1984, pp 115-116.
19. Tenkanen, M.; Hausalo, T.; Siika-aho, M.; Buchert, J.; Viikari, L.; *Proceedings of the 8th International Symposium on Wood and Pulping Chemistry*, Helsinki, Finland, 1995, Vol. III, pp 189-194.
20. Bertaud, F.; Sundberg, A.; Holmbom, B.; *Carbohydrate Polymers* **2002**, *48*, 319-324.

Chapter 10

Specific Antibodies for Immunochemical Detection of Wood-Derived Hemicelluloses

Arja Lappalainen¹, Maija Tenkanen², and Jaakko Pere¹

¹VTT Biotechnology, P.O. Box 1500, FIN-02044 VTT, Espoo, Finland

²Current address: Department of Applied Chemistry and Microbiology, University of Helsinki, P.O. Box 27, FIN-00014, Helsinki, Finland

Antibodies raised against wood-derived hemicelluloses can be used for chemical mapping of pulp fibres. Polyclonal antibodies were produced against cell wall carbohydrates, i.e. xylan, mannan and pectin, using both oligosaccharides coupled to BSA and polymeric carbohydrates as antigens. The antisera were checked for their specificity using ELISA techniques. In general, oligosaccharide-BSA conjugates were more antigenic and established higher affinities against the tested antigens as compared with the corresponding polymeric hemicelluloses. Applicability of the antisera was further tested on pulp fibres of known chemical composition. Labelling patterns of pulp fibres were in agreement with available information on the surface chemistry of fibres. FITC conjugate was shown to be suitable for delignified samples whereas AlexaFluor 633 label can also be used on lignin-containing material.

Native wood fibres are composed mainly of cellulose, hemicellulose, lignin and extractives. Both the pulping method and the bleaching sequence applied affect the chemical composition of fibre surfaces. The technical properties of paper, such as bonding ability, are largely governed by the surface chemistry of fibres. FTIR (Fourier Transformed Infrared Spectroscopy) and ESCA (Electron Spectroscopy for Chemical Analysis) have been applied for gross analysis of pulp and paper, but these methods do not provide information on the surface distribution of chemical components (lignin, cellulose, xylan, glucomannan, extractives) (1-4). Microscopy offers a link between chemistry and structure, with methods for distinctive and specific staining or labelling of pulp components. There exist dyes for detecting lignin (5-7) and pectin (8,9), but problems have been encountered in differentiation between the main carbohydrates, i.e. cellulose, xylan and glucomannan.

There is a clear need for a specific labelling method for carbohydrates on heterogenous fibres. Antibodies can be used as specific markers for carbohydrates. Oligosaccharides derived from xylan by acid hydrolysis (10) and from xyloglucan by cellulase hydrolysis (11) have been used as antigens for production of polyclonal antibodies. Polymeric carbohydrates have also been used as antigens for antibody production (12-14).

Xylan has a backbone of β (1 \rightarrow 4) linked xylose residues which are partially substituted in woods by α -linked 4-*O*-methylglucuronic acid and/or *L*-arabinofuranosidase residues at C-2 and at C-3, respectively. The most abundant hemicellulose in hardwood is *O*-acetyl-(4-*O*-methylglucurono)xylan, whereas arabino(4-*O*-methylglucurono)xylan forms the main part of softwood hemicellulose (15,16). Therefore, the methylglucuronic acid xylo-oligomer is one of the most characteristic units in wood xylans. During kraft pulping the structure of xylan is modified. Some of the arabinose side-groups are degraded and the MeGlcA side-groups are converted into 4-deoxy- β -*L*-threo-hex-4-enopyranosyluronic acid (hexenuronic acid, HexA) side-groups (17,18).

In this paper preparation of antigens and production as well as testing of antibodies raised against different hemicelluloses will be described and examples of their application in chemical mapping of pulp fibres will be presented. Hemicelluloses from different sources were subjected to enzymatic hydrolysis and the oligosaccharides formed were separated and coupled to a carrier protein prior to immunisation of rabbits.

Materials and methods

Hemicelluloses

The xylans used were non-substituted linear xylan from beech (Lenzing AG, Austria), 4-*O*-methylglucuronoxylan from birch (MeGlc-xylan) (Roth, Germany). Hexenuronic acid xylan (HexA-xylan) was alkali treated 4-*O*-

methylglucuronic acid xylan (19), kindly supplied by Tapani Vuorinen, HUT, Finland. *O*-Acetyl-4-*O*-methylglucuronoxylan was prepared from beechwood holocellulose by DMSO extraction (20) and kindly supplied by Jürgen Puls, BFH, Germany and arabinoxylan from oat spelts was purchased from Sigma. The mannans used were *O*-acetyl-galactoglucomannan isolated from spruce, kindly provided by Bjarne Holmbom, Åbo Akademi, Finland, acetylated glucomannan (Konjac, Megazyme) and non-substituted mannan from ivory nuts (Megazyme). Pectin from citrus peels and polygalacturonic acid (PGA) were purchased from Fluka (Switzerland) and Koch-Light (UK), respectively.

Enzymes

The enzymes needed for xylan and mannan hydrolysis originated from *Trichoderma reesei*; endo-1,4- β -xylanase I and II, β -xylosidase and endo-1,4- β -mannanase were produced and purified as described previously (21-23).

Preparation and purification of oligosaccharides

Different xylo- and manno oligosaccharides were prepared by enzymatic hydrolysis by xylanase and mannanase, respectively (Fig. 1). MeGlcAXyl₃ was prepared from 4-*O*-methylglucuronoxylan, AraXyl₄ from oat spelts arabinoxylan and Xyl₃ from linear xylan. β -Xylosidase was added in the hydrolysis of 4-*O*-methylglucuronoxylan to remove all the non-substituted xylose units from the non-reducing end of the xylo oligosaccharides. HexAXyl₃ was isolated from enzymatic hydrolysate of birch kraft pulp (24). GalMan₂ and Man₂ were prepared from locust bean gum and linear mannan, respectively. Hydrolyses were carried out in 5 mM sodium acetate buffer at pH 5 with high enzyme dosages (2000 - 10 000 nkat/g) for 48 h at 40 °C.

Oligosaccharides formed in enzymatic hydrolyses were separated by anion exchange chromatography and/or gel filtration (Fig. 2). The acidic oligosaccharides derived from xylans were isolated by anion-exchange chromatography (Dowex 1x2, Fluka) as described earlier (24,25). The fractions containing the acidic oligosaccharides were pooled, concentrated by evaporation and the salts were removed by gel filtration (BioGel P-2, Bio-Rad, USA) using water as eluent. The preparations obtained consisted mainly of tetrasaccharides, carrying either a MeGlcA (MeGlcAXyl₃) or a HexA (HexAXyl₃), respectively. Neutral oligosaccharides (AraXyl₄, Xyl₃, GalMan₂ and Man₂) were purified by gel filtration (BioGel P-2, Bio-Rad) using water as eluent. The fractions containing the oligosaccharides were pooled and lyophilised before further use. The purification of oligosaccharides was followed by TLC (26) and the purity was analysed by HPLC equipped with an anion exchange column (Carbo-Pac PA1, Dionex, USA) (26) using previously isolated oligosaccharides as

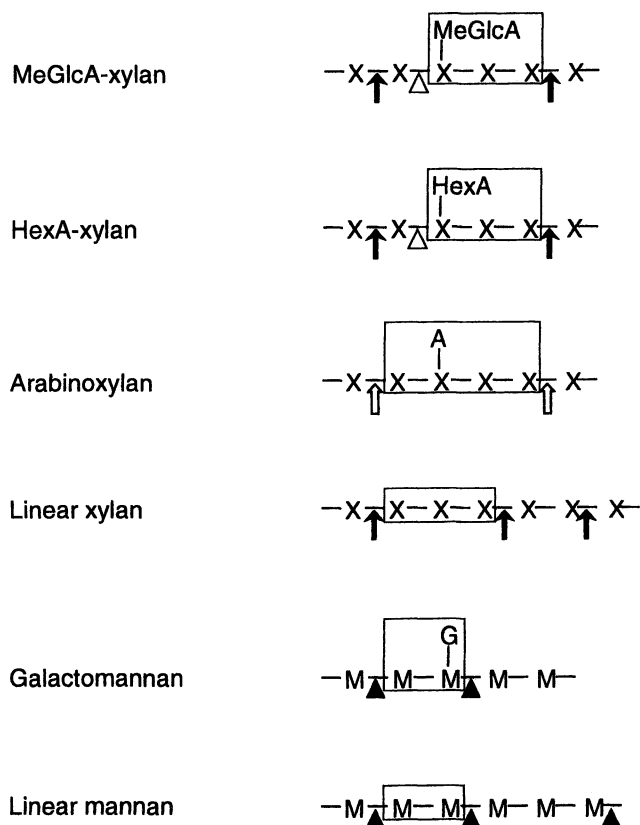


Figure 1. Enzymatic hydrolyses of different xylans (-X-X-) and mannans (-M-M-) by T. reesei enzymes. The purified oligosaccharides are shown in the boxes. Hydrolysis points of enzymes are marked: \uparrow endo-1,4- β -xylanase II, Δ β -xylosidase, \hat{v} endo-1,4- β -xylanase I, \blacktriangle endo-1,4- β -mannanase, X β -D-xylopyranose unit, M β -D-mannopyranose unit, A α -L-arabinofuranoside unit, G β -D-galactopyranose unit, MeGlcA α -D-4-O-methylglucuronic acid, HexA hexenuronic acid

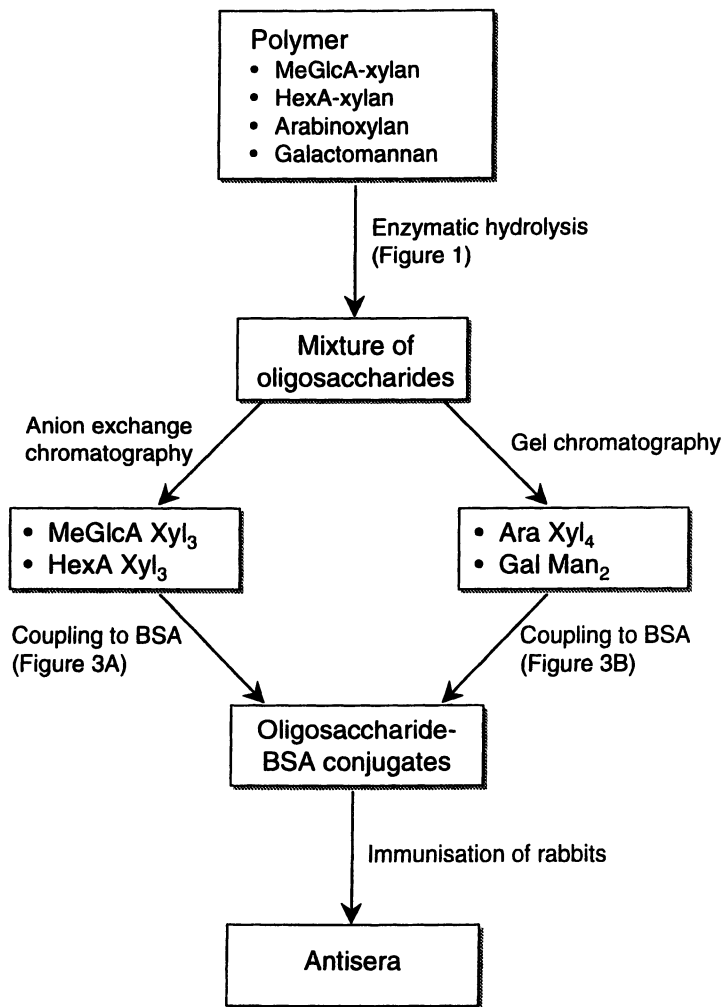


Figure 2. Preparation of antisera.

qualitative standards (25-27). The structure of AraXyl₄ was verified by ¹H NMR spectroscopy (25).

Characteristics of the poly- and oligosaccharides used as antigens are listed in Table I.

Preparation of oligosaccharide-protein conjugates

MeGlcAXyl₃ and HexAXyl₃-oligosaccharides were coupled to BSA (bovine serum albumin, fraction V, Sigma) and to OA (ovalbumin, chicken egg, Sigma) with 1-ethyl-3-(3-dimethylaminopropyl) carbodi-imide hydrochloride (EDC, Sigma) according to the method of Lönngren *et al.* (28) (Fig. 3A). The sugar-BSA and/or sugar-OA conjugates of AraXyl₄, GalMan₂, Xyl₃ and Man₂ were prepared by the method of Gray (29) (Fig 3B). Carbohydrate and protein contents in the conjugates were determined by the phenol-sulphuric acid method (30) and the Lowry method (31), respectively.

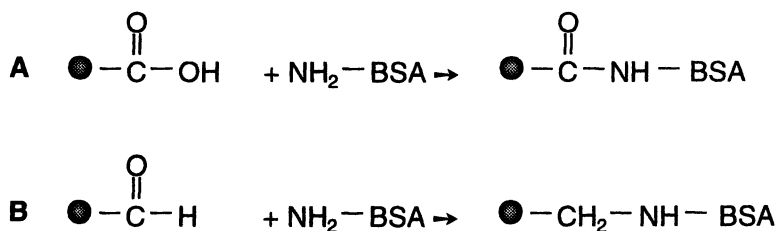


Figure 3. Preparation of antigens by coupling oligosaccharides (●) to BSA via the carboxyl group (A) or the aldehyde group (B).

Production of antibodies

Polyclonal antisera against oligosaccharide-BSA conjugates and corresponding polymeric hemicelluloses as well as pure BSA were obtained by immunisation of rabbits for 2.5 months (University of Kuopio, Finland). The antigens were emulsified with 1 ml of Freund's adjuvant (Difco Laboratories, USA) prior to injection intradermally 4-5 times into rabbits at 3 week intervals. The total amounts of antigens used were: 37 mg MeGlcAXyl₃-BSA, 35 mg HexAXyl₃-BSA, 60 mg AraXyl₄-BSA, 60 mg GalMan₂-BSA, 200 mg MetGlcA-xylan, 100 mg HexA-xylan, 36 mg Ac-glucomannan, 20 mg pectin, 17 mg polygalacturonic acid and 10 mg BSA. The sera were collected after

Table I. Poly- and oligosaccharides used as antigens.

<i>Antigen</i>	<i>Source</i>	<i>Structure</i>
<i>Xylan components</i>		
MeGlcA-xylan	Birch, commercial (Roth)	4- <i>O</i> -MeglCA groups attached to xylan backbone
HexA-xylan	Alkali treatment of MeGlcA-xylan	HexA groups attached to xylan backbone
MeGlcAXyl ₃	Enzymatic hydrolysis of MeGlcA-xylan	4- <i>O</i> -MeglCA group attached to xylotriose
HexAXyl ₃	Enzymatic hydrolysis of birch kraft pulp	HexA group attached to xylotriose
Ara Xyl ₄	Enzymatic hydrolysis of oat spelt arabinoxylan	Arabinose attached to xyloetraose
<i>Mannan components</i>		
Ac-glucomannan	Konjac, commercial (Megazyme)	Acetylated glucomannan Glucose:Mannose = 40:60
GalMan ₂	Enzymatic hydrolysis of locust bean gum	Galactose unit attached to mannobiose
<i>Pectins</i>		
Pectin	Citrus peel, commercial (Fluka)	Poly-D-galacturonic acid methyl ester
Polygalacturonic acid	Koch-Light	demethylated

centrifugation and used without further purification. Preimmune sera were collected from the rabbits prior to the first injection of antigens.

Testing of antisera

Immunodiffusion in an agar plate

Double diffusion (Ouchterony) was carried out using 1 % agar gel in 25 mM sodium diethylbarbiturate-HCl buffer, pH 8.2 (32). The antiserum (10 μ l) was placed in the center well in an agar plate. The polymeric hemicelluloses and oligosaccharide-OA conjugates (10 μ l, 1 mg carbohydrate/ml) were placed in the peripheral wells. The plate was incubated at room temperature for 24 h.

Enzyme-linked immunosorbent assay (ELISA)

The ELISA-method was applied both on nitrocellulose paper (dotblot) and on microtiter plates. Polymeric hemicelluloses, oligosaccharides cleaved thereof, oligosaccharide-OA conjugates (1 μ l, 1 mg /ml) and carrier proteins (BSA and OA, 1 μ l, 1 mg/ml) were dotted on nitrocellulose paper and probed with antibody for their reaction, identified with goat anti-rabbit IgG (Sigma) conjugated with alkaline phosphatase and finally detected by staining with a Protoblot kit (Promega, USA) (33). Microtiter plate (Nunc 96 Microwell™ plates, Nalge Nunc International, Denmark) wells were coated either with the oligosaccharide-OAs (1 μ g /well) or with the polymeric hemicelluloses (50 μ g/well) (34). Serial dilutions of the antisera were made and pipetted into wells, where they reacted with the conjugate and substrate of alkaline phosphatase for 2 hours and 30 min, respectively. Release of p-nitrophenol during the alkaline phosphatase reaction was measured at 405 nm with a Multiscan apparatus (ThermoLabsystems Oy, Finland). The absorbance values obtained were approximately ranked to four categories according to the strength of the immunoreaction: neutral \pm , minor +, medium ++ and high +++. For control purposes the reactions with OA were also checked. Some of the antisera gave a slight positive reaction with OA and this was taken into account in the evaluation of the results.

Immunolabelling of pulp fibres

Chemical (kraft) and mechanical pulp (TMP) fibres (unbleached and bleached) were obtained from Finnish pulp mills. Hemicellulose profiles on the surfaces of chemical and mechanical pulp fibres were modified by enzymatic treatments. Extensive treatments with xylanase or mannanase (5000 nkat/g) were

performed at pH 5 for 24 hours. Solubilised carbohydrates (xylan/mannan) were analysed by HPLC (35).

Immunolabelling for microscopy

Pulp fibres were preincubated in 50 mM phosphate buffered saline (PBS, pH 7.0) overnight. The fibres were blocked with 5% FCS (fetal calf serum, ICN Biomedicals, USA) in PBS for 15 min prior to incubation with the diluted antisera (1/50 in PBS + 5% FCS) for 2 h at room temperature. The fibres were washed three times with PBS + 5% FCS before incubation for 1 h at 30°C with the anti-rabbit IgG (whole molecule) conjugated to FITC (Sigma) or with AlexaFluor 633 labelled goat anti-rabbit IgG (Molecular Probes, USA).

The labelled fibres were thoroughly washed with PBS and distilled water before mounting on glass slides and examination either by fluorescence microscopy (Olympus BX50, Olympus Optical Co, UK) or by confocal laser microscopy (CLSM) (Bio-Rad 2000).

Results and discussion

Preparation of antigens

In order to obtain antibodies against most characteristic groups in the wood and pulp hemicelluloses, oligosaccharides thereof were prepared by enzymatic hydrolysis (Fig. 1). Acidic xylo-oligosaccharides carrying either MeGlcA or HexA sidegroups were isolated from the hydrolysis mixture by anion-exchange and gel chromatography (Fig. 2). The isolated MeGlcA- and HexA-xylo-oligosaccharides contained mainly tetrasaccharides. Due to the hydrolysis mechanism of *T. reesei* xylanase II a small amount of HexAXyl₂ was also present. These oligosaccharides were not further separated. The neutral oligosaccharides were purified by gel filtration. The purification of oligosaccharides was monitored by TLC and verified by HPLC analysis.

Because oligosaccharides are rather small molecules to be used as antigens, they were chemically linked to an inert carrier protein, BSA. For specificity testing of the antisera the oligosaccharides were also coupled to ovalbumin (OA) to avoid positive reactions and cross-reactivity due to antibody clones raised against epitopes in the BSA molecule.

The acidic oligosaccharides were coupled to protein through the carboxyl group (Fig. 3 A). The coupling reaction involves activation of the carboxyl group of the sugar derivative by reaction with a water-soluble carbodiimide to

give an acylisourea, which further reacts with accessible nucleophiles in the protein, e. g. ϵ -amino groups of lysine residues, forming amide linkages (peptide bonds). Neutral oligosaccharides are coupled to protein through the aldehyde group by reductive amination with cyanoborohydride (Fig. 3 B). The oligosaccharide-BSA and oligosaccharide-OA conjugates were analysed for carbohydrates prior to immunisation and testing of antisera in order to verify the adequate coupling of oligosaccharides to the carrier protein molecules. According to the results the amount of bound carbohydrates varied between 6.2 and 11.9 % (w/w).

Polymeric hemicelluloses were used for immunisation as such without coupling to a carrier protein molecule and the chemical composition or purity of the commercial polymers were not analysed.

Characterization of antisera

The antisera obtained were first tested using the double diffusion (Ouchterlony) technique. Only oligosaccharide-OAs gave weak precipitation lines against the corresponding oligosaccharide-BSA antisera (results not shown). The reaction between polymeric hemicelluloses and the corresponding antisera were too weak to give any precipitation lines. The results indicated that the double diffusion method was not sensitive enough for testing of the antisera.

Dot blot technique was also used in the preliminary testing of the antisera. The samples were dotted on nitrocellulose paper and serial dilutions of the antisera (1:25, 1:50, 1:100, 1:200) were added. Anti-oligosaccharide-BSA antisera recognised well the corresponding oligosaccharides-OAs of similar structure (results not shown), without clear cross-reactivity with other compounds tested. The reactivity of antisera raised against polymeric hemicellulose was weaker than that of the corresponding oligosaccharide-BSA conjugate. However, the results were only qualitative, because comparison of the intensities of the spots was rather difficult. This might be due to partial diffusion of the dotted polysaccharides out of nitrocellulose membranes under the experimental conditions used. Strong reaction between anti-oligosaccharide-BSA antisera and BSA alone was an indication of high antigenicity of BSA in the immunisation of rabbits as compared with the carbohydrate moiety in the oligosaccharide-BSA conjugates.

Finally, testing of the antisera was performed in microtiter plates using the ELISA method. The antisera were tested for their reactivity against their own antigen as well as against other hemicellulosic oligosaccharides linked to ovalbumin and solely against polymeric hemicelluloses (Table II). All antisera recognized well their own antigen, but a few of them cross-reacted slightly with other cell wall components. Antisera raised against BSA-linked xylo-

Table II. Specificity of the antisera against wood-derived components as determined by ELISA.

<i>Tested compound</i>	<i>Antisera against</i>									
	MeGlcA-xylan	HexA-xylan	MeGlcA-Xyl ₃	HexA-Xyl ₃	Ara-Xyl ₄	Ac-gluco-mannan	Gal-Man ₂	Pectin	PGA	
<i>Xylans</i>										
MeGlcA-xylan	+	+	+	+	±	-	-	-	-	-
HexA-xylan	+	+	+	+	±	-	-	-	-	-
Ac-gluconoxylan	-	-	±	±	-	-	-	-	-	-
MeGlcAXyl ₃	+	++	+++	++	++	-	++	±	±	-
HexAXyl ₃	±	+	+++	++	++	-	++	-	-	-
Ara Xyl ₄	-	-	-	±	+	-	-	-	-	-
Xyl ₃	-	-	+	+	+	-	-	-	-	-
<i>Mannans</i>										
Ac-glucomannan	+	+	-	-	+	+++	+	-	-	-
Ac-galactoglucomannan	-	-	-	-	-	+	+	+	±	-
GalMan ₂	+	±	-	-	±	-	+++	-	-	-
Man ₂	±	-	-	-	±	-	-	-	-	-
<i>Pectins</i>										
Pectin	+	+	-	-	-	-	-	+++	++	++
PGA	+	+	-	-	-	-	-	-	++	++

oligosaccharides showed higher *in vitro* affinities in ELISA than those raised against xylan polysaccharides.

The reactivity of the anti-MeGlcAXyl₃ was strong and it recognised well xylotriose and the polymeric xylans in addition to its own antigen (MeGlcAXyl₃). Cross-reactivity was further tested by labelling experiments on pulp fibres. Unfortunately, antisera against HexA-xylan and HexAXyl₃-BSA were not specific, and they were highly cross-reactive with anti-MeGlcAXyl₃. Labelling of hexenuronic acids on oxygen and hydrogen peroxide bleached TCF pulp was unsuccessful and a similar labelling pattern as with anti-MeGlcAXyl₃ was obtained on ECF kraft pulp, which did not contain hexenuronic acid groups in the xylan (18). One reason to cross-reactions between anti-MeGlcAXyl₃-BSA and anti-HexAXyl₃-BSA might be that the linkage from oligosaccharide to BSA was via the carboxyl group (Fig. 3A) and not via the aldehyde group. Therefore methylglucuronic acid and hexenuronic acid groups could not act as free and intact epitopes during immunisation. For some reason the reactions of anti-AraXyl₄ antiserum were unsatisfactory and it recognised other oligosacchrides (MeGlcAXyl₃ and HexAXyl₃) better than its own antigen (AraXyl₄). Furthermore, anti-AraXyl₄ antiserum also gave reactions with mannans. Thus, specific antisera for each sidegroup present in xylans could not be produced.

Interestingly, anti-GalMan₂ gave a slight positive reaction with MeGlcAXyl₃, perhaps due to a conformational similarity. However, no labelling was observed on bleached birch kraft fibres which contain only minute amount of glucomannan, whereas in similar conditions bleached softwood kraft fibres were intensively labelled (results not shown).

Some confusion in the results might have been due to different binding affinities of the tested compounds, i.e. oligosaccharide-OA conjugates versus polysaccharides, on plate material. The OA conjugates were expected to bind accurately on the well bottoms, but binding of polymeric hemicelluloses might have been more variable and evidently depended on the nature of the polymeric hemicellulose.

Preimmune sera and anti-BSA sera did not give positive reactions with any of the tested components.

Application to immunolabelling of fibre surfaces

In the next phase the antisera were tested for their specificity and applicability in immunolabelling of pulp fibres of known chemical composition. Extensive enzymatic removal of the target hemicellulose, with a xylanase or mannanase, prior to labelling was used to check the intensity of labelling as compared with intact fibres. Commercial anti-rabbit IgGs conjugated either to FITC or to AlexaFluor 633 were used as fluorescent dyes for labelling of delignified bleached kraft fibres and lignified mechanical pulp fibres, respectively. The conjugate carrying AlexaFluor 633 was used to avoid

autofluorescence from lignin and the fibres were examined under a CLSM supplied with an argon laser. Anti-MeGlcAXyl₃ was the most potential for immunolabelling of xylan on fibre surfaces. When performed on native birch pulp fibres, the fibres were rather evenly labelled (Fig. 4a). After the xylanase treatment and removal of 25% of original xylan the overall intensity of the label was significantly decreased, indicating clearly the sensitivity of the antibody to the amount of xylan on the fibre surface (Fig. 4b). No labelling of fibres was detected either with the preimmune serum or when the primary antibody was omitted from the labelling procedure (results not shown).

The extent of xylan labelling varied to some extent between individual fibres; some fibres were labelled faintly and their neighbours more intensively. In the latter case the label was not distributed evenly on fibres, but more intense labelling was observed on deformed parts of fibres, e.g. around kinks and nodes (Fig. 4a). This might be due to true chemical variation on different parts of the fibres or to variation of accessibility of xylan to the antibody. Softwood kraft fibres were also labelled with anti-MeGlcAXyl₃, but the labelling intensity was weaker than with hardwood fibres (results not shown). This is in keeping with surface chemistry, because the surface of softwood kraft fibres contains less xylan than hardwood fibres (18).

Xylan oligosaccharides coupled to BSA gave rise to antisera with higher affinity for both isolated antigens (in ELISA) and polymeric hemicellulosics on fibres. This is exemplified in Figures 4a and 4c for anti-MeGlcAXyl₃ and anti-xylan antibody in the labelling of xylan on birch fibres.

According to the ELISA test anti-PGA also reacted slightly with different xylans and galactomannan in addition to different pectins, which might be due to contamination in the commercial PGA preparation used. However, anti-PGA did not show any labelling when tested on softwood kraft pulp fibres, which contained low amounts of pectin but were rich in xylan and glucomannan. On unbleached TMP fibres, anti-PGA antisera together with AlexaFluor 633 resulted in intense labelling of pectin around pits of spruce fibres (Fig. 5a). Contrary to the distribution of pectin, glucomannan on bleached TMP fibres (spruce) was revealed as dispersed and dotted areas on fibre surfaces when labelled with anti-GalMan₂ -antibody (Fig. 5b).

In this work the main attention was paid to producing polyclonal antisera against characterised oligosaccharides derived from different hemicelluloses to be used in chemical mapping of pulp fibres. The reason for this strategy was that polymeric carbohydrates are not very antigenic, and the specificity of an antiserum against a polymeric antigen is difficult to determine. Specificity testing of anti-oligosaccharide-BSA antisera with ELISA worked rather well and the authenticities of the observed cross-reactions were further tested with pulps of defined chemical composition. In general, labelling of fibres was in agreement with the available information on fibre surface chemistry. However, thorough evaluation of the specificity of the antisera is a key issue in obtaining reliable results when the antisera are applied on complex fibrous substrates.

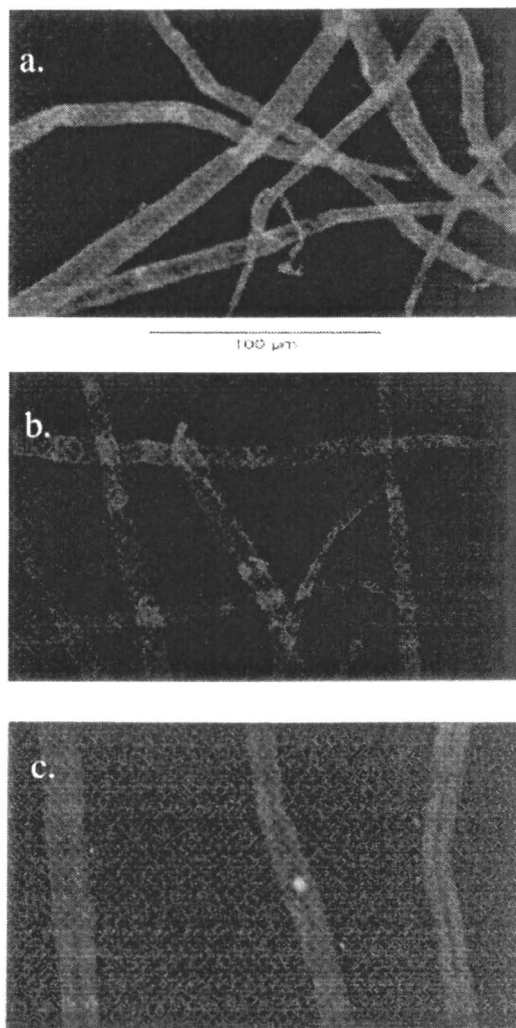


Figure 4. Immunolabelling of bleached birch kraft pulp with anti-MeGlcAXyl₃ prior to (a) and after removal of 25% of original xylan by extensive xylanase treatment (b) and after labelling with anti-xylan antibody (polymeric xylan as antigen) (c). FITC was used as the fluorescent conjugate.

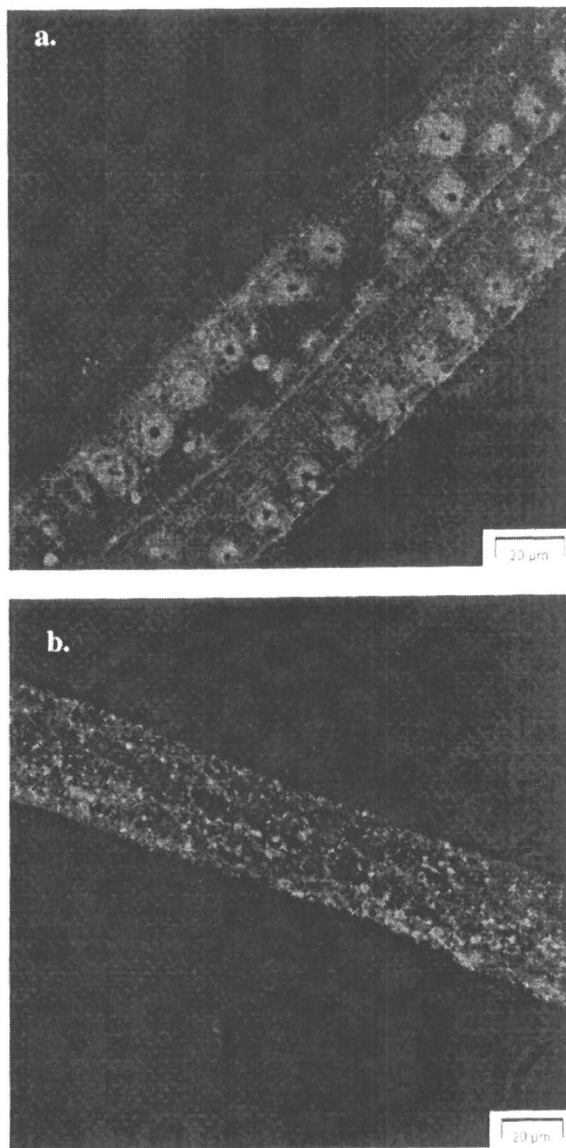


Figure 5. Labelling of pectin (a) and glucomannan (b) on unbleached (a) and bleached (b) spruce TMP fibres with anti-PGA antibody (a) and anti-GalMan₂ antibody (b), respectively, using AlexaFluor 633 as the fluorescent conjugate.

Acknowledgements

The authors thank Mariitta Svanberg for microscopical work and Maija Tikka for technical assistance. Anita Teleman is thanked for NMR analysis and Marjukka Perttula for HPLC analysis. The work was partially financed by the National Technology Agency (Tekes).

References

1. Sweeny, K. *Tappi J.*, **1989**, *72*, 171-174.
2. Laine, J., Stenius, P., Carlsson, G.; Ström, G. *Cellulose* **1994**, *1*, 145-160.
3. Johansson, L.-S., Campbell, J.M., Koljonen, K.; Stenius, P. *Appl. Surface Sci.*, **1999**, *144-145*, 92-95.
4. Ristolainen, M., Alén, R., Malkavaara, P.; Pere, J. *Holzforschung*, **2002**, *56*, 513-521.
5. Bland, D., Foster, R.; Logan, A. *Holzforschung*, **1971**, *25*, 137-142.
6. Fergus, B.; Goring, D. *Holzforschung*, **1970**, *24*, 118-124.
7. Gurr, E.; *The rational use of dyes in biology*; Leonard Hill, London, UK, 1965.
8. Jensen, W.; *Botanical histochemistry*; W. H. Freeman & Co, San Francisco, CA, 1962.
9. Reeve, R.; *Stain Technol.* **1959**, *26*, 209-211.
10. Takahashi, N.; Sumiya, K. *Wood Res.* **1990**, *77*, 8-17.
11. Sone, Y.; Sato, K. *Biosci. Biotech Biochem.* **1994**, *58*, 2295-2296.
12. Moore, P. J. In *Modern Methods of Plant Analysis*, Liusklus, T.; Jarkoon, A., Eds.; Plant Fibers, New Series, Springer-Verlag, Berlin, Germany, 1989, Vol 10, pp. 70-88.
13. Knox, J. P., Lindstead, P. J., King, J., Cooper, C.; Roberts, K. *Planta* **1990**, *181*, 512-521.
14. Westermark, U.; Vennigerholz, F. In: The 8th International Symposium on Wood and Pulping Chemistry, June 6-9, Helsinki, Finland, Proceedings, Vol I, 1995, 101-106.
15. Shimizu, K. In: *Wood and Cellulosic Chemistry*, Hon, D. N.-S.; Schiraishi, N.; Eds, Dekker, New York, USA, 1991, pp. 177-214.
16. Sjöström, E. In: *Wood Chemistry: Fundamentals and Applications*, Academic Press, New York, 1993, pp. 140-161.
17. Teleman, A., Harjunpää, M., Tenkanen, M., Buchert, J., Hausalo, T., Drakenberg, T.; Vuorinen, T. *Carbohydrate Res.* **1995**, *272*, 55-71.
18. Buchert, J., Teleman, A., Harjunpää, V., Tenkanen, M., Viikari, L.; Vuorinen, T. *Tappi J.* **1995**, *78*, 125-130.
19. Teleman, A., Hausalo, T., Tenkanen, M.; Vuorinen, T. *Carbohydr. Res.* **1996**, *280*, 197-208.

20. Hägglund, E., Lindberg, N.; McPherson, J. *Acta Chem Scand.* **1956**, *67*, 1160-1164.
21. Tenkanen, M., Puls, J.; Poutanen, K. *Enzyme Microb. Technol.* **1992**, *14*, 566-574.
22. Poutanen, K.; Puls, J. *Appl. Microbiol. Biotechnol.* **1988**, *28*, 425-432.
23. Stålbrand, H., Siika-aho, M., Tenkanen, M.; Viikari, L. *J. Biotechnol.* **1993**, *29*, 229-242.
24. Teleman, A., Siika-aho, M., Sorsa, H., Buchert, J., Perttula, M., Hausalo, T.; Tenkanen, M. *Carbohydr. Res.* **1996**, *293*, 1-13.
25. Teleman, A., Harjunpää, V., Hausalo, T., Sorsa, H., Viikari, L.; Tenkanen, M., In: *Biotechnology in the Pulp and Paper Industry*, Srebotnik, E.; Messner, K.; Eds.; Proc. 6th Int. Conf. Biotechnology in the Pulp and Paper Industry, Facultas-Universitätsverlag, Vienna, Austria, 1996, pp. 131-134.
26. Tenkanen, M.; Siika-aho, M. *J. Biotechnol.* **2000**, *78*, 149-161.
27. Tenkanen, M., Makkonen, M., Perttula, M., Viikari, L.; Teleman, A. *J. Biotechnol.* **1997**, *57*, 191-204.
28. Lönngrén, J., Goldstein, I. J.; Niederhuber, J. E. *Arch. Biochem. Biophys.* **1976**, *175*, 661-669.
29. Gray, G. R. *Methods in Enzymol.* **1997**, *50*, 155-160.
30. Dubois, M., Gilles, K. A., Hamilton, J. K. Rebers, P. A.; Smith, F. *Anal. Chem.* **1956**, *28*, 350-356.
31. Lowry, O., Rosebrough, N. H., Parr, A.L.; Randell, R. J. *J. Biol. Chem.* **1951**, *193*, 265-275.
32. Mancini, G., Carbonara, A. O.; Heremans, J. F. *Immunochemistry* **1965**, *2*, 235-254.
33. Towbin, H., Staehelin, T.; Gordon, J. *Proc. Natl. Acad. Sci. U.S.A.* **1979**, *76*, 4350-4354.
34. Engvall, E.; Perlman, P. *J. Immunol.* **1972**, *109*, 129-135.
35. Buchert, J., Siika-aho, M., Bailey, M., Puls, J. Valkeajärvi, A., Pere, J.; Viikari, L. *Biotechnol. Techn.* **1993**, *7*, 785-790.

Chapter 11

Isolation and Properties of Xylan: Rediscovery and Renewable Resource

Robert H. Marchessault

Department of Chemistry, McGill University, 3420 University, Room 201,
Montreal, Quebec H3A 2A7, Canada

In the past 50 years wood chemists have learned much about the composition and physical properties of hardwood xylans. Partially acetylated glucuronoxylans are model native hardwood xylans. They exhibit thermoplasticity, film forming properties, crystallization potential and are oriented in the secondary cell wall. Their crystal structure has been determined and the hydration of this crystalline polysaccharide has been defined. The structural regularity of these abundant polysaccharides can be interpreted using the principle of optical superposition.

Introduction

In 1943 the Chemistry Department at McGill University set a strong course for the study of carbohydrates and wood polysaccharides when Clifford B. Purves became E.B. Eddy Professor of Industrial and Cellulose Chemistry at McGill, and Director of Wood chemistry research in the Pulp & Paper Research Institute of Canada. About ten years later he was joined by Dr. T.E. Timell from Sweden and hemicellulose analysis prevailed for the next decade. Timell focused his attention on wood hemicellulose and generously collaborated with the writer since he was a consultant for American Viscose Corp. where I was employed. My immediate superior was Dr. Wayne Sisson and his experience in x-ray diffraction on cellulose organic polymers encouraged me to learn that technique and apply it to wood hemicelluloses (1,2).

American Viscose was the dominant rayon company at the time and well-purified dissolving grade wood cellulose was constantly improved thanks to fundamental research on methods of carbohydrate analysis. Purves had originally studied at St. Andrews University where Haworth, Hirst, Purdy and Irvine pioneered the methylation techniques which were essential for chemical structure determination.

The rayon business eventually went through a serious downturn and investment in fundamental research related to cellulose and its purification were neglected. Today, in the Green Chemistry era, sustainability concepts and focus on renewable resources means that natural polysaccharides such as xylan are being rediscovered not only in wood but also in all kinds of biomass. In essence, biomass is destined to be a source of carbon for the world's plastics industry. The search for sustainability will promote this replacement.

Molar Rotation of Xylans

Since the days of Pasteur and Freudenberg, the value of optical rotation: $[\alpha]_D$, as a means of characterizing polysaccharides has been appreciated. Timell isolated and purified glucuronoxylans and arabinoxylans to provide a series of samples whose optical rotation could be recorded in 10% aqueous sodium hydroxide. Figure 1 is a schematic of the molecular structure of the 4-O-methylglucuronoxylans which he isolated with a variable content of uronic acid. Figure 1 also shows the Equation which we used to account for the observed molar rotation of xylans (3).

As can be seen in Figure 2 the plots of reduced molar rotation for the fractions which varied in their xylose/aldobiuronic ratio are linear. However, the slope for the arabinoxylans and glucuronoxylans are of opposite sign, in keeping with the different chemistry of the uronic acid linkage and the arabinose to the xylan backbone. In both cases the slope represents the molar rotation of the disaccharide unit in the chain (3) and since the α -D-configuration of 4-O-methylglucuronosyl xylose is well established, the opposite slope favors the assignment of a α -L-configuration for the arabinosyl xylose unit, which is known to contain an L-arabinofuranose sugar.

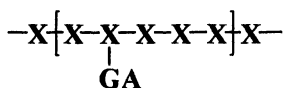
These linear plots are essentially physical proofs of structure of the respective polysaccharides and can be used for analytical purposes. Someone once referred to the Equation in Figure 1 as the "Marchessault equation" which I accept humbly but in fact the derivation follows directly from the teachings of C.S. Hudson and K. Freudenberg, used for proof of structure of cellulose. However, the optical rotation of the neutral xylan chain, derived from these data, is much greater than that of cellulose.

Crystalline Structure and Conformation of a (4-O-methylglucuronoxylan)

Since native xylans are partially acetylated they dissolve in water and can be cast into flexible films. Strips of these films were hot-stretched into oriented fibers and deacetylated with alkaline methanolic solutions to obtain x-ray fiber diagrams from which to derive a unit cell and observe the pitch of the xylan chain along the fiber axis. Figure 3 shows the derived left-handed helical conformation of the chain corresponding to 3 residues per turn within a distance of 14.85Å (4). The handedness of the pitch was further confirmed as improved x-ray fiber diagrams became available. The structure responsible for this fiber diagram is a xylan dihydrate and in fact glucuronoxylans are water sensitive and take up increasing amounts of water with relative humidity. The baseplane of the unit cell of xylan hydrate is shown in Figure 4 where the hexagonal unit cell is built around a column of water. The opening shown by the circle in Figure 4 most likely can accommodate the randomly occurring uronic acid substituents so that the latter co-crystallize, as it were, with the xylan chain in the unit cell. Nevertheless, this was not part of our proposed hydrate unit cell which is shown in Figure 5 with the helical hydrogen bonded water chain (5).

The pronounced susceptibility of xylan to hydration is nature's method of plasticizing and the random acetyl groups assist further by preventing crystallization. Polarized infrared spectroscopy provided evidence that the xylan chains are oriented along the tree axis and one can conclude that this is equivalent to axial orientation in the fiber. (6)

The schematic in Figure 6, illustrates the proposed crystalline and non-crystalline state of xylan in the S2 layer of fibers. The crystalline xylan state develops when deacetylation happens without xylan removal or when epitaxial



Let:

- n be number of unsubstituted xylose units
 m be molar rotation of xylose unit
 u be molar rotation of aldobiuronic acid
 σ be (xylose / aldobiuronic) ratio
 ϕ be the molar rotation of a xylan chain with a ratio σ

$$\frac{\phi}{n(1 + 1/\sigma)} = \frac{m \cdot n + u \cdot n/\sigma}{n(1 + 1/\sigma)} = [\alpha]_D \left(132 + \frac{190.35}{\sigma + 1}\right)$$

Figure 1. Schematic of glucuronoxylan chain segment and optical superposition equation to fit the observed rotation $[\alpha]_D$ to glucuronic acid content.

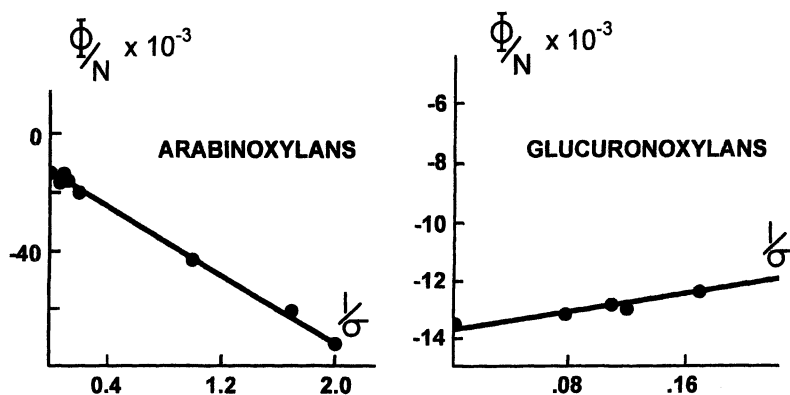


Figure 2. Reduced molar rotation plot as a function of $1/\sigma$ for arabino and glucuronoxylans. (Adapted from ref. 3)

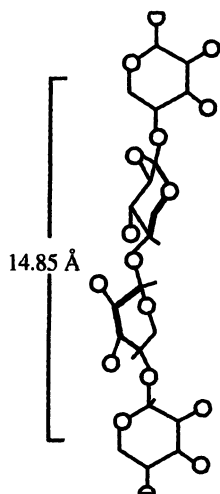


Figure 3. Crystalline conformation of threefold symmetry helix, 3, xylan hydrate chain with 14.85 Å pitch. (.Adapted from ref. 4)

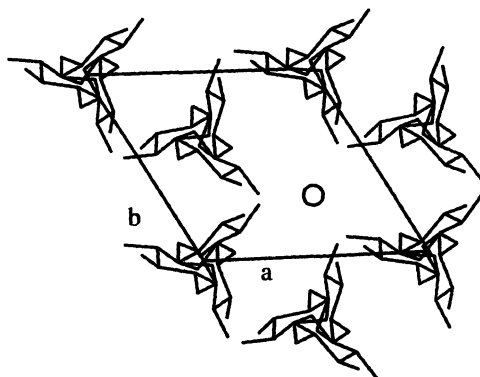


Figure 4. Baseplane unit cell projection of white birch xylan hydrate. The unit cell is indexed as hexagonal: $a=b=9.16 \text{ \AA}$; c (fiber axis) = 14.85 \AA . The circle represents the position of the water column.(By permission from ref. 5)

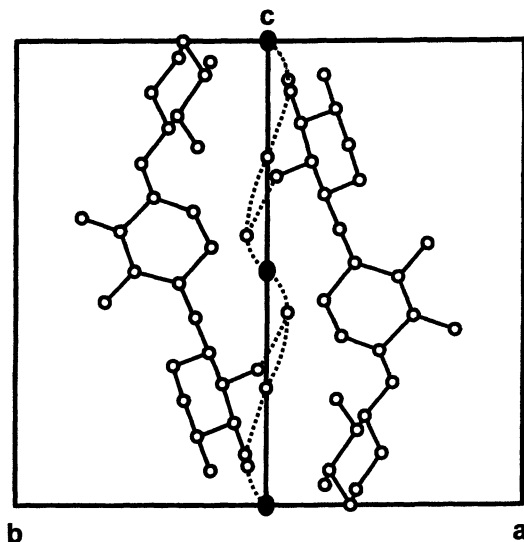


Figure 5. Projection of lefthanded 3, helices of xylan hydrate onto 110 plane. Helical dotted line represents hydrogen-bonded water chain. Twofold rotation axes, relating antiparallel chains, are shown. (By permission from ref. 5)

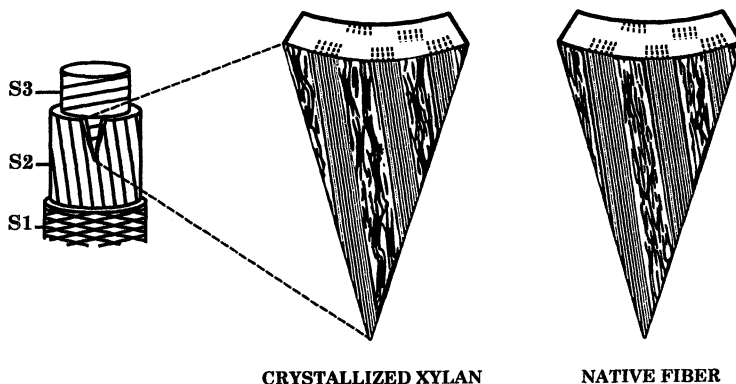


Figure 6. Schematic of oriented xylan in secondary wall of hardwood xylan for native state and crystalline state. (Adapted from Ph.D. thesis of W.J. Settineri, College of Forestry, Syracuse N.Y. , 1966)

crystallization of xylan, due to redeposition, happens during pulping. Different extents of these two organizations can exist in wood depending on history of the material and location.

Thermoplasticity of Xylan

Perhaps the closest approach to a true “native xylan from wood” has been the native O-acetyl xylan from hardwood which is extracted from a holocellulose with dimethyl sulfoxide. A sample extracted from white birch and having: one 4-O-methyl glucuronic acid group and 3.6 acetyl per 10 xylose units, served to make films whose thermoplasticity was studied. The number average molecular weight was 25,000 g/mol and it is assumed that a linear chain is involved. By drying a 10-20% aqueous solution on a glass plate, a flexible film is obtained which can be used for stretching into oriented filmstrips or for study of thermoplasticity (7). A differential thermal analysis study shows that this film (7), conditioned to room relative humidity, displays endothermic behavior over a broad temperature range from 60 to 225°C with a maximum at 150°C.

Since the x-ray diffraction pattern of the starting film is essentially non-crystalline, both before and after heating, it can be assumed that the change in chemical composition is not great and that one is witnessing the disappearance of water from the xylan hydrate non-crystalline state. The large endotherm in the DTA curve is most probably related to a distinct softening point for the xylan film which is shown in the thickness-temperature curve in Figure 7. This curve was recorded with a commercial apparatus where the sample is in contact, under pressure, with the thermostat oil and the weight loss, between 15-20% by weight, is mainly due to loss in water.

The thermoplasticity phenomenon was also displayed by the arabinoglucurono-xylan films from white pine, but the latter were far more extensible than the native O-acetyl counterparts from white birch. For example, while the white birch O-acetyl xylan could extend no more than 50%, the white birch samples readily allowed up to 200% stretch. There is little doubt that the heterogeneity of the xylans hinders crystallization but the well-established fact that hydrated and dry crystalline states exist should help to understand many of the unusual features of these materials.

Conclusions

Polysaccharides have found a wide range of value-added uses. Similarly, starch as an easily isolated pure high molecular weight substance is used industrially both as a fermentation substrate and as a macromolecular substance. Up to now, hemicelluloses have not achieved this same usage. The low

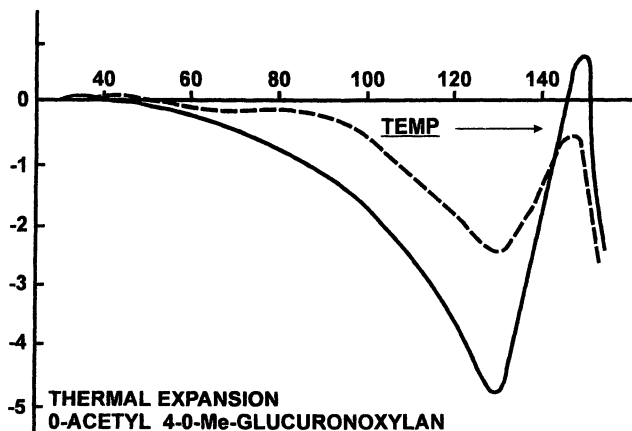


Figure 7. Thickness – temperature curves for *O*-acetyl-4-*O*-methyl glucuronoxylans. Plasticity develops at “flow point”. (Adapted from ref. 7)

molecular weight has been a handicap and the heterogeneity of structure also. Nevertheless, as a carbon source, these features are less important. Hemicelluloses have been studied as a substrate for fermentation and it is estimated that the substrate cost for use in producing the bacterial polyester: poly(3-hydroxybutyrate), PHB, would be similar to that of cane molasses and half that of bulk glucose (8).

The development of enzymatic methodology for chemical modification of polysaccharides offers promise of preparing value-added oligomers of xylan. These oligomers custom made to act as macromonomers, could contribute a new “green” family of chiral polymer building blocks.

Acknowledgments

The writer is pleased to recognize the important contribution of T.E. Timell (9).

References

1. Marchessault, R.H.; Timell, T.E. *J. Phys. Chem.* **1960**, 43, 85-100.
2. Bowering, W.D.S.; Marchessault, R.H.; Timell, T.E. *Svensk Papperstidn.* **1961**, 64, 191-194.
3. Marchessault, R.H.; Holava, H.; Timell, T.E. *Can J. Chem.* **1963**, 41, 1612-1618.

4. Settineri, W.J.; Marchessault, R.H. *J. Polymer Sci.* **1965**, C-11, 253-264.
5. Nieduszynski, I.A.; Marchessault, R.H. *Biopolymers* **1972**, 11, 1335-1344.
6. Marchessault, R.H.; Liang, C.Y. *J. Polymer Sci.* **1962**, 59, 357-378.
7. Marchessault, R.H. In *Chimie et Biochimie de la Lignine, de la Cellulose et des Hemicelluloses*; Les Imprimeries Réunies de Chambéry, France, **1964**, pp. 287-301.
8. Ramsay, J.; Hassan, A.M-C.; Ramsay, B. *Can. J. Microbiol.* **1995**, 41 Supplement 1, 262-266.
9. Timell, T.E., *Adv. in Carb. Chem.* **1964**, 19, 247-299; *ibid* **1965**, 20, 410-482.

Chapter 12

Contribution of the Molecular Architecture of 4-*O*-Methyl Glucuronoxylan to Its Aggregation Behavior in Solution

Johannes P. Roubroeks¹, Bodo Saake², Wolfgang G. Glasser³,
and Paul Gatenholm¹

¹Biopolymer Technology, Department of Materials and Surface Chemistry,
Chalmers University of Technology, SE-412 58, Göteborg, Sweden

²Institute of Wood Chemistry and Chemical Technology of Wood, Federal Research
Centre of Forestry and Forest Products, 21031 Hamburg, Germany

³Department of Wood Science and Forest Products, Virginia Polytechnic
and State University, Blacksburg, VA 24061-0323

Alkali extracted glucuronoxylan from aspen wood, showed a polydisperse fractionation pattern after size exclusion chromatography. The glucuronic acid distribution along the chain showed that sparsely substituted glucuronoxylan chains contributed to aggregate formation while removal of lignin moieties decreased aggregation. It was observed that glucuronoxylan contained both bound-and unbound lignin. The unbound lignin was mainly syringyl in the erythro form.

1. Introduction

There has been a considerable interest in the interactions between different polymeric constituents of the cell wall. In the approximation of comparing wood to reinforced composites, the fibrillar skeleton of cellulose is embedded in an amorphous matrix, consisting of lignin and hemicellulose (Frey-Wyssling, 1968)(1). Both the cellulose skeleton and the matrix have an enormous impact on chemical, physical and mechanical properties.

In recent literature, it has been emphasized that the cell wall design is basically a helicoidal pattern analog to cholesteric order (Roland et al., 1987; Satiat-Jeunemaitre, 1987; Neville, 1993)(2,3,4). The helicoidal wall pattern and its consolidation have been extensively described by Reis et al. (1994)(5). The tight interaction between glucuronoxylan and cellulose with colloidal gold labelling (Reis et al., 1992)(6) confirms the occurrence of a charged coat, along the microfibrils that is likely to play an important role in assembly. The existence of chemical linkages between lignin and hemicelluloses have been suggested (Watanabe et al., 1993; Košíková and Ebringerová, 1994) (7,8), and the interaction between hydrophobic and hydrophilic moieties creates possibilities for the design of functional nanostructures according to the concept of supramolecular assembly (Akiyoshi et al., 2000) (9).

The major component of the secondary walls of dicotyledons is glucuronoxylan. They constitute 20-35% of the dry weight of woody tissues (Zinbo and Timell, 1965)(10). Glucuronoxylans are composed of a linear backbone of (1-4)- β -linked xylopyranosyl residues, substituted with short mobile side chains. This could be α -glucuronic acid (or its methyl ester) mainly at O-2. The distribution of these side groups is in average one per ten xylose residues (Jacobs et al., 2002)(11). Native glucuronoxylan is acetylated in O-2 and/or O-3 and the acetyl content is around 70% (Aspinall, 1980; Carpita and Gibeaut, 1993)(12,13). The degree of substitution determines the solubility of the polymer and also affects the capability of interact with other polymers (Reis et al., 1994)(5). The molecular properties of xylans from various wood species have been elucidated by static light scattering experiments (Goring and Timell, 1969) (14). These authors already reported about the colloidal character of the xylan solution. The tendency for xylans to form associated material in aqueous solutions was also reported by Blake and Richards (1971)(15). Solubility of xylans in water containing salts, in comparison to dissolution in organic solvents like DMSO or THF have shown that light scattering signals were removed or shifted and the distribution of xylan became more Gaussian than in the water system (Glasser et al., 2000; Saake et al., 2001)(16,17). The amphiphilic behaviour of glucuronoxylans can also be derived from the hypothesis that glucuronoxylan could play a key role in the twisted morphogenesis of the cell

walls (Nieduszinski and Marchessault, 1972; Reis et al., 1994)(5,18). It has been suggested that during the secondary wall deposition, when cellulose and glucuronoxylan meet in the periplasm, glucuronoxylan probably acts as a surfactant around the microfibrils allowing their assembly in cholesteric mesophase (Reis et al., 1994)(5). Helicoidal morphogenesis and the lignification process are correlated (Eriksson et al., 1988; Vian et al., 1992)(19,20). The anisotropic construction of cellulose-glucuronoxylan can form a host structure for lignin precursors. Due to internal electrostatic repulsion, gaps appear and lignin can be inserted which leads to neutralisation of the anionic environment and interactions can be established (Reis et al., 1994)(5). In a study performed by Joseleau and Gancet (1981)(21) it was shown that the enzymatic degradation of xylan initiated a depolymerization of lignin which was completed by mild alkaline hydrolysis and this suggests a possible position of glucuronoxylan as a crosslinking agent between lignin blocks.

Lignin carbohydrate complexes (LCC) as introduced by Björkman (1952)(22) contain both, hydrophilic carbohydrates and more hydrophobic lignin. The formation of a micelle based on LCC has been suggested by Yaku et al. (1979)(23). The interaction between lignin and carbohydrate determines the formation of micelles.

We have been working with alkali extracted glucuronoxylan from aspen wood (*Populus tremula*) (Gustavsson et al., 2001)(24), for a considerable time and extensive chemical analysis of its components has been performed (Gustavsson et al., 2001; Teleman et al., 2000; Dahlman et al., 2000; Jacobs et al., 2002)(11,24,25,26). Preliminary results which showed that glucuronoxylan in solution had a colloidal appearance and its peculiar behaviour in solution has led to the hypothesis that high molecular weight glucuronoxylan entities observed in size exclusion chromatography represents aggregates. We therefore aim to fractionate the assumed heterogeneous glucuronoxylan preparation into more distinct molecular entities and to understand how the different fractions influence the solubility.

2. Materials and Methods

2.1 Materials

Aspen wood chips (*Populus tremula*) were obtained from Rockhammars Bruk (Frövi, Sweden) and ground in an 8-inch Sprout Waldron 105-A refiner.

After a prehydrolysis step (0.05 M HCl, pH 1.4, 2h at 70°C), the solution was cooled to room temperature and adjusted to pH 10.2 with ammonium hydroxide. After a sequential extraction with ammonium hydroxide, alkaline ethanol and alkaline water (both at room temperature and elevated temperature (70°C), the filtrates were bleached (50% H₂O₂, 2 days, 40°C). After ultrafiltration and spray drying a glucuronoxylan with a weight average molecular weight (\overline{M}_w) of 15,700 g/mol was obtained (Glasser et al., 2000; Gustavsson et al., 2001)(16,24).

2.2 Carbohydrate analysis

The carbohydrate composition (neutral carbohydrates and uronic acid residues) was determined by the use of enzymatic hydrolysis and a subsequent capillary zone electrophoresis as described elsewhere (Dahlman et al., 2000)(26). The amount of lignin was determined gravimetrically and spectrophotometrically (Kaar and Brink, 1991)(27).

2.3 High-Performance Size Exclusion Chromatography combined with Multiple Angle laser Light Scattering detection

For the separation of glucuronoxylans in the water system a HPSEC-UV-MALLS-RI system consisted of a Waters 2690 with online degasser, autosampler and column oven (Waters Milford, MA, USA) and two serially connected columns (TSK gel G6000 WXL and TSK gel GMPWXL, TosoHaas, Stuttgart, Germany) were used. The eluent was 0.1 M NaNO₃ containing 0.01% NaN₃ at 0.5 ml/min. Detectors were refractive index (Optilab DSP, Wyatt Technology Corp., Santa-Barbara, CA, USA), UV monitor (Shimadzu SPD-10A/vp, Shimadzu Corp. Kyoto, Japan) and multi angle laser light scattering (MALLS; Dawn DSP equipped with a He-Ne laser at 632.8 nm, Wyatt Technology Corp., Santa-Barbara, CA, USA). Columns and RI detector were controlled at 50°C.

Samples (typically 2.0-2.5 mg/ml) were filtered (0.45 µm) before injection of 100 µl. Data for molecular weight determination was analysed using ASTRA software (version 4.73.03, Wyatt Technology Corp., Santa-Barbara, CA, USA) based on a dn/dc of 0.110.

In the DMSO-water system (90:10) with 0.05 M LiBr, three serially connected columns were used: Gram 30, 100 and 3000 (PSS). The detector

system consisted of a UV detector (PLLC 1200), and a RI detector (Shodex RI-71). The flow rate was 0.4 ml/min at 60°C. Molecular weights were calculated from the viscosity and RI-signals by universal calibration using pullulan standards.

2.4 pH-fractionation

Glucuronoxylan (1g) was weighed into a 75 ml tube with 50 ml 0.5 M NaOH (pH 13.47). After extraction (16 h, room temperature), the material was centrifuged (2500 rpm, 20 min) and the supernatant decanted and adjusted to pH 13 with 0.5 M HCl. This procedure was followed for each step, decreasing the pH scale by a value of 0.5. The final supernatant was dialysed (cut-off 10,000) and freeze dried. All pellets obtained during the fractionation were air dried and analysed for weight average molecular weight and glucuronic acid content by MALDI-TOF-MS and Capillary Zone Electrophoresis.

2.5 Lignin extraction

A total volume of 43 mL pyridine/HAc/H₂O (9:1:4) was added to a sample of glucuronoxylan (1g). After extraction under continuous stirring for 1h at room temperature, the sample was centrifuged at 4000 rpm and the supernatant decanted. The pellet was treated once more with a similar volume of the extractant. The supernatants were combined and chloroform was added (1:1.3). After separation of the chloroform phase, the water phase was washed once more with a similar volume of chloroform. The chloroform phases were combined and all phases were dried by rotavaporation. To remove pyridine from the phases, all fractions were sequentially washed by ethanol-toluene-ethanol, adapted from Lundquist et al. (1990)(28).

2.6 ¹H-NMR

NMR spectroscopy was performed on a Varian VXR 300 S spectrometer (Varian Inc., Palo Alto, CA, USA) operating at 25°C. The dried chloroform phase was acetylated with pyridine and acetic acid anhydride. After extensive washing with ethanol, toluene and ethanol, diethyl ether was applied which rendered the acetylated material insoluble while contamination could be

removed. The dried material (0.5 mg) was dissolved in 0.7 mL CDCl_3 (δ_{H} 7.26 ppm) was used as internal reference.

3. Results and Discussion

3.1 Fractionation of glucuronoxyylan

Glucuronoxyylan was dissolved in aqueous media (0.1 M NaNO_3) and organic solvent (DMSO/ water) and applied to size exclusion chromatography in combination with refractive index and multi-angle laser light scattering detection (SEC-RI-MALLS). The elution profile of glucuronoxyylan dissolved in 0.1 M NaNO_3 (Figure 1A) shows three populations by RI-detection. A low molecular weight fraction at $V_e = 21.8$ mL, and two fractions at $V_e = 19.3$ mL and $V_e = 15.3$ mL with approximate equal polymer concentration. Light scattering detection observes a signal at the lowest elution volume ($V_e = 14.4$ mL) while the other two signals fail to produce a light scattering response. The separation into distinct fractions by SEC is unusual for polymers, but has been repeatedly described with heteropolysaccharides and other polyelectrolytes. This separation could be caused by a molecular weight distribution, differences in charge density or the ability to aggregate.

Differences in charge density and the propensity to aggregate can be eliminated or reduced by examining the elution behaviour in a non-aqueous solvent. When glucuronoxyylan was dissolved in DMSO/water (9:1) the RI response shows a Gaussian distribution (Figure 1B). A similar observation was made by Glasser et al. (17) where a multi-peak xylan mixture by SEC has a uniform molecular weight distribution as a THF soluble derivative (hydroxypropylated). It should be noted that the column system is different and therefore a direct comparison with the elution volume scale in figure 1A is not possible. Moreover, the DMSO dissolved fraction scatters light and therefore the \overline{M}_w could be calculated. The value 15,582 g/mol, is in good agreement with the \overline{M}_w 15,700 g/mol determined by SEC-MALDI-TOF-MS (Gustavsson et al., 2001)(26). More interesting however, is the combination of SEC with RI- and UV detection (Figure 1A,B). Glucuronoxyylan in 0.1 M NaNO_3 (Fig. 1A) shows that all previous described fractions with RI response show a UV response. The fraction with $V_e = 19.3$ mL relates to an UV signal which appears as a shoulder in a larger signal ($V_e = 19.3$ mL and 20.7 mL respectively). However, this larger

amplitude has no apparent RI response. This might be explained with the molar extinction coefficient. The UV absorbing substance appears to be very low in concentration, but it contains entities with a high molar extinction coefficient and therefore this entity contributes more to the UV signal. Whether the fraction at $V_e = 21.8\text{mL}$ has a corresponding UV signal is difficult to determine. There seems to be some overlap, but it fails to have an exact match. The opposite effect, a relatively high concentration of a UV absorbing substance with a low molar extinction coefficient, could be responsible for this peak. The two fractions, $V_e = 15.3\text{mL}$ and 19.3mL , carry both carbohydrate and a UV absorbing substance. We can therefore conclude that two complexes occur with widely varying molecular weight and also one UV fraction alone. When DMSO was used as a solvent (Fig. 1B) the shoulder at 18 mL (19.3 mL in Fig. 2A) has increased and the UV signal at 14.8 mL has disappeared. This might be interpreted as a close attachment of the UV absorbing substance to the carbohydrate which now moves into a more Gaussian distribution. The UV signal at 19.6 mL (20.7 mL in Fig. 1A) has also increased somewhat, and we can therefore conclude that the UV absorbing signal at 14.8 mL in Fig. 1A has been redistributed into fractions at $V_e = 18.0\text{ mL}$ and 19.6 mL (Fig. 1B). The UV absorbing material is most likely lignin. The role of lignin impurities in aggregation phenomena has already been suggested by Saake et al. (2001)(17). The lignin content in untreated hardwoods amounts to 18-22% (Puls and Schuseil, 1993)(29), whereas the residual lignin in the alkaline extracted and bleached aspen glucuronoxylan was determined to be 5% (Gustavsson et al., 2001)(24).

The possibility of an interaction between glucuronoxylan and lignin could give rise to aggregation behaviour in solution. However, one could not rule out the contribution of H-bonding between polysaccharide chains. We therefore perform a fractionation of the heterogeneous glucuronoxylan structure.

3.2 The effect of intermolecular H-bonding on aggregate formation

In this experiment the glucuronoxylan was dissolved in 0.5 M NaOH ($\text{pH}_{\text{begin}} 13.47$) and the pH was decreased in steps of 0.5 . The pellets that were obtained after fractionation were dried and analysed by capillary zone electrophoresis (CZE) and MALDI-TOF-MS. The results are shown in Figure 2. Those steps where no pellet was obtained are omitted. It can be observed that a decrease in pH corresponds to an increase of the glucuronic acid content. It appears that the unsubstituted xylan chains, the least acidic fractions, are selectively removed in the earlier stages of the pH fractionation. These sparsely substituted xylan chains are expected to be responsible for the intermolecular H-bonding in solution, as has been observed for cellulose chains. Furthermore it

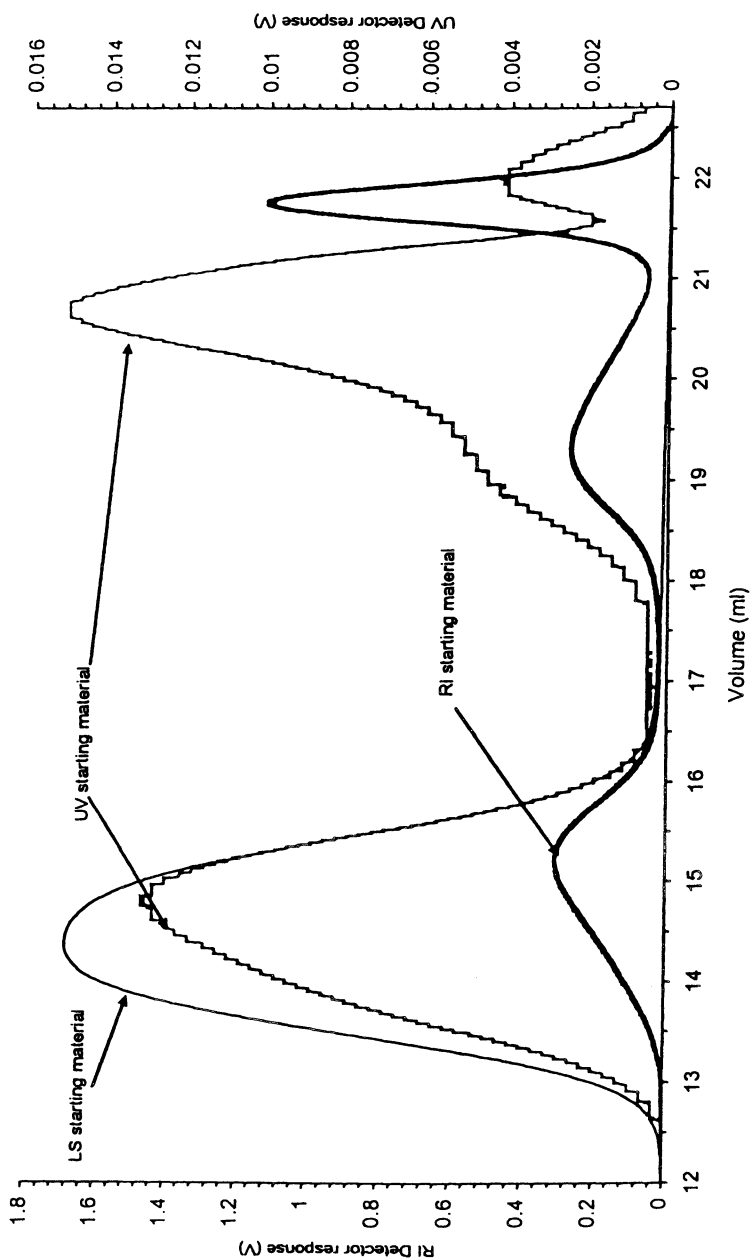


Figure 1A: SEC-UV-MALLS-RI of the aspen glucuronoxylan in 0.1 M NaNO_3

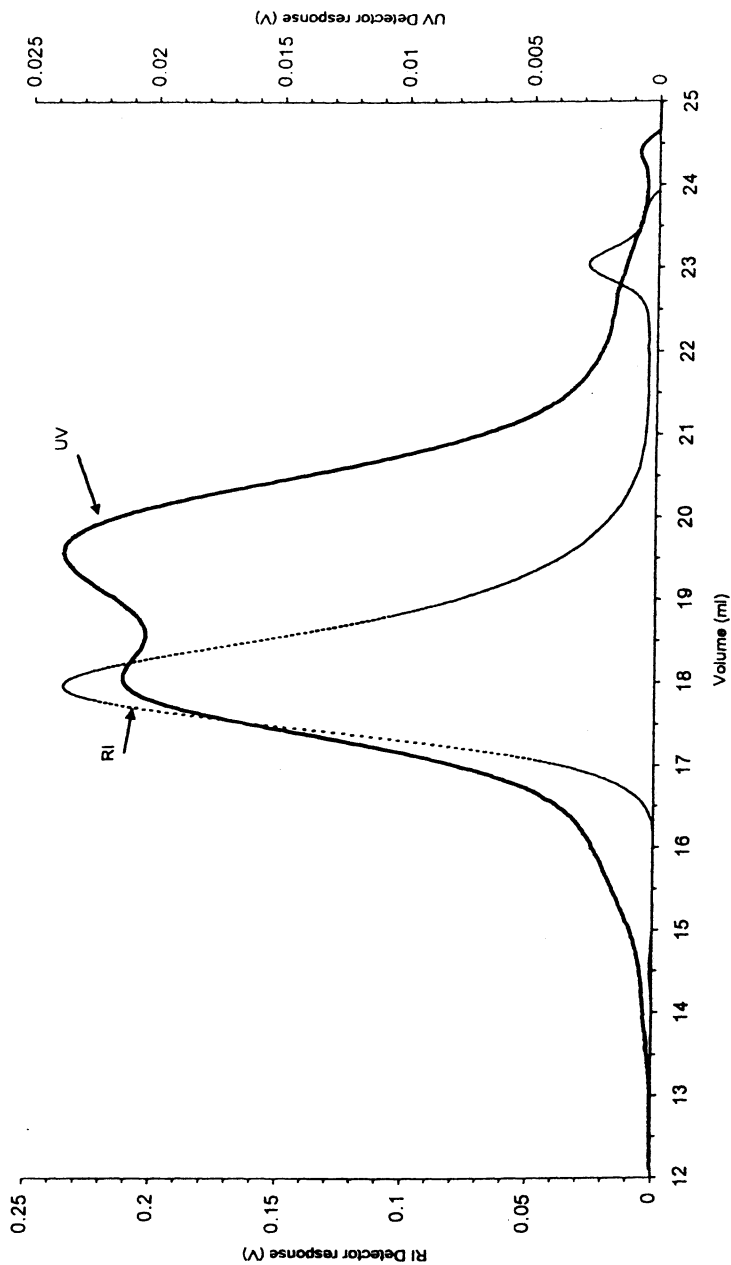


Figure 1B: SEC-UV-Ri of aspen glucuronoxylan in DMSO/water (9:1)

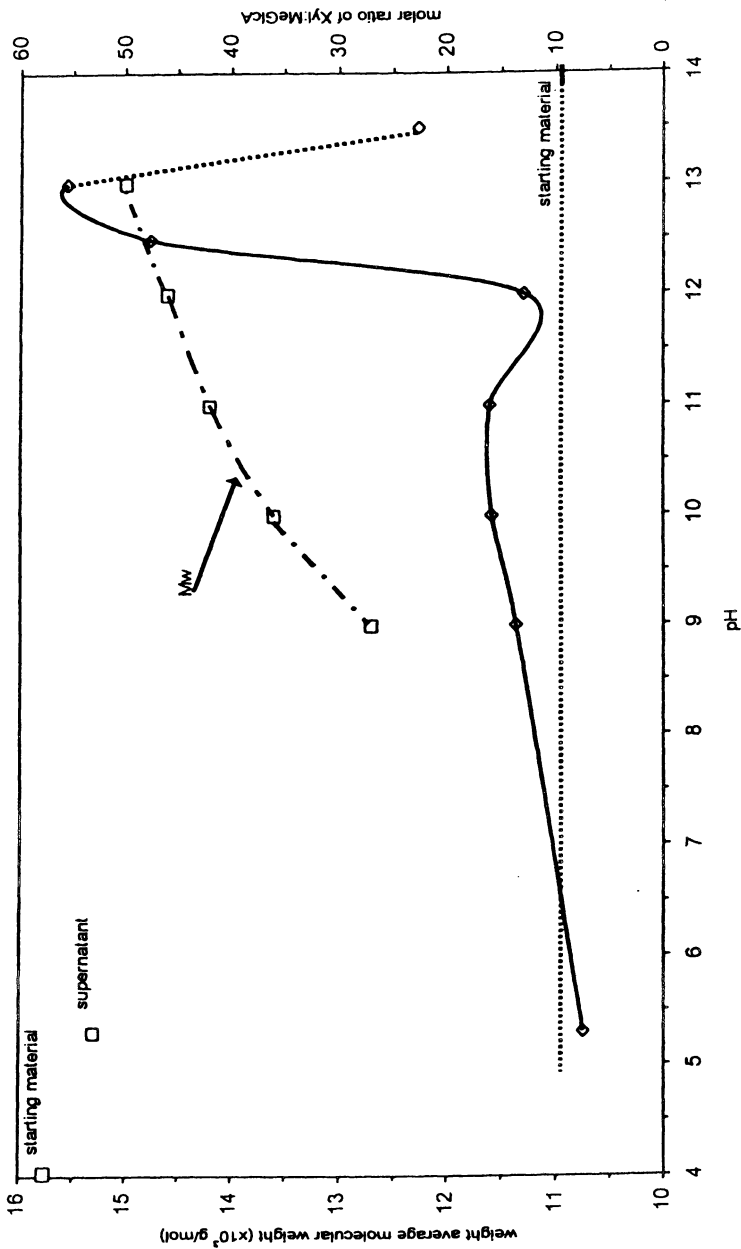


Figure 2: pH fractionation of aspen glucuronoxylan. The dotted line represents the glucuronic acid content of the starting material.

can be seen that the glucuronic acid content in the final extraction step is slightly higher than the glucuronic acid content in the starting material. This might be interpreted as an enrichment of those structures that have a higher substitution degree. The starting glucuronoxylan is heterogeneous in fine structure, but through the procedure of pH fractionation, the remaining fraction have become more homogeneous.

The sample with a molar ratio of Xyl:MeGlcA of 22.7 at pH 13.5 is not really part of the pH fractionation, since this represents the pellet that is not soluble in 0.5 M NaOH. It also appears as if the molecular weight is decreasing with increasing glucuronic acid content, but the molecular weight of the supernatant is close to the molecular weight of the starting material. This indicates the heterogeneity of the sample. The fraction which fails to precipitate pH<9 is displayed after SEC-MALLS in Figure 3. The starting material shows the familiar three populations by RI of which only the highest molecular weight scatters light (see also Fig. 1A). Following pH fractionation, the pH<9 soluble material (with the highest glucuronic acid content) has the same populations, with the exception that the fraction at highest elution volumes in the starting material has been eliminated, possibly by fractionation or dialysis. Only the population with the highest molecular weight displays light scattering and has increased in intensity. The shoulder which develops in the RI signal at $V_e=14$ mL could be responsible for this increase in the light scattering signal. It could be suggested that removal of the sparsely substituted xylan chains results in enrichment of the xylan chains with higher glucuronic acid substitution and since the UV signal appears to shift to lower elution volumes (the peak coincides with the shift in RI) there appears to be a more pronounced effect of the substances that absorb UV. This indicates that aggregate formation is not mainly influenced by intermolecular H-bonding. A positive side effect is that the refractive index signal for the contamination at low molecular weight has disappeared. This is probably due to the fractionation or the extensive dialysis. Since intermolecular H-bonding does not seem to contribute directly to aggregate formation, it was suggested that lignin moieties are responsible for this effect.

3.3 Lignin extraction

The presence of 5% lignin as determined by Gustavsson et al. (24) and the shift of lignin to higher elution volumes on size-exclusion chromatography, when the elution in DMSO was compared to elution in 0.1 M NaNO₃, resulted

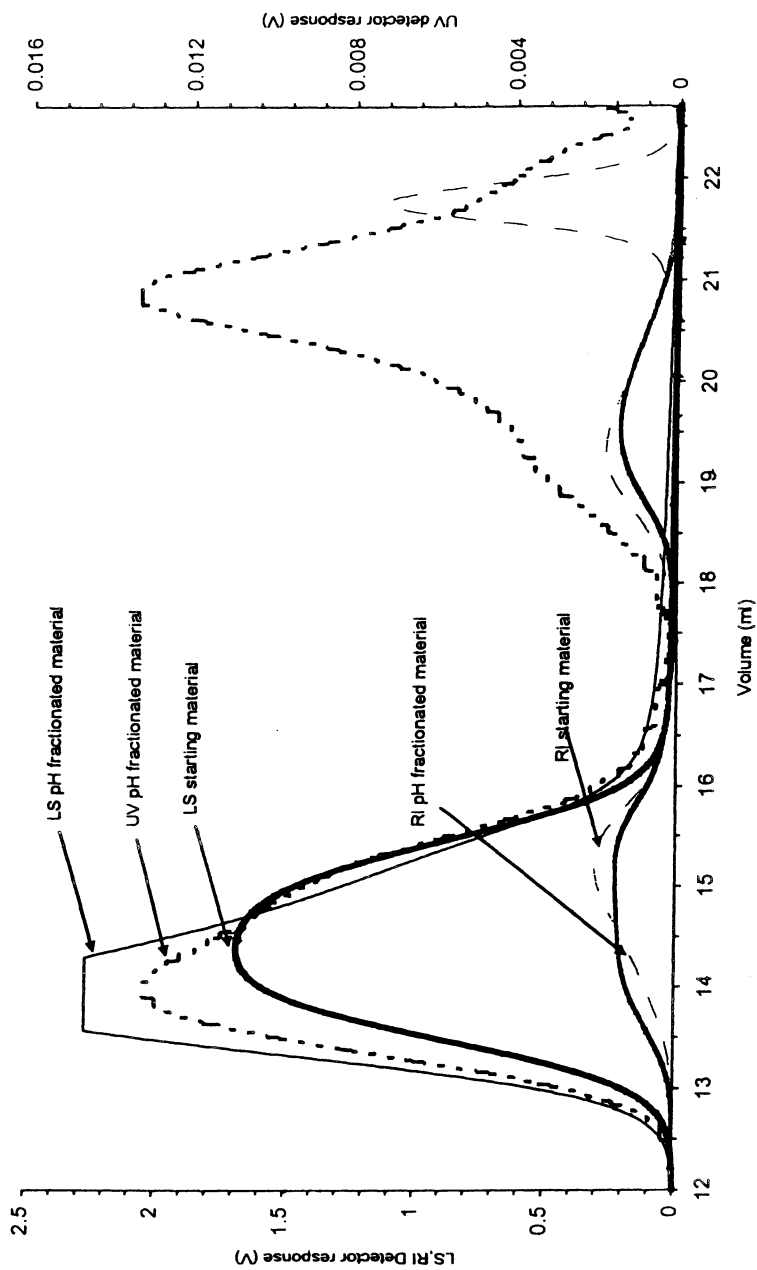


Figure 3: SEC-RI-MALLS of the supernatant after pH fractionation in comparison to the starting material

in the attempt to extract lignin by the use of solid-liquid extraction, followed by a liquid-liquid extraction.

The glucuronoxylan was extracted twice with a mixture of pyridine/HAc/H₂O. The residue contained 90.9% of the starting material. The supernatant was separated with the aid of chloroform and a pyridine- and a chloroform phase were obtained. After washing and extensive drying the pyridine fraction (6.0%) was shown to contain low molecular weight fragments of xylan with possibly some connected lignin as indicated by FT-IR. The chloroform fraction (3.1%) however, contained mainly lignin and possibly some extractives. It was observed that the bands at 1500-1510, 1465 and 1425 cm⁻¹ were relatively strong, which indicated a larger contribution of the lignin moiety. The acetylated lignin was identified by ¹H-NMR (Figure 4). Signals were assigned according to the literature (Lundquist, 1992)(30). The signal at 1.94 ppm derived from aliphatic acetate and at 2.13 ppm derived from benzylic acetate in erythro forms of β-O-4 structures of syringyl ether type, as well as a signal at 6.58 ppm and 6.0 ppm, belonging to aromatic protons in syringyl and erythro forms respectively, could indicate that the lignin has a high syringyl content in the erythro form, which has been identified previously in aspen wood (Bardet et al., 1998)(31).

The elution profile of glucuronoxylan after lignin extraction is depicted in Figure 5. In comparison to the starting material (Figure 1A), there is a slight decrease in the RI signal and somewhat shifted to higher elution volumes. This fraction is still detected by LS, although there seems to be an apparent shift of the position of the peak maximum to lower elution volumes. Also notable is that the populations detected by RI have decreased from three to two, with the fraction at $V_e=21.8$ mL eliminated. The largest change occurs in the UV signals. (a) reduction of the signal at $V_e=14.8$ mL to a more pronounced polydisperse fraction with a peak at $V_e=13.9$ mL and a shoulder at $V_e=15.7$ mL (b) The shoulder in the UV signal of the starting material at $V_e=19.3$ mL has developed into a peak which closely follows the RI signal. On the other hand, there is the UV signal at $V_e=20.7$ mL which has disappeared almost completely. This might indicate that some lignin can be removed, lignin that appears to be 'unbound' and some lignin that remains in close vicinity of the carbohydrate; lignin that is 'bound'. The results are consistent with the hypothesis that glucuronoxylans occur as mixtures of molecules containing both a copolymer architecture with 'bound' lignin and 'unbound' extractable lignin. The lignin-glucuronoxylan complex has a \overline{M}_w of 15.700 g/mol and it associates to particles with a \overline{M}_w of 1.7×10^7 that scatter light. This shows that the aggregation number is higher than 1000. The 'unbound' lignin might be able to participate in the aggregate formation and this might be the effect that is observed (UV signal) with solvent exchange of aqueous to non-aqueous in Figure 1B.

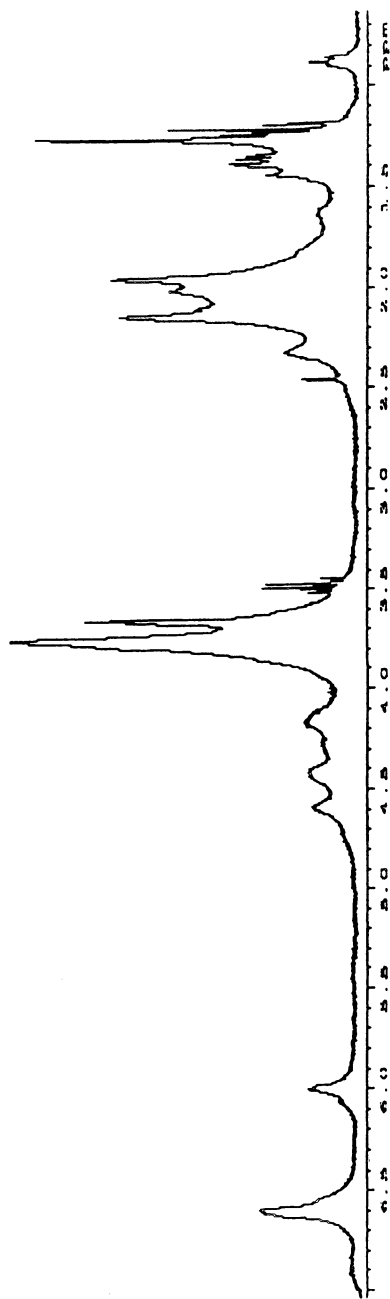


Figure 4: $^1\text{H-NMR}$ of lignin isolated from aspen. The lignin is acetylated and CDCl_3 was used as an internal standard

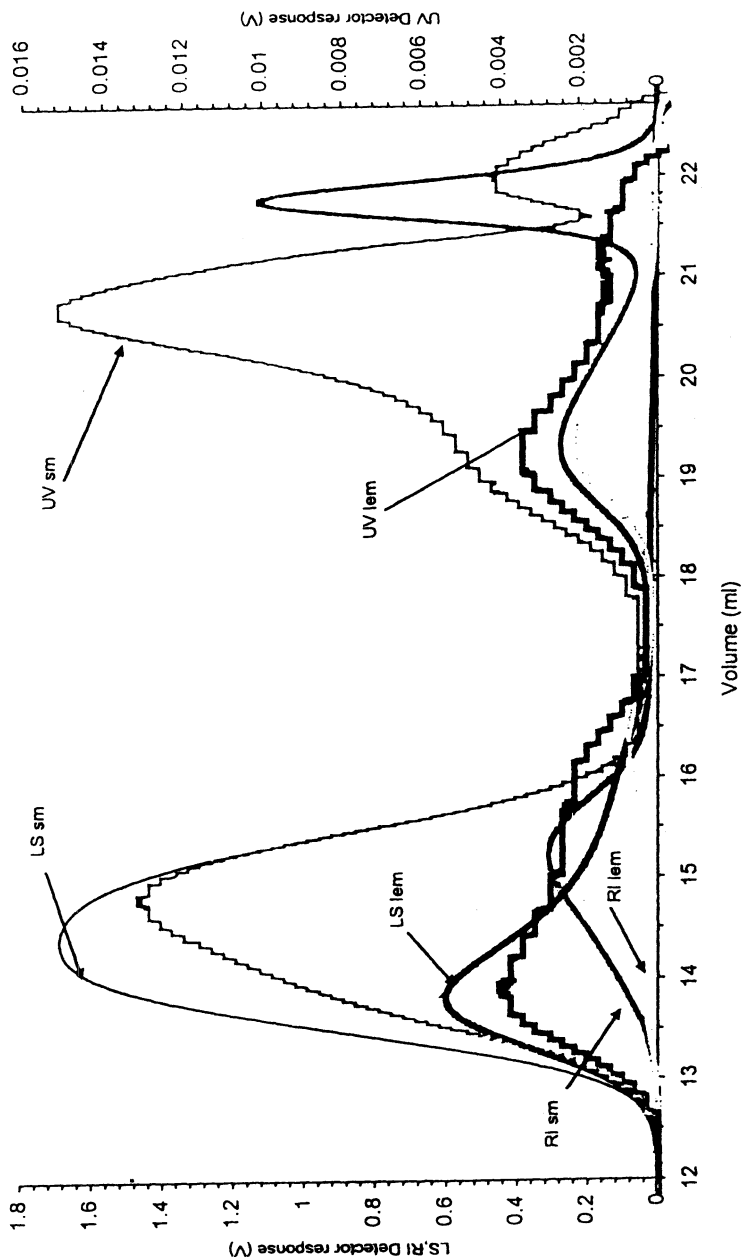


Figure 5: SEC-UV-MALLS-RI of lignin extracted material (lem) in comparison to the starting material (sm).

Conclusions

Glucuronoxylan in aqueous solvents exhibits polydispersity with a peak molecular weight of 1.7×10^7 g/mol which represents aggregates. This peak is not visible when a non aqueous solvent like DMSO is used. Fractionation by pH on the heterogeneous glucuronoxylan showed that the sparsely substituted glucuronoxylan chains do not contribute to aggregate formation, since the material after fractionation displays even larger aggregates than the starting material. This material showed a slightly higher glucuronic acid content of the remaining xylan chains and a more pronounced UV signal. The extraction of lignin from this material showed that the aggregates were almost removed, which indicates that lignin is the main contributor to aggregate formation. It was also evident that the lignin moiety consisted of a bound- and unbound fraction. The unbound lignin was mainly syringyl in the erythro form.

Literature cited

- (1) Frey-Wyssling, A. *Wood Sci. Technol.* **1968**, vol 2, 73-83
- (2) Roland, J.C., Reis, D., Vian, B., Satiat-Jeunemaître, B., and Mosiniak, M. *Protoplasma*, **1987**, vol 140, 75-91
- (3) Satiat-Jeunemaître, B. *Biol. Cell*, **1987**, vol 59, 89-96
- (4) Neville, A.C. *Biology of fibrous composites. Development beyond the cell membrane*. Cambridge University press, Cambridge, UK, **1993**
- (5) Reis, D., Vian, B., and Roland, J.C. *Micron*, **1994**, vol 25, 171-187
- (6) Reis, D., Roland, J.C., Mosiniak, M., Darzens, D., and Vian, B. *Protoplasma*, **1992**, vol 166, 21-34
- (7) Watanabe, T., M. Karina, Y. Sudiyani, T. Koshijima, and M. Kuwahara. *Wood Res.* **1993**, vol 79, 13-22
- (8) Košíková, B., and A. Ebringerová. *Wood Sci. Technol.* **1994**, vol 28, 291-296
- (9) Akiyoshi, K., Kang, E-C., Kurumada, S., Sunamoto, J., Principi, T., and Winnik, F.M. *Macromolecules* **2000**, vol 33, 3244-3249
- (10) Zinbo, M., and Timell, T.E. *Sv. Papperstid.* **1965**, vol 68, 647-662
- (11) Jacobs, A., Larsson, P.T., and Dahlman, O. *Biomacromolecules* **2001**, vol 2, 979-990

- (12) Aspinall, G.O. In: *The Biochemistry of Plants: A comprehensive treatise*, Preiss, J. (ed.), Academic Press, New York, **1980**, Vol. 3, pp 473-500
- (13) Carpita, N., and Gibeaut, D.M. *Plant J.*, **1993**, vol 3, 1-30
- (14) Goring, D.A.I., and Timell, T.E. *J. Phys. Chem.* **1969**, vol.64, 1426-1430
- (15) Blake, J.D., and Richards, G.N. *Carbohydr. Res.* **1971**, vol. 18, 11-21
- (16) Glasser, W.G., Kaar, W.E., Jain, R.K., and Sealey, J.E. *Cellulose*, **2000**, vol. 7, 299-317
- (17) Saake, B., Kruse, T., and Puls, J. *Biores. Technol.* **2001**, vol 80, 195-204
- (18) Nieduszynski, I.A., and Marchessault, R.H. *Biopolymer*, **1972**, vol 11, 1335-1344
- (19) Eriksson, I., Lidbrandt, O., and Westermark, U. *Wood Sci. Technol.*, **1988**, vol 22, 251-257
- (20) Vian, B., Roland, J.C., Reis, D, and Mosiniak, M. *IAWA Bull.* **1992**, vol 13, 269-282
- (21) Joseleau, J-P., and Gancet, C. *Sv. Papperstid.* **1981**, vol 84, R123-R127
- (22) Björkman, A. *Sv. Papperstid.* **1957**, vol 60, 243-251
- (23) Yaku, F., Tsuji, S., and Kosijima, T. *Holzforschung*, **1979**, vol 33, 54-59
- (24) Gustavsson, M., Bengtsson, M., Gatenholm, P., Glasser, W.G., Teleman, A., and Dahlman, O. In: *Biorelated Polymers- Sustainable Polymer Science and Technology*, Chiellini, E., Gil, M.H.M., Buchert, J., Brauneegg, G., Gatenholm, P., and Van Der Zee, M. (eds.), Kluwer Academic-Plenum Publishers, London, UK, **2001**, pp. 41-51
- (25) Teleman, A. Lundqvist, J., Tjerneld, F., Stålbrand, H., and Dahlman, O. *Carb. Res.* **2000**, vol 329, 807-815
- (26) Dahlman, O., Jacobs, A., Liljenberg, A., and Olsson, I. A. *J. Chromatogr. A.* **2000**, vol 891, 157-174
- (27) Kaar, W.E., and Brink, D.L. *J. Wood Chem. Technol.* **1991**, vol 11, 465-477
- (28) Lundquist, K., Simonson, R., and Tingsvik, K. *Nordic Pulp Paper Res. J.* **1990**, vol 5, 107-113
- (29) Puls, J., and Schuseil, J. In: *Hemicellulose and Hemicellulases*, Coughlan, M.P., and Hazlewood, G.P. (eds.), Portland Press, London, UK, **1993**, p. 1-27
- (30) Lundquist, K. In: *Methods in Lignin Chemistry*, Lin, S.Y., and Dence, C.W. (eds.), Springer-Verlag, Heidelberg, Germany, **1992**, pp. 242-249
- (31) Bardet, M., Robert, D., Lundquist, K., and von Unge, S. *Magn. Reson. Chem.* **1998**, vol. 36, 597-600

Chapter 13

The Softening Behavior of Hemicelluloses Related to Moisture

Anne-Mari Olsson and Lennart Salmén*

Swedish Pulp and Paper Research Institute, STFI, Box 5604,
SE-11486 Stockholm, Sweden

The properties of hemicelluloses and especially their softening are important for the performance of paper products; softening temperatures of hemicelluloses have earlier been determined under various conditions. However, there is a lack of mechanical spectroscopic data needed for characterizing their behavior in products under the conditions of use, i.e. their mechanical frequency dependence under moist conditions. In this study a method of humidity scans in mechanical spectroscopy was used to characterize the mechanical performance of a xylan and a glucomannan in relation to load frequency, temperature and humidity. Two transitions were found; a weak one at 20 to 40% relative humidity, RH, and a major at 50 to 90 %RH. For the xylan, the activation energy of this major softening was determined to be 400 kJ/mol at a moisture ratio of 26%, a reasonable value for the glass transition of a hydrogen-bonding polymer. The xylan had its glass transition temperature at a somewhat higher humidity than did the glucomannan: at 50°C and 1 Hz it occurred at 76 %RH as compared to 65 %RH for the glucomannan.

Introduction

The properties of the hemicelluloses within the composite material of the wood cell wall are important for the performance of wood and paper products, especially with regard to the influence of moisture. In fact, the interaction between water and wood fibers leading to swelling and softening may to a great extent be related to the properties of the hemicelluloses (1).

Dynamic mechanical measurements on moist wood show a weak transition above room temperature that has been postulated to be related to the hemicelluloses (2). Due to the highly reinforced fiber wall structure with cellulose fibrils in a crosslinked lignin matrix, only a weak softening is expected as a result of the hemicellulose transition (3). Despite this moderate effect on fiber elasticity, transitions of the hemicelluloses give an increased mobility within the cell wall, and this can lead to important property changes within the fiber wall. In order to characterize such a hemicellulose transition, studies have earlier been performed on alkali-extracted hemicelluloses (4,5). Although the structure of extracted hemicelluloses differs somewhat from the native ones, results from measurements on the extracted materials give the best possibilities so far for drawing conclusions about the behavior of the hemicelluloses in wood.

For alkali-extracted hemicelluloses, the softening under dry conditions ranges from 150°C to 220°C (5-7). Factors that may influence the position of this glass transition are related to the structure of the polymer such as degree of branching, type of sidegroups and backbone linkages (8). The molecular weight of the polymer and degree of crystallinity are also important (8). In general the glass transition approaches a limiting value at a degree of polymerization, DP, of several hundred (9,10). This has also been demonstrated from studies on oligosaccharides related to the wood polymers (11).

Water acts as a plasticizer and increases the mobility of the hygroscopic hemicellulose macromolecules, and this leads to a lower glass transition temperature under moist conditions. Measurements (4) as well as calculations (6) show a decrease to approximately 50°C at 20% water content. In other carbohydrates water also shows a strong softening effect (12,13).

Earlier measurements on the moist transitions of extracted hemicelluloses were made by differential scanning calorimetry (DSC) (4). This enables the glass transition to be studied from a thermodynamic point of view, but information relevant for mechanical considerations such as the effect of load frequency is lacking. Some measurements in temperature scans in dynamic mechanical tests have been performed on carbohydrates such as amylopectin (13-15). The problem with such measurements on moist samples is the evaporation of water at the high temperatures. To avoid such problems, a technique for humidity scans

in dynamic mechanical analysis, DMA, has been developed where the relative humidity, RH, surrounding the sample is changed at a constant rate while the temperature is kept constant. Using this method the softening mechanisms of some extracted hemicelluloses has been characterized in terms of load frequency in humidity scans from 1 to 95 %RH at temperatures from 30°C to 80°C. The moisture content of the sample corresponding to a given relative humidity has been determined separately in sorption experiments from 0 to 90 %RH at 20°C to 50°C. This has made it possible to determine the activation energy of the glass transition of extracted hemicellulose at different moisture contents.

Experimental

Material

A wood xylan was prepared from birch fibers that had been subjected to acetone extraction and chlorite delignification. The xylan fraction was extracted with a solution of 6.5% KOH in a nitrogen atmosphere at 20°C for 3.7 hours. The extract was acidified and the xylan was precipitated with ethanol.

A commercial glucomannan extracted from *Amorphophallus Konjac* was also tested.

Some chemical characteristics of the samples are listed in table I. The amount of methyl-gluconic acid was determined by conductometric titration. The xylan was mainly composed of xylose units with only a few sidegroups. Also, the glucomannan contained few sidegroups, in contrast to the glucomannans within the wood. The molecular weights were determined by SEC/MALDI-MS (size-exclusion chromatography/matrix-assisted laser desorption/ionization time-of-flight mass spectroscopy) (16). The high molecular weight

Table I. Relative Composition (%) of the Hemicelluloses Used

	<i>Xylan</i> <i>Betula Verrucosa</i>	<i>Glucomannan</i> <i>Amorphophallus Konjac</i>
<i>Arabinose</i>	0.2	0.4
<i>Xylose</i>	98.7	0.1
<i>Mannose</i>	0.6	60.5
<i>Galactose</i>	0.2	0.5
<i>Glucose</i>	0.2	38.5
<i>Me-GluU/xyl</i>	1/10	-
<i>Molecular weight</i>	8700	35000

for glucomannan might be somewhat overestimated due to aggregation (being difficult to dissolve), but it is definitely higher than that of the xylan sample.

Mechanical Testing

The mechanical testing was performed with a Perkin Elmer DMA 7, where a dynamic and a static load were applied to the samples. The extracted hemicelluloses were impregnated onto mechanically inert glass fiber braids that were tested in tension. The loading was done with dynamic strains not greater than 0.05% of different frequencies and with a static load that was 120% of the dynamic load. Measurements were made at constant temperature in humidity scans with the relative humidity of the surrounding air increasing at a constant speed from 1 to 90 %RH. The loads applied to the sample, the deformation and the phase angle were recorded, and the modulus and the damping were calculated. A softening humidity was determined by analogy with the softening temperature from temperature scans at the onset of the decrease in storage modulus with increasing humidity (17).

Humidity Generation

Humidity scans from 1 to 90 %RH at temperatures from 30°C to 80°C were generated by a computer-controlled humidifier (Tecnequip Enterprises Pty. Ltd.). The humid air was achieved by mixing dry and fully saturated air streams heated to the chosen temperature. Humidity ramps of 1 or 0.1%RH/minute were used, with an airflow of 1.4 l/min. The rate of the ramps did not affect the position or shape of the main transition of the material. However, a softening at low relative humidity was affected why measurements at the rate of 0.1%RH/minute were used in this case. A schematic view of the testing system is shown in Figure 1.

Water Sorption Testing

Moisture sorption isotherms at different temperatures from dry to 90 %RH at temperatures up to 50°C were determined with a DVS dynamic vapor sorption equipment from Surface Measurement Systems Ltd. This device generates a moist atmosphere by mixing dry and saturated air streams generated at different constant temperatures. A microbalance registers the weight changes throughout the sorption process. The amount of water is given as moisture ratio, i.e. gram water per gram dry material.

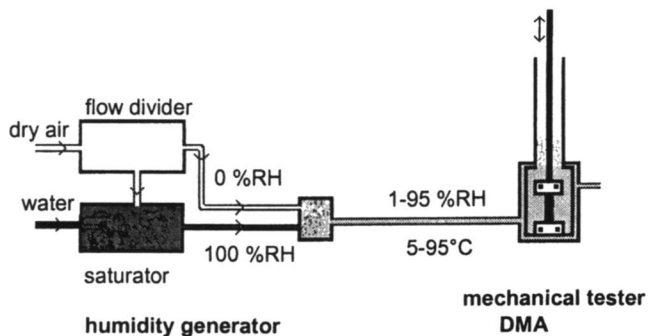


Figure 1. The set-up for the mechanical testing in humidity scans.

Results

The softening behavior of hemicelluloses in a humidity scan of 0.1%RH/min is exemplified in Figure 2 for the birch xylan at 60°C at a load frequency of 1 Hz. With increasing moisture content in the material the mobility of the polymer chains increased, evident as a drop in the storage modulus.

The modulus of the xylan showed two transitions; a weak one at about 20 %RH and a major one at 74 %RH. The first softening could have been caused by mobility of the glucuronic acid groups or by movements within the carbohydrate rings of the main chain of the birch xylan. The later softening was probably due to the glass transition of the main chain. The damping behavior of the material, shown as $\tan \delta$, supported the idea that this change in material properties was caused by a glass transition of the xylan polymer. The position of the softening has been defined in the present work as the onset of the drop in the storage modulus, as exemplified in Figure 2. This is one of many ways used to determine the transition point in polymers (13,17).

Load frequency, temperature, and moisture content all affect the position of the softening of a hygroscopic polymer. In Figure 3, the softening humidity of the birch xylan is given as a function of the load frequency at different temperatures measured in humidity scans of 1%RH/min. A higher frequency, as well as a lower temperature, shifted the softening to higher relative humidity levels. The scatter in the measured data at the lower temperatures can be attributed to measuring difficulties at high relative humidities.

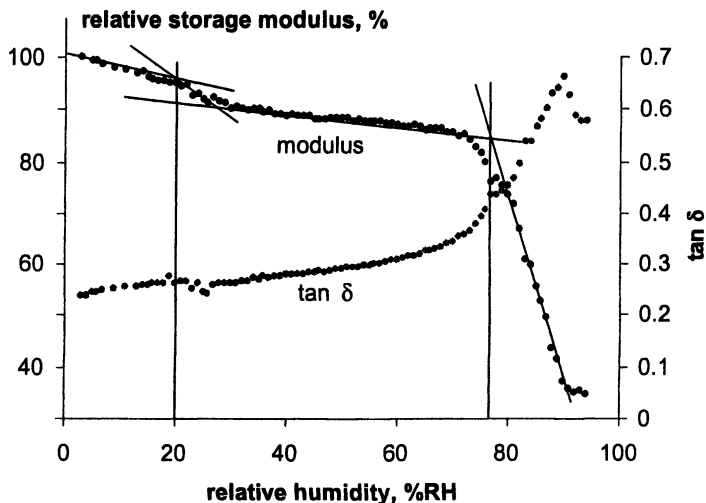


Figure 2. The relative storage modulus and the mechanical damping, $\tan \delta$, as functions of relative humidity for birch xylan at 1 Hz and 60°C. Scanning rate 0.1 %RH/min. The method of determining the softening humidity is indicated.

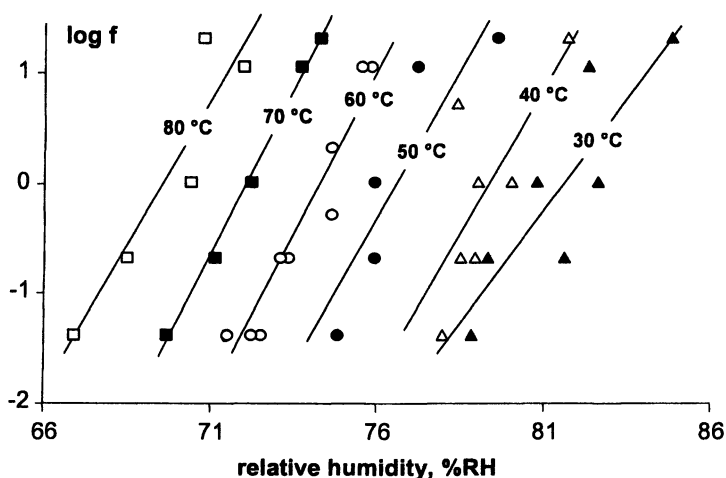


Figure 3. The softening point of the birch xylan at various temperatures shown in a diagram of the logarithm of the loading frequency versus the relative humidity. The lines are based on a linear regression of the data for each temperature.

Sorption isotherms of xylan at different temperatures are shown in Figure 4. It is evident that the moisture content at a given relative humidity decreased with increasing temperature. The decreasing moisture content with increasing temperature is typical for carbohydrates, as also reported for cellulose (18) and for wood (19).

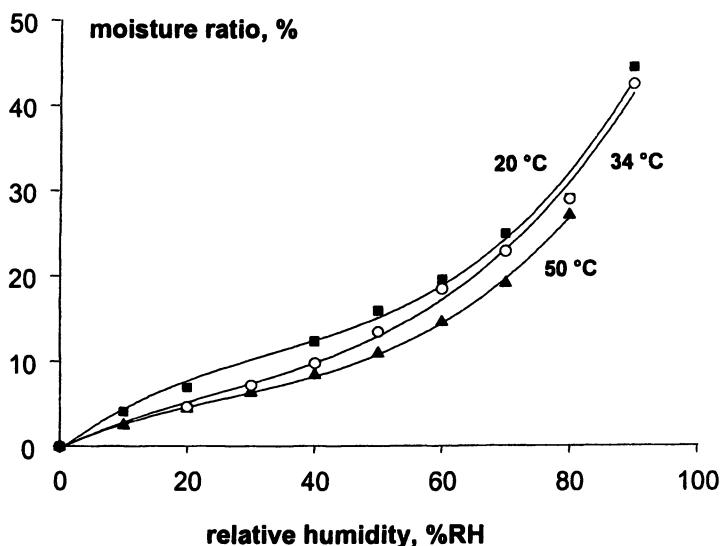


Figure 4. Water sorption isotherms obtained for birch xylan during absorption at different temperatures.

From sorption isotherms such as those in Figure 4 it is possible to transform the relative humidity x-axis of Figure 3 to a moisture ratio axis (utilizing functions of moisture content as a function of temperature at various relative humidities). The results of such calculations are shown in Figure 5 where the softening point measured as the logarithm of the load frequency is plotted versus the moisture ratio for different temperatures. As seen in the figure, there is a somewhat lower scatter in the data when moisture content is used. The 95% confidence interval of the moisture ratio determinations was 0.35%.

The data in Figure 5 may then be converted to Arrhenius plots (8) that show the logarithm of the load frequency versus the inverse of the temperature of the softening constructed at a given moisture ratio, as indicated by the procedure in Figure 6.

Figure 7 shows Arrhenius plots for the softening at different moisture ratios for the birch xylan obtained by this procedure. At higher moisture ratios the slope of the Arrhenius curve is lower. From such a slope an apparent activation energy, ΔH_a , for the softening process can be calculated as;

$$\Delta H_a = 2.303 \cdot R \cdot (\Delta \log f) / \Delta (1/T_g)$$

where R is the gas constant (8.3143 J/mol*K), and T_g is the temperature of the softening in Kelvin.

In this case for xylan, the activation energy was found to be around 500 kJ/mol at a moisture ratio of 16%, decreasing to 400 kJ/mol at a moisture ratio of 26%, as shown in Figure 8. The standard deviation in the determinations of the activation energy was about 40 kJ/mol.

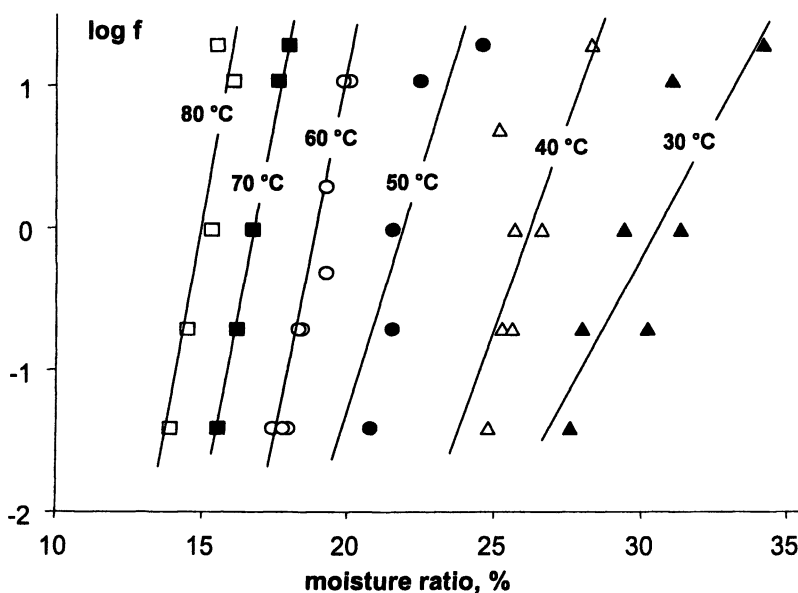


Figure 5. Softening points for the birch xylan at various temperatures shown in a diagram of the logarithm of the loading frequency versus moisture ratio, converted from Figure 3 using the isotherms in Figure 4. The 95% confidence interval for the moisture ratio determinations of the softening points was 0.35%. The lines are based on a linear regression of the data for each temperature.

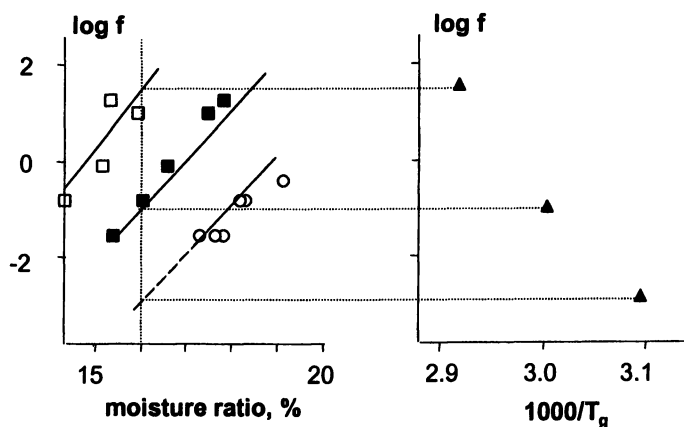


Figure 6. Illustration of the procedure for converting softening points as a function of moisture ratio to an Arrhenius plot, showing the logarithm of the load frequency versus the reciprocal of the softening temperature at a moisture ratio of 16% in the birch xylan. The left part of the figure is a partial view of Figure 5.

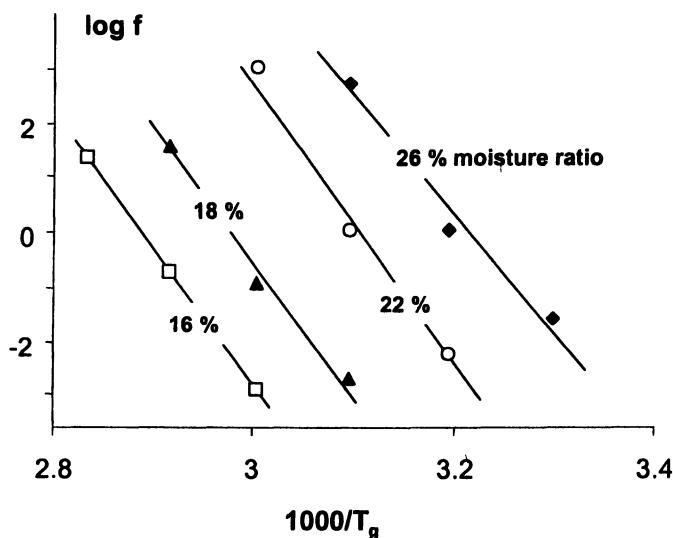


Figure 7. Arrhenius plots for the glass transition of birch xylan at different moisture ratios. The values are derived from the results in Figure 5.

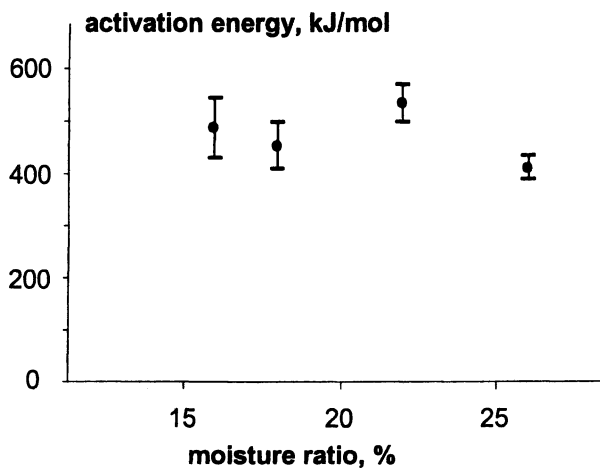


Figure 8. The apparent activation energy, ΔH_a , for the glass transition of xylan as a function of the moisture ratio of the xylan. The standard deviation of the activation energy was about 40 kJ/mol as indicated by the error bars.

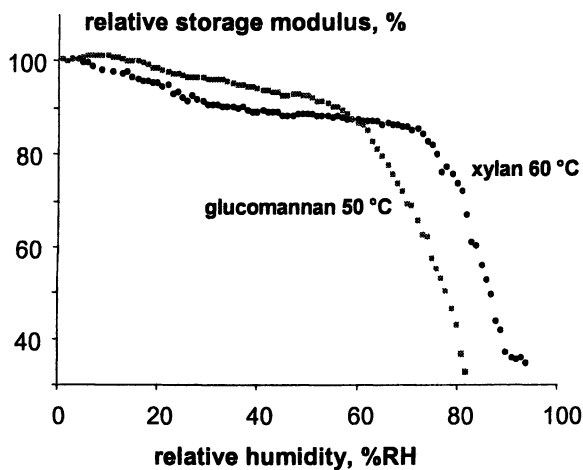


Figure 9. The relative elastic modulus of glucomannan from *Amorphophallus Konjac* at 50°C and birch xylan at 60°C as a function of relative humidity at a load frequency of 1 Hz, in humidity scans of 0.1 %RH/min.

For the glucomannan extracted from *Amorphophallus Konjac*, the modulus curves at 50°C at a load frequency of 1 Hz and a humidity rate of 0.1 %RH/min is compared to that of xylan in Figure 9. As in the xylan, a weak transition occurred at low relative humidity and a glass transition at 60 to 70 %RH. Also, for the glucomannan the transitions shifted to lower relative humidities with increasing temperature.

Figure 10 shows the derived values of the glass transition temperature for the birch xylan and the glucomannan as a function of moisture ratio compared with data for the transition temperature for softwood hemicelluloses taken from literature (4). In the xylan, the glass transition temperature at 50°C and 1 Hz occurred at 76 %RH, which corresponded to a moisture ratio of 22%, whereas for the glucomannan at 50°C and 1 Hz it occurred at 65 %RH, corresponding to a moisture ratio of 16%.

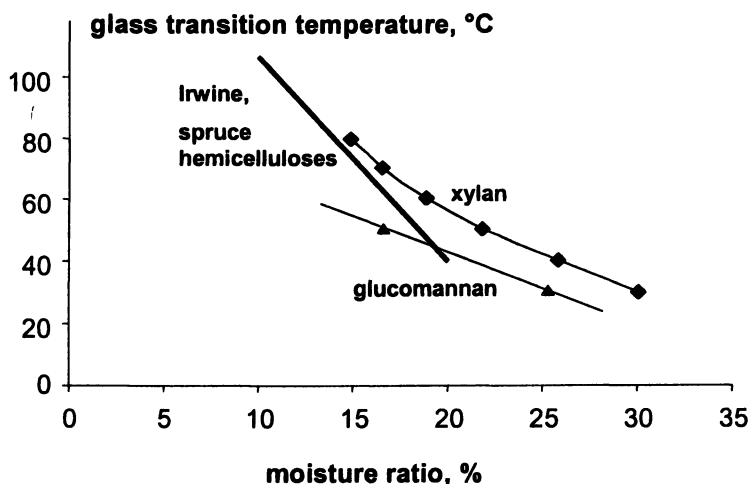


Figure 10. Glass transition temperature versus moisture content for the xylan and glucomannan compared to values from literature (4).

Discussion

This paper has presented a method of studying the softening, or glass transition, of hygroscopic polymers by using humidity scans at constant temperatures. In extracted hemicelluloses, here xylan and glucomannan, a

distinct decrease in the storage modulus accompanied by a clear peak in the damping, $\tan \delta$, with increasing relative humidity clearly indicated the occurrence of a glass transition. For both these hemicelluloses, a weak transition was also evident at a lower relative humidity.

As seen in Figure 10, the glass transition temperature obtained here with dynamic mechanical testing particularly for the xylan was somewhat higher compared to literature values. These earlier values were obtained for moist hemicellulose from spruce samples using DSC with a considered testing frequency in the region of $1 \cdot 10^{-4}$ Hz (20). The higher testing frequency of 1 Hz in the dynamic mechanical measurements used here is the probable explanation for the higher values for the xylan transition detected here.

For both the xylan and the glucomannan, the observation that the water uptake reached a moisture ratio of 30% at 80 %RH indicates that they must be considered as nearly or completely amorphous (21). The relatively low molecular weight of the xylan should mean that, in contrast to the glucomannan, its glass transition should be 10 to 20 degrees below its limiting T_g considering the molecular weight dependence determined from oligosaccharides (11). Also, the xylan should have a higher content of sidegroups than the glucomannan examined, generally meaning a lower glass transition (12). Thus, the probable cause of the difference between the softenings of xylan and glucomannan should in this respect be attributed to differences in the backbone structures of these hemicelluloses.

The apparent activation energy of the xylan transition was found to decrease with increasing moisture ratio, from around 500 kJ/mol at a moisture ratio of 16% to a value of 400 kJ/mol at a moisture ratio of 26%. These values are of the magnitude expected for a transition due to main chain motion involved in the glass transition of a polymer (22). The frequency dependence of the transition, together with the magnitude of the activation energy, provide a strong support for this being the glass transition of the xylan polymer. The decrease in activation energy with increasing moisture content is also in line with the behavior of synthetic polymers with increasing plasticizer content.

The properties of extracted hemicelluloses probably differ somewhat from those of the hemicelluloses in the wood, although the general features are probably similar. It is evident that the softening, the glass transition, of hemicelluloses occurs at rather high relative humidities at normal room temperatures, above 65 to 70 %RH. The differences in softening seen between the glucomannan and the xylan also indicate that the structure has an important influence on the position of the softening, although they are still located in the high humidity region. In wood or pulp samples, where a mixture of hemicelluloses affects the properties, it is thus not surprising that the softening is less distinct. It has also been possible to model the general decrease in stiffness of fibers and papers from rather imprecise data of extracted hemicelluloses, with

the right magnitude for their softening (23). Nevertheless, it is clear that the effect of the stiffness decrease in the RH region for wood, fibers and paper must be attributed to the softening, glass transition, of the hemicelluloses.

The fact that both the hemicelluloses showed a weak transition at lower relative humidities is of great interest for the ductility of the fiber material. In general, materials with a secondary transition exhibit an increasing ductility when passing such a transition. Further studies of the structural causes for this transition within hemicelluloses are, however, necessary, in order to be able to relate this transition to product property changes.

Conclusions

By mechanical spectroscopy in humidity scans it was shown that hemicelluloses exhibit a true glass transition at high humidities at room temperature with an apparent activation energy of 400 to 500 kJ/mol. With increasing moisture content, this activation energy is lowered in the same manner as for plasticized synthetic polymers. The softening clearly occurs in a range of temperatures and humidities such that this softening must be the cause of the changes in the properties of paper and wood occurring in the corresponding environment and what is experienced in the daily use of these materials.

References

1. Salmén, L. In *MRS Symp; Caulfield D.F., Passaretti, J. D., Sobczynski, S. F., Eds.: Pittsburg, 1990; Vol. 197, pp 193-201.*
2. Kelley, S. S.; Rials, T. G.; Glasser, W. G. *J. Mater. Sci.* **1987**, *22*, 617-624.
3. Salmén, L.; Olsson, A.-M. *J. Pulp Pap. Sci.* **1998**, *24*, 99-103.
4. Irvine, G. M. *Tappi J.* **1984**, *67*, 118-121.
5. Marchessault, R. H. In *Chimie et biochimie de la lignine, de la cellulose et des hémicelluloses*; Les imprimeries réunies de chambéry: Grenoble, 1964; pp 287-301.
6. Back, E. L.; Salmén, L. *Tappi J.* **1982**, *65*, 107-110.
7. Shigematsu, M.; Morita, M.; Sakata, I. *Jpn. Wood Res. Soc.* **1992**, *38*, 199-203.
8. Sperling, L. H. In *Introduction to Physical Polymer Science*; J. Wiley: New York, 1986.
9. Fox, T. G.; Folry, P. *J. Appl. Phys.* **1950**, *21*, 581-591.
10. Cowie, J. M. G.; Henshall, S. A. E. *Europ. Pol. J.* **1976**, *12*, 215-218.

11. Alfthan, E.; de Ruvo, A.; Brown, W. *Polymer* **1973**, *14*, 329-330.
12. Bizot, H.; Le Bail, P.; Leroux, B.; Davy, J.; Roger, P.; Buleon, A. *Carbohydr. Polym.* **1997**, *32*, 33-50.
13. Kalichevsky, M. T.; Jaroszkiewicz, E. M.; Ablett, S.; Blanshard, J. M. V.; Lillford, P. J. *Carbohydr. Polym.* **1992**, *18*, 77-88.
14. Kalichevsky, M. T.; Jaroszkiewicz, E. M.; Blanshard, J. M. V. *Polymer* **1993**, *34*, 346-358.
15. Kalichevsky, M. T.; Blanshard, M. V. *Carbohydr. Polym.* **1993**, *20*, 107-113.
16. Jacobs, A.; Lundqvist, J.; Stålbrand, H.; Tjerneld, F.; Dahlman, O. *Carbohydr. Res.* **2002**, *337*, 711-717.
17. Hagen, R.; Salmén, L.; Lavebratt, H.; Stenberg, G. *Polymer Testing* **1994**, *13*, 113-128.
18. Wahba, M.; Nashed, S. *J. Text. Inst.* **1957**, *48*, T1-T20.
19. Kelsey, K. E. *Aust. J. Appl. Sci.* **1957**, *8*, 42-54.
20. Boyer, R. F. *Encyclopedia of polymer science and technology*; John Wiley & Sons; 1977; Vol. 2.
21. Berthold, J.; Rinaudo, M.; Salmén, L. *Colloides and Surfaces* **1996**, *A 112*, 119-131.
22. Boyer, R. F. *Rubber Chem. Technol* **1963**, *36*, 1303-1418.
23. Salmén, L.; Kolseth, P.; De Ruvo, A. *J. Pulp Pap. Sci.* **1985**, *11*, 102-107.

Chapter 14

Self-Assembly Behavior of Some Co- and Heteropolysaccharides Related to Hemicelluloses

Alan Esker¹, Ulrike Becker², Sylvie Jamin², Shinji Beppu²,
Scott Rennekar², and Wolfgang Glasser^{2,*}

Departments of ¹Chemistry and ²Wood Science and Forest Products,
Virginia Polytechnic and State University, Blacksburg, VA 24061-0323

The self-assembly behavior of a series of fluorinated cellulose ester copolymers with different F-substituents and with varying cellulose propionate (CP) molecular weight, and that of several xylan-rich hetero-polysaccharides and their derivatives, were examined in relation to their critical micelle concentration (CMC) and their interaction with model cellulosic surfaces. The F-containing CP derivatives had a telechelic architecture based on mono-functional CP segments of well-defined size; their F-content varied with the type of fluoro-alcohol group. The model cellulosic surface consisted of Langmuir-Blodgett films prepared from trimethylsilyl (TMS) cellulose in accordance with work by Schaub et al. Surface adsorption (“docking”) of water-soluble xylan derivatives was studied by surface plasmon resonance (SPR) spectroscopy. Surface deposition was also examined by atomic force microscopy (AFM). The results suggest that the CMC varies with both the chemical structure and the molecular weight of the amphiphile, and that cationic substituents and an enhanced hydrophilic/hydrophobic balance contribute to make the most strongly adsorbing water-soluble xylan on a cellulose surface. However, other xylans also adhere to, or self-assemble on a model cellulosic surfaces. Several hypothetical aggregate structures are presented.

Introduction

Self-assembly and self-organization are terms that describe the behavior of molecules as the purposeful response to environmental conditions. As such, self-assembly represents a form of smartness or intelligence (1,2). In the case of macromolecules, self-assembly behavior manifests itself in such spontaneous processes as the formation of aggregates in solution and the segregation of molecules at surfaces. Aggregation of copolymers occurs in solvents when one component is preferentially solvated over another component (3). This condition produces structures variably described as micelles, worm-like structures, lamellae, bi-layers, sheets, crew-cut micelles and vesicles (4,5). For AB di-block copolymers, the aggregation is usually limited to the formation of micelles similar to the ones observed in small-molecule surfactants (6). The micelles are formed by hiding the insoluble block in the core, thereby preventing precipitation.

We have previously synthesized a series of fluorine (F)-containing cellulose derivatives that have exhibited clear evidence of self-assembly in non-aqueous, organic solvent environments (7). The introduction of F-atoms into cellulose had originally been attempted with the aim of promoting compatibility between cellulose and synthetic polymers. The incorporation of fluorine into cellulose was accomplished by adding single F-atoms onto the backbone, or by covalently coupling F-containing substituents as grafts to the backbone (8-10).

F-containing cellulose derivatives are inherently amphiphilic molecules having a hydrophobic moiety (the F-substituent) covalently attached to a hydrophilic moiety (the cellulose backbone) (11). Similar amphiphiles on the basis of polysaccharides have been reported by Sunamoto et al. (12-15) and Uraki et al. (16, 17). Using water-soluble pullulan derivatized with cholesteryl substituents, Sunamoto et al. were able to study such features as the permeability of a polysaccharide-coated liposome as well as the fluidity of the liposomal membrane (12); the formation by self-aggregation of nanosize hydrogel particles in water (13); the complexation of an antitumor drug (adriamycin) in these hydrogel particles (14); and the macromolecular complexation of bovine serum albumin with these self-assembled nanoparticles (15).

Uraki et al., by contrast, was able to determine that the cellulose from unbleached organosolv pulp fibers (from acetic acid pulping), that is made water-soluble by hydroxypropylation, self-assembles into micellar structures on account of its inherent co-polymerization with (hydrophobic) lignin (16, 17). The amphiphilic hydroxypropyl cellulose-hydroxypropyl lignin copolymers of Uraki et al. are similar in architecture to isolated lignin-carbohydrate complexes, such as glucuronoxylans, that are associated with residual lignin fragments. Numerous studies have been dedicated to the nature

of this association in the past and, while there continues to be debate over the true nature of the bond (or bonds), there no longer is conflict over the fact that covalent bonds exist between the (hemicellulosic) carbohydrate portion and the lignin fraction (see other chapters in this book).

Fluorinated cellulose esters, cholesteroylated pullulan, lignin (derivative)-containing hydroxypropyl cellulose, and lignin-carbohydrate complexes (i.e., lignin-containing glucuronoxylan, or simply "xylan", a widely represented hetero-polysaccharide in the plant kingdom) all have in common amphiphilic character and self-assembly behavior. Since only the first two types of molecules (i.e., the cellulose ester and the pullulan derivatives) are structurally designed by synthesis whereas the latter are subject to isolation from biocomposites that are frequently poorly described in structure and composition, an attempt is made in this study to define some molecular parameters important for self-assembly. This approach employs F-containing cellulose ester derivatives that (a) are "blocky" (or telechelic) in architecture, and (b) have variable molecular dimensions and substituent types.

Amphiphiles self-assemble differently in solution than at solid surfaces. The behavior of xylans at cellulosic surfaces (pulp fibers) has recently come under investigation by Henriksson and Gatenholm (19) who demonstrated that pulp fibers gain as much as 20% in weight when suspended in aqueous alkaline solutions of xylan at elevated temperature. Scanning electron microscopy (SEM) and atomic force microscopy (AFM) images revealed that the so-treated fibers contained particles (aggregates) within the cell wall structure of the fibers after treatment.

In order to achieve the overall goal of establishing the fundamental factors affecting adsorption to cellulose surfaces, two distinct steps are required. First, Langmuir Blodgett (LB) films (20) of regenerated cellulose are used to produce uniform surfaces that allow us to understand the physico-chemical underpinnings of adsorption without the morphological complications of a fiber surface. Second, the uniform cellulose layers, prepared on gold substrates, allow us to use surface plasmon resonance (SPR) experiments to monitor the adsorption of water-soluble polysaccharide derivatives onto the model cellulose surfaces.

Langmuir Blodgett (LB)-films of cellulose derivatives have been prepared in the past (21-25). Trimethylsilyl (TMS) cellulose dissolved in chloroform has been shown to form monolayers at the air-water interface (21). The layer has been shown to be transferrable onto solid hydrophobic surfaces. Multi-layered thin films of TMS cellulose can be easily desilylated using HCl vapors, producing a regenerated cellulose film with well-defined thicknesses and surface roughnesses. Such films have variably been used for studying self-assembly phenomena, immobilization tests of biomolecules (23), and determining surface energies of uncontaminated cellulose (21).

Surface plasmon resonance (SPR) is an optical technique that offers real time *in situ* analysis of dynamic events at solid surfaces and thus is capable of defining dimensional parameters of adsorbed mass, and rates of adsorption and desorption for a range of molecular interactions (26). While SPR has been widely utilized for biological applications, it is a relatively novel approach for studying adsorption in cellulosic systems. Hence, a brief description of the underlying principles and system requirements for SPR measurements is warranted. At the interface between a dielectric substance and metal, there exists a surface plasmon, a charge density that propagates longitudinally between the two media. For surface plasmons to exist at such an interface, the real parts of the dielectric constants of the two media must be of opposite sign. This condition is met in the near infrared (NIR) region for the air/metal and water/metal interfaces. At a critical angle, p-polarized laser light reflected at the interface of the two media interacts with the surface plasmon. A portion of the energy of the reflected light is coupled to the oscillating surface plasmon causing a decrease in intensity of the reflected light (parallel to absorption of energy in infrared spectroscopy). The critical angle will change as a function of the refractive index of the second medium, which is dependent on the thickness of the adsorbate. Gold is usually used as the metal coating on which the material to be studied is deposited. A schematic illustration of a typical SPR instrument can be found in Green et al. (26).

The objectives of the current study therefore dealt with exploring (a) the relationship between molecular parameters (block size and substituent type) and self-assembly behavior in F-containing cellulose esters (i.e., copolysaccharides), and (b) the self-assembly at solid surfaces (i.e., the “docking” behavior) of amphiphilic xylan molecules (i.e., heteropolysaccharides) at well-defined cellulose surfaces.

Materials and Methods

I. Materials:

Cellulose propionate was obtained from Eastman Chemical Company, Kingsport, TN. The mono-functional segments were synthesized in our laboratory as described previously (27, 28). Briefly, per-propionylated cellulose ester (CTP) was hydrolyzed with HBr in propionic anhydride and isolated by precipitation in water. The partially hydrolyzed CTP-oligomers were converted from the OH- to the NCO-terminated CTP derivatives by treatment with toluene diisocyanate (TDI) (27). The NCO-terminated, monofunctional segments were then reacted with various fluoro-alkyl alcohols to yield F-containing CTP telechelic copolymers. This procedure has been

employed previously for the purpose of studying surface segregation processes at cellulose ester surfaces (7).

Xylan was obtained from various biomass resources, including peanut hulls and rice husks, yellow poplar wood and rye straw using a method described previously (18). Cationic xylan was prepared by reacting xylan in aqueous alkali solution (pH 10 to 11) with glycidyl trimethyl ammonium chloride at 50°C for eight hours. The protocol followed work by Pulkkinen et al. with isolated lignin (29). The water-soluble reaction product was purified and isolated by membrane filtration and freeze-drying. It had an N-content of 2.30 wt.% corresponding to a DS of 0.3.

An anionic xylan derivative was produced by carboxymethylation of xylan in homogeneous 1N alkali solution using the sodium salt of chloroacetic acid, according to Gustavsson et al. (30). After 3 hr. at 70°C, the reaction mixture was adjusted to pH 10 with HCl and precipitated in ethanol.

A fluorine (F)-containing cationic xylan derivative was prepared by first reacting xylan in mildly alkaline aqueous solution with glycidyl-2, 2, 3, 3, 4, 4, 5, 5, 6, 6, 7, 7-dodeca-fluoroheptyl ether at 50° for two hours before further derivatizing the reaction product by the addition of additional alkali and the glycidyl trimethyl ammonium chloride reagent mentioned above. The reaction product was isolated, following neutralization and membrane filtration, by freeze-drying.

II. Methods:

Determination of critical micelle concentration (CMC) for cellulose ester derivatives: The CMC was determined by measuring the surface free energy of low concentration-oligomer solutions. The F-containing cellulose ester derivatives were not cleanly soluble in any organic solvent, but formed turbid solutions in a variety of solvents, including acetone and THF. The xylan derivatives formed similarly turbid solutions in water. The two types of polysaccharide derivatives thereby exhibited both differences and similarities: they had vastly different solubility characteristics (organic solvent vs. water), and they formed colloidal solutions at low concentration on account of their bipolar structural characteristics. Cellulose esters were therefore measured in THF, and xylan derivatives were analyzed in water. For every oligomer or polymer, a 1% (w/v) solution in THF or water was made (stock solution), which was subsequently diluted as necessary. The surface free energy of the solutions were measured using a Cahn balance. A clean, round glass slide was connected to the beam of the balance, and the force was measured when the glass slide was lowered into the solution. Every measurement was carried out in triplicate. The value of the CMC was determined as percent (w/v) of oligomer or polymer in solution.

Determination of critical micelle concentration (CMC) for xylan derivatives: Surface tension measurements for the aqueous xylan solutions were made using the tensiometer from the Langmuir Blodgett trough system used below (KSV 2000). The surface tension was determined by the Wilhelmy plate technique using a sand blasted platinum plate. The xylan solutions were measured in a specially designed glass beaker that was cleaned with sulfuric acid. The temperature was held constant at 22.5°C by circulating thermostated water through the exterior of the beaker.

Langmuir Blodgett (LB) film preparation: The LB films of regenerated cellulose were prepared in accordance with an earlier publication by Schaub et al. (21). Trimethylsilyl (TMS) cellulose (Jena Biosciences, Ltd.) was used as chloroform-soluble derivative that was spread on the water surface of an LB-trough (KSV 2000) as a monomolecular film (20). A hydrophobic glass slide with a gold coating on one side was used as the SPR-suitable substrate for LB-film deposition.

Adsorption (docking) experiments by surface plasmon resonance (SPR): SPR-experiments were conducted on cellulose films prepared from a 40-layer film of TMS cellulose deposited by the LB method on glass slides coated with chromium and gold. The film on the glass side was removed with chloroform, and the film on the gold side was desilylated. The slide was then introduced into the SPR-apparatus. A refractive index matching oil was used to couple the back of the substrate to the SPR instrument. An oval plastic gasket was positioned on the slide, and the cell was placed on top. The cell was linked by two tubing lines to a pump. Both lines can be placed into the same solution to avoid pumping air during the transition to a second solution. The solutions used were prepared with distilled, deionized water. All solutions were prepared at concentrations of 10, 40, 100, 200, 1000, 2000, and 4000 mg L⁻¹. The solutions were allowed to run in the cell until the signal indicated the establishment of near-equilibrium conditions. This situation usually required not more than a few minutes. Water was eluted for a few minutes before the line was switched to a solution of higher concentration. Adsorption due to this more concentrated solution thus occurred on top of the already adsorbed solids from the previous solution. This means that the solute present in the 10 mg L⁻¹-solution adsorbed on a clean cellulose surface, but all other solutions were adsorbed on top of what had already been absorbed from the solution with the next lower concentration. The solutions were run through the cell on the gold slide at a flow rate of 0.45 mL min⁻¹, and the changes in the resonant angle, which can be related to the thickness, were recorded every 10 s.

Atomic Force Microscopy (AFM) image acquisition: AFM measurements were conducted on films cast on mica slides. The films were coated with self-assembling substances by immersion in the respective solutions at room temperature and stored at 4 C. AFM measurements were conducted in tapping mode on a Digital Instruments Dimension 3000 Scope, with a Nanoscope IIIa

controller. Several samples using at least two different silicon nitride tips were used for each film in order to exclude artifacts.

Results and Discussion

Self-Assembly Measurements in Solution: The critical micelle concentration (CMC) is the characteristic solution concentration at which solubilized single molecules aggregate into micellar structures. A number of parameters, including osmotic pressure, conductivity, turbidity and surface tension experience dramatic changes at the CMC. One method of determining the CMC involves surface tension measurements using a Wilhelmy plate. The CMC of various F-terminated cellulose ester oligomers and of xylans were determined in THF and water, respectively.

The F-terminated cellulose esters varied by size of the cellulose ester (cellulose propionate, CP) segment, which ranged between the degree of polymerization (DP) of 15 and 70; and it varied by type of F-containing end group, which was either a trifluoroethoxy, octafluoropentoxy, or perfluorooctanoxo end group (Table I and Figure 1). The xylan derivatives varied by substituent type and functionality: there was an *anionic* derivative, a *cationic* derivative, and an *F-containing cationic* derivative (Figure 2).

Table I: Overview of block-like (telechelic) cellulose ester copolymers. (S. Figure 1 for structure).

Sample designation	DP of CP Block ^a	End-group type	Number of F-atoms in substituent	F-content (%) ^b	CP mass per endgroup (g/mole) ^c
T ₁₅ ^d -TF ^e	15	Trifluoro	3	0.87	4950
T ₁₅ -PF	15	Perfluoro	13	3.63	4950
T ₁₅ -OF	15	Octafluoro	8	2.29	4950
T ₃₀ -TF	30	Trifluoro	3	0.45	9900
T ₃₀ -PF	30	Perfluoro	13	1.91	9900
T ₃₀ -OF	30	Octafluoro	8	1.19	9900
T ₇₀ -TF	70	Trifluoro	3	0.18	23000
T ₇₀ -PF	70	Perfluoro	13	0.78	23000
T ₇₀ -OF	70	Octafluoro	8	0.48	23000

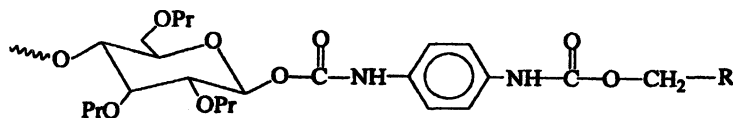
^a Calculated from molecular weight data

^b Calculated as atomic % of F-atoms on all atoms of the sample, excluding protons

^c Calculated from GPC data

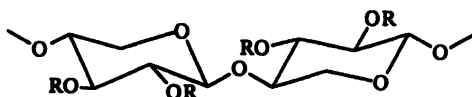
^d Indicates DP of CP-block

^e Indicates type of end-group



where R = - CF₃ (trifluoro)
 - CF₂CF₂CF₂CF₂H (octafluoro)
 - CH₂CF₂CF₂CF₂CF₂CF₂CF₃ (perfluoro)

Figure 1. Structural schemes of F-containing cellulose ester copolymers.



XYLAN DERIVATIVES

R = H and some lignin (10-15% by wt.), Xylan
 R = -CH₂-CH(OH)-CH₂-N⁺(CH₃)₃Cl⁻, Cationic Xylan
 R = -CH₂-CO₂H, Anionic Xylan
 R = -CH₂-CH(OH)-CH₂-N⁺(CH₃)₃Cl⁻/
 -CH₂-CH(OH)-O-CH₂-(CF₂)₆-H,
 F-containing Cationic Xylan

Figure 2. Structural schemes of water-soluble xylan derivatives used for adsorption studies on cellulosic LB-surfaces.

The presence of amphiphilic cellulose esters and xylan derivatives in THF and water, respectively, causes a decrease in the surface free energy for the solution as the surface-active molecules adsorb at the air/solution interface. By measuring the change in surface tension as a function of bulk solution concentration, it is possible to estimate the critical micelle concentration (CMC), the point where surfactant molecules self-assemble into larger aggregates. For small molecule surfactants, these aggregates possess well-defined sizes, shapes, and large aggregation numbers, the number of molecules needed to make the micelle. For polydisperse polymeric amphiphiles, the "micellar" sizes, shapes, and aggregation numbers, are more poorly defined.

In general, polymeric species exhibit aggregation numbers that are typically much smaller than regular small-molecule surfactants in accord with the closed-association model for micelle formation (31). As a consequence, the transitions seen in Figure 3, where "surface tension" is plotted as a function of bulk solution concentration are not as sharp as one might find for typical small molecule surfactants like sodium dodecylsulfate (31). In principle, the change in surface tension with respect to bulk solution concentration can also be used to obtain the surface concentration of the surfactant, Γ_2 , through the Gibbs adsorption isotherm:

$$\Gamma_2 = -\frac{1}{RT} \left(\frac{\partial \gamma}{\partial \ln a_2} \right) \quad [1]$$

$$\lim_{c_2 \rightarrow 0} \Gamma_2 = -\frac{1}{RT} \left(\frac{\partial \gamma}{\partial \ln c_2} \right) \quad [2]$$

where γ is the surface tension of the solution, a_2 is the activity of the solute, c_2 is the concentration of the solute, R is the gas constant, and T is the temperature. Plotting the data in Figure 3 as a function of $\log c_2$ would provide a slightly better interpretation of the data with respect to the estimation of the CMC, and calculation of Γ_2 . However, the absence of activity data, the fact that we have polydisperse samples, and the lack of actual γ values for the CTP series of polymers, precludes such a detailed analysis.

Figure 3A, shows "wetting force" as a function of bulk solution concentration for T₇₀-TF in THF. Here, "wetting force" is the mass of a round glass plate in contact with a CTP solution as measured by a Cahn balance. As the mass is proportional to the surface tension one gets in a true Wilhelmy plate method, Figure 3A is equivalent to a plot of γ vs. c_2 . From the plot, it is clear that there is a transition from one-type of linear behavior at low concentration to a different linear regime at higher concentration. At low CTP concentrations, $a_2 \cong c_2$ and $\Gamma_2 \propto (\partial\gamma/\partial \ln c_2)$. At higher concentrations, $a_2 \approx$ a constant independent of c_2 so $(\partial\gamma/\partial \ln c_2)$ grossly distorts the fact that the chemical potential of the solute is not significantly changing with increasing solute concentration. Hence, the intersection of these two regimes provides a qualitative measure of the CMC. For the CTP series, two distinct trends (Figures 4 & 5) are noted:

- 1) the CMC depends on the type of F-end group used, $CMC_{\text{octafluoro}} > CMC_{\text{trifluoro}} > CMC_{\text{perfluoro}}$; and
- 2) the CMC increases with the degree of polymerization.

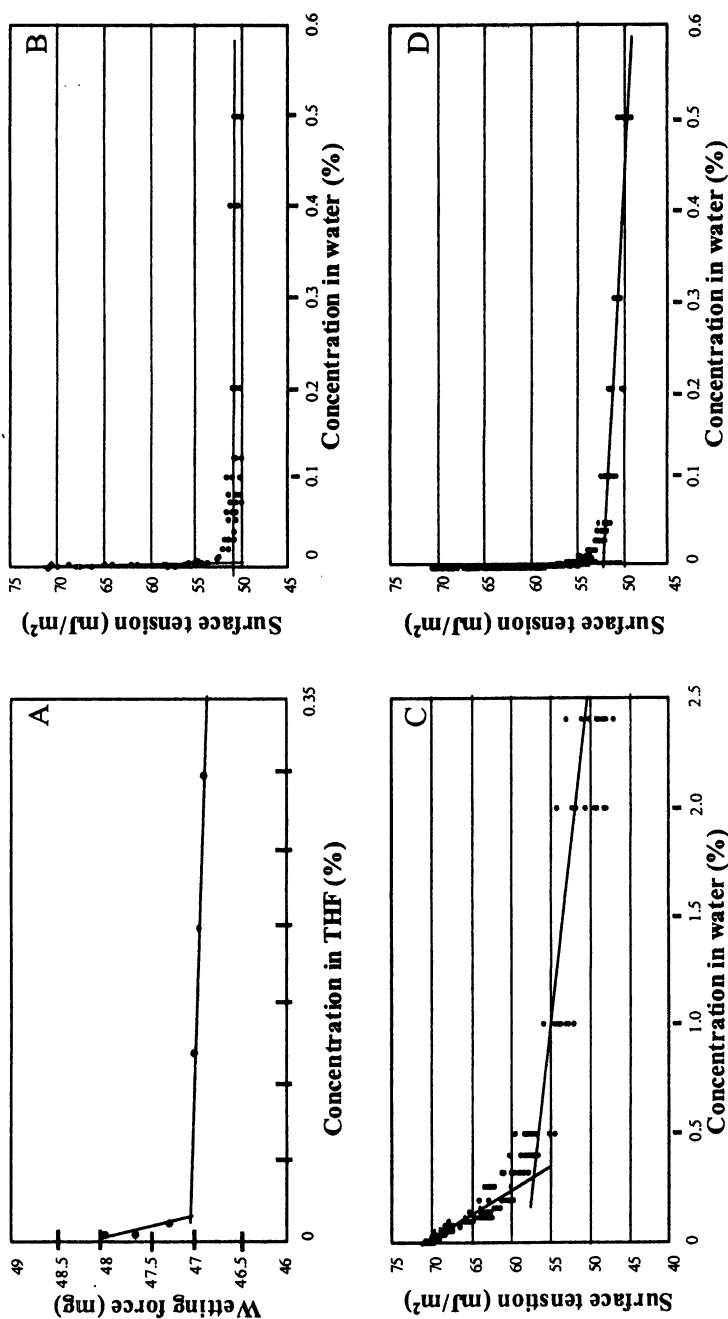


Figure 3. Illustration of critical micelle concentration (CMC) measurement results using the modified Wilhelmy plate method. CMC is obtained as the intercept of the linear portion of two slopes relating wetting force (or surface tension) to analyte concentration. (A) Typical telechelic fluorinated cellulose ester copolymer (T_{70} -TF) (data are averages of three measurements with a variation of ± 0.25); (B) xylan from rye straw (data variation as shown); (C) xylan from yellow poplar; and (D) hydroxypropyl xylan derivative.

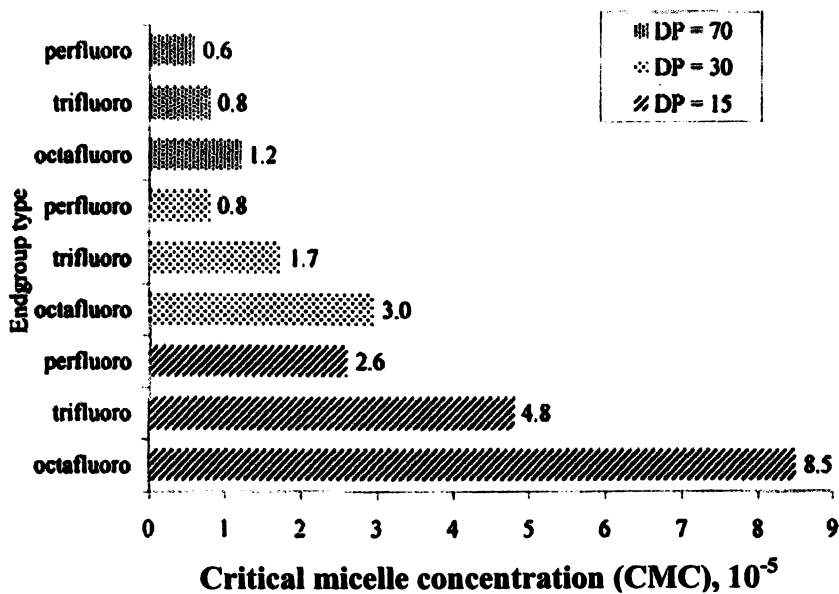


Figure 4. CMC values obtained with F-containing, telechelic cellulose ester copolymers having variable substituent type and variable cellulose ester-molecular size (expressed in DP).

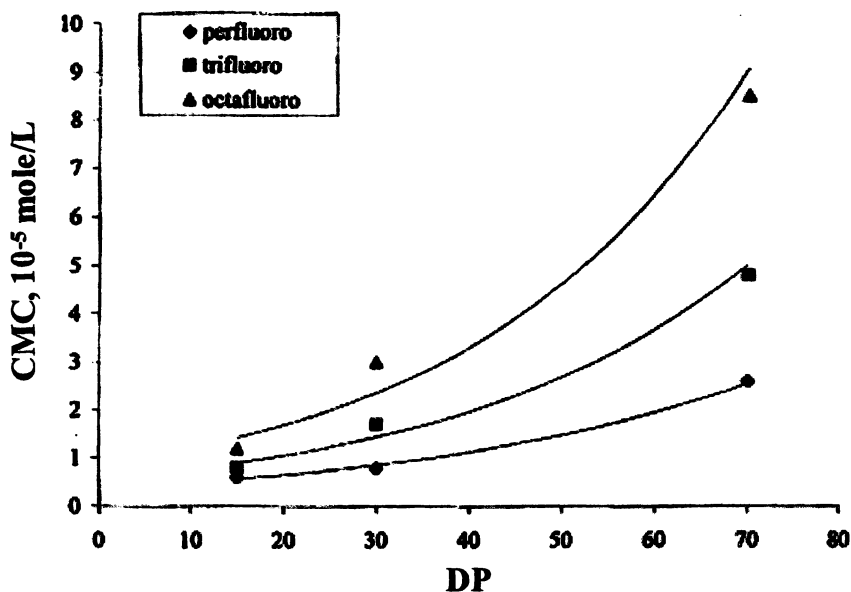


Figure 5. Dependence of CMC on the DP of the cellulose ester block for different F-containing end groups.

Both effects can be rationalized in terms of the balance between "hydrophobic" and "hydrophilic" interactions. As the CTP is more THF compatible than the fluorinated end groups, CTP represents the "hydrophilic" part of the molecule. Hence, as the molecular weight of CTP \uparrow , THF compatibility \uparrow , and a bigger CMC is observed in response to the increased "hydrophilic" character of the molecule. For the effect of fluorination, it is important to note that the F-endgroups represent the "hydrophobic" part of the molecule in THF. For trifluoro vs. "perfluoro" endgroups, it is clear that the "perfluoro" group is more "hydrophobic" than the fluorinated methyl end group, hence a lower CMC is expected and observed. However, one might also rationalize that the octafluoro end group should lie between the trifluoro and "perfluoro" derivative based solely on the number of F atoms. The reason that the CMC for the CTP with octafluoro end groups is actually bigger than CTP with trifluoro or "perfluoro" endgroups appears to be due to a strong dipole residing on the terminal C-H bond. The polarity of the C-H bond arises from the fact that strongly electronegative F substituents reside on the same carbon as well as on the adjacent carbon atoms. This strong dipole may allow the $\text{CF}_2\text{-H}$ terminus to engage in secondary interactions that significantly enhance the polymer-solvent compatibility, thereby resulting in a larger CMC. This hypothesis is consistent with the observation that ω -hydroxy functional quaternary ammonium bolaform surfactants have a significantly larger CMC than the corresponding non-hydroxylated surfactants (32). This difference was explained with the ability of the hydroxy-terminus to hydrogen bond with the solvent.

Even though the CTP polymers with fluorinated end groups were only soluble in THF, their ability to aggregate in solution offered insight into how one might change the structure of xylan-rich heteropolysaccharides, or simply "xylan" for short, to produce water-soluble amphiphilic molecules. To this end, a series of xylan-rich heteropolysaccharides and their more water-soluble hydroxypropyl (HP) and acetoxypopyl (AP) derivatives (33) were prepared. As these materials were water soluble, it was possible to easily measure the true surface tension of the aqueous solutions by the Wilhelmy plate method. Hence, Figures 3B-3D, show γ as a function of the bulk solution concentration. Overall, the xylan-rich heteropolysaccharides and their HP and AP derivatives exhibited a wide range of CMC values ($0.01\text{-}5.0 \text{ g}\cdot\text{L}^{-1}$). However, these three plots are representative examples for two important trends:

1. Xylan obtained from different sources or isolation procedures exhibits extremely different CMC values (Figure 3B vs. 3C);
2. In general, HP or AP xylan derivatives (33), produced sharp transitions in surface tension with respect to bulk solution concentration and distinct CMC values (Figure 3D), whereas most (Figure 3D), but not all (Figure 3B), xylan isolated from natural

sources do not exhibit sharp changes in surface tension with changing bulk solution concentration and hence have less definitive CMC values.

Weak transitions, like the one in Figure 3C, are indicative of ill-defined aggregates in solution with small aggregation numbers. Nonetheless, the fact that xylans with different lignin-levels (Figure 3B) or chemical modification by HP or AP derivatives (Fig. 3D) could alter and sharpen the CMC provided encouragement that xylan-derivatives could be made that would adsorb ("dock") more strongly on a cellulose surface.

Self-Assembly Measurements at Solid Surfaces: Surface plasmon resonance (SPR) spectroscopy produces observations regarding the adsorption of solid (colloidal) mass at smooth surfaces from solution (26). LB films of regenerated cellulose represent multilayered architectures of cellulose molecules, with each layer having the thickness of a single cellulose molecule (4.2 Å) (34). These films and their structures have previously been described in the literature (21-26). The usual 40 to 60-layered films have an overall thickness of 15 to 20 nm, and they are totally clear and transparent. These films produce a contact angle with water of between 23 and 55° (21, 23).

SPR-experiments using the instrumental arrangement described by Green et al. (26) provide experimental observations related to film thickness (in pixel-values) on a time or concentration scale. Film thickness in pixels is determined by measuring the location of the baseline after correcting for changes in the bulk refractive index of the film due to changes induced by the solvent. Film thickness in pixels is related to a distance dimension according to a complicated relationship involving the response coefficient of the adsorbed substance, a reflection angle value, and many other parameters. Since the coefficient of the specific solutes have not been determined, no rigorous relationship can be established at this time. Nevertheless, an approximate thickness measure can be derived from the knowledge that each cellulose layer has a thickness of 4.2Å (34). By measuring the change in resonant angle in pixels for films with different numbers of cellulose layers (0, 10, 20, 40, and 60 layers), an approximate relationship between number of pixels and film thickness can be established. A conversion factor of 0.49 pixels/Å has been established experimentally.

Several water-soluble, xylan-rich hetero-polysaccharides and their derivatives were measured in this way with respect to their self-assembly behavior at cellulosic LB film surfaces (i.e., "docking" behavior). The corresponding experimental results are summarized in Figure 6. The structure of the xylan derivatives used is given in Figure 2.

Xylan itself is a hetero-polysaccharide that forms colloids at low solution concentration. Results indicate that a little xylan is adsorbed, slowly, at

concentrations above the CMC (Figure 6). By adding cyclodextrin to the xylan colloidal solution, xylan becomes more water soluble (as judged by the unaided eye), and the adsorption behavior as revealed by SPR changes (Figure 6). Very little xylan is adsorbed with the change in resonant angle leveling-off point at around 3 pixels. This value corresponds to a film $\approx 1.5\text{\AA}$ thick. As this value is too small to be consistent with a homogeneous monolayer, the surface must be weakly populated by “micellar” aggregates. When cyclodextrin is present, the same adsorbed amount is reached at a lower bulk solution concentration and the maximum adsorption plateaus at a slightly higher value (Figure 6). Anionically-modified xylan (CMX) shows behavior similar to that of xylan with cyclodextrin: rapid adsorption to a submonolayer adsorbed film (Figure 6).

Based on the above results, it was clear that more drastic changes in xylan structure were required to promote adsorption (“docking”). Hence cationic and F-containing xylan derivatives were examined given the strong “hydrophobic” effect seen for F-containing CTP derivatives. Cationically-

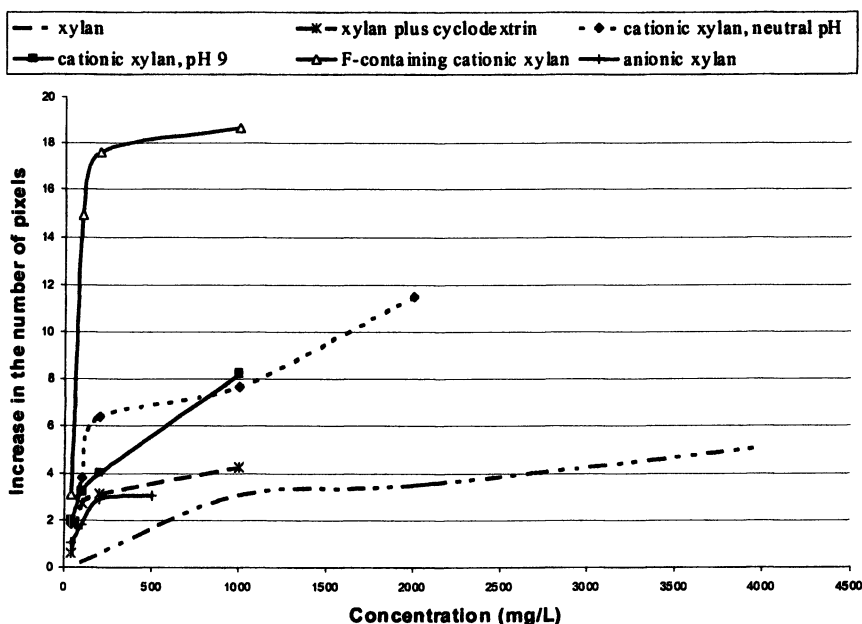


Figure 6. Results of an SPR-analysis monitoring film thickness (in pixels, whereby 2 pixels correspond approximately to 1 Å) on a concentration-scale for several xylan derivatives (peanut hull xylan served as starting material).

modified xylan is more strongly adsorbed by the cellulose surface with a sharp change in resonant angle to a value of approximately 8 pixels at concentrations below 0.1 g L^{-1} (Figure 6). Given the thickness of a cellulose layer, 4.2 \AA (34), this change in resonant angle, 8 pixels $\approx 4 \text{ \AA}$, maybe close to monolayer coverage. Another interesting feature is that anionic, cationic, and xylan plus cyclodextrin films all reach their plateau adsorption value below 0.1 g L^{-1} (Figure 6). Moreover, the driving force for enhanced adsorption of cationic xylan on cellulose does not seem to be solely driven by change as the adsorbed amount was independent of pH over a limited but important range.

Enhanced adsorption (“docking”) was not unexpected as the cationic functional groups can ionically bond to surface anionic functionalities present on regenerated cellulose films. This phenomenon is an effect similar to cationically modified starch being used for paper sizing (35). Nonetheless, as noted above, this effect is smaller than expected, hence the CTP results drove us to also try incorporating F-substituents onto the cationic xylan.

Figure 6 also shows that the adsorption behavior of cationic xylan can be further enhanced by introducing F-containing functionality into the molecule. X-ray photoelectron spectroscopy (XPS) experiments used to obtain the amount of F present on the polymer provided an estimated degree of substitution (DS) of approximately 0.1 (i.e., 1 F-substituent per 10 anhydroxylose units). Hence, even a small amount of F-substituents causes a substantial change in the amount of cationic xylan adsorbed. Based on the change in resonant angle, 18 pixels, adsorbed layer, on the order of 9 \AA , forms at low bulk solution concentrations. Hence, both ionic and hydrophobic interactions must be important for xylan adsorption on cellulose surfaces.

AFM Analysis of LB-Film Surfaces: The use of the same films employed for SPR experiments in subsequent AFM-experiments was made impossible by the use of a refractive index-adjusting oil that was found to interfere with AFM observations. For this reason, separate LB-films of regenerated cellulose were used in adsorption experiments in which films on glass (instead of gold) slides were suspended in water-soluble polysaccharide solutions of different composition and different concentration. Each adsorption experiment lasted for several hours at room temperature, followed by thorough washing of the surface with deionized water. The resulting surfaces were examined by AFM in the height as well as the phase-mode. The results reveal different levels of adsorption for water-soluble polysaccharides in the form of film-like coatings or nanosize particles and agglomerates. The fluorinated cationic xylan derivative appears to produce a textured surface with nanosize particles (Figure 7). Hence, even though F-containing xylan showed the strongest adsorption (“docking”) behavior, the textured surface supports the conclusion that adsorption of the xylan derivatives produces submonolayer coverage, and that adsorption occurs largely through “micellar” aggregates.

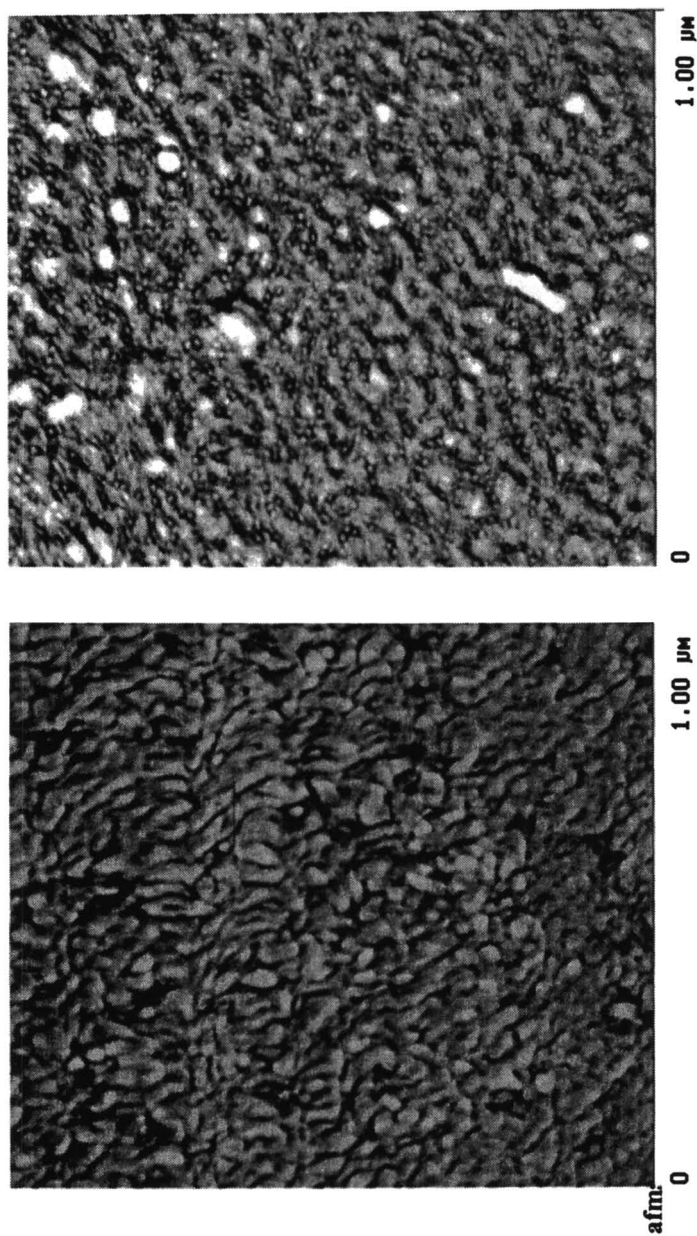


Figure 7. AFM height image (left) and phase images (right) of a 40-layer cellulose LB film treated with an aqueous solution of the F-containing cationic xylan derivative. Note the spherical particles deposited on the image on the right side.

Hypothetical Structures of Self-Assembled Micellar Aggregates: Various schematic models representing the possible structures of polysaccharidic and F-containing polymers have been advanced in the recent past. Some of these structures are illustrated in Figure 8. While it is too early to speculate on the specific structure of hemicellulose-like polysaccharides, it is apparent that both chemical structure and molecular size influence micellation, and this assembly is consistent with several of the aggregate models proposed for a variety of amphiphilic molecules.

The self-aggregation of telechelic copolymers with F-containing substituents has been pictured as the formation of jellyfish-like structures (7) in accordance with a proposition of Eisenberg et al. (4) (Figure 8A) for diblock copolymers. The extensive work on cholesteroylated pullulan (copolysaccharide) by Sunamoto et al. (12-15) has resulted in the model of a spherical nanoparticle transformed into a hydrogel by hydrophobic interactions (Figure 8B). Only one cholesteryl substituent in 100 anhydro-glucose repeat units of pullulan is sufficient to produce a gel structure. Uraki et al. (16, 17) present a similar vision for their hydroxypropylated unbleached organosolv pulp cellulose (Figure 8C). Recent work by Hillmyer and Lodge (11) advanced the idea of a self-aggregated structure varying with the magnitude of the polymer-polymer interaction parameter, χ . Whether the phases of the copolymers separate weakly or strongly depends on values of both χ and the molecular size of the respective copolymer components (in our case, the DP of the cellulose ester segment, Figure 5). A spherical aggregate structure results when the two copolymer components differ modestly in compatibility (i.e., have a low χ -value), and a more oblate, disk-like or sheet-like structure will result when χ rises (Fig. 8D). Thus, it can be expected that xylan-rich heteropolysaccharides produce self-aggregates with different structures, and that these differences depend on both molecular size and chemical structure, especially in relation to substitution patterns with non-polar groups.

Conclusions

1. Mono-functional, F-terminated cellulose ester oligomers in THF were found to self-assemble into micellar structures at concentrations of between 10^{-4} to 10^{-5} moles L^{-1} . The CMC depended on both the chemical nature of the oligomer (i.e., type of F-containing end group) and the size of the CTP-segment.

2. Langmuir Blodgett (LB) films of regenerated cellulose represent a uniform and a highly ordered cellulose surface well-suited for adsorption studies.

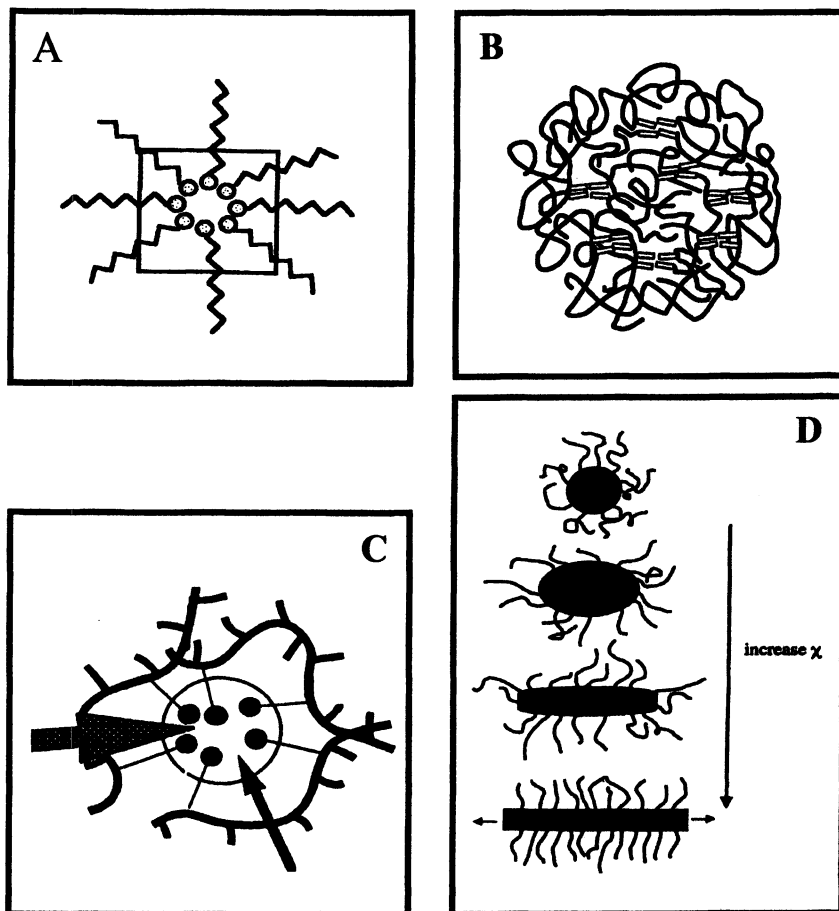


Figure 8. Several conceptual illustrations of the hypothetical structures of self-assembled macromolecular aggregates. (A) Micelles formed by blocky F-containing cellulose ester copolymers in THF-solution; (B) Schematic polycore model of cholesteroylated pullulan; (C) self-aggregate of hydroxypropylated unbleached (acetic acid-based organosolv) pulp cellulose; and (D) micellar structures changing from spherical (top) to sheet-like (bottom) with increasing polymer-polymer interaction parameter (χ). ((A) Reproduced with permission from reference 7. Copyright 1998 American Chemical Society. (B) Reproduced with permission from reference 13. Copyright 1995 Japanese Academy. (C) Reproduced with permission from reference 16. Copyright 1997 Walter de Gruyter. (D) Reproduced with permission from reference 11. Copyright 2002 John Wiley & Sons, Inc.)

3. The adsorption of polysaccharide derivatives on LB-surfaces of cellulose can be studied by SPR in relation to solute structure and concentration.

4. The amount of adsorbed xylan (heteropolysaccharide) is promoted by cationic functionality as well as by enhancing the amphiphilic character with strongly hydrophobic (F-containing) substituents.

5. AFM images corroborate the SPR results and demonstrate the deposition of nano-particles on the cellulose surfaces with submonolayer coverage.

6. The results are consistent with a variety of hypothetical models of self-assembled structures that depend on both the chemical composition (i.e., compatibility of different copolymer components), as well as molecular size.

Acknowledgment

Financial support for this study was provided by the USDA under its NRI program, contract # 9902352. Helpful discussion of the study by Prof. Paul Gatenholm and Hanno Roebroks, Chalmers University of Technology, are greatly appreciated.

References Cited

1. Simmons, W. C. In *Smart Materials Technologies*. W. C. Simmons, I. A. Aksay, and D. R. Huston, eds. Proc. SPIE, SPIE:Bellingham, WA, Vol. 3040, 1997, pg. 2-7.
2. Polla, D. L., W. P. Robbins, T. Tamagawa, C. Ye. *Mat. Res. Soc. Symp. Proc.*, 276, 1992.
3. Bellare, J. R., T. Kaneko, and D. F. Evans. *Langmuir* 4, 1988, 1066.
4. Zhang, L., H. Shen, and A. Eisenberg. *Macromolecules* 30, 1997, 1001.
5. Lin, Z. *Langmuir* 12, 1996, 1729.
6. Kikuchi, A., and T. Nose. *Polymer* 37(26), 1996, 5889.
7. Becker, U., J. G. Todd, and W. G. Glasser. *Surface Segregation Phenomena in Blends of Cellulose Esters*. Chapter in Cellulose Derivatives: Modification, Characterization, and Nanostructures, Th. J. Heinze and W. G. Glasser, eds., ACS Symp. Ser. No. 688, 315-331 (1998).
8. Frazier, C. E., and W. G. Glasser. 1995. Intramolecular effects in cellulose mixed benzyl ethers blended with poly(ϵ -caprolactone). *J. Appl. Polym. Sci.*, 58(6):1063-1075.

9. Sealey, J. E., C. E. Frazier, G. Samaranayake, and W. G. Glasser. 2000. Novel cellulose derivatives. V. Synthesis and thermal properties of esters with trifluoroethoxy acetic acid. *J. Polymer Sci.: Pt. B: Polym. Physics* 38 (3), 486-494.
10. Glasser, W. G., U. Becker, and J. G. Todd. 2000. Novel cellulose derivatives. VI. Preparation and thermal analysis of two novel cellulose esters with fluorine-containing substituents. *Carbohydrate Polymers* 42, 393-400.
11. Hillmyer, M. A., Lodge, T. P. Synthesis and self-assembly of fluorinated block copolymers. *J. Polymer Sci.: Pt. A*, 40, 2002, 1-8
12. Sunamoto, J., Sato, T., Taguchi, T., and Hamazaki, H. Naturally occurring polysaccharide derivatives which behave as an artificial cell wall on an artificial cell liposome. *Macromolecules* 25, 1992, 5665-5670.
13. Akiyoshi, K., S. Deguchi, H. Tajima, T. Nishikawa, and J. Sunamoto. Self-assembly of hydrophobized polysaccharide. *Proc. Japan Acad.* 71, 1995, Ser. B, 15-19.
14. Akiyoshi, K., Taniguchi, I., Fukui, H., and Sunamoto, J. Hydrogel nanoparticle formed by self-assembly of hydrophobized polysaccharide. Stabilization of adriamycin by complexation. *Eur. J. Biopharm.* 42 (4), 1996, 286-290.
15. Nishikawa, T., Akiyoshi, K., and Sunamoto, J. Macromolecular complexation between serum albumin and the self-assembled hydrogel nanoparticle of hydrophobized polysaccharides. *J. American Chem. Soc.* 118 (26), 1996, 6110-6115.
16. Uraki, Y., K. Hashida, and Y. Sano. Self-assembly of pulp derivatives as amphiphilic compounds: Preparation of amphiphilic compound from acetic acid pulp and its properties as an inclusion compound. *Holzforschung* 51, 1997, 91-97.
17. Uraki, Y., Hanzaki, A., Hashida, K., and Sano, Y. Self-assembly of pulp derivatives as amphiphilic compounds: verification of molecular association and complexation with low and high molecular mass compounds. *Holzforschung* 54, 2000, 535-540.
18. Glasser, Wolfgang G., William E. Kaar, Rajesh K. Jain, and James E. Sealey. 2000. Isolation options for non-crystalline heteropolysaccharides (HetPS).(Part 5 of "Steam-Assisted Fractionation of Biomass"-series). *Cellulose* 7(3), 299-317.
19. Henriksson, A., and P. Gatenholm. Controlled assembly of glucuronoxylans onto cellulose fibres. *Holzforschung* 55, 2001, 494-502.
20. Petty, M. C. *Langmuir-Blodgett films, an introduction.* Cambridge University Press, 1996.

21. Schaub, M., G. Wegner, G. Wenz, A. Stein and D. Klemm. Ultrathin films of cellulose on silicon wafers. *Advanced Materials* 5(12), 1993, 919-923.
22. Basque, P., A. de Gunzbourg, P. Rondeau, and A. M. Ritcey. Monolayers of cellulose ethers at the air-water interface. *Langmuir* 12, 1996, 5614-5619.
23. Loscher, F., T. Ruckstuhl, T. Jaworek, G. Wegner and S. Seeger. Immobilization of biomolecules on Langmuir-Blodgett films of regenerative cellulose derivatives. *Langmuir* 14(10), 1998, 2786-2789.
24. Mao, L., and A. M. Ritcey. Preparation of cellulose derivative containing carbazole chromophore. *J. Appl. Polym. Sci.* 74, 1999, 2764-2772.
25. Mao, L., and A. M. Ritcey. Langmuir-Blodgett films of cellulose ethers containing carbazole. *Macromol. Chem. Phys.* 201, 2000, 1718-1725.
26. Green, R. J., R. A. Frazier, K. M. Shakesheff, M. C. Davies, C. J. Roberts, and S. J. B. Tendler. Surface plasmon resonance analysis of dynamic biological interactions with biomaterials. *Biomaterials* 21, 2000, 1823-1835.
27. de Oliveira, W., and W.G. Glasser. 1994. Novel cellulose derivatives. II. Synthesis and characteristics of mono-functional CP segments. *Cellulose*, 1(1), 77-86.
28. Glasser, W. G., and U. Becker. 1999 (app'd in 2000). About the hydrolysis of cellulose propionate to segments with low DP. *Cellulose* 6(4), 283-28.
29. Pulkkinen, E., A. Maekelae, and H. Makkonen. Preparation and testing of cationic flocculants from Kraft lignin. In *Lignin – Properties and Materials*, W. G. Glasser and S. Sarkanen, eds., ACS Symp. Ser. No. 397, 1989, 284-293.
30. Gustavsson, M., M. Bengtsson, P. Gatenholm, W. Glasser, A. Teleman, and O. Dahlman. Isolation, characterisation and material properties of 4-O-methylglucuronoxylan from aspen. Chapter in *Biorelated Polymers – Sustainable Polymer Science and Technology*, E. Chiellini, H. Gil, G. Braunegg, J. Buchert, P. Gatenholm, and M. van der Zee, Eds., Kluwer Academic/Plenum Publishers, New York, 2001, pg. 41-52.
31. Evans, D., and H. Wennerstrom. *The colloidal domain*. Wiley-VCH, 1999.
32. Davey, T. W., W. A. Ducker, and A. R. Hayman. 2000. Aggregation of ω -Hydroxy Quaternary Ammonium Bolaform Surfactants. *Langmuir* 16, 2430-2435.

33. Jain, Rajesh K., M. Sjöstedt, and W. G. Glasser. 2001. Thermoplastic xylan derivatives with propylene oxide. *Cellulose* 7(4), 319-336.
34. Buchholz, V., G. Wegner, S. Stemme, and L. Oedberg. *Adv. Mater.* 8, 1996, 399-402.
35. Maximova, N., Laine, J., and Stenius, P. Adsorption of lignin-cationic starch complexes on the cellulose fibers. Proc. 7th European Workshop on Lignocellulosics and Pulp, Turku/Abo, Finland, August 26-29, 2002, 127-130.

Chapter 15

Sorption of Mannans to Different Fiber Surfaces: An Evolution of Understanding

Tea Hannuksela and Bjarne Holmbom

Process Chemistry Group, Åbo Akademi University, Porthaninkatu 3,
Turku, Åbo 20500, Finland

Mannans are sorbed to a high extent onto chemical pulps, giving the fibers and the formed sheet superior properties. This paper reviews the use of mannans in papermaking, both as additives and as naturally present polysaccharides. The effect of mannans in mechanical pulping and papermaking, including the interaction with colloidal wood resin droplets, is, furthermore, discussed.

Introduction

Sorption of mannans onto fiber surfaces has received much attention throughout the years. Today, the interest still remains but the focus has slightly changed and evolved with the needs and demand of industry. The present paper focuses on mannan sorption in the production of pulp and paper, even if sorption also plays an important role in other fields of industry (textile, food etc.).

We will begin by listing the mannans in question and setting out some milestones in the history of mannans in papermaking. Towards the end, we will briefly discuss other properties of mannans and put more emphasis on the interactions of mannans in mechanical pulping and papermaking, which is also the main focus of research, in the present field, at our laboratory.

Different types of mannans

The term “mannans” usually refers to polysaccharides built up of a backbone of mannose units. The ones discussed in the present paper are all natural mannans, either extracted from gum plants or from wood. The most commonly used gum *galactomannans* (GMs) in papermaking are locust bean gum and guar gum. They are both built up of a backbone of (1→4)-linked β -D-mannopyranosyl units, with single (1→6)-linked α -D-galactopyranosyl units as side groups (1). Guar gum GMs are highly substituted along the whole backbone - approximately six out of ten mannose units carry a galactose group. Locust bean gum, on the other hand, has fewer galactose side groups which are not regularly distributed over the backbone, but rather exist in uniform blocks, thus also creating regions that are completely unsubstituted (1). Even if both gums are galactomannans, their structure renders their properties and interactions somewhat different.

Softwood mannans are *galactoglucomannans* (GGMs) built up of a backbone of (1→4)-linked β -D-mannopyranosyl units, alternated with occasional (1→4)-linked β -D-glucopyranosyl units. Varying amounts of (1→6)-linked α -D-galactopyranosyl units are found as single side groups. Softwood GGMs are additionally partly acetylated at positions 2 or 3 of the mannose units. The acetylated GGMs (AcGGM) are, however, easily deacetylated in alkaline conditions which renders the polysaccharides less water-soluble due to a higher degree of orientation through intermolecular bonding. The deacetylated GGMs (DeacGGMs) may even crystallize with time (2).

Hardwood mannans are glucomannans, which are built up of a backbone of only mannose and glucose units, *i.e.* they have no galactose side groups. Recently, hardwood mannans have also been found to carry acetyl groups (3).

Mannans in chemical pulping and papermaking

The first scientific publications on mannans as beater and wet-end additives were very much practically oriented. They focused on the obtained effects rather than the phenomenon behind. The need of a deeper understanding came into the picture some time later, when the practical use of mannans was already rather well established. The attention was then turned to wood mannans naturally present in pulp, with an attempt of increasing the yield. Today, a large interest lies in elucidating the interactions between mannans and cellulose in wood itself, as well as between mannans and other interfaces in pulp suspensions than cellulose.

Mannans as beater additives

Different kinds of vegetable mucilages were already used in ancient Egypt as glue during mummification (4) and in Japan as an additive, or more precisely as a fiber-dispersing agent, in the production of the exquisite long-fibered Japanese paper (5). Hundreds of years later, mannans are still used in papermaking in order to obtain the same results – bonding, strength and homogeneity.

Initially, natural mannans, mainly locust bean gum, were used as beater additives in the papermaking process for their ability to produce pulps with the same properties as highly beaten pulps, but at much shorter beating times (6). This was later explained, assuming sorption took place also inside the fibers, by an increased swelling and flexibility of the fibers, which resulted in fibrillation during refining rather than cutting (7). Shorter beating times enabled the use of also short-fibered wood for the manufacturing of paper. Furthermore, a shorter beating time in itself also ameliorated the properties of the pulp (better formation and faster drainage) as well as that of the formed paper; lower shrinkage, higher porosity and opacity, better compressibility, and on the whole, better strength properties at lower costs, and at higher paper machine speeds (5). An increased retention of fines has also been reported upon mannan addition (8). Later on, after the large-scale cultivation and commercialization of guar gum in 1953 in the United States, guar gum replaced the use of locust bean gum in papermaking (8). Extensive fundamental research was undertaken in order to learn more about the outstanding properties of mannans, for it was mannans, more than other polymers that gave the best results. Regarding the mechanism lying behind sorption, it was stated already in 1950 by Swanson (5) that the fibers became coated by a hydrogel layer of mucilage which gave the fibers their excellent properties. Gruenhut (9) suggested that the mannan polymers align on the fiber surfaces with the cellulose chain and form hydrogen bonds, when structural conformations allow it. Gruenhut also found that sorption of mannans to fiber surfaces was dependent on the mannan structure – a less branched GM being sorbed to a higher degree. Leech (10) pointed out one year later that mannans increased paper strength by increasing the strength of the bonds, but also through better formation and by creating a larger bonding area.

Several papers were published where more detailed experiments had been conducted in order to understand the effect of different parameters, such as mannan structure and concentration, pulp consistency, temperature and pH (11, 12, 13). The results are somewhat varying depending on the used mannan and the experimental conditions, which in turn depend on the final interest of the research. Dugal and Swanson (14) published a paper in 1972 regarding the effect of the galactose content on the properties of the formed paper. They found the GM to give the best paper strength properties at optimal mannose to galactose

ratios, usually between 2 and 3, except for the tear strength that was optimal at lower ratios.

Little by little, the interest in mannan as a beater and wet-end additive seemed to decrease from a scientific point of view. The interest in natural mannans did not disappear completely, but was rather shifted towards research on the properties of mannans in solution and in mixtures with other polysaccharides, something which mainly served the food industry, but that could also be applied to papermaking, as we will discover later on.

The use of mannans as wet-end additives has decreased with the years, along with the line of new, more specific additives. Chemically modified mannans (15) have, however, gained new interest and become worthy competitors.

Dissolved wood mannans

Some years after the upswing in the use of mannans as beater additives, mannan sorption studies started to focus on wood based mannans that were naturally present in the pulp itself and which were dissolved into the process water during processing and cooking. A retention or sorption of the dissolved mannans on the fibers in the formed sheet increased the yield and was thus economically desirable. Furthermore, sorption of wood mannans, like gum GMs, also ameliorates the strength properties of the formed sheet (16).

The first scientific publications concerning sorption of dissolved wood mannans onto fibers were written by Most (17) in 1957, and in 1960, focused on glucomannans, by Annergren and Rydholm (18). They suggested that fragments of glucomannans, dissolved during alkaline impregnation in sulfite pulping, were resorbed onto cellulose surfaces, such as cotton linters, which decreased their otherwise excessive degradation in the cooking liquor. They further pointed out that the resorption was primarily set off by a deacetylation of the glucomannan. The effect of acetyl groups was investigated in detail some years later by Laffend and Swenson (19) who found that sorption of deacetylated glucomannan increased with increasing mannan concentration, while the sorption of acetylated glucomannan leveled out at higher concentrations. Handsheets containing deacetylated glucomannans gave slightly better strength properties than the acetylated, both, nonetheless, remarkably superior to the blank (7).

It is, however, not only mannans that sorb to cellulose surfaces. Also wood xylans are able to do so, but only after partial degradation of the hemicellulose itself as well as of the fiber surface, which takes place, for instance, during kraft cooking. As a considerable part of the chemical pulps are produced from hardwoods, such as birch in Northern Europe, which contain considerable amounts of xylans rather than mannans, the resorption of xylans received a lot

more attention than that of mannans. Furthermore, during kraft cooking of softwood, with appreciable amounts of mannan instead of xylan, the deacetylation of the mannans causes a rapid resorption and stabilization on the fiber surfaces as described above. The resorption of mannans in chemical pulping is, thus, not of great concern. Clayton and Phelps (20) compared the sorption of glucomannans with birch xylans and found that sorption of mannans was twice as high as that of modified birch xylans. A large study on both wood xylan and mannan sorption onto cotton fibers was conducted under conditions representative of a kraft cook (21, 22). The sorption of both polysaccharides was shown to be of physical type, *i.e.* through hydrogen bonding, by calculating the activation energies for sorption.

The sorption studies became more and more fundamental and new sophisticated techniques were employed for the purpose. These results will, therefore, be discussed in a new chapter, as they mainly involve the mechanism of sorption. Some additional results of mannan sorption onto chemical pulps will be presented in the section "Mannans in mechanical pulping and papermaking".

Mechanism of sorption

The sorption of mannans onto fibre surfaces has often simply been described as a process involving four steps (12). The first involves the diffusion or transport of the polysaccharide to the fibre surface. This process is governed by the collision frequency induced either by Brownian motion or turbulent transport. Attachment or sorption of the polysaccharide to the fibre surface, in the second step, is a direct consequence of collision, if the polymer – sorbent attraction is higher than the polymer – solvent attraction. As a third step, the polysaccharides will undergo certain rearrangements or reconfigurations after the attachment at the fibre surface, during which polysaccharides are also believed to diffuse into the fiber. The last step involves the reverse of steps 1 to 3 or the detachment of the polysaccharide from the fibre surface. The extent of desorption is, however, believed to be quite limited.

The extensive research in mannan sorption brought little by little forward a hypothesis of the mechanism of sorption. It was already stated above (21) that sorption involved hydrogen bonding between hydroxyl groups on the cellulose chain and polar groups on the polysaccharide. Due to the almost identical conformation of mannose and glucose, apart from the conformation at C2, crystallization could be anticipated. It had been observed earlier that the sorption of glucomannans increased with the crystallinity of cotton indicating that a more ordered structure of the sorbent enhanced sorption (22). In 1978 Chanzy *et al.* (23) visualized the crystallization of pure mannan on cellulose microfibrils in a shish-kebab morphology, determined by X-ray analysis, where the mannan

crystals (the kebabs) grow perpendicularly on the cellulose microfibrils (the shish, or stick). The mannan in the crystal is, nevertheless, parallel with the cellulose chain axis. In a later study (24), they found that crystals of glucomannans were less perfect than those of pure mannan, and that the disorganization increased with the amount of glucose. Crystals of low-molar-mass glucomannans could, nonetheless, also be grown on cellulose microfibrils in the shish-kebab morphology.

For mannans containing galactose side groups, the situation is a little different as these groups will hinder a close contact between the two backbones, and thus also complete crystallization. The so called co-crystallization of mannans with cellulose microfibrils (often of bacterial origin) has been investigated in detail recently in order to understand the role and interactions of mannans in the living plant cell wall. Whitney *et al.* (25) found through solid-state NMR analysis that unsubstituted mannan segments in glucomannans and galactomannans were able to bind to cellulose and interfered thus with the crystallization of bacterial cellulose. Glucomannans disrupted the cellulose crystallinity much more than galactomannans, while galactose-rich GM did not almost interact with cellulose at all. Newman and Hemmingson (26) furthermore found, also through NMR analysis, that it was not only the unsubstituted mannose units that interacted with cellulose, but also the ones with galactose substituents, whereas the galactose units themselves did not show any sign of interaction.

Iwata *et al.* (27) observed by X-ray analysis that out of different glucans, xylans and galactans, it was indeed the mannans that showed the highest affinity towards bacterial cellulose. The sorption mechanism of different hemicelluloses is, moreover, not necessarily the same. Uhlin *et al.* (28) found that bacterial cellulose crystallized in a different form in the presence of wood hemicelluloses than in their absence (I_{β} , rather than I_{α}). Furthermore, xylans and mannans seemed to interact with cellulose in different ways – xylans co-crystallized with cellulose producing defects in the crystalline structure, while mannans mainly decreased the crystallite size and thus also the over all degree of crystallinity. Xylan and mannan chains have been shown to undergo different conformational transitions upon sorption (29). The mannans were able to form a two-fold helix and lay down on the cellulose chain quite nicely and seemed to interact with two cellulose chains, while xylan took on a three-fold molecular axis and could, therefore, not sorb as efficiently. Larsson *et al.* (30) showed through solid-state NMR analysis that xylans can, anyhow, interact directly with cellulose surfaces. Tetramers were the smallest polymers to sorb onto cellulose surfaces (29).

As most of the work done in the field has not used crystallographic methods to measure the interactions between mannans and cellulose, the terms “sorption” or “adsorption” are preferred. The association of mannans with cellulose should perhaps rather be described as a partial crystallization of the two polymers.

Mono- or multi layer sorption

Whether mannans are able to sorb on surfaces other than pure cellulose, has also been looked into. Mannan sorption has been described by both mono- and multi-layer theories, adopted from gas- or electrolyte adsorption theories. In reality, the situation is more complex as polysaccharides are very large and have a random coil formation in solution, and are therefore initially likely to attach to the fiber surface in this conformation. Due to the galactose side groups, the polysaccharide will not be able to lay down completely flat on the fiber surface even after certain rearrangements and there will probably be loops and tails spreading out from the fiber surface (22).

Multi-layer sorption, on the other hand, would have to involve an interaction between mannan chains themselves. Mannan sorption seems, however, to be built up of two stages; firstly, the initial very rapid sorption, followed by a much slower sorption phase, which may be the multilayer sorption (20). A change in the mannan conformation after sorption may perhaps enable or facilitate mannan – mannan interactions and allow multilayer sorption. Studies at our laboratory on sorption of mannans onto bleached kraft pulp (BKP) showed that sorption of a high-molar-mass GM was not affected by the presence of a layer of presorbed low-molar-mass GM, and vice versa (31). Furthermore, sorption onto mechanical pulp fibers, which already contain high amounts of hemicelluloses and probably little, if any free cellulosic surfaces, has also been achieved with certain mannans. This point will be further discussed in the next chapter.

Sorption equilibrium is often not reached even after long sorption times (17) indicating that sorption of mannans is a rather dynamic process, involving reorganization, diffusion into the fiber wall, etc. On the other hand, mannan sorption is essentially irreversible. Desorption would involve a simultaneous release of all hydrogen bonds between the mannan chain and the sorbent, a situation that is rather unlikely.

Finally there is the possibility of mannan deposition onto the fiber surfaces involving firstly an association/aggregation of the mannans in solution prior to deposition onto the fiber surface. This point will also be discussed in more detail in the next chapter. However, in order to understand mannan interactions better, we need to briefly look at another research area – the interactions of mannans in solution.

Properties and interactions of mannans in solution

Different mannans have been used in the food industry already for years due to their excellent thickening, binding and stabilizing properties. Guar gum GMs are fairly soluble in water and behave as non-Newtonian solutions. GM solutions

are stable in a wide pH range and they are also resistant to salts (4), which is one of the reasons for their wide popularity. GMs alone in solution do not show inter-chain interactions, *i.e.*, they do not form gels. High concentrations of multivalent ions may, however, provoke gel formation. Borates and transition metal ions are, therefore, used to crosslink the GMs into commercially useful gels (4).

GMs may also form gels with other polysaccharides, such as xanthans (which are also non-gelling alone) (32) - the most interactive mannans being the ones with the fewest galactose side groups (33). The interactions are not completely understood and several mechanisms have been presented, but the interactions are basically dependent on the structure and conformation of both polysaccharides as well as on the thermodynamic conditions (34).

Mannans are able to sorb both onto hydrophilic and hydrophobic particles, such as minerals and talc, respectively, and form bridges between the particles. For this reason, mannans (normally charged) are used as flocculating agents in water cleaning systems, or in mineral separation from ores. Such interactions have been proposed to be governed by hydrogen bonding as well as chemical interactions (35).

Mannans are also used as stabilizing agents for emulsions in the food industry. Traditionally, it has been believed that in order to stabilize oil droplets, mannans need a presorbed layer of surfactant, such as proteins, which the mannans can interact with. Alternatively, the stabilization is said to be produced by the increased viscosity, brought on by the mannans (36). Both of the theories may be true in the studied cases, but mannans are, nonetheless, also able to give steric stabilization in the absence of surfactants, and at very low concentrations. Garti and Reichman (37) found that GMs were indeed slightly surface active by measuring their surface tension in solution as well as the interfacial tension with different oils. It has, furthermore, been established, for certain oligosaccharides, that depending on their conformation, they may in fact develop hydrophobic sites thanks to the methine groups (CH) (38).

Wood mannans have also been shown to sterically stabilize colloidal wood resin droplets. Applied studies at our laboratory showed that it was mainly the molar mass of the mannan that governed the stabilization of wood resin - the larger the polymer, the better was its stabilizing properties (39).

Mannans in mechanical pulping and papermaking

In mechanical pulping and papermaking, none of the wood constituents are intentionally removed from the pulp during processing. However, during refining or grinding of wood (mainly spruce in Northern Europe), considerable amounts of acetylated GGMs (AcGGM) are dissolved into the process water (40).

Softwoods, furthermore, contain sticky resinous substances, familiarly called wood resin or wood pitch, which are also released into the process waters as colloidal droplets. In pure water, wood resin droplets are electrostatically stabilized, but in the presence of salts or certain chemicals, the droplets aggregate and may deposit. This is naturally detrimental for the runnability of a paper machine, as well as for the quality of the formed paper. Fortunately, the concurrently dissolved GGMs are able to sterically stabilize the wood resin droplets against electrolyte induced aggregation (41, 42). It has, furthermore, been shown that even when aggregation occurs, the deposition tendency of the aggregates is reduced (43). It is, thus, clear that the presence of dissolved mannans in mechanical pulping and papermaking process waters is highly desirable, and that removal through sorption onto fiber surfaces should be minimized.

The strength of mechanical pulps is also increased after mannan sorption. One explanation is the increased hydrophilicity of the fibers, due to coverage of lignin by mannans, and thus an increased hydrogen bonding ability (44).

Next, we will focus on a laboratory study of mannan sorption onto both mechanical and chemical pulps that are relevant in the production of wood-containing papers, as chemical pulps are often also added as reinforcement fibers. The sorption experiments were performed with GGMs isolated from spruce, or enzymatically modified guar gum GGMs. The amount of sorbed mannan was calculated by measuring the amount of mannan left in solution by acidic methanolysis followed by GC analysis.

Sorption onto mechanical pulp fibers

A large part of the produced thermomechanical pulp (TMP) is subjected to alkaline peroxide bleaching (PB). As described earlier, GGMs are deacetylated under alkaline conditions, *i.e.* also during peroxide bleaching. Deacetylation dramatically increases sorption of GGMs, even onto TMP fibers. After a laboratory bleaching and subsequent agitation, about 60% of all dissolved GGMs were sorbed (45). This means that after a bleaching stage, there will only be small amounts of mannans in solution for stabilization purposes. If chemical pulp is additionally introduced in the mixing chest, the remaining GGMs will sorb onto the pulp leaving virtually no GGM left in solution. In order to overcome this problem, other natural mannans, such as guar gum GGMs, may be added, or part of the GGM-rich process water taken aside and reintroduced at appropriate locations. For realizing this, fundamental knowledge of mannan sorption onto different pulps is needed.

Studies at our laboratory showed that hardly any AcGGMs sorbed to spruce TMP (46). This is natural as GGMs are dissolved from the pulp in the first place.

Softwood TMP fibers, unbleached or bleached, are not believed to have any clean cellulose surfaces, as dissolved GGMs would directly sorb onto these areas if such were exposed. Sorption of AcGGMs was also not increased after peroxide bleaching of the fibers for the same reason. Sorption of unmodified guar gum GMs was also low onto all TMP samples (45). After an enzymatic degradation to lower molar masses, the sorption was not either improved. However, after removal of galactose side groups, the sorption onto TMP was increased, and increased further with time (~50% sorbed after 24 h). Sorption of the galactose-poor GMs was, nonetheless, lower on PB-TMP, due to “presorbed” GGMs from peroxide bleaching, which may slow down the subsequent sorption of other mannans, perhaps by blocking of pores.

Separately deacetylated GGMs were sorbed to TMP fibers to a high degree, and, as for the galactose-poor GMs, deacetylated GGMs were sorbed to a lower extent to PB-TMP due to the “presorbed” GGMs from peroxide bleaching.

The high extent of sorption of certain mannans onto TMP indicates that mannans are also able to sorb onto “unclean” surfaces, *i.e.* without exposed cellulose surfaces, or that the sorption may indeed be a deposition on the fiber surface after self-association, which can happen with galactose-poor GMs (33), or partial crystallization after deacetylation of GGMs, or simply due to concurrent factors affecting the mannan solubility upon mixing of mannans with fibers.

Aggregation on fiber surfaces has been observed for xylans (47). The size and amount of deposited xylan particles could be governed by experimental conditions, such as temperature, pH and time, as well as the number of glucuronic acid side groups (48). Xylans are, nevertheless, charged and will therefore behave differently from neutral mannans. Microscopic methods should be used in order to visualize whether deposition can take place also for mannans under certain conditions.

Sorption onto chemical pulps

Results obtained at our laboratory (31) agreed well with the literature. AcGGMs were sorbed to BKP at a high rate, and after deacetylation, almost all mannan was sorbed, even at very high GGM concentrations. The sorption of acetylated GGMs was slightly increased at high salt and GGM concentrations.

The sorption of AcGGM was found to be dependent on the type of pulping method used, *i.e.* lignin-retaining or lignin-removing, indicating that AcGGMs were preferentially sorbed onto cellulosic fibers (Figure 1) (46). Bleaching, whether it attacked lignin or not, did not affect sorption. Ishimaru and Lindström (49) studied the sorption of a commercial polygalactomannan to different pulps and observed that it was preferentially sorbed onto chemical pulps rather than

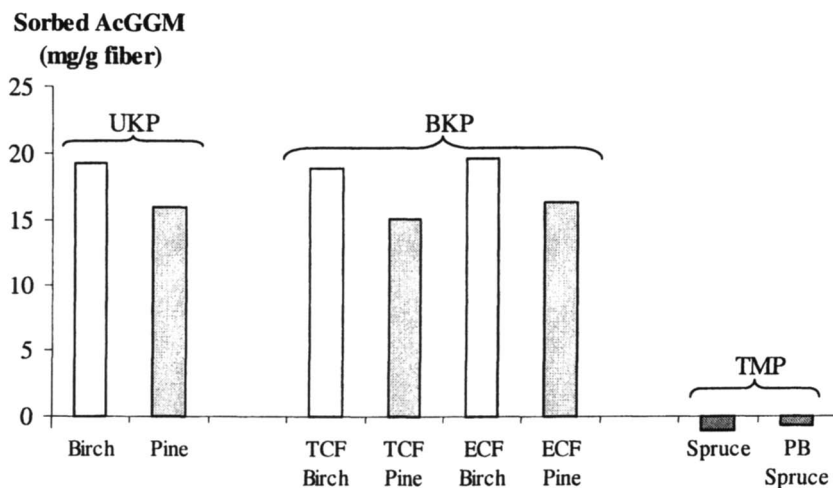


Figure 1. Sorption of acetylated GGMs onto different pulps after 4 h, 25°C, pH 7, 0.01 M NaCl, 1% consistency (46). Complete sorption at 23.3 mg/g. TCF= totally chlorine free, ECF=elemental chlorine free.

mechanical pulps. They did not either see any great differences between sorption onto unbleached (UKP) and BKP.

The type of wood fiber used also affected GGM sorption; hardwoods generally sorbing more than softwoods (Figure 1). Hardwood mechanical pulps may, in fact, have clean cellulose surfaces as they do not contain large amounts of GGMs. The relationship is, however, not straightforward, owing to the different fiber structure and composition between hardwoods and softwoods.

Regarding the effect of mannan structure on sorption, studies with enzymatically modified guar gum GGMs, showed that it was mainly the number of galactose side groups that affected sorption, rather than the molar mass (31). Temperature, pH and salt addition did not affect GM sorption, under conditions that are normal during mechanical pulping and papermaking. The degree of beating of the BKP did not either affect sorption - differences were only found with unbeaten pulps or when using low-molar-mass GGMs.

In conclusion, if mannans were to be added to the process waters as stabilizers for wood resin, their sorption to fiber surfaces ought to be minimal. Of the mannans studied at our laboratory, the unmodified guar gum GM sorbed the least to cellulosic fibers, and hardly at all to mechanical pulp fibers. Preliminary results (39) from deposition tests with wood resin emulsions also indicated that unmodified guar gum GGMs were the best stabilizers and gave the

lowest amount of deposition. If mechanical process waters were to be recycled, they should be withdrawn before peroxide bleaching when the content of acetylated GGMs is the highest, for deacetylated GGMs sorb too easily and are inadequate wood resin stabilizers.

Conclusions

Mannan sorption studies have a long history. It was initially studied in order to determine the beneficial properties that mannans gave upon addition as beater additives. Later on, the increase in yield through sorption of wood mannans during chemical pulping was studied. More recently the focus has turned to mannan and cellulose interaction in the living plant cells. All this, as well as information from the food, textile, pharmaceutical and cosmetics industries, have helped in understanding the interaction of mannans with other surfaces, or interfaces, than cellulose. For instance, in mechanical pulping and papermaking, mannans act as steric stabilizers and detackifiers of wood resin droplets. In conclusion it can be stated that mannans possess an extraordinary ability to interact with different kinds of surfaces, something which could be exploited to a higher degree in the pulp and papermaking industry. Expenses for additives could also be reduced if GGMs in process waters were efficiently recycled. Mannans are, furthermore, neutral polymers and will not give detrimental effects upon accumulation in process waters due to closure of water systems. Natural mannans will not consume other chemical additives, or be sensitive to changes in pH or salt concentrations.

Finally, as AcGGMs seem to sorb preferentially onto cellulose surfaces, sorption studies might also be used as an easy technique for measuring the presence of accessible surface cellulose.

Acknowledgements

Financial support from the international PhD Program in Pulp and Paper Science and Technology in Finland (PaPSaT) is gratefully acknowledged. Dr Antoinette O'Sullivan is, furthermore, thanked for linguistic assistance. This study was partly conducted within the European Commission "Pitch"-project (QLK5-CT-1999-01357). This work is part of the activities at the Åbo Akademi Process Chemistry Group within the Finnish Centre of Excellence Program (2000-2005) by the Academy of Finland.

References

1. Baker, C.; Whistler, R. *Carbohydr. Res.* **1975**, *45*(1), 237-243.
2. Katz, G. *Tappi* **1965**, *48*(1), 34-41.
3. Teleman, A.; Antonsson, M.; Tenkanen, M.; Jacobs, A.; Dahlman, O. *Carbohydr. Res.*, in press.
4. Maier, H.; Anderson, M.; Karl, C.; Magnuson, K.; Whistler, R. In *Industrial gums: polysaccharides and their derivatives*; Whistler, R.; Bemiller, J. N., Eds.; Academic Press: London, 1993; pp 181-227.
5. Swanson, J. *Tappi* **1950**, *33*(9), 451-463.
6. Shiever, E.; Webb, M.; Swanson, J. *Tappi* **1950**, *33*(12), 578-586.
7. Laffend, K.; Swenson, H. *Tappi* **1968**, *51*(3), 141-143.
8. Goldstein, A.; Alter, E.; Seaman, J. In *Industrial Gums*; Whistler, R. Ed.; Academic Press: New York, 1973, pp 303-321.
9. Gruenhut, N. *Tappi* **1953**, *36*(7), 297-301.
10. Leech, H. *Tappi* **1954**, *37*(8), 343-349.
11. Keen, J.; Opie, J. *Tappi* **1957**, *40*(2), 100-104.
12. Russo, V.; Thode, E. *Tappi* **1960**, *43*(3), 209-218.
13. Opie, J.; Keen, J. *Tappi* **1964**, *47*(8), 504-507.
14. Dugal, H.; Swanson, J. *Tappi* **1972**, *55*(9), 1362-1367.
15. Burnfield, K. *Proceedings*, Papermakers Conference, Chicago, IL; TAPPI, 1995; pp 209-214.
16. Suurnäkki, A.; Oksanen, T.; Kettunen, H.; Buchert, J., Technical Research Centre of Finland, unpublished results.
17. Most, D. *Tappi* **1957**, *40*(9), 705-712.
18. Annergren, G.; Rydholm, S. *Svensk Papperstidn.* **1960**, *63*(18), 591-600.
19. Laffend, K.; Swenson, H. *Tappi* **1968**, *51*(3), 118-123.
20. Clayton, D.; Phelps, G. *J. Polymer Sci., Pt. C* **1965**, (11), 197-220.
21. Hansson, J.-Å. *Svensk Papperstidn.* **1970**, *73*(3), 49-53.
22. Hansson, J.-Å. *Holzforschung* **1970**, *23*(3), 77-83.
23. Chanzy, H.; Dube, M.; Marchessault, R. *Tappi* **1978**, *61*(7), 81-82.
24. Chanzy, H.; Grosrenaud, A.; Joseleau, J-P.; Dube, M.; Marchessault, R. *Biopolymers* **1982**, *21*(2), 301-319.
25. Whitney, S.; Brigham, J.; Darke, A.; Reid, J.; Gidley, M. *Carbohydr. Res.* **1998**, *307*(3-4), 299-309.
26. Newman, R.; Hemmingson, J. *Carbohydr. Polym.* **1998**, *36*(2/3), 167-172.
27. Iwata, T.; Indrarti, L.; Azuma, J. *Cellulose* **1998**, *5*(3), 215-228.
28. Uhlin, K.; Atalla, R.; Thompson, N. *Cellulose* **1995**, *2*(2), 129-144.
29. Kroon-Batenburg, L.; Leeftang, B.; van Kuik, J. A.; Kroon, J. Presented at the 223rd ACS National Meeting, Orlando, FL, 2002, CELL-148.
30. Larsson, P.; Hult, E.-L.; Wickholm K.; Petterson E.; Iversen T. *Solid State Nucl. Magn. Reson.* **1999**, *15*(1), 31-40.

31. Hannuksela, T.; Tenkanen, M.; Holmbom, B. *Cellulose* **2002**, 9(3-4), 251-261.
32. Lopes Da Silva, J.; Gonçalves, M.; Doublier, J.; Axelos, M. In *Gums and Stabilizers for the Food Industry*; Phillips, G.; Williams, P.; Wedlock, D., Eds.; IRL Press: London, 1994; Vol 7, pp 301-305.
33. Dea, I.; Clark, A.; McCleary, B. *Food Hydrocolloid* **1986**, 1(2), 129-140.
34. Rinaudo, M.; Milas, M.; Bresolin, T.; Ganter, J. *Macromol. Symp.* **1999**, 140, 115-124.
35. Rath, R.; Subramanian, S.; Laskowski, J. *Langmuir* **1997**, 13(23), 6260-6266.
36. Bergenståhl, B. In *Gums and Stabilizers for the Food Industry*; Philips, G.; Wedlock, D.; Williams, P, Eds.; IRL Press: Oxford, UK, 1988; Vol 4, pp 363-369.
37. Garti, N.; Reichman, D. *Food Hydrocolloid* **1994**, 8(2), 155-173.
38. Sundari, S.; Balasubramanian, D. *Prog. Biophys. Mol. Biol.* **1997**, 67(2/3), 183-216.
39. Hannuksela, T.; Holmbom, B. *Proceedings*, 7th European Workshop on Lignocellulosics and Pulp, Turku, Finland, 2002, pp 131-134.
40. Thornton, J.; Ekman, R.; Holmbom, B.; Örså, F. *J. Wood Chem. Technol.* **1994**, 14(2), 159-175.
41. Sundberg, K.; Holmbom, B. *Pap. Puu* **1997**, 79(1), 50-54.
42. Sihvonen, A.; Sundberg, K.; Sundberg, A.; Holmbom, B. *Nord. Pulp Pap. Res. J.* **1998**, 13(1), 64-67.
43. Otero, D.; Sundberg, K.; Blanco, A.; Negro, C.; Tijero, J.; Holmbom, B. *Nord. Pulp Pap. Res. J.* **2000**, 15(5), 607-613.
44. Holmbom, B.; Åman, A.; Ekman, R. *Proceedings*, 8th International Symposium on Wood and Pulping Chemistry, Helsinki, Finland, 1995, pp 597-604.
45. Hannuksela, T.; Holmbom, B. Åbo Akademi University in Finland, unpublished material.
46. Hannuksela, T; Fardim, P.; Holmbom, B., submitted for publication in *Cellulose*.
47. Henriksson, Å.; Gatenholm, P. *Holzforschung* **2001**, 55(5), 494-502.
48. Mora, F.; Ruel, K.; Comtat, J.; Joseleau, J-P. *Holzforschung* **1986**, 40(2), 85-91.
49. Ishimaru, Y.; Lindström, T. *J. Appl. Polym. Sci.* **1984**, 29(5), 1675-1691.

Chapter 16

Effect of Cellulose Substrate on Assembly of Xylans

Åsa Linder and Paul Gatenholm*

Biopolymer Technology, Department of Materials and Surface Chemistry,
Chalmers University of Technology, SE-412 96 Göteborg, Sweden

Cellulosic materials with various specific surface areas, crystallinity and morphology were autoclave treated in solutions of 4-*O*-methyl glucuronoxylan isolated from birch by alkali extraction. Treatment resulted in “decoration” of the cellulose surfaces with particle-like xylan assemblies of various sizes. The amount of xylan retained on the cellulose was proportional to the accessible surface area of the cellulose substrate as determined by adsorption of the dye Congo Red. Visualization of xylan treated cellulose substrates by immunolabelling and confocal laser microscopy showed that the xylan retained was located not only on the surfaces but also in pores. Formation of xylan surface assemblies was dependent on the cellulose substrate morphology. Fibril-like cellulose I surfaces induce the organization of xylan molecules into globular shaped structures, while the cellulose II surfaces result in formation of less well-defined and more elongated xylan structures. This study shows that treatment of cellulose with glucuronoxylans is a convenient way to modify the surface morphology of cellulose.

The hierarchical organization of biological materials has become an important source of inspiration for material scientists. Biological processes such as biosynthesis successfully transform carbon dioxide and water into high performance structural materials using solar energy, the annual growth of more than 170 billion metric tons of biomass being a good example. Biomass is an enormous asset, and there is an increased interest in developing new materials based on this renewable resource.

Wood is a biological structural material that has been extensively studied. The cell walls of wood are advanced composite materials, where load-carrying cellulose microfibrils associated with a matrix of hemicelluloses and lignin form complex hierarchical structures (1). The stiffness and strength of the cell wall is highly dependent both on the orientation of and the associations between the cellulose microfibrils (2). Hemicelluloses, *e.g.* glucomannans and xyloglucans, have been shown to associate strongly with cellulose microfibrils (3,4). Polysaccharides with a β -1,4-linked backbone have been found to be particularly effective in modifying the aggregation behavior of celluloses (5-8). On the basis of these observations Atalla and co-workers have proposed that the hemicelluloses in plants play the role of regulators of the tertiary structure during assembly of the cellulose microfibrils into the cell wall (5,6). Furthermore, the strong associations between hemicelluloses and cellulose enable the hemicelluloses to provide linkages between cellulose and lignin thereby effectively cross-link and stabilize the cell walls. For instance, Vincent has proposed a mechanism for xylan to bridge two microfibrils (2). The linear xylose backbone allows a partial alignment and formation of hydrogen bonds to a cellulose microfibril, but the side groups prevent a complete association. This enables the other unsubstituted end of the xylan chain to align with a second microfibril, effectively joining the two. The interactions between xylans and cellulose have been well documented. Taylor and Haigler have shown that, during the assembly of the cell wall, the synthesis and deposition of xylan are intimately linked with that of cellulose (9). The tendency of xylans to reabsorb onto the cellulose fibers during alkaline pulping is well documented (10-12) and evidence of crystallization of deacetylated xylan in the presence of cellulose has been presented by Marchessault *et al* (13). In conclusion, cellulose and xylans interact strongly with each other, and a greater understanding of these interactions is crucial in the development of new advanced materials based on wood polymers.

We recently reported that cellulose fiber surfaces can be surface modified with glucuronoxylans isolated from birch (14). We have shown in autoclave experiments that it is possible to control the amount of xylan retained on the cellulose surface as well as the surface topography by careful variation of the experimental conditions (time and temperature of the autoclave treatment and pH of the xylan solution). The largest retention of xylan was found at high

temperature and pH (170°C, pH 10). The xylans retained on the cellulose surfaces formed nano and micro-sized particles, hereafter referred to as “surface decoration”. Surface modification of lignocellulosic fibers with xylan also indicated that the surface chemistry of the fibers has an effect on the retention of xylan. Xylan modified lignocellulosic fibers show improved wetting and liquid spreading properties, which is very interesting for absorption type applications (15). In the present study we have investigated the effect of the cellulose substrate surface area, crystallinity and morphology on the decoration of cellulose surfaces with glucuronoxylans.

Experimental

Cellulose materials

The cellulose materials used as substrates were native fibers from cotton and wood, and regenerated celluloses such as fibers, membranes and film. The cotton linters were from Munktell filter paper No. 5 produced by STORA Filter Products, Grycksbo, Sweden. The wood fibers were from a dissolving grade pulp (approx. 90% cellulose) produced from softwood by Domsjö Sulphite Mill in Örnsköldsvik, Sweden. The regenerated cellulose materials used were lyocell fibers produced by Lenzing AG in Austria, membrane filters from Schleicher & Schuell in Germany (Prod. No. RC58, RC60 and RC61, corresponding to pore sizes 0.2 μm , 1.0 μm and 3.0 μm , respectively) and cellophane film from UCB Films, UK (Prod. No. 350POO). In addition, a polypropylene (PP) membrane with a pore size of 0.2 μm produced by Enka Corporation, Germany, was used. Prior to use the substrates were purified by a sequential extraction of methanol, acetone, and water, in an ultrasonic bath for 15 minutes. After extraction, the substrates were dried at 50°C for 2 h.

Autoclave experiments

4-*O*-methyl glucuronic acid xylan, separated from birchwood by alkaline extraction, purchased from Sigma, Germany (Prod. No. X-0502), was used without further purification. Nuclear Magnetic Resonance (NMR) analysis showed that the xylan consisted of linear β -(1 \rightarrow 4)-linked D-xylopyranose units with 4-*O*-methyl-D-glucuronic acid groups, α -(1 \rightarrow 2)-linked to the xylose units (16). The average degree of substitution was one uronic acid residue per eleven

xylose units. Solutions were prepared by the addition of 3.0 g xylan to 60 ml NaOH solution (pH 10), followed by heating to 95°C for 15 minutes. After cooling, the solution was adjusted to pH 10 using NaOH. The solution and substrate were transferred to a glass ampoule, which was subsequently placed in a stainless steel autoclave and heated to 170°C in an oven. For the polypropylene membrane the temperature in the oven was 140°C to avoid melting the substrate. After autoclaving the substrate was washed with hot water, filtered on a Büchner funnel and vacuum dried at 50°C for 2 h before weighing. The amount of xylan on the substrate was expressed as the percentage increase in weight according to Equation 1:

$$\text{Amount of xylan (\%)} = 100 \frac{w_2 - w_1}{w_1} \quad (1)$$

where w_1 and w_2 represent the weight of the dry substrate before and after autoclave treatment, respectively. A control was run for each experiment using pure NaOH solution (pH 10) instead of xylan solution. The control was used to determine weight loss, if any, of the substrate caused by the autoclaving.

Surface characterization

Scanning electron microscopy (SEM) was used to study the substrates before and after autoclaving. The surfaces were coated with gold prior to analysis in a Zeiss DSM 940A, operated at 10 kV. The surface morphology of the fibrous substrates was examined using atomic force microscopy (AFM) in the tapping mode. Single fibers were removed from the surfaces of the samples and mounted on magnetic holders using sticky tabs to prevent the fibers from moving during the analysis. The equipment used was a Digital Instrument Dimension 3000 Large Sample AFM with a type G Scanner. A standard silicon tip was used for the analysis, which was done in air.

Specific surface area

The specific surface areas of the cellulose substrates were evaluated by determining the maximum amounts of adsorption of the Congo red dye (Direct Red 28, purchased from Riedel-de Haën, Germany) following the procedure of

Inglesby and Zeronian (17,18). The substrates were dyed for 24 h at 60°C with a liquid ratio of 100:1 at various concentrations ranging from 0.5% of the weight of the substrate (ows) to 5.0% ows with Congo red. NaCl (20% ows) was added as an electrolyte. Substrate weights were corrected for moisture content. After dyeing the cellulose material was removed from the solutions by centrifugation at 2,000 rpm for 5 min, and the amount of Congo red in the dye bath was measured at 492 nm using a Perkin Elmer UV/VIS Spectrometer Lambda 20. The maximum amount of adsorbed Congo red was calculated using Equation 2 derived from Langmuir's adsorption theory (19):

$$\frac{[E]}{[A]} = \frac{1}{K_{ads} [A]_{max}} + \frac{[E]}{[A]_{max}} \quad (2)$$

where [E] (mg/ml) is the concentration of Congo red at adsorption equilibrium, [A] (mg/g cellulose sample) is the amount of Congo red adsorbed to the cellulose surface, [A]_{max} (mg/g cellulose sample) is the maximum amount of adsorption of Congo red to the cellulose surface and K_{ads} is the adsorption equilibrium constant. The specific surface, A_{sp}, is then expressed as:

$$A_{sp} = \frac{[A]_{max} N_A A_{CR}}{10^{21} M_w} \quad (3)$$

where M_w is the molecular weight of Congo red (653 g/mol), N_A is Avogadro's constant and A_{CR} is the area occupied by one Congo red molecule (1.73 nm² as calculated by Ougiya *et al.* (19)).

Immunolabelling of fibers

The distribution of xylan on cellulose fibers from dissolving pulp was analyzed using a technique for detection and visualization of wood fiber components developed at VTT Biotechnology and Food Research, Espoo, Finland (20). The method involves specific labelling of xylan with antibodies produced using the oligosaccharide MeGlcAXyl₂₋₃ linked to BSA as antigens. For study with confocal laser microscopy the fibers were treated with antibodies which were then visualized by a fluorescent labelled secondary antibody. The anti-rabbit IgG was conjugated to FluoroTMCyTM5 (Amersham Pharmacia Biotech, Uppsala, Sweden) which gives fluorescence at 638 nm.

Crystallinity

The type and degree of crystallinity of the cellulose materials were investigated using wide-angle x-ray diffraction (WAXD). Diffractograms were recorded in the reflection geometry on a Siemens D5000 diffractometer using CuK_α radiation. Diffractograms were taken between 5° and $40^\circ(2\theta)$ at a rate of $1^\circ(2\theta)$ per minute and a step size of $0.1^\circ(2\theta)$. The crystallinity ratio (Cr.R.) was calculated by a formula used by Buschle-Diller and Zeronian (21):

$$\text{Cr.R.} = 1 - \frac{I_1}{I_2} \quad (4)$$

where I_1 is the intensity at the minimum (between $2\theta = 18^\circ$ and 19° for cellulose I and between $2\theta = 13^\circ$ and 15° for cellulose II) and I_2 is the intensity of the crystalline peak at the maximum (between $2\theta = 22^\circ$ and 23° for cellulose I and between $2\theta = 18^\circ$ and 22° for cellulose II).

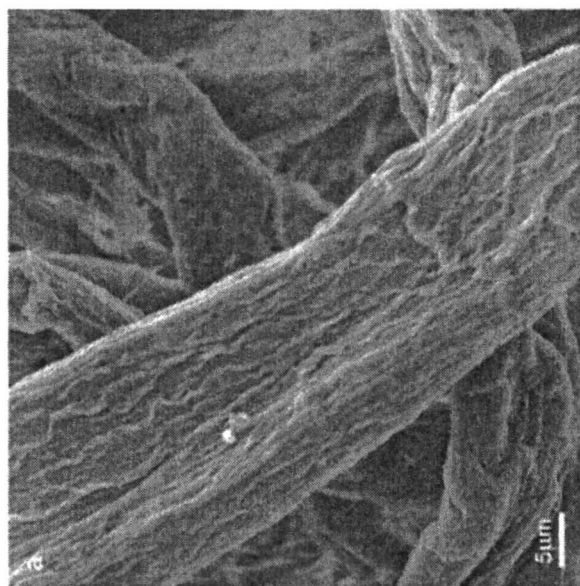
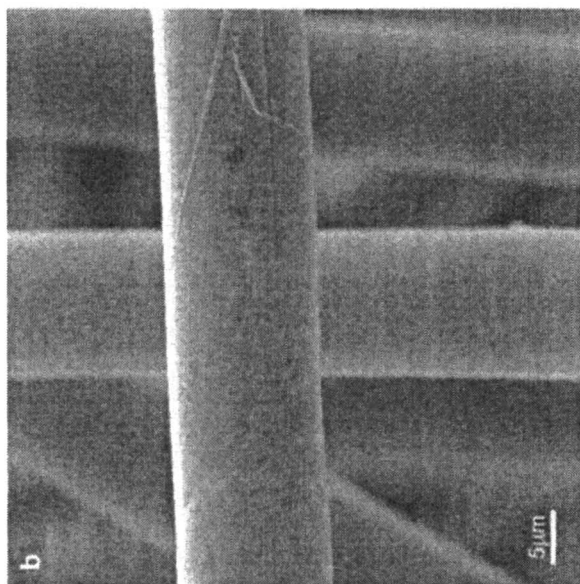
Results and discussion

Surface characterization of substrates

The untreated cellulose substrates were examined by scanning electron microscopy prior to the autoclave experiments. The dissolving pulp (Figure 1a) and the cotton fibers have textured surfaces with clearly visible fibrils. The lyocell fibers on the other hand are nearly devoid of surface features (Figure 1b). The cellophane film has a completely flat surface with a few spherical shaped inhomogeneities, while the cellulose membranes display distinct porous structures. The $1.0 \mu\text{m}$ cellulose membranes were clearly inhomogeneous, with large flat areas interspersed with porous structures.

Retention of xylan

The various cellulose substrates and the polypropylene membrane were autoclaved in the presence of a NaOH solution of birch xylan (pH 10). Weight increases were found for all substrates except the PP membrane after exposure to the xylan solution for 3 h. Table I summarizes the amounts of xylan retained



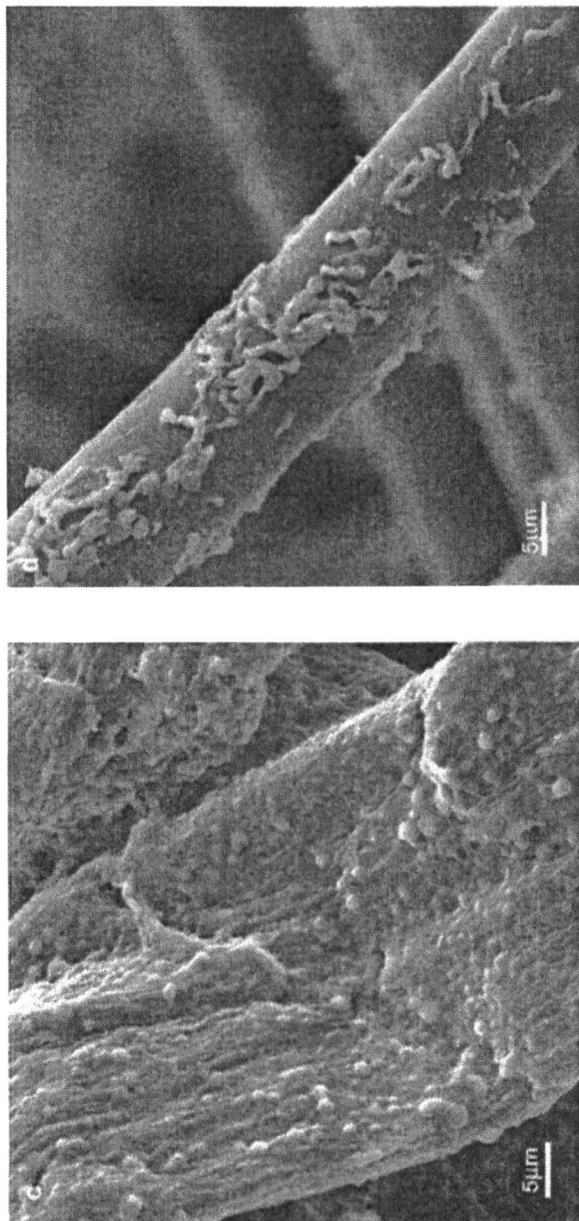


Figure 1. High magnification scanning electron micrographs of untreated cellulose substrates and substrates with retained xylan: (a) dissolving pulp reference, (b) lyocell reference, (c) dissolving pulp with xylan (24.4%), and (d) lyocell with xylan (16.8%). Magnification 2000x. Weight increase of substrates corresponding to amount of retained xylan is shown in parentheses.

on the various substrates. No evidence of xylan retention on the PP membrane was found, indicating a preferential xylan retention on cellulose. The amount of xylan varies among the studied substrates, the largest amounts of xylan being attached onto the wood pulp fibers and the 0.2 μm cellulose membranes. It is also worth noting that the autoclave results in the case of the 1.0 μm membranes reveal quite a large scattering, probably as a consequence of the heterogeneity of these membranes.

Table I. Average amount of xylan retention, specific surface area (A_{sp}) and crystallinity ratio (Cr.R.) of the various cellulose substrates.

<i>Cellulose substrate</i>	<i>Xylan retention [%]</i>	<i>A_{sp} [m^2/g]^{a,b}</i>	<i>Cr.R.</i> ^c
Dissolving pulp	23.6 \pm 0.9	135	0.72 (I)
Cotton linters	19.0 \pm 1.5	67.9	0.85 (I)
Lyocell fibers	16.8 \pm 0.8	100	0.42 (II)
Cellophane	13.7 \pm 0.8	48.1	0.80 (II)
0.2 μm membrane	21.9 \pm 3.3	(220)	0.66 (II)
1.0 μm membrane	12.1 \pm 5.7	(236)	0.65 (II)
3.0 μm membrane	10.8 \pm 1.2	(268)	0.69 (II)

^aLiterature values quoted for surface areas determined by Congo Red are 18- 44 m^2/g for cotton (17,18) and 110 m^2/g for bleached kraft pulp (19).

^bRegression gives R^2 values of 0.97-0.99

^cType of crystallinity (Cellulose I or II) shown in parenthesis.

It is of interest to know if retention of xylan onto cellulose is limited to the external surfaces of the substrates, or if the xylan also penetrates into the pores of the substrates. A new analysis, involving specific labelling of xylan with antibodies in combination with confocal laser microscopy (CLM), was used to investigate where the xylan is located (20). Dissolving pulp before and after autoclaving with xylan was treated with antibodies. The labelled fibers were then reacted with a fluorescent labelled secondary antibody and visualized by CLM. Figure 2 shows confocal microscopy images of reference (Fig 2a-b) and xylan-treated (Fig 2c-d) dissolving pulp fibers labeled with antibodies against MeGlcAXyl_{2,3}. The areas of the fiber containing xylan appear in light grey in the images. The xylan treated fibers clearly have more label than the fibers that were not treated in the autoclave. The small amount of label on the untreated fibers corresponds well with the low residual concentration of xylan in the dissolving pulp after pulping and bleaching, approximately 7 g/kg pulp. Figure 2c shows one optical section of a xylan treated fiber, and in Figure 2d about 20 optical sections are combined (approx. 0.5 μm between sections). There is clearly much more label when optical sections from different layers of the fiber

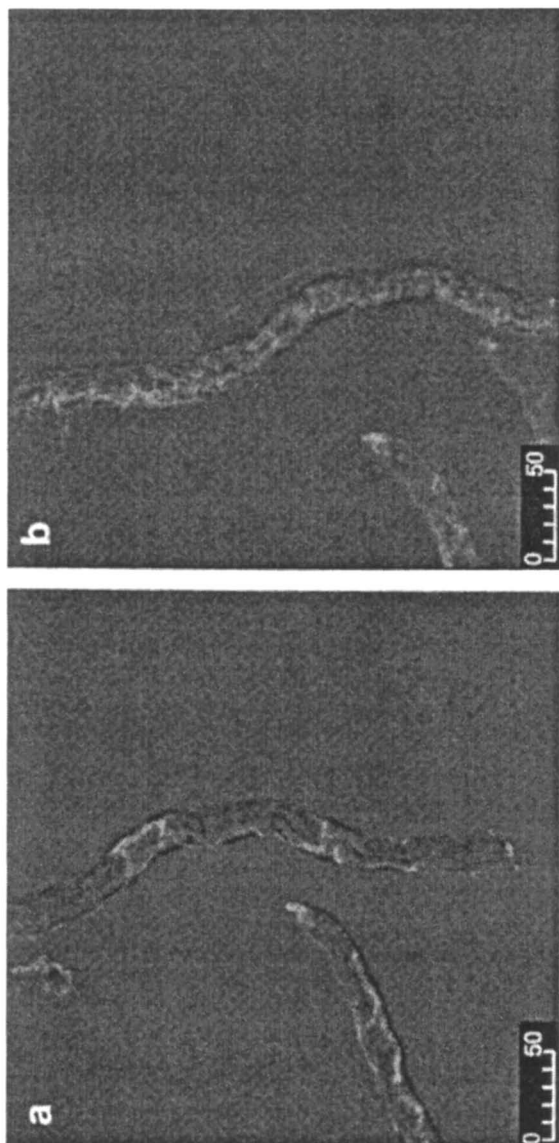
are combined, proving the xylan to be located not only on the external surface of the fiber but also on the internal surfaces and/or in the pores. The determination of the available surface area of the cellulose substrates is thus of interest to be able to verify the effect of cellulose structure on xylan retention.

Surface area of cellulose substrates

The specific surface areas of the various cellulose substrates in the wet state were measured using the method of dye adsorption. It has been demonstrated by Yoshida *et al.* that the Langmuir isotherm can be utilized satisfactorily for the adsorption of direct dyes onto cellulose at low dye concentrations (22). If the adsorption of the dye follows the Langmuir adsorption theory, the adsorbate has most likely been adsorbed as a monolayer and the specific surface area of the cellulose can thus be determined from the maximum amount of adsorption of the dye. The adsorbate used in this study was the direct dye Congo red, and the area occupied by one molecule was set to 1.73 nm² as calculated by Ougiya *et al.* (19). Table I shows the specific surface areas (A_{sp}) of the cellulose surfaces, as calculated by Equation 3. Dye adsorption onto the lyocell fibers and the cellophane film resulted in quite high values of $[A]_{max}$, indicating that these regenerated substrates exhibit nano-scale porosity in the wet state. All of the cellulose substrates except for the cellulose membranes exhibited a Langmuir type behavior. Regardless of whether the deviation for the membranes reflects formation of multilayers or a completely different type of adsorption, the result is an overestimation of the specific surface areas of the membranes. Still, the values determined for the specific surface areas of the other substrates correspond quite well with values found in the literature for dye adsorption studies (17,19). It is known that the size of the adsorbate molecule has a significant influence on the accessible surface area, which leads to the conclusion that only a fraction of the surface area is available for sorption of the xylan molecules. The Congo red molecule is about 2.5 nm in length along its longitudinal axis, while a fully extended xylan chain with DP 50-100 has a maximum length of 25-50 nm (23). Österberg *et al.* also reported dynamic light scattering results suggesting that xylan molecules aggregate in solution (23). These xylan aggregates have even larger hydrodynamic radii and thus the fraction of cellulose surface area accessible to them is even smaller.

Accessibility of cellulose for xylan

All of the fibrous cellulose samples and the cellophane film conform to a linear relationship with larger surface areas corresponding to higher amounts of



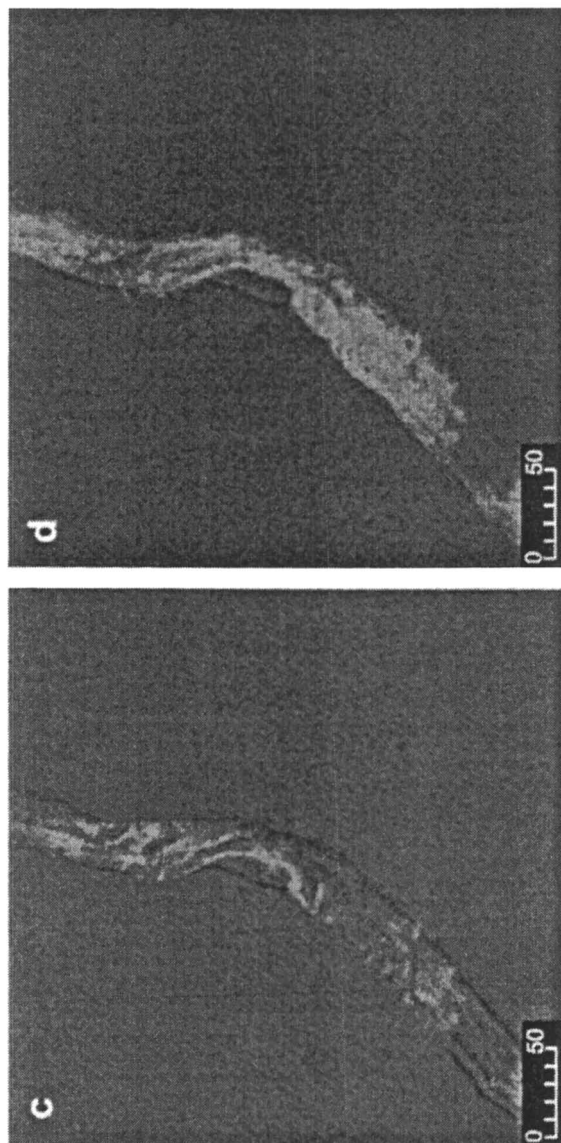


Figure 2. Confocal microscopy images of dissolving pulp fibers from spruce after labeling with antibodies: (a) reference fiber, one optical section, (b) reference fiber, combined sections, (c) xylan treated fiber, one optical section, and (d) xylan treated fiber, combined sections. The combined sections represent about 20 optical sections of the fiber, 0.5 μm between each.

retained xylan (Figure 3). The specific surface area of the cellulose membrane could not be determined satisfactorily by dye adsorption, but it has been shown for cellulose fibers that the surface area in pores is inversely related to the pore diameter (24). Thus the relationship between the surface area and the amount of xylan retained is probably also valid for the cellulose membranes since the amount of xylan was twice as high for the 0.2 μm membrane as compared to the 3.0 μm membrane. The deviations from linearity in Figure 3 are most likely an effect of the surface area of the cellulose substrates accessible to xylan, consisting not only of the external area but also of the area associated with pores, making the pore sizes very important. For instance, the dependence of the xylan accessible area on pore size explains the higher amounts of xylan found on cotton in comparison with lyocell fibers, since the former has been reported to have larger pore sizes than regenerated cellulose fibers (25). All of the substrates used in this study have been reported to contain pores that should be large enough to accommodate at least the low molecular weight fraction of the dissolved xylan (26-28), especially at the high temperatures and alkaline conditions of the autoclave treatments. The results of the immunolabelling study support this conclusion.

Surface topography of cellulose treated with xylan

The surface topography of the xylan treated cellulose substrates was analyzed with scanning electron microscopy (SEM) and atomic force microscopy (AFM). The wood pulp fibers (Figure 1c) and the cotton fibers (both cellulose I) have similar appearances in SEM images. A thin layer of xylan seems to cover the surfaces and well-defined globular structures are formed in some areas. The xylan structures on the regenerated cellulose substrates (cellulose II), *e.g.* the lyocell fibers (Figure 1d), have a completely different appearance. The xylans form elongated structures, much less clearly defined than the structures on the native cellulose fibers.

The difference in the appearance of the micrometer-sized xylan structures between the native and regenerated cellulose substrates may depend on either the degree of molecular ordering in the cellulose substrates, providing that the crystallinity of the substrate induces organization of the xylan, or on the morphological features of the surfaces, *e.g.* the presence or absence of fibrils. To be able to discriminate between these two possibilities, the crystallinity ratio (Cr.R.) of the cellulose substrates was determined using wide-angle x-ray diffraction (WAXD). The results are shown in Table I. The highest crystallinity ratio (0.85) was found for cotton linters, while the value for the wood pulp fibers was somewhat lower. The lowest crystallinity ratio was found for the lyocell fibers (0.42). However, no direct correlation was found between the

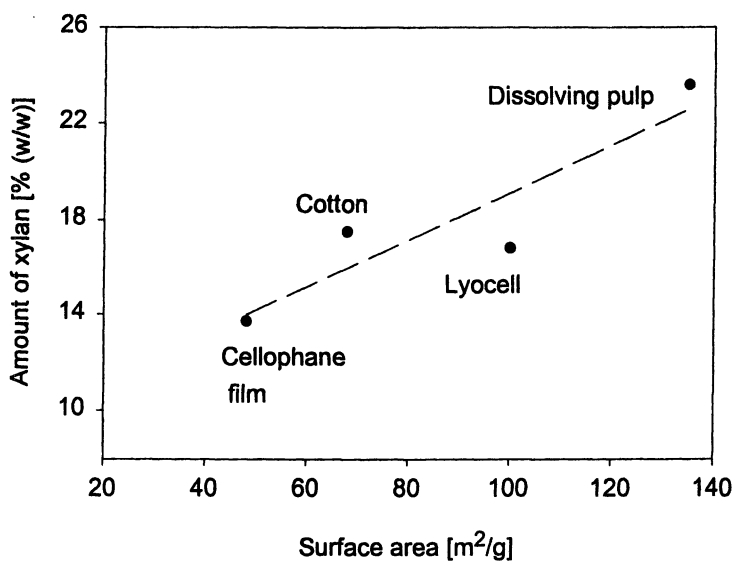


Figure 3. Average amount of xylan retained as a function of the specific surface area of the cellulose substrates. Line shows the result of linear regression ($R^2=0.83$).

relative crystallinity of the substrates and the type of xylan structures they induce.

The untreated and xylan treated substrates were all investigated with atomic force microscopy in the tapping mode. The appearance of the areas with a xylan layer was similar on all substrates. Figure 4 shows AFM phase images of the dissolving pulp fibers with and without xylan. The untreated dissolving pulp fiber (Figure 4a) has well ordered microfibrils of 20 to 40 nm and the fiber surface is relatively smooth. The surface of the fiber with xylan in Figure 4b looks completely different with a layer of bump-like particle structures that can easily be distinguished from the microfibrils beneath. The layer is quite thin, in the order of tens of nanometers, and is thus probably not connected to the micrometer-size xylan structures seen in the SEM images.

In conclusion, the appearance of the micrometer-sized structures formed by the xylans seems to be related to the morphology of the cellulose substrate rather than the degree of crystallinity. The crystal structure of the cellulose substrate (cellulose I or II) is not unimportant but its influence is indirect, through the absence of fibril-like surface features that can induce the formation of xylan structures on the regenerated substrates (cellulose II). On a nanometer scale, the xylan layer looks similar on all of the cellulose substrates, supporting the conclusion that the cellulose surfaces studied are different on the micro scale but quite similar on the nano and molecular levels.

Mechanism of xylan retention on cellulose

Several aspects of the process of the retention of xylan on cellulose surfaces during autoclave treatment are in agreement with features that have been observed in macromolecular adsorption (29): a strong dependence of adsorbed amounts on the available surface area, large adsorption hysteresis (*i.e.* difference in the rate of adsorption and desorption), and the existence of larger amounts of adsorption than flat layers would be expected to contain. If the surface area that would be occupied by the amount of xylan retained on the various substrates is estimated using Equation 3 and the xylan chains are approximated with xylopyranose rings ($M_{w_{xylos}} \sim 130$ g/mol, $A_{xylos} \sim 0.2$ nm²), the result is specific surface areas at least twice as large as those obtained by Congo red adsorption. The conclusion is that not all of the xylan chains can be in contact with the cellulose surface. Eirich has proposed various models of macromolecular chain deposition at a solid-solvent interface (29), including a model where a chain adsorbed by short sections extends loops of random length into the solution. This model is consistent with the characteristics of xylan retention on cellulose, since partially adsorbed xylan chains extending into the solution in the wet state would most likely collapse onto the surface during drying to form globular

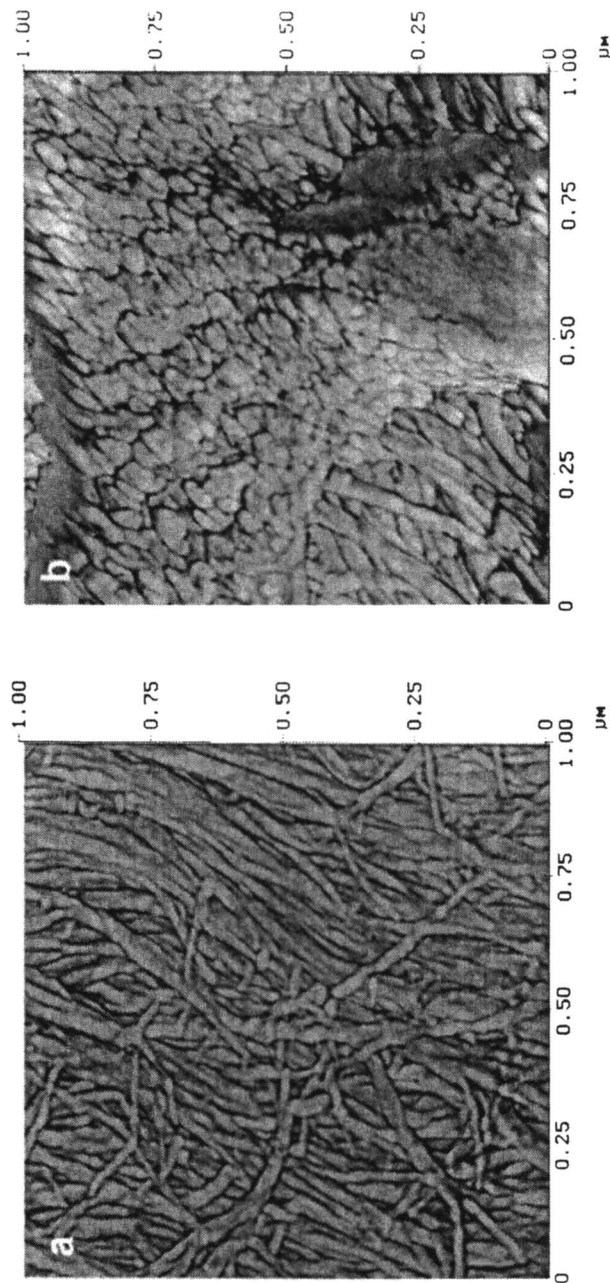


Figure 4. AFM phase images of dissolving pulp: (a) untreated fiber, and (b) fiber with retained xylan.

shaped structures such as those shown by AFM analysis. However, the nanometer-size particle structures seen in AFM images are too large to be composed of single xylan chains, indicating that the structures are either made up by association of several xylan molecules at the surface or that adsorption occurs in the form of xylan aggregates from solution. Both of these mechanisms are possible but the adsorption of colloidal xylan aggregates is likely to be the most important process, based on the amount of xylan retained and the evidence for xylan aggregation in solution (23). The micrometer-size particle structures seen in SEM could then be the result of localized additional adsorption of xylan aggregates, maybe guided by the morphology of the underlying cellulose substrate.

Conclusions

This study showed preferential retention of xylan on cellulose surfaces compared to polypropylene surfaces. The linear relationship found between the accessible surface area of the cellulose and the amount of xylan on the surface after autoclaving indicate that the deposition of xylan onto cellulose surfaces occurs by an adsorption type of process. The appearance of the xylan particle structures formed was found to differ significantly between the native and regenerated celluloses. We believe that the differences in the xylan structures are caused by variations in the morphology of the cellulose substrates, *i.e.* the presence or absence of fibril-like surface features, thereby reflecting variations in the hierarchical organization of the celluloses. The versatility with regard to cellulose substrate and the possibilities to closely control the process make adsorption of xylan onto cellulose interesting not only for surface decoration of cellulosic fibers but also for preparation of new materials based on polymers from biomass.

Acknowledgements

The financial support from the Foundation for Strategic Research (SSF), Forest Products Industry Research College program, is gratefully acknowledged. The authors also thank Dr. Maija Tenkanen and Arja Lappalainen for providing the immunolabeling analysis results. The Nils and Dorthi Troëdsson Foundation is acknowledged for funding the purchase of our AFM instrument. Thanks also to Anders Mårtensson for skillful assistance in the SEM and AFM work.

References

1. Reis, D.; Vian, B.; Roland, J. C. *Micron* **1994**, *25*, 171-187.
2. Vincent, J. F. V. *J. Exp. Biol.* **1999**, *202*, 3263-3268.
3. Hayashi, T.; Ogawa, K.; Mitsuishi, Y. *Plant Cell Physiol.* **1994**, *35*, 1199-1205.
4. Chanzy, H.; Dube, M.; Marchessault, R. H. *Tappi* **1978**, *61*, 81-82.
5. Atalla, R. H.; Hackney, J. M.; Uhlin, I.; Thompson, N. S. *Int. J. Biol. Macromol.* **1993**, *15*, 109-112.
6. Hackney, J. M.; Atalla, R. H.; VanderHart, D. L. *Int. J. Biol. Macromol.* **1994**, *16*, 215-218.
7. Tokoh, C.; Takabe, K.; Fujita, M.; Saiki, H. *Cellulose* **1998**, *5*, 249-261.
8. Whitney, S. E. C.; Brigham, J. E.; Darke, A. H.; Reid, J. S. G.; Gidley, M. *J. Plant J.* **1995**, *8*, 491-504.
9. Taylor, J. G.; Haigler, C. H. *Acta Bot. Neerl.* **1993**, *42*, 153-163.
10. Yllner, S.; Enström, B. *Svensk Papperstidn.* **1956**, *59*, 229-232.
11. Yllner, S.; Enström, B. *Svensk Papperstidn.* **1957**, *60*, 449.
12. Hansson, J. A.; Hartler, N. *Svensk Papperstidn.* **1969**, *72*, 521-530.
13. Marchessault, R. H.; Settineri, W. J.; Winter, W. *Tappi* **1967**, *50*, 55-59.
14. Henriksson, Å.; Gatenholm, P. *Holzforschung* **2001**, *55*, 494-502.
15. Henriksson, Å.; Gatenholm, P. *Cellulose* **2002**, *9*, 55-64.
16. Gabriellii, I.; Gatenholm, P.; Glasser, W. G.; Jain, R. K.; Kenne, L. *Carbohydr. Polym.* **2000**, *43*, 367-374.
17. Inglesby, M. K.; Zeronian, S. H. *Cellulose* **1996**, *3*, 165-181.
18. Inglesby, M. K.; Zeronian, S. H. *Cellulose* **2002**, *9*, 19-29.
19. Ougiya, H.; Hioki, N.; Watanabe, K.; Morinaga, Y.; Yoshinaga, F.; Samejima, M. *Biosci., Biotechnol., Biochem.* **1998**, *62*, 1880-1884.
20. Lappalainen, A.; Tenkanen, M. *VTT Symp.* **2000**, *207*, 219-222.
21. Buschle-Diller, G.; Zeronian, S. H. *J. Appl. Polym. Sci.* **1992**, *45*, 967-979.
22. Yoshida, H.; Kataoka, T.; Maekawa, M.; Nango, M. *Chem. Eng. J. (Lausanne)* **1989**, *41*, B1-B9.
23. Österberg, M.; Laine, J.; Stenius, P.; Kumpulainen, A.; Claesson, P. M. *J. Colloid Interface Sci.* **2001**, *242*, 59-66.
24. Sommers, R. A. *Tappi* **1963**, *46*, 562-569.
25. Focher, B.; Marzetti, A.; Sarto, V.; Beltrame, P. L.; Carniti, P. *J. Appl. Polym. Sci.* **1984**, *29*, 3329-3338.
26. Stone, J. E.; Treiber, E.; Abrahamson, B. *Tappi* **1969**, *52*, 108-110.
27. Duchesne, I.; Daniel, G. *Nord. Pulp Pap. Res. J.* **1999**, *14*, 129-139.
28. Maloney, T. C.; Paulapuro, H. *J. Pulp Pap. Sci.* **1999**, *25*, 430-436.
29. Eirich, F. R. *J. Colloid Interface Sci.* **1977**, *58*, 423-436.

Chapter 17

Interaction between Cellulose I and Hemicelluloses Studied by Spectral Fitting of CP/MAS ¹³C-NMR Spectra

Per Tomas Larsson

STFI AB, P.O. Box 5604, SE-114 86 Stockholm, Sweden
(email: tomas.larsson@stfi.se)

A review of our work with spectral fitting of CP/MAS ¹³C-NMR spectra recorded on isolated cellulose I, on a mixtures of cellulose I and xylan and, on kraft pulps is given. The conceptual model for cellulose I used by us is presented. References demonstrating the validity of the spectral fitting model is given. Results from kraft pulps containing hemicelluloses are presented and interpretations discussed based on results obtained from a model system that is a mixture of colloidal sols of isolated cellulose I and xylan. It is concluded that the method used is powerful enough to study, diagnose and monitor interactions between cellulose I and hemicelluloses.

Studying interactions at the supermolecular level, between cellulose I (the dominating form of native cellulose) and hemicelluloses in wood fibers and in wood fiber based products such as paper pulps and paper is a formidable task. Still, it is an interesting area since current and future commercial use of wood fibers can benefit from a clear understanding of how the supermolecular characteristics of cellulose I and hemicelluloses affect chemical and physical properties of commercial products.

In our work CP/MAS ^{13}C -NMR (Cross-Polarization Magic Angle Spinning Carbon-13 Nuclear Magnetic Resonance) spectroscopy together with spectral fitting has been the method used for studying interactions between cellulose I and hemicelluloses. A necessary prerequisite for this approach is a reliable interpretation of cellulose I spectra.

The interpretation of cellulose I spectra is based on enriched cellulose I samples, i.e. some sample preparation is necessary before interpretable CP/MAS ^{13}C -NMR spectra can be recorded on cellulose I. This is equally true for the samples where interactions between cellulose I and hemicelluloses are to be studied. The choice of sample preparation procedure may change the *in vivo* properties and the *in vivo* behavior of the polysaccharides to a varying extent.

This résumé consists of five parts. The first part presents the general characteristics of CP/MAS ^{13}C -NMR spectra recorded on isolated cellulose I. A presentation of the conceptual model of isolated cellulose I and the vocabulary that we use, are given in part two. Part three discusses the spectral fitting procedure used for isolated cellulose I and give references to results that demonstrate its validity. In part four results from paper pulps containing hemicelluloses are presented and finally, in part five possible interpretations of the results from the paper pulps are discussed by comparison with a model system consisting of a mixture of colloidal sols of isolated cellulose I and xylan.

CP/MAS ^{13}C -NMR spectra recorded on cellulose I

The CP/MAS ^{13}C -NMR spectra recorded on cellulose I enriched samples exhibit a large variation depending on the origin of the sample and the preparation procedure used (1-17) as shown in Figure 1.

Typical CP/MAS ^{13}C -NMR spectra recorded on isolated cellulose I are made up of four signal clusters originating from the six carbons in the anhydroglucose unit. The C1 cluster centered around 105 ppm, the C4 cluster centered around 87 ppm the C2, C3 and C5 clusters centered around 73 ppm and the C6 cluster centered around 63 ppm. The fine structure of each signal cluster is due to the supermolecular structure of cellulose I. All chemical shifts reported here are determined by using glycine as an external standard.

The information content in this fine structure is high, but the accessibility of the information is limited by the severe overlap of the cellulose I signals. In order

to obtain quantitative information on the supermolecular structure of cellulose, some post-acquisition processing of the spectra is necessary.

The general characteristics of the signal clusters differ substantially, the C4 signal cluster (80-92 ppm) is unique in the sense that it is the most resolved spectral region containing signals from a single atom in the anhydroglucose unit (6,16). This makes the C4 region the preferred target for spectral fitting.

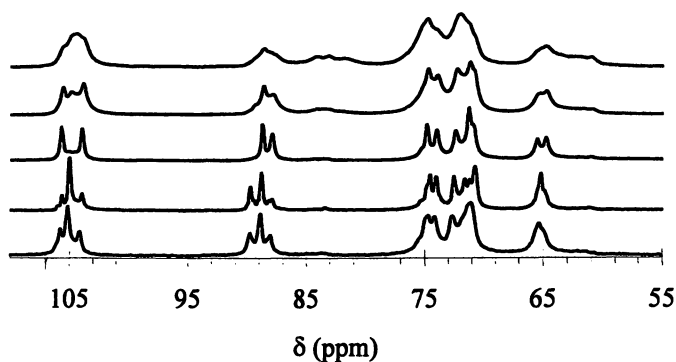


Figure 1. CP/MAS ^{13}C -NMR spectra recorded at 7.05 T on cellulose I isolated from different sources and one kraft pulp. From bottom to top the sources are Valonia, Cladophora, Halocynthia, and cotton linters. The top spectrum is bleached birch kraft pulp that contains hemicelluloses. (Reproduced with permission from reference 16. Copyright 1999).

In order to perform spectral fitting, two prerequisites are needed, the signal intensities must be shown to represent amounts present in the sample (quantitatively) and a reasonable model for the structural elements present in the sample is needed for assignments.

A model for isolated cellulose I

The polyglucan chains (β -(1 \rightarrow 4) linked D-glucan units) that make up one cellulose I *fibril* have all the same sense of direction, all reducing ends points in the same direction. Fibrils have cross-sections of varying shape with widths in the range from a few nanometers to a few tenths of nanometers (18-20). The

terms micro fibril and elementary fibril are also found in the literature and are here considered synonymous to the term fibril used herein.

Within the cell wall, fibrils may aggregate into *fibril aggregates*. The fibrils typically aggregate with main axes parallel or anti-parallel. The shape of fibril aggregate cross-sections may be of any form with widths in the range of several tenths of nanometers (18-21).

A fibril aggregate is considered a distinct object with a boundary. The boundary layer consist of fibril surfaces in direct contact with e.g. surrounding water. Due to the direct contact with water the polyglucan chains at the fibril aggregate boundary possess a characteristic behavior. These kinds of surfaces are herein referred to as *accessible fibril surfaces* (AS) (8,11).

The formation of fibril aggregates leads to a situation where some fibril surfaces are in direct contact. At such contact zones, intermolecular bonds may not develop to the same state found in the crystal lattice of cellulose I. Hence, the contact zone is some kind of geometrical discontinuity. The polyglucan chains at such contact zones may possess a characteristic behavior and are herein referred to as *inaccessible fibril surfaces* (IS) (11). There are other situations that may lead to the formation of inaccessible fibril surfaces, three such situations are discussed below.

Direct association of hemicelluloses to accessible fibril surface present at the fibril aggregate boundary transform accessible fibril surface to inaccessible fibril surface with the accompanying change in behavior of the affected polyglucan chains.

In the case of non-perfect fibril aggregation, cavities within the fibril aggregate may exist. Such inter-fibril cavities expose fibril surface not directly involved in fibril aggregate formation. If such cavities are filled with hemicelluloses, direct contact between fibril surface and hemicelluloses within the fibril aggregate is possible, leading to the formation of inaccessible fibril surface.

Another possibility for the presence of inaccessible surfaces is distortions within the fibril, interior surfaces. Some mechanical treatment of wood fibers shows a strong impact on CP/MAS spectra (22). Distortions of the cellulose I structure within the fibril, distributed along the fibril, may also constitute zones of geometrical discontinuities.

Direct contact between fibril surfaces, fibril surfaces in contact with other cell wall polymers (at the fibril aggregate boundary or within the fibril aggregate) and interior surfaces are all considered causes for the presence of inaccessible fibril surfaces. Herein they are all referred to as inaccessible fibril surfaces (IS) (11).

In a sense, accessible fibril surfaces and inaccessible fibril surfaces are both geometrical discontinuities compared to the crystal lattice of cellulose I. The polyglucan chains at both kinds of surfaces may exist in conformations distinct

from that found in crystalline cellulose. The question then arises whether this difference in conformation is present in the polyglucan chains at the surface layers only, or penetrates deeper into the fibril structure. If it is believed that such a difference in conformation diminishes gradually, going from the surface layer to the fibril interior, yet another form of cellulose may be present. Such cellulose form exist within the fibril, is considered highly ordered but non-crystalline (as judged by NMR) and herein referred to as *para-crystalline* cellulose (PC) (10, 11,23)

The remaining polyglucan chains in the fibril constitute the *crystalline* cellulose (C) (cellulose I α or cellulose I β) (1-3) and are located in the fibril interior.

We consider the AS, IS, PC and C forms of cellulose the most important features of a model for interpreting CP/MAS ^{13}C -NMR spectra recorded on a

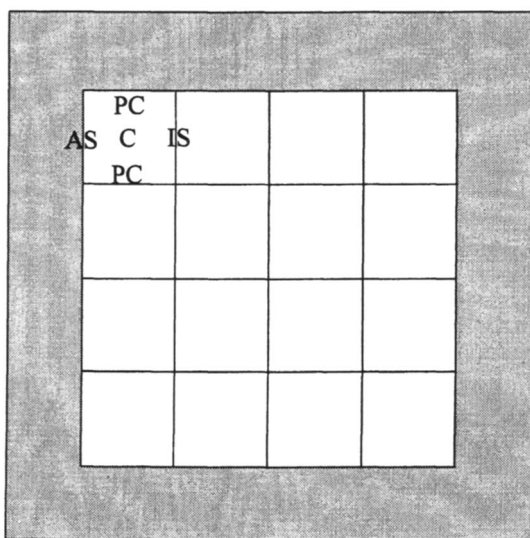


Figure 2. Features of the SFAM. A diagrammatic picture showing how the SFAM models a cross-section through a fibril aggregate (16 fibrils surrounded by water). White squares are cross-sections through the individual cellulose I fibrils, gray color represents water. Polyglucan chains (not shown explicitly) are perpendicular to the plane of the paper. Annotations within the figure show some example positions of the different cellulose forms, C=crystalline cellulose, PC=para-crystalline cellulose, AS=accessible fibril surface, IS=inaccessible fibril surface.

system of aggregated cellulose I fibrils. The Square Fibril Aggregate Model (SFAM) consist of the above mentioned cellulose forms and three simplifying assumptions: 1 The fibrils are assumed to have square cross-sections, 2 the fibril aggregates are assumed to have square cross-sections and, 3 the aggregation is assumed to be perfect, i.e. no cavities exist within the fibril aggregate. The SFAM achieves computational simplicity at the expense of sacrificing the complexity characteristic of real cellulose I systems. The SFAM is, of course, an over-simplification, but it is still a reasonable approximation for interpreting spectra of isolated cellulose I. A diagrammatic representation of the SFAM is shown in Figure 2.

Fitting CP/MAS ^{13}C -NMR spectra

Our work (10) has substantiated the work on the quantity of CP/MAS ^{13}C -NMR spectra recorded on dry cellulose (4,24). Using polyethylene as an internal standard, spectra recorded on dry and water saturated cellulose samples were shown to be quantitative for a range of contact times (10). Typically, the spectra subjected to fitting are recorded on water saturated cellulose samples (>30 % water w/w) since this improves the quality of the spectra.

The mathematical model used for fitting CP/MAS ^{13}C -NMR spectra recorded on isolated cellulose I use different line-shapes for different forms of cellulose. Signals from crystalline forms of cellulose I are fitted using Lorentzian line-shapes and the remaining signals, from less ordered forms of cellulose, are fitted using Gaussian line-shapes (10).

Performing spectral fitting on the C4 region of quantitative spectra recorded on isolated cellulose I, in conjunction with chemical modifications of the cellulose has allowed for the assignment of the less ordered forms of cellulose (11). Apart from the signals from cellulose I α and cellulose I β , signals can be assigned to para-crystalline cellulose (11), accessible fibril surfaces (2,11,13,15,25) and, inaccessible fibril surfaces (11,17). The assignments of the spectral C4 region are shown in Table I and Figure 3.

The reason for the presence of two signals originating from accessible fibril surfaces, in the C4 region of spectra recorded on isolated cellulose I, is not known. Two suggestions are that it is due either to the two-fold screw axis of the polyglucan chains at the accessible fibril surfaces or that the cellulose I fibril have two pairs of non-equivalent surfaces.

Using the above shown assignments and line-shapes, spectral fitting has been performed on spectra recorded on cellulose I isolated from different sources. Using SFAM, the obtained relative signal intensities have been used to estimate average lateral fibril dimensions and average lateral fibril aggregate dimensions (11,15,21,25,26). The obtained dimensions are in agreement with

Table I. Fitting the C4 region of spectra recorded at 7.05 T on cellulose isolated from cotton linters

<i>Assignment</i>	δ (ppm)	<i>FWHH</i> ^a (Hz)	<i>Relative Intensity</i> (%)	<i>Line-shape</i>
I α (C)	89.6 ^b	31 (2.0) ^c	3.4 (0.4)	Lorentz
I(α + β) (C)	88.8	29 (0.5)	19 (0.9)	Lorentz
Para-crystalline (PC)	88.5	158 (1.5)	32 (1.9)	Gauss
I β (C)	88.0	56 (1.4)	20 (1.3)	Lorentz
Accessible fibril surfaces (AS)	84.3	57 (3.3)	2.6 (0.2)	Gauss
Inaccessible fibril surfaces (IS)	84.0	318 (8.0)	20 (0.8)	Gauss
Accessible fibril surfaces (AS)	83.4	61 (3.3)	3.1 (0.3)	Gauss

^a Full Width at Half Height

^b Errors are smaller than 0.05 ppm

^c Values in parentheses are standard errors

NOTE: The results of a non-linear least squares fitting of the C4 region of the CP/MAS ¹³C-NMR spectrum recorded on cellulose isolated from cotton linters by HCl(aq) hydrolysis (Reproduced with permission from reference 16. Copyright 1999).

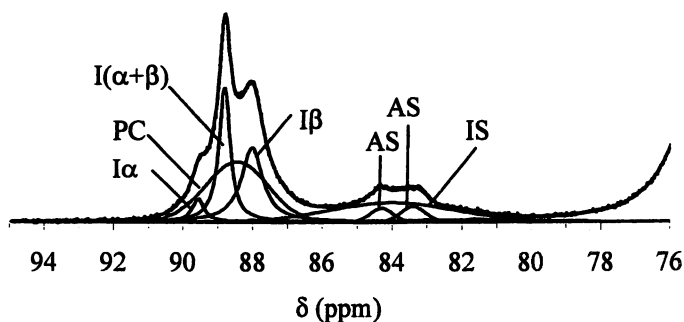


Figure 3. Fitting the C4 region of a CP/MAS ¹³C-NMR spectrum recorded on cellulose I isolated from cotton linters by HCl(aq) hydrolysis (2.5M HCl(aq) 100 °C 17h, yield about 80 %. After hydrolysis the cellulose is a colloidal sol). The experimental spectrum is shown as a broken line. The fitted spectral lines and their superposition are shown as solid lines. The broken line of the experimental spectrum is partially hidden by the superimposed fitted curves. See Table I for annotations.

dimensions estimated by microscopy (11,21,26). This agreement, between NMR and microscopy results, is only possible if the CP/MAS ^{13}C -NMR spectra are quantitative and the spectral assignments are correct.

Despite the coarseness of the SFAM its ability to extract reasonable estimates for average lateral fibril dimensions and average lateral fibril aggregate dimensions is quite surprising (11,21,26). It is worth emphasizing that lateral dimensions can only be estimated by the SFAM in isolated cellulose I samples.

In cellulose I systems with large lateral dimensions of fibrils and fibril aggregates the relative intensity of the AS and IS signals are small, presenting a signal-to-noise problem, which makes estimates uncertain. The mathematical formulation of the SFAM (11) also becomes less 'sensitive' at large lateral dimensions. Practical limitations sets an upper bound on the sizes that can be determined by the SFAM at about 50-100 nm. Hence, CP/MAS ^{13}C -NMR spectroscopy can be considered a tool selective with respect to supermolecular structure.

Some difficulties encountered when fitting CP/MAS ^{13}C -NMR spectra recorded on paper pulps and mixtures of cellulose I and hemicelluloses need to be mentioned. In these spectra additional signals (compared to isolated cellulose I) occur and these signals are assumed to be of Gaussian shape. The cellulose I spectra has been shown to be quantitative for the used contact time (10), but this is not necessarily the case for the hemicelluloses. Signal overlap is more frequent in spectra recorded on paper pulps and mixtures. The fitting procedure is very stable and reproducible in most situations but due to numerical limitations it cannot distinguish closely positioned signals of similar widths in cases where the difference in position is small compared to signal widths. Spectral fitting require spectra of high signal-to-noise ratio. This results in long acquisitions times (typically 'over night' acquisitions). If acquisition is performed without the use of a lock signal compensating for magnetic field-drift a stable magnet is necessary.

In spite of these difficulties we have been able to show that spectral fitting of CP/MAS ^{13}C -NMR spectra can be used to study, monitor and diagnose interactions between cellulose I and hemicelluloses.

Hemicelluloses in kraft pulps

CP/MAS ^{13}C -NMR spectra recorded on kraft pulps contain additional signals as compared to spectra recorded on isolated cellulose I, as shown in Figure 4 and Figure 5.

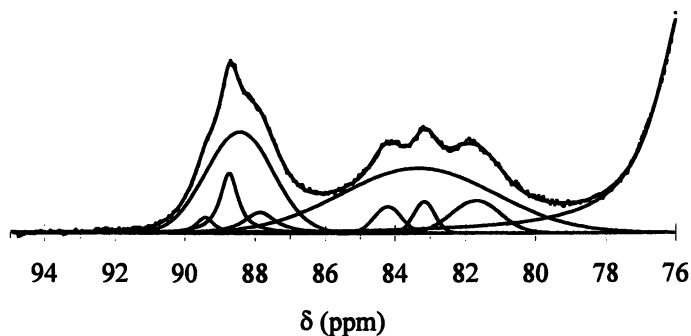


Figure 4. Spectral fitting of the C4 region of a bleached birch kraft pulp HCl(aq) hydrolyzed at 100 °C for 10 minutes. The broken line represents the experimental spectrum. The fitted curves and their superposition are shown as solid lines. The broken line of the experimental spectrum is partially hidden by the superimposed fitted curves.

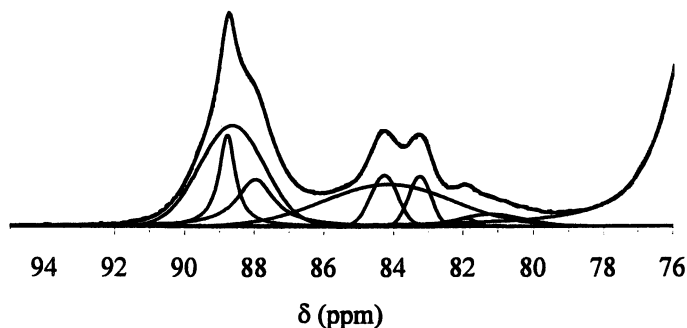


Figure 5. Spectral fitting of the C4 region of a chlorite delignified spruce kraft pulp. The experimental spectrum is shown as a broken line. The fitted curves and their superposition are shown as solid lines. The broken line of the experimental spectrum is partially hidden by the superimposed fitted curve. (Reproduced with permission from reference 16. Copyright 1999).

During acid hydrolysis of bleached birch kraft pulp (Figure 4) spectra were recorded at different stages of the hydrolysis and subjected to spectral fitting. The fitting results were compared with the corresponding results from chemical analysis of the carbohydrate content. This study made it possible to correlate spectral changes to the removal of hemicelluloses (mainly xylan). The relative signal intensities at about 82 and 84 ppm were seen to decrease as a consequence of the hydrolysis. Based on this the interpretation was made that hemicelluloses in kraft pulps give contribution to the relative signal intensity at about 82 and 84 ppm (11).

In Figure 5 the signal pattern (two signals) in the 80-82 ppm region of spruce kraft pulp is seen to be different compared to that found in bleached birch kraft pulp (one signal in the 80-82 ppm region) in Figure 4. It is well known that the hemicelluloses found in birch and spruce differ (18), and this may be the cause for the different results obtained when fitting the two pulp spectra. This deserves to be noted since the spectral fitting method is able to make a distinction between the two pulps based on the composition and/or structure of the hemicelluloses present.

When studying kraft cooking of spruce wood, using CP/MAS ^{13}C -NMR and spectral fitting, a change in signal pattern from hemicelluloses was observed and interpreted as being due to some form of restructuring of the hemicelluloses in the cell/fiber wall (21).

The cellulose I – xylan model system

Isolated cellulose I and xylan extracted from bleached birch pulp was mixed in order to study the process opposite to the removal of hemicelluloses from bleached kraft pulp by acid hydrolysis (16). The spectrum of hydrated xylan is shown in Figure 6.

In Figure 7 the C4 spectral region recorded on cellulose I and the C4 spectral region recorded on the cellulose I-xylan mixture are shown.

A comparison between the results obtained when fitting a spectrum recorded on isolated cellulose I with results obtained when fitting a spectrum recorded on the mixture of isolated cellulose I and xylan is shown in Figure 8. The mixing was done by heating a mixture of colloidal sols of isolated cellulose I and isolated xylan for 48 h at 90 °C (excess of water present at all times). The mixture was then centrifuged and placed in a NMR rotor and spectra were recorded.

From spectra recorded on the mixture of cellulose I and xylan (data not shown) it was apparent that substantial amounts of xylan unaffected by the presence of cellulose was present and the reason for this is not known but it may be due to saturation effects or incomplete mixing.

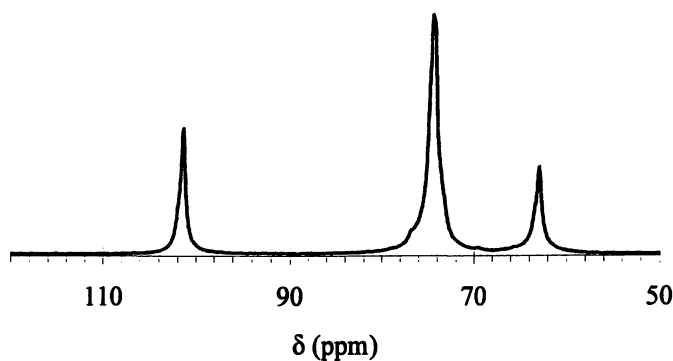


Figure 6. The CP/MAS ^{13}C -NMR spectrum recorded on xylan isolated from bleached birch kraft pulp. The xylan sample is a colloidal sol (Reproduced with permission from reference 16. Copyright 1999).

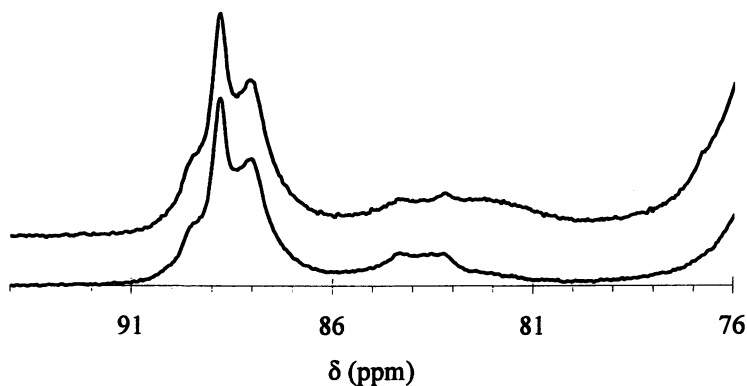


Figure 7. The C4 region from spectra recorded on cellulose I isolated from cotton linters (bottom) and the C4 region recorded on a mixture of isolated cellulose I (70 % w/w) and xylan (30 % w/w) (top). Both spectra were recorded at 7.05 T and the xylan was isolated from bleached birch kraft pulp. (Reproduced with permission from reference 16. Copyright 1999)

As can be seen from Figure 1 and Figure 6 the C4 region of isolated cellulose I is the only region that is not overlapped by signals from isolated xylan. From Figure 3, Figure 6 and Figure 7 it is apparent that no discernable signal maximum is present in the 80-82 ppm region of the spectra recorded on isolated cellulose I and no discernable signal maximum is present in the 80-82 ppm region of the spectra recorded on isolated xylan.

From Figure 8 it is seen that the major difference, due to the addition of xylan, is the presence of a new signal at 82.0 ppm (X), an increase in relative signal intensity at 84.0 ppm (IS), and a decrease in relative signal intensity at 83.4 ppm, one of the signals from accessible fibril surfaces (AS). Other changes are also present but less statistically significant as illustrated by the error bars in Figure 8.

Reference experiments showed that no detectable spectral changes occurred in the spectra of cellulose or in the spectrum of xylan when they were heated (48 h 90 °C in water) separately (16).

The tendencies for the relative signal intensities at 82 ppm and 84 ppm are the opposite to that observed during the acid hydrolysis of bleached birch kraft pulp.

One possible interpretation of the data shown in Figure 8 is the direct association of xylan onto accessible cellulose fibril surfaces present at e.g. fibril aggregate boundaries. In this case some or all of the water at the accessible fibril surfaces would be displaced by xylan, converting accessible fibril surface to inaccessible fibril surfaces. In spectra this should increase the signal intensity at 84.0 ppm from inaccessible fibril surfaces (IS) and decrease the signal intensity from accessible fibril surfaces (AS). From Figure 8 it is seen that signal intensity from inaccessible fibril surfaces increases (IS at 84.0 ppm) and that signal intensity from accessible fibril surfaces decreases (AS at 84.3 and 83.4 ppm). The intensity decrease is only slight in the signal at 84.3 ppm but more pronounced in the signal at 83.4 ppm. Some explanation for this difference in signal intensity decrease found between the two signals originating from accessible fibril surfaces would be gratifying.

¹³C T₁-measurements on cellulose I in water have shown that the two AS signals are characterized by different relaxation times (84.3 ppm T₁=19 s, 83.4 ppm T₁=11 s) (11). Taking into account the two-fold screw axis of the polyglucan chains in cellulose I, the presence of two different kinds of C4 sites on the accessible fibril surfaces is possible. If it is assumed that one of the two kinds of C4 sites is, on the average, in closer proximity to the surrounding water these C4 atoms can be interpreted as the origin for the signal at 83.4 ppm. The shorter T₁ indicates that these C4 atoms interact more strongly with the surrounding (mobile) water and are believed to be the C4 atoms most affected when water at accessible fibril surfaces is displaced by xylan.

Another possible interpretation of the data shown in Figure 8 is the presence of two types of accessible fibril surfaces (e.g. two pairs of accessible fibril surfaces that are structurally dissimilar). In this case, consistency with the

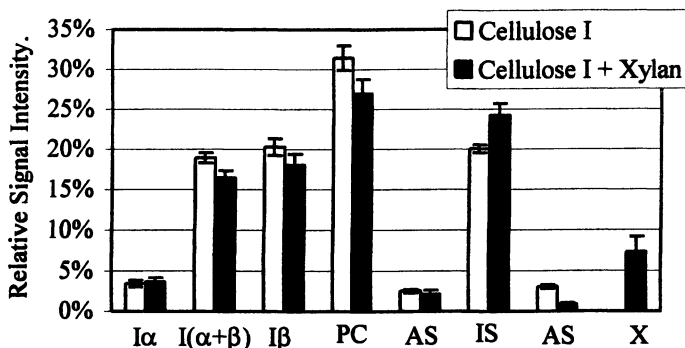


Figure 8. A comparison between spectral fitting results from the C4 region of isolated cellulose I and spectral fitting results from the C4 region of a mixture of isolated cellulose I (70 % w/w) and xylan (30 % w/w). The xylan was isolated from bleached birch kraft pulp. Error bars represent the standard error. Signal positions are: I α 89.6 ppm, I(α + β) 88.8 ppm, PC 88.5 ppm, I β 88.0 ppm, AS 84.3 ppm, IS 84.0 ppm, AS 83.4 ppm, and xylan X 82.0 ppm (Reproduced with permission from reference 16. Copyright 1999)

experimental findings is obtained by assuming that xylan is preferentially adsorbed onto one of the two types of surfaces (16). In terms of this interpretation a detailed account for the differences in ^{13}C T_1 relaxation times observed, for the two accessible fibril surface signals, is more difficult.

Since the signal at 82.0 ppm (X) is not present in neither the spectrum recorded on isolated cellulose I nor in the xylan spectrum it can unambiguously be assigned as a signal resulting from the interaction between cellulose I and xylan.

Whether the signal intensity at 82.0 ppm originates from cellulose I or xylan (or both) is not known. Studies on xylan have shown that it possesses structural polymorphism (27) and that drying or replacement of water in the xylan structure with other small molecules (28) can induce changes in the xylan CP/MAS ^{13}C -NMR spectra such that signal intensity becomes present in the 80-85 ppm region. X-ray results (29) show that when xylan is adsorbed to cellulose I surfaces there is a competition between the preferred three-fold helical axis of xylan and the imposed two-fold helical axis of the polyglucan molecules in cellulose. Such a change in the conformation of the xylan backbone could explain the presence of NMR signal intensity from xylan in the 80-85 ppm region. This suggests that the signal at 82.0 ppm originates from xylan.

Comparing the spectra of kraft pulps (Figure 4 and Figure 5) with the results from the model system (Figure 8) it is apparent that in the kraft pulps the signals from accessible fibril surfaces are of similar intensity although substantial

amounts of hemicelluloses are present in both kraft pulps. This is not the case in the model system. Although no immediate explanation for this difference can be given, it should be born in mind that the kraft pulp fibers originate from a system that once was assembled under biosynthetic control, which clearly is not the case for the model system.

References

1. Atalla, R. H.; VanderHart, D. L. *Science*, **1984**, *223*, 283-285.
2. VanderHart, D. L.; Atalla, R. H. *Macromolecules*, **1984**, *17*, 1465-1472.
3. VanderHart, D. L.; Atalla, R. H. *ACS Symp. Ser.*, **1987**, *340*, 88-118.
4. Teeäär, R.; Serimaa, R.; Paakkari, T. *Polymer Bull.* **1987**, *17*, 231-237.
5. Sterk, H. *Carbohydr. Res.*, **1987**, *164*, 85-95.
6. Yamamoto, H.; Horii, F. *Macromolecules*, **1993**, *26*, 1313-1317.
7. Newman, R. H. *J. of Wood Chem. and Tech.*, **1994**, *14(3)*, 451-466.
8. Newman, R. H. *Holzforshung*, **1998**, *52*, 157-159.
9. Larsson, P. T.; Westermark, U.; Iversen, T. *Carbohydr. Res.*, **1995**, *278*, 339-343.
10. Larsson, P. T.; Wickholm, K.; Iversen, T. *Carbohydr. Res.*, **1997**, *302*, 19-25.
11. Wickholm, K.; Larsson, P. T.; Iversen, T. *Carbohydr. Res.*, **1998**, *312*, 123-129.
12. Belton, P. S.; Tanner, S. F.; Cartier, N.; Chanzy, H. *Macromolecules*, **1989**, *22*, 1615-1617.
13. Newman, R. H.; Ha, M.-A.; Melton, L. D. *J. Agric. Food Chem.*, **1994**, *42*, 1402-1406.
14. Newman, R. H. *Cellulose*, **1997**, *4*, 269-279.
15. Ha, M.-A.; Apperley, D. C.; Evans, B. W.; Huxham, I. M.; Jardine, W. G.; Viëtor, R. J.; Reis, D.; Vian, B.; Jarvis, M. C. *The Plant Journal*, **1998**, *16(2)*, 183-190.
16. Larsson, P. T.; Hult E.-L.; Wickholm, K.; Pettersson, E.; Iversen, T. *Solid State Nuclear Magnetic Resonance*, **1999**, *15*, 31-40
17. Newman, R. H.; Hemmingson, J. A.; *Cellulose*, **1994**, *2*, 95-110.
18. Fengel, D.; Wegener G. *Wood Chemistry, Ultrastructure, Reactions*. Walter de Gruyter, Berlin, New York, **1989**
19. Krässig, H. A. *Cellulose, Structure Accessibility and Reactivity*, Gordon and Breach Science Publishers, Amsterdam, **1996**
20. Atalla, R. H. *Celluloses, Comprehensive natural products chemistry*; Barton, D.; Nakanishi, K; Meth-Cohn, M. Eds.; v. 3 *Carbohydrates and their derivatives including tannins, cellulose, and related lignins*; Pinto, B. M. Ed.; Elsevier Science, Oxford, **1999**.

21. Hult, E.-L. *CP/MAS ^{13}C -NMR Spectroscopy Applied to Structure and Interaction Studies on Wood and Pulp Fibers*, Doctoral Dissertation, Royal Institute of Technology, Stockholm, 2001.
22. Wormald, P.; Wickholm, K.; Larsson, P. T.; Iversen, T. *Cellulose*, 1996, 3, 141-152.
23. Kulshreshtha, A. K.; Dweltz, N. E. *J. Polym. Sci.*, 1973, 11, 487-497.
24. Horii, F.; Hirai, A.; Kitamura, R. *J. Carbohydr. Chem.*, 1984, 4, 641-662.
25. Newman, R. H. *Holzforschung*, 1992, 46, 205-210.
26. Duchesne, I. *Electron Microscopic and Spectroscopic Studies on the Surface Ultrastructure of Kraft Pulp Fibers*, Doctoral Dissertation, Swedish University of Agricultural Sciences, Uppsala, 2001.
27. Chanzy, H; Dube, M; Marchessault R. H. *Polymer*, 1970, 20, 1037-1039.
28. Teleman, A; Larsson, P. T.; Iversen, T. *Cellulose*, 2001, 8, 209-215.
29. Leeflang, B. R.; van Kuik, J. A.; Kroon, J. *CELL 148 in 223rd ACS National Meeting*, American Chemical Society, Orlando Florida USA, April 7-11, 2002.

Chapter 18

Interaction between Cellulose and Xylan: An Atomic Force Microscope and Quartz Crystal Microbalance Study

Arja Paananen¹, Monika Österberg^{2,*}, Mark Rutland³, Tekla Tammelin²,
Terhi Saarinen², Kirsi Tappura^{1,4}, and Per Stenius²

¹VTT Biotechnology, P.O. Box 1500, Espoo, Finland

²Laboratory of Forest Products Chemistry, Helsinki University of Technology,
Espoo, Finland

³Surface Chemistry, Royal Institute of Technology and Institute for Surface
Chemistry, Stockholm, Sweden

⁴Current address: VTT Information Technology, Tampere, Finland

The atomic force microscope (AFM) colloidal probe technique has been used to investigate forces between cellulose beads as well as cellulose beads and mica in aqueous solution, and the interaction between cellulose surfaces in xylan solutions. Several observations of the behaviour of the cellulose beads were made. Swelling of the beads in aqueous solutions is rather slow. Thus, it is important to let the beads equilibrate before measurements. The beads are somewhat compressed when forced together to constant compliance, but relax back to their original shape in a few minutes. A long-range electrostatic repulsion between cellulose and mica occurs on approach. The xylan concentration in solution affects the forces between two cellulose surfaces. When the concentration increases from 10-100 mg/l more xylan adsorbs slowly and irreversibly on the cellulose leading to an increasingly long-range and stronger repulsion between the surfaces on approach. Adhesion between the layers is very low and seems to be due to entanglement of polymer chains. Studies of the adsorption of xylan (100 mg/l) on cellulose films with a quartz crystal microbalance with dissipation (QCM-D) verify that a thick, water-swollen layer of xylan is formed by slow adsorption. It has been proposed that adsorbed xylan on fibre surfaces increases paper strength. We conclude that this must be associated with the behaviour of the adsorbed layers of xylan on drying.

Introduction

The role and behaviour of hemicelluloses in papermaking, especially the interaction between hemicellulose and cellulose, are still subjects of debate. Most studies dealing with cellulose-hemicellulose interaction have so far been bulk experiments using pulp samples. They have given information on the role of hemicelluloses and hydrogen bonding in fibril aggregation and wood polymer association (1-5). Studies of the behaviour of xylan during hardwood pulping indicate that dissolved xylan adsorbs onto the cellulose fibres if the pH is lowered at some stage (6). It has also been proposed that xylan on the fibre surfaces improves paper strength (7). Our recent surface force apparatus (SFA) approach gave a more detailed understanding of the behaviour of xylan (8). Details of hemicellulose-cellulose association at the molecular level were theoretically calculated by Kroon-Batenburg et al. (9). Nevertheless, the kinetics of adsorption of xylan, the structure of the adsorbed layers and their effect on interactions between cellulose surfaces are still not fully understood.

Investigation of cellulose systems in closer detail requires the choice of representative cellulose model surfaces for the experiment. A spin-coated cellulose surface on mica was the first model surface used in studies of forces in papermaking systems (10). This work was followed by other SFA studies using Langmuir-Blodgett (LB) films of cellulose (11-14). These films are noticeably smoother and more stable than spin-coated surfaces. In studies using the atomic force microscope (AFM) colloidal probe technique (Ducker et al. (15)), interaction forces were measured either between two cellulose beads (16,17) or between cellulose beads and spin-coated cellulose surfaces (18,19).

Currently available cellulose beads are usually of variable origin and, hence, published reports often include some characterization of their surfaces. However, a thorough investigation of their behaviour in aqueous solutions has, to our knowledge, not yet been published. Cellulose is a soft, compliant material, which swells in neutral solutions, and even more extensively at higher pH. Hence, force measurements are not as straightforward as when using hard materials such as, e.g., mica and silica. It is important to know if the surfaces are modified as a consequence of pushing the surfaces together and how rapidly a bead relaxes back to its original shape after a full force measurement cycle (approach followed by separation).

In this study the AFM colloidal probe technique was used to investigate the forces between cellulose beads in aqueous solutions of simple electrolyte and xylan. Particular attention was paid to the behaviour of the cellulose beads. The adsorption kinetics and characteristics of adsorbed xylan on cellulose was studied with a quartz crystal microbalance with dissipation (QCM-D).

Experimental section

Materials

Crosslinked cellulose beads were obtained from Kanebo Co. (Japan). The beads consisted of mainly type II cellulose with crystallinity 5-35% and diameters between 20-50 μm (17). The surface topography of several beads was measured by AFM (NanoScope III, Digital Instruments, California) in water and in 1mM NaCl at pH 10. The surface roughness was approximately 30 nm for beads with diameters from 30 to 35 μm (Figure 1). Images of beads taken in wet and dry stage by optical microscope showed that swelling changes the diameter by 5 to 20%. The diameters used in force calculations were those of swollen beads. The LB cellulose films used in QCM-D experiments were prepared by depositing 30 layers of trimethylsilyl cellulose (TMSC) on polystyrene coated quartz crystals at a constant surface pressure of 20 mN/m. A Langmuir trough from KSV Instruments, Finland, was used for the depositions. The TMSC surface was held above an aqueous 10% hydrochloric acid solution for 3 min to regenerate the cellulose prior to measurements. More details on the synthesis of TMSC and preparation and properties of the LB cellulose films are found in (11,20). The crystals were AT-cut polystyrene coated quartz crystals supplied by Q-Sense AB ($f_0 \approx 5$ MHz. and $C = 0.177$ $\text{mg m}^{-2} \text{Hz}^{-1}$).

The xylan was commercial birch xylan (4-O-methylglucuronoxylan from Roth, M_w 14 400 g/mol, DP 100). It contains 7.8 % α -D-methylglucuronic acid side groups and is alkali soluble. NaCl, NaOH and HCl were all of analytical grade. Solutions were prepared in doubly distilled water (Millipore). The mica was muscovite mica (Electron Microscopy Sciences, FT. Washington).

Sample preparation for force measurements

Single cellulose spheres were glued (epoxy glue, UHU+) to the end of an AFM cantilever (silicon nitride, tipless cantilevers from Digital Instruments with a nominal spring constant of 0.12 N/m) in the following way. The AFM head was set as for the measurements with a tipless cantilever mounted to the head. The cantilever was first dipped into glue on a glass support so that a small spot of glue attached onto the cantilever, and then a sphere was picked from another glass support. The spring constant was determined by the thermal method during sample preparation (21). Cellulose beads were attached to the sample support on a thin layer of glue on glass. Cantilevers and sample supports with cellulose beads were dried in a desiccator. New samples and solutions were prepared just prior to each force measurement.

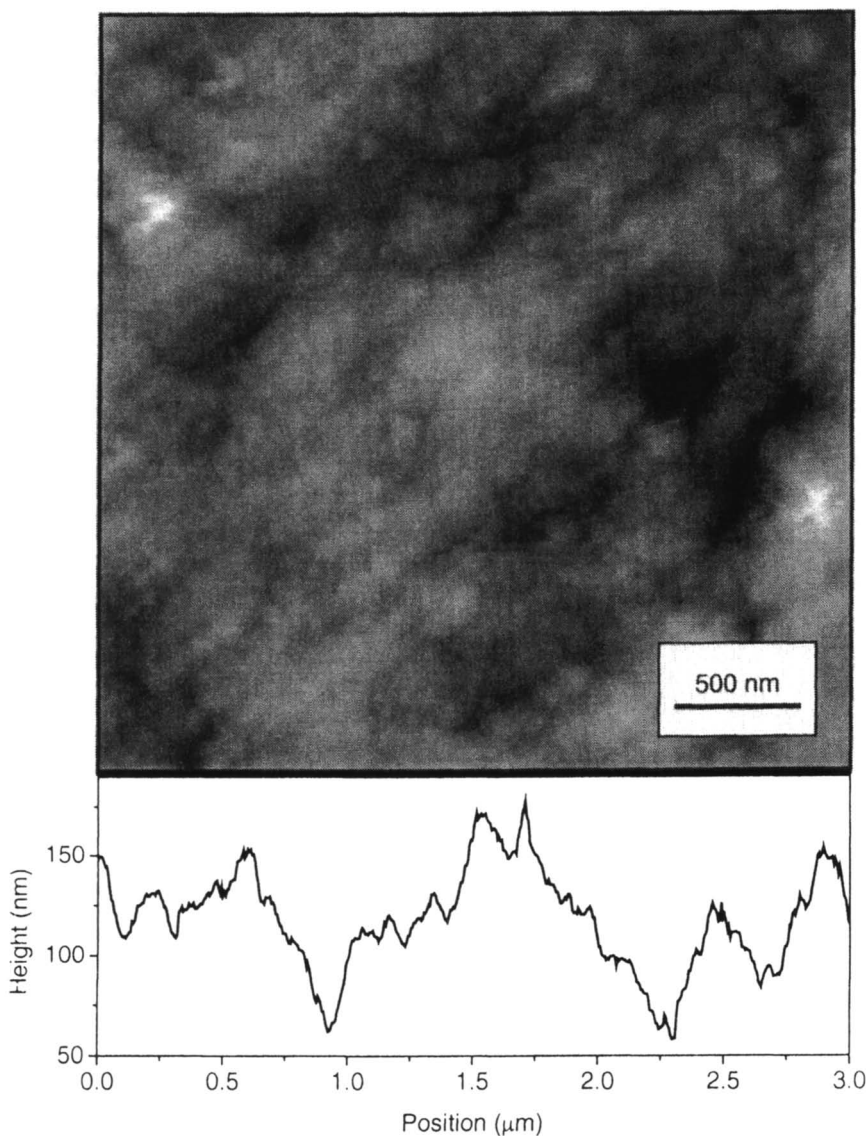


Figure 1. A $3 \times 3 \mu\text{m}$ AFM image of a cellulose bead surface in the reference solution (pH 10 and 1 mM NaCl) measured in tapping mod). The line profile was obtained diagonally across the image.

Force measurements

The force measurements were done by the colloidal probe technique in contact mode using a NanoScope III MultiMode AFM (Digital Instruments, California) equipped with a fluid cell and a scanner E, vertical engagement, using an O-ring. When measuring forces between cellulose beads, the bead attached to the cantilever was placed directly on top of a bead on the sample support. The position of the bead was checked using the optical microscope of the AFM instrument.

The forces between cellulose beads and mica in water and in 1 mM NaCl at pH 10 were measured. The behaviour of the beads was monitored for at least 6 h, using different loading forces and varying time gaps between consecutive force curves. In order to get representative force curves, at least three different spots on the mica were selected and several force curves were taken on each spot. The measuring velocity was 50 nm/s and the ramp size was 500 nm.

Cellulose-cellulose interaction forces were measured in a reference solution (1 mM NaCl, pH 10) and in xylan solutions (10, 50 and 100 mg xylan/l in 1 mM NaCl, pH 10) starting from the reference and continuing with growing xylan concentration. All measurements were done at pH 10 to ensure that xylan was soluble. After changing the xylan concentration the system was allowed to stabilize for 1 h before measurements. Different loading forces were used and the time gap between consecutive force curves was varied from 0.5 to 10 min. The reproducibility of the force curves was checked by shifting the cantilever horizontally in less than 1 μm steps between measurements. Thus, the force curves were centered at slightly different spots on the lower bead, but still on the central area of the beads.

In desorption experiments the xylan solutions were replaced by a fresh reference solution. The system was allowed to stabilize for 0.5 h and the desorption of xylan was monitored for 1 h.

The raw data in NanoScopeIII format were converted into voltage vs. sample-displacement data in ASCII format using a Scanning Probe Image Processor (SPIP, Image Metrology, Denmark) and further handled in Excel. The cantilever sensitivity value was determined separately for each measurement from the force curve obtained when using maximum loading force. The deflection was calculated by dividing the deflection voltage by the cantilever sensitivity. The separation between the sample and the cantilever was taken as the sum of the deflection and the height signal. Forces were calculated as the product of the spring constant and the deflection (Hooke's law). The forces reported here are normalised by the radii of the interacting spheres (R_1 and R_2). The normalised force is related to the interaction free energy W_f between flat surfaces by the Derjaguin approximation (22)

$$F(D) = 2\pi \frac{R_1 \cdot R_2}{R_1 + R_2} W_f \quad (1)$$

where $F(D)$ is the force as function of distance D .

Quartz Crystal Microbalance

Adsorption of xylan was studied with a quartz crystal microbalance, the QCM-D instrument from Q-Sense, Gothenburg, Sweden (23).

Without adsorbate the crystal oscillates at a resonant frequency f_o , which is lowered to f when material adsorbs on the crystal. If the adsorbed mass is evenly distributed, rigid and small compared to the mass of the crystal, $\Delta f = f_o - f$ is related to the adsorbed mass by the Sauerbrey equation

$$\Delta m = -\frac{C \cdot \Delta f}{n} \quad (2)$$

where Δm is the adsorbed mass per unit surface, n is the number of the overtone used in the measurement (in the present case $n = 3$) and C is a constant. Dissipation of energy leads to damping of the amplitude of the oscillation with a decay rate that depends on the viscoelastic properties of the system. The change in the dissipation factor $\Delta D = D_o - D$ when material is adsorbed can be measured. D_o is the dissipation factor of the pure quartz crystal immersed in the solvent and D is the dissipation factor when material has been adsorbed. D is defined by

$$D = \frac{E_{diss}}{2\pi \cdot E_{stor}} \quad (3)$$

where E_{diss} is the energy dissipated during one oscillation cycle and E_{stor} is the total energy stored in the cycle. Using appropriate models Δf and ΔD can be interpreted in terms of adsorbed mass, layer thickness and viscoelastic properties of the adsorbed layer (24).

100 mg/l xylan in 1 mM NaCl at pH 10 was used in the measurements of adsorption on LB-cellulose. The cellulose coated crystals were kept in reference solution (1 mM NaCl at pH 10) at least 12 hours to ensure equilibrium swelling of the cellulose film and to stabilize the oscillation of the crystal.

Results

Behaviour of cellulose beads during force measurements in aqueous solution

The behaviour of the cellulose beads during force measurements was studied by measuring the forces between a cellulose bead and a flat macroscopic mica surface. This system was chosen since the properties of mica in aqueous solutions are well known. The fact that mica is hard and can be cleaved to reveal a perfectly smooth and clean surface just prior to the measurements also makes the interpretation of the results easier.

The effect of swelling

The effect of swelling of the cellulose beads on the interactions in 1 mM NaCl at pH 10 is shown in Figure 2. Three positions on the mica surface per swelling time was studied. The forces at different positions were very reproducible. The repulsion between the surfaces 2 h after immersion is more long-range and stronger than after 1 h. After 2 h the forces are very reproducible at least up to 6 h after immersion. This indicates that the swelling in electrolyte solutions at this pH is rather slow and, hence, it is important to let the surfaces equilibrate in the solution for at least 2 h before any force measurements. The swelling in pure water was also slow, reproducibility was reached after 4 h.

The effect of loading force

Figure 3 shows that the loading force did not have any effect on the cellulose-mica interaction, measured 6 h after immersion. The loading forces used were ~ 0.6 mN/m (low) and ~ 1.7 mN/m (high). However, the cellulose surface is compliant and part of the repulsion measured on approach (Figure 3a) is due to compression of the cellulose sphere. Note that a region of constant compliance was not reached when the low loading force was used. Hence, it is important that force curves measured using low loading force are analysed using sensitivity values from measurements with high force.

The adhesion was very low both in pure water and in electrolyte solution at pH 10. It varied between 0 and 0.04 mN/m at different contact positions. Figure 3b shows that the adhesion did not depend on the loading force. The profile of the force-distance curve is, on the other hand, rather interesting. Usually, when

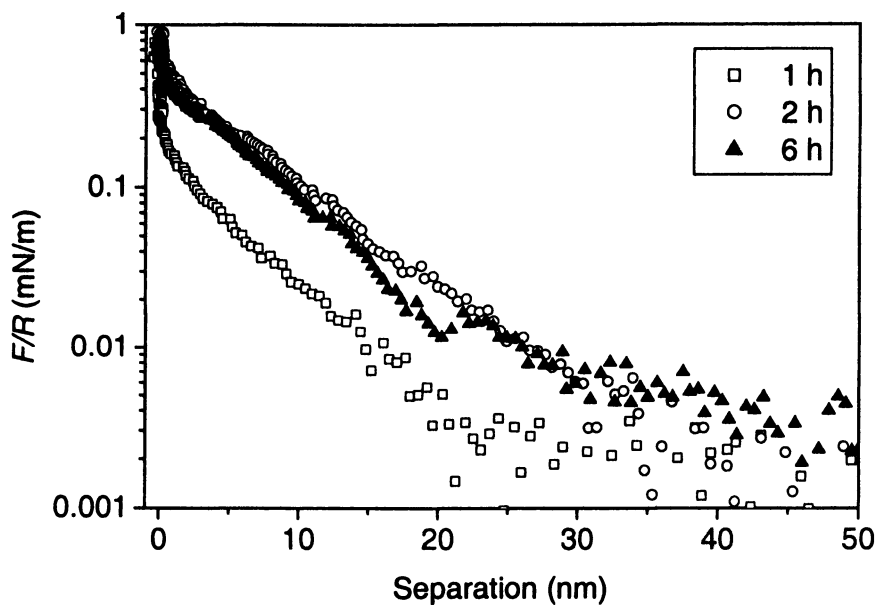


Figure 2. The force, normalised by the radius of curvature, as function of surface separation, between a cellulose bead and a mica surface in 1 mM NaCl at pH 10. The forces measured on approach 1 h (\square), 2 h (\circ) and 6 h (\blacktriangle) after introducing the sphere into water are shown. Each curve was recorded several times at different spots on the mica surface; since the curves were very reproducible only one curve for each time is shown.

the surfaces are separated from adhesive contact in force measurements, the contact distance remains constant until suddenly, when the force gradient exceeds the spring constant, the surfaces jump apart to a large separation. In these experiments, however, the surfaces often separated gradually and minima in the force curve occurred at rather large distances, about 40-50 nm. A likely interpretation is that a few cellulose chains stick strongly to the mica surface and are pulled out from the sphere during separation. A similar behaviour was observed between cellulose and alkyd resin (25).

The recovery of the cellulose surface between force measurements was also studied. If the force curves were recorded right after one another, no adhesion was observed on separation, and the shape of the approach curves varied. If, on the other hand, the surfaces were allowed to relax for a few minutes between measurements, reproducible curves were obtained in both directions. A time gap of five minutes between consecutive force curves seemed to be long enough for the cellulose surface to recover.

The effect of electrolyte concentration

In Figure 4 the forces between cellulose and mica in water are compared with the forces in 1 mM NaCl at pH 10. The forces were fitted to the DLVO theory using the parameters in Table I. The fitting was done based on the algorithm described by Bell et al. (26) for the boundary condition of constant charge. For the forces in the reference solution only the surface potentials of the surfaces at large distances were used as fitting parameters. In the case of interactions across water also the Debye length (κ^{-1}) was used as fitting parameter.

The forces at large separation fit well to the theory, indicating that they are dominated by an electrostatic repulsion. At distances below 50 nm the forces across pure water are less repulsive than predicted by theory. A not very distinct repulsive force maximum is found at a separation of about 5 nm. At smaller separations the force becomes less repulsive due to the presence of an attractive force contribution, until the compliance takes over. Probably the assumption of constant charge is no longer valid at these short distances and thus the repulsion is lower than predicted by the theory.

The fitting suggests a surface potential of -48 mV for mica and -4 mV for cellulose in water (Table 1). This corresponds to an area/charge of 164 nm² for the mica surface and 2260 nm² for cellulose. In the reference solution the surface potentials are slightly lower, as expected since the electrolyte concentration is higher.

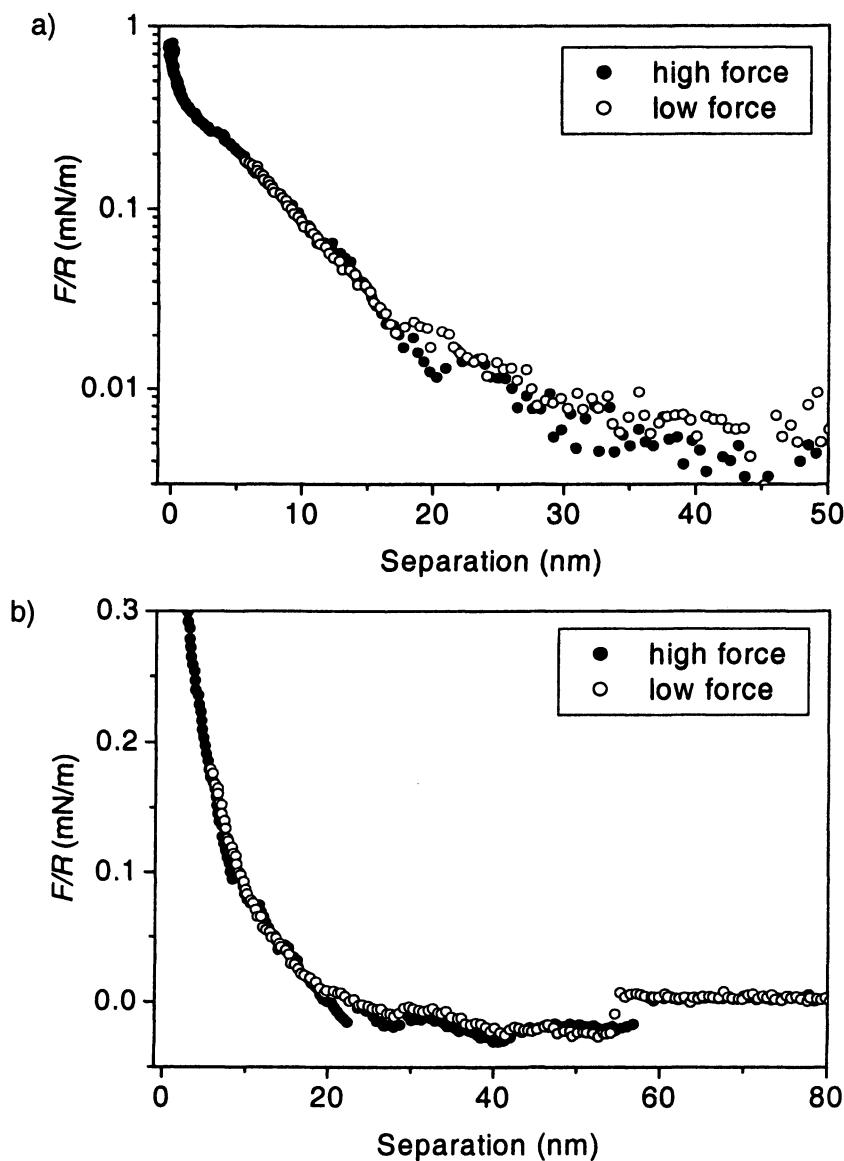


Figure 3. The effect of loading force on the interactions between a cellulose sphere and a mica surface across an 1 mM NaCl-solution at pH 10. The repulsion on approach (a) and the weak adhesion observed on separation (b) are shown. The force was normalised by the radius of curvature of the cellulose sphere.

The potentials in water are lower than what is usually reported for mica (-80 mV (27-29)) and cellulose (10-20 mV (14,17,30)). However, in a previous study we also found that the surface charge of cellulose was lowered in the presence of a highly charged surface like mica (14).

Table I. Parameters Used when Fitting Data to DLVO Theory

<i>system</i>	A^a (10^{-20} J)	ψ_1 (mV)	$Area/q_1^b$ (nm^2)	ψ_2 (mV)	$Area/q_2^b$ (nm^2)	κ^{-1} (nm)
<i>cellulose-mica in water</i>	2.2	-48	164	-4	2260	39.6
<i>cellulose-mica reference</i>	2.2	-40	50	-4	554	9.6
<i>Cellulose- cellulose 50 mg/l xylan</i>	0.8 ^c	-25	85	-25	85	9.6
<i>Cellulose- cellulose 100 mg/l xylan</i>	0.8	-55	34	-55	34	9.6

^aHamaker constant, ^bArea/charge, ^cfrom (30)

Interaction between cellulose and xylan

The forces between two cellulose spheres across a solution containing xylan were measured for different xylan concentrations (10, 50, and 100 mg/l) in 1 mM NaCl, pH 10 (reference). When the compliance behaviour of the cellulose beads was taken into account and the forces were scaled by the effective radius of curvature of the immersed beads, the force measurements became very reproducible. This is illustrated in Figure 5, where approach curves in reference solution from three separate force experiments are shown.

Cellulose-cellulose interaction in varying xylan concentrations

The forces between the cellulose surfaces in different xylan solutions are shown in Figure 6. Before the addition of xylan a weak repulsion extending to 5-10 nm occurs on approach (Figure 6a). Figure 6b shows that there is a weak adhesion (0.1-0.4 mN/m) on separation. As in the case of cellulose against mica, the separation curve was sometimes saw-tooth shaped, indicating entanglement of the cellulose chains. The attractive minima occur at rather large distances, e.g. 40-50 nm.

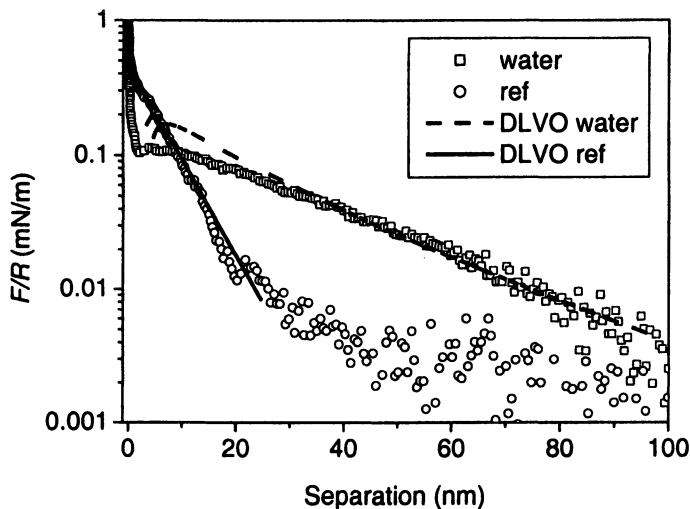


Figure 4. The force, normalised by the radius of curvature, as function of surface separation, between a cellulose sphere and a mica surface in water (\square) and in 1 mM NaCl at pH 10 (\circ). The lines are the best fit to the DLVO theory assuming constant charge using the parameters in Table 1.

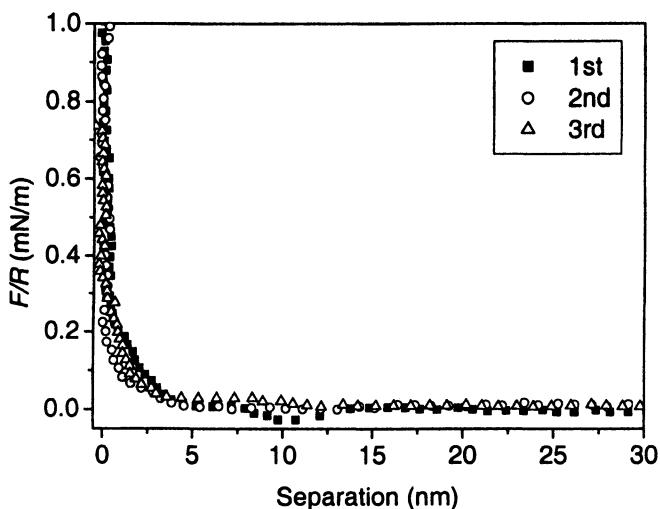


Figure 5. The force, normalised by the radius of curvature, as function of surface separation, between two cellulose surfaces across a 1 mM NaCl solution at pH 10. The force curves were measured on approach in three different experiments.

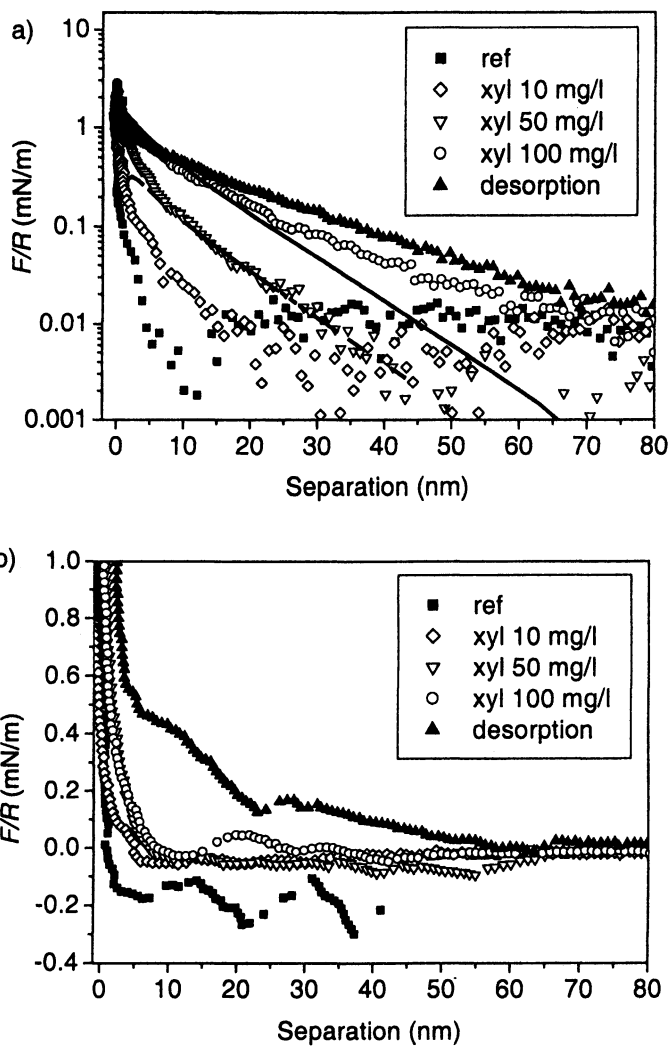


Figure 6. The forces measured on approach (a) and separation (b) between two cellulose beads across xylan solutions at different xylan concentrations (0-100 mg/l). The forces after changing the solution in the chamber back to the reference solution are also shown (\blacktriangle). The lines are the best fit to the DLVO theory assuming constant charge using the parameters in Table 1.

When 10 mg/l xylan was added the repulsion on approach increased slightly. Adhesion on separation was about the same as before addition of xylan. However, the attractive minima were occasionally found at distances larger than 100 nm. When the concentration of xylan in the solution was increased to 50 mg/l the repulsive forces increased and adhesion decreased to less than 0.1 mN/m. At the highest xylan concentration (100 mg/l) the repulsion on approach was even more long-range and stronger than before and interactions on separation were also repulsive. Evidently the xylan does adsorb onto the cellulose surface although both surfaces are negatively charged. In the concentration range studied, adsorption increases with the xylan concentration.

An attempt was made to fit the forces to the DLVO theory. When the xylan concentration was 10 mg/l or less the forces were so low that it was not possible to get reliable estimations of the surface potential. When the xylan concentration was 50 mg/l the long-range forces fitted rather well to the theory assuming a surface potential of -25 mV at long distances (corresponding to an area/charge of 85 nm²). The Debye length was calculated from the electrolyte concentration in solution and the Hamaker constant (A) for cellulose in water was taken from (31). The forces at distances below 6 nm are more repulsive than predicted. Thus, the long-range forces seem to be mainly electrostatic while steric repulsion due to interpenetration of the xylan layers becomes dominating at shorter distances. At the highest xylan concentration the fit to the theory was poor. The results suggest that the area/charge decreases to about 30 nm², but now steric forces seem to dominate also at long distances. Thus, no firm conclusions can be drawn about the charge density of the surfaces. However, it is logical that it increases when more xylan adsorbs.

After measurements in high xylan concentrations the solution in the measuring chamber was changed back to pure reference solution. The repulsion on approach did not change, implying that the xylan does not desorb.

Within one series of experiment the effect of increasing xylan concentration was always the same. On the other hand, the absolute strength of the interaction was clearly different when repeating measurements with new surfaces. This may be due to the kinetics of xylan adsorption. Variations in adsorption times could lead to different adsorbed amount of xylan and thus different magnitudes of repulsion.

Adsorption kinetics of xylan adsorption on cellulose

To verify the conclusions about the adsorption of xylan on cellulose drawn from the force measurements the adsorption kinetics of xylan on cellulose was studied using QCM-D. Figure 7 shows the change in frequency, Δf , and dissipation, ΔD as a function of time when xylan is adsorbed from a 100 mg/l solution in 1 mM NaCl at pH 10 on LB-cellulose. Figure 8 shows a plot of ΔD vs Δf for the xylan adsorption.

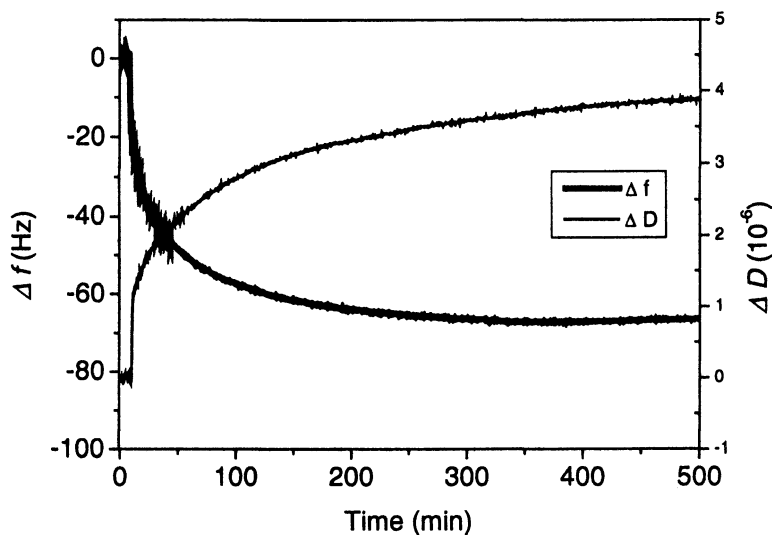


Figure 7. The frequency and dissipation shift vs. time for 100 mg/l xylan in 1 mM NaCl at pH 10 on LB-cellulose. The addition of reference solution is made after 500 minutes. $f_0 = 5$ MHz, $n=3$.

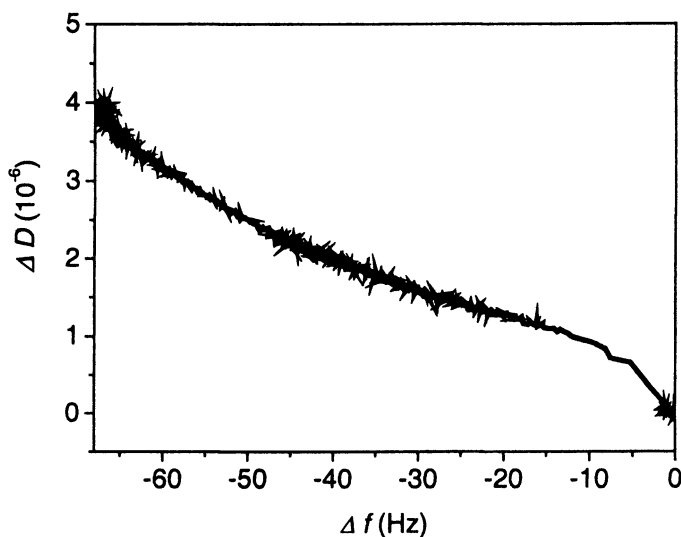


Figure 8. The change in dissipation factor as a function of the change in frequency for the xylan adsorption. $f_0 = 5$ MHz, $n=3$.

The adsorption is rather slow, probably due to the rigid conformation of the xylan molecule. The rate of change in the adsorbed amount becomes very low after about 3 h but a plateau on the adsorption curve is not reached until after several hours. However, the results confirm, as already concluded from the AFM experiments, that xylan does adsorb onto cellulose. The dissipation increases continuously with time. Using eq (2) the adsorbed amount is found to be about 3.0 mg m^{-2} . However, the assumption that the layer is rigid (assumed when Sauerbrey equation is used to calculate the adsorbed amount) is not a very good approximation for this layer. The fact that dissipation rises non-linearly with increasing adsorption (Figure 8), indicates a non-rigid layer that contains water associated with the xylan, which makes the layer softer. The adsorbed mass of xylan in such a layer cannot be calculated accurately from the Sauerbrey equation. A deeper analysis would require measurements at several overtones and xylan concentrations, which is beyond the scope of this paper. However, the increase in dissipation is not very dramatic, i.e. the amount of water that softens the layer is probably not very large and the layer must own substantial elasticity. Hence, although eq (2) underestimates the adsorbed mass it probably gives a reasonable indication of its magnitude.

Discussion

Behaviour of cellulose beads in aqueous solution

Our experiments using cellulose beads present several aspects of how these beads behave and how these observations should be taken into account during force measurements.

The swelling of the beads is rather slow, and hence, stabilisation of the interacting cellulose surfaces is crucial in order to get reproducible results of a cellulose system representing a state of equilibrium. Hence, we let the cellulose beads stabilise in pure water overnight and in reference solution (1 mM NaCl, pH 10) for 3 h before measurements in cellulose-cellulose systems. These are longer times than reported previously (18).

The swelling also affects the normalisation of the forces, which depends on whether one uses radii that are determined for wet or dry beads. In our experiments the adhesive forces observed between two cellulose beads in electrolyte solution at pH 10 are lower than the forces reported previously (17). A possible explanation is that in the normalisation of the force we used the radius of the beads determined after at least 2 h incubation in electrolyte solution (and overnight in pure water). This radius is 5-20 % larger than the radius of dry

spheres used in earlier reports and, hence, results in lower values of the normalized force, F/R . Due to the roughness of the cellulose beads the actual contact area between the interacting surfaces can be smaller than for perfectly smooth surfaces. Thus, also variation in roughness between cellulose beads used in separate studies may lead to differences in magnitude of the measured forces.

Carambassis et al. (17) and Zauscher et al. (18) reported different regimes, e.g. electrostatic and electrosteric, seen in the approach curves in the interaction between cellulose surfaces. Such behaviour is not as clearly seen in our results. This could be explained, again, by the swelling behaviour of cellulose. It is likely that the fully swollen and stabilised surfaces are softer than surfaces that are still swelling, and hence, the distance at which a electrostatically dominated interaction changes into a sterically dominated is not as distinct.

Determination of the sensitivity value in measurements between soft surfaces is very important. At low loading forces the region of small distances is partially affected by surfaces moving together and partially by indentation, and hence, constant compliance is not fully reached. Sometimes it is necessary to measure gently, if the studied surfaces cannot endure high loading forces. Nevertheless, in order to obtain realistic values the force curves measured using low loading force must be analysed using sensitivity values from measurements with high force.

The recovery of the cellulose surfaces between consecutive force measurements was found to require at least five minutes. This is related to the previous publications (17,18) that reported on the effect of the approach speed and relaxation of the cellulose chains, as well as hydrodynamic effects involved. The slow recovery of the cellulose beads between force runs may also explain why we in this work observed adhesion between cellulose surfaces at pH 10 in contrast to previous observations (17).

Driving forces of adsorption

Our experiments give no direct evidence of the nature of the interactions that bind the xylan to the surfaces. However, the following observations can be made.

Although both the cellulose surface and the xylan have a negative charge, the xylan adsorbs onto the cellulose beads. Further, the cellulose-xylan interaction is strong enough to prevent desorption upon dilution. It is also strong enough so that two adsorbed layers in contact separate without desorption, although entanglement of the layers clearly occurs when they are kept in contact. On the other hand, the layers are swollen with water (as indicated by the QCM results) and adhesion between them is very weak.

Formation of hydrogen bonds between xylan and cellulose has often been cited as the driving force of adsorption (*I*). In aqueous solution, this would require that the bonds are stronger than hydrogen bonds between water and cellulose, and those between water and xylan. There are numerous sites on both xylan and cellulose that could lead to such bonds. Hence, if this were indeed the case, attachment of xylan should be very strong and, consequently, the layer should be very flat. Also, one would then expect hydrogen bonds between xylan molecules to be effective. Both the swollen layers and the weak adhesion between them indicate that it is unlikely that this mechanism is of importance. Most probably, the driving force is a combination of the inherent entropy increase associated with the release of solvent molecules when polymers are adsorbed and weak van der Waals' attraction. Note that the solubility of xylan at pH 10 is still rather low, so that even weak attraction could promote substantial adsorption.

The plot of ΔD vs Δf for the xylan adsorption (Figure 8) shows that ΔD rises steeply when the first molecules are adsorbed. As the adsorbed amount increases the gradient of ΔD becomes lower, i.e. when more material is adsorbed its contribution to dissipation becomes lower. In other words, the dissipative mechanisms become less effective, which would indicate formation of a more elastic layer. This could be due to closer packing of the xylan, or perhaps to slow exchange of smaller molecules for larger ones.

Forces between xylan-coated cellulose spheres

We found that the repulsion between cellulose surfaces across a xylan solution becomes stronger and more long-range when the xylan concentration in solution increases in the concentration range 10-100 mg/l. Evidently more xylan adsorbs onto the cellulose surfaces. When more xylan adsorbs onto the weakly charged cellulose, the charge density of the surface increases. Thus an increased electrostatic repulsion is expected. On the other hand, the increase in layer thickness could also lead to an increased steric repulsion between protruding xylan chains.

The fitting to the DLVO theory suggested that at intermediate xylan concentration (50 mg/l) the long-range forces were electrostatic. At distances below 6 nm the forces are more repulsive than predicted by the theory. This deviation suggests that the repulsion is steric. Adding the fact that the xylan molecules are charged, and thus, there must also be repulsive electrostatic interactions, means that the forces are both steric and electrostatic. The term "electrosteric" could be used to describe the forces in this regime. At high xylan concentration the forces were more long-range than predicted by a simple DLVO theory. This suggests that steric interactions dominate at all distances. The steric

repulsion could be due to individual xylan molecules protruding out from the surface or xylan aggregates adsorbed on the surface making the xylan layer thick.

The force curves were recorded 1-2 h after changing the xylan concentration. The QCM-D measurements suggested that the adsorption reached a plateau value only after about 3 h. No firm conclusions can be drawn about the nature of the interactions between the xylan-coated surfaces based on these experiments. The effect of electrolyte concentration should be investigated to clarify whether the forces are purely electrostatic or not. This is done in an ongoing study.

In previous force measurements we found that the interactions between xylan-coated mica surfaces were dominated by steric forces (8). In that work we argued that due to the stiffness of the xylan molecule, fitting to other theories of polymer interaction is not straightforward. The adsorbed xylan layer was rather thick in that study. However, in another investigation (32) it was found that electrostatic repulsion dominated the interactions between xylan-coated mica surfaces at large distances. In that case the adsorption of xylan was very limited and the layer thin. These results agree with our conclusions that steric factors become dominating when the adsorption of xylan increases.

Comparison to bulk experiments using cellulose fibres

In bulk experiments the interaction between cellulose and hemicellulose is often described as sorption rather than adsorption, implying that xylan may also be embedded into the fibre interior. There is no indication of sorption of xylan into the cellulose beads in our experiments. Such sorption would certainly imply changes in the effective radii of the bead with xylan concentration. It has been shown in the studies of sorption of xylan on birch kraft pulp that the xylan content on the fibre surfaces is much larger than in the bulk fibres (33). We therefore believe that our experiments are of direct relevance to the adsorption behaviour of xylan in chemical pulps. For mechanical pulps, with large amounts of lignin and extractive material in the surface, the situation will be different.

Relevance of results to papermaking

It should be stressed that the conclusions above do not eliminate the possibility that hydrogen bonds may be of great importance in *dry* systems, such as dried fibre networks (paper). But they show rather unequivocally that, even in weakly alkaline solutions at low ionic strength, where both cellulose and fibres carry a low negative charge,

- there is long-range repulsion between cellulose surfaces, whether they are covered by xylan or not,

- once the surfaces have been brought into contact, the adhesion between them on separation is very weak, whether they are covered by xylan or not.

Thus, any real effect of xylan on paper strength (interfibre bonding) must be primarily associated with processes that take place on drying. The formation of thick xylan layers on adsorption indicate that dry xylan may perhaps act as a "glue" between the fibres by increasing the contact area between them.

Conclusions

The swelling in electrolyte solution and the recovery of the cellulose beads after force measurements is slow. This is important to consider when planning an experiment using these cellulose beads.

Xylan adsorbs onto the surface of cellulose giving rise to a long-range repulsion between the surfaces. Adsorption probably is mainly driven by entropy increase and van der Waals interactions. Repulsion is the stronger, the higher the xylan concentration is in solution. Adhesion between the surfaces decreases upon adsorption of xylan. It has repeatedly been reported that sorption of xylan increases paper strength and that this is due to formation of hydrogen bonds. We conclude that this effect cannot be due to formation of such bonds in wet paper and that improvement of strength must be due to effects of xylan on fibre bonds during drying of paper.

Acknowledgements

The work was partially financed by the Commission of the European Communities (FAIR CT96-1624) and partially by the Academy of Finland. Johan Fröberg from the Institute of Surface Chemistry is thanked for providing the software for fitting the DLVO theory for uneven potentials to experimental data. Jaakko Pere from VTT Biotechnology is thanked for fruitful discussions.

References

1. Mora, F.; Ruel, K.; Comtat, J.; Joseleau, J.-P. *Holzforschung* **1986**, *40*, 85-91.
2. Salmén, L.; Olsson, A.-M. *J. Pulp Paper Sci.* **1998**, *24*, 99-103.
3. Åkerholm M., S. L. *Polymer* **2001**, *42*, 963-969.
4. Duchesne, I.; Hult, E.-L.; Molin, U.; Daniel, G.; Iversen, T.; Lennholm, H. *Cellulose* **2001**, *8*, 103-111.
5. Henriksson, Å.; Gatenholm, P. *Holzforschung* **2001**, *55*, 494-502.
6. Yllner, S.; Enström, B. *Sv. Papperstidn.* **1956**, *59*, 229-232.

7. Buchert, J.; Teleman, A.; Harjunpää, V.; Tenkanen, M.; Viikari, L.; Vuorinen, T. *Tappi J.* **1995**, *78*, 125-130.
8. Österberg, M.; Laine, J.; Stenius, P.; Kumpulainen, A.; Claesson, P. M. *J. Colloid Interface Sci.* **2001**, *241*, 59-66.
9. Kroon-Batenburg L.M.J.; Leeftang, B. R.; van Kuik, J. A.; Kroon, J. *223rd ACS National Meeting*; American Chemical Society : Washington, D. C.
10. Neuman, R. D.; Berg, J. M.; Claesson, P. M. *Nordic Pulp Pap. Res. J.* **1993**, *8*, 96-104.
11. Holmberg, M.; Berg, J.; Rasmusson, J.; Stemme, S.; Ödberg, L.; Claesson, P. *J. Colloid Interface Sci.* **1997**, *186*, 369-381.
12. Holmberg, M.; Wigren, R.; Erlandsson, R.; Claesson, P. M. *Colloids Surf. A: Physicochem. Eng. Aspects* **1997**, *129-130*, 175-183.
13. Österberg, M.; Claesson, P. M. *J. Adhesion Sci. Technol.* **2000**, *14*, 603-618.
14. Österberg, M. *J. Colloid Interface Sci.* **2000**, *229*, 620-627.
15. Ducker, W. A.; Senden, T. J.; Pashley, R. M. *Langmuir* **1992**, *8*, 1831.
16. Rutland, M. W.; Carambassis, A.; Willing, G. A.; Neuman, R. D. *Colloids Surf. A: Physicochem. Eng. Aspects* **1997**, *123-124*, 369-374.
17. Carambassis, A.; Rutland, M. W. *Langmuir* **1999**, *15*, 5584-5590.
18. Zauscher, S.; Klingenberg, D. J. *J. Colloid Interface Sci.* **2000**, *229*, 497-510.
19. Zauscher, S.; Klingenberg, D. J. *Colloids Surf. A: Physicochem. Eng. Aspects* **2001**, *178*, 213-229.
20. Österberg, M. PhD thesis, Royal Institute of Technology, Stockholm, Sweden, 2000.
21. Hutter, J. L.; Bechhoefer, J. *Rev. Sci. Instrum.* **1993**, *64*, 1868-1873.
22. Derjaguin, B. *Kolloid Zeit.* **1934**, *69*, 155-164.
23. Rodahl, M.; Höök, F.; Krozer, A.; Brzezinski, P.; Kasemo, B. *Rev. Sci. Instrum.* **1995**, *66*, 3924.
24. Voinova, M. V.; Rodahl, M.; Jonson, M.; Kasemo, B. *Physica Scripta* **1999**, *59*, 391.
25. Carambassis, A. PhD thesis, University of Sydney, Sydney, Australia 2000.
26. Bell, G. M.; Peterson, G. C. *J. Colloid Interface Sci.* **1972**, *41*, 542-566.
27. Pashley, R. M. *J. Colloid Interface Sci.* **1981**, *83*, 531-546.
28. Pashley, R. M. *J. Colloid Interface Sci.* **1981**, *80*, 153-162.
29. Claesson, P. M.; Herder, P. C.; Stenius, P.; Eriksson, J. C.; Pashley, R. M. *J. Colloid Interface Sci.* **1986**, *109*, 31-39.
30. Poptoshev, E.; Rutland, M. W.; Claesson, P. M. *Langmuir* **2000**, *16*, 1987-1992.

31. Bergström, L.; Stemme, S.; Dahlfors, T.; Arwin, H.; Ödberg, L. *Cellulose* **1999**, *6*, 1-13.
32. Claesson, P. M.; Christenson, H. K.; Berg, J. M.; Neuman, R. D. J. *Colloid Interface Sci.* **1995**, *172*, 415.
33. Suurnäkki, A.; Heijnesson, A.; Buchert, J.; Westermark, U.; Viikari, L. *8th Int. Sym. On Wood and Pulping Chem*; p 237.

Chapter 19

Enzymatic Tailoring of Hemicelluloses

Maija Tenkanen

Department of Applied Chemistry and Microbiology, University of Helsinki,
P.O. Box 27, FIN-00014 Helsinki, Finland

The functional and technical properties of hemicelluloses are not only dependent on their chemical composition. They are largely governed by the structure of the polymer, e.g. the degree and pattern of substitution as well as the degree of polymerisation. Specific chemical modification of these properties is often difficult. Enzymes are valuable tools for modification of natural biopolymers such as hemicelluloses. They are generally very specific and thus can be used for targeted modifications. Several hydrolytic enzymes are available to be utilized as selective scissors. They can be used for controlled modification of the composition and the type of substitution, or the degree of polymerisation by hydrolysing desired glycosidic linkages. Combining hemicellulases in simultaneous or step-wise fashion enlarges the possibilities. However, each individual enzyme is unique and its action on the target polymer must be carefully evaluated prior to use. The enzymes forming new glycosidic linkages are not yet available for in vitro modifications of hemicelluloses. Although the various hydrolytic enzymes already offer a useful palette of enzymatic tools, many potential new enzymes, such as glycosyltransferases and oxidases, will certainly be available in the future after their discovery and production in larger scale.

Introduction

Vast quantities of lignocelluloses are produced every year, constituting the main source of renewable organic material available on earth. Wood has conventionally been used as a building material and for fibre production for paper and textiles. Grasses and cereals are used for animal feeding and as components in the human diet. Due to shortage of natural oil and continuous accumulation of forest and agricultural side-streams, transformation of biomass into useful products is becoming a more important issue.

Plant cell wall polysaccharides are the main organic compounds found in nature. They are divided into three groups: cellulose, hemicelluloses, and pectic substances (1,2). Cellulose is a linear and long homopolymer consisting of 1,4-linked β -D-glucopyranosyl residues. Its main function is to ensure the rigidity of the plant cell wall. Hemicelluloses constitute the second most abundant plant material after cellulose. They are highly hydroscopic and have an influence on the flexibility of cell walls.

Hemicelluloses are a structurally heterogenic group of polysaccharides, which vary in their monosaccharide composition, glycosidic linkage content, substitution pattern and degree of polymerisation (Table I) (3). The primary structure of hemicelluloses depends on the type of plant and may even vary between different parts of the same plant (3-5). The term hemicellulose itself is not very clear. It is rather loosely defined as plant cell wall polysaccharides which are closely associated with cellulose (6). Hemicelluloses are often water soluble in native form but extractable in larger amounts only with alkaline solutions due to the complex multilayer structure of the cell walls.

The structural characteristics, such as the construction of the backbone and the type and degree of branching, affect the physical properties of polymers, e.g. solubility, viscosity and crystallinity. Thus it is foreseen that the development of more efficient utilization and novel applications of hemicelluloses require targeted tailoring of their properties.

Due to the complex structures of hemicelluloses, several different enzymes are involved in their enzymatic degradation and modification (Table II) (7-10). Enzymes are nature's own catalysts, which act in mild conditions. Consequently, the use of enzymes offers an excellent alternative to engineer the properties of hemicelluloses in a controlled way. This paper discusses properties of hemicellulases and the possibilities for enzyme-aided modifications of hemicelluloses.

Composition of hemicelluloses

Hemicelluloses are usually classified according to the main sugar residue in the backbone (Table I). Xylans and mannans are the two main groups of hemicelluloses and they exist in large quantities in lignified plant tissues in the secondary cell wall. The most abundant hemicelluloses are xylans, which are

Table I. Classification of the main hemicelluloses

<i>Hemi-cellulose</i>	<i>Main sugars in the backbone</i>	<i>Linkage in the backbone</i>	<i>Main sugars in the side groups / chains</i>	<i>Polymer Types</i>
Xylans	D-Xylose	β -1,4	L-Arabinose 4-O-Methyl-D-glucuronic acid (Glucuronic acid)	Arabinoxylans Glucuronoxylans Arabinoglucuronoxylans
Gluco-mannans (Mannans)	D-Mannose D-Glucose	β -1,4	D-Galactose	Glucomannans Galactoglucomannans (Mannans) (Galactomannans)
Arabinans	L-Arabinose	α -1,5	L-Arabinose (D-Galactose)	Arabinans
Galactans	D-Galactose	β -1,4	L-Arabinose D-Galactose D-Glucuronic acid	Arabino-1,4-galactans (Type I)
		β -1,3	Same substituents as mentioned above	Arabino-1,3/6-galactans (Type II)
Glucans	D-Glucose	β -1,4	D-Xylose D-Galactose (L-Arabinose) L-Fucose	Xyloglucans
		and β -1,3	No substituents	1,3-1,4- β -Glucans

Table II. Hemicellulolytic enzymes

<i>Substrate</i>	<i>Enzyme</i>	<i>Enzyme commission number</i>	<i>Linkage hydrolysed</i>
Xylan			
Backbone	Endoxylanase	3.2.1.8	Internal β -1,4
	Exoxylanase	Not classified yet	Terminal β -1,4
Side groups	α -Arabinosidase	3.2.1.55	Terminal α -1,2, α -1,3
	α -Glucuronidase	3.2.1.131	Terminal α -1,2
	Acetyl xylan esterase	3.1.1.72	Ester bond
Oligomers	β -Xylosidase	3.2.1.37	Terminal β -1,4
Glucomannan			
Backbone	Endomannanase	3.2.1.78	Internal β -1,4 after Man
	Endoglucanase	3.2.1.91	Internal β -1,4 after Glc
Side groups	α -Galactoside	3.2.1.22	Terminal α -1,6
	Acetyl mannan esterase	Not classified	Ester bond
Oligomers	β -Mannosidase	3.2.1.25	Terminal β -1,4 after Man
	β -Glucosidase	3.2.1.21	Terminal β -1,4 after Glc
Arabinan			
Backbone	Endoarabinanase	3.2.1.99	Internal α -1,5
Side groups and oligomers	α -Arabinosidase	3.2.1.55	Terminal α -1,2, α -1,3, α -1,5
Galactan			
Backbone	Endo-1,4-galactanase	3.2.1.89	Internal β -1,4
	Endo-1,3-galactanase	Not identified yet	Internal β -1,3
Side groups	α -Arabinosidase	3.2.1.55	Terminal α -1,2, α -1,3, α -1,5
Side groups and oligomers	1,6-Galactanase	Not classified	Internal and terminal β -1,6
	β -Galactosidase	3.2.1.23	Terminal β -1,3, β -1,4, β -1,6
Xyloglucan			
Backbone	Endoglucanase	3.2.1.91	Internal β -1,4
Side groups	α -Xylosidase	Not classified	Terminal α -1,6
	β -Galactosidase	3.2.1.23	Terminal β -1,2
	α -Arabinosidase	3.2.1.55	Terminal α -1,2
	α -Fucosidase	3.2.1.63	Terminal α -1,2
Oligomers	β -Glucosidase	3.2.1.21	Terminal β -1,4
	Xyloglucosidase	Not classified	Terminal β -1,4 in Xyl substituted Glc

present in all terrestrial plants and comprise up to 30% of the cell wall material of annual plants (grasses and cereals), 15-30% of hardwoods and 5-10% of softwoods (5,11). Glucomannans exist mainly in softwoods (15-25%) (11). Xyloglucans are abundant components of the primary cell wall (up to 20%), but their amount in the secondary wall is negligible. Mixed linked β -glucans are important cell wall components in a number of grasses and cereals (1,2).

Arabinans and galactans are generally minor constituents and are often closely associated with pectin in the primary cell wall. One exception is larchwood, which is rich in arabinogalactan (10-25%) (11). Arabinans and galactans are found in larger quantities in some tubers, bulbs and seeds such as sugar beet, potato, soybean and rapeseed (1,2). Some of them are classified as pectic substances rather than as hemicelluloses (3,4,12). Furthermore, structurally similar polysaccharides, such as galactomannans in locust bean and guar, and arabinogalactan in acacia, occur as reserve polysaccharides, and are thus not classified as hemicelluloses (2,3). These polysaccharides are generally called plant gums and are used in the food and other industries as thickening agents. Highly substituted arabinoxylans present in cell walls of grain endosperms are often referred to as cereal gums or pentosans rather than as hemicelluloses.

Xylans possess a 1,4-linked β -D-xylopyranosyl backbone, which is lanced at irregular intervals with groups of 4-O-methyl- α -D-glucopyranosyl-uronic acid and/or α -L-arabinofuranosyl units linked by 1,2- and 1,3-glycosidic linkages. Many xylans also carry esterified side groups, mainly acetyl groups. Esterified phenolic acids, such as ferulic acid, are found in xylans from annual plants (3-5,13). Xylans are further classified based on their side groups i.e. as arabinoxylans (cereal endosperms), glucuronoxylans (hardwoods) and arabinoglucuronoxylans (softwoods, straws, husks, stems) (Table I).

The main mannans in the cell walls of higher plants are glucomannans. The backbone is composed of randomly alternating 1,4-linked β -D-mannopyranosyl and β -D-glucopyranosyl units. α -D-Galactopyranosyl side groups are attached to mannose units via 1,6-bonds. Mannans may also carry acetyl side groups (3,4,14,15). Mannans with a polymannose backbone are found in tubers, roots and seeds (3). Based on their carbohydrate composition mannan-polymers are generally divided into mannans (ivory nut), glucomannans (konjac root, hardwoods), galactomannans (guar, locust bean) and galactoglucomannans (softwoods) (Table I).

Arabinans consist predominantly of α -L-arabinofuranosyl residues, which are linked in the backbone by 1,5-linkages and to side groups by 1,2- and 1,3-linkages (2,12). Galactans are grouped into two main structural types. Type I is composed of a 1,4-linked β -D-galactopyranosyl backbone, which is substituted mainly at C-6 and C-3 with α -L-arabinofuranosyl side groups, and in some cases also with β -D-galactopyranosyl units. Type II galactans have a highly branched 1,3-linked β -D-galactopyranosyl backbone with side chains consisting of 1,6-linked β -D-galactopyranosyl units. Both α -L-arabinofuranosyl and β -D-arabinopyranosyl residues are also present (2,12). Arabinans and galactans can further carry esterified phenolic acids.

In addition to cellulose, plant cell walls also contain other β -glucans. The most common are xyloglucans and mixed linked β -glucans (1,3-1,4- β -glucans), both consisting of a backbone of β -D-glucopyranosyl units. In 1,3-1,4- β -glucans, glucopyranosyl residues are joined by alternating 1,3- and 1,4-linkages (2). Mixed linked glucans are linear polymers. The xyloglucan backbone has the same structure as cellulose, containing only 1,4-linkages. The glucan chain is substituted at C-6 by α -D-xylopyranosyl units, some of which carry further β -D-galactopyranosyl or occasionally α -L-arabinofuranosyl residues. α -L-Fucopyranosyl may be attached to some of the galactose units. Xyloglucans may also carry acetyl groups. The xylose units are distributed in the glucan backbone according to a regular pattern. Generally two or three out of four glucose units carry a xylose side group (2,16).

Enzymatic reactions

Enzymes are specific catalysts, which normally act in mild conditions. Due to the complex structures of hemicelluloses, several different enzymes are involved in their degradation in nature (Table II). Microorganisms often produce a wide range of different hemicellulases, which act in synergism to degrade hemicelluloses completely into monosaccharides. Thus these "natural" enzyme solutions are not suitable for targeted modifications. Individual enzyme components can be isolated from the mixtures. The other, usually more economic option is to modify microorganisms genetically so that they produce the target enzyme as much as possible and do not produce unwanted enzymes. These tailored enzyme mixtures can often be used as such without further purification.

Polymer-acting enzymes may be roughly classified into three different types. Endoglycanases, such as endoxylanases, endomannanases, endoarabinanases, endogalactanases and endoglucanases hydrolyse internal linkages in the backbone and produce a set of different linear and substituted /branched oligosaccharides. Side groups are removed by exoglycosidases, often also called accessory enzymes. These include for example α -arabinosidases, α -glucuronidases, α -galactosidases, β -galactosidases and α -xylosidases. The enzymes in the third class are also exoglycosidases, such as β -xylosidases, β -mannosidases, β -glucosidases, β -galactosidases and α -arabinosidases. They act on backbone sugar units in oligosaccharides by removing terminal monosaccharides from the non-reducing end of the oligosaccharides. Some of them may also act on side groups. There are only a few reports on exoglycanases which are able to liberate terminal mono- or oligosaccharides from the backbones of polymeric hemicelluloses. Because many hemicelluloses are esterified, several esterases, such as acetyl and feruloyl esterases, are also involved in their degradation.

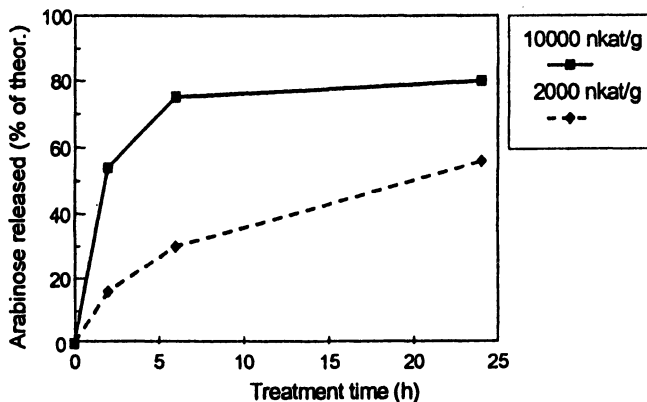


Figure 1. Removal of arabinose side groups from softwood arabinoglucuronoxylan by the α -arabinosidase pl 8.5 from *Aspergillus terreus* (19)

Hemicellulases are generally very specific towards one type of glycosidic linkages connecting particular monosaccharides. However, there exist a few exceptions. One such enzyme is the endoglucanase I from *Trichoderma reesei*, which acts equally well on β -1,4-glucosidic and β -1,4-xylosidic linkages, thus being able to hydrolyze cellulose, glucomannans and xylans (17). Glucopyranose and xylopyranose are structurally similar except that xylose lacks the C-6. In addition some enzymes have been found to liberate both β -D-galactosyl and α -L-arabinosyl units, which in pyranose form have the same ring structure but the latter lacks again the C-6 (18). These examples indicate that some enzymes are able to accommodate similar sugars in their active site instead of just one.

The degree of an enzymatic reaction is easily controlled by choosing a suitable enzyme dosage and/or treatment time. Figure 1 illustrates a typical example of this. Half of the arabinose side groups can be liberated in few hours using high enzyme loading. If less enzymes is utilized, the same result is obtained with a longer hydrolysis time. However, complete reaction normally requires rather high enzyme dosages, as the degree of hydrolysis levels off during prolonged reactions. Enzyme reactions are also rather easy to terminate by increasing temperature. The temperature needed depends on the enzyme used. Some microorganisms produce thermophilic enzymes, which tolerate up to 80°C.

Backbone hydrolyzing enzymes

The degree of polymerization (DP) can easily be reduced by enzymatic treatment. The best results are obtained if the starting material is completely water soluble because then the enzyme reaction proceeds in a homogenous way. If the hemicellulose sample is only partially water soluble, enzymes act first on

the soluble part and may hydrolyze this fraction into short oligosaccharides, while the insoluble part is attacked much more slowly resulting in a heterogenous distribution of end products as can be seen in Figure 2. Due to the easy termination of enzyme-catalyzed processes, products with varying DP can be manufactured. Not all enzymes act in a similar way. Some endoglycanases possess more random action mechanisms than others. Randomly acting enzymes result in very rapid reduction of viscosity and decrease in DP.

Degree of substitution (DS) also affects the homogeneity of the enzyme hydrolysis. If the backbone is highly substituted, endo-acting enzymes do not have sufficient space in the backbone to cut at regular intervals. An example of this is shown in Figure 3, in which two different galactomannans were treated with endomannanase. The action of endoglycanases may be enhanced by the accessory enzymes. However, removal of side groups is not always desired as it may affect the functional properties of the hemicellulose in question. Side group-cleaving enzymes can be used simultaneously with or prior to endoglycanases by stepwise fashion, resulting in most cases in different results, especially when the decrease in substitution decreases the solubility.

Shorter and shorter oligosaccharides are formed when the hydrolysis of the backbone is allowed to proceed further. The side groups in substituted hemicelluloses have different effects on various endoglycanases. Some endoglycanases are able to hydrolyze close to the substitution but others require more unsubstituted backbone units for their action. Good examples of this are endoxylanases, some of which produce xylotriase carrying methylglucuronic acid in the non-reducing end xylose unit, whereas others produce internally substituted xyloetraose and xylopentaose (22). Similar differences have been observed in the case of arabinose-substituted xylooligo-saccharides (23). Endomannanases are also found to differ in their action pattern on galacto- and glucomannans (24,25). Specific oligosaccharides may, for example, be used as building blocks of new man-made biodegradable polymers.

Enzymes for side groups

Each type of side group in hemicelluloses is hydrolyzed by one specific class of enzymes (Table II). One enzyme can, however, act on various hemicelluloses. For example α -arabinosidases may remove arabinose side groups from arabinoxylans, arabinogalactans and arabinans as can be seen from Table III. Even though enzymes catalyze the hydrolysis of the same linkage they may differ in their specificity to the rest of the molecule, e.g. some α -arabinosidases are more active on xylans whereas others are more active on galactans (Table III). Beldman et al. (27) have indeed classified α -arabinosidases into six different groups on the basis of their substrate specificities. In addition to the structure of the backbone, the degree of substitution as well as the type of other closely situated side groups have an effect on the action of accessory enzymes.

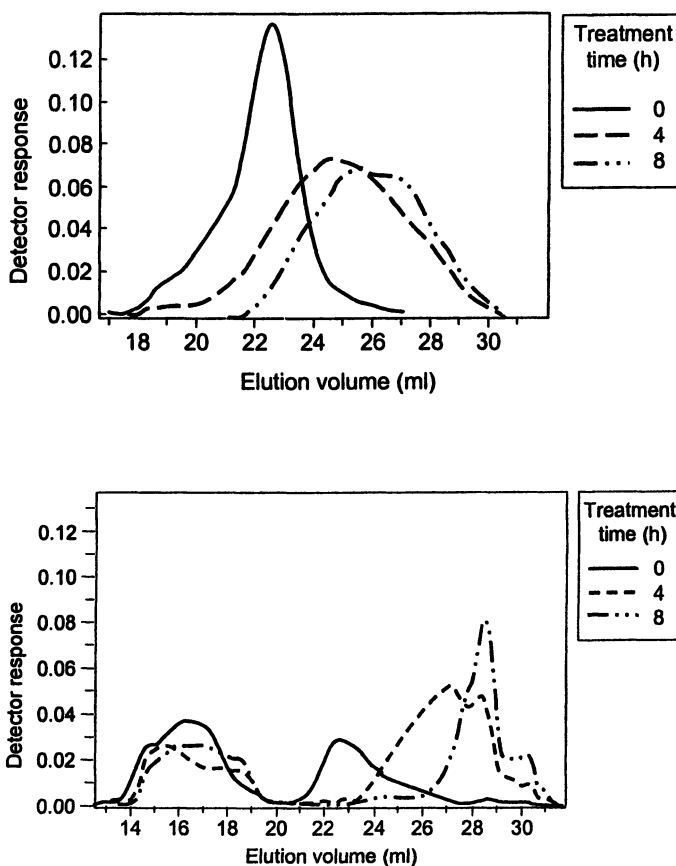


*Figure 2. Hydrolysis of completely (top) and partially water soluble (bottom) xylan with an endoxylanase preparation (20 nkat/g) from *T. reesei* as analyzed by size exclusion chromatography in which large molecules are eluted first. (Reproduced with permission from reference 20. Copyright 2001 Elsevier)*

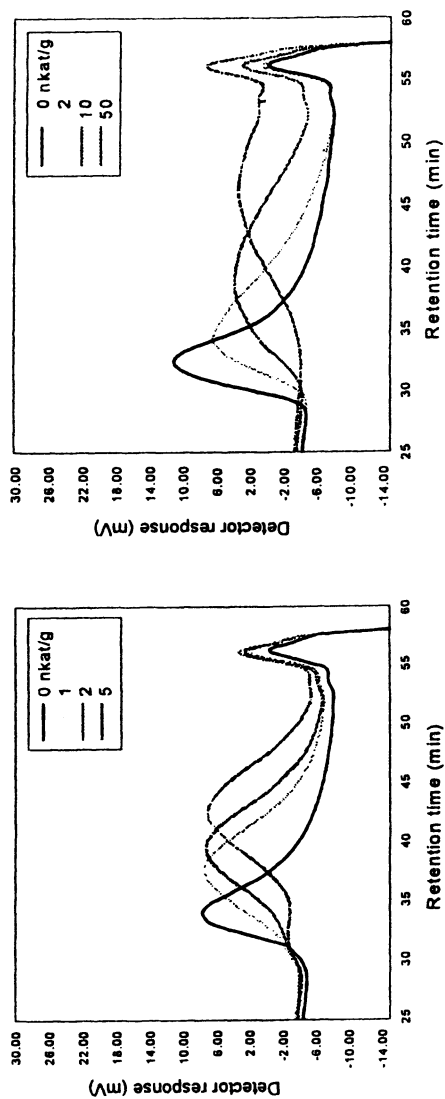


Figure 3. Hydrolysis of locust bean, Gal:Man = 1:4 (left) and guar, Gal:Man = 1:5 (right) galactomannan by endomannanase of *T. reesei* for 2 h. Analysis with size exclusion chromatography. Large molecules are eluted first (21).

Table IV. Comparison of action of *Trichoderma reesei* and *Schizophyllum commune* α -glucuronidases. 1000 nkat / g xylan was incubated for 24h (28,29).

Enzyme source	Methylglucuronic acid liberated from glucuronoxylan (% of theor)		
	Alone	with xylanase	with xylanase and β -xylosidase
<i>T. reesei</i>	1	3	79
<i>S. commune</i>	40	86	not measured

Not all accessory enzymes are capable of acting on polymeric substrates. Many of them function only in synergy with backbone hydrolyzing enzymes and have the highest activity towards oligomeric substrates. One such example is shown in Table IV. The α -glucuronidase from *Trichoderma reesei* is active only towards small oligosaccharides that are formed by hydrolysis with endoxylanase and β -xylosidase, whereas the enzyme from *Schizophyllum commune* is able to act on polymeric xylan. The latter enzyme can thus only be used for modification of the properties of polymeric xylan. One microorganism may also produce several enzymes which possess activity towards the same glycosidic linkage but differ in their ability to act on polymeric substrate. Figure 4 compares the action of three different α -galactosidases from *Penicillium janthinellum* on galactomannans. Only AGL I acted well on the polymeric substrate. The effect of degree of substitution is also seen in this figure, as locust bean gum containing

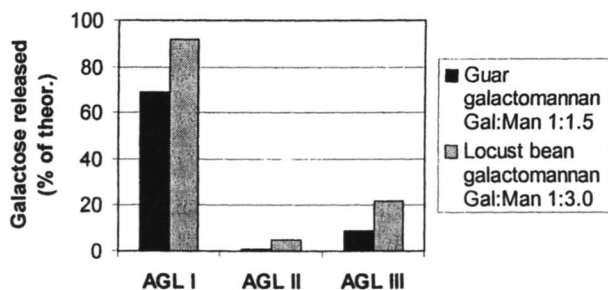


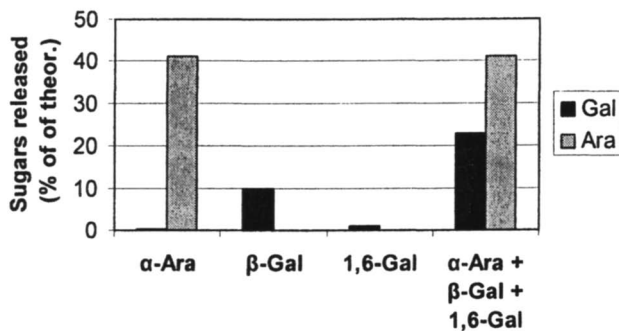
Figure 4. Action of three different α -galactosidases AGL I, AGL II and AGL III from *Penicillium janthinellum* on two galactomannans having different degrees of substitution. 5000 nkat of α -galactosidase / gram of mannan was incubated for 24h (30).

Table III. Release of arabinose from arabinoxylans, arabinogalactans and arabinan by different *Aspergillus* α -arabinosidases. 0.5 mg enzyme / g substrate was incubated for 5 h (2h for AXH) (26).

Enzyme source	Release of arabinose from (% of theor)				
	Arabino-xylan from wheat flour	Arabino-glucuronoxylan from softwood	Arabino-1,4-galactan	Arabino-1,3/6-galactan	Arabinan
<i>A. niger</i>					
Ara B	7	3	50	5	16
<i>A. terreus</i>					
Ara pI 7.5	9	6	22	1	12
<i>A. terreus</i>					
Ara pI 8.5	21	11	48	10	15
<i>A. awamori</i>					
AXH	30	23	0	0	0

less galactose was attacked more efficiently than the more highly substituted guar gum.

Accessory enzymes may not only work in synergy with backbone hydrolyzing enzymes. Enzymes acting on different side groups can also show cooperation with each other as different side groups may block the accessibility of one another. Such an example is illustrated in Figure 5. The action of α -arabinosidase was not enhanced by the presence of β -galactosidase and 1,6-galactanase but the removal of galactose side groups was clearly improved by the mixture of accessory enzymes.



*Figure 5. Liberation of arabinose and galactose from arabinose-1,3/6-galactan by three side-chain-acting enzymes; α -arabinosidase, β -galactosidase and 1,6-galactanase from *Aspergillus niger* (18,31).*

In contrast to glycanases, most esterases are known to be rather unspecific enzymes. Therefore some esterases are able to act on several different hemicelluloses, as shown in Table V, whereas others are more specific and act only on one type of hemicellulose (33). Thus, one esterase may be useful in the treatment of several different hemicelluloses.

Even though the classification of enzymes appears rather simple and straightforward in Table II, each individual enzyme is unique in its specificity towards the substrate molecule. The action of enzymes must therefore be thus carefully evaluated with the target substrates to know whether they are useful for desired modifications.

Table V. Action of three different esterases on acetylated xylan and glucomannan. 4 mg of esterase / g was incubated for 24 h (32).

<i>Enzyme source</i>	<i>Acetic acid from</i>	
	<i>(% of theor)</i>	
	<i>Xylan</i>	<i>Glucomannan</i>
<i>T. reesei</i> AXE	80	0
<i>A. oryzae</i> AGME	17	67
<i>A. oryzae</i> FE	81	90

Enzymatic modifications

The solubility and rheological properties of the polymers are related to their structure, e.g. to the degree of polymerization as well as to the degree of substitution. The solubility normally increases when the degree of polymerization is decreased, and decreases after removal of substituents, leading to an increase in viscosity or a precipitation of the polymer. Thus enzymes offer excellent means for modification of these properties.

A possible use of enzymes is to upgrade a cheaper raw material to a more valuable product. One such, patented already twenty years ago, is to change the composition of guar galactomannan, which has a galactose to mannose ratio of 1:1.5, to resemble locust bean galactomannan with a Gal:Man ratio of 1:3.0 using an α -galactosidase treatment (Table VI). Galactomannan from guar gum is more than tenfold cheaper than galactomannan from locust beans, but has poorer gelling properties.

Figure 6 shows how the viscosity of a galactomannan solution increases until a certain point, after which it decreases due to the poor solubility of the resultant polymers. Similar modifications can also be carried out with other

Table VI. Modification of guar gum galactomannan with high galactose content by α -galactosidase. Treatment time 5h (31).

<i>α-Galactosidase dosage (nkat/g)</i>	<i>Gal : Man ratio After the treatment</i>
0	1 : 1.5
200	1 : 1.9
500	1 : 2.4
1000	1 : 3.1

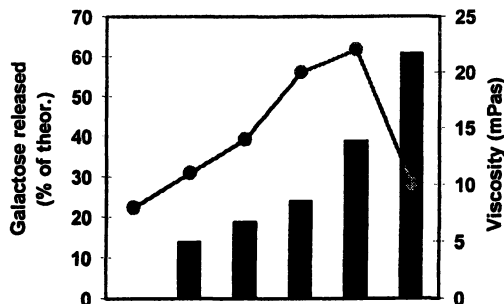


Figure 6. Effect of enzymatic removal of galactose side groups (bars) on the viscosity (line) of galactomannan solution (21).

hemicelluloses. Better controllability of the viscosity of hemicellulose solutions is desired in many of the potential future applications in the food, pharmaceutical and chemical industries.

The precipitation of xylan and mannan due to removal of side groups is demonstrated in Figure 7. Substituents hinder the close association between backbone sugar units and thus restrict the formation of tight hydrogen bonds between them. Removal of side groups results in a more close association of hemicelluloses and they start to precipitate, and may even crystallize. Polyxylan and α -mannan are known to organize into crystalline structures (36,37).

If water-insoluble polymers, such as cellulose or wood fibres are present in the solution, precipitating hemicelluloses attach easily onto the surfaces. This also occurs in current processing of lignocellulosic materials such as in alkaline pulping, during which acetyl groups in xylan and mannan are removed, with the result that hemicelluloses are associated more tightly with cellulose in pulp than in wood fibres. Hemicelluloses are indeed important for the paper technical properties of pulp fibres (38).

Absorption of water soluble hemicelluloses to the cellulose surface is also improved by lowering the content of side groups, as is illustrated in Figure 8. Less substituted mannan adsorbs clearly better on cellulose than highly substituted mannan. The binding efficiency was mainly governed in this case by DS, as decrease of the polymerization by endomannanase did not affect the sorption (39). Endoglycanase treatment may thus be used for example to treat polysaccharides which result in highly viscose solutions, and are thus difficult to handle and adsorb unevenly. Better control of the absorption properties as well as of processes opens up new possibilities to use hemicelluloses for coatings, absorbents, composites etc.

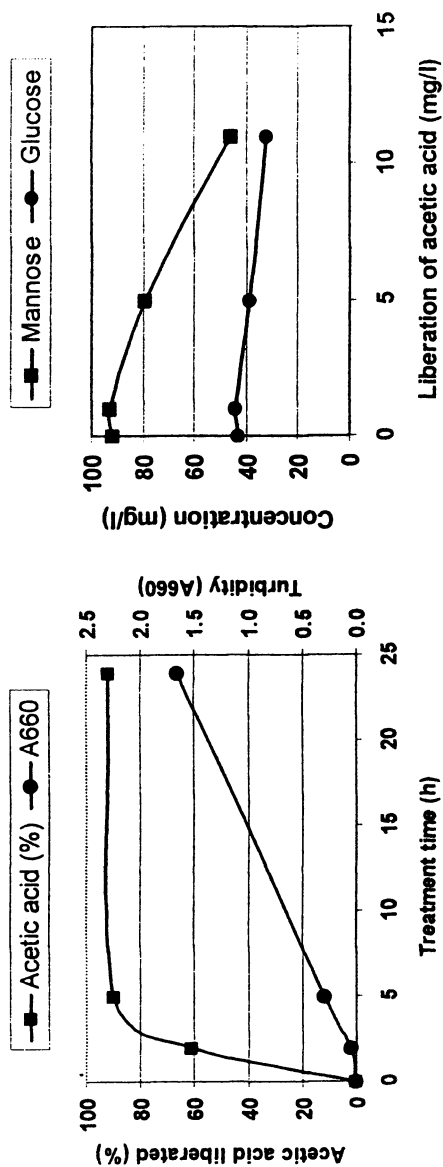


Figure 7. Effect of enzymatic removal of acetyl side groups from xylan (left) and from glucomannan (right) on their solubility. On the right the enzyme treatment was performed in a solution containing wood fibres. During deacetylation, part of the glucomannan adsorbed on fibres. (Reproduced with permission from references 34 and 35. Copyright 1990 and 1994 Springer-Verlag)

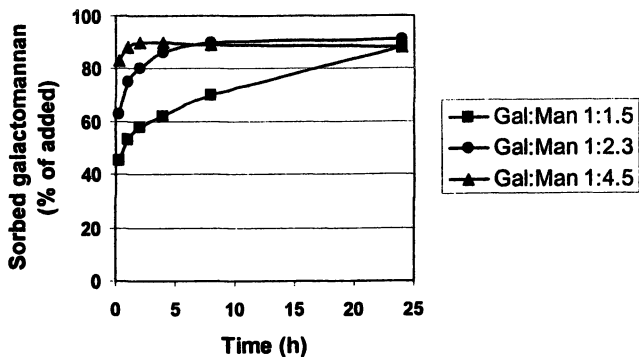


Figure 8. Sorption of guar gum galactomannan (Gal:Man 1:1.5) and two α -galactosidas-treated galactomannans with reduced degree of substitution on wood pulp. (Reproduced with permission from reference 37. Copyright 1979 Kluwer)

Hemicellulose-acting esterases may also be utilized in the future for regioselective removal of acetyl, or other esterified groups, in chemically esterified hemicelluloses. Different acetyl xylan esterases have recently been shown to possess distinct regioselective modes of action against cellulose acetate, cleaving the acetyl substituents in the C-2 and/or C-3-position (40). This kind of specificity is difficult to obtain by conventional chemical methods and it will enable the manufacture of more defined esterified polysaccharides.

The utilization of various hydrolases for the modification of hemicelluloses in large scale is, however, still restricted due to the limited industrial availability of the enzymes discussed above. Endoxylanases, endomannanases and endoglucanases can be obtained in substantial quantities from the enzyme producers. However, other backbone-hydrolyzing enzymes are not available without side-activities and thus cannot yet be used for selective modifications. The only accessory enzyme currently on the market is α -galactosidase. New enzyme products containing other hemicellulases are still needed before the enzymatic tailoring of hemicelluloses can be performed in industrial scale.

New potential enzymes for the future

The enzymes forming new glycosidic linkages are involved in the synthesis of hemicelluloses and exist in all plants. They are, however, not yet available for in vitro modifications of hemicelluloses. Plant polysaccharide synthetases are still poorly characterized and only a few of the enzymes participating in the synthesis of hemicelluloses have been isolated and characterized (41). Furthermore, even fewer of them have been cloned and produced in another host organism in significant amounts.

The hemicellulose-synthesizing enzymes are by definition transferases, which transfer the glycosyl residues from the activated donors, nucleoside diphosphate sugars such as UDP-xylose and GDP-mannose, onto a growing polysaccharide backbone or as a side group. The requirement of the activated sugar donor also restricts the use of these enzymes in large scale unless efficient methods for the production of activated sugars are developed. Some of the transferases have been found to act in synergy, such as the mannosyltransferase and galactosyltransferase in the synthesis of galactomannan (42). The degree of substitution of the synthesized galactomannan could be regulated in vitro by adjusting the relative concentrations of GDP-mannose and UDP-galactose (42). However, in the future the manipulation of hemicellulose structures may be more feasible through modification of biosynthetic processes in vivo rather than using synthetic enzymes in vitro.

Few known enzymes are able to form glycosidic linkages between polysaccharides. One such enzyme is xyloglucan endotransglycosylase (XET), which catalyzes the cleavage of the backbone in xyloglucan, and attaches the non-reducing end of the formed molecule either to water (hydrolysis) or another xyloglucan molecule (transferase reaction) (43). XETs are highly specific for xyloglucan and do not act on cellulose. This type of crosslinking enzyme would be a very interesting tool in the future.

Another completely different type of future enzymes are the oxidases, which are able to oxidize selectively the hydroxyl groups in polymers. An example of this type of enzyme is galactose oxidase, which transforms the hydroxyl group in C-6 to the aldehyde group (44). This enzyme has been known for over 30 years, but its use in the modification of galactomannans has been restricted due to the lack of a suitable industrial enzyme preparation. The possible applications of galactose oxidases are discussed in more detail in another chapter in this book. Hitherto this is the only known oxidase to act on hemicelluloses, but hopefully more enzymes of this type will be discovered in the future.

Acknowledgements

Matti Siika-aho is thanked for the previously unpublished data presented here.

References

1. Aspinall, G.O.; *Polysaccharides*; Pergamon Press: New York, 1970, pp. 103-115.
2. Aspinall, G.O.; In: Preiss, J., Ed.; *The Biochemistry of Plants*; vol 3; Academic Press Inc.: New York, 1980, pp. 437-500.

3. Aspinall, G.O. *Adv. Carboh. Chem.* **1959**, *14*, 429-468.
4. Timell, T.E. *Wood Sci. Technol.* **1967**, *1*, 45-70.
5. Wilkie, K.C.B.; *Adv. Carboh. Chem. Biochem.* **1979**, *36*, 215-264.
6. Schulze, E.; *Berichte der Deutsche Chemische Gesellschaft*, **1891**, *24*, 2277-2287.
7. Dekker, R.F.H.; In: Higuchi, T., Ed.; *Biosynthesis and Biodegradation of Wood Components*; Academic Press Inc.: Orlando, 1985, pp. 505-533.
8. Coughlan, M.P.; Hazelwood, G.P., *Hemicellulose and Hemicellulases*; Portland Press: London, 1993.
9. Warren, R.A.J. *Annu. Rev. Microbiol.*, **1996**, *50*, 183-212.
10. Biely, P.; *Trends. Biotechnol.*, **1985**, *3*, 286-290.
11. Sjöström, E. *Wood Chemistry, Fundamentals and Applications*; Academic Press Inc.: New York, 1981.
12. Schols, H.A.; Voragen, A.G.J., In: Whitaker, J.R., Voragen, A.G.J., Eong, D.W.S., Eds.; *Handbook of Food Enzymology*; Marcel Dekker, Inc.: New York, 2003, pp. 829-843.
13. Mueller-Harvey, I.; Hartley, R.D.; Harris, P.J.; Curzon, E.H. *Carbohydr. Res.* **1986**, *148*, 71-85.
14. Matsuo, T.; Mizuno, T. *Agric. Biol. Chem.* **1974**, *38*, 465-466.
15. Teleman, A.; Antonsson, M.; Tenkanen, M.; Jacobs, A.; Dahlman, O. *Carbohydr. Res.* **2003**, in press.
16. Vincken, J.-P.; York, W.S.; Beldman, G.; Voragen, A.G.J. *Plant Physiol.* **1997**, *114*, 9-13.
17. Biely, P.; Vršanská, M.; Claeysens, M. *Eur. J. Biochem.* **1991**, *200*, 157-163.
18. Luonteri, E.; Laine, C.; Uusitalo, S.; Teleman, A.; Siika-aho, M.; Tenkanen, M.; *Carbohydr. Polym.*, **2003**, in press.
19. Luonteri, E.; Siika-aho, M.; Tenkanen, M.; Viikari, L. *J. Biotechnol.*, **1995**, *38*, 279-291.
20. Saake, B.; Krause, Th.; Puls, J. *Bioresource Technol.* **2001**, *80*, 195-204.
21. Siika-aho, M. unpublished results.
22. Biely, P.; Vršanská, M.; Tenkanen, M.; Kluepfel, D. *J. Biotechnol.* **1997**, *57*, 151-166.
23. Kormelink, F.J.M.; Gruppen, H.; Viëtor, R.J.; Voragen, A.G.J. *Carbohydr. Res.* **1993**, *249*, 355-367.
24. Tenkanen, M.; Makkonen, M.; Perttula, M.; Viikari, L.; Teleman, A.. *J. Biotechnol.*, **1997**, *57*, 191-204.
25. McCleary, B.V. *Phytochemistry* **1979**, *18*, 757-763.
26. Luonteri, E.; Beldman, G.; Tenkanen, M.; *Carbohydr. Polym.*, **1998**, *37*, 131-141.
27. Beldman, G., Schols, H.A., Pitson, S.M., Searle-vanLeeuwen, M.J.F.; Voragen, A.G.J. *Adv. Macromol. Carbohydr. Res.* **1997**, *1*, 1-64.
28. Siika-aho, M.; Tenkanen, M.; Buchert, J.; Puls, J.; Viikari, L.; *Enzyme Microb. Technol.*, **1994**, *16*, 813-819.

29. Tenkanen, M.; Siika-aho, M.; *J. Biotechnol.*, **2000**, *75*, 149-161.
30. Luonteri, E.; Tenkanen, M.; Viikari, L. *Enzyme Microbiol. Technol.* **1998**, *22*, 192-198.
31. Tenkanen, M. unpublished results.
32. Tenkanen, M. *Biotechnol. Appl. Biochem.* **1998**, *27*, 19-24.
33. Tenkanen, M.; Eyzaguirre, J.; Isoniemi, R.; Faulds, C.B.; Biely, P.; In: Mansfield, S.; Saddler, J., Eds.; *ACS Symp. Ser.*, 2003, in press.
34. Poutanen, K.; Sundberg, M.; Korte, H.; Puls, J. *Appl. Microbiol. Biotechnol.* **1990**, *33*, 506-510.
35. Thornton, J.; Tenkanen, M.; Ekman, R.; Holmbom, B.; Viikari, L. *Holzforchung*, **1994**, *48*, 436-440.
36. Marchessault, R.H.; Settineri, W.J. *J. Polymer Sci.* **1965**, C-11, 253-264.
37. Chanzy, H.; Dubé, M.; Marchessault, R.H.; Revol, J.-F.; *Biopolymers* **1979**, *18*, 887-898.
38. Schönberg, C.; Oksanen, T.; Suurnäkki, A.; Kettunen, H.; Buchert, J. *Holzforchung*, **2001**, *55*, 639-644.
39. Hannuksela, T.; Tenkanen, M. Holmbom, B., *Cellulose*, **2002**, *9*, 251-261.
40. Altaner, C.; Saake, B.; Tenkanen, M.; Eyzaguirre, J.; Faulds, C.B.; Biely, P.; Viikari, L.; Siika-aho, M.; Puls, J. submitted.
41. Gregory, A.; Bolwell, G.P.; In: Barton, D.; Nakanishi, K.; Meth-Cohn, O., Eds.; *Comprehensive Natural Products Chemistry*; vol 3; Elsevier: Oxford, 1999, pp. 599-615.
42. Edwards, M.; Bulpin, P.V.; Dea, C.M.; Reid, J.S.G.; *Planta* **1989**, *178*, 41-51.
43. Fry, S.C.; Smith, K.F.; Renwick, K.F.; Martin, D.J.; Hodge, S.K.; Matthews, K.J. *Biochem. J.* **1992**, *282*, 821-828.
44. Avigad, G.; Amaral, D.; Asensio, C.; Horecker, B.L.; *J. Biol. Chem.* **1962**, *237*, 2736-2743.

Chapter 20

Chemical Functionalization of Xylan: A Short Review

Thomas Heinze¹, Andreas Koschella¹, and Anna Ebringerová²

¹Department of Chemistry (FB9), Bergische University of Wuppertal,
Gauss Strasse 20, D-42097 Wuppertal, Germany

²Institute of Chemistry, Slovak Academy of Sciences, Dubravská cesta 9,
Bratislava, SK-842 38, Slovakia

Typical functionalization reactions of xylan are reviewed. Moreover, comments about the analytical characterization of the xylan derivatives are given and some structure-property relationships are discussed.

The hemicellulose xylan belongs to the most abundant biopolymers present in wood and other plants such as grasses, cereals, and herbs. The xylan structure is rather complex. Depending on the natural source of the xylan, varying contents of glucose, xylose, mannose, galactose, arabinose, fucose, glucuronic acid, and galacturonic acid can be found. The backbone consists mainly of β -1 \rightarrow 4-linked xylose units (*1*). Recently, xylan gains increasing importance as basis for new biopolymeric materials and functional polymers by chemical modification reactions. Moreover, agricultural wastes like cobs, blades, leaves are always available and interesting raw-products.

In the present article, important functionalization methods for the preparation of xylan derivatives are discussed. In addition, examples for the structure analysis and applications are given.

Xylan esters

Carboxylic acid esters of xylan are prepared under typical conditions used for polysaccharide esterification, i.e., activated carboxylic acid derivatives are allowed to react with the polymer both heterogeneously and homogeneously (Figure 1). The heterogeneous esterification of oakwood sawdust and wheat bran

hemicelluloses (extracted with alkaline media) with an excess of octanoyl chloride under different conditions including the use of bases and co-solvents was described (2). The conversion was characterized by the weight increase of the products and the ester content by a saponification method. A solid esterified material and a liquid fraction were isolated after a solvent-free reaction. The liquid fraction was separated into an insoluble part (acetylated cellulose) and soluble hemicellulose and lignin. Moreover, the values of the degree of substitution (DS) of the products after fractionation steps showed that products of high DS are soluble in the reaction medium and, therefore, DS values of solubilized parts are higher compared to the non-dissolved material. The conversion of hemicellulose and wood is accompanied by polymer degradation induced by acidic hydrolysis due to the HCl. The amount of liquefied fraction is diminished in the presence of pyridine.

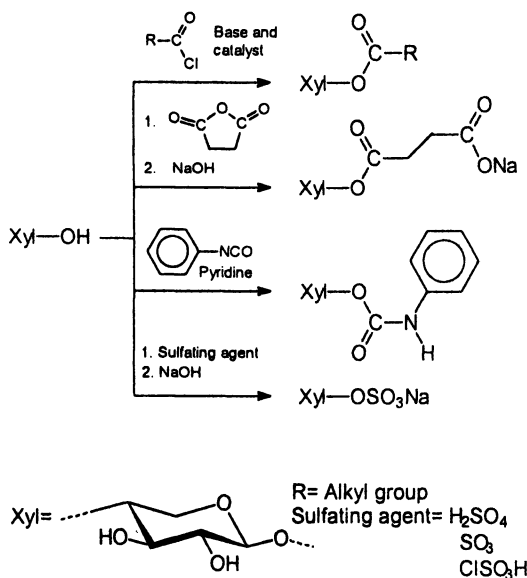


Figure 1. Introduction of ester groups into xylan.

The homogeneous acylation of the hemicellulose is mostly carried out in the solvent *N,N*-dimethylformamide (DMF) in combination with LiCl. Hemicellulose extracted from poplar wood chips was acylated with various carboxylic acid chlorides in DMF/LiCl applying triethylamine and 4-*N,N*-dimethylaminopyridine (DMAP) as base and catalyst (3, Table 1). Depending on

the molar ratio of acyl chloride and anhydroxylose unit, DS values in the range from 0.32 to 1.51 were obtained under moderate reaction conditions (temperature <75°C, time up to 45 min).

Table 1: Conditions and degree of substitution (DS) of esterified hemicellulose.

<i>Carboxylic acid chloride</i>	<i>Conditions</i>				<i>Product</i>
	<i>Molar ratio^a</i>	<i>Temp. (°C)</i>	<i>Time (min)</i>	<i>TEA^b (%)</i>	<i>DS</i>
Acetyl	3:1	45	30	242	0.63
Butyryl	3:1	75	35	280	1.15
Octanoyl	3:1	75	40	280	1.17
Decanoyl	2:1	65	30	150	0.44
Decanoyl	3:1	75	40	220	1.21
Stearoyl	2:1	65	30	110	0.40
Stearoyl	3:1	75	40	180	1.22
Stearoyl	3:1	75	45	280	1.51
Oleoyl	2:1	65	30	110	0.32
Oleoyl	3:1	75	40	180	1.17

^aMolar ratio of carboxylic acid chloride to anhydroxylose unit.

^bPercentage of triethylamine based on the weight of the hemicellulose (w/w).

SOURCE: Adapted from reference 3.

Wheat straw hemicellulose stearates were synthesized in DMF/LiCl by using 1-3 eq. acid chloride in the presence of triethylamine or pyridine and DMAP (4). DS values between 0.18 and 1.71 were obtained depending on the reaction conditions. A maximum DS of 1.71 was realized with 3 eq. acylating reagent after 30 min at 75°C. It was found that the polymer degradation is lower than 8% at short reaction times and temperatures below 75°C. A notable degradation occurs during the acylation at 85°C.

The DMF/LiCl system was also used for the acetylation of hemicellulose B isolated from wheat straw (5). Hemicellulose B is accessible after potassium hydroxide extraction of the delignified wheat straw, neutralization, and ethanol precipitation of remaining liquid. This material contains 73.5% xylose, 12.2% arabinose, and small amounts of other sugars (glucose, galactose, and rhamnose). The reaction of hemicellulose with 0.8 eq. acetic anhydride per mole hydroxyl group was carried out in a highly swollen system in the presence of DMAP as catalyst within a reaction time of 2-72 h and temperatures from 60 to 90°C leading to DS values in the range from 0.59 to 1.25. The highest DS was

obtained after 60 h at 85°C. The acetylated hemicelluloses are soluble in tetrahydrofuran, hexane or another solvents of varying polarity depending on the DS and form films after casting the solution and evaporation of the solvent. SEC measurements show that the polymer degradation is low at reaction temperatures of 60–85°C. Increasing temperatures and prolonged reaction times lead to a significant degradation. Moreover, the acetylated hemicellulose was found to be thermally more stable than the non-esterified material.

The conversion of water-soluble wheat straw hemicellulose with succinic anhydride in aqueous alkaline solutions yields carboxyl groups containing products (6). The DS values of the products are rather low (<0.26) due to side-reactions in the aqueous medium. Despite the low functionalization, the thermal stability is increased and applications as thickening agents and metal ion binders are proposed.

The treatment of oat spelt xylan with phenyl- or tolyl isocyanate in pyridine leads to the fully functionalized corresponding carbamates (7). Xylan-3,5-dimethylphenylcarbamate shows a high chiral recognition ability which is even better than known from cellulose derivatives for some chiral drugs (8).

Xylan sulfates are mostly studied with regard to their biological activities. Usually, sulfuric acid, sulfur trioxide or chlorosulfonic acid are employed as sulfating agents alone or in combination with alcohols, amines or chlorinated hydrocarbons as reaction media (9).

The reaction of beech wood xylan in N_2O_4 /DMF with SO_2 or SO_3 yields sulfuric acid half esters of low DS (0.17–0.55) compared with the sulfation of cellulose due to the absence of reactive primary hydroxyl groups in the xylan structure (10). Moreover, algal cell wall microfibril homoxylan (β -1 \rightarrow 3-xylan) was sulfated with SO_3 -pyridine under mild conditions and investigated with regard to the sulfation regioselectivity by means of different NMR techniques (11).

Cationic xylan ethers

Cationic groups are usually introduced into xylan by the formation of ether bonds applying various reagents (Figure 2). Mostly, the polymer is reacted with prebuilt cationic reactants bearing halogens or epoxide rings as reactive moieties. Furthermore, it is possible to react the polymer with epichlorohydrin yielding a chlorohydroxypropyl group which can be quarternized subsequently by reaction with a tertiary amine. Investigations were directed not only towards the use of isolated and purified polymers as starting material but also to non-purified mixtures of biopolymers like wood sawdust or sugar cane bagasse containing xylan, cellulose, and lignin.

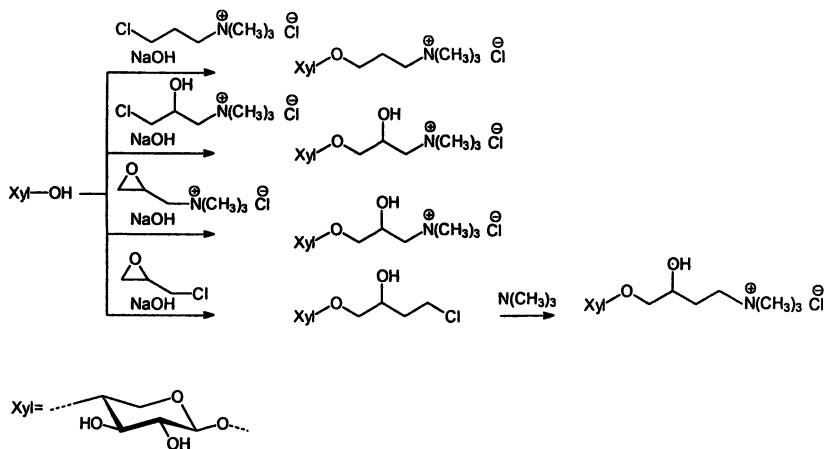


Figure 2. Reaction pathways for the introduction of cationic moieties into xylan.

Antal *et al.* (12) reported the etherification of beech sawdust with 3-chloro-2-hydroxypropyltrimethylammonium chloride (CHTMAC). Subsequent extraction steps with water, aqueous sodium chlorite and sodium hydroxide solution and ethanol lead to a fractionation of the trimethylammonium-2-hydroxypropyl (TMAHP) sawdust into TMAHP-cellulose, -hemicellulose, and -lignin. It was demonstrated that the main part of the modified hemicellulose can be extracted with water directly from the modified sawdust because of the increasing solubility in polar solvents. Furthermore, the hemicellulose was found to be the most reactive components followed by lignin and cellulose. Thus, the authors have developed a method for the preparation of xylan derivatives directly from natural sources. The exchange capacity of the TMAHP-xylan is higher compared to TMAHP-derivative of lignin and cellulose.

Large quantities of bagasse, as a plant residue from sugar cane, are formed as a by-product of the production of sugar in tropical countries. The cationization of sugar cane bagasse was studied with regard to a possible separation in lignin and hemicellulose dependent on the alkylating agent (13). CHTMAC and 1,3-bis(3-chloro-2-hydroxypropyl)imidazolium sulfate (BCHIS) were used as reagents yielding cationic derivatives of cellulose, hemicellulose, and lignin. The ratios of the extractable materials changed after the cationization (Table 2). For instance, unmodified bagasse contains 12.7% water soluble hemicellulose while 21.8% of the TMAPH derivative can be extracted. Crosslinked polymers were obtained with BCHIS as a bifunctional reagent. A small amount of water-soluble derivative obtained was discussed to be only monofunctionalized polymer. The cationic modification of the bagasse causes degradation of the polymers. The weight average molecular weight of water-soluble hemicellulose was 11085 gmole^{-1} before and 1854 gmole^{-1} after reaction

Table 2: The yields of fractions obtained with unmodified bagasse and after reaction with 3-chloro-2-hydroxypropyl-trimethylammonium chloride.

<i>Bagasse</i>		<i>TMAHP-bagasse</i>	
<i>Fraction^a</i>	<i>Yield (%)</i>	<i>Fraction^a</i>	<i>Yield (%)</i>
Ethanol lignin	7.9	TMAHP-EL	9.6
Residue after EL extraction	91.5	TMAHP-residue after EL extraction	90.9
Water-extracted hemicellulose	12.7	Water-extracted TMAHP-hemicellulose	21.8
Residue after WH extraction	59.9	TMAHP-residue after WH extraction	69.9
Alkali-soluble hemicellulose	17.9	Alkali-soluble TMAHP-hemicellulose	3.5
Residue after AH	41.9	TMAHP-residue after AH	37.2

^aEL= Ethanol lignin; WH= water-soluble hemicellulose; AH= alkali-soluble hemicellulose; TMAHP= trimethylammonium-3-hydroxypropyl
SOURCE: Adapted from reference 13 (© 1997).

with CHTMAC. The degradation is combined with a decrease of the polydispersity from 2.9 to 1.1.

Antal *et al.* investigated aspen wood flower as raw material for the alkylation with CHTMAC (14). Nearly 50% of the existing xylan was converted in TMAHP-xylan. Water- and ethanol soluble parts were extracted. It is worth to mention that the addition of TMAHP-xylan to spruce sulfite pulp improves the mechanical properties remarkably.

More recently, the quarternization of xylan isolated from beech wood, corn cobs, and rye bran was investigated (15). The reactions were carried out with a sodium hydroxide activated xylan and CHTMAC as alkylating reagent. The results show clearly that the DS of TMAHP groups depends on the molar ratios CHTMAC/xylan and NaOH/CHTMAC as well as on the xylan type used (Table 3).

The DS_{TMAHP} was determined by means of elemental analysis. The purification of the products is very difficult due to the fact that electrostatic interactions between the quaternary ammonium moieties and carboxyl groups may prevent the complete removal of degradation products and nitrogen containing impurities. Therefore, the nitrogen content may not be appropriate for the determination of the DS.

Cationic xylan improve the paper making properties of pulp (16). Xylan samples from beech wood (4-*O*-methyl glucurono xylan, GX) and corn cobs (arabino-(4-*O*-methyl glucurono) xylan, AGX) were converted into TMAHP

derivatives by treating the sodium hydroxide activated polymer with CHTMAC. In order to characterize the retention behavior, a pulp slurry was treated with different concentrations of TMAHP-derivatives of xylan. The turbidity of the water after dynamic dewatering was determined. It was found that a low content of 0.25% TMAHP-GX in the pulp slurry is the most effective concentration. TMAHP-GX acts as a flocculant for the pulp fibers which improves the sheet formation due to a microfloculation. In contrast, synthetic polymers does not show this effect. The flocculation properties of the xylan derivatives are influenced by the DS while the structure of the polymer backbone depending on the natural origin of the xylan does not play an important role. This may be of industrial importance because the properties of the xylan based flocculants are not affected by the raw material. Moreover, the authors point out that the polymer chain of xylan is more similar to cellulose (except the lack of the CH₂OH group) than starch and galactomannan. Therefore, xylan shows a natural affinity to cellulose which is the reason for the good flocculation behavior due to the irreversible adsorption onto cellulose fibers.

The determination of the functionalization pattern is of great interest due to the understanding of structure-property-relationships. Ebringerová *et al.* described the characterization of TMAHP-derivatives of xylan using NMR- and IR spectroscopy (15, 17). The introduction of TMAHP residues leads to remarkable changes in the FTIR spectra. Namely, a band at 1475 cm⁻¹ appears which was assigned to bending vibrations of methyl and methylene groups of the TMAHP moiety. The ratio of bands at 1475 and 985 cm⁻¹ and the nitrogen content determined by means of elemental analysis agrees quite well. Consequently, FTIR spectroscopy may be used for the quantitative analysis of TMAHP-derivatives of xylan. ¹³C NMR spectroscopic measurements of the polymers lead to spectra with broad peaks. Moreover, many peaks were observed due to the complex structure of the polysaccharide backbone. In fact, the primary structural features of the xylan was not altered during the modification. The assignment of methylene groups could be achieved by using the DEPT technique. Better results were obtained after complete hydrolytic chain degradation and separation of the components by means of preparative chromatography.

Oxidized Xylan Derivatives

Oxidation is an important tool for the introduction of carbonyl and carboxyl functions into biopolymers. The tendency of the oxidation of polysaccharides depends substantially on the nature of the oxidants and the conditions. Most of the oxidants known from the low-molecular organic chemistry produce both carbonyl and carboxyl functions to a varying extent depending on the

experimental conditions (9). Moreover, even so-called selective oxidation reactions will result in more or less depolymerization of the macromolecules. In principle, xylan as polyhydroxy compounds bearing secondary hydroxyl groups can be oxidized to 2-keto-, 3-keto- and 2,3-diketo xylan neglecting the transformation of the end groups.

Moreover, 2,3-dialdehyde xylan may be obtained in the well-known glycol cleavage oxidation of vicinal diol units with sodium periodate, which can be further oxidized to give 2,3-dicarboxyl xylan. Figure 3 summarizes the structures of the possible oxidized repeating units.

The biodegradation of various carboxylic group containing polymers was studied by Matsumura *et al.* (18-20). The aim of this work was to develop compounds which are biologically degradable detergents. Thus, xylan from oat

Table 3: Quarternization of xylan in relation to the molar ratios of reactants.

Xylan ^a	Molar ratios ^b		N (%)	DS _Q ^c	DS ^d	Yield (g/g) ^e
	CHTMAC/Xyl	NaOH/CHTMAC				
BWX	1.00	0.80	0.82	0.10	0.09	0.72
	1.00	1.20	3.42	0.59	0.51	1.14
	1.00	1.40	3.07	0.50	0.44	1.05
	1.00	2.00	2.27	0.34	0.29	0.98
BPX	1.00	4.10	0.98	0.12	0.10	0.78
	4.00	0.80	1.33	0.15	0.14	1.01
	4.00	1.10	2.06	0.26	0.25	1.17
	4.00	1.60	3.27	0.49	0.46	1.32
CCX	4.00	2.10	2.08	0.37	0.35	1.04
	4.00	1.00	2.48	0.28	0.25	1.13
	4.00	1.20	3.10	0.47	0.39	1.29
	7.00	2.00	2.24	0.31	0.28	1.24
	17.00	1.80	2.34	0.33	0.29	1.37

^aBWX= beech wood xylan, BPX= beech pulp xylan, CCX= corn cob xylan.

^bCMAHC= 3-chloro-2-hydroxypropyl-trimethylammonium chloride, NaOH as 17.5% aqueous solution

^cDegree of substitution of cationic groups.

^dDegree of substitution related to the total molar amount of all sugar constituents.

^eProduct weight related to the starting sample weight.

SOURCE: Adapted from reference 15 (© 1994).

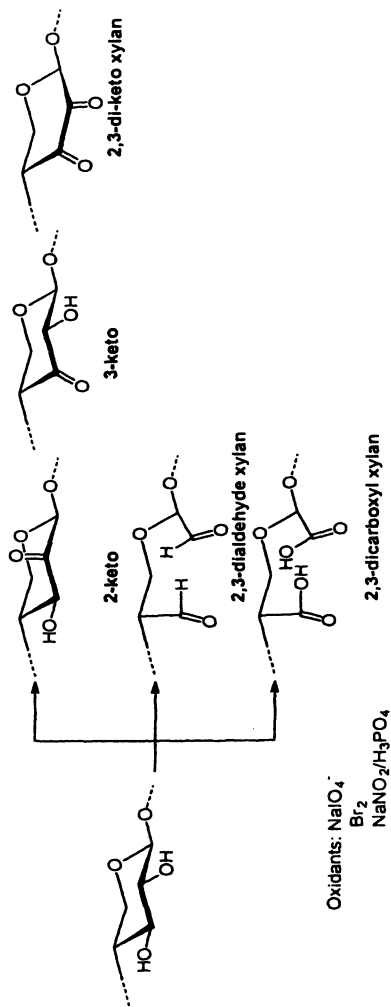


Figure 3. Typical repeating units of oxidized xylan.

spelts (commercially available from Sigma Chemical Co.) as well as cellulose and starch were oxidized to 2,3-dicarboxylic polysaccharides in a two step procedure by using $\text{HIO}_4/\text{NaClO}_2$ as oxidants. Xylan was treated with periodic acid for 6 h at 4°C to obtain 2,3-dialdehyde xylan with 39 mole% dialdehyde groups. Subsequent treatment with sodium chloride for 24 h at 20°C and 1 h at 50°C leads to sodium 2,3-dicarboxylic xylan with 39 mole% dicarboxylate moieties. A set of oxidized samples with a content of dicarboxylate functions in the range from 29 to 53 mole% was synthesized by varying the reaction time.

The biodegradability of these polyanions was compared with artificial poly(carboxylic acids). An important result was the fact that the biodegradability is improved if the polymer chain contains functionalities like hydroxyl, ether, ester or carbonyl groups as well as sugar residues. The biodegradability and detergency is improved by the introduction of carboxylic groups (18, Table 4). Poly(sodium acrylate) was used as reference in a five day biochemical oxygen demand measurement (BOD_5). No oxygen consumption was measured for the reference substance. It was found that the BOD_5 decreases with increasing content of dicarboxylic units in the polymers used.

Matsumura *et al.* showed also that the biodegradability of oxidized xylan and amylose by α -amylases and xylanases depends on the degree of oxidation (21). In the case of amylose, a content of at least 50% non-oxidized glucopyranose units is necessary for the degradation by amylase. Xylan is biodegradable with a content of more than 70% xylopyranose units. These results indicate that enzymatic degradation occurs if the content of oxidized repeating units is in a range in which the polymer still contains blocks of non oxidized sugar residues. It was found that the biodegradability of xylan derivatives was higher than that of oxidized amylose but amylose may have a higher carboxyl content than xylan in order to gain enzymatic degradation.

Andersson *et al.* investigated the oxidation of xylan and cellulose with sodium nitrite in orthophosphoric acid (22). This oxidant is known to attack primary hydroxyl groups yielding carboxylic acid groups, i.e., in case of cellulose 6-carboxyl cellulose is formed (23, 24). Consequently, an oxidation of xylan should not occur due to the absence of a primary hydroxyl group. NMR measurements of the oxidized xylan indicate that the polymer is preferentially oxidized to 2-ulose residues. Oxidation at C-3 occurs to a very low extent only. The peak assignment could be performed using 2D-COSY experiments. The result is in agreement with the fact that esterification of the O-2 is faster compared to O-3. In addition, the low oxidation at C-3 was revealed by means of the more sensitive sugar analysis after borohydride reduction compared to NMR measurements.

The neutral xylan fraction from *Palmaria decipiens* was treated with aqueous bromine solution (25). This xylan contains 1→4- as well as 1→3-linked sugar units. Carbonyl groups are formed which was revealed by means of FTIR (ν_{CO} at 1741 cm^{-1}) and NMR spectroscopy. The peaks found in the ^{13}C -NMR spectrum were assigned (Table 5). The presence of C=O was also revealed

Table 4. Five-day biochemical oxygen demand (BOD₅) as measured by the oxygen consumption method

<i>Xylan</i> ^a	<i>ThOD</i> ^b (mg O/g)	<i>BOD</i> ₅ (mg O/g)	<i>BOD</i> ₅ / <i>ThOD</i> (%)
10500 (29)	918	258	28.1
19900 (39)	839	240	26.6
32200 (39)	836	140	16.7
17700 (45)	794	111	14.0
8520 (53)	737	126	17.1
9020 ^c	935	0	0

NOTE: ^aThe polymer code indicates the number-average molecular weight (M_n) and its relative dicarboxylate content in mole-% in parentheses.

^bThOD: Theoretical oxygen demand.

^cPSA-9020: Poly(sodium acrylate). $M_n = 9020$, $M_w/M_n = 1.8$. Activated sludge, obtained from a municipal sewage plant in Yokohama city, was used for this test.

SOURCE: Adapted from reference 20.

chemically by reactions with *p*-chloroaniline or bovine serum albumin followed by reduction to the corresponding amine with sodium cyanoborane. The oxidation occurs at C-2 only as determined by means of GLC after reductive cleavage, reduction and peracetylation.

The sodium periodate oxidation of xylan isolated from *Palmaria decipiens* yields 2,3-dialdehyde xylan (26). The dialdehyde moieties can be converted into a Schiff base type compound by the reaction with *p*-chloroaniline (Figure. 4).

Imine structures are known to be ligands for the complexation of metal ions. Thus, the Schiff base type compounds obtained from 2,3-dialdehyde xylan coordinates copper(II) in a complex. The complexes were characterized by means of spectroscopic methods (IR, UV/VIS, cyclic voltammetry).

Conclusions

Despite the discussed progress in the field of xylan chemistry, a large number of challenges remain to take full advantage of xylan's great assets. Future advancements will be based on the synthesis of functional polymers both with new functionalities and tailored combinations of different groups as well as with a well-defined and pre-set primary structure both on the level of the repeating unit and the polymer chain. Essential steps on this way include both improved isolation of pure polymeric xylan from the natural sources, and the development of analytical tools for the determination of structural features of xylan products. The availability and outstanding structures of xylan, e.g., two hydroxyl groups

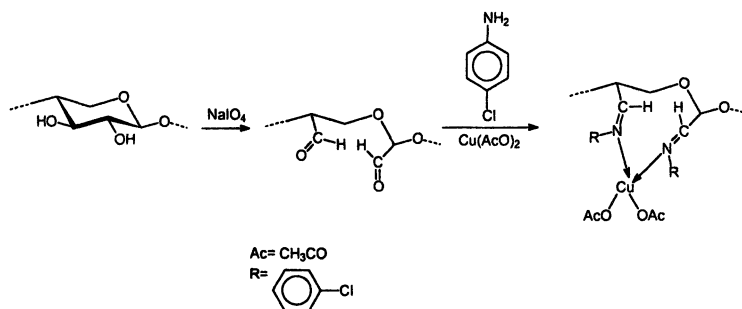


Figure 4. Complexation of copper(II) by a ligand synthesized from xylan
(Adapted from reference 26)

Table 5. Chemical shift assignments for the ¹³C-NMR spectra of xylan and its bromine-oxidized derivative (25).

<i>β</i> -D-Xylopyranosyl residue	Chemical shift (ppm)						
	C-1		C-2		C-3	C-4	C-5
	1→3	1→4	1→3	1→4			
Xylan							
3-O-substituted	104.08	102.50	73.39	73.39	84.39	68.61	65.78
4-O-substituted	104.08	102.50	74.02	73.64	74.62	77.29	63.80
Br₂ oxidized derivative							
3-O-substituted	104.05	102.48	73.56	73.56	84.28	68.51	65.75
4-O-substituted	104.05	102.48	74.15	74.15	74.54	77.22	63.80
CO	203.73						

per repeating unit suitable for chemical functionalization and supramolecular structure formation make the polymers available by functionalization reactions an interesting class of polymeric materials whose attractiveness is expected to rise in the future.

References

1. Ebringerová, A.; Heinze, Th. Xylan and xylan derivatives - biopolymers with valuable properties, 1. *Macromol. Rapid Commun.* **2000**, *21*, 542-556.
2. Thiebaud, S.; Borredon, M. E. Analysis of the liquid fraction after esterification of sawdust with octanoyl chloride – production of esterified hemicelluloses. *Biores. Technol.* **1998**, *63*, 139-145.
3. Sun, RunCang; Fang, J.M.; Tomkinson, J.; Hill, C.A.S. Esterification of hemicelluloses from poplar chips in homogeneous solution of N,N-dimethylformamide/Lithium chloride. *J. Wood Chem. Technol.* **1999**, *19(4)*, 287-306.
4. Sun, R.C.; Fang J. M.; Tomkinson, J. Stearoylation of hemicelluloses from wheat straw. *Polym. Degrad. Stab.* **2000**, *67*, 345-353.
5. Fang, J. M.; Sun, R. C.; Tomkinson, J.; Fowler, P. Acetylation of wheat straw hemicellulose B in a new non-aqueous swelling system. *Carbohydr. Polym.* **2000**, *41*, 379-387.
6. Sun, Runcang; Sun, X. F.; Bing, X. Succinoylation of Wheat Straw Hemicelluloses with a Low Degree of Substitution in Aqueous Systems. *J. Appl. Polym. Sci.* **2002**, *83*, 757-766.
7. Vincendon, M. Xylan derivatives: aromatic carbamates. *Makromol. Chem.* **1993**, *194*, 321-328.
8. Okamoto, Y.; Noguchi, J.; Yashima, E. Enantioseparation on 3,5-dichloro- and 3,5-dimethylphenylcarbamates of polysaccharides as chiral stationary phases for high-performance liquid chromatography. *React. Functional Polym.* **1998**, *37*, 183-188.
9. Klemm, D.; Philipp, B.; Heinze, T.; Heinze, U.; Wagenknecht, W. *Comprehensive Cellulose Chemistry*; Wiley-VCH: Weinheim, 1998.
10. Philipp, B.; Nehls, I.; Wagenknecht, W. ¹³C-N.M.R. spectroscopic study of the homogeneous sulphation of cellulose and xylan in the N₂O₄-DMF system. *Carbohydr. Res.* **1987**, *164*, 107-116.
11. Yamagaki, T.; Tsuji, Y.; Maeda, M.; Nakaknishi, H. NMR Spectroscopic Analysis of Sulfated β-1,3-Xylan and Sulfation Stereochemistry. *Biosci. Biotech. Biochem.* **1997**, *61*, 1281-1285.
12. Antal, M.; Ebringerová, A.; Simkovic, I. New Aspects in Cationization of Lignocellulose Materials. II. Distribution of Functional Groups in Lignin, Hemicellulose, and Cellulose Components. *J. Appl. Polym. Sci.* **1984**, *29*, 643-650.

13. Simkovic, I.; Mlynár, J.; Alföldi, J.; Micko, M. M. New Aspects in Cationization of Lignocellulose Materials. XI. Modification of Bagasse with Quarternary Ammonium Groups. *Holzforschung* **1990**, *44*(2), 113-116.
14. Antal, M.; Ebringerová, A.; Micko, M.M. Kationisierte Hemicellulosen aus Espenholzmehl und ihr Einsatz in der Papierherstellung. *Papier* **1991**, *45*, 232-235.
15. Ebringerová, A.; Hromádková, Z.; Kacuráková, M.; Natal, M. Quarternized xylan: synthesis and structural characterization. *Carbohydr. Polym.* **1994**, *24*, 301-308.
16. Antal, M.; Ebringerová, A.; Hromádková, Z. Struktur und papiertechnische Eigenschaften von Aminoxylanen. *Papier* **1997**, *5*, 223-226.
17. Ebringerová, A. Hromádková, Z. Zur Substituentenverteilung in kationischen Xylanderivaten. *Angew. Makromol. Chem.* **1996**, *242*, 97-104.
18. Matsumura, S.; Yoshikawa, S. *Biodegradable Poly(carboxylic acid) Design In: Agricultural and Synthetic Polymers Biodegradability and Utilization Development*; American Chemical Society, Cellulose, Paper, and Textile Division: Washington, DC, ACS Symposium series 433, XI, 323, 5, 1990; p 124.
19. Matsumura, S.; Maeda, S.; Yoshikawa, S. *Molecular design of biodegradable poly(carboxylic acid) In: Polymeric materials science and engineering*, American Chemical Society, Division of Polymeric Materials Science and Engineering, Washington, DC, **62**, 1990, p 984.
20. Matsumura, S.; Maeda, S.; Yoshikawa, S. Molecular design of biodegradable functional polymers, 2, Poly(carboxylic acid) containing xylopyranosediyl groups in the backbone. *Makromol. Chem.* **1990**, *191*, 1269-1274.
21. Matsumura, S.; Nishioka, M.; Yoshikawa, S. Enzymatically degradable poly(carboxylic acid) derived from polysaccharide. *Makromol. Chem. Rapid Commun.* **1991**, *12*, 89-94.
22. Andersson, R.; Hoffman, J.; Nahar, N.; Scholander, E. An n.m.r. study of oxidation of cellulose and (1→4)-β-D-xylan with sodium nitrite in orthophosphoric acid. *Carbohydr. Res.* **1990**, *206*, 340-346.
23. Painter, T. J. Preparation and periodate oxidation of C-6-oxycellulose: conformational interpretation of hemiacetal stability. *Carbohydr. Res.* **1977**, *55*, 95-103.
24. Heinze, Th.; Klemm, D.; Schnabelrauch, M.; Nehls, I. *Properties and following reactions of homogeneously oxidized cellulose In: Cellulosics: Chemical, Biochemical and Material Aspects*, Eds. Kennedy, J. F., Phillips, G. O., Williams, P. A., and Horwood, E., New York, 1993, p 340.
25. Jerez, J. R.; Matsuhira, B.; Urzúa, C.C. Chemical modifications of the xylan from *Palmaria decipiens*. *Carbohydr. Polym.* **1997**, *32*, 155-159.
26. Barroso, N. P.; Costamagna, J.; Matsuhira, B.; Villagran, M. El xilano de *palmaria decipiens*: Modificación química y formación de un complejo de Cu(II). *Bol. Soc. Chil. Quim.* **1997**, *42*, 301-306.

Chapter 21

Preparation and Characterization of Arabinoxylan Esters

**Charles M. Buchanan¹, Norma L. Buchanan¹, John S. Debenham¹,
Paul Gatenholm², Maria Jacobsson², Michael C. Shelton¹,
Thelma L. Watterson¹, and Mathew D. Wood¹**

¹Research Laboratories, Eastman Chemical Company, P.O. Box 1972,
Kingsport, TN 37662

²Chalmers University, Goteborg, Sweden

Arabinoxylan was isolated from corn fiber as a highly branched, water-soluble polysaccharide composed of xylose, arabinose, galactose, glucuronic acid and glucose. Treatment of this arabinoxylan with a C2-C4 aliphatic anhydride using methanesulfonic acid as a catalyst conveniently provided the corresponding arabinoxylan esters. The arabinoxylan esters were isolated as high molecular weight, amorphous solids with glass transition temperatures ranging from 61 to 138 °C. The glass transition temperatures were found to be highly dependent on the degree of substitution and upon the type of substituent. The arabinoxylan esters are thermally stable to near 200 °C but undergo significant and rapid thermal degradation when heated above the onset of thermal degradation.

Introduction

Hemicellulose is generally defined as being polysaccharides that can be extracted by water or aqueous alkali from plant tissue (1,2). Hemicellulose can be comprised of a wide variety of monosaccharides including xylose, arabinose, glucose, galactose, mannose, fucose, glucuronic acid, and galacturonic acid depending upon the source. The most common hemicelluloses, largely found in hardwood or annual plants, are comprised of a 1,4- β -D-xylopyranosyl main chain with a varying number of side chains based on L-arabinofuranosyl, 4-O-methyl-D-glucuronopyranosyl, D,L-galactopyranosyl, or D-glucuronopyranosyl units. Hemicellulose isolated from hardwood and annual plants differ from one another. The main hemicelluloses found in hardwood are partially acetylated (4-O-methyl-D-glucuronopyranosyl)-D-xylans and these are often simply called xylans. The hemicelluloses found in annual plants such as maize, rice, oats, sunflower, rye, barley, and wheat, are generally more structurally diverse and complex. These plant hemicelluloses have a 1, 4- β -D-xylopyranosyl main chain that can be heavily branched with Xylp- Araf-, Galp- mono-, di, and trisaccharide side chains. These plant hemicelluloses can be neutral or acidic depending on if they contain 4-O-methyl-D-glucuronopyranosyl or D-glucuronopyranosyl substituents. Generally, the two predominant monosaccharides in these annual plant hemicelluloses are xylose and arabinose and they are thus termed arabinoxylans.

Isolation of hemicellulose from wood and annual plants has been investigated for many years (3). The pulping industry would seem to be a most viable source of hemicellulose. In reality, along with the lignin matrix, the hemicellulose is partially or completely degraded during the pulping process (3). Alternative methods exist for extraction of wood hemicellulose, but they are not likely to be reduced to commercial practice in the near future (4). Because wood hemicellulose cannot be easily isolated in polymeric form by conventional pulping methods, the material properties of these polysaccharides have not been fully defined and exploited. Annual plants have proven to be a rich source of hemicellulose (3). However, many of the early methods developed for extraction of hemicellulose from annual plants were not efficient and did not cleanly provide the targeted polysaccharides. Consequentially, a simple commercial process for extraction and isolation of annual plant hemicellulose has never been completely realized. However, significant effort has been recently expended in developing more efficient methods that would enable isolation of hemicellulose from a variety of plant sources (3,4,5).

Perhaps in part due to the lack of commercial supply, hemicellulose has found relatively little industrial utility. The reported industrial applications for plant hemicellulose include their use as viscosity modifiers, gelling agents, tablet binders, or wet strength additives (1). Recently, there has been interest in the use

of hemicellulose as a nutraceutical (6), in chiral separations (7), and as an HIV inhibitor (8). More often, the hemicellulose is hydrolyzed to a mixture of monosaccharides which can be converted to chemicals such as furfural, erythritol, or xylitol or used as fermentation feedstock for making chemicals such as ethanol or lactic acid (9).

While preparation of ether derivatives of arabinoxylans is relatively straight forward (10, 11, 12), synthesis of fully substituted, high molecular weight ester derivatives is not. The classical method for preparing ester derivatives of this type entails the use of base catalysis and polar solvents such as formamide (13,14,15,16). The reported reaction times were typically very long and it was very difficult to obtain complete esterification of the various types of hemicelluloses. Presumably, these methods were developed out of concern that acid catalyzed esterification of these hemicelluloses would lead to cleavage of acid sensitive glycosidic linkages and loss in molecular weight.

With this background, we recently disclosed a method for the isolation of a highly purified, high molecular weight arabinoxylan from corn fiber (10). In addition to our interest in the properties of the parent arabinoxylan, we were also very interested in preparing ester and ether derivatives of this polysaccharide and examining their physical properties. In this context, we describe the methods we have developed for esterification of arabinoxylan from corn fiber and characterization of these new polysaccharide derivatives.

Experimental Section

Modulated differential scanning calorimetry (MDSC) curves were obtained using a Universal V2.4F TA spectrometer. First scan MDSC heating curves were obtained by heating at $5\text{ }^{\circ}\text{C min}^{-1}$ to the desired temperature. Second scan MDSC heating curves were obtained by first cooling the sample after the first heating in the instrument over ca. 17 min. The sample was then heated at $5\text{ }^{\circ}\text{C min}^{-1}$ to the desired temperature.

Differential scanning calorimetry (DSC) curves were obtained using a Universal V3.1E TA spectrometer. The DSC heating curves were obtained by first heating at $20\text{ }^{\circ}\text{C min}^{-1}$ to the desired temperature followed by cooling the sample in the instrument over ca. 17 min. The 2nd scan DSC heating curves were then obtained by heating the sample at $20\text{ }^{\circ}\text{C min}^{-1}$ to the desired temperature.

The thermal stability of the arabinoxylan and arabinoxylan esters were determined by thermogravimetric analysis (TGA) using a Universal V3.1E TA spectrometer. Typically, the sample was heated under air from 20 to 400°C at $20\text{ }^{\circ}\text{C min}^{-1}$.

Molecular weights were determined using a Waters Model 150C high temperature gel permeation chromatograph equipped with an RI detector. For arabinoxylan, the operating temperature was 25 °C and the mobile phase was 0.001 M NaOH on a PL-gel aqueous column. The molecular weights are reported relative to pullulan standards. For the arabinoxylan esters, the operating temperature was 40 °C and the mobile phase was NMP with 1 wt% acetic acid on a PL-gel mixed bed column. The molecular weights are reported relative to polystyrene equivalents.

NMR spectra were collected using a JEOL Model Eclipse+ 600 NMR spectrometer. The sample (10 mg) was dissolved in 0.5 mL of DMSO- d_6 containing TFA- d and added to a 5-mm OD NMR tube. The spectra were collected at 80 °C. Chemical shifts for the proton NMR spectra were referenced to DMSO- d_6 at 2.49 ppm.

Acetic, propionic, and butyric anhydrides were obtained from Eastman Chemical Company. The purity of each anhydride was greater than 99.9%. Methanesulfonic acid (MSA) and trifluoroacetic anhydride (TFAA) were obtained from Aldrich and were used as received.

Isolation of Arabinoxylan

Corn fiber (466.7 g, dry wt.) and distilled water (4000 mL) were added to a 5000 mL 3-necked round-bottomed flask equipped with an overhead stirrer, a condenser, and a thermometer attached to a Therm-O-Watch temperature controller. The pH of the mixture was adjusted to a pH of 8.5 with NaOH. The mixture was heated with stirring to 80 °C and was held at this temperature with stirring for approximately 15 minutes. Amylase (GC 521, 16.7 mL, Genencor, Palo Alto, CA) and protease (Protex 6L, 10.0 mL, Genencor, Palo Alto, CA) were added to the mixture simultaneously. The mixture was stirred for 2.5 hours at 80 °C with no attempt to control pH. The mixture was filtered through a 1 mm pore size Buchner funnel. The retained fiber was washed with eight 2000 mL portions of hot water (45 – 55 °C) followed by a single 2000 mL wash with distilled water. After drying at 60 °C in a vacuum oven, 229.1 g of destarched, proteolyzed corn fiber was obtained.

Destarched, proteolyzed corn fiber (168 g dry weight) and 2.4 L of 0.83 M NaOH were added to a 5 L 3-necked round-bottomed flask equipped with an overhead stirrer, a condenser, and a thermometer attached to a Therm-O-Watch temperature controller. The mixture was stirred for 2 h while maintaining the reaction temperature between 94–99 °C. The heterogeneous reaction mixture was filtered through a 70–100 μm glass frit funnel that was kept in an oven at 63 °C. The solids were washed with 1 L of H₂O followed by a second wash of 1.5 L H₂O. The combined filtrate was concentrated to 600 mL before adding 2.9 L of

acetic acid, which gave a white precipitate. The solids were allowed to settle for 3 h before all but ca. 300 mL of the solution was decanted from the solids. The hemicellulose was then isolated by filtration and washed with EtOH. After drying, 67.4 g of arabinoxylan was obtained as a mixture of hemicellulose A and B.

A solution of corn fiber arabinoxylan containing both insoluble hemicellulose A (2.1 wt% by GPC) and soluble hemicellulose B (97.9 wt%) was prepared by dissolving 30 g of arabinoxylan in 1385 g of H₂O at pH 7. The solution was centrifuged at 3100 X g for 1 h. The solution was decanted from the solids and the solids were washed extensively with H₂O. The liquids were filtered through a 3.5-5.0 μm glass frit funnel before concentrating to a 7.2 wt% solids solution. A portion (56.6 g) of the solution was poured slowly into 350 mL of glacial acetic acid. The resulting slurry was stirred for 30 min then transferred to a 40-50 μm glass frit funnel. The liquids were allowed to drain before adding fresh (350 mL) glacial acetic acid. After removing the liquids, the solids were washed with three 200 mL portions of EtOH before drying at 80 °C under vacuum, which gave 3.4 g (83% recovery) of hemicellulose B as a white solid. Carbohydrate analysis indicated that the arabinoxylan was composed of 47.2 mol% xylose, 33.4 mol% arabinose, 11.6 mol% galactose, 6.6 mol% glucuronic acid, and 1.2 mol% glucose.

The hemicellulose A separated above by centrifugation was extracted in a soxlet extractor with pH 7 H₂O for 7 days. The remaining solids were then dried at 80 °C under vacuum for 48 h. This provided 0.62 g (2.1 wt % based on the weight of starting arabinoxylan) of a tan solid.

General Procedure for Preparation of Arabinoxylan Acetate

To 55.4 g of aqueous arabinoxylan (Hemi B, 7.2 wt% arabinoxylan) was slowly added 350 mL of glacial acetic acid while stirring. The white precipitate that formed was allowed to stand for ca. 45 min before the liquids were decanted. Fresh glacial acetic acid was added (3 X 100 mL), and the solids were allowed to stand in the acetic acid for 5-10 min before decanting the liquids. After the 3rd exchange, the acetic acid wet white solids (51 mL of acetic acid) were transferred to a 100 mL 3-neck round bottom flask equipped for mechanical stirring. To the acetic acid wet arabinoxylan was added 20 mL of acetic anhydride. The flask was immersed in a preheated 50 °C oil bath and the slurry was stirred for 10 min before adding 45 mg of MSA in 1 mL of glacial acetic acid. Within 10 min, all of the solids were dissolved in the reaction media except for a few small particles. One hour after adding the MSA, the homogeneous reaction mixture was filtered through a 10-15 μm glass fritted funnel. The filtrate was then poured into 250 mL of 8 wt% aqueous acetic acid

while stirring vigorously followed by 200 mL of deionized water. The solids were isolated by filtration and washed with deionized water until the filtrate reached a pH of 7. The solids were then dried at 60 °C and 50 mm Hg. This provided 4.71 g of a white solid. Proton NMR revealed that the solid was an arabinoxylan acetate having a degree of substitution of 2.11.

General Procedure for Preparation of Arabinoxylan Propionate or Butyrate

To 57.1 g of aqueous arabinoxylan (Hemi B, 7.2 wt% arabinoxylan) was slowly added 350 mL of glacial acetic acid while stirring. The white precipitate that formed was allowed to stand for ca. 30 min before the liquids were decanted. Fresh glacial acetic acid was added (100 mL), and the solids were allowed to stand in the acetic acid until the solids hardened before decanting the liquids. Butyric acid was then added to the solids (3 X 100 mL) and the solids were allowed to stand in the butyric acid for 5-10 min before decanting. After the 3rd exchange, solids were transferred to a 40-60 μm glass fritted funnel and the solids were washed with butyric acid (10 X 100 mL). Each time the liquids were allowed to slowly drain before applying a vacuum to remove the remaining excess liquids. The butyric acid wet white solids (31 mL of butyric acid) were transferred to a 100 mL 3-neck round bottom flask equipped for mechanical stirring. To the butyric acid wet arabinoxylan was added 31.7 mL of butyric anhydride. The flask was immersed in a preheated 50 °C oil bath and the slurry was stirred for 10 min before adding 47.5 mg of MSA in 5 mL of butyric acid. After 1.5 h, no reaction was evident so the reaction temperature was increased to 60 °C. After 2.7 h total reaction time, an additional 45.9 mg of MSA in 1 mL of butyric acid was added to the reaction. Four hours after beginning the reaction, the solution viscosity was observed to increase significantly. The reaction was allowed to proceed for 14.5 h before the reaction mixture was filtered through a 10-15 μm glass fritted funnel. The filtrate was then added to an equal volume of MeOH. Water (100 mL) was then added slowly to the MeOH containing filtrate, which gave a white sticky solid. The liquids were decanted and the sticky solid was taken up in 80 mL of MeOH and 120 mL of acetone. Water (100 mL) was then added slowly which gave a slightly tacky white solid. This solid was taken up in 125 mL of acetone and poured into 80/20 water/MeOH giving a hard white solid. The solids were washed with 1.5 L of 80/20 water/MeOH before drying at 60 °C and 50 mm Hg. This provided 4.69 g of a white solid. Proton NMR revealed that the solid was an arabinoxylan butyrate having a degree of substitution of 2.01.

Results and Discussion

Recently, we described in detail the process we developed for isolation of the arabinoxylan, from corn fiber (10). Briefly, the process involves first treating the corn fiber with a combination of amylase and protease to remove the starch and protein. Treatment of the destarched, proteolyzed corn fiber with 0.5-1.5 M NaOH at 70-100 °C results in the solubilization of the arabinoxylan, which can be separated, from the cellulose component by filtration. The aqueous arabinoxylan solution is concentrated, preferably by ultrafiltration as this also lowers the salt concentration, before precipitating with acetic acid. The arabinoxylan is isolated by filtration and washed with an alcohol to remove residual water and acetic acid. The arabinoxylan isolated by this process is comprised of two components, hemicellulose A and B. Hemicellulose B, the desirable component, is a high molecular weight polysaccharide (>500,000) soluble in water over the entire pH range. Hemicellulose A is a lower molecular weight polysaccharide (<25,000) that is soluble in water only at a pH greater than ca. 10. The arabinoxylan we isolate typically contains about 2-5 wt% hemicellulose A. However, hemicellulose A can be readily separated from hemicellulose B by taking advantage of the differences in solubility at pH 5-7 (*vide supra*).

Esterification of Corn Fiber Arabinoxylan

Acid catalyzed esterification of corn fiber arabinoxylan potentially offers the most efficient and cost effective means for preparing arabinoxylan esters. Consequentially, we examined the esterification of corn fiber arabinoxylan using H₂SO₄ and MSA as acid catalysts in the esterification of polysaccharides. We also examined TFAA as a “promoter or impeller” in the esterification of corn fiber arabinoxylan (17,18). From our prior experiences, we know MSA can be a very effective catalyst in esterification of polysaccharides and, at moderate temperatures, MSA promotes little molecular weight loss. Although widely used in the esterification of polysaccharides, H₂SO₄ can cause rapid loss of polysaccharide molecular weight. It has been shown that TFAA promoted esterification of cellulose provides very high molecular weight cellulose esters (17). Additionally we have also examined the impact of activation on the esterification of corn fiber arabinoxylan. As noted above, after extraction into a basic aqueous medium, we isolate corn fiber arabinoxylan by precipitation with acetic acid. Relative to dried corn fiber arabinoxylan, our anticipation was that this acetic acid wet arabinoxylan would be more easily esterified.

Figures 1 and 2 provide representative examples of the changes in molecular weight and carbohydrate composition during prolonged MSA and H₂SO₄

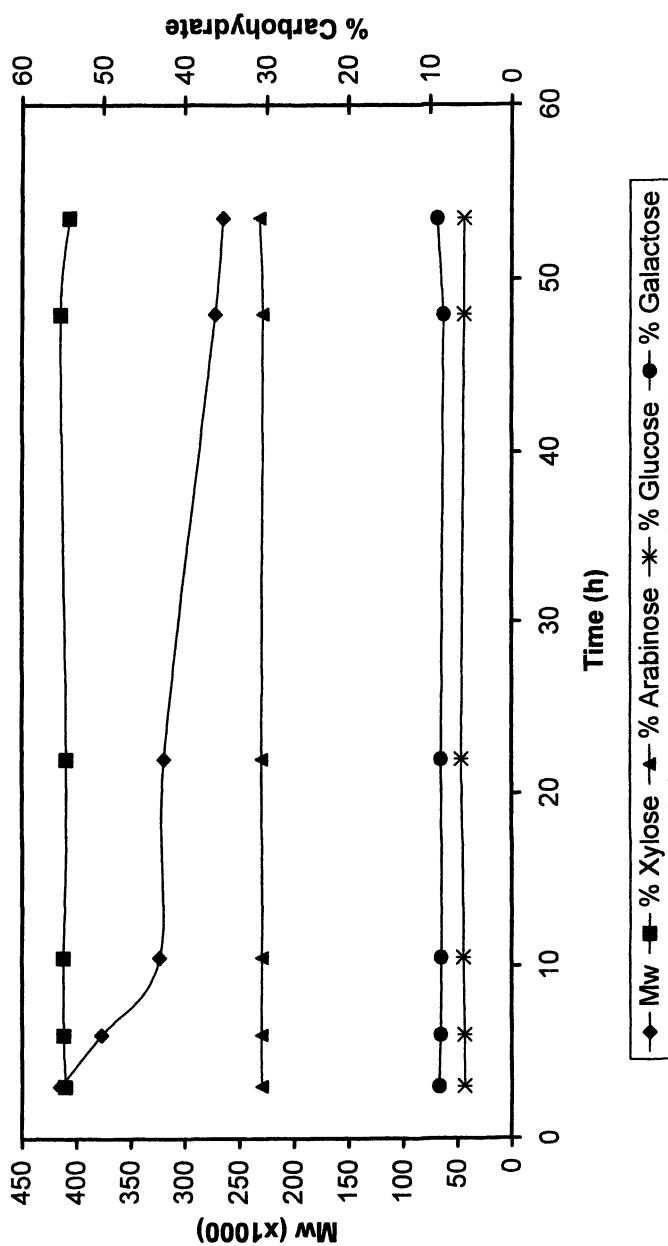


Figure 1. The change in weight-average molecular weight and the carbohydrate composition over an extended time period during acetylation of corn fiber arabinoxylan using 0.65 wt% MSA at 25 °C. Reproduced with permission from reference 19. Copyright 2002 Elsevier Science Ltd.

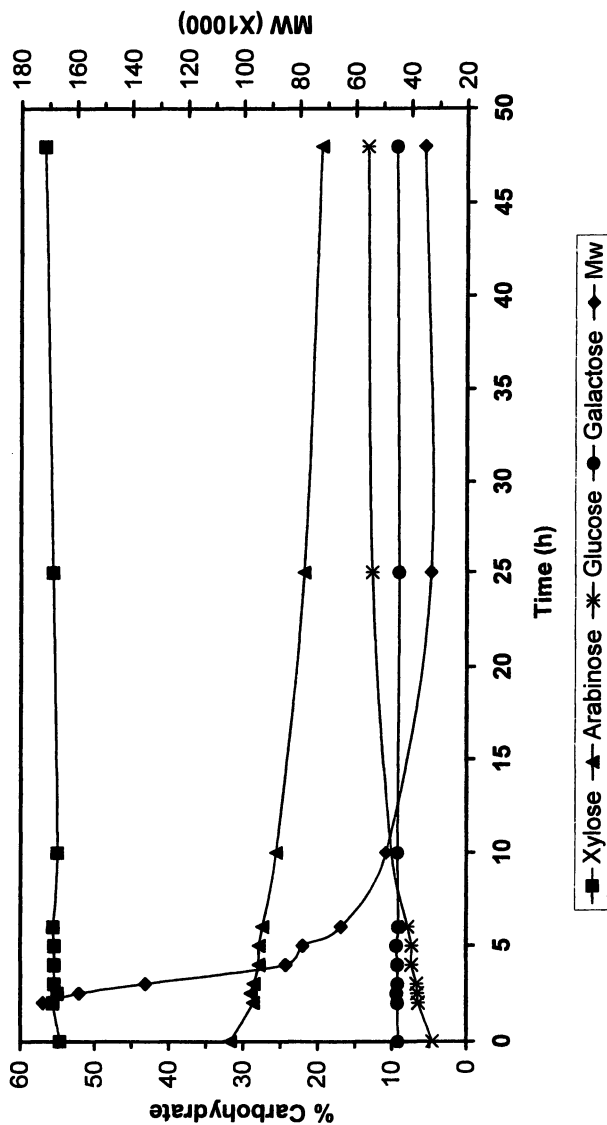


Figure 2. The change in weight-average molecular weight and the carbohydrate composition over an extended time period during acetylation of corn fiber arabinosylan using 0.65 wt% H_2SO_4 at 35 °C. Reproduced with permission from reference 19. Copyright 2002 Elsevier Science Ltd.

catalyzed acetylation of corn fiber arabinoxylan. In both experiments, the first data point was taken at the point at which the arabinoxylan was fully soluble in the reaction medium. The observed changes in molecular weight and carbohydrate composition are due to prolonged exposure to the reaction conditions. In the case of MSA, there was essentially no change in carbohydrate composition after 53.5 h of exposure to the reaction conditions. The molecular weight of the arabinoxylan acetate (AXA) at 3 h was 415,000 and this dropped to 323,000 after 10.5 h. From 10.5 h to 53.5 h, the molecular weight only decreased from 323,000 to 265,000. In contrast, with H_2SO_4 , the molecular weight initially determined at 2 h for the AXA was 172,000. The molecular weight of the AXA in the H_2SO_4 catalyzed reaction declined very rapidly reaching 48,900 after 10 h. Interestingly, even with prolonged exposure to the reaction medium over the range of reaction temperatures and concentrations of H_2SO_4 examined, the molecular weight of the AXA plateaued near 35,000. With regard to the carbohydrate composition of the AXA prepared by H_2SO_4 catalysis, the mol % arabinose was observed to decrease while the percentage of xylose and galactose remained essentially constant. The initial ratio of xylose/arabinose increased from 1.7 to 2.9. This would suggest preferential cleavage of the arabinose from the arabinoxylan.

The data contained in Table I demonstrate the importance of activation and other aspects of the esterification of corn fiber arabinoxylan. Entry 1 illustrates the MSA catalyzed esterification of non-activated, dried corn fiber arabinoxylan. Relative to the reaction of acetic acid activated arabinoxylan with acetic anhydride, which requires only 1 h for complete esterification (entry 6), significant solids (48 wt% of starting material) were present after a reaction time of 4.5 h. After removing the unreacted solids, the AXA was isolated by precipitation. Characterization of the AXA revealed that the molecular weight and the DS were comparable to that obtained from acetic acid activated arabinoxylan (cf. entries 1 and 6). Hence, while the DS and MW were essentially the same, relative to acetic acid activated arabinoxylan, esterification of non-activated arabinoxylan leads to a lower product yield and longer reaction times. In the case of entries 2-5, the arabinoxylan was precipitated with acetic acid, the acetic acid was removed by washing with EtOH, and the arabinoxylan was stored wet in EtOH. Prior to esterification, the EtOH was exchanged for acetic acid. At low concentration of MSA (entries 2, 3), all of the arabinoxylan was not solubilized and the solids had to be removed by filtration prior to precipitation. Furthermore, the DS indicated that the arabinoxylan was not fully esterified and the molecular weight was observed to decrease. At higher concentrations of catalyst (entries 4, 5), the DS indicated that the arabinoxylan was fully esterified but the MW was significantly diminished. With the exception of entry 12, the remaining entries in Table I are for arabinoxylan that was precipitated with acetic acid and used directly in the esterification reaction. Using 1.1 wt% MSA

as the catalyst, an AXA was prepared having a DS of 1.99 and a molecular weight of 485,000 (entry 6).

Table I. Reaction Conditions for Esterification of Arabinoxylan and Product Characterization

Entry	Starting Material (g) ¹	Ester	Catalyst, Promoter	Reaction Temperature (°C)	Reaction Time (h)	Yield (g)	% Metals ² SM /Product	DS (¹ H)	Mw (10 ⁴)
1 ³	B, 1.7	C2	23 mg MSA	50	4.5	1.24	0.05/ND	2.09	58.6
2 ⁴	B, 0.7	C2	4 mg MSA	35(1h), 50(2h)	3.0	0.68	1.6/ND	1.58	43.6
3 ⁴	B, 0.7	C2	9 mg MSA	35(0.5h), 50(3h)	3.5	0.87	1.6/ND	1.76	24.3
4 ⁴	B, 0.7	C2	246 mg MSA	35	3.0	0.86	1.6/ND	2.24	10.4
5 ⁴	B, 0.7	C2	511 mg MSA	35	2.5	0.88	1.6/ND	2.33	12.7
6 ⁵	B, 4.0	C2	45 mg MSA	50	1.0	4.71	0.05/ND	1.99	48.5
7 ⁵	B, 4.0	C3	46 mg MSA	50	3.3	5.58	0.05/ND	2.06	58.8
8 ⁵	B, 4.1	C4	93 mg MSA	60	14.5	4.69	0.05/ND	2.15	42.5
9 ⁵	B, 4.0	C2	12 mL TFAA ⁶	50	1.0	5.70	0.1/0.1	2.10	48.6
10 ⁵	B, 4.0	C2	10 mL TFAA ⁶	50	3.5	5.11	0.05/ND	2.09	29.5
11 ⁵	B, 9.1	C2	12 mL TFAA ⁶	49	1.0	4.80	56.6/0.3 ⁷	2.10	28.1
12 ⁵	A, 4.0	C2	12 mL TFAA ⁶	50	1.0	0.30	ND	-	-
13 ⁵	A+B, 4.0	C2	12 mL TFAA ⁶	54	1.0	2.20	57.8/11.7	2.19	17.3
14 ⁵	A+B, 4.0	C2	12 mL TFAA ⁶	64	1.0	2.20	57.8/15.8	2.22	6.76

1. A = Hemicellulose A, B = Hemicellulose B, A+B = hemicellulose A (ca. 3 wt%) and B. Based on dry weight of arabinoxylan.

2. The metals for entries 2-5, 10-13 were determined by ash analysis. The metals for entries 6-9 were determined by ICP. ND = not determined.

3. No activation.

4. The arabinoxylan was precipitated and stored wet in EtOH. The EtOH was exchanged for acetic acid prior to esterification.

5. The arabinoxylan was water activated.

6. No attempt was made to optimize the amount of TFAA.

7. The product was initially precipitated with water. The precipitate was taken up in acetone and reprecipitated in 10% aqueous acetic acid.

SOURCE: Reproduced with permission from reference 19. Copyright 2002 Elsevier Science Ltd.

After exchanging the acetic acid for propionic acid, an arabinoxylan propionate (AXP) was prepared at the same catalyst loading but a longer reaction time was required (entry 7). In the case of arabinoxylan butyrate (AXB, entry 8), relative to AXA (cf. entry 6), a higher concentration of catalyst, a higher temperature, and longer reaction time was required to achieve a high DS. Most interestingly, the molecular weight of the AXB remained comparable to AXA and AXP (entries 6, 7) despite the more harsh conditions.

When TFAA was used as a promoter for the esterification of corn fiber arabinoxylan instead of catalytic amounts of MSA, acetic acid activated arabinoxylan was successfully acetylated. The AXA was essentially identical to that obtained from MSA catalyzed esterification (cf. entries 6 and 9). With TFAA, when the reaction time was extended from 1 h to 3.5 h, the molecular weight was observed to drop from 486,000 to 295,000 (entry 10). Entry 11 illustrates TFAA promoted acetylation of a corn fiber arabinoxylan having a high salt content. The high salt content of the arabinoxylan is due to the method of isolation (10). Entry 11 demonstrates that it is not necessary to highly purify the arabinoxylan prior to esterification as the salts can be removed from the product during precipitation of the arabinoxylan ester.

As noted earlier, the hemicellulose A component of corn fiber arabinoxylan has very limited solubility in water at a pH less than ca. 10. Entry 12 illustrates that hemicellulose is also quite difficult to esterify. The hemicellulose was allowed to swell in pH 7 water before exchanging the water for acetic acid. Using the same reaction conditions used for esterification of the hemicellulose B component (cf. entries 9 and 12), essentially no esterification was observed. This difficulty in esterifying the hemicellulose A component extends to esterification of mixtures of hemicellulose A and B (entries 13 and 14). Treatment of a mixture of hemicellulose A and B with acetic anhydride in the presence of TFAA resulted in a decreased product yield and an AXA with a much lower molecular weight. Clearly, it is advantageous to separate hemicellulose A and B prior to esterification of corn fiber arabinoxylan.

Characterization of Arabinoxylan Esters

Figure 3 provides a typical ^1H NMR spectrum for an AXA. Due to the severe overlap and broad resonances in the proton and carbon-13 NMR spectra of these arabinoxylan esters, no structural details for the arabinoxylan esters could be obtained by NMR spectroscopy. However, the DS for the arabinoxylan esters could be easily determined from the ^1H NMR spectra according to the equation:

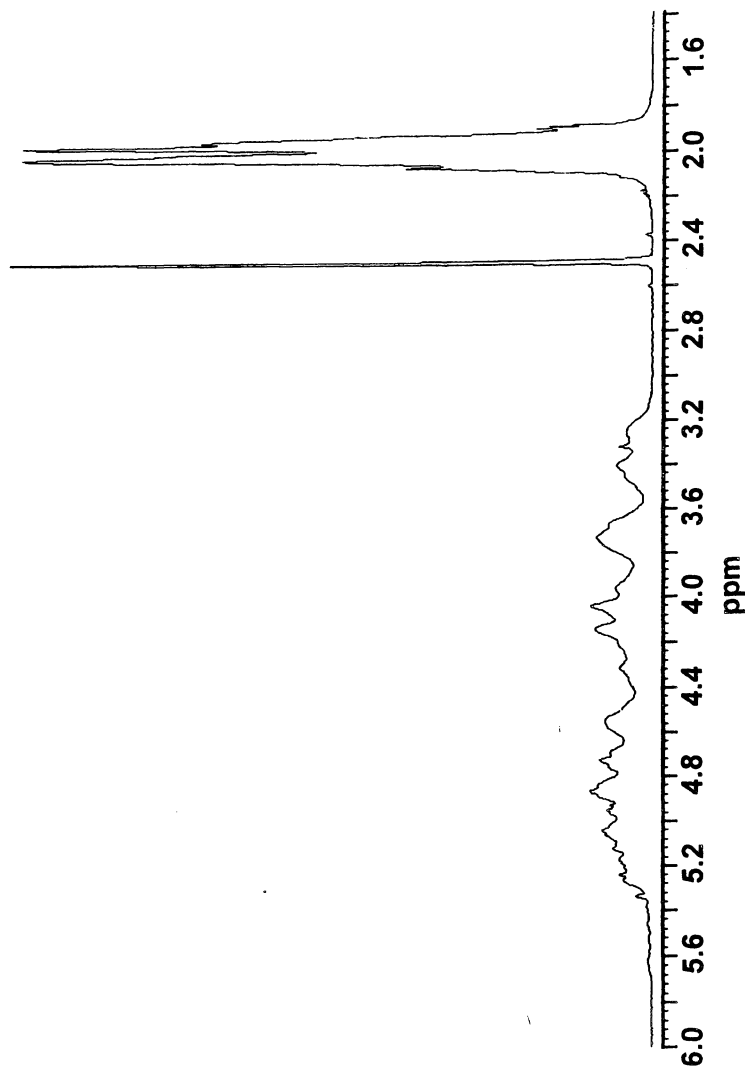


Figure 3. ^1H NMR spectrum (DMSO- d_6 , 80 °C) of an arabinoxylan acetate. Reproduced with permission from reference 19. Copyright 2002 Elsevier Science Ltd.

$DS = (\text{ester methyl proton integral}/3)/(\text{carbohydrate ring proton integral}/6.2).$

The value of 6.2 for the number of carbohydrate ring protons is based on the carbohydrate and linkage analysis of the parent arabinoxylan. Fully substituted arabinoxylan esters with a high molecular weight typically had a DS in the range of 2.0-2.1. In the case of arabinoxylan esters, where the molecular weight was significantly lowered during the esterification, the observed DS tended to be higher.

As the data contained in Table I show, it was possible to obtain arabinoxylan esters with weight-average molecular weights near 500,000. Poor activation and, to a lesser degree, higher reaction temperatures and longer reaction times lead to lower molecular weights. Figure 4 shows typical GPC traces for AXA, AXP, and AXB. Also included is a typical GPC trace for the parent arabinoxylan. As can be seen, the parent arabinoxylan has a relatively uniform molecular weight dispersion ($M_w/M_n = 4-5$) while the polydispersity of the arabinoxylan esters are typically larger ($M_w/M_n = 7-17$). Particularly prominent is a tail toward a higher MW in each GPC trace for the arabinoxylan esters. The abrupt drop in MW, relative to the parent arabinoxylan, for arabinoxylan esters isolated immediately after all of the arabinoxylan has been solubilized in the reaction mixture, the consistency of a molecular weight during prolonged reactions, and the relative insensitivity of molecular weight to substituent type suggest that the observed change in MW in moving from the parent arabinoxylan to arabinoxylan ester is likely due to a change in polymer aggregation rather than being the result of chain cleavage.

We do point out that, due to the differences in solubility of the arabinoxylan and arabinoxylan ester, different standards and columns were used in determining the molecular weight of the arabinoxylan and the arabinoxylan esters. It is possible that the column and standard differences could contribute to the observed differences in the molecular weight of the arabinoxylan and the arabinoxylan ester at the point of the first sampling. However, as we have discussed, the consistent molecular weight of the arabinoxylan esters prepared using MSA over a prolonged reaction time relative to molecular weight of the arabinoxylan esters prepared using H_2SO_4 clearly indicates that MSA is the preferred catalyst for preparing arabinoxylan esters.

Figure 5 provides typical TGA spectra for the parent arabinoxylan, AXA, AXP, and AXB. The onset of degradation for all three of the ester derivatives lies near 225 °C. However, the rate of degradation after onset decreases as the chain length of the substituent increases. For AXA, AXP, and AXB, 10 wt% weight loss was reached at 277, 286, and 309 °C, respectively. Relative to the parent arabinoxylan, the thermal stability of the arabinoxylan esters was increased.

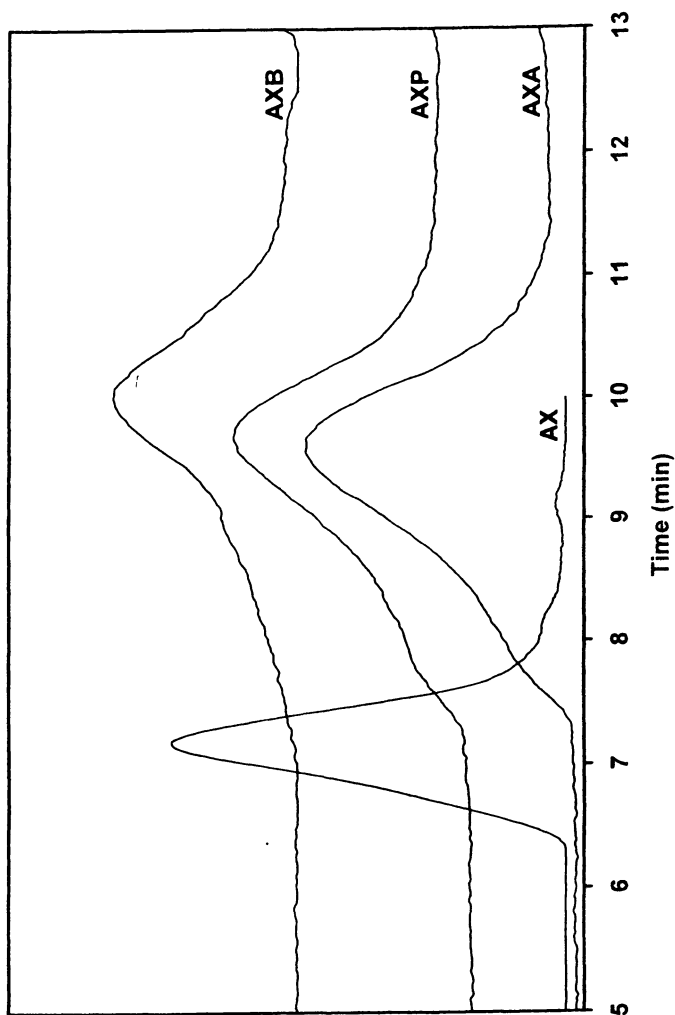


Figure 4. GPC curves for unmodified corn fiber arabinoxylan (AX) and for the acetate (AXA), propionate (AXP), and butyrate (AXB) esters of the arabinoxylan. Reproduced with permission from reference 19. Copyright 2002 Elsevier Science Ltd.

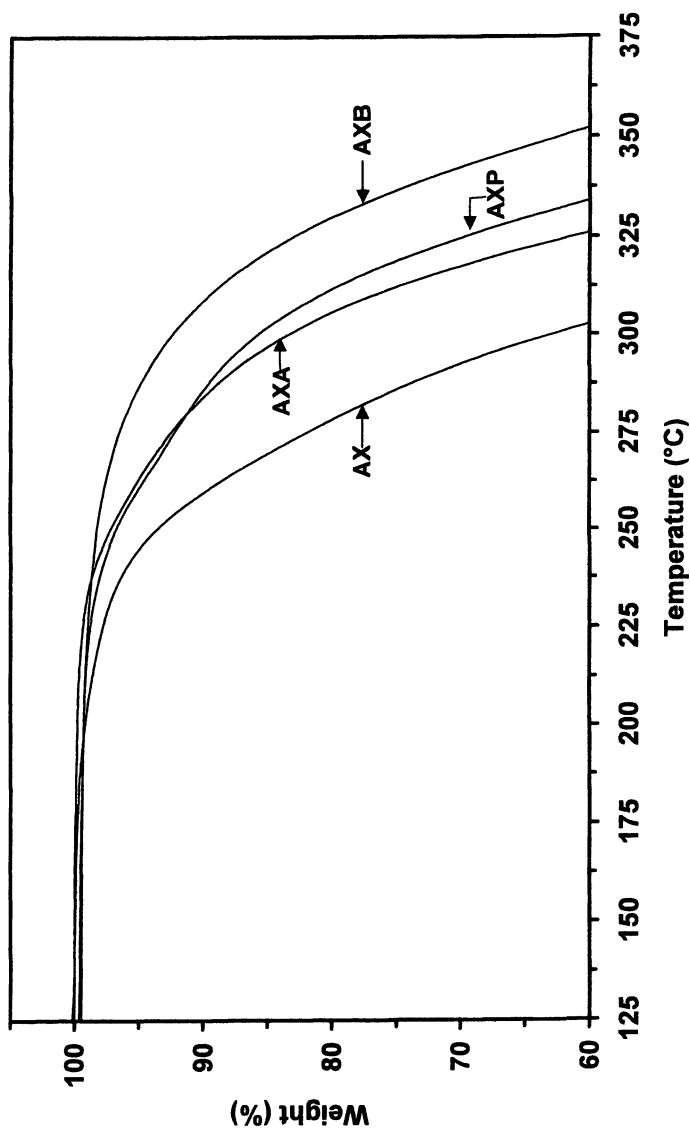


Figure 5. TGA spectra for unmodified corn fiber arabinoxylan (AX) and for the acetate (AXA), propionate (AXP), and butyrate (AXB) esters of the arabinoxylan. To remove the effects of residual moisture, the TGA spectra for AX and AXA were normalized to 100 wt% at 140 °C. Reproduced with permission from reference 19. Copyright 2002 Elsevier Science Ltd.

The DSC spectra provided in Figure 6 illustrates the sensitivity of the T_g of AXA to the thermal history of the sample. When a sample of AXA was heated from 0 to 170 °C at 20 ° min⁻¹, a T_g of 138 °C was observed in the 1st heating curve. After cooling in the instrument to 0 °C, the sample was heated to 220 °C and a T_g of 136 °C was obtained in this 2nd heating curve. The sample was once again cooled, heated to 170 °C, cooled, and heated to 170 °C. A T_g of 115 °C was obtained in both the 3rd and 4th heating scan. It was mildly surprising that even though we remained below the decomposition onset, the T_g of the AXA dropped quite significantly. This data indicates that a reproducible T_g of AXA can only be obtained if the sample is kept under the onset of thermal degradation. It should also be noted that a T_m is not observed for AXA in any of these DSC experiments and there is no change in ΔC_p between the 1st and 2nd heating curves for samples where the 1st scan is stopped at 170 °C. This suggests that AXA is amorphous or that the T_m lies above the decomposition temperature. Characterization of AXP and AXB revealed that they were also sensitive to thermal degradation.

Figures 7 and 8 illustrate the effect of type of substituent and DS on the T_g of these arabinoxylan esters. In the series of parent arabinoxylan, AXA, AXP, and AXB, the respective T_g 's are 198, 138, 97, and 61 °C. In the case of arabinoxylan acetates, as the DS decreased, the observed T_g increased. That is, the T_g of these arabinoxylan esters decreases as the length of the side chain and the total DS increases. The decrease in T_g with increasing DS is likely the result of a decrease in polymer-polymer interactions arising from hydrogen bonding. The decrease in T_g as the length of the side chain increases is likely due to both a decrease in polymer-polymer interactions and to an increase in free volume.

Conclusions

In this account, we have shown that aliphatic C2-C4 esters of corn fiber arabinoxylan can be readily and rapidly prepared using MSA as an acid catalyst. These arabinoxylan esters typically have high molecular weights and are amorphous solids. Thermal characterization of these arabinoxylan esters revealed that the T_g 's of the arabinoxylan esters are rapidly and significantly depressed when the arabinoxylan esters are heated to near the onset of thermal degradation. Additionally, the T_g 's of the arabinoxylan esters are highly dependent on the DS and substituent type. Furthermore, in a separate account (19), we have shown that these arabinoxylan esters can be incorporated into blends with cellulose esters.

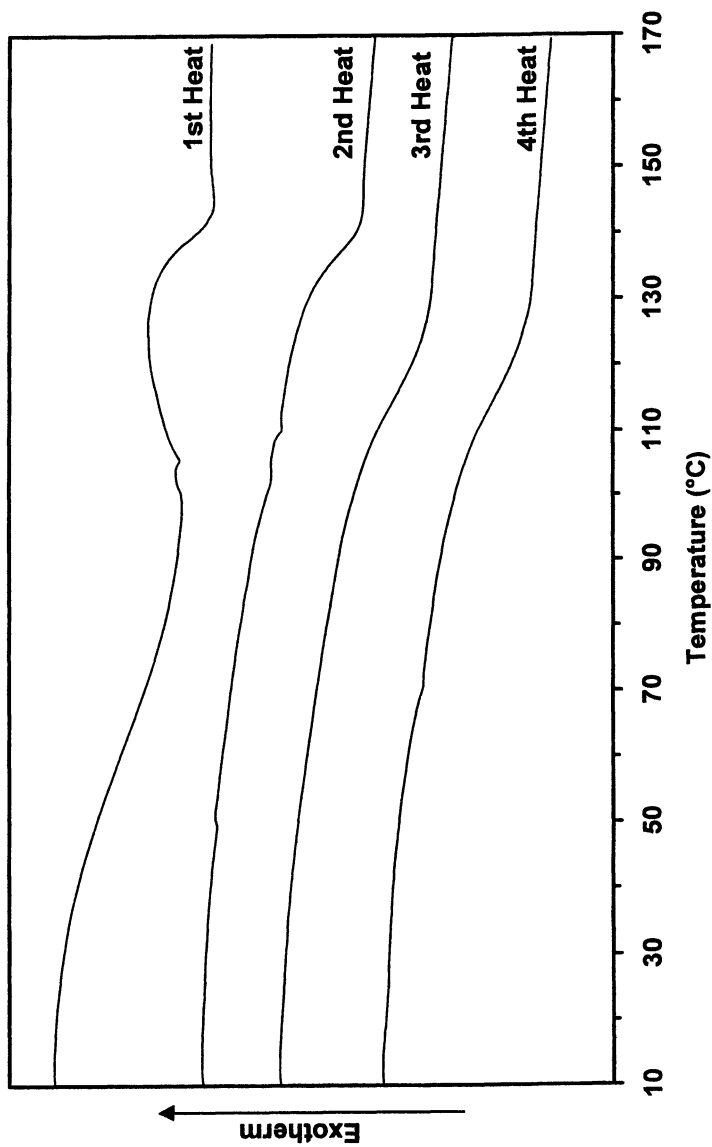


Figure 6. DSC spectra of AXA (1st scan, 0 to 170 °C; 2nd scan, 0 to 220 °C; 3rd scan, 0 to 170 °C; 4th scan, 0 to 170 °C). Reproduced with permission from reference 19. Copyright 2002 Elsevier Science Ltd.

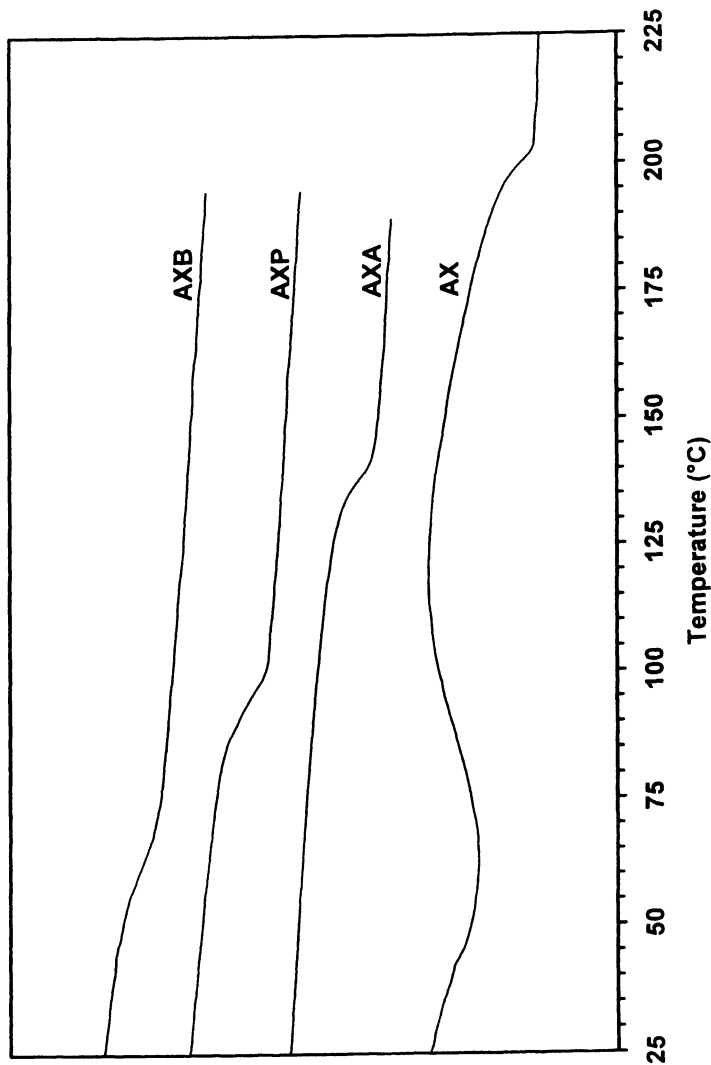


Figure 7. Modulated DSC spectra (1st scan, reversing component) for unmodified corn fiber arabinoxylylan (AX) and for the acetate (AXA), propionate (AXP), and butyrate (AXB) esters of the arabinoxylylan. Reproduced with permission from reference 19. Copyright 2002 Elsevier Science Ltd.

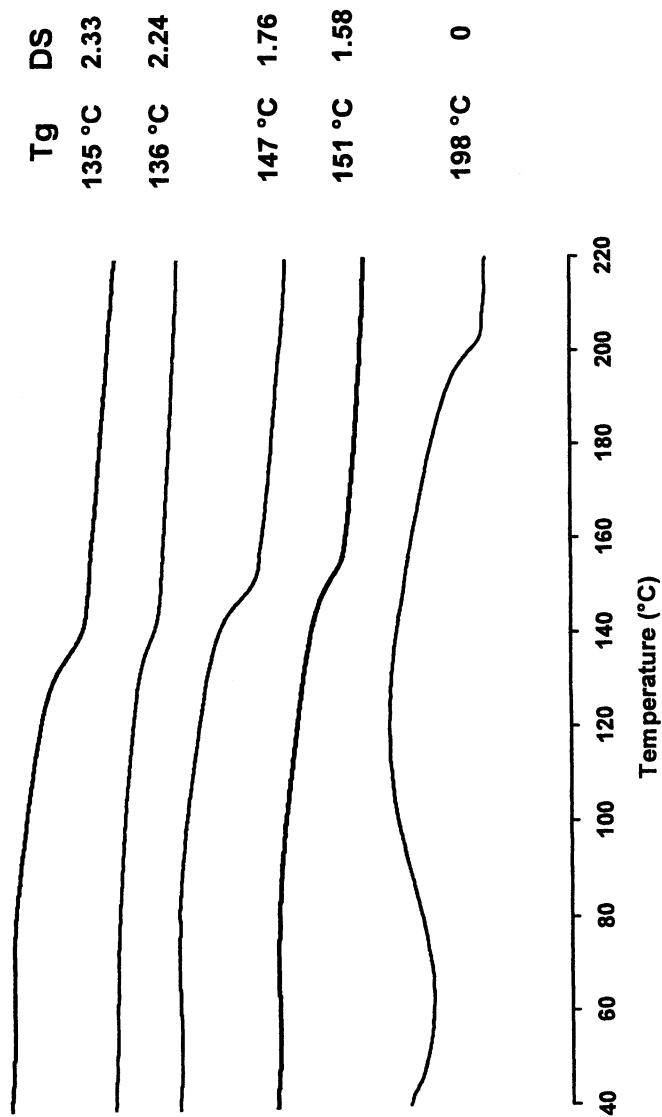


Figure 8. Modulated DSC spectra (1st scan, reversing component) for a series of AXA with different degrees of substitution. Reproduced with permission from reference 19. Copyright 2002 Elsevier Science Ltd.

References

1. Whistler, R. L. *Industrial Gums, Third Edition* Academic Press, New York, 1993, pp. 295-308.
2. Gabriellii, I.; Gatenholm, P.; Glasser, W. G.; Jain, R. K.; Kenne, L. *Carbohydrate Polymers* **2000**, *43*, 367.
3. Ebringerova, A.; Heinze, T. *Macromol. Rapid. Commun.* **2000**, *21*, 542.
4. Glasser, W. G.; Kaar, W. E.; Jain, R. K.; Sealey, J. E. *Cellulose*, **2000**, *7*, 299.
5. Doner, L. W.; Hicks, K. B. *Cereal Chem.* **1997**, *74*, 176.
6. Sugawara, M.; Suzuki, T.; Totsuka, A.; Takeuchi, M.; Ueki, K. *Starch/Stärke* **1994**, *46*, 335.
7. Okamoto, Y.; Kawashima, M.; Hatada, K. *J. Am. Chem. Soc.* **1984**, *106*, 5357.
8. Magerstaedt, M.; Meichsner, C.; Schlingmann, M.; Schrinner, E.; Walch, A.; Wiesner, M.; Winkler, I. DE 3,921,761, 1991.
9. Heikkila, H.; Alen, R.; Kauko, S.; Lindroos, M.; Nurmi, J.; Sarmala, P.; Tylli, M. US Patent 6,262,318, 2001.
10. Buchanan, C. M.; Buchanan, N. L.; Debenham, J. S.; Shelton, M. C.; Wood, M. D.; Visneski, M. J.; Arumugam, B. K.; Sanders, J. K.; Lingerfelt, L. R.; Blair, L. US Patent 6,352,845, 2002.
11. Jain, R. K.; Sjostede, M.; Glasser, W. G. *Cellulose*, **2001**, *7*, 319.
12. Fang, J. M.; Fowler, P.; Tomkinson, J.; Hill, C. A. S. *Carbohydrate Polymers*, **2002**, *47*, 285.
13. Carson, J. F.; Maclay, W. D. *J. Am. Chem. Soc.* **1946**, *68*, 1015.
14. Carson, J. F.; Maclay, W. D. *J. Am. Chem. Soc.* **1948**, *70*, 293.
15. Renard, C. M. G. C.; Jarvis, M. C. *Carbohydrate Polymers*, **1999**, *39*, 201.
16. Fang, J. M.; Sun, R. C.; Tomkinson, J.; Fowler, P. *Carbohydrate Polymers*, **2000**, *41*, 379.
17. Buchanan, C. M.; Parker, S. W. WO 9114709, 1991.
18. Morooka, T.; Norimoto, M.; Yamada, T.; Shiraishi, N. *J. Appl. Polym. Sci.* **1984**, *29*, 3981.
19. Buchanan, C. M.; Buchanan, N. L.; Debenham, J. S.; Gatenholm, P.; Jacobsson, M.; Shelton, M. C.; Waterson, T. L.; Wood, M. D. *Carbohydrate Polymers*, **2003**, *52*, 345.

Chapter 22

New Hemicellulose-Based Hydrogels

Margaretha Söderqvist Lindblad, Ann-Christine Albertsson,
and Elisabetta Ranucci

Department of Fibre- and Polymer Technology, Royal Institute of Technology,
SE-100 44 Stockholm, Sweden (email: aila@polymer.kth.se)

Different kinds of hemicellulose-based hydrogels have been made by radical polymerization using hydrosoluble hemicellulose from spruce chips with a number-average molecular weight and polydispersity of 2400 and 1.5 respectively. 80% of the hemicellulose was galactoglucomannan and the remainder mainly 4-*O*-methylglucuronoxylan. Hemicellulose/poly(2-hydroxyethyl methacrylate) based hydrogels were prepared by polymerization in water of 2-hydroxyethyl methacrylate with hemicellulose modified with well-defined amounts of methacrylic functions. The chemical modification of hemicellulose was performed in dimethyl sulfoxide using 2-[(1-imidazolyl) formyloxy]ethyl methacrylate as modifying agent. The kinetics of the modification reaction were monitored by ¹H NMR. The degree of modification of the hemicellulose used for the hydrogel synthesis varied from 10% to 40%. The ratio of modified hemicellulose to 2-hydroxyethyl methacrylate in the hydrogels was 1:1 by weight. The resulting hydrogels were elastic, homogeneous, soft, transparent and easily swollen in water.

Introduction

The industrial exploitation of products from renewable sources and the design of new bioactive and biocompatible polymers capable of exerting a temporary therapeutic function are two diverse research areas currently considered to be strategic by the international scientific community. In the field of biocompatible polymers, poly(2-hydroxyethyl methacrylate) (PHEMA) and polysaccharides are among the most popular and widely investigated.

We have previously reported the design of mixed hydrophilic/hydrophobic hydrogels containing PHEMA and polysaccharide segments, in which the polysaccharide structure is a hydrosoluble hemicellulose with a comparatively low molecular weight obtained from spruce chips by a steam explosion technique and fractionated by size exclusion chromatography (SEC) (1). In this paper we summarize earlier work and add some new results concerning controllability.

According to the classical definition, hemicelluloses are heterogeneous cell wall polysaccharides, which are normally extractable by a relatively concentrated aqueous alkaline solution. Hemicelluloses constitute 20-30% of the total bulk of annual and perennial plants and are consequently among the most abundant native polymers in the world. The hydrosoluble hemicellulose we are using occurs also in waste streams in the forest industry and can thus be obtained as a by-product from pulp and paper production. An additional benefit of using hemicelluloses is their biodegradability.

Hydrogels are three-dimensional networks of polymers in which large amounts of water are present. The most characteristic property of hydrogels is that they swell in the presence of water and shrink if the water is removed. The extent of swelling is determined by the nature – hydrophilicity - of the polymer chains and the crosslinking density. For a long time, both PHEMA (2) and polysaccharides (3) have been proposed as suitable materials for use as matrices for hydrogel preparation and, particularly, for use in key applications such as drug release systems and tissue engineering. Hemicelluloses obtained from birch (constitutes mainly of xylan with glucuronic acid functionalities) have also been used in hydrogel synthesis by direct reaction with chitosan under acid conditions (4).

Our approach is first to modify soluble hemicellulose to a low extent with methacrylation carried out in dimethyl sulfoxide (DMSO) to increase the reactivity of the hemicellulose. Then we polymerize the modified hemicellulose with 2-hydroxyethyl methacrylate (HEMA) in water under mild conditions. The basic idea is to demonstrate the feasibility of exploiting renewable resources to

build up new polymeric materials amenable to production and to processing by conventional techniques and applicable as specialty polymers, e.g. as biomaterials.

For the methacrylation of polysaccharides, several examples of dextran modification have been reported, for instance using maleic anhydride (5), methacryloyl chloride (6) or glycidyl methacrylate (7) as modifiers. Here we report the use of 2-[(1-imidazolyl) formyloxy]ethyl methacrylate (HEMA-Im) as an efficient and more convenient agent for the methacrylation of polysaccharides (8).

Hemicellulose preparation

Fractionation of spruce chips

The hemicellulose fraction used for hydrogel synthesis was produced according to a procedure developed at Lunds Institute of Technology in Sweden, (Figure 1) (9).

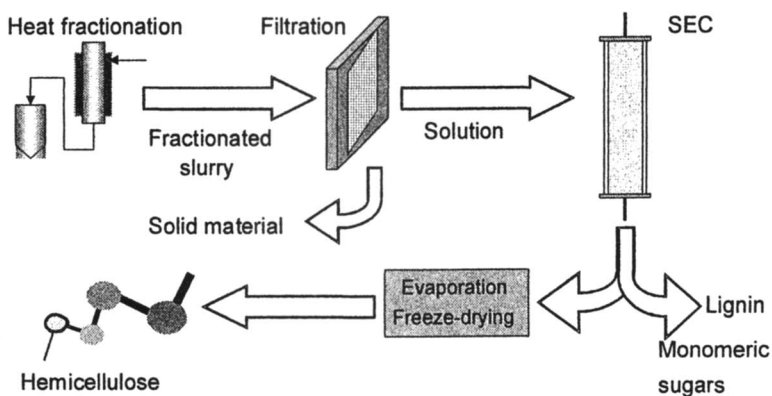


Figure 1. Fractionation of spruce for the production of hemicellulose for hydrogel synthesis. (Thanks to Magnus Palm, LTH for the outline.)

Heat fractionation by steam treatment of the spruce chips was carried out at 190 – 200°C for 2-5 min. The raw product was first filtered to eliminate solid material together with precipitated lignin and then fractionated, using water as eluent, by preparative SEC (Index 50 column filled with Superdex 30 preparative grade, Amersham Pharmacia Biotech, flow rate 12 ml/min, height of filtration bed 29 cm and diameter 10 cm). The hemicellulose fraction was collected and after evaporation it was recovered by freeze-drying as a white and fluffy solid, which was completely soluble in water. The yield of the whole procedure was approximately 50% with respect to the total amount of hemicelluloses in spruce.

Characterization of the hemicellulose fraction

The main hemicellulose component in spruce wood is galactoglucomannan (Figure 2) and it was also the main component in the hemicellulose fraction used here. The carbohydrate composition, according to enzymatic hydrolysis and subsequent capillary zone electrophoresis (10), was 80% galactoglucomannan (galactose/glucose/mannose: 16:28:100) and 20% other polysaccharides (mainly 4-*O*-methylglucuronoxylan). In native spruce the ratio between galactoglucomannan and 4-*O*-methylglucuronoxylan is about 2:1 (11). This means that our hemicellulose contains somewhat more galactoglucomannan than the native one do. The sugar composition is in accordance with the sugar composition in native galactoglucomannan (12). The approximate degree of acetylation of the galactoglucomannan was 0.3, determined by ¹H NMR (13). This means that our hemicellulose had about the same degree of acetylation as native galactoglucomannan in spruce. The number-average molecular weight and the polydispersity of the galactoglucomannan were 2400 and 1.5, as determined by analytical SEC, calibrated with specially fractionated galactoglucomannan characterized by MALDI-TOF spectrometry (14). The hemicellulose fraction also contained traces of aromatic compounds, shown by ¹H NMR spectra. All analytical data are average values from two heat fractionation batches.

The solubility in water of the hemicellulose fraction was 500 mg/ml and it was also soluble in organic solvents such as DMSO (>20 mg/ml) and *N,N*-dimethylformamide (>20 mg/ml). The good solubility properties are probably due to the retained acetyl groups since side groups prevent polysaccharides from aggregating with each other (15).

Modification of hemicellulose

Methacrylation

The hemicellulose was modified by reaction with HEMA-Im in DMSO at 45°C with triethylamine as catalyst. HEMA-Im was prepared by the reaction of HEMA with 1,1'-carbonyldiimidazole in chloroform. The synthetic pathway for the methacrylation is outlined in Scheme 1.

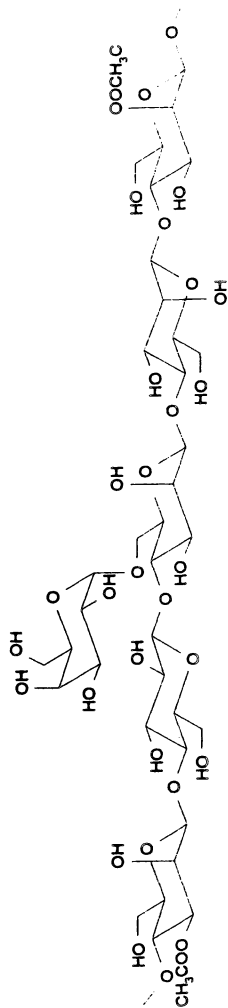
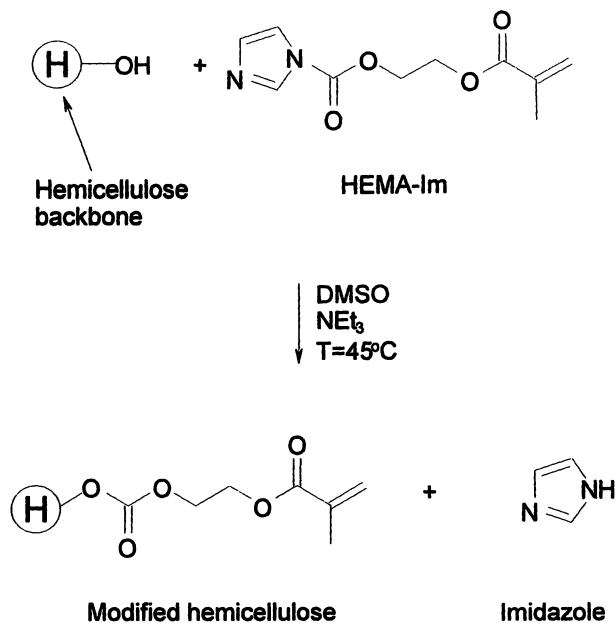


Figure 2: Galactoglucomannan.



Scheme 1

The advantages of this procedure are its facility, superior stability and relative insensitivity at room temperature to traces of moisture. HEMA-Im is also compatible with most solvents and the reaction gives imidazole, which is neither harmful nor chemically aggressive towards hemicelluloses.

Kinetic experiments

In order to determine the exact reaction times necessary to reach specific degrees of substitution, kinetic experiments were carried out, on an 11 mg scale in an NMR tube under controlled temperature conditions. ^1H NMR spectra were recorded at 500 MHz on a Bruker DMX 500 using Bruker software. The samples were dissolved in deuterated DMSO in sample tubes 5 mm in diameter. Non-deuterated DMSO ($\delta=2.50$) was used as an internal standard. Figure 3 and 4

shows the ^1H NMR spectra of a typical reactive mixture composed of 0.08 M hemicellulose (with respect to the repeating unit), 0.1 M HEMA-Im and 0.02 M triethylamine, after 0 h (Figure 3) and after 23 h (Figure 4). Assignments, with references to the structures, are for clarity reported in Scheme 2.

Figure 3 shows the diagnostic peaks of HEMA-Im when practically only the reactive reagents are present. The range of resonances of the hemicellulose protons is also visible, as well as peaks from triethylamine and DMSO. Figure 4 shows in addition the diagnostic peaks of imdazole (peaks k and l), which is the by-product of the condensation reaction between HEMA-Im and hemicellulose.

Conversion of HEMA-Im was evaluated by following the decrease in the imidazolyl peak at 8.25 ppm (peak a, -H) with respect to the peak at 1.86 ppm (peak h, $-\text{CH}_3$), as internal standard. This gives the equation for conversion of HEMA-Im: $1 - I_a / (I_h/3)$.

The results of the kinetic experiments performed in duplicate are reported in Figure 5.

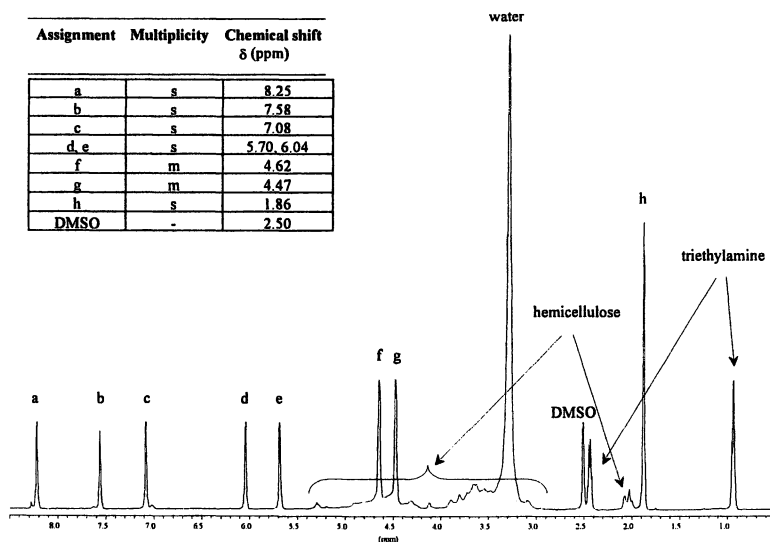


Figure 3. ^1H NMR spectrum (45°C , 500 MHz, $\text{DMSO}-d_6$) of reactive mixture composed of hemicellulose (0.08 M with respect to the repeating unit), Hema-Im (0.1 M) and triethylamine (0.02 M) after 0 h. (Reproduced from reference 1, with permission from WILEY-VCH.)

Assignment	Multiplicity	Chemical shift δ (ppm)
a	s	8.25
b	s	7.58
c	s	7.08
d, e	s	5.70, 6.04
f	m	4.62
g	m	4.47
h	s	1.86
i	s	12.13
k	s	7.65
l	s	7.02
m	s	4.32
DMSO	-	2.50

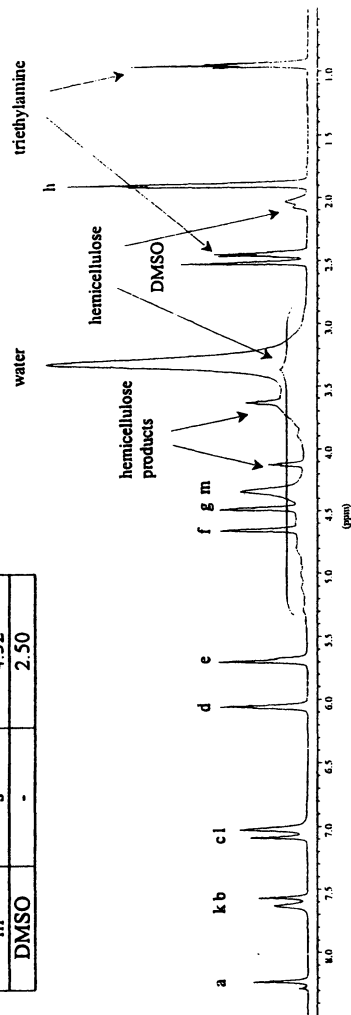
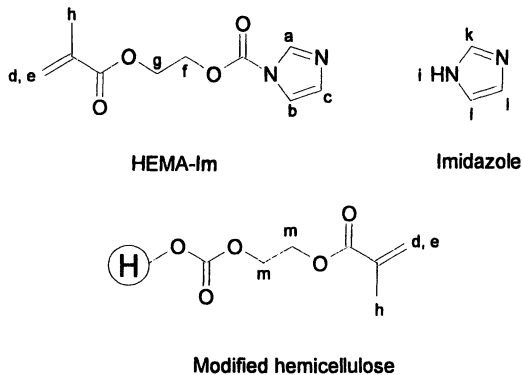


Figure 4. ^1H NMR spectrum (45°C , 500 MHz, $\text{DMSO}-d_6$) of reactive mixture composed of hemicellulose (0.08 M with respect to the repeating unit), Hema-Im (0.1 M) and triethylamine (0.02 M) after 23 h. (Reproduced from reference 1, with permission from WILEY-VCH.)



Scheme 2

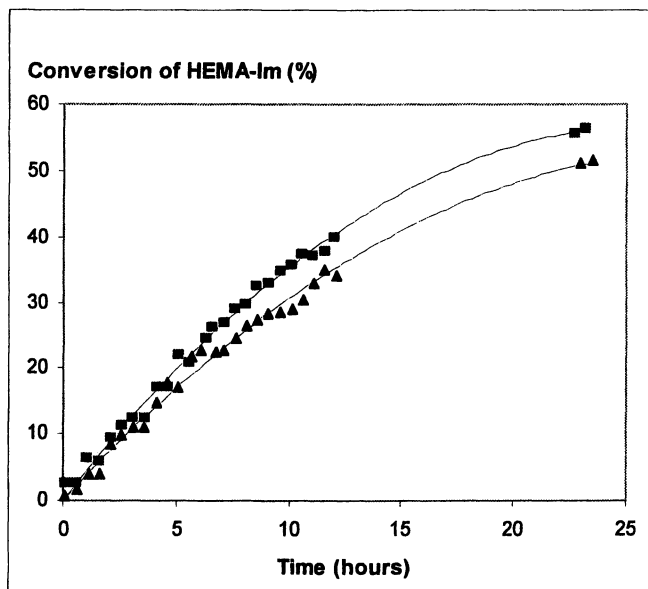


Figure 5. Conversion versus time for the reaction between hemicellulose (0.08 M with respect to the repeating unit) and HEMA-Im (0.1 M) carried out in DMSO at 45°C; ▲, ■: duplicate series; catalyst: triethylamine (0.02 M). (Reproduced from reference 1, with permission from WILEY-VCH.)

The methacrylation reaction reached a conversion value of approximately 55% after 23 h. Adequate values for hydrogel synthesis (ca. 10–30% conversion) were reached after 3–7 hours. These results also indicate that the reproducibility and controllability of the condensation reaction are rather good.

Up-scaled runs of the methacrylation reaction confirmed the preliminary results. The time needed to reach a certain conversion of HEMA-Im was shorter, probably due to stirring that could be used when the reaction was carried out on a larger scale (1.4 g hemicellulose). To reach 10–30% conversion of HEMA-Im, ca. 1–5 hours were needed on this larger scale.

The up-scaled procedure also allowed a purification procedure to be established. Purification involved precipitating the reactive mixture twice in ethyl acetate to eliminate unreacted low-molecular weight reagents, and continuous extraction with diethyl ether in a Soxhlet apparatus to remove residual ethyl acetate and DMSO.

Hydrogel preparation

Synthesis

Hydrogel was synthesized by first preparing the reactive aqueous solution by mixing modified hemicellulose with HEMA in water in the desired amounts. A weight ratio of hemicellulose/HEMA/water equal to 1:1:2 was used (Scheme 3). Initially hemicellulose with a degree of modification of ca. 16% was used. The degree of modification was given by multiplying the conversion of HEMA-Im by the concentration of hemicellulose and dividing by the concentration of HEMA-Im. The degree of modification implies consequently that, on average, slightly more than two sugar monomers in each hemicellulose polymer chain have a methacrylic function. The redox initiator, a mixture of ammonium peroxodisulfate and sodium pyrosulfite, was finally added at 0.8 wt.-% with respect to the two reagents. The solution was then injected into a 1 mm thick mold and reacted at 40°C for 30 min. An elastic, soft and transparent hydrogel was obtained which was easily swollen in water at room temperature. The hydrogel seemed to be homogenous.

Controllability

To study the controllability and reaction rate of the hydrogel synthesis, hydrogels with different initiator concentrations were prepared. We started with

abilities. Several modified hemicelluloses with modification degrees between 10% and 40% were used. All degrees of modification gave soft, transparent and elastic hydrogels. It is accordingly possible to prepare hydrogels from hemicellulose with widely different degrees of modification. This project will continue with studying effects on viscoelasticity, diffusion etc depending on different cross-linking densities.

Conclusions

This work demonstrates the feasibility of using material derived from renewable sources to build up new polymeric structures having potential applications as specialty polymers. The results demonstrate that soluble hemicellulose, with a low molecular weight prepared by steam explosion from spruce chips, are easily purified and efficiently modified by a methacrylation reaction in DMSO. The degree of modification is easy to control. Hemicelluloses, modified to different extents, can lead to a variety of different reactive modified hemicelluloses capable of participating in radical polymerization reactions for the preparation of hydrogels. The rate of the radical polymerization can be controlled by varying the initiator concentration. All the hydrogels were elastic, soft and easily swollen in water. They were also transparent and seemed to be homogeneous.

These results are encouraging and represent the basis for future investigations on the physical, chemical and biological properties of these and related compounds.

Acknowledgement

Financial support from VINNOVA (PROFYT program) is gratefully acknowledged. We wish to thank Guido Zacchi and Magnus Palm, LTH, for performing the steam explosion treatments and for help with SEC separations. Olof Dahlman, Anna Jacobs and Anita Teleman, STFI, are gratefully thanked for the characterization of the hemicellulose fraction with capillary zone electrophoresis, SEC/MALDI-TOF mass spectrometry and ^1H NMR spectroscopy. We also thank Ulla Jacobsson, KTH, for help with the Bruker DMX 500 instrument.

References

1. Söderqvist Lindblad, M.; Ranucci, E.; Albertsson, A.-C. *Macromol. Rapid Commun.* **2001**, *22*, 962.
2. Davies, P. A.; Huang, S. J.; Nicolais, L.; Ambrosio, L. In *High Performance Biomaterials*; Szycher, M., Ed.; Technomic: Basel, **1991**; pp 343-367.

3. Chen, J.; Jo, S.; Park, K. *Carbohydr. Polym.* **1995**, *28*, 69.
4. Gabrielli, I.; Gatenholm, P. *J. Appl. Polym. Sci.* **1998**, *69*, 1661.
5. Kim, S.-H.; Won, C.-Y.; Chu, C. C. *J. Biomed. Mater. Res.* **1999**, *46*, 160.
6. Kim, I.-S.; Jeong, Y.-I.; Kim, S.-H. *Int. J. Pharm.* **2000**, *205*, 109.
7. Hennink, W. E.; Talsma H.; Borchert, J. C. H.; De Smedt, S. C.; Demeester, J. *J. Control. Release* **1996**, *39*, 47.
8. Ranucci, E.; Spagnoli, G.; Ferruti, P. *Macromol. Rapid Commun.* **1999**, *20*, 1.
9. Junel, L. Licentiate Thesis, Lunds Institute of Technology, Lund, **1999**.
10. Dahlman, O.; Jacobs, A.; Liljenberg, A.; Olsson, A. I. *J. Chromatogr., A* **2000**, *891*, 157.
11. Sjöström, E. *Wood Chemistry – Fundamentals and applications*, 2nd ed., Academic Press: London, **1993**, p 249.
12. Sjöström, E. *Wood Chemistry – Fundamentals and applications*, 2nd ed., Academic Press: London, **1993**, p 63.
13. Lundqvist, J.; Teleman, A.; Junel, L.; Zacchi, G.; Dahlman, O.; Tjerneld, F.; Stålbrand, H. *Carbohydr. Polym.* **2002**, *48*, 29.
14. Jacobs, A.; Dahlman, O. *Biomacromolecules* **2001**, *2*, 894.
15. Dea, I. C. M.; Clark, A. H.; McCleary, B. V. *Carbohydr. Res.* **1986**, *147*, 275.

Chapter 23

Production of Oxidized Guar Galactomannan and Its Applications in the Paper Industry

Sybe Hartmans^{1,2}, Hielke T. de Vries^{1,3}, Peter Beijer¹, Richard L. Brady^{1,4},
Michaela Hofbauer^{1,5}, and Alfred J. Haandrikman¹

¹Hercules European Research Center, Barneveld, The Netherlands

²Current address: DSM Food Specialties, Delft, The Netherlands

³Current address: Noviant, Nijmegen, The Netherlands

⁴Current address: Hercules Research Center, 1313 Market Street, Wilmington, DE 19894

⁵Current address: Eastman Chemicals, Middelburg, The Netherlands

Guar is a readily available galactomannan that can be selectively oxidized using the enzyme galactose oxidase. Application of oxidized guar as a wet-end additive in papermaking results in improved strength properties due to acetal and hemi-acetal bonding of the aldehyde groups in oxidized guar with cellulose. Until recently the availability and price of galactose oxidase prevented the development of an economically viable process for the production of oxidized guar. This chapter focuses on galactose oxidase production, the multi-enzyme approach used to produce oxidized guar and examples of potential applications in the paper industry.

Guar gum

Guar gum (also called guaran) is a galactomannan extracted from the seed of the leguminous shrub *Cyamopsis tetragonoloba*, where it plays a role as water store and reserve material. *Cyamopsis tetragonoloba* is mainly cultivated in India and Pakistan and is extremely drought resistant.

Guar gum consists of a (1→4)-linked β -D-mannopyranose backbone with α -D-galactosyl residues attached on the O-6 position of about 65% of the mannose residues (Figure 1). There has been some debate about the substitution pattern of the galactosyl side groups in guar gum (i.e. random versus block wise) in the past. Using an approach initially devised by McCleary which exploits the specificity of a purified endo- β -mannanase from *Aspergillus niger*, Daas *et al.* (1) have convincingly shown that the substitution pattern of the galactosyl groups in guar gum is block wise.

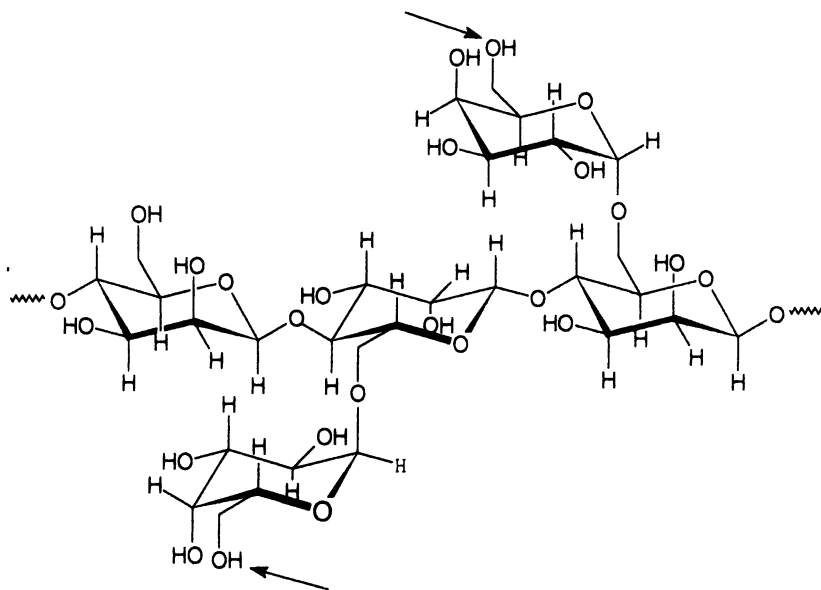


Figure 1. Segment of a guar molecule. The C-6 hydroxyl groups of the galactosyl side-chains that can be oxidized by galactose oxidase are marked with an arrow.

Functionality

Guar gum is an economical thickener and stabilizer. It hydrates fairly rapidly in cold water to give highly viscous pseudoplastic solutions of generally greater low-shear viscosity when compared with other hydrocolloids and much greater than that of locust bean gum. Locust bean gum, a galactomannan with a lower galactose content than guar gum, is less soluble and has a lower viscosity than guar gum as it has fewer galactose branch points. Locust bean gum differs from guar gum in that it forms thermally irreversible weak gels by association of the galactose deficient regions. These unsubstituted areas also allow interaction with cellulose and xanthan with which it shows viscosity synergy (2).

Enzymatic modification of galactomannans

Several enzymes can be used to modify galactomannans resulting in altered physical properties. Mannanases can be used to cleave the backbone resulting in a reduced average molecular weight and altered viscosifying properties.

A more interesting enzymatic modification, from an economical point of view, is treatment of guar gum with α -galactosidase. Enzymatic removal of part of the galactose side-groups results in stretches of unsubstituted polymannose backbone. In this way a polysaccharide is obtained which is similar to locust bean gum, which currently is 15-times more expensive than guar gum.

The third enzymatic activity that can be used to modify galactomannans is galactose oxidase to generate oxidized galactomannans.

Oxidized guar

Treatment of guar with galactose oxidase results in so-called oxidized guar in which some or most of the C-6 hydroxyl groups of the galactosyl side-chains (Figure 1) have been oxidized to aldehyde functionalities. Oxidized guar can be used as an additive in papermaking to improve strength properties due to acetal and hemi-acetal bonding of the aldehyde groups of oxidized guar with cellulose.

The product of the oxidation of aqueous solutions of guar gum and other galactose bearing polysaccharides using galactose oxidase was first patented by F. J. Germino in 1967 (3). Germino described the use of the oxidized products of polysaccharides in the manufacture of paper or tobacco sheets. Germino only used galactose oxidase, and consequently he observed only a relatively low degree of oxidation with a maximum of 4.6% carbonyl groups after incubating guar with galactose oxidase for 24 hours. The limited degree of oxidation is

probably due to inactivation of galactose oxidase due to hydrogen peroxide accumulation as a result of the galactose oxidase activity.

In 1987 Chiu of National Starch and Chemical Corporation described the production of aldehyde-containing heteropolysaccharides by treating galactoglycoside starch ethers with galactose oxidase (4). To increase the operational stability of the galactose oxidase Chiu added catalase to remove the hydrogen peroxide that is produced as a result of galactose oxidase activity. In a patent published in 1996 on the preparation of aldehyde cationic polysaccharides Chiu *et al.* describe an example of guar oxidation where an aldehyde level of 13.5% was obtained (5).

Analysis of oxidation levels in oxidized guar

Several methods have been used to determine the degree of oxidation of guar treated with galactose oxidase. In the earlier studies (e.g. Chiu) the carbonyl content of oxidized guar was determined with iodometric titration. Other methods that have been used are based on determination of the galactose/mannose ratio after chemical hydrolysis of the oxidized guar. The oxidized galactose groups do not survive the hydrolysis conditions so that the galactose content after hydrolysis is a reflection of the galactose groups that were not oxidized.

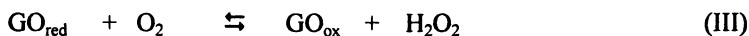
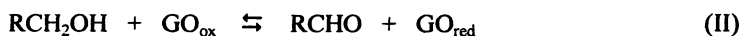
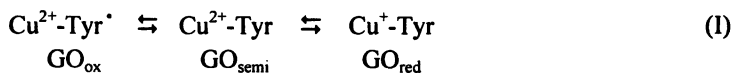
In a more elegant method that we now use routinely, the oxidized guar is reduced with sodium borodeuteride before hydrolysis. After hydrolysis and a second reduction with sodium borodeuteride and acetylation, the acetylated alditols are analyzed with GC-MS. Galactitols with 2 deuterium atoms are derived from oxidized galactose groups, whereas non-oxidized galactose groups contain one deuterium atom after this treatment. The percentage of galactitols with 2 deuterium atoms compared to the total galactitol is defined as the degree of oxidation. Guar that is completely oxidized (100% galactitols with 2 deuterium atoms, or no galactose present after hydrolysis of non-reduced oxidized guar) will have a carbonyl content that equals the galactose content of guar of about 40% (7).

An alternative method allowing on-line monitoring of the oxidation reaction involves the measurement of oxygen consumption. For short reaction times this can be done by monitoring the change in the dissolved oxygen concentration in the reaction mixture with an oxygen electrode. Reactions involving the consumption of more oxygen can be monitored in closed bottles fitted with an OxiTop® (a registered trademark of Wissenschaftlich-Technische Werkstätten GmbH) measuring head with a piezoelectric pressure sensor to monitor the pressure drop due to oxygen consumption. In this manner we could monitor the reaction kinetics of guar oxidation on-line during a period of several

hours or days. The calculated degree of oxidation of samples taken at the end of OxiTop® experiments correlated well with the degree of oxidation determined with the GC-MS method.

Galactose oxidase

Galactose oxidase (GO) is a mononuclear radical-coupled copper enzyme which catalyzes the oxidation of primary alcohols using molecular oxygen, producing aldehydes and H₂O₂. Galactose oxidase can be present in three oxidative states (6,7): The active oxidized form with a tyrosine radical in the active site, the reduced form which results from the two electron redox reaction by which a primary alcohol is converted to an aldehyde (Cu, tyrosine), and an intermediate semi-form containing tyrosine. The three oxidation states can be defined as in equation I.



In the catalytic cycle the two-equivalent reduction of GO_{ox} with RCH₂OH (eq. II) is followed by the reaction with O₂ (eq. III). Autoredox processes result in substantial conversion of GO_{ox} to GO_{semi} resulting in the so-called "native" mix with approximately 95% inactive or semi form of the enzyme and approximately 5% active enzyme (8). The literature describes several different techniques for oxidizing the semi (inactive) form of galactose oxidase to the active form. It is possible to obtain a fully activated galactose oxidase from the equilibrium mixture by a chemical oxidation, e.g., by ferricyanide. Chemical oxidants such as ferricyanide are useful for a single activation cycle to obtain substantially 100% active enzyme for analytical purposes. However, in a synthetic application, these oxidants are consumed in every enzyme reactivation cycle. Thus, a large excess of oxidant with respect to galactose oxidase must be added to the system to achieve long-term activation.

Effect of horseradish peroxidase on galactose oxidase activity

It has also been published that the activity of galactose oxidase is enhanced in the presence of horseradish peroxidase (HRP). This is illustrated in the

Figures 2 and 3 for the oxidation of guar gum. In Figure 2 the necessity of catalase is also clearly demonstrated. In the absence of catalase GO is completely inactivated after about 15 minutes.

Figure 3 shows that by adding HRP the oxidation rate of guar gum by GO is enhanced. In the presence of HRP more than 40% of the galactose groups in the guar are oxidized after three hours, while in the absence of HRP the same amount of GO oxidizes less than 10% of the galactosyl side-chains.

By adding horseradish peroxidase much less galactose oxidase is required to obtain the same level of guar oxidation (9). This finding was an important step towards developing an economically viable process for preparing oxidized guar for papermaking applications. However, the availability of GO is very limited and the cost of the commercially available material was still too high for commercialization of the oxidized guar technology.

Heterologous production of galactose oxidase

Galactose oxidase is produced by the fungus *Dactylium dendroides*, recently renamed as a *Fusarium* spp. The amounts of enzyme produced by the wild-type *Fusarium* strains are, however, low.

Therefore we looked into the possibilities of more efficient galactose oxidase production systems in collaboration with Dr. McPherson of Leeds University and others.

The galactose oxidase gene from *Fusarium* was cloned and characterized by McPherson *et al.* (10). The full-length *Fusarium* gene encoding galactose oxidase (GO) yields as a protein of 639 amino acids (72.8 kDa). The gene contains a leader sequence encoding 41 amino acids consisting of a pre- and a pro-region. The pre-region (18 amino acids) directs the galactose oxidase to the outside of the *Fusarium* cell and is cleaved off during translocation of GO over the cell wall. The pro-region (23 amino acids) is probably cleaved off by a copper-mediated autocatalytic process outside the cell (11). Mature GO has a molecular weight of 68.9 kDa.

Various expression hosts were evaluated for the heterologous production of GO. We, and others (12), found that in spite of the post-translational modifications that are necessary to obtain active GO, efficient expression of GO was possible using the *Pichia pastoris* expression system that is commercially available from Invitrogen, Carlsbad, CA.

In our optimized fermentation protocols we were able to produce almost a 100-fold more enzyme using *Pichia pastoris* as expression host compared to fermentations using the wild-type *Fusarium* strain.

The combination of the horseradish peroxidase activation (Figure 3) with the heterologous production of galactose oxidase has reduced the enzyme cost for the production of oxidized guar with several orders of magnitude.

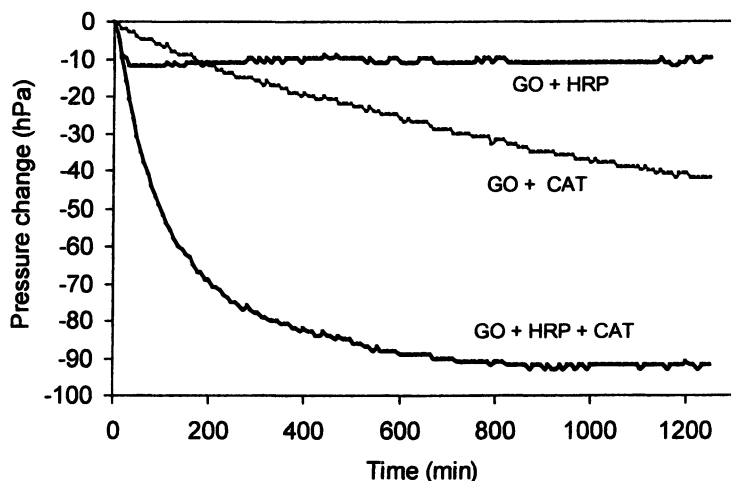


Figure 2. Oxidation of low molecular weight guar gum (5% w/v) monitored in bottles with an OxiTop[®] measuring head at pH 7 and room temperature with galactose oxidase (GO) in the presence or absence of Horse Radish Peroxidase (HRP) and Catalase (CAT).

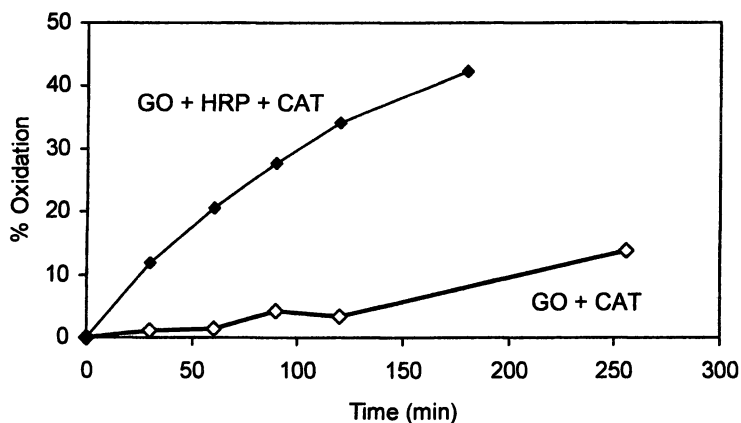


Figure 3. Effect of adding Horseradish Peroxidase (HRP) to the Galactose Oxidase (GO) – Catalase (CAT) enzyme mixture in the oxidation of low molecular weight guar gum (5% w/v) at room temperature and pH 7.

Applications of oxidized guar

An increase in the dry tensile strength of paper products can be achieved either by mechanical processes to insure adequate formation of hydrogen bonding between the hydroxyl groups of adjacent papermaking fibers, or by the inclusion of certain dry strength additives e.g. a galactomannan such as guar gum. Strength additives that are added prior to the papermaking (wet-end addition) should preferably have cationic functionalities so that they are easily retained by the cellulose fibers, which are naturally anionic. Figure 4 shows that the aldehyde functionality, introduced by galactose oxidase treatment, significantly increases the effect of cationic guar (Hydroxypropyl trimethyl ammonium chloride guar gum) on paper strength.

The much lower strength of Thermo-mechanical Pulp (TMP) in comparison with Softwood Kraft Pulp (SWK) can be compensated for by adding a strength additive e.g. oxidized cationic guar. The strength increase obtained by addition of 0.75-1.0 % of oxidized cationic guar (45% oxidation) to a pulp mixture of 80% TMP and 20% SWK results in paper with a strength that is better than paper prepared with 50/50 TMP/SWK (Figure 4). This can be very interesting from an economic point of view because TMP is much cheaper than SWP due to the higher pulp yield of the thermo-mechanical pulping process in comparison with the Kraft pulping process.

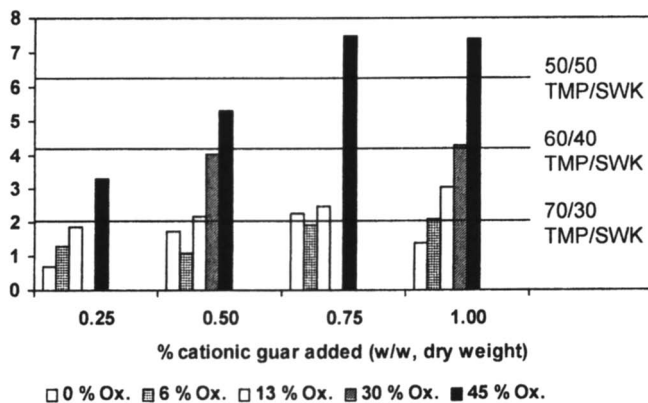


Figure 4. Dry tensile strength increase (N) of sheets prepared with 80/20 TMP/SWK and different dosages of cationic oxidized guar (0.25 – 1%) of various degrees of oxidation (0-45%) compared to a base sheet prepared without guar addition. Horizontal lines show the strength increase of sheets prepared with different ratio's of Thermo-mechanical Pulp (TMP) and Softwood Kraft Pulp (SWK) compared to the base sheet prepared with 80/20 TMP/SWK.

Figure 5 shows how the addition of 0.5% of oxidized neutral guar to bleached kraft pulp (50% hardwood, 50% softwood) results in a 27% increase in dry strength. The oxidized guar actually performs better than Kymene® 557H synthetic resin of Hercules Incorporated. This clearly shows that also neutral oxidized guar has a lot of potential in the production of high performance papers.

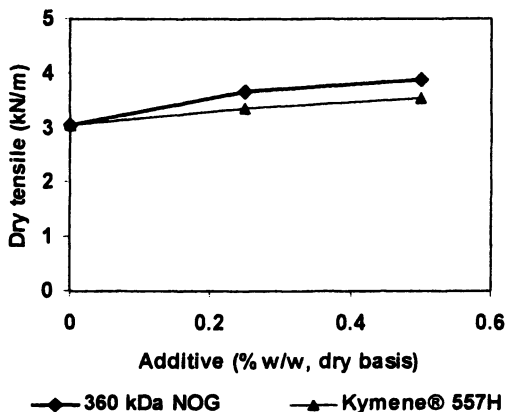


Figure 5. Dry strength of paper prepared with oxidized guar (42% oxidation) with an average MW of 360 kDa or a conventional dry strength additive, Kymene® 557H. Pulp: 50/50 hardwood/softwood bleached kraft, paper ~ 65 gsm sheet, Papermaking: pH 7.5 for Kymene® and pH 5.5 for oxidized guar.

Besides application as a dry strength additive oxidized guar can also be used as a temporary wet strength additive. Temporary wet strength is in fact important in products such as toilet tissue and facial tissue. In these products wet strength is only required for a short period of time, e.g. 5 minutes during use. Subsequently the wet strength should be lost rapidly to prevent clogging of the sewer system.

Additionally, due to the increased demand for paper and the emergence of paper recycling, there is a need to produce paper which is more readily repulpable. For example, paperboard products which are recycled must be defibered and repulped in neutral water without requiring, expensive or extraordinary processing requirements and to cope with permanent wet strength resins.

The hemi-acetal bond that can be formed between the aldehyde groups in oxidized guar and hydroxyl groups of cellulose fibers is reversible under wet conditions. Therefore paper made with oxidized guar with improved strength properties when dry, will loose strength during (prolonged) soaking in water.

Figure 6 shows some examples of wet strength decay for paper made with neutral oxidized guar or a typical wet strength additive (polyamide-amine epichlorohydrin resin, PAE), and a control without any additive.

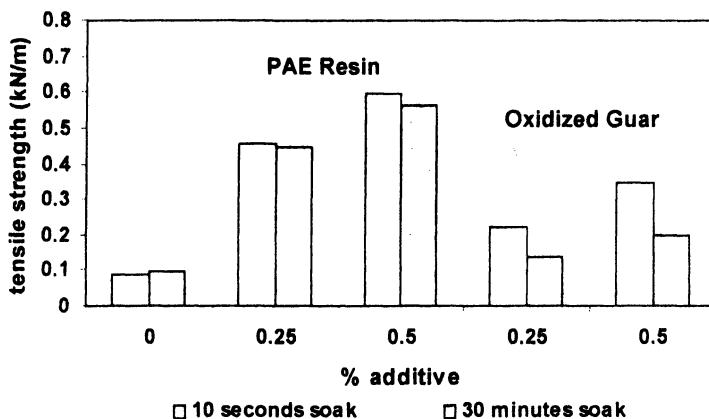


Figure 6. Wet tensile strength after 10 seconds and 30 minutes soaking time of paper prepared with 0.25% or 0.50 % polyamide-amine epichlorohydrin resin or oxidized guar

Paper prepared with the PAE wet strength resin does not lose much strength upon prolonged soaking in water. Soaking paper prepared with neutral oxidized guar for 30 minutes in water results in about 40% loss of the strength present after 10 seconds of soaking. After 30 minutes of soaking in water the wet strength of the paper prepared with 0.25% neutral oxidized guar approaches the value of the control paper without any additive.

Conclusions

By producing galactose oxidase (GO) with the heterologous production host *Pichia pastoris* it is possible to realize a significant reduction in the cost of the enzyme. By adding horseradish peroxidase and catalase the catalytic efficiency and operational stability of GO is significantly enhanced. These two factors will increase the viability of a number of possible applications of GO. The examples given above are limited to the oxidation of guar and cat-ionic guar for papermaking applications. There are, however, a number of other potential applications.

Donnelly (13) describes the use of galactose oxidase in combination with catalase for the oxidation of guar gum to produce products with various viscosities or gels under mild conditions for food applications. Oxidized guar gum and locust bean gum can also be used as precursors for various chemically modified polysaccharides. Yalpani and Hall exploited the aldehyde functionality to attach various functional groups via reductive amination, oxidation, and reduction (14). Oxidized guar can also be further oxidized chemically to obtain a

poly-carboxylic acid that can be applied as a thickening agent with altered rheological properties (15).

Galactose oxidase has also been shown to be capable of oxidizing aldehydes to the carboxylic derivative.

Kelleher and Bhavanandan showed that raffinose was partly converted to 6"-carboxyraffinose when treated with galactose oxidase and catalase (16). More recently it was shown that UDP-galactose could be oxidized to UDP-GalA with a yield of more than 95% in the presence of high levels of galactose oxidase and catalase, at prolonged incubation times (17).

Formation of carboxyl groups on oxidized guar has not yet been demonstrated, but it is conceivable that these are formed upon prolonged incubation of guar with a high dosage of galactose oxidase.

Another aspect that we have not yet looked into is the possibility of further tailoring the properties of oxidized guar by using α -galactosidase to create stretches of unsubstituted polymannose backbone which might have an impact on the interaction of the modified oxidized guar with cellulose.

Acknowledgements.

The authors would like to thank Mike McPherson (Leeds University) and Bea Penninkhof, Corien Tel, Andries Hanzen and Peter Burgers (Analytical Sciences Department, Hercules European Research Center) for their contributions.

References

1. Daas, P.J.H.; Schols, H.A.; de Jongh, H.J.H. *Carbohydr. Res.* **2000**, *329*, 609-619.
2. Grant Reid, J.S.; Edwards, M.E. In *Food polysaccharides and their Applications*; Stephen, A.M., Ed. Marcel Dekker, Inc. New York, NY, 1985, pp 155-186.
3. Germino, F.J. U.S. Pat. No. 3,297,604, 1967.
4. Chiu, C.W. U.S. Pat. No. 4,663,448, 1987.
5. Chiu, C.W.; Jeffcoat, R.; Henley, M.; Peek, L. U.S. Pat. No. 5,554,745, 1996.
6. McPherson, M.J.; Parsons, M.R.; Spooner, R.K.; Wilmot, C.M. In *Handbook of Metalloproteins*; Wieghardt, K.; Huber, R.; Poulos, T.L.; Messerschmidt, A. Eds. John Wiley & Sons Ltd. Bern, 2001 pp. 1272-1283.
7. Whittaker, M.M.; Whittaker, J.W. *J. Biol. Chem.* **1988**, *263*, 6074-6080.
8. Saysell, C.G.; Borman, C.D.; Baron, A.J.; McPherson, M.J.; Sykes, A.G. *Inorg. Chem.* **1997**, *36*, 4520-4525.

9. Busink, R.; Verbeek, M.A.M.; Haandrikman, A.J.; Hofbauer, M.; Vaessen-van Hoven, H.W.C. U.S. Pat. Appl. No. 2002102661, 2002.
10. McPherson, M.J.; Ogel, Z.B.; Stevens, C.; Yadav, K.D.; Keen, J.N.; Knowles, P.F. *J. Biol. Chem.* **1992**, *267*, 8146-8152.
11. Rogers, M.S.; Baron, A.J.; McPherson, M.J.; Knowles, P.F.; Dooley, D.M. *J. Am. Chem. Soc.* **2000**, *122*, 990-991.
12. Whittaker, M.M.; Whittaker, J.W. *Protein Expr. Purif.* **2000**, *20*, 105-111.
13. Donnely, M.J. In *Carbohydrate Biotechnology Protocols*; Burke, C., Ed.; Humana Press; Totowa, NJ, 1999; 79-88.
14. Yalpani, M.; Hall, L.D. *J. Polym. Sci.* **1982**, *20*, 3399-3420.
15. Frolini, E.; Reed, W.F.; Milas, M.; Rinaudo, M. *Carbohydr. Polym.* **1995**, *27*, 129-135.
16. Kelleher, F.M.; Bhavanandan, V.P. *J. Biol. Chem.* **1986**, *261*, 11045-11048.
17. Basua, S.S.; Dotsona, G.D.; Raetz, C.R.H. *Anal. Biochem.* **2000**, *280*, 173-177.

Author Index

- Albertsson, Ann-Christine, 347
Anderson, L., 66
Andersson, A., 66
Becker, Ulrike, 198
Beijer, Peter, 360
Beppu, Shinji, 198
Brady, Richard L., 360
Buchanan, Charles M., 326
Buchanan, Norma L., 326
Dahlman, Olof B., 66, 80
de Vries, Hielke T., 360
Debenham, John S., 326
Ebringerová, Anna, 312
Erasmý, N., 52
Esker, Alan, 198
Gatenholm, Paul, 167, 236, 326
Glasser, Wolfgang G., 167, 198
Haandrikman, Alfred J., 360
Hägglund, P., 66
Hannuksela, Tea, 222
Hartmans, Sybe, 360
Heinze, Thomas, 312
Hofbauer, Michaela, 360
Holmbom, Bjarne, 222
Jacobs, Anna, 66, 80
Jacobsson, Maria, 326
Jamin, Sylvie, 198
Jorda, J., 38
Kabel, Mirjam A., 108
Kiemle, David J., 122
Koschella, Andreas, 312
Kruse, Th., 52
Lappalainen, Arja, 140
Larsson, Per Tomas, 254
Lindblad, Margaretha
 Söderqvist, 347
Linder, Åsa, 236
Lundqvist, J., 66
Mais, Ursula, 94
Marchessault, Robert H., 158
Maréchal, P., 38
Mayo, Kelly E., 122
Nordström, Maria, 80
Olsson, Anne-Mari, 184
Österberg, Monika, 269
Paananen, Arja, 269
Palm, M., 66
Pere, Jaakko, 140
Pontalier, P.-Y., 38
Puls, Juergen, 24, 52
Ranucci, Elisabetta, 347
Rennekar, Scott, 198
Rigal, L., 38
Roubroeks, Johannes P., 167
Rutland, Mark, 269
Saake, Bodo, 24, 52, 167
Saarinen, Terhi, 269
Salmén, Lennart, 184
Schmekal, E., 52
Schols, Henk A., 108
Shelton, Michael C., 326
Sixta, Herbert, 94
Stålbrand, H., 66
Stenius, Per, 269
Stipanovic, Arthur J., 122
Sun, RunCang, 2
Sun, X. F., 2
Tammelín, Tekla, 269
Tappura, Kirsi, 269
Teleman, A., 66
Tenkanen, Maija, 140, 292
Tjerneld, F., 66
Tomkinson, J., 2
Voragen, Alphons G. J., 108
Watterson, Thelma L., 326
Wood, Mathew D., 326
Zacchi, G., 6

Subject Index

A

O-acetyl-galactoglucomannan (AcGGM)

- content in softwood, 3, 67
- difficulties in fractionation, 67–68
- dissolved in process water during pulping, 229–230
- enzymatic hydrolysis, 73
- influence of pH during heat fractionation, 74–75
- isolation of AcGGM, 72
- microwave heat fractionation, 70, 72, 74–76
- molecular weight determination, 70, 71*f*, 73–74

recovery of *O*-acetyl-galactoglucomannan by steaming, 30

sorption onto chemical pulps, 231–232

structure, 67, 72–73

See also Galactoglucomannans; Glucomannans; Mannans

Acetyl groups

- degree of acetylation (DS), 68
- in wood hemicelluloses, 6

See also *O*-acetyl-galactoglucomannan (AcGGM)

AcGGM. *See* *O*-acetyl-galactoglucomannan

Adsorption

- adsorption (docking) experiments by surface plasmon resonance (SPR), 203, 210–212

driving forces of xylan adsorption on cellulose beads, 285–286

kinetics of xylan adsorption on cellulose, 282–284, 286

- xylan adsorption measurement by quartz crystal microbalance, 274
- xylan adsorption to cellulose surfaces, 200, 210–212

AFM. *See* Atomic force microscopy

Amphiphilic molecules

- fluorine (F)-containing cellulose derivatives, 199–200, 205
- pullulan, 199

Antibodies, production, 145

Antigens

- poly- and oligosaccharides used as antigens, 145, 146*t*, 148
- preparation of oligosaccharide-protein conjugates, 145, 148–149

Antisera

- enzyme-linked-immunosorbent assay (ELISA), 147, 149–152
- immunodiffusion testing, 147, 149
- immunolabelling of pulp fibres, 147–148, 151–152, 153*f*–154*f*
- preparation, 144*f*, 145, 147

Applications of hemicelluloses

- guar gum galactomannans, use as thickener and stabilizer, 362
- industrial uses of hemicelluloses, 327–328

mannans, as beater additives, 224–225

mannans, as flocculating agents, 229

mannans, as stabilizing agents for emulsions, 229

oat spelts, uses, 53

oxidized guar for improvement of strength in papermaking, 362, 367–369

pharmaceutical uses of hemicelluloses, 4–5, 53

- poly- and oligosaccharides used as antigens, 145, 146*t*, 148
- trimethylammonium-2-hydroxypropyl (TMAHP) xylan, use as beater additive, 14
- uses for wheat straw hemicelluloses, 3
- xylans, commercial uses, 4
- xylans, pharmaceutical uses, 4, 53
- Arabinans, 294*t*, 296
- Arabinoxylans
- arabino-(4-*O*-methylglucurono)-xylan in softwood, 83, 141
 - arabinoxylan from oat spelt, 56
 - arabinoxylans from cereal cell walls, 43
 - content in cereals, 53
 - degree of substitution, effect on thermal stability of arabinoxylan esters, 342, 344*f*–345*f*
 - diferulic acid (diFA) cross-linking of arabinoxylans to lignin, 7, 8*f*
 - differential scanning calorimetry (DSC), 328, 342, 343*f*
 - effects of reaction conditions for esterification of arabinoxylan, 335–337
 - ether linkage to lignins, 9–10
 - gel permeation chromatography (GPC), 329, 339, 340*f*
 - isolation of arabinoxylan, 329–330, 332
 - methanesulfonic acid (MSA) used as catalyst, 330–331, 332, 333*f*, 335–337
 - 4-*O*-methylglucuronoarabinoxylan, 6*f*
 - modulated differential scanning calorimetry (MDSC), 328, 342, 344*f*–345*f*
 - preparation of arabinoxylan acetate, 330–331
 - preparation of arabinoxylan esters, 328, 330–331
 - preparation of arabinoxylan propionate, 331
 - proton NMR (¹H-NMR) spectrum of arabinoxylan acetate, 337–339
 - separation of hemicellulose A and B, 332
 - thermal stability, 328, 339, 341–342, 344*f*–345*f*
 - thermogravimetric analysis (TGA), 328, 339, 341*f*
 - trifluoroacetic anhydride (TFAA) as promoter of esterification, 332, 336*t*, 337
 - weight-average molecular weight and carbohydrate composition changes during acetylation, 333*f*–334*f*, 335, 336*t*, 339
- See also* Xylans
- Aspen wood (*Populus tremula*), 169–170, 317
- Atomic force microscopy (AFM)
- AFM colloidal probe technique for measurement of interaction forces, 270, 273–274, 275–278
 - cellulose bead surfaces, 271, 272*f*
 - Langmuir Blodgett (LB) films, 203–204, 212, 213*f*, 270
 - surface modification of cellulose fibers with xylans, 248, 250, 251*f*
- B**
- Bagasse (from sugar cane), 316–317, 319*f*
 - Barley straw, 3
 - BCHIS (1,3-bis(3-chloro-2-hydroxypropyl)imidazolium sulfate), 316–317
 - Beater additives, 14, 224–225
 - Biosynthesis of hemicelluloses, 3, 297, 308–309
 - Birch (*Betula verrucosa*)
 - composition of birch xylan, 186*t*
 - CP/MAS ¹³C-NMR spectra of xylan from bleached birch kraft pulp, 264*f*

- hydrogels made from birch hemicelluloses, 348
- MALDI-TOF MS spectrum of *O*-acetyl-glucomannan from birch, 83, 84*f*
- size exclusion chromatography of birch extracts, 31–33
- storage modulus and mechanical damping as functions of relative humidity, 188, 189*f*
- Bovine serum albumin (BSA), 140, 145, 148–149
- Brewery's spent grain
composition of hemicellulosic extracts, 110–111
- MALDI-TOF spectrum of endoxylase I-digested brewery's spent grain, 116–117
- O*-acetyl substituted xylo-oligosaccharides, 110–111, 117–118
- structural characteristics of xylo-oligosaccharides in hydrolysates, 116–118
- structure of xylans, 109–110
- BSA (bovine serum albumin), 140, 145, 148–149

C

- Capillary zone electrophoresis (CZE), 173
- ¹³C-NMR (carbon NMR). *See under* Nuclear magnetic resonance (NMR) spectroscopy
- Cell wall constituents and structure, 168, 237, 293
- Cellulose
cellulose-xylan model system, 263–267
- CP/MAS ¹³C-NMR spectra of cellulose I, 255–256, 259–261
- crystallinity of cellulose fibers, 241, 244, 258
- mannan crystallization on cellulose microfibrils, 226–227
- mechanism of xylan retention on cellulose, 250, 252
- model for isolated cellulose I fibrils, 256–259
- xylan adsorption to cellulose surfaces, 200
- See also* Atomic force microscopy; Cellulose beads; Fibrils (cellulose I); Fluorine (F)-containing cellulose ester derivatives; Surface modification of cellulose fibers with xylan
- Cellulose beads
behavior in aqueous solutions, 275–279, 280*f*, 284–285
- behavior in xylan solutions, 279–282, 283*f*
- driving forces of xylan adsorption, 285–286, 288
- effects of electrolyte concentration, 277, 279, 280*f*
- effects of loading force, 275, 277, 278*f*, 285
- effects of swelling, 275, 276*f*, 284–285, 288
- force measurements by AFM, 271, 273
- forces between xylan-coated cellulose beads, 286–287
- kinetics of xylan adsorption on cellulose, 282–284, 286
- surface typography by AFM, 271, 272*f*
- Cellulose I. *See* Fibrils
- Cereal straws
acetylation in, 6
- effect of straw/bran ratio in twin screw extrusion, 43–46
- hemicellulose content, 3
- hemicellulose structure, 5
- size exclusion chromatography (SEC) of wheat straw extracts, 31–33

utilization of hemicelluloses, 4
 viscosity of extracts from wheat bran
 and wheat straw, 42–43, 46
 xylan extraction from wheat straw
 and wheat bran, 41–42, 48–50
 Cereals, arabinoxylan content, 53
 Chiu, C. W., 363
 CHTMAC (3-chloro-2-
 hydroxypropyltrimethylammonium
 chloride), 316–318
 Classification of hemicelluloses, 293–
 294
 Corn cobs, 109–111
 Coumaric acid. *See p*-Coumaric acid
 (PCA)
 Critical micelle concentration (CMC)
 definition, 204, 205
 determination of critical micelle
 concentration, 202, 203, 204–210
 wetting force, 206, 207*f*
 Cross-polarization magic angle
 spinning carbon-13 nuclear
 magnetic resonance (CP/MAS ¹³C-
 NMR). *See under* Nuclear magnetic
 resonance (NMR) spectroscopy
 Crystallinity of cellulose fibers, 241,
 244, 258

D

Degree of polymerization (DP) of
 hemicelluloses, 31, 305
 Degree of substitution (DS) of
 hemicelluloses
 degree of acetylation, 68
 effect on solubility, 305–306, 307*f*,
 313
 effect on thermal stability of
 arabinoxylan esters, 342, 344*f*–
 345*f*
 Derjaguin approximation, 273–274
 Differential scanning calorimetry
 (DSC), 185, 328, 342, 343*f*
 Dimethyl sulfoxide (DMSO), as
 solvent for methacrylation, 348,
 352–356
 Dissolving pulps
 acid sulfite cooking, 95
 alkali-insoluble R-fractions, 96, 99–
 100, 104*f*
 alkali-soluble S-fractions, 96, 99–
 100, 104*f*
 beechwood sulphite pulp (BS),
 98
 carboxyl groups, 100
 Eucalyptus prehydrolysis kraft pulp
 (EK), 98
 4-*O*-methylglucuronic acid
 (40MeGlcA) residues, 102–103,
 106
 press lye (PL) characteristics, 99*t*,
 102
 R values (R18 and R10), 98
 specification of starting materials,
 98*t*
 structural characterization by FT-IR
 spectroscopy, 103, 104*t*
 structural characterization by solid-
 state NMR spectroscopy, 104–
 105
 viscosity and molecular weight of
 hemicellulose fractions, 96, 100–
 101
 xylan degradation during viscose
 process, 95
See also Viscose process
 DLVO (Derjaguin, Landau, Verwey
 and Overbeek) theory, 273–274,
 277, 279*t*, 286
 DMF/LiCl (*N,N*-dimethylformamide
 with lithium chloride) solvent, 15–
 16, 313, 314
 Docking. *See* Adsorption
 DSC. *See* Differential scanning
 calorimetry
 Dynamic mechanical analysis (DMA),
 186

E

Electron spectroscopy for chemical analysis (ESCA), 141

Enzymatic modifications, 305–308, 362–366

See also Enzymes; Guar gum galactomannans; Modification of hemicelluloses

Enzyme-linked immunosorbent assay (ELISA), antisera specificity testing, 147, 149–152

Enzymes

accessory enzymes, 297, 304

α -arabinosidases from *Aspergillus*, 302, 303*t*

backbone hydrolyzing enzymes, 298–299, 300*f*

catalase, 363, 365, 366*f*

classification of hemicellulolytic enzymes, 295*t*, 297

effect of enzyme dosage, 298

endoglycanases (backbone hydrolyzing enzymes), 297, 298, 301*f*

esterases, 297, 304, 305*t*, 308

exoglycosidases (side-group hydrolyzing enzymes), 299, 302–305

galactose oxidase (GO), 309, 362–366

α -galactosidases, 302, 308, 362

α -glucuronidases, 302

hemicellulases from microorganisms, 297

hemicellulose-synthesizing enzymes, 308–309

horseradish peroxidase (HRP), 364–365, 366*f*

mannanases, 362

specificity, 298

xyloglucan endotransglycosylase (XET), 309

xylopyranose, 298

ESCA. *See* Electron spectroscopy for chemical analysis

Eucalyptus wood, 110–111, 112–113, 118

Extensin, 9

F**Ferulic acid (FA)**

cross-links between lignin and hemicelluloses, 7

diferulic acid (diFA) cross-linking of arabinoxylans to lignin, 7, 8*f*

ester linkage to hemicelluloses, 7, 296

ether linkage to lignin, 7

ferulyl groups attached to xylan, 6*f*, 7

Fibrils (cellulose I)

accessible fibril surfaces (AS), 257–258

crystalline cellulose (C), 258

description, 256–257

direct contact with hemicellulose, 257

fibril aggregates, 257

inaccessible fibril surfaces (IS), 257–258

para-crystalline cellulose (PC), 258

square fibril aggregate model (SFAM), 258*f*, 259

Fluorine (F)-containing cellulose ester derivatives

amphiphilic character, 199–200

block-like (telechelic) cellulose ester copolymers, 204*t*

critical micelle concentration (CMC), 205–210

introduction of fluorine atoms, 199, 201–202

self-assembly measurements at solid surfaces, 210–212

self-assembly measurements in solution, 204–210

structure, 204, 205*f*, 214, 215*f*

Freudenberg, K, 159, 160

Furfural, 133, 134*f*

Furrier transformed infrared spectroscopy (FTIR)
 carbonyl groups in xylan derivatives, 321
 pulp and paper analysis, 140–141
 TMAHP-derivatives of xylan, 318

G

Galactans, 294*t*, 296

Galactoglucomannans (GGMs)

characteristics, 223

content in softwood, 3, 296

deacetylation during in alkaline conditions, 230

galactomannan from spruce, 350, 351*f*

mechanism of sorption to fiber surfaces, 227

sorption onto chemical pulps, 232–233

sorption onto thermomechanical pulp (TMP) fibers, 230–231

See also *O*-acetyl-

galactoglucomannan;

Glucomannans; Guar gum

galactomannans; Mannans

Galactose oxidase (GO), 309, 362–366

Gel permeation chromatography (GPC), 329, 339, 340*f*

Germino, F. J., 362

Glucans, 294*t*, 296, 297, 309

Glucomannans (GMs)

Amorphophallus Konjac

glucomannan, 186*t*, 193*f*, 194

characteristics, 81, 223, 294*t*, 296

content in softwood, 296

effect on properties of paper, 224–225

enzymatic modifications of galactomannans, 305–306

gel formation, 229

locust bean gum galactomannans, 223, 224

MALDI-MS spectrum of alkali-treated glucomannan from spruce wood, 81–82

MALDI-MS spectrum of *O*-acetyl-glucomannan from spruce wood, 82, 84*f*

MALDI-TOF MS spectrum of *O*-acetyl-glucomannan from birch, 83, 84*f*

mechanism of sorption to fiber surfaces, 226–227

See also *O*-acetyl-

galactoglucomannan (AcGGM);

Guar gum galactomannans

Glucuronoxylans

aggregate formation, 173, 176–178, 179–180

colloidal character of xylan solutions, 168, 169

ester linkages of *p*-coumaric acid to arabinoglucuronoxylans, 7, 9*f*

fractionation, 172–173, 174*f*–175*f*

high-performance size exclusion chromatography with multiple

angle laser light scattering

detection and refractive index

detectors (HPSEC-UV-MALLS-

RI), 170–171, 172–173, 174*f*–175*f*

lignin extraction, 171, 177–181

MALDI-TOF MS analysis, 83, 85–88, 173, 176*f*

4-*O*-methylglucuronoxylan graft copolymers, 14

4-*O*-methylglucuronoxylan structure and molar rotation, 159–164

pH fractionation, 173, 176–178

solubility, 168–169

structure, 159–164, 168

GPC. *See* Gel permeation chromatography

Guar gum galactomannans, 223, 228–229, 305

analysis of oxidation levels in oxidized guar, 363–364

applications of oxidized guar, 362, 367–369

catalase for removal of hydrogen peroxide, 363, 365, 366f
 compared to locust bean gum, 223, 362

Cyamopsis tetragonoloba, 361
 effect of horseradish peroxidase (HRP), 364–365, 366f
 modification with galactose oxidase (GO), 305, 309, 362–366

modification with α -galactosidase, 362

modification with mannanases, 362
 oxidized guar for improvement of strength in papermaking, 362, 367–369

use as thickener and stabilizer, 362

See also *O*-acetyl-galactoglucomannan (AcGGM); Galactoglucomannans; Glucomannans

Guaran. *See* Guar gum galactomannans

H

Heat fractionation process (steaming)
 degradation of hemicelluloses, 28, 30–31, 32f

degree of polymerization (DP) of hemicelluloses after steaming, 31

hemicelluloses from steaming pretreatment, 30–33

lability of 4-*O*-methyl-glucuronic acid residues, 30*t*, 31

pilot plants, 25, 32f, 33

recovery of *O*-acetyl-galactoglucomannan, 30

use in pulp production, 25, 28

HEMA (2-hydroxyethyl methacrylate), 348–349

HEMA-Im (2-[(1-imidazolyl)formyl]ethyl methacrylate), 349, 350, 352–356

Hemicellulolytic enzymes. *See* Enzymes

Hemicelluloses, general information classification, 293–294

composition, 3, 293, 296–297, 327

content in cereals and straw, 3

definition of hemicelluloses, 3, 24, 67, 293, 327

Hexenuronic acid (4-deoxy- β -L-threo-hex-4-enopyranosyluronic acid, HexA), methylglucuronic acid (MeGlcA) side-groups, 141–142

High performance anion exchange chromatography and pulsed amperometric detection (HPAEC-PAD), 96, 105*t*, 123, 125

High performance anion exchange chromatography (HPAEC), 111–114

High-performance size exclusion chromatography with multiple angle laser light scattering detection and refractive index detectors (HPSEC-UV-MALLS-RI), 170–171, 172–173, 174f–175f

HPAEC-PAD. *See* High performance anion exchange chromatography and pulsed amperometric detection

Hydrogels

2-hydroxyethyl methacrylate (HEMA) in methacrylation of polysaccharides, 348–349

birch hemicelluloses in hydrogels, 348

controllability, 356–358

heat fractionation of spruce for production of hemicellulose for hydrogel production, 349–350

hydrogel synthesis, 356, 357f

2-[(1-imidazolyl)formyl]ethyl methacrylate (HEMA-Im) in methacrylation of polysaccharides, 349, 350, 352–356

kinetic studies of methacrylation of hemicellulose, 352–353, 354f–355f, 356

methacrylation of hemicellulose, 348–349, 350, 352–356

poly(2-hydroxyethyl methacrylate) (PHEMA)-based hydrogels, 15, 348
 properties, 348
 radical polymerization reactions, 357, 358
¹H-NMR (proton NMR). *See under* Nuclear magnetic resonance (NMR) spectroscopy
 Hydroxycinnamic acids, 9–10, 11–12
See also Ferulic acid (FA); *p*-Coumaric acid (PCA)
 Hydroxymethylfurfural (HMF), 111, 133

I

Immunolabelling of pulp fibres, 147–148, 151–152, 153*f*–154*f*, 240
 Isolation of hemicelluloses
 AcGGM, 72
 alkaline hydrolysis, 11–13, 53
 alkaline peroxide extraction, 13, 54
 isolation of arabinoxylan, 329–330, 332
 liquid/solid ratio (L/S) required in wheat bran extraction, 39, 43, 46–47
 microwave heat fractionation, 70, 72
 steam explosion method, 12, 54
 ultrasound-assisted extraction, 12
See also Pulping processes; Twin screw extrusion

L

Langmuir Blodgett (LB) films
 atomic force microscopy (AFM), 203–204, 212, 213*f*
 in self-assembly measurements, 210, 212
 preparation from trimethylsilyl (TMS, TMSC) cellulose, 203, 271

preparation from trimethylsilyl (TMS) cellulose, 200
 surface force apparatus (SFA), 270
 Lignin
 acetylated lignin identification by ¹H NMR, 171–172, 179, 180*f*
 content in oat spelts, 56
 diferulic acid (diFA) cross-linking of arabinoxylans to lignin, 7, 8*f*
 effects on isolation of hemicellulose, 11–12
 ether linkage to arabinoxylans, 9–10
 extraction from glucuronoxylan, 171, 177–181
 ferulic acid (FA) cross-links between lignin and hemicelluloses, 7
 lignin carbohydrate complexes (LCC), 169, 200
p-Coumaric acid (PCA) ester-linkages to lignin, 8*f*

M

Maize stems, hemicellulose content, 3
 MALDI-TOF MS. *See* Matrix assisted laser desorption/ionization time-of-flight mass-spectrometry
 Mannans
 affinity toward bacterial cellulose, 227
 mechanism of sorption to fiber surfaces, 226–229
 mono- or multi- layer sorption, 227
 poly- and oligosaccharides used as antigens, 145, 146*t*
 preparation and purification of oligosaccharides from mannans, 142, 143*f*–144*f*
 properties and interactions in solutions, 228–229
 resorption of dissolved wood mannans, 225–226
 sorption onto chemical pulp fibers, 231–233

- sorption onto mechanical pulp fibers, 230–231, 231–231
- types of mannans, 223, 296
- use as beater additives, 224–225
- use as flocculating agents, 229
- use as stabilizing agents for emulsions, 229
- wet-end additives, 225
- See also* *O*-acetyl-galactoglucomannan (AcGGM); Galactoglucomannans; Glucomannans; Guar gum galactomannans
- Matrix assisted laser desorption/ionization time-of-flight mass-spectrometry (MALDI-TOF MS)**
- advantages of MALDI-TOF-MS method, 81, 102
- analysis of AcGGM fractions, 69, 71*f*, 73
- analysis of glucuronoxylans, 83, 85–88, 173, 176*f*
- analysis of hexenuronoxylans, 88–89
- MALDI-TOF spectrum of endoxylase I-digested brewery's spent grain, 116–117**
- SEC prior to MALDI-MS analysis (SEC/MALDI-MS), 71*f*, 73–74, 89–93**
- spectrum of *O*-acetyl-glucomannan from birch, 83, 84*f*
- spectrum of alkali-treated glucomannan from spruce wood, 81–82
- spectrum of press lye, 102
- MDSC. *See* Modulated differential scanning calorimetry**
- Methacrylation of hemicelluloses, 348–356**
- See also* Hydrogels
- Methanesulfonic acid (MSA), 330–331, 332, 333*f*, 335–337**
- Methylglucuronic acid (MeGlcA) side-groups**
- 4-*O*-methylglucuronic acid (4OMeGlcA) residues in dissolving pulps, 102–103, 106
- 4-*O*-methylglucuronic acid substituted xylo-oligosaccharides, 110–111
- 4-*O*-methylglucuronic acid substituted xylo-oligosaccharides in *Eucalyptus* wood hydrolysates, 118
- modification to hexenuronic acid during pulping, 141
- Micelles. *See* Critical micelle concentration**
- Modification of hemicelluloses**
- acetylation of hemicelluloses, 16–17
- N*-bromosuccinimide (NBS), use as catalyst, 16–17
- chemical modification, 13–17
- effects on hydrophobic capacity, 13, 16
- hemicellulose/poly(2-hydroxyethyl methacrylate) (PHEMA)-based hydrogels, 15, 348
- methacrylation, 348–349, 350, 352–356
- 4-*O*-methylglucuronoxylan graft copolymers, 14
- pentosan polysulfate (PPS), 15
- shortcomings of hemicelluloses, 13
- trimethylammonium-2-hydroxypropyl (TMAHP) xylan, 14
- See also* Enzymatic modifications; Guar gum galactomannans; Hydrogels
- Modulated differential scanning calorimetry (MDSC), 328, 342, 344*f*–345*f***
- MSA. *See* Methanesulfonic acid**
- N**
- Nuclear magnetic resonance (NMR) spectroscopy**

- carbon NMR (^{13}C -NMR)
 ester bond between lignin and glucuronic acid by ^{13}C -NMR spectroscopy, 11*f*
 oxidized xylan derivatives, 321–322, 323*t*
 TMAHP derivatives of xylans, 318
 xylo-oligosaccharides (XOS), 115–116
- cross-polarization magic angle spinning carbon-13 nuclear magnetic resonance (CP/MAS ^{13}C -NMR)
 cellulose I spectra, 259–261
 cellulose-xylan model system, 263–267
 characteristics of spectra, 255–256
 hemicelluloses, spectra, 261–263
 interaction of cellulose and xylan, 263–267
 model for isolated cellulose I, 255–259
 xylan, spectra, 264*f*
- proton NMR (^1H -NMR)
 acetylated lignin identification, 171–172, 179, 180*f*
 AcGGM molecular weight determination, 69, 74
 advantages over HPLC and HPAEC-PAD, 123, 125
 arabinose (Ara) determination by NMR, 127, 130*f*
 arabinoxylan acetate, 337–339
 cellobiose, 133
 common sugars, spectrum, 127, 128*f*–130*f*
 disadvantages of NMR method, 125
 furfural, 133, 134*f*
 D-galactose (Gal) determination, 127, 130*f*
 D-glucuronic acid (GluA) determination, 127, 131*f*, 132
 hydrolyzed balsam fir, spectrum, 136*f*
 hydrolyzed willow wood (*Salix sp.*), spectrum in acidic D_2O , 124*f*, 126–127
 influence of acid concentration on water peak chemical shift, 126
 kinetic studies of methacrylation, 352–354
 repeatability, 132
 sample preparation, 125–126
 sugar composition of hydrolyzed wood samples, 135–137
 sugars, "absolute" concentration determination, 137–138
 sugars, conformation of, 126, 127*t*
 sugars, quantification of model sugar compounds, 126–135
 D-xylose (Xyl) determination by NMR, 127
- O**
- Oat spelts
 arabinoxylan from oat spelt, 56
 carbamates from oat spelt xylan, 315
 composition of oat spelts from different sources, 56–57
 hydrolysis residues, 56*t*, 57*t*, 62*t*
 lignin content, 56
 non-pressurized alkaline extraction, 57–58
 oxygen aided alkaline extraction, 58–64
 temperature, effects on xylan extracts, 57–58
 uses, 53
 xylan composition, 53
 xylan extraction and precipitation, 54–55
- Oligosaccharide-protein conjugates, preparation, 145
- Organosolv pulping
 Alcell process, 26
 degradation of hemicelluloses, 26–28
 Organocell process, 26–28

- solvents and general information, 25–26
- Ovalbumin (OA)
preparation of oligosaccharide-protein conjugates, 145, 148–149
- specificity of oligosaccharide-OA antisera, 149

P

- p*-Coumaric acid (PCA)
ester-linkages to
arabinoglucuronoxylans, 7, 9*f*
p-coumaryl groups attached to xylan, 6*f*
- Paper pulps
effects of cationic xylan derivatives, 317–318
removal of hemicelluloses, 25, 35
- Pentosan polysulfate (PPS),
pharmaceutical use, 15
- Pharmaceutical uses of
hemicelluloses, 4–5, 53
- Poly(3-hydroxybutyrate) (PHB), 165
- Pullulan, 199, 200
- Pulping processes
kraft pulping, 25, 98, 264*f*, 367–368
paper pulps, 25, 35
sulfite pulping, 25, 95
thermomechanical pulping, 34, 230–231
- See also* Dissolving pulps; Heat fractionation process; Organosolv pulping; Viscose process
- Purves, Clifford B., 159

Q

- Quartz crystal microbalance, 274, 282–284, 286, 287

R

- Rice straw, 3
Rye straw, 3

S

- Sauerbrey equation approximation, 274
- Scanning electron microscopy (SEM), 239, 241, 242*f*–243*f*, 248, 250
- SEC. *See* Size exclusion chromatography (SEC)
- Self-assembly of molecules
aggregation of copolymers, 199
critical micelle concentration, effect on self assembly, 204
self-assembly behavior, 199
self-assembly measurements at solid surfaces, 210–212
self-assembly measurements in solution, 204–210
xylan adsorption to cellulose surfaces, 200
- SEM. *See* Scanning electron microscopy
- SFAM (square fibril aggregate model), 258*f*, 259
- Size exclusion chromatography (SEC)
O-acetyl-galactoglucomannan (AcGGM), 70, 71*f*, 73–74
birchwood and wheat straw extracts, 31–33
high-performance SEC with multiple angle laser light scattering detection and refractive index detectors (HPSEC-UV-MALLS-RI), 172–173, 174*f*–175*f*
SEC prior to MALDI-MS analysis (SEC/MALDI-MS), 71*f*, 73–74, 89–93
xylans from oat spelts, 55
- Softening behavior of hemicelluloses
activation energy, 191, 192*f*–193*f*

- dynamic mechanical analysis (DMA), 186
- dynamic mechanical measurements on moist wood, 185
- effects of temperature, humidity and loading frequency on softening point, 188, 189f
- glass transition, 185–186, 192f, 194–196
- load frequency, effect of, 185–186
- mechanical testing in humidity scans, 187, 188f
- moisture ratio, effect on softening point, 190–191, 192f
- relative humidity, effect of, 188, 189f
- softening under dry conditions, 185
- storage modulus and mechanical damping as functions of relative humidity, 188, 189f, 193f, 194
- water, softening effect, 185
- water sorption testing, 187, 190
- SPR. *See* Surface plasmon resonance
- Spruce (*Picea abies*)
- carbohydrate composition of aqueous phase of Organocell process, 26–28, 29f
 - characterization of hemicellulose fraction, 350, 351f
 - heat fractionation for production of hemicellulose for hydrogel production, 349–350
- Square fibril aggregate model (SFAM), 258f, 259
- Steaming. *See* Heat fractionation process
- Stirred-reactor xylan extraction, 39, 42, 46–48
- Straw hemicelluloses, structure, 5
- Structure of hemicelluloses
- effect on physical properties, 293
 - ester linkage of lignin to glucuronic side chains, 9–10
 - ether linkage of lignin to arabinoxylans, 9–10
 - ferulic acid cross-links between lignin and hemicelluloses, 7, 8f
 - ferulyl groups attached to xylan, 6f, 7
 - glucuronoxylan structure, 159–164, 168
 - linkage to secondary wall proteins, 9
 - 4-*O*-methylglucuronoarabinoxylan, 6f
 - p*-coumaryl ester linkages to arabinoglucuronoxylans, 7, 9f
 - p*-coumaryl groups attached to xylan, 6f, 7
 - straw hemicelluloses, 5
 - xylan structure, 109–110, 141, 159–163, 168
 - β -1,4-linked-D-xylopyranosyl main chain, 5, 141
- Sugars found in hemicelluloses, 3, 123, 126, 127t, 312
- "Surface decoration." *See* Surface modification of cellulose fibers with xylan
- Surface force apparatus (SFA), 270
- Surface modification of cellulose fibers with xylan
- accessibility of cellulose for xylan, 245, 248, 249f
 - autoclave experiments, methods, 237–239
 - effect of pore size, 248, 249f
 - mechanism of xylan retention on cellulose, 250, 252
 - retention of xylan, 241, 244–245, 246f–247f
 - surface area of cellulose substrates, 239–240, 245
 - surface characterization by atomic force microscopy (AFM), 248, 250, 251f
 - surface characterization by scanning electron microscopy (SEM), 239, 241, 242f–243f, 248, 250
 - surface topography of cellulose treated with xylan, 248, 250
- See also* Xylans
- Surface plasmon resonance (SPR), 200–201, 203, 210–212
- Sustainability concept, 159

T

Thermogravimetric analysis (TGA),
339, 341*f*

Thermomechanical pulping, 34, 230–
231

Timmell, T. E., 159

TMAHP. *See* Trimethylammonium-2-
hydroxypropyl xylan

Trimethylammonium-2-
hydroxypropyl (TMAHP) xylan, 14,
316–318

Twin screw extrusion

effect of quantity of soda, 43–46

effect of straw/bran ratio, 43–46

extraction method for wheat straw
and wheat bran, 39–41

xylan extraction yields, 43–45

U

Ultrafiltration, 41–42, 48–50

V

Viscose process

acid sulfite cooking, 95

hemicellulose accumulation during
steeping, 95

hemicelluloses from steeping liquor,
25, 34, 95–96

specification of starting materials,
98*t*

steeping process, 95

xylan degradation during viscose
process, 95

See also Dissolving pulps

Viscosity, 42–43, 46, 60, 96, 100–101

W

Wheat bran

composition, 38

composition of hemicellulosic
extracts, 42–48, 110–111

liquid/solid ratio (L/S) in extraction,
39, 43, 46–47

O-acetyl substituted xylo-
oligosaccharides, 110–111

stirrer-reactor xylan extraction, 39,
42

structure of xylans, 109–110

twin-screw extrusion, 39–41, 42, 43

Wheat straw

composition of hemicellulosic
extracts, 42–48

hemicellulose content, 3

hemicellulose stearates from wheat
straw, 314

hemicellulose structure, 5

succinic anhydride reaction with
wheat straw hemicellulose, 315

twin-screw extrusion, 39–41, 43

uses for wheat straw hemicelluloses,
3

Wood resin, 230

X

Xylan esters

carbamates from oat spelt xylan, 315

carboxylic acid esters, 312–315, 319,
321

complexation of copper (II) by a
ligand synthesized from xylan,
322, 323*f*

degree of substitution, effects of
reaction conditions, 314–315

DMF/LiCl (*N,N*-dimethylformamide
with lithium chloride) solvent,
313, 314

hemicellulose B acetylation, 314–
315

hemicellulose stearates from wheat
straw, 314

introduction of ester groups, 313*f*

succinic anhydride reaction with
wheat straw hemicellulose, 315

- thermal stability, 315
 xylan sulfates, 315
- Xylan ethers**
 bagasse reaction with CHTMAC and 1,3-bis(3-chloro-2-hydroxypropyl)imidazolium sulfate (BCHIS), 316–317, 319†
 etherification with 3-chloro-2-hydroxypropyltrimethylammonium chloride (CHTMAC), 316–318
 introduction of cationic groups into xylan, 315–318, 319†
 quarternization of xylan, 317, 319†
 trimethylammonium-2-hydroxypropyl (TMAHP) derivatives, 316–318
- Xylans**
O-acetyl-(4-*O*-methylglucurono)-xylan in hardwood, 83, 141
 adsorption to cellulose surfaces, 200, 210–212
 aggregation on fiber surfaces, 231
 alkalinity, effects on xylan extracts, 58–60
 anionic xylan, 202, 205†
 arabino-(4-*O*-methylglucurono)-xylan in softwood, 83, 141
 biodegradability of xylan derivatives, 319, 321
 bleaching, 55, 62–64
 bridges between cellulose microfibrils, 237
 carboxylic acid esters, preparation, 312–315
 cationic xylan, 202, 205†
 commercial uses, 4
 composition of hemicellulosic extracts from wheat bran and wheat straw, 42–48
 composition of xylans from oat spelts, 53
 CP/MAS ¹³C-NMR spectra of xylan from bleached birch kraft pulp, 264†
 crystalline structure, 160–164
 crystallization on cellulose microfibrils, 237
 degradation during derivative preparation, 95, 315, 316–317
 diferulic acid (diFA) cross-linking of arabinoxylans to lignin, 7, 8†
 driving forces of xylan adsorption on cellulose beads, 285–286
 ester linkages of *p*-coumaric acid to arabinoglucuronoxylans, 7, 9†
 ether linkage of arabinose side chains to ligninoxylans, 9–10
 ether linkage of arabinoxylans to lignin, 9–10
 extraction and precipitation from oat spelts, 54–55
 ferulyl groups attached to xylan, 6†, 7
 film properties, 43, 46, 164–165
 forces between cellulose beads in xylan solutions, 279–282
 introduction of cationic groups into xylan, 315–318, 319†
 kinetics of xylan adsorption on cellulose, 282–284, 286
 MALDI-MS analysis of glucuronoxylans, 83, 85–88
 MALDI-MS analysis of hexenuronoxylans, 88–89
 mechanism of xylan retention on cellulose, 250, 252
 4-*O*-methylglucuronoarabinoxylan, 6†
 molar mass of xylan from oat spelt, 53, 57–58, 60, 63†
 molar rotation, 159–160, 161†
 non-pressurized alkaline extraction, 57–58, 60–64
 oxidized xylan derivatives, 318–323
 oxygen aided alkaline extraction, 58–64
p-coumaryl groups attached to xylan, 6†, 7
 pharmaceutical uses, 4, 53
 poly- and oligosaccharides used as antigens, 145, 146†, 148

- preparation and purification of
oligosaccharides from xylans, 142,
143*f*–144*f*
- pressure, effects on xylan extracts,
60–62
- quarternization of xylan, 317
- resorption of dissolved wood xylans,
225–226, 237
- retention on cellulose fibers, 241,
244–245, 246*f*–247*f*
- stirred-reactor xylan extraction, 39,
42, 46–48
- structure, 109–110, 141, 159–163,
294*t*
- temperature, effects on xylan
extracts, 57–58, 61
- thermoplasticity, 164, 165*f*
- thickness-temperature curve, 164,
165*f*
- twin-screw extrusion extraction
methods, 38–42
- ultrafiltration, 41–42, 48–50
- viscosity of extracts from oat spelts,
60
- viscosity of extracts from wheat bran
and wheat straw, 42–43, 46
- xylan content in hardwood, 3, 294
- xylan content in wheat bran, 38
- β -1,4-linked-D-xylopyranosyl main
chain, 5, 141, 296, 312
- See also* Arabinoxylans;
Glucuronoxylans; Softening
behavior of hemicelluloses;
Surface modification of cellulose
fibers; Xylan esters; Xylan ethers
- Xylo-oligosaccharides (XOS)
arabinose substituted, 110–111
from depolymerization of xylans
during hydrothermal treatment,
109
- in hydrolysates after hydrothermal
treatment, 110–111
- 4-*O*-methylglucuronic acid
substituted, 110–111
- separation and identification,
chromatographic methods, 111–
114, 114–116
- Xylose, 6, 109, 127
- See also* Xylans